Lower Hassayampa River Watercourse Master Plan

River Behavior Report

Volume 5

Prepared for

Flood Control District of Maricopa County

2801 W. Durango Street
Phoenix, AZ 85009

Prepared by

JE FULLER
HYDROLOGY & GEOMORPHOLOGY, INC.

8400 S. Kyrene Road, Suite 201
Tempe, AZ 85284
www.jefuller.com

April 2006

Lower Hassayampa River Watercourse Master Plan

River Behavior Report

Prepared for

Flood Control District of Maricopa County

2801 W. Durango Street
Phoenix, AZ 85009

Prepared by

JE FULLER
HYDROLOGY & GEOMORPHOLOGY, INC.

8400 S. Kyrene Road, Suite 201
Tempe, AZ 85284
www.jefuller.com

Registered Geologist
Certificate No. 38732
Jonathan E. Fuller
Date Signed 4-7-06
Arizona U.S.A.

April 2006

Lower Hassayampa River Watercourse Master Plan

River Behavior Report

Prepared for

Flood Control District of Maricopa County

2801 W. Durango Street
Phoenix, AZ 85009

Registered Professional Engineer (Civil)
CERTIFICATE NO. 36246
JONATHAN E. FULLER
Date Signed 4-7-06
ARIZONA, U.S.A.

Prepared by

JE FULLER
HYDROLOGY & GEOMORPHOLOGY, INC.

8400 S. Kyrene Road, Suite 201
Tempe, AZ 85284
www.jefuller.com

Registered Geologist
CERTIFICATE NO. 38732
JONATHAN E. FULLER
Date Signed 4-7-06
ARIZONA, U.S.A.

April 2006

TABLE OF CONTENTS

CHAPTER 1 – RIVER BEHAVIOR REPORT INTRODUCTION
1.1 Purpose 1-1
1.2 Report Organization 1-1
1.3 Report Overview & Objectives 1-2
1.3.1 Field Reconnaissance Analysis 1-2
1.3.2 Geomorphic Analysis 1-3
1.3.3 Bed Elevation Analysis 1-3
1.3.4 Sediment Transport Analysis 1-4
1.3.5 Lateral Migration Analysis 1-4
1.3.6 Sediment Trend Analysis 1-5
1.4 Data Sources 1-5
1.5 Reach Designation 1-5
1.5.1 Hassayampa River Reach 1: Gila River to SPRR Bridge 1-5
1.5.2 Hassayampa River Reach 2: SPRR Bridge to I-10 Bridge 1-6
1.5.3 Hassayampa River Reach 3: I-10 Bridge to Jackrabbit Wash 1-6
1.5.4 Hassayampa River Reach 4: Jackrabbit Wash to Wagner/Daggs Wash 1-6
1.5.5 Hassayampa River Reach 5: Wagner/Daggs Wash to CAP Siphon 1-6
1.5.6 Jackrabbit Wash 1-6

CHAPTER 2 – FIELD RECONNAISSANCE REPORT
2.1 Objectives 2-1
2.2 Field Data Collected 2-2
2.3 Active Channel Conditions 2-2
2.3.1 Hassayampa River Reach 1: Gila River to SPRR Bridge 2-3
2.3.2 Hassayampa River Reach 2: SPRR Bridge to I-10 Bridge 2-10
2.3.3 Hassayampa River Reach 3: I-10 Bridge to Jackrabbit Wash 2-16
2.3.4 Hassayampa River Reach 4: Jackrabbit Wash to Wagner/Daggs Wash 2-25
2.3.5 Hassayampa River Reach 5: Wagner/Daggs Wash to CAP Siphon 2-30
2.4 Floodplain Conditions 2-35
2.4.1 Hassayampa River Reach 1: Gila River to SPRR Bridge 2-36
2.4.2 Hassayampa River Reach 2: SPRR Bridge to I-10 Bridge 2-43
2.4.3 Hassayampa River Reach 3: I-10 Bridge to Jackrabbit Wash 2-49
2.4.4 Hassayampa River Reach 4: Jackrabbit Wash to Wagner/Daggs Wash 2-57
2.4.5 Hassayampa River Reach 5: Wagner/Daggs Wash to CAP Siphon 2-61
2.5 Historical Flood Evidence 2-67
2.5.1 Avulsions 2-67
2.5.2 Flotsam 2-67
2.5.3 Sediment Deposits 2-68
2.6 Structures Investigation 2-72
2.6.1 Bank Protection 2-73
2.6.2 Bridges 2-74
2.6.3 Levees 2-79
2.6.4 At-Grade Road Crossings 2-81
2.6.5 Irrigation and Siphon Crossings 2-82
2.6.6 Power Line Towers and Poles 2-83

2.7 Sediment Data 2-88
2.7.1 Channel Bed Sediments 2-88
2.7.2 Channel Bank Sediments 2-88
2.7.3 Floodplain Sediments 2-92
2.8 Field Evidence of Vertical Channel Change 2-92
2.8.1 Headcuts and Tailcuts near Sand and Gravel Mines 2-92
2.8.2 Headcuts on Floodplain and Tributary Terraces 2-95
2.8.3 Long-Term Degradation in Reach 1 2-95
2.8.4 Evidence of Aggradation 2-96
2.8.5 Natural Grade Control 2-97
2.9 Summary 2-97

Chapter 3 GEOMORPHIC ANALYSIS REPORT 3-1
3.1 Purpose 3-1
3.2 Stream Classification 3-1
3.2.1 Brice Classification System 3-2
3.2.2 Rosgen Classification System 3-4
3.3 Geomorphic Mapping 3-7
3.3.1 Geomorphic Mapping and Lateral Stability 3-7
3.3.2 Methodology 3-8
3.3.3 Geomorphic Units 3-10
3.4 Geomorphic Surface Age Analysis 3-15
3.4.2 Results 3-25
3.5 Historical Analysis 3-32
3.5.1 Functional Surfaces 3-32
3.5.2 Results 3-58
3.5.3 Historical Avulsions 3-58
3.6 Empirical Geomorphic Analysis 3-61
3.6.1 Hydraulic Data 3-61
3.6.2 Hydraulic Geometry/Regime Equations 3-63
3.6.3 Allowable Velocity 3-75
3.6.4 Conclusions 3-79
3.7 Summary 3-79

CHAPTER 4 – BED ELEVATION ANALYSIS
4.1 Introduction 4-1
4.2 Scour 4-1
4.2.1 Methodology 4-2
4.2.2 Discussion & Results 4-5
4.2.3 Long-Term Scour 4-9
4.3 Equilibrium slope 4-9
4.3.1 Methodology 4-10
4.3.2 ADWR Equation 4-10
4.3.3 AMAFCA Equation 4-12
4.3.4 Schoklitsch Equation 4-13
4.3.5 Meyer-Peter, Muller Equation 4-13
4.3.6 Shields Diagram Method 4-14
4.3.7 Results 4-14

4.3.8 Summary 4-17
4.4 Armoring 4-17
4.4.1 Methodology 4-17
4.4.2 Meyer-Peter, Muller Bedload Transport Function 4-18
4.4.3 Competent Bottom Velocity 4-18
4.4.4 Shields Diagram 4-18
4.4.5 Yang Incipient Motion 4-19
4.4.6 Depth to Armor Equation 4-19
4.4.7 Results 4-19
4.4.8 Conclusions 4-20
4.5 Comparison of Armoring, Scour, and Equilibrium Slope 4-21
4.5.1 Conclusion 4-22
4.6 Bed Change Analysis 4-22
4.6.1 Data Sources 4-22
4.6.2 Cross Section Profile Analysis 4-22
4.6.3 Longitudinal Profile Analysis 4-58
4.6.4 Conclusions 4-68
4.7 Summary 4-69

CHAPTER 5 – SEDIMENT TRANSPORT ANALYSIS
5.1 Sediment Data 5-1
5.2 Sediment Transport Function 5-2
5.3 Model Hydrology 5-3
5.3.1 Hassayampa River 5-3
5.4 Sediment Inflow 5-8
5.4.1 Methodology 5-8
5.4.2 Jackrabbit Wash 5-9
5.4.3 Wagner Wash and Daggs Wash 5-9
5.4.4 Other Tributaries 5-9
5.5 HEC-6 Sediment Transport Modeling 5-9
5.5.1 Model Limitations 5-10
5.5.2 HEC-6 Model Parameters 5-12
5.5.3 HEC-6 Model Scenarios 5-16
5.5.4 HEC-6 Modeling Results 5-28
5.6 Reach Equation Analysis 5-28
5.6.1 Transport functions 5-28
5.6.2 Safe Yield Recommendation 5-33
5.7 In-Stream Mining Impact Analyses 5-33
5.7.1 Methodologies 5-33
5.7.2 Model Geometry Data 5-34
5.7.3 Flow Hydrograph 5-35
5.7.4 Sediment Data 5-36
5.7.5 ADOT Procedure 5-36
5.7.6 HEC-6 5-37
5.7.7 In-Stream Mining Impact Analysis Summary 5-40
5.8 Summary 5-40

CHAPTER 6 – LATERAL MIGRATION ANALYSIS

6.1 Objectives 6-1
6.2 Historical Channel Change Analysis 6-1
6.2.1 Single-Event Channel Change Analysis 6-1
6.2.2 Long-Term Channel Change Analysis 6-2
6.2.3 Width Change Analysis 6-3
6.2.4 Summary 6-3
6.3 Historical Flood Impact Analysis 6-8
6.3.1 Flood Chronology 6-8
6.3.2 Impacts of Historical Floods 6-9
6.3.3 Lateral Migration Constraints 6-9
6.4 Locational Probability Analysis 6-11
6.4.1 Methodology 6-11
6.4.2 Results and Interpretation 6-12
6.5 Erosion Hazard Zones 6-19
6.5.1 Methodologies 6-19
6.5.2 Severe Erosion Hazard Zone 6-27
6.5.3 Lateral Migration Erosion Hazard Zone 6-27
6.5.4 Long-Term Erosion Hazard Zone 6-28
6.5.5 Erosion Zone Delineation at the Pleistocene-Active Channel Contact 6-28
6.5.6 Erosion Hazard Zone Delineation 6-29
6.6 Jackrabbit Wash Erosion Hazard Delineation 6-29
6.6.1 Summary 6-30

CHAPTER 7 – SEDIMENT TREND ANALYSIS

7.1 River Behavior Trends: Vertical Channel Change 7-1
7.1.1 Functional Surface Analysis 7-1
7.1.2 Geomorphic Mapping 7-2
7.1.3 HEC-6 Modeling 7-3
7.1.4 Sediment Transport Calculations 7-4
7.1.5 Observed River Responses 7-4
7.1.6 Aggradation/Degradation Trend 7-5
7.2 River Behavior Trends: Lateral Channel Change 7-5
7.2.1 Functional Surface Analysis 7-6
7.2.2 Geomorphic Mapping 7-6
7.2.3 HEC-6 Modeling 7-7
7.2.4 Sediment Transport Calculations 7-7
7.2.5 Observed Lateral Channel Responses 7-7
7.2.6 Lateral Movement Trends 7-9
7.3 Implications of Sediment Trends 7-9
7.3.1 Flood Response 7-9
7.3.2 Natural Channel Controls 7-9
7.3.3 Encroachment & Channelization 7-9
7.3.4 Bridge Crossings 7-10
7.3.5 Sand & Gravel Mining 7-11
7.3.6 Watershed Urbanization 7-11
7.4 Recommendations for Future Sediment Analyses 7-12
7.5 Summary 7-12

CHAPTER 8 - SUMMARY
8.1 General Recommendations 8-1

CHAPTER 9 – REFERENCES

CHAPTER 10 - GLOSSARY

LIST OF FIGURES

CHAPTER 1 – RIVER BEHAVIOR REPORT INTRODUCTION
Figure 1-1. Map showing the Hassayampa River Reach 1 extent. 1-7
Figure 1-2. Map showing the Hassayampa River Reach 2 extent. 1-8
Figure 1-3. Map showing the Hassayampa River Reach 3 extent. 1-9
Figure 1-4. Map showing the Hassayampa River Reach 4 extent. 1-10
Figure 1-5. Map showing the Hassayampa River Reach 5 extent. 1-11

CHAPTER 2 – FIELD RECONNESSIANCE REPORT
Figure 2-1. Reach 1 photograph showing the active channel pattern and features2-4
Figure 2-2. Reach 1 active channel field photos 2-5
Figure 2-3. Reach 1 cutbank locations..... 2-6
Figure 2-4. Reach 1 cutbank field photos 2-7
Figure 2-5. White Tanks Wash confluence 2-8
Figure 2-6. Reach 1 structure photos..... 2-9
Figure 2-7. Reach 2 photograph showing channel pattern and features..... 2-10
Figure 2-8. Reach 2 vegetation field photos 2-11
Figure 2-9. Reach 2 cutbank locations..... 2-12
Figure 2-10. Reach 2 cutbank field photos 2-13
Figure 2-11. Reach 2 active channel field photos 2-15
Figure 2-12. Reach 3 photograph showing channel pattern and features..... 2-16
Figure 2-13. Reach 3 channel and bank vegetation..... 2-18
Figure 2-14. Reach 3 cutbank locations..... 2-19
Figure 2-15. Reach 3 cutbank field photos 2-20
Figure 2-16. Tonopah-Salome Hwy pre- and post-Dec 2004 flows..... 2-21
Figure 2-17. Sand & gravel mines near Tonopah-Salome Highway 2-22
Figure 2-18. Sand & gravel pit outflow channel 2-23
Figure 2-19. Reach 3 active channel field photos. 2-24
Figure 2-20. Reach 4 photograph showing channel pattern and features..... 2-25
Figure 2-21. Reach 4 Wagner Wash/Daggs Wash confluence 2-26
Figure 2-22. Reach 4 channel and bank vegetation..... 2-27
Figure 2-23. Reach 4 cutbank locations..... 2-28
Figure 2-24. Reach 4 cutbank field photos 2-29
Figure 2-25. Reach 5 photograph showing channel pattern and features..... 2-30
Figure 2-26. Reach 5 channel and bank vegetation..... 2-31
Figure 2-27. Reach 5 cutbank locations..... 2-32
Figure 2-28. Reach 5 cutbank field photos 2-33
Figure 2-29. Reach 5 active channel field photos 2-34
Figure 2-30. Reach 1 Ql surface 2-38
Figure 2-31. Field photos of Late Pleistocene surface - Reach 1..... 2-39
Figure 2-32. Levees upstream of SPRR Bridge 2-40
Figure 2-33. Reach 1 floodplain field photos upstream of the SPRR Bridge..... 2-41
Figure 2-34. Reach 1 floodplain field photos downstream of the SPRR Bridge 2-42
Figure 2-35. Locations of headcuts in Reach 2..... 2-44
Figure 2-36. Locations of potential avulsions in Reach 2..... 2-45
Figure 2-37. Photos of headcuts and potential avulsion locations in Reach 2 2-45

Figure 2-38. Reach 2 floodplain vegetation 2-47
Figure 2-39. Photos of structures in the Reach 2 floodplain 2-48
Figure 2-40. Reach 3 tributary terraces 2-50
Figure 2-41. Locations of headcuts in Reach 3 2-51
Figure 2-42. Locations of potential avulsion in Reach 3 2-52
Figure 2-43. Photos of headcuts and a potential avulsion location in Reach 3 2-52
Figure 2-44. Reach 3 disturbed floodplain areas 2-53
Figure 2-45. Reach 3 floodplain vegetation 2-54
Figure 2-46. Reach 3 floodplain structure field photos 2-56
Figure 2-47. Runoff and sediment intercepted by White Tanks Wash 2-57
Figure 2-48. Reach 4 headcut locations 2-59
Figure 2-49. Reach 4 potential avulsion locations 2-59
Figure 2-50. Reach 4 geomorphic feature field photos 2-60
Figure 2-51. Reach 4 floodplain vegetation 2-61
Figure 2-52. Reach 5 headcut locations 2-63
Figure 2-53. Example of headcuts originating from avulsion channels 2-63
Figure 2-54. Example of long-term headcut migration 2-64
Figure 2-55. Reach 5 potential avulsion locations 2-64
Figure 2-56. Vegetative cover on Reach 5 floodplain surfaces. 2-65
Figure 2-57. CAP siphon excavated area 2-66
Figure 2-58. Reach 5 sand and gravel mine complex 2-67
Figure 2-59. High terrace flotsam locations 2-69
Figure 2-60. Field photos of flotsam on high terrace surfaces 2-70
Figure 2-61. Locations of 1890 flood deposits 2-71
Figure 2-62. Field photos of 1890 high terrace deposit 2-71
Figure 2-63. Typical locations of slackwater deposits 2-72
Figure 2-64. CAP canal bank stabilization 2-73
Figure 2-65. Field photos of CAP canal bank stabilization 2-74
Figure 2-66. Field photos of the Old US Highway 80 Bridge 2-75
Figure 2-67. Field photos of railroad bridge 2-77
Figure 2-68. Field photos of the Interstate 10 Bridges 2-78
Figure 2-69. Field photos of Reach 1 levees 2-79
Figure 2-70. Levees upstream of railroad bridge 2-80
Figure 2-71. Reach 2 levee 2-80
Figure 2-72. Reach 4 levee 2-81
Figure 2-73. Arlington Canal siphon 2-82
Figure 2-74. Field photos of power poles at Baseline Road 2-83
Figure 2-75. Field photos of power line towers in Reach 2 2-84
Figure 2-76. Reach 3 power pole alignment 2-84
Figure 2-77. Reach 5 field photos of the southern power line alignment towers 2-85
Figure 2-78. Reach 5 field photos of the northern power line alignment towers 2-87
Figure 2-79. Field photos of channel bed sediments 2-89
Figure 2-80. Low terrace channel bank sediments 2-90
Figure 2-81. High terrace channel bank sediments 2-90
Figure 2-82. Tributary terrace channel bank sediments 2-91
Figure 2-83. Pleistocene terrace channel bank sediments 2-92
Figure 2-84. Headcut upstream of the Pioneer Sand gravel pit. 2-94
Figure 2-85. Tailcut channel downstream of the Hansen gravel pit. 2-95

Figure 2-86. Hassayampa River at the Naramore Road crossing.....2-96
Figure 2-87. Photos of incised Hassayampa River near the Gila River conf.....2-96

CHAPTER 3 – GEOMORPHIC ANALYSIS REPORT

Figure 3-1. Idealized Sketch of Riverine Terraces and Ages.....3-8
Figure 3-2. Field photographs of active channel surfaces.....3-11
Figure 3-3. Field photographs of active bar surfaces.....3-12
Figure 3-4. Field photographs of low terrace surfaces.....3-13
Figure 3-5. Field photograph of high terrace surface.....3-13
Figure 3-6. Field photographs of tributary deposit surfaces.....3-14
Figure 3-7. Soil pit location map.....3-18
Figure 3-8. Reach 1 mapped geomorphology.....3-26
Figure 3-9. Reach 2 mapped geomorphology.....3-27
Figure 3-10. Reach 3 mapped geomorphology.....3-28
Figure 3-11. Reach 4 mapped geomorphology.....3-29
Figure 3-12. Reach 5a mapped geomorphology.....3-30
Figure 3-13. Reach 5b mapped geomorphology.....3-31
Figure 3-14. Reach 1 active channel surfaces.....3-34
Figure 3-15. Reach 2 active channel surfaces.....3-35
Figure 3-16. Reach 3 active channel surfaces.....3-36
Figure 3-17. Reach 4 active channel surfaces.....3-37
Figure 3-18. Reach 5a active channel surfaces.....3-38
Figure 3-19. Reach 5b active channel surfaces.....3-39
Figure 3-20. Reach 1 bar surfaces.....3-40
Figure 3-21. Reach 2 bar surfaces.....3-41
Figure 3-22. Reach 3 bar surfaces.....3-42
Figure 3-23. Reach 4 bar surfaces.....3-43
Figure 3-24. Reach 5a bar surfaces.....3-44
Figure 3-25. Reach 5b bar surfaces.....3-45
Figure 3-26. Reach 1 floodplain terrace surfaces.....3-46
Figure 3-27. Reach 2 floodplain terrace surfaces.....3-47
Figure 3-28. Reach 3 floodplain terrace surfaces.....3-48
Figure 3-29. Reach 4 floodplain terrace surfaces.....3-49
Figure 3-30. Reach 5a floodplain terrace surfaces.....3-50
Figure 3-31. Reach 5b floodplain terrace surfaces.....3-51
Figure 3-32. Reach 1 tributary deposit surfaces.....3-52
Figure 3-33. Reach 2 tributary deposit surfaces.....3-53
Figure 3-34. Reach 3 tributary deposit surfaces.....3-54
Figure 3-35. Reach 4 tributary deposit surfaces.....3-55
Figure 3-36. Reach 5a tributary deposit surfaces.....3-56
Figure 3-37. Reach 5b tributary deposit surfaces.....3-57
Figure 3-38. 1951 channel avulsion near Baseline Road.....3-59
Figure 3-39. 1951 channel avulsion near Tonopah-Salome Highway.....3-60

CHAPTER 4 – BED ELEVATION ANALYSIS

Figure 4-1. I-10 Westbound Bridge 100-year HEC-RAS bridge scour plot. 4-7
Figure 4-2. I-10 Eastbound Bridge 100-year HEC-RAS bridge scour plot. 4-7
Figure 4-3. Union Pacific Railroad Bridge 100-year HEC-RAS bridge scour plot....4-8
Figure 4-4. Old US 80 Bridge 100-year bridge scour plot. 4-8
Figure 4-5. Cross-Section 27.61 Profile Comparison.....4-24
Figure 4-6. Cross-Section 26.67 Profile Comparison.....4-25
Figure 4-7. Cross-Section 25.72 Profile Comparison.....4-26
Figure 4-8. Cross-Section 24.77 Profile Comparison.....4-27
Figure 4-9. Cross-Section 24.20 Profile Comparison.....4-28
Figure 4-10. Cross-Section 23.63 Profile Comparison.....4-29
Figure 4-11. Cross-Section 22.59 Profile Comparison.....4-30
Figure 4-12. Cross-Section 21.46 Profile Comparison.....4-31
Figure 4-13. Cross-Section 20.51 Profile Comparison.....4-32
Figure 4-14. Cross-Section 19.75 Profile Comparison.....4-33
Figure 4-15. Cross-Section 19.28 Profile Comparison.....4-34
Figure 4-16. Cross-Section 18.62 Profile Comparison.....4-35
Figure 4-17. Cross-Section 17.58 Profile Comparison.....4-36
Figure 4-18. Cross-Section 16.53 Profile Comparison.....4-37
Figure 4-19. Cross-Section 15.59 Profile Comparison.....4-38
Figure 4-20. Cross-Section 14.45 Profile Comparison.....4-39
Figure 4-21. Cross-Section 13.32 Profile Comparison.....4-40
Figure 4-22. Cross-Section 12.37 Profile Comparison.....4-41
Figure 4-23. Cross-Section 11.43 Profile Comparison.....4-42
Figure 4-24. Cross-Section 10.50 Profile Comparison.....4-43
Figure 4-25. Cross-Section 9.74 Profile Comparison.....4-44
Figure 4-26. Cross-Section 9.08 Profile Comparison.....4-45
Figure 4-27. Cross-Section 8.51 Profile Comparison.....4-46
Figure 4-28. Cross-Section 7.75 Profile Comparison.....4-47
Figure 4-29. Cross-Section 6.52 Profile Comparison.....4-48
Figure 4-30. Cross-Section 5.48 Profile Comparison.....4-49
Figure 4-31. Cross-Section 5.00 Profile Comparison.....4-50
Figure 4-32. Cross-Section 4.53 Profile Comparison.....4-51
Figure 4-33. Cross-Section 3.53 Profile Comparison.....4-52
Figure 4-34. Cross-Section 2.48 Profile Comparison.....4-53
Figure 4-35. Cross-Section 1.49 Profile Comparison.....4-54
Figure 4-36. Cross-Section 1.11 Profile Comparison.....4-55
Figure 4-37. Cross-Section 0.54 Profile Comparison.....4-56
Figure 4-38. Longitudinal Profile of Hassayampa River 4-59
Figure 4-39. Historical Longitudinal Profile Plot 4-60
Figure 4-40. Reach 5 Longitudinal Profile.....4-61
Figure 4-41. Reach 4 Longitudinal Profile.....4-62
Figure 4-42. Reach 3 Longitudinal Profile.....4-63
Figure 4-43. Reach 2 Longitudinal Profile.....4-64
Figure 4-44. Reach 1 Longitudinal Profile.....4-65
Figure 4-45. Slope Change by Reach, 1957-2004.....4-67

CHAPTER 5 – SEDIMENT TRANSPORT ANALYSIS

Figure 5-1. Sediment gradation curve 5-2
Figure 5-2. Long-Term Hydrographs 5-4
Figure 5-3. 100-Year Hydrographs 5-5
Figure 5-4. Flow Distribution in Leveed Reach 5-7
Figure 5-5. Sediment Inflow Rating Curve for the Hassayampa River 5-8
Figure 5-6. Hydraulics Calibration 5-14
Figure 5-7. Downstream Rating Curve 5-16
Figure 5-8. Sediment Inflow model calibration 5-19
Figure 5-9. Manning's N model calibration 5-20
Figure 5-10. Influence of Tributary sediments 5-21
Figure 5-11. Average Bed Change – Base Conditions Model 5-23
Figure 5-12. Initial and Final Average Bed Elevations (1 of 3) 5-23
Figure 5-13. Initial and Final Average Bed Elevations (2 of 3) 5-24
Figure 5-14. Initial and Final Average Bed Elevations (3 of 3) 5-24
Figure 5-15. Manning's n value sensitivity 5-25
Figure 5-16. Sediment Inflow Sensitivity 5-26
Figure 5-17. Particle size sensitivity 5-27
Figure 5-18. Particle size sensitivity 5-27
Figure 5-19. Reach limits 5-29
Figure 5-20. Sediment Transport Capacity by Subreach 5-31
Figure 5-21. Cross Section for Pit Occupying Entire Floodplain. 5-34
Figure 5-22. Cross Section for Pit Occupying Part of Channel 5-35
Figure 5-23. Cross Section for Pit Located in Floodway Fringe. 5-35
Figure 5-24. Gravel Pit Analysis – Pit Occupying Full Width Of Channel 5-38
Figure 5-25. Gravel Pit Analysis – Pit Located At One Side Of Channel 5-39
Figure 5-26. Gravel Pit Analysis – Pit Located At Middle Of Channel 5-39

CHAPTER 6 – LATERAL MIGRATION ANALYSIS

Figure 6-1. Right bank lateral migration summary 6-4
Figure 6-2. Left bank lateral migration summary 6-5
Figure 6-3. Lower Hassayampa lateral migration summary 6-6
Figure 6-4. Width change analysis summary 6-7
Figure 6-5. Major tributary avulsion locations 6-10
Figure 6-6. Alma School Road Bridge abutment erosion. 6-11
Figure 6-7. Locational Probability for Reach 1 6-13
Figure 6-8. Locational Probability for Reach years) 6-14
Figure 6-9. Locational Probability for Reach years) 6-15
Figure 6-10. Locational Probability for Reach years) 6-16
Figure 6-11. Locational Probability for Reach years) 6-17
Figure 6-12. Locational Probability for Reach years) 6-18
Figure 6-13. Hydraulic data spatial plots 6-23
Figure 6-14. Velocity data spatial plots 6-24
Figure 6-15. Depth data spatial plots 6-25
Figure 6-16. Depth-velocity product data spatial plots 6-26
Figure 6-17. Lower Hassayampa River Erosion Hazard Zones - Reach 1 6-31
Figure 6-18. Lower Hassayampa River Erosion Hazard Zones - Reach 2 6-32
Figure 6-19. Lower Hassayampa River Erosion Hazard Zones - Reach 3 6-33

Figure 6-20. Lower Hassayampa River Erosion Hazard Zones - Reach 4 6-34
Figure 6-21. Lower Hassayampa River Erosion Hazard Zones - Reach 5a 6-35
Figure 6-22. Lower Hassayampa River Erosion Hazard Zones - Reach 5b 6-36
Figure 6-23. Jackrabbit Wash Erosion Hazard Zone 6-37

LIST OF TABLES

CHAPTER 2 – FIELD RECONNESSIANCE REPORT
Table 2-1. Reach 1 Surface-Type Distribution 2-37
Table 2-2. Reach 2 Surface-Type Distribution 2-43
Table 2-3. Reach 3 Surface-Type Distribution 2-49
Table 2-4. Reach 4 Surface-Type Distribution 2-58
Table 2-5. Reach 5 Surface-Type Distribution 2-62
Table 2-6. Reach 2 - cutbank erosion distance 2-83

CHAPTER 3 – GEOMORPHIC ANALYSIS REPORT
Table 3-1. Brice Stream Classification System 3-2
Table 3-2. Rosgen classification data 3-4
Table 3-3. Soil analysis summary 3-19
Table 3-4. Channel Pattern Relationships 3-66
Table 3-5. Observed and Expected Channel Characteristics 3-73
Table 3-6. Fortier & Scobey Table of Permissible Canal Velocities (ft/s) 3-76
Table 3-7. Suggested Maximum Permissible Mean Channel Velocities 3-77
Table 3-8. Corps of Engineers Erosive Velocity Data 3-77
Table 3-9. Flood Velocities 3-78
Table 3-10. Allowable Velocity Results 3-78

CHAPTER 4 – BED ELEVATION ANALYSIS
Table 4-1. Scour Estimates (ft) 4-6
Table 4-2. HEC-RAS 100-Year Bridge Scour Estimates (ft) 4-6
Table 4-3. ADWR Equilibrium Slope Results (ft) 4-15
Table 4-4. Equilibrium Slope Analysis Results (Slope in ft/ft) 4-16
Table 4-5. Armoring Analysis Results 4-20
Table 4-6. Comparison of Armoring, Scour, and Equilibrium Slope Estimates 4-21
Table 4-7. Sources of historical topography 4-22
Table 4-8. Historical Channel Slopes 4-66
Table 4-9. Historical Channel Slopes By Reach 4-66

CHAPTER 5 – SEDIMENT TRANSPORT ANALYSIS
Table 5-1. Transport function equation data 5-3
Table 5-2. Model Limitations 5-12
Table 5-3. 1987 and 2004 Topography Comparisons 5-18
Table 5-4. Sediment load passing through the system 5-22
Table 5-5. Long-Term Hydrograph Discretizations 5-30
Table 5-6. 100-year Event Hydrograph Discretizations 5-30
Table 5-7. Long-Term Reach-By-Reach Bed Change (ft) 5-32
Table 5-8. 100-Year Event Reach-By-Reach Bed Change (ft) 5-32
Table 5-9. HEC-6 Reach-By-Reach Net Bed Change 5-33
Table 5-10. Pit Analyses Parameters (ft) 5-34
Table 5-11. ADOT Procedure Pit Analysis Results 5-36

CHAPTER 6 – LATERAL MIGRATION ANALYSIS

Table 6-1. Maximum single-event channel change summary 6-2
Table 6-2. Cumulative channel change summary 6-2
Table 6-3. List of floods and subsequent aerial photo coverage 6-8
Table 6-4. Historical Flood Impacts on the Active Corridor 6-9

APPENDICES

APPENDIX 5.1 – Field forms
APPENDIX 5.2 – Soil description sheets
APPENDIX 5.3 – Results of geomorphic mapping & soils analysis
APPENDIX 5.4 – Sediment sample gradation data
APPENDIX 5.5 – HEC-6 vs. RAS comparison tables
APPENDIX 5.6 – ADOT scour example details

CHAPTER 1 - RIVER BEHAVIOR REPORT INTRODUCTION

1.1 Purpose

The purpose of a watercourse master plan (WCMP) is to identify and develop a plan and technical guidance for managing flood hazards, lateral migration of the watercourse, and the cumulative impacts of existing and future development in the floodplain. Authority to perform watercourse master planning is granted in Arizona Revised Statutes Title 48 (ARS 48-3609). This River Behavior Report was prepared to support the Lower Hassayampa River Watercourse Master Plan (LHWCMP).

The purpose of the river behavior analysis was to compile, analyze, and present the best available information representative of the historical and existing fluvial processes for the Lower Hassayampa River, and to synthesize this information for the purpose of providing insight into the potential future behavior of the system. To date, the Hassayampa River is one of only a few remaining undammed major watercourses in Arizona. This free-flowing condition has resulted in a more "natural" condition of the river and floodplain than those found in many other river systems in the state. Development pressure within the Lower Hassayampa River watershed and numerous permit applications for new in-stream aggregate mine necessitated a working understanding of the river, both past and present, so that any proposed future changes to the system can be adequately understood and incorporated into a future watercourse master plan.

1.2 Report Organization

The River Behavior Report prepared in support of the LHWCMP was organized around six primary types of analyses, each of which are discussed separately in the following chapters:

- Chapter 2: Field Reconnaissance Analysis
- Chapter 3: Geomorphic Analysis
- Chapter 4: Bed Elevation Analysis
- Chapter 5: Sediment Transport Analysis
- Chapter 6: Lateral Migration Analysis
- Chapter 7: Sediment Trend Analysis

In addition to the technical analyses, the following chapters were included to summarize the results and present supplemental and supporting information:

- Chapter 8: Summary & Recommendations
- Chapter 9: References
- Chapter 10: Glossary

The River Behavior Report primarily addresses the historical and expected behavior of the Lower Hassayampa River. While erosion hazard zones were defined for Jackrabbit Wash based on application of the Level 3 Limited Detailed Methodology defined in the

Flood Control District of Maricopa County's (District) draft Erosion Hazard Zone Delineation and Development Guidelines (JEF, 2004), the District's scope of services did not authorized application to Jackrabbit Wash of most of the types of analyses applied to the Hassayampa River. Therefore, unless specifically noted, this report focuses on the Lower Hassayampa River, from the CAP Siphon to the Gila River confluence.

1.3 Report Overview & Objectives

An overview and summary of the specific objectives for each of the types of technical analyses presented in Chapters 2 to 7 are summarized below.

1.3.1 Field Reconnaissance Analysis

Geomorphology is a field-based science of observation that relies heavily on the judgment and interpretation of the investigator. Although a significant amount of geomorphic information can be obtained by non-field-based analyses (such as aerial photo interpretation), a detailed field assessment is critical for understanding the river system, verifying mapping, and ground-truthing landform interpretations. Therefore, the LHWCMP study included a significant number of field visits, systematic detailed field observations, and photo-documentation of field conditions. The following types of field visits were performed:

- Initial Reconnaissance Trips. Reconnaissance was performed by project personnel with expertise in hydraulic engineering, hydrologic modeling, sedimentation engineering, floodplain management, land planning, environmental management, resource management, biology, and archaeology.

- Detailed Field Investigations. Field investigations were conducted by geomorphologists from JE Fuller/Hydrology & Geomorphology, Inc. (JEF), and consisted of observing key features of the study area, preparing systematic field notes, and obtaining photographs of channel and floodplain conditions. The results of these field investigations are presented in Chapter 2 (Field Reconnaissance Analysis).

- Detailed Soil Investigations. Soil investigations were conducted by JEF geomorphologists, and consisted of examination and description of 25 soil pits in channel and floodplain areas. The results of the soil investigation are described in Chapter 3 (Geomorphic Analysis).

- Follow-Up Trips. Additional field tours were conducted with the entire LHWCMP team to present findings to District staff and stakeholders.

- Flood Visit. A field visit was conducted during flooding in late December 2004. JEF staff documented and photographed changes to the river prior to the flood event.

The objective of the field reconnaissance analysis was to observe and document channel and floodplain conditions for use in calibrating and verifying the results of the

geomorphic and sedimentation analyses. Most of the field data are presented in Chapter 2.

1.3.2 Geomorphic Analysis

The primary purpose of the geomorphic analysis was to identify the current and historical geomorphology of the Lower Hassayampa River within the study area. This goal was accomplished through the following tasks:

- Stream Classification. Two proven methods of stream classification were employed (Brice and Rosgen) for comparison. Stream classification techniques are used to identify channel processes expected to impact or be impacted by future urbanization of the watershed and river corridor.

- Geomorphic Mapping. Detailed mapping of geomorphic landforms within the geologic floodplain was performed to identify geologically recent lateral channel movement and sediment distributions, and to characterize potential future channel movement.

- Empirical Geomorphic Analyses. Empirical geomorphic relationships were used to characterize and assess channel pattern, channel plan form, and channel geometry, and to predict expected lateral and vertical channel movement.

The results of the geomorphic analysis are presented in Chapter 3.

1.3.3 Bed Elevation Analysis

The purpose of the bed elevation change analysis was to determine historical changes in bed elevation from a variety of data sources, and compare historical trends with computational methods that predict future changes. The methods used for the LHWCMP included the following:

- Scour Estimates. Local and general scour depths were estimated using standard equations and hydraulic data obtained from HEC-RAS modeling developed for the LHWCMP.

- Equilibrium Slope Analysis. The potential for long-term scour was assessed by applying a variety of equilibrium slope equations.

- Armoring Analysis. Analytical techniques to predict the ability of the river to resist scour by armoring were applied to the study reach.

- Historical Topographic Data. Changes in channel bed elevations shown on historical topographic maps, stream gauge rating curves, hydraulic model cross sections, and as-built plans were evaluated to detect changes in bed elevation.

- Longitudinal Profile Analysis. The longitudinal profile of the river was examined to identify anomalies and irregularities that might indicate future channel change.

- Field Observations. Field data were used to verify the reasonability of scour estimates determined by the methods listed above.

The results of the bed elevation analyses are presented in Chapter 4.

1.3.4 Sediment Transport Analysis

The objective of the sediment transport analysis was to simulate the long-term streambed profile response to the Lower Hassayampa River based on natural and existing conditions within the river corridor. This objective was accomplished via the following tasks:

- HEC-6 Modeling. HEC-6 sediment transport modeling of the river was prepared and verified using historical channel bed elevation changes. Models predicting future response to the 100-year design flood and the historical flood series were prepared and evaluated. Sensitivity analyses of upstream sediment supply, tributary sediment inflow, roughness, and transport function were prepared.

- Sediment Continuity Routing. Spreadsheet based sediment continuity modeling was also prepared using HEC-RAS hydraulic data and the sediment transport functions applied in the HEC-6 model.

- Mining Impact Analysis. Techniques for evaluating the potential impacts of in-stream aggregate mining were applied and assessed for the study reach.

The results of the sediment transport analysis are presented in Chapter 5.

1.3.5 Lateral Migration Analysis

The objectives of the lateral migration analysis were to estimate the potential for future lateral migration of the Lower Hassayampa River and to develop regulatory erosion hazard zone boundaries within the study area. The lateral migration analysis relied on the results from the analyses described above in conjunction with the following methodologies:

- Historical Channel Position Analysis. Changes in channel position, channel morphology, and channel pattern were described and quantified using semi-rectified historical aerial photographs.

- Channel Locational Probability Analysis. GIS-based mapping and analysis techniques were applied to determine locational probability statistics describing the frequency of channel position within the geologic floodplain over the period of photographic record.

- Impacts of Historical Flood Events. Channel changes occurring in response to specific large floods were described and quantified using the semi-rectified historical aerial photographs.

Erosion hazard zones were also developed for Jackrabbit Wash from the Central

Arizona Project Siphon to the Hassayampa River confluence. The results of the lateral migration analysis are presented in Chapter 6.

1.3.6 Sediment Trend Analysis

The purpose of the sediment trend analysis was to develop a management tool based on the results of the analyses described above that could be used to evaluate the impacts on future activities and infrastructure in the channel corridor. The sediment trend focused on predicting the following potential channel responses:

- Aggradation/Degradation
- Lateral Movement
- Response to Urbanization and Channelization

The results of the sediment trend analysis are presented in Chapter 7.

1.4 Data Sources

The methods used to assess the river behavior in the LHWCMP study area relied on a variety of existing information, field data, and new analyses. Information from a variety of sources was collected and synthesized for use in each of the six primary analyses. A brief list of the types of data collected is shown below, segregated by data type. A detailed summary of the project data collection effort is discussed in the *Lower Hassayampa River Watercourse Master Plan Data Collection Report* (JEF, 2005).

1.5 Reach Designation

For the river behavior analyses, the LHWCMP study area was considered in five reaches. The reaches were subdivided based on natural geomorphic or geographic features such as tributaries, manmade structures such as bridges, and hydraulic characteristics identified by HEC-RAS modeling. The purpose of the reach divisions was to isolate impacts on the river of features such as bridges and tributaries (or vice-versa). Reach descriptions are provided below along with maps illustrating the reach limits (Figure 1-1 to Figure 1-5).

1.5.1 Hassayampa River Reach 1: Gila River to SPRR Bridge

Hassayampa River Reach 1 extends from the southern study area limit to just upstream of the Southern Pacific Railroad (SPRR) Bridge, corresponding to river miles (RM) 0.82 and 4.63 in the WEST Consultants HEC-RAS model, respectively. For the river behavior analysis, the southern study area limit was defined as the Gila River regulatory floodway boundary.

Reach 1 contains the river segments with the most significant long-term human impacts that include channelization, channel straightening, agricultural leveling of the floodplain, and impending urbanization. Other significant manmade features that define Reach 1 include the following:

- SPRR Bridge
- Old US Route 80 (US 80) Bridge
- Farm Levees – US 80 to Gila River floodplain

- Buckeye Canal Outfall & Irrigation Tailwater
- Arlington Canal Siphon

1.5.2 Hassayampa River Reach 2: SPRR Bridge to I-10 Bridge

Hassayampa River Reach 2 extends from Reach 1 (RM 4.63) to just downstream of the Interstate 10 (I-10) Bridges (RM 10.21). The active channel in this reach has a single channel pattern, whereas upstream of Reach 2 the channel alternates between single channel and braided forms. The lower limit was defined at 1.5 miles below the I-10 Bridges to include the effect of the I-10 Bridges in Reach 3.

1.5.3 Hassayampa River Reach 3: I-10 Bridge to Jackrabbit Wash

Reach 3 extends from Reach 2 (RM 10.21) to just upstream of the Jackrabbit Wash confluence (RM 15.68). The upstream limit was defined to help isolate the effects of Jackrabbit Wash on channel morphology. The initial geomorphic interpretation indicated that the impact of Jackrabbit Wash on the Hassayampa River did not extend further downstream than Baseline Road. The lower limit of Reach 3 was extended 1.5 miles downstream of the I-10 Bridges to account for the geomorphic impact of the bridges on the river.

1.5.4 Hassayampa River Reach 4: Jackrabbit Wash to Wagner/Daggs Wash

Reach 4 extends from Reach 3 (RM 15.68) to immediately upstream of the Daggs Wash/Wagner Wash confluence (RM 21.65). These limits were selected to isolate the effects of the two major tributaries on the Hassayampa River. The Daggs Wash and Wagner Wash confluences are the major geomorphic features in Reach 4.

1.5.5 Hassayampa River Reach 5: Wagner/Daggs Wash to CAP Siphon

Reach 5 extends from Reach 4 (RM 21.65) to the upstream limit of the LHWMCP study area (RM 27.89). Reach 5 has the widest floodplain in the LHWCMP study area. Also, the general geographic orientation of the river changes at the approximate mid-point of Reach 5. The change in orientation creates map presentation issues, so Reach 5 was divided into two subreaches (5a and 5b), as shown in Figure 1-5. Most of the maps in the river behavior report use the 5a/5b division, although, from an analysis standpoint Reach 5 was considered as one continuous reach.

1.5.6 Jackrabbit Wash

Jackrabbit Wash was considered as a single reach from the upstream LHWCMP study limit at the CAP Siphon to the confluence with Jackrabbit Wash, and included the breakout reach identified in the WEST LHWMCP Hydraulics Report.

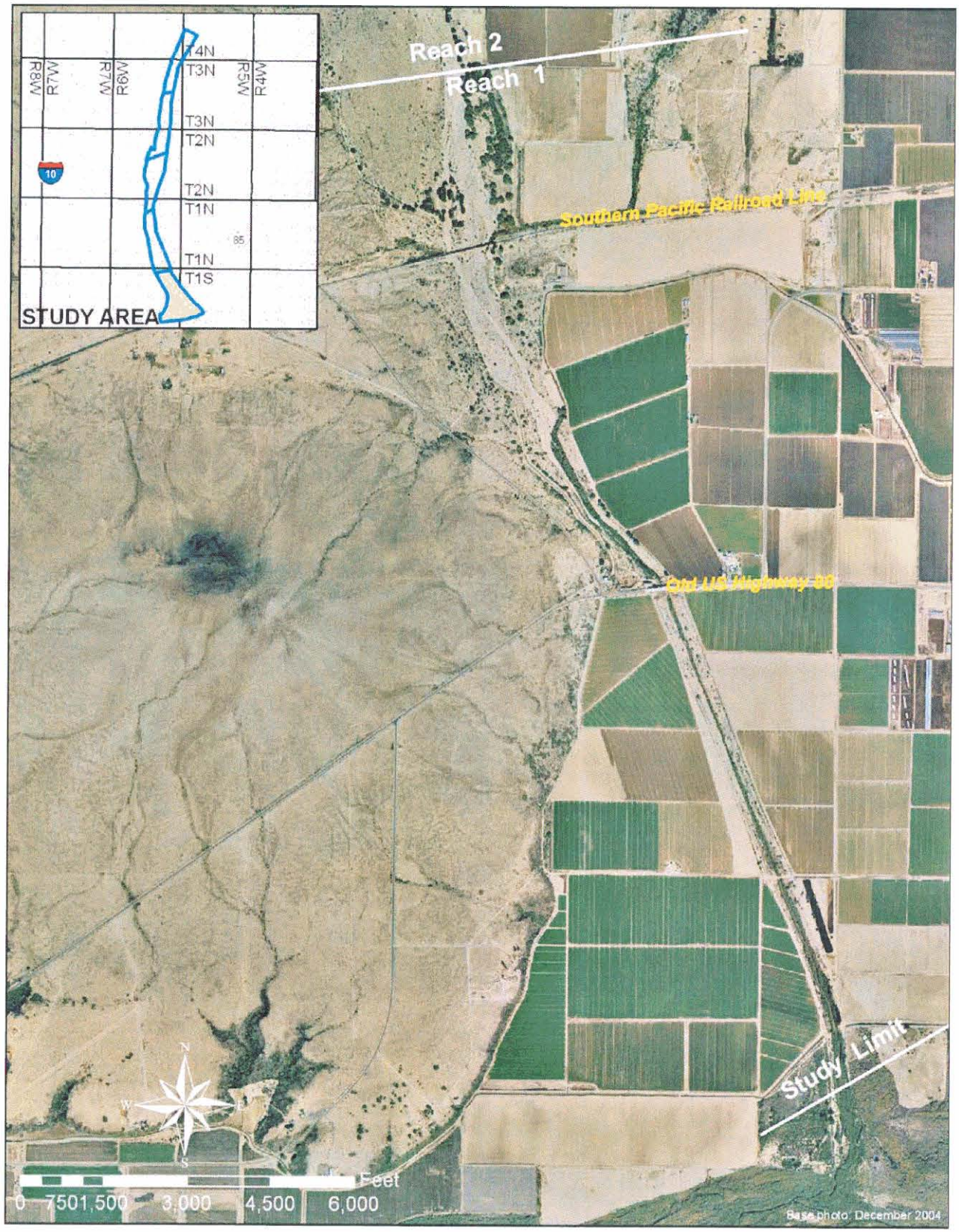

Figure 1-1. Map showing the Hassayampa River Reach 1 extent.

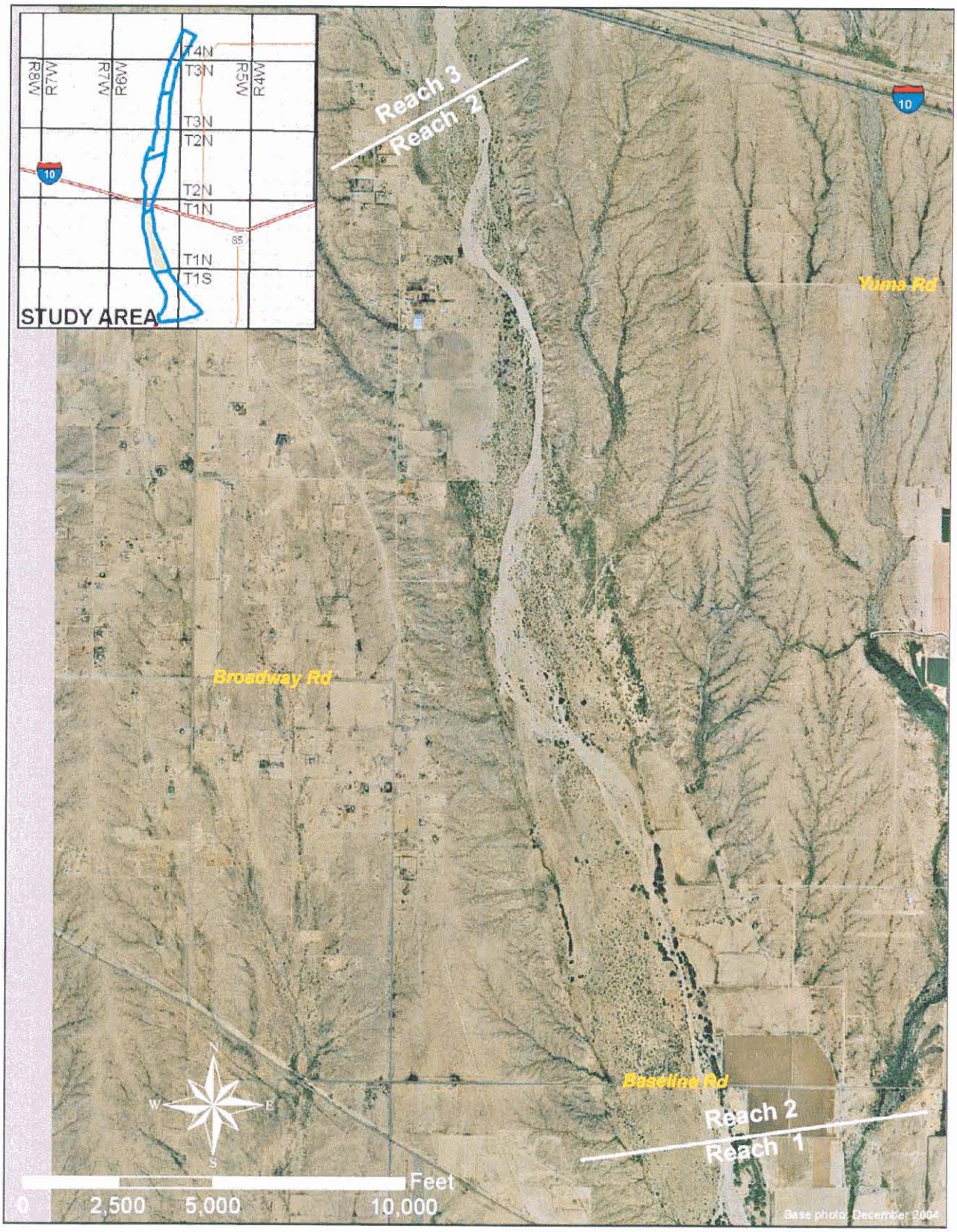

Figure 1-2. Map showing the Hassayampa River Reach 2 extent.

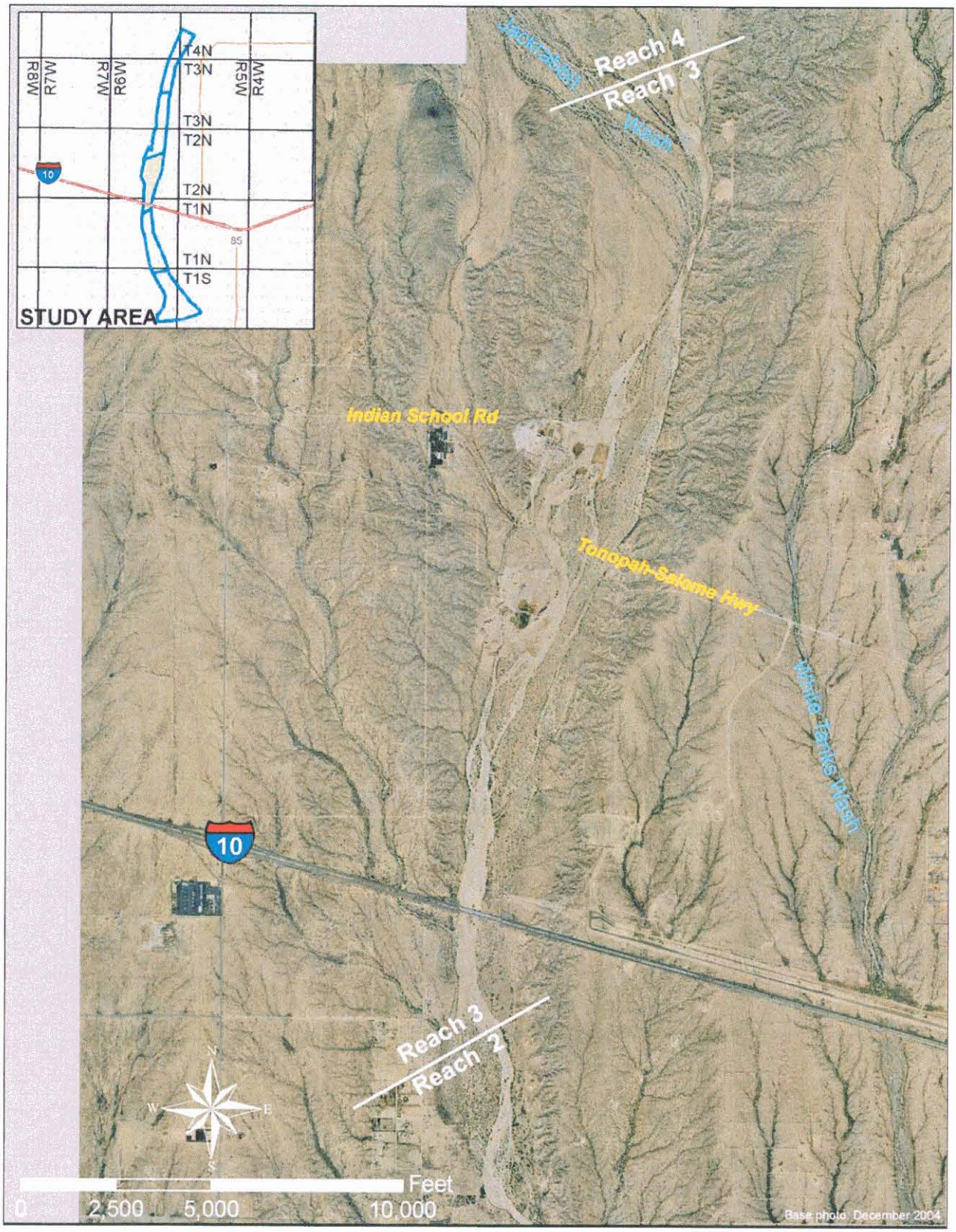

Figure 1-3. Map showing the Hassayampa River Reach 3 extent.

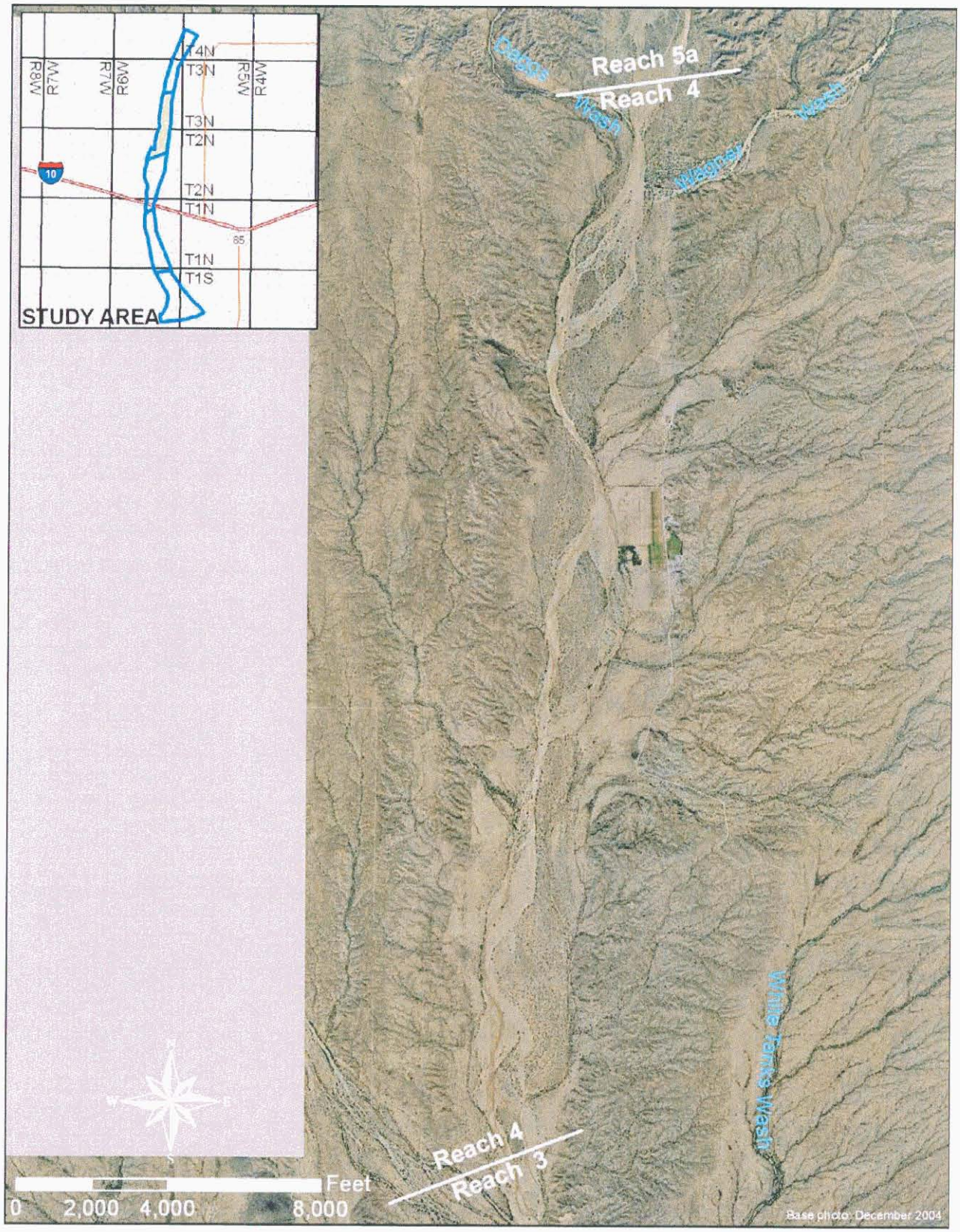

Figure 1-4. Map showing the Hassayampa River Reach 4 extent.

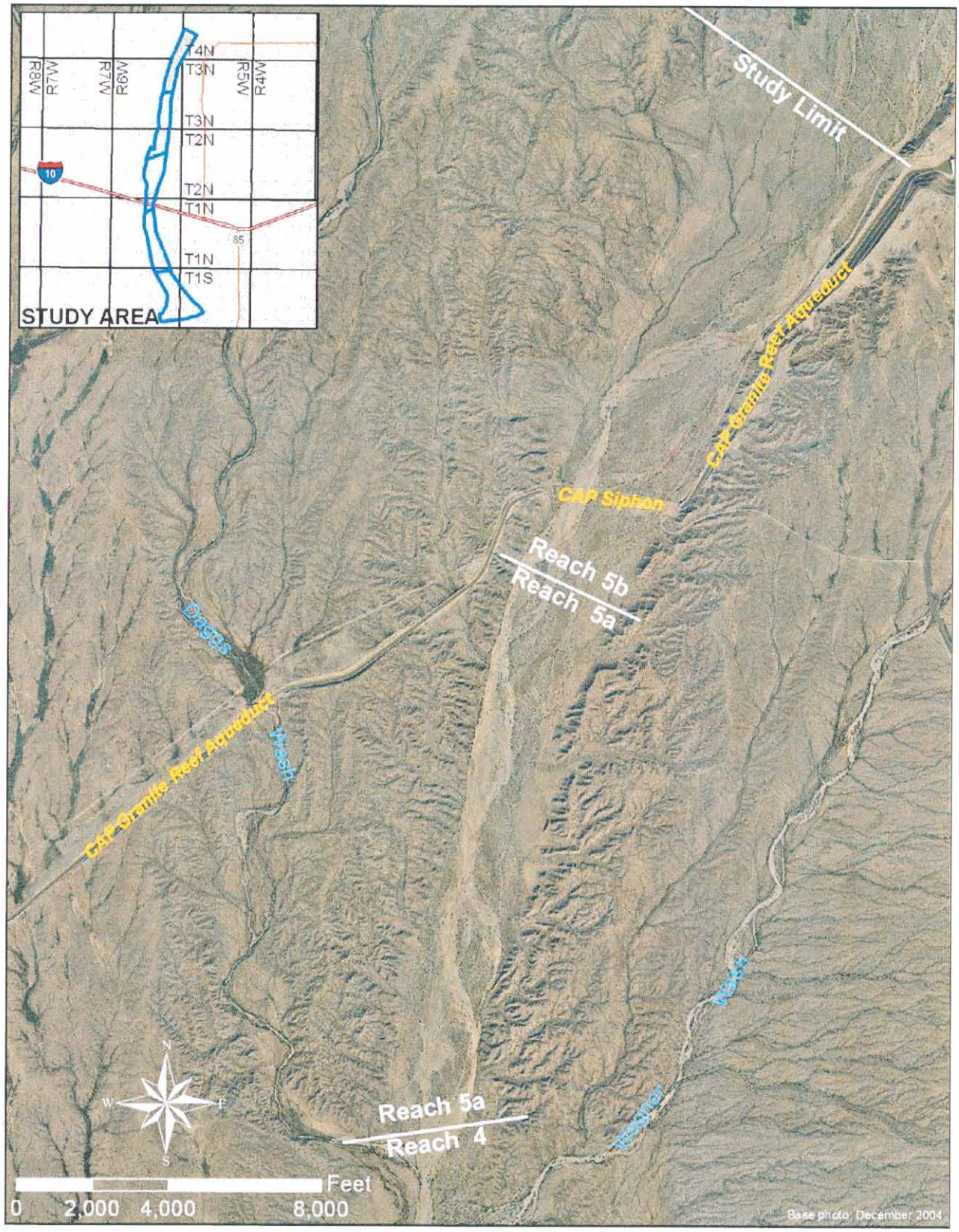

Figure 1-5. Map showing the Hassayampa River Reach 5 extent.

CHAPTER 2 - FIELD RECONNAISSANCE REPORT

Geomorphology is a field-based science of observation that relies heavily on the judgment and interpretation of the investigator. Although a significant amount of geomorphic information can be obtained by non-field-based analyses (such as aerial photo interpretation), a detailed field assessment is critical for understanding the river system, verifying mapping, and ground-truthing landform interpretations. Therefore, the LHWCMP study included a significant number of field visits, systematic detailed field observations, and photo-documentation of field conditions. More than 1,400 field photographs were collected and are provided within the GIS deliverable and technical appendices to this report.

The field data summarized in this chapter are presented by subreach within the following general categories:

- Active Channel Conditions
- Floodplain Conditions
- Evidence of Historical Floods
- Manmade Structures
- Sediment Data

Field visits to the LHWCMP study area were conducted over a period from June 2004 to November 2005. Initial field visits consisted of driving the study reach to observe general conditions and identify areas that required detailed field analyses. Subsequent detailed field visits consisted of walking the active channel and floodplain areas, photographing and mapping key geomorphic and geographic features, and recording descriptions of the existing channel and floodplain conditions. Locations for soil pits and sediment samples were also identified during the field mapping visits. The field reconnaissance tasks also included the soils pit analyses described in Chapter 3.

2.1 Objectives

The primary objective of the field reconnaissance analysis was to observe and document channel and floodplain conditions for use in calibrating and verifying the results of the geomorphic and sedimentation analyses. The secondary objectives of the field work included the following:

- Documenting stream conditions
- Identifying evidence of recent or historical lateral erosion
- Identifying evidence of recent or historical degradation or aggradation
- Identifying stream responses to human impacts or structures
- Identifying evidence of the 1891 Walnut Grove Dam failure flood
- Identifying natural grade control or natural lateral erosion control
- Inventorying river conditions near manmade structures constructed within the floodplain
- Identifying geomorphic features, their characteristics, and function

2.2 Field Data Collected

The following channel characteristics relevant to lateral erosion and channel stability were observed and recorded in the field:

- Cutbanks – location, height, and characteristics
- Headcuts – density, extent, and depth
- Avulsion Potential – overbank areas at risk of avulsion
- Bank Sediments – composition, cohesiveness, and resistance to erosion
- Floodplain Sediments – composition, surficial features, and relative age
- Bedrock – location and extent
- Vegetation – channel, bank, floodplain, type, and density
- Structures – utility towers, levees, bridges, bank protection, and road crossings
- Disturbed Areas – areas directly altered by human activity
- Soil Development – degree of development: clay and carbonate accumulation, reddening

Examples of the forms used to systematically collect information in the field are provided in Appendix 5.1, and include a structure impacts form and a soil pit analysis form. All areas with bank protection, bridges, levees, at-grade roadway crossings, irrigation and siphon crossings, and power line towers and poles were inventoried by collecting the information shown on the structures form. The soils pit form was adapted from Birkeland (1984). Field photos were also logged on the forms. Much of the field data were transferred to the GIS.

2.3 Active Channel Conditions

The active channel is defined as the part of the floodplain that most frequently conveys runoff and that conveys the most runoff and sediment during floods. The active channel serves as the primary sediment transport corridor, and is contrasted to portions of the floodplain dominated by sediment deposition. The active channel is usually the topographically lowest feature within the geologic floodplain. Vegetation in the active channel is typically very sparse to absent, with some seasonal variation, and is subject to periodic removal by floods. Within the LHWCMP study reach, the active channel width varies considerably, from 100 to 900 feet. Active channel sediment consists of moderately to poorly sorted medium-coarse sand with minor amounts of gravel and cobbles.

At the time of the field mapping, the active channel comprised approximately 6% of the Holocene[1] floodplain. The active channel width varies from approximately 900 feet near the Tonopah-Salome Highway to less than 100 feet at the Jackrabbit Wash and Wagner Wash/Daggs Wash confluence in Reach 4. The active channel pattern was variable and alternated between braided and single channels. General channel characteristics that were observed and documented during the field investigations are listed below with a brief explanation as to their significance. Descriptions are segregated by the reaches defined in Chapter 1, and by the following four subject areas:

[1] Holocene – a geologic Epoch representing the past 10,000 years

1. Channel Width, Pattern, and Sinuosity – The active channel width provides insight into the relative lateral channel stability. Where the river is narrow, the width may indicate a physical constraint or barrier to erosion. Channel width is often a function of streamflow frequency and magnitude, the size and type of transported sediment, and the composition of the bed and bank materials (Ritter, 1979). Abrupt changes in channel width may indicate a disequilibrium condition. Channel patterns reflect the river's effort to dissipate energy and balance sediment transport during flow. Specific channel patterns are caused by characteristics such as slope, discharge, and sediment load. Channel patterns can be classified as straight, meandering, or braided. A straight channel extending a significant distance probably experienced some type of manmade control. Meandering and braided channels generally reflect a less manmade control, more natural condition. Channel sinuosity reflects the degree of meandering, and is computed from the ratio of stream length to valley length. Under natural conditions, a river will increase or decrease its sinuosity to balance the energy between stream power and sediment load such that it neither degrades nor aggrades (Schumm, 1977).

2. Channel and Bank Vegetation – Channel vegetation provides information on the relative frequency of flow, the frequency channel erosion, and the occurrence of channel avulsions. The absence of vegetation or the presence of only fast-growing annual vegetative species usually indicates more frequent or recent lateral erosion and high flow velocities than found in channels containing more established vegetation suites. The presence of bank vegetation generally indicates a higher degree of channel stability than is found in non-vegetated banks. Bank vegetation can increase bank stability because roots help bind the bank sediment and because the plant canopy increases roughness (lowering velocities). Vegetation type and density are key factors for bank stability.

3. Cutbanks – The presence of cutbanks generally suggests lateral instability of the active channel. Locations, heights, and characteristics of cutbanks were mapped and described during the field investigations.

4. Structure Impacts – Manmade structures can adversely impact the channel morphology and future channel behavior. Conversely, natural channel changes can adversely impact manmade structures. At minimum, manmade structures provide a reference point from which to measure progressive channel changes. Channel features at and near structures observed during the field visits were inventoried to identify clues about the existing and future channel stability. Impacts of structures on the active channel are discussed below. Impacts of the river on the structures themselves are discussed in Section 2.6 of this chapter.

2.3.1 Hassayampa River Reach 1: Gila River to SPRR Bridge

Most of the Reach 1 active channel corridor has been significantly modified by human activity. The channel downstream from Old US 80 to the Gila River confluence has been channelized and leveed at least since the 1930's, according to long-time

residents.[2] Irrigation return flow that enters the Hassayampa River between the SPRR Bridge and the Old US 80 Bridge results in near-perennial flow that creates active channel characteristics that differ from the rest of the study area.

2.3.1.1 Channel Width, Pattern, and Sinuosity

Channel width is relatively consistent throughout Reach 1, ranging from about 400 feet immediately upstream of the leveed reach, to just over 100 feet within the leveed area. The channel pattern consists of a single channel, except for of a small split-flow area which forms a small low-flow island just downstream of the railroad bridge. Sinuosity is very low, and was measured at 1.00, indicating that the channel has been artificially straightened as part of the channelization.

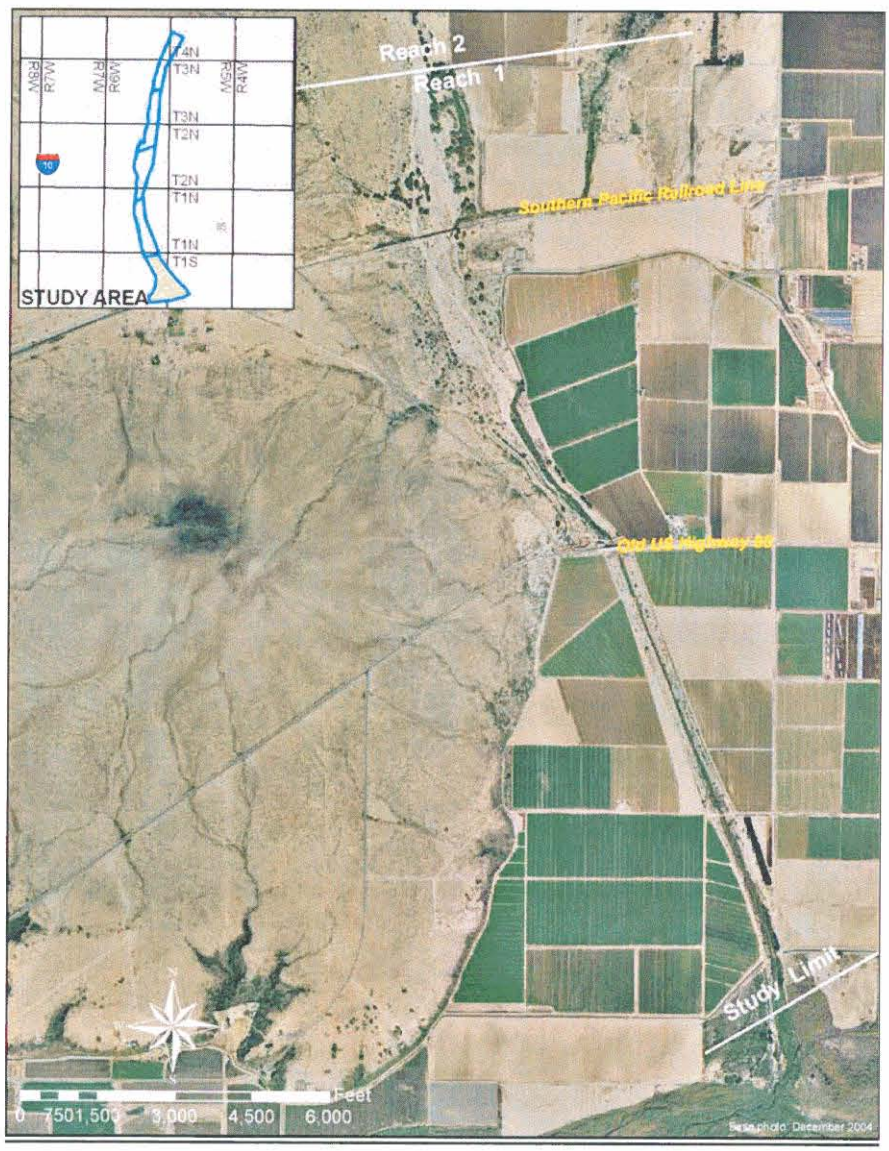

Figure 2-1. Reach 1 photograph showing the active channel pattern and features

[2] Personal communication with Mike and Marie Johnson on December 7, 2004.

2.3.1.2 Channel and Bank Vegetation

Upstream of the irrigation tailwater outfall, in-channel vegetation is sparse and characterized predominantly by desert dicoria. Bank vegetation is generally sparse with a few limited areas of dense vegetation. Bank vegetation is composed primarily of tamarisk with some desert broom and snakeweed. The channelized reach below the irrigation return flow outfall is characterized by very dense bank vegetation, primarily tamarisk. Figure 2-2 shows field photos of the channel and bank vegetation in Reach 1.

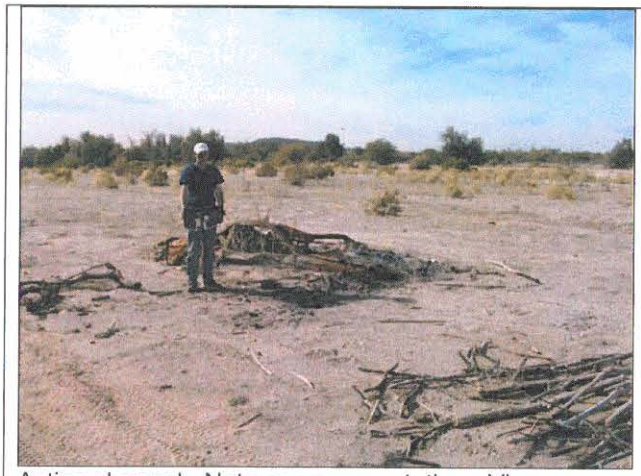

Active channel. Note sparse vegetation. View upstream.

Active channel. Note sparse vegetation and obvious navigability challenges. View upstream.

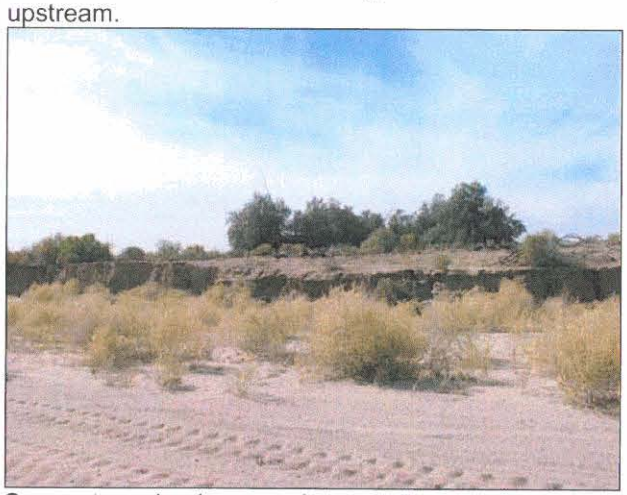

Sparse to no bank vegetation, resulting in a vertical cutbank. View right bank.

Active channel within the channelized reach. Note dense bank vegetation. View downstream.

Figure 2-2. Reach 1 active channel field photos

2.3.1.3 Cutbanks

The banks of the active channel upstream of the channelized area are near vertical and vary between two to three feet in height, becoming higher near the channelized reach. The right bank is between six and 10 feet high at the upstream end of the channelized reach. Within the channelized reach a low flow channel exists within the active channel corridor. The low-flow channel banks are two to three feet high. A low, 40 to 80 feet wide terrace abuts the low flow channel. The terrace characteristics are similar to the active channel characteristics, suggesting frequent inundation. The banks of the low terrace rise steeply to the top of the levees. Bedrock crops out in the active channel corridor in the channelized reach indicating vertical control for at least a portion of Reach 1. The property owners upstream of Old US 80 recalled blasting through a lava layer to deepen the channel at some time in the past. Figure 2-3 shows the locations of cutbanks as observed during the field investigations. The hatched lines define the extent of the cutbanks and the numeric identifiers represent the bank heights in feet. Figure 2-4 shows field photos of cutbanks in Reach 1.

Figure 2-3. Reach 1 cutbank locations

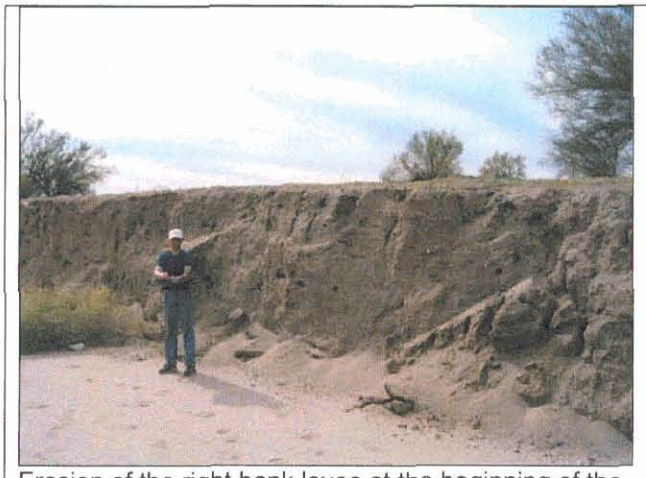

Erosion of the right bank levee at the beginning of the channelized subreach.

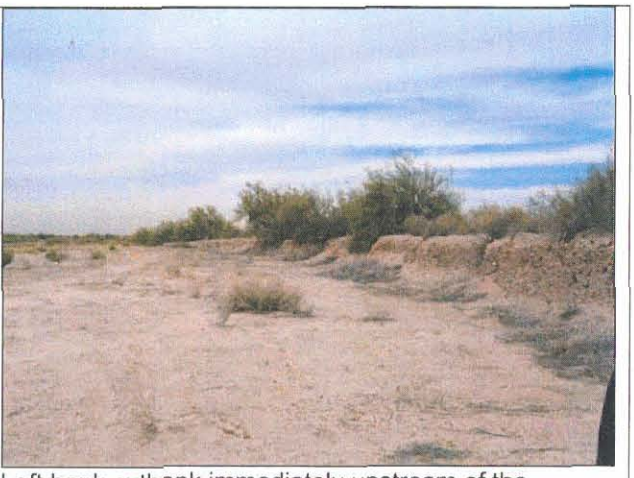

Left bank cutbank immediately upstream of the channelized subreach. View upstream.

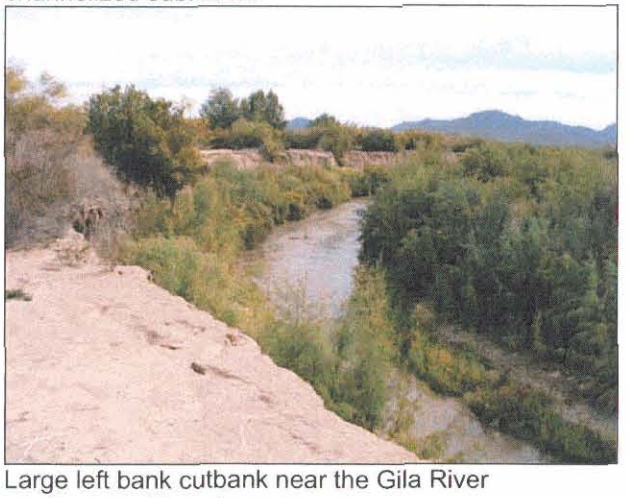

Large left bank cutbank near the Gila River confluence. View downstream.

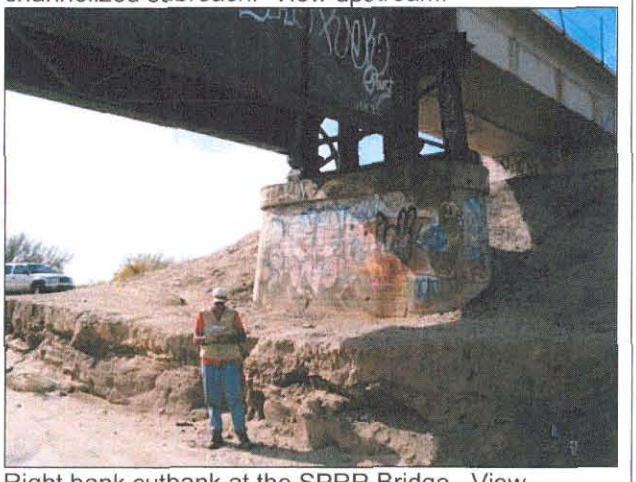

Right bank cutbank at the SPRR Bridge. View downstream.

Figure 2-4. Reach 1 cutbank field photos

The historical confluence of White Tanks Wash and the Hassayampa River was located in Reach 1 just upstream of the SPRR embankment. The earliest available aerial historical photograph (1934) shows a large tributary deposit at the mouth of White Tanks Wash. This deposit is similar to other active tributary deltas found in the study area (e.g., Jackrabbit Wash, Daggs Wash, and Wagner Wash). These active tributary deltas appear to control the lateral position of the Hassayampa River active channel, discussed in detail later in this chapter. Comparing the tributary delta characteristics with the historical White Tanks Wash deposits suggests that White Tanks Wash also provided lateral control of the active channel in the past. However, by 1964, much of the White Tanks Wash delta had been removed and/or graded for agriculture. In 1974, the Buckeye FRS #1 in 1974 along the I-10 alignment upstream of Reach 1 effectively diverted White Tanks Wash from its original confluence, removing the potential for any future lateral control of the active channel. Figure 2-5 shows the active channel and tributary delta evolution of this area.

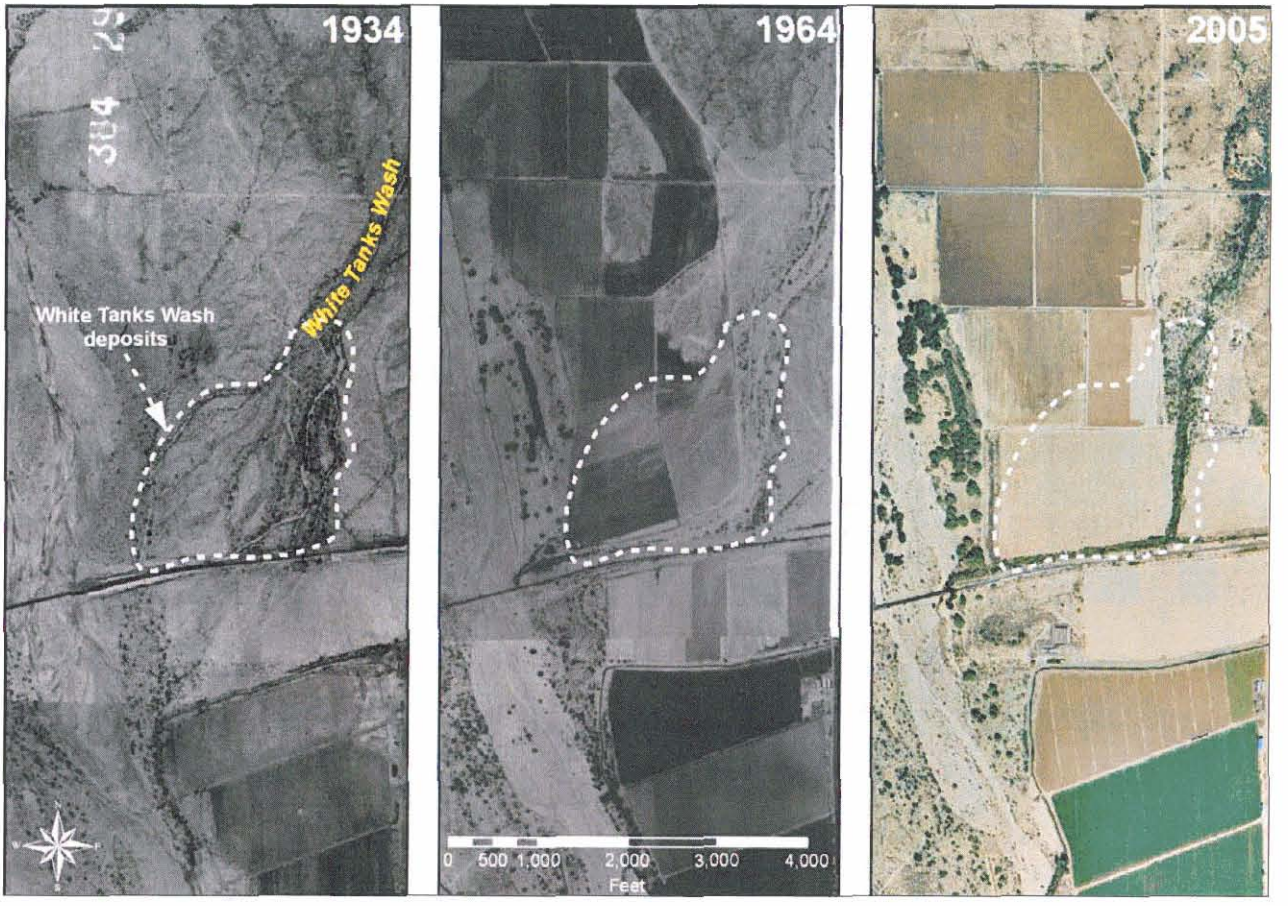

Figure 2-5. White Tanks Wash confluence

2.3.1.4 Structure Impacts

The following four major structures are located in Reach 1:

- Southern Pacific Railroad (SPRR) Bridge
- Old US 80 Bridge
- Farm Levees within the channelized reach
- Arlington Canal siphon

Field evidence indicated the two bridges had minor impact on the present active channel. The levees have a significant impact in that they constrain the active channel to a fixed location, not allowing for natural meandering or braiding. The Old US 80 Bridge was determined by others to be a scour critical structure. Recently, soil cement lining was added to the bridge section to protect against scour and prevent lateral migration (Figure 2-6). The soil cement lining also provides grade control for reaches immediately upstream. The Arlington Canal siphon has no discernable impact on the (already) leveed and narrowed channel section. Figure 2-6 shows field photos of the structures in Reach 1.

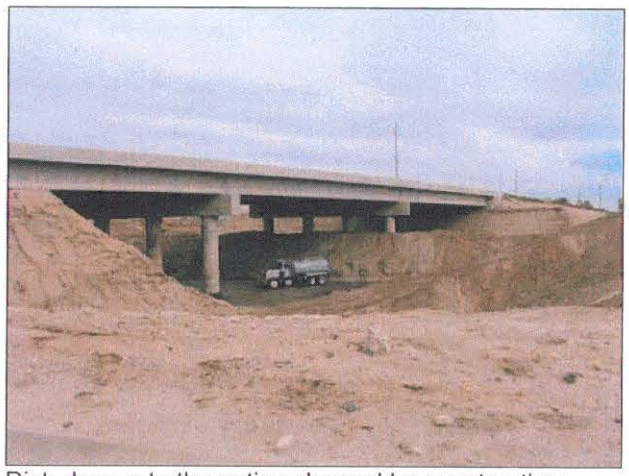

Disturbance to the active channel by construction activity. View upstream.

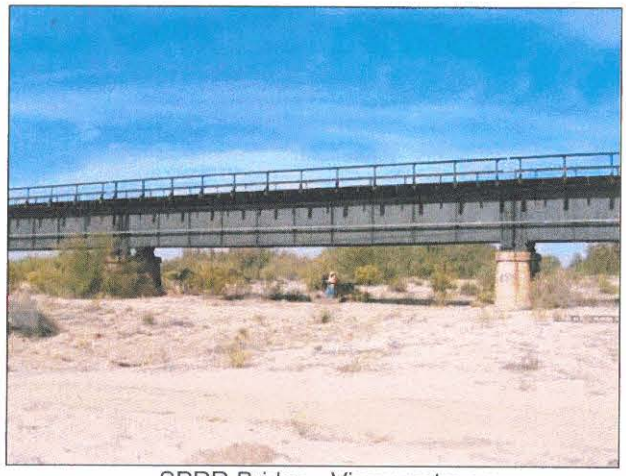

SPRR Bridge. View upstream.

Bedrock outcrop near the active channel within the channelized reach. View slightly upstream.

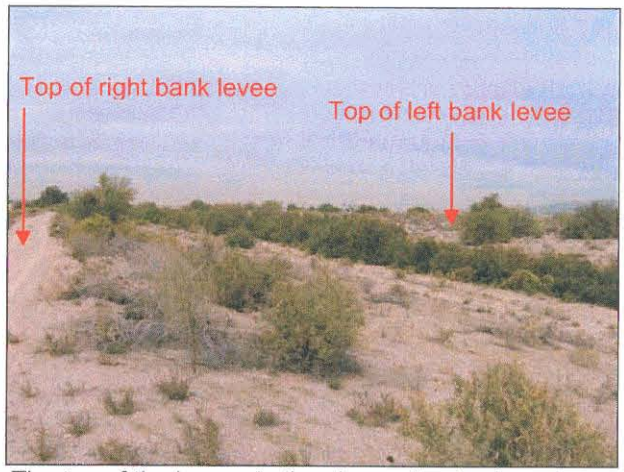

The top of the levees in the channelized subreach. View north.

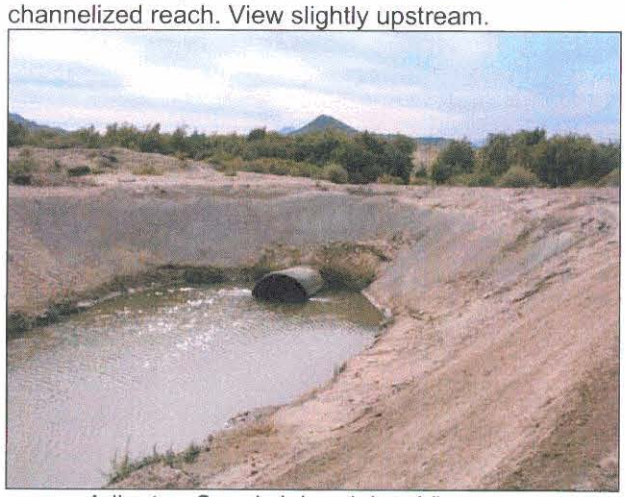

Arlington Canal siphon inlet. View west.

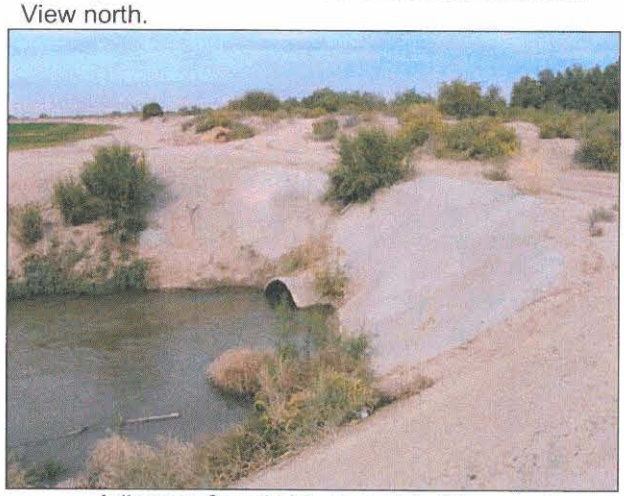

Arlington Canal siphon outlet. View north.

Figure 2-6. Reach 1 structure photos

2.3.2 Hassayampa River Reach 2: SPRR Bridge to I-10 Bridge

Reach 2 extends from just downstream of the Interstate 10 Bridge to just upstream of the SPRR Bridge. At the time of the field investigation, the active channel corridor appeared relatively undisturbed. That is, no evidence of man-made alterations to channel such as in-channel sand and gravel mining, realignments, road crossings or channelization was found. The minor exception was a 300-foot section of the left bank located about one mile upstream of the Reach 2/Reach 1 boundary where trash was dumped over the active channel bank.

2.3.2.1 Channel Width, Pattern, and Sinuosity

The active channel in Reach 2 varies from about 100 feet to 600 feet wide. The channel pattern consists mostly of a single channel with two minor divided flow areas located near the midpoint of the reach. Sinuosity was measured at 1.08, higher than that of Reach 1 or Reach 3. Three large wavelength, low amplitude meanders occur in the upper half of Reach 2, although the lower half of Reach 2 is nearly straight and significantly narrower.

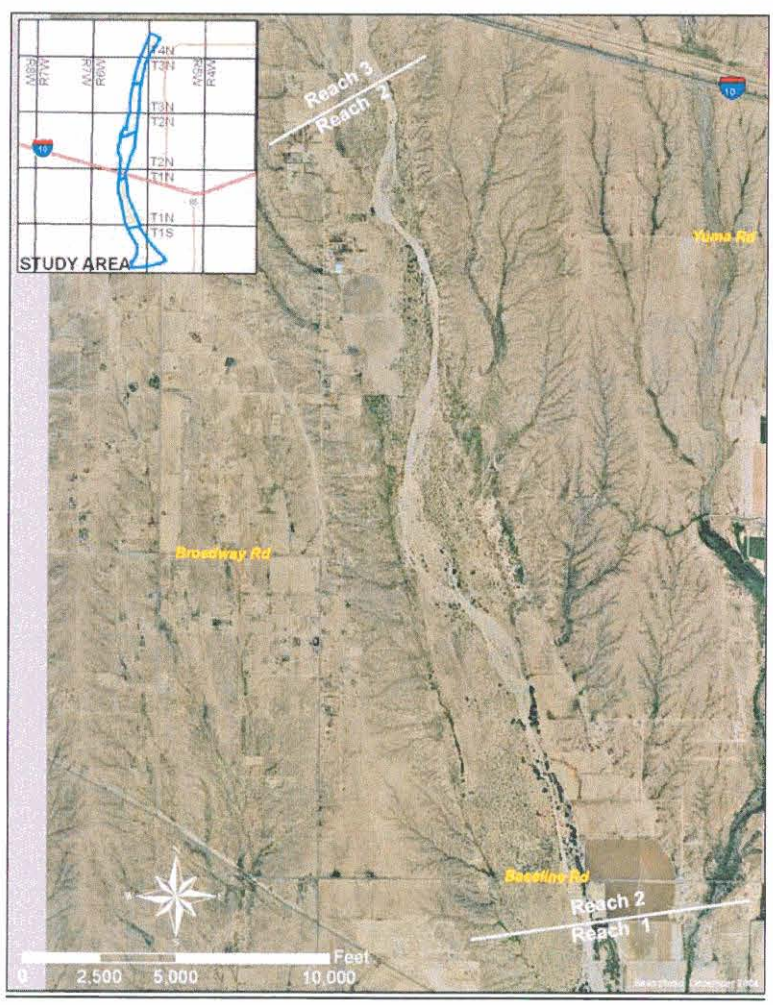

Figure 2-7. Reach 2 photograph showing channel pattern and features

2.3.2.2 Vegetation

In-channel vegetation in Reach 2 consisted of sparse Desert dicoria, similar to that of Reach 1 upstream of the irrigation return flow outfall. Bank vegetation density was highly variable and ranged from dense, tamarisk dominated areas to sparse, low-brush areas to no vegetation present. Bank vegetation, when present, was composed primarily of tamarisk, desert broom, and snakeweed with occasional palo verde trees. The line of tall trees near the left bank visible in Figure 2-7 is not located within the active channel, but instead occurs along agricultural fields and canal laterals in the floodplain. Figure 2-8 shows field photos of channel and bank vegetation in Reach 2.

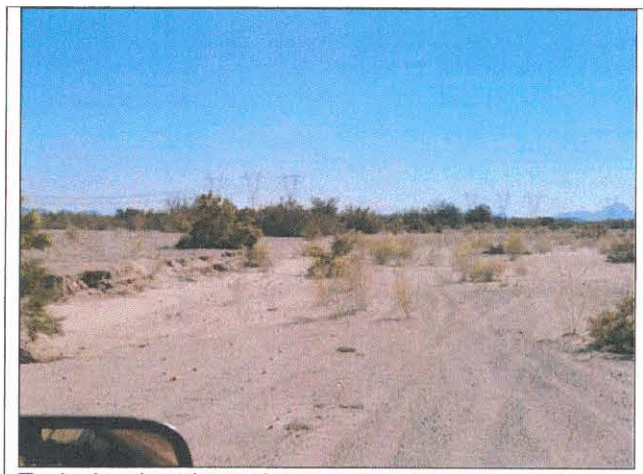

Typical active channel vegetation. View downstream.

Example of no vegetation present in the low-flow portion of the active channel. View downstream.

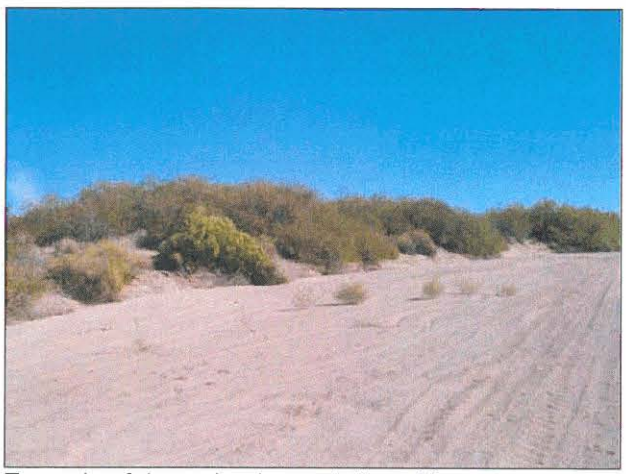

Example of dense bank vegetation. View downstream.

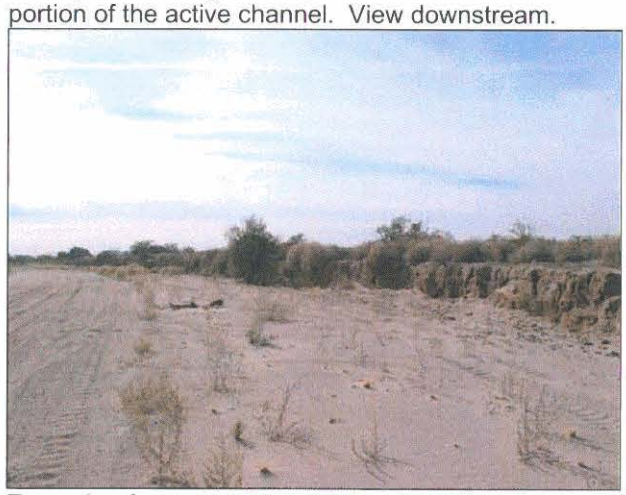

Example of sparse to no bank vegetation. View downstream.

Figure 2-8. Reach 2 vegetation field photos

2.3.2.3 Cutbanks

Vertical cutbanks occured frequently in Reach 2 and varied from two to five feet in height. Two areas in Reach 2 contained high (>5 feet) vertical cutbanks, both located on the outside of large bends in the active channel. The bank materials in all of the cutbanks exposed in Reach 2 are composed of non-cohesive, highly erodible, fine-grained alluvium. Figure 2-9 shows the locations of cutbanks in Reach 2 at the time of the field investigation (images extend downstream to upstream, left to right). The hatched lines define the extent of the cutbanks and the numeric identifiers represent the bank heights in feet. Figure 2-10 shows field photographs of cutbanks.

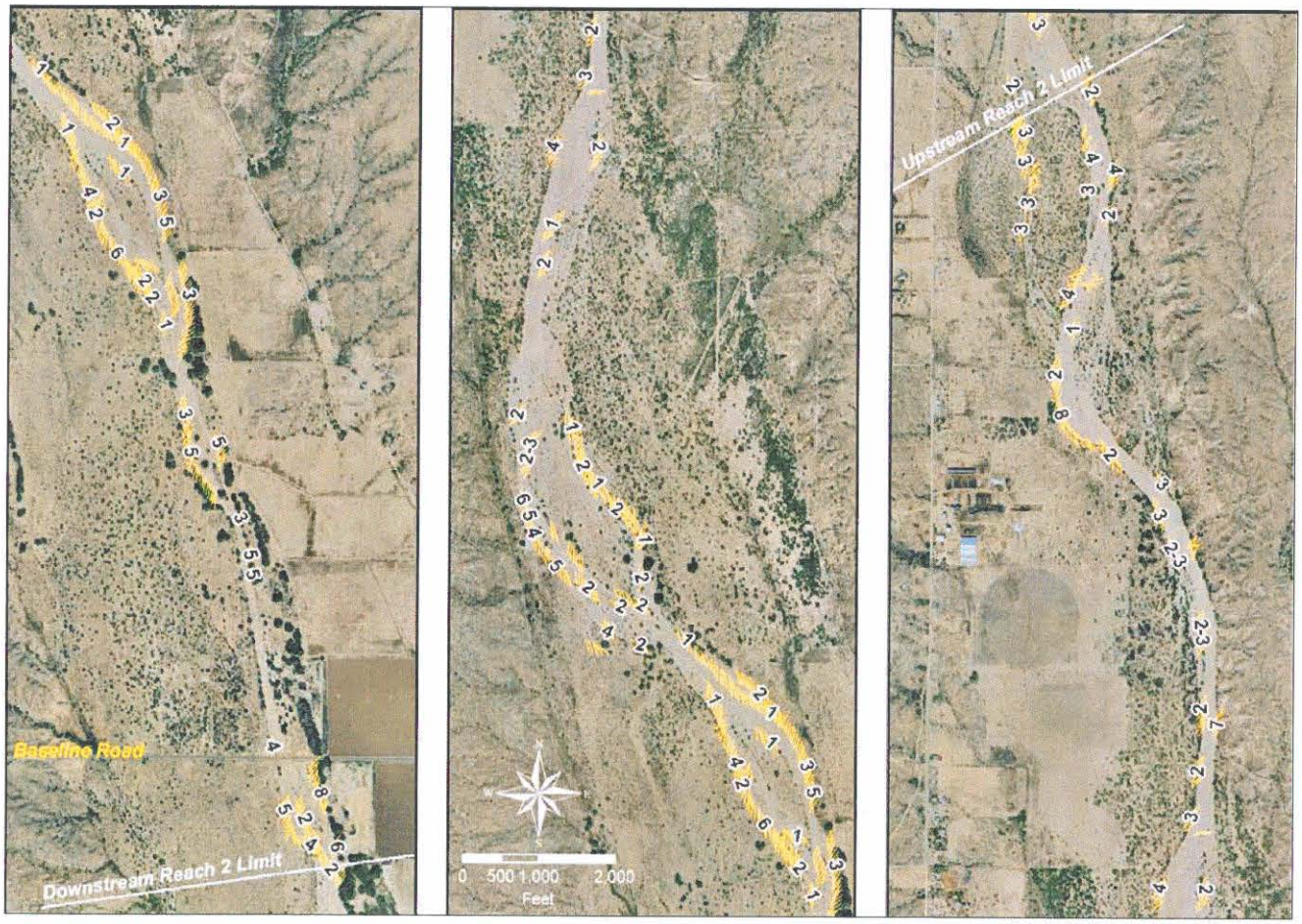

Figure 2-9. Reach 2 cutbank locations

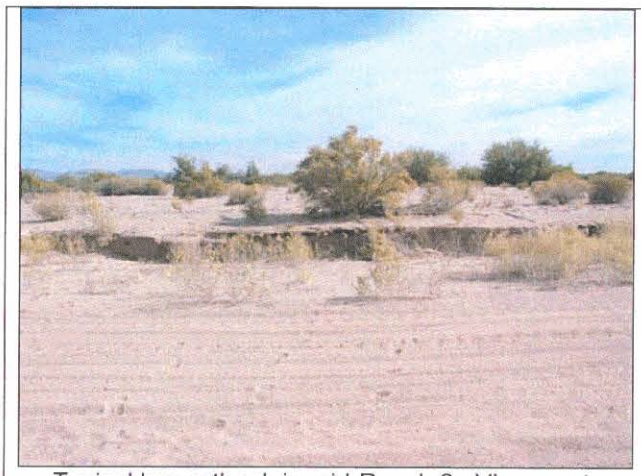

Typical low cutbank in mid-Reach 2. View west.

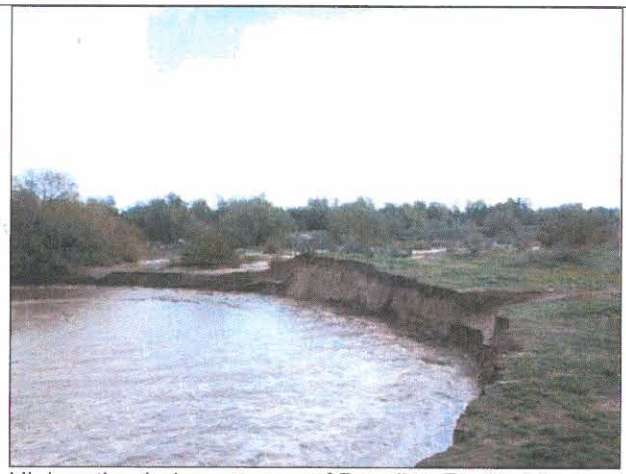

High cutbank downstream of Baseline Road. View downstream

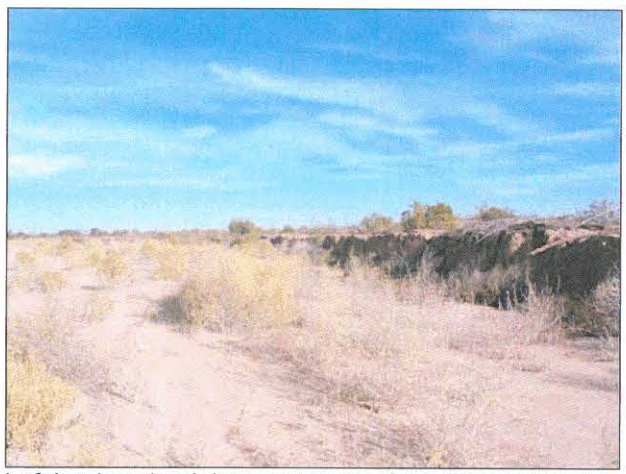

Left bank cutbank just upstream of the Reach 2 limit. View upstream.

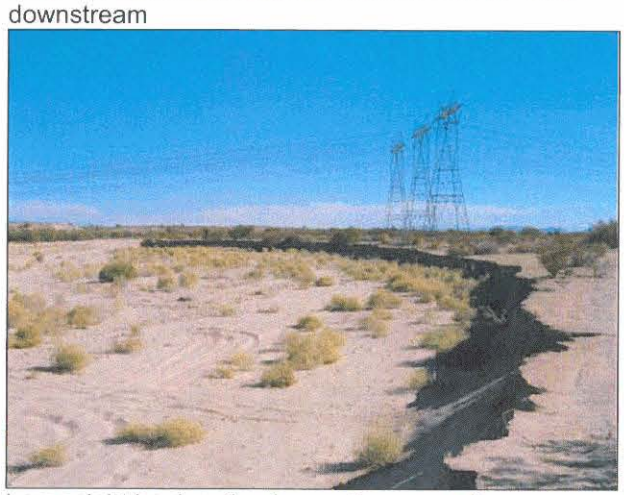

Large right bank cutbank near the power line alignment. View downstream.

Figure 2-10. Reach 2 cutbank field photos

2.3.2.4 Structure Impacts

The following major structures intersect the active channel corridor in Reach 2:

- Multi-tower Power Line
- Baseline Road At-Grade Crossing
- Single Overhead Utility Line

The structures in Reach 2 are shown in Figure 2-11. The multi-tower alignment consists of a set of three towers, located approximately one mile south of the upstream reach limit and crossing the active channel in a southwest to northeast orientation. Within this alignment two sets of towers were located in the floodplain west of the active channel, and one set was located east of the active channel. No towers were located within the active channel. Therefore, the multi-tower crossing was considered to have no impact on the active channel, although, given the lateral erosion toward the closest tower shown in Figure 2-11, the active channel may soon have an impact on the towers. The overhead utility line at Baseline Road appears to have no obvious impact on the active channel at the two places where power poles are located within the active channel.

Baseline Road provides a measure of grade control for the channel during small floods, but tends to be eroded by scour or buried by deposition during significant flows. The crossing shows no evidence of adverse impact on the active channel outside of the right-of-way. The roadway elevation was at grade with the low-flow channel. No evidence of scour downstream of the roadway was observed during field visits.

Multi-tower power line in the right-overbank floodplain. View south.

Power line towers on the eastern Pleistocene terrace. View south.

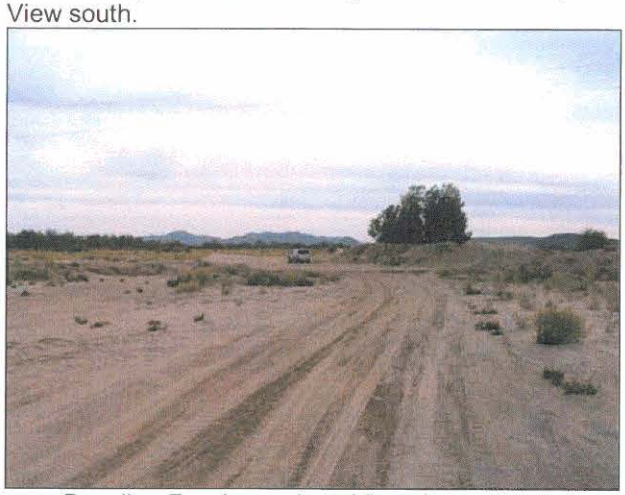

Baseline Road crossing. View downstream.

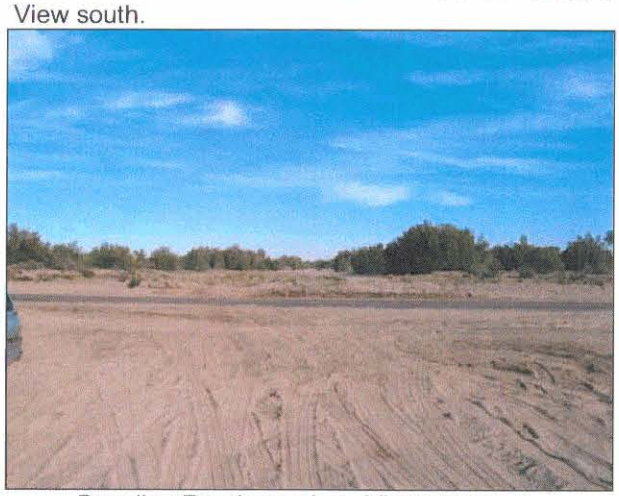

Baseline Road crossing. View upstream.

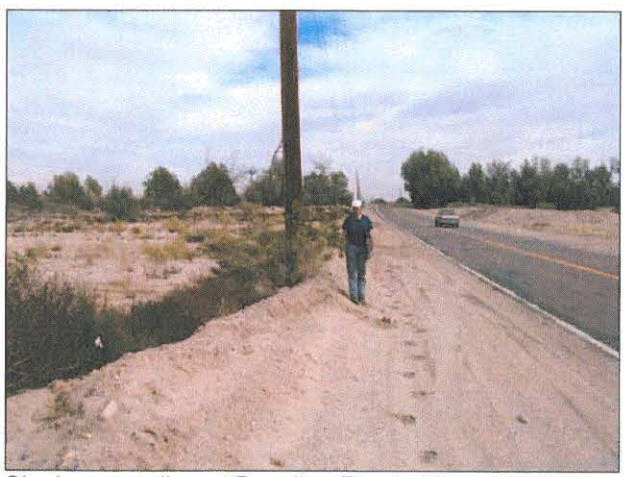

Single-power line at Baseline Road. View east from right overbank.

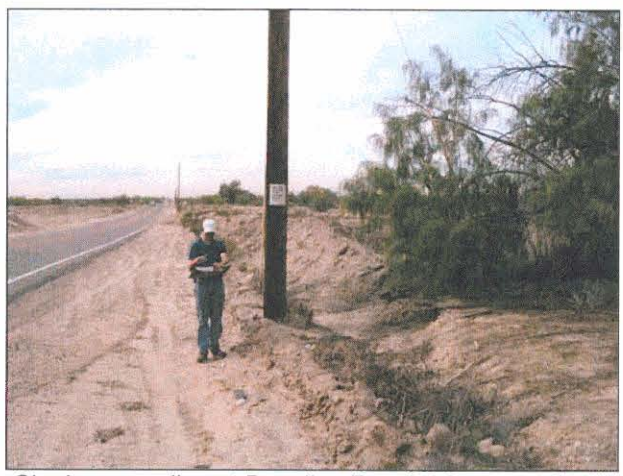

Single-power line at Baseline Road. View west from left overbank.

Figure 2-11. Reach 2 active channel field photos

2.3.3 Hassayampa River Reach 3: I-10 Bridge to Jackrabbit Wash

Reach 3 extends from just upstream of the Jackrabbit Wash confluence to just downstream of the I-10 Bridges. The reach was highly disturbed at the time of the field investigation due to the presence of multiple active sand and gravel mining operations. The active channel characteristics within Reach 3 are heavily influenced by Jackrabbit Wash and the mining activity.

2.3.3.1 Channel Width, Pattern, and Sinuosity

The active channel width varies from about 900 feet near the mining district north of the Tonopah-Salome Highway to about 100 feet near the Jackrabbit Wash confluence, making it one of the narrowest reaches within the LHWMCP study area.

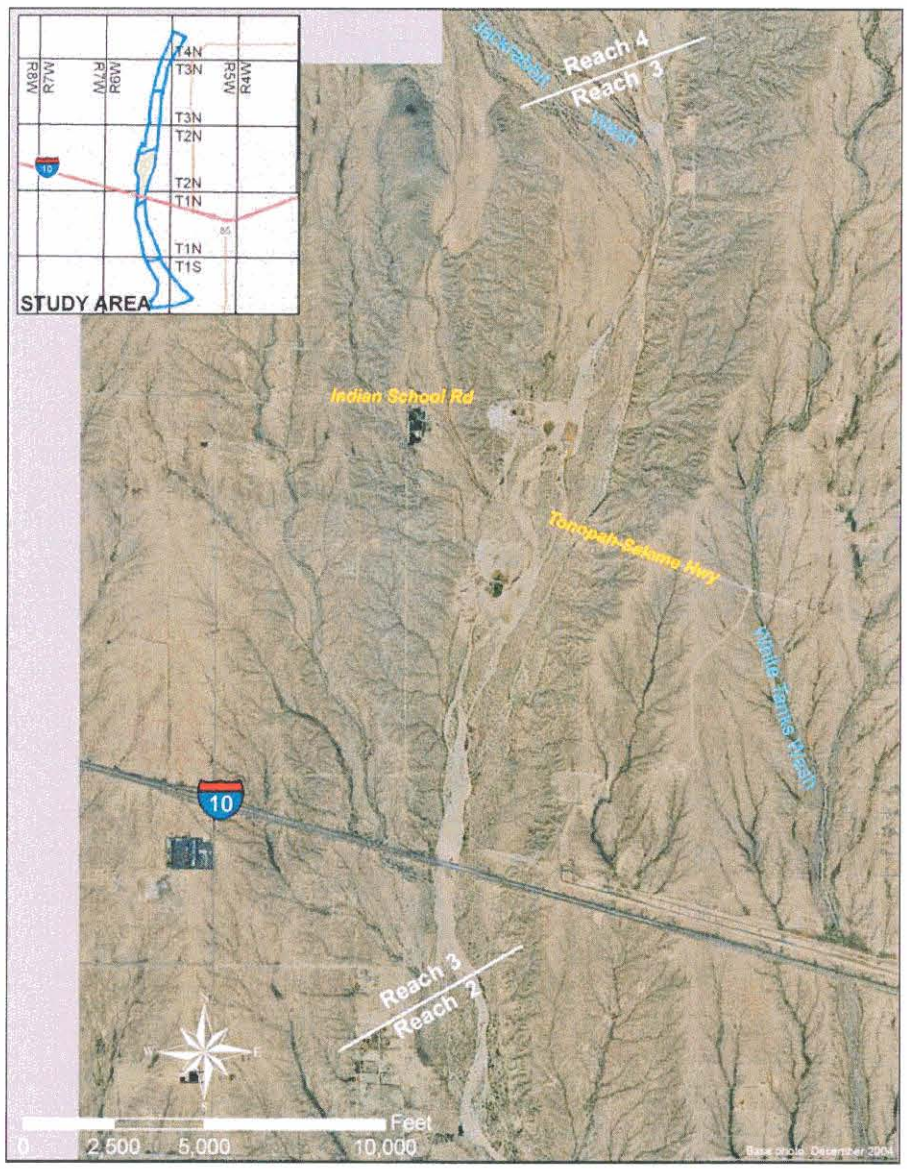

Figure 2-12. Reach 3 photograph showing channel pattern and features.

Transgressive sediment deposition from Jackrabbit Wash has created a deltaic fan that narrows and constrains the Hassayampa River active channel, and forces it against the Pleistocene terrace scarp opposite the Jackrabbit Wash delta. Soils analysis from the Jackrabbit Wash fan indicated the Hassayampa River has been constrained to its present location for hundreds to thousands of years, as described in the soils analysis in Chapter 3. The apparent age of the delta deposits suggests that Jackrabbit Wash provides lateral control of the Hassayampa River active channel. Downstream of the Jackrabbit Wash confluence, the Hassayampa River channel has a braided pattern with multiple flow splits and varying channel widths. The braided channel pattern is expected downstream of the delta constriction where concentrated energy within the constriction is dissipated by rapid expansion of the channel. The single channel pattern is reestablished just upstream of the I-10 Bridges. Measuring sinuosity in Reach 3 was complicated by the braided channel pattern, but was estimated at approximately 1.05.

2.3.3.2 Vegetation

Channel vegetation in Reach 3 is consistent with that described for Reach 2, and consists of sparsely distributed desert dicoria. Tamarisk was far less abundant in Reach 3 than in Reaches 1 and 2, and becomes less frequent to non-existent further upstream, suggesting that the source of the invasive tamarisk species was the Gila River and that migration is in the upstream direction. The dominant bank vegetation in Reach 3 is palo verde, snakeweed, and desert broom. In areas where the active channel was directly adjacent to a tributary deposit, the dominant bank vegetation was creosote. Overall, bank vegetation was generally sparse. Bare banks with no vegetation were frequent. Figure 2-13 shows field photos of channel and bank vegetation in Reach 3.

Typical active channel vegetation in Reach 3. View downstream.

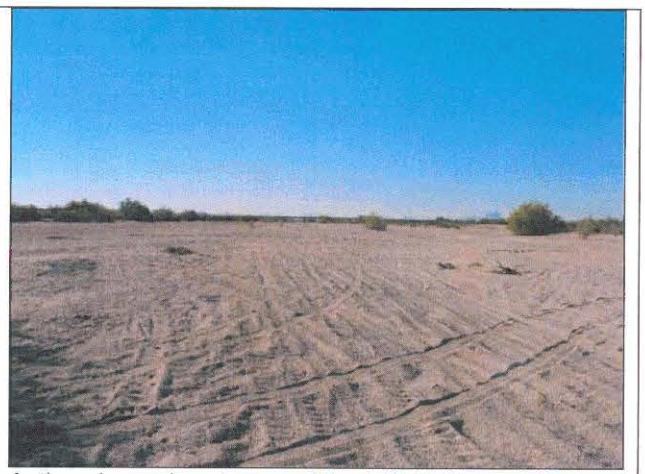

Active channel upstream of the I-10 Bridges. View downstream.

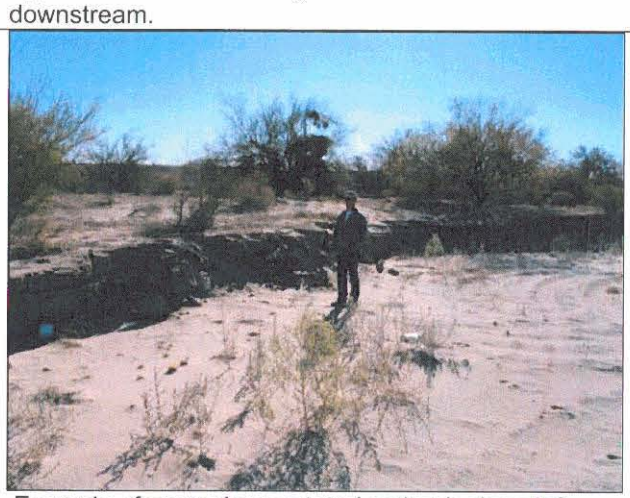

Example of sparsely vegetated cutbank along left bank. View downstream.

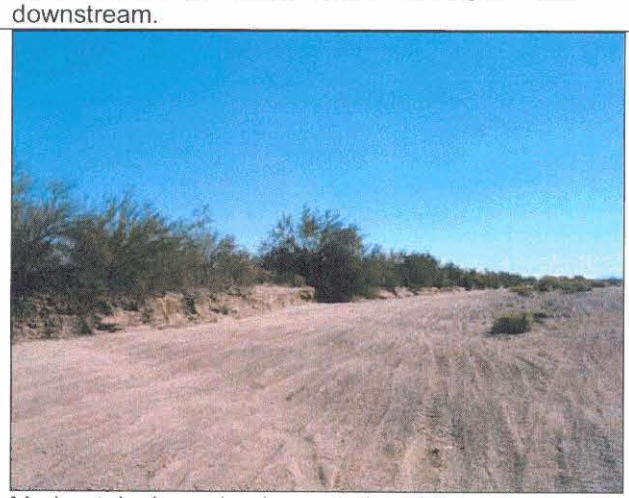

Moderately dense bank vegetation. View downstream.

Figure 2-13. Reach 3 channel and bank vegetation

2.3.3.3 Cutbanks

Vertical cutbanks are just as prevalent in Reach 3 as in Reach 2; however, their lateral extent was generally less. Typical cutbank heights are two to four feet, with cutbanks of up to five to eight feet observed near the in-stream sand and gravel operations. Figure 2-14 shows the locations of cutbanks mapped during the field investigations. The hatched lines define the extent of the cutbanks and the numeric identifiers represent the bank heights in feet. Figure 2-15 presents field photos of cutbanks in Reach 3.

Figure 2-14. Reach 3 cutbank locations

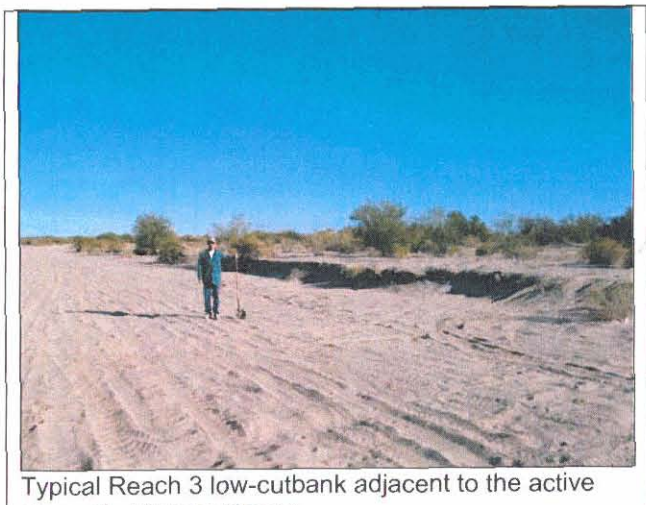

Typical Reach 3 low-cutbank adjacent to the active channel. View upstream.

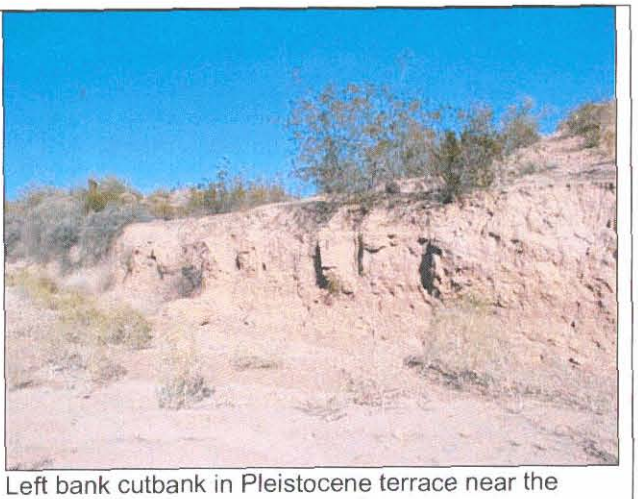

Left bank cutbank in Pleistocene terrace near the Jackrabbit Wash confluence. View east.

Figure 2-15. Reach 3 cutbank field photos

2.3.3.4 Structure Impacts

The following major structures impacting the Reach 3 active channel were identified:

- I-10 Bridges
- Tonopah-Salome Highway At-Grade Crossing
- Sand and Gravel Mines
- Overhead Utility Line

Field investigation of the I-10 Bridges suggests they have no adverse impact on the active channel. During early field investigations, several low-flow channels intersected the Tonopah-Salome Highway. Many of these channels were blocked by roadway embankment fill. After the small floods in late December 2004, follow-up field investigation determined the roadway embankment had had no effect on the active channel, as the roadway crossing was destroyed at every low-flow channel intersection location. Figure 2-16 shows before and after photographs of the Tonopah-Salome Highway crossing.

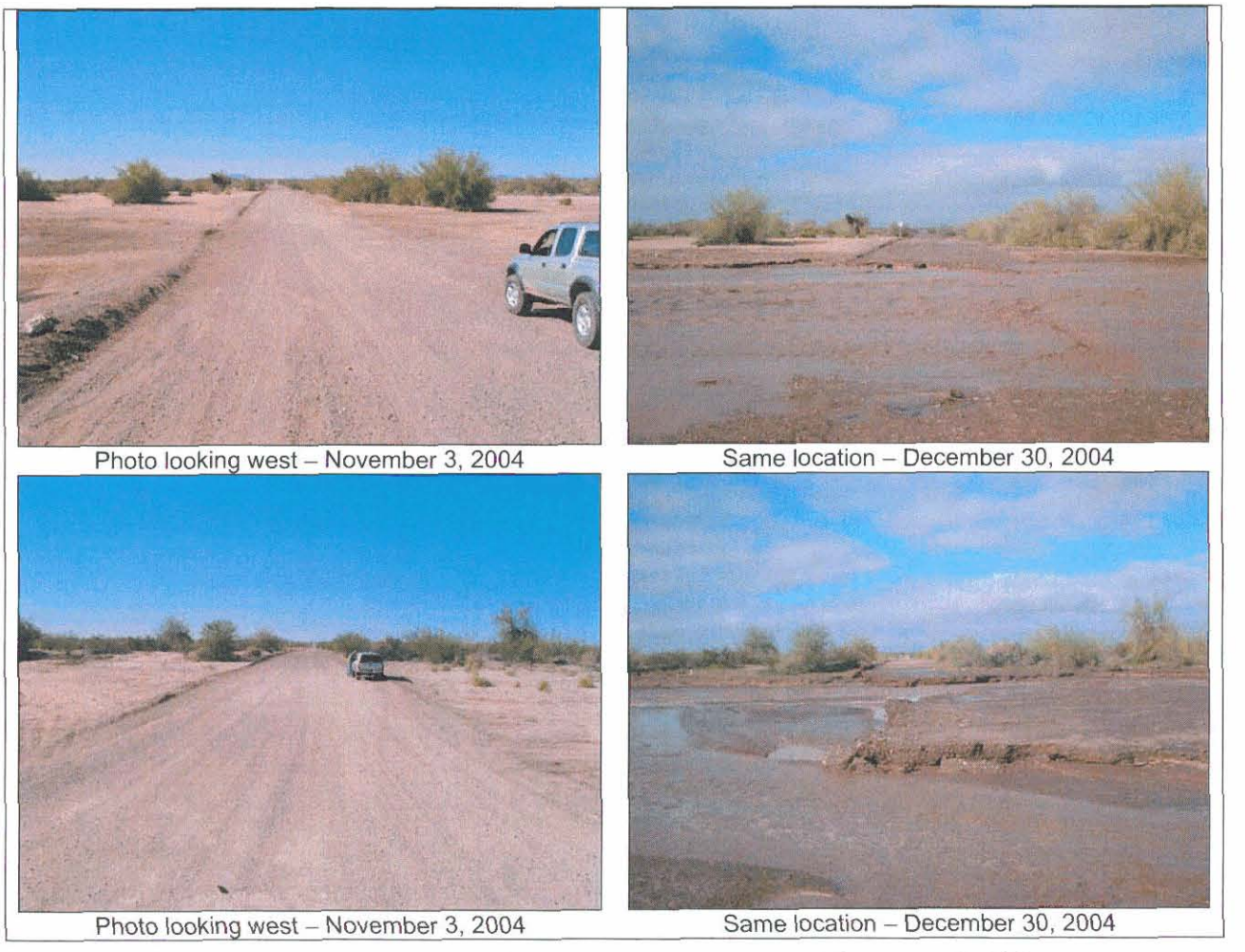

Figure 2-16. Photos of the Tonopah-Salome Highway pre- and post-December 2004 flows

At the time of the field investigation, two active sand and gravel mines were in operation in Reach 3. The mines are located along river, right immediately upstream and downstream of the Tonopah-Salome Highway crossing. The upstream operation has about a 40-acre footprint. The downstream operation has about a 73-acre footprint. Figure 2-17 is an aerial view of each mining operation and its position relative to the active channel. As shown in Figure 2-17, both mines directly flank the active channel, suggesting they would intercept at least a portion of the flow during floods, as occured during the December 2004 floods, potentially altering the channel's location and/or geometric characteristics. During that flood, runoff exiting the downstream pit into the western braid created additional scour and lateral erosion. Figure 2-18 shows the out flow channel location and photographs taken during the field investigation. The process of clear-water discharge from the downstream end of the mining pits will likely continue in the above described overflow channel in addition to other locations resulting in both lateral and vertical changes to the active channel within Reach 3. Additional field photographs are shown in Figure 2-19.

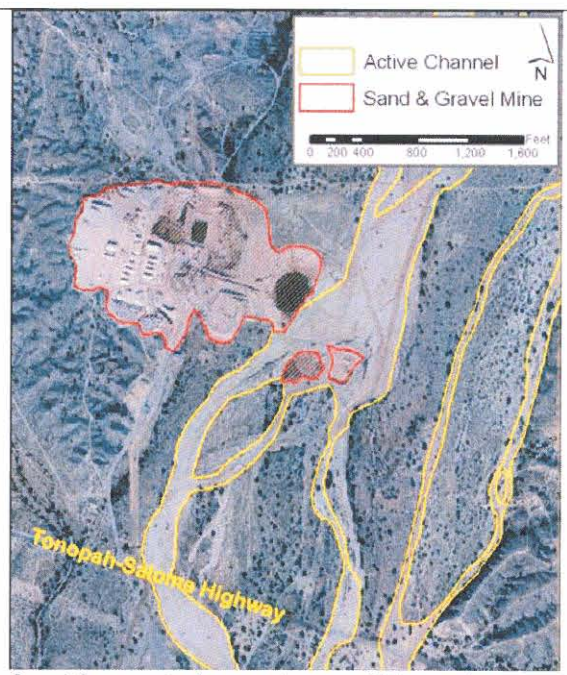

Sand & gravel mine upstream of Tonopah-Salome Highway

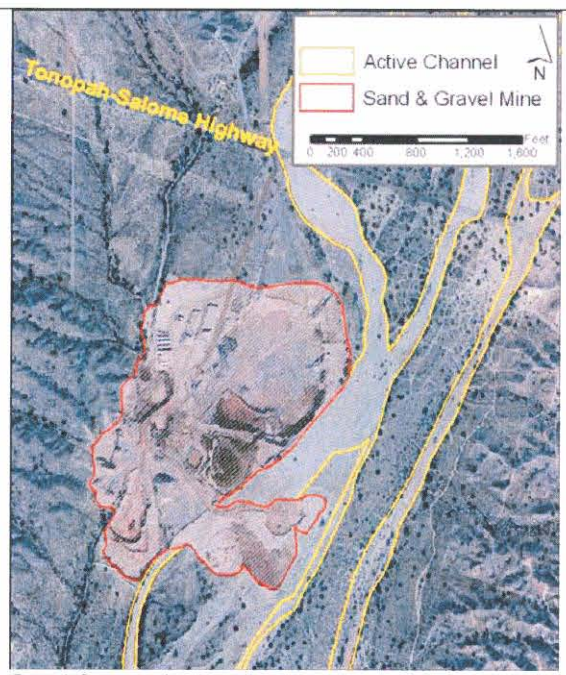

Sand & gravel mine downstream of Tonopah-Salome Highway

Figure 2-17. Sand & gravel mines near Tonopah-Salome Highway

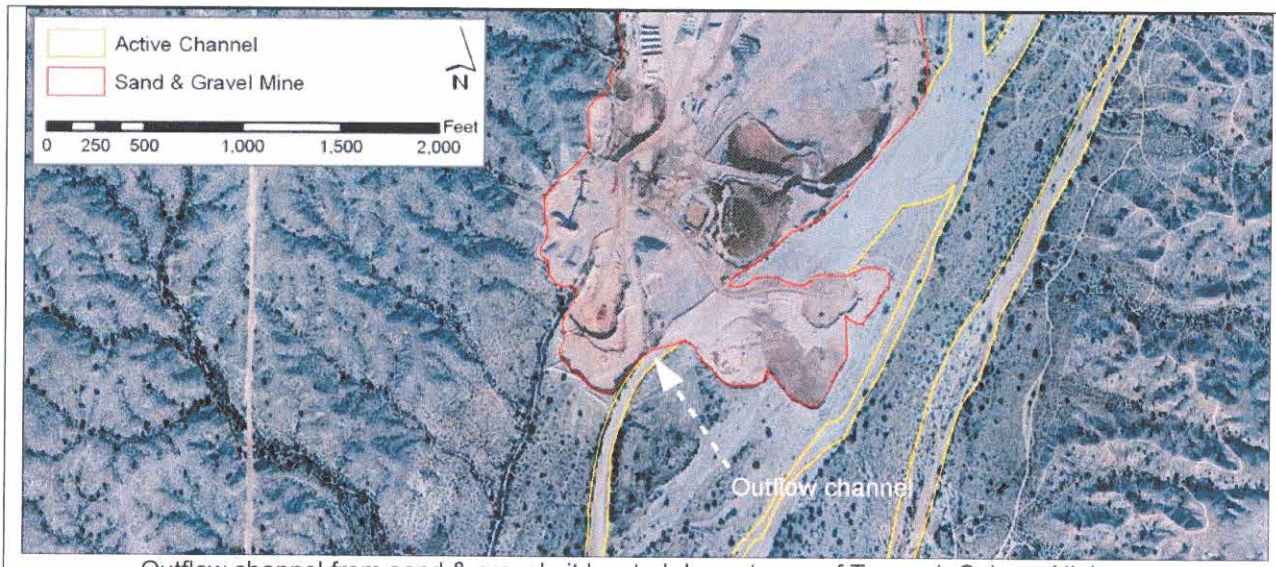

Outflow channel from sand & gravel pit located downstream of Tonopah-Salome Highway

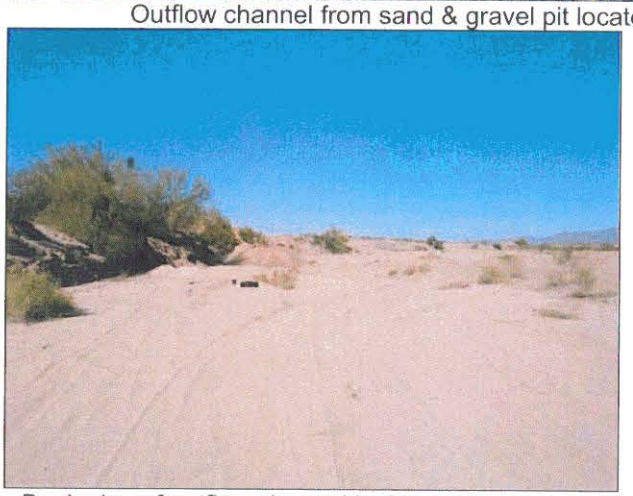

Beginning of outflow channel looking upstream at mining pit.

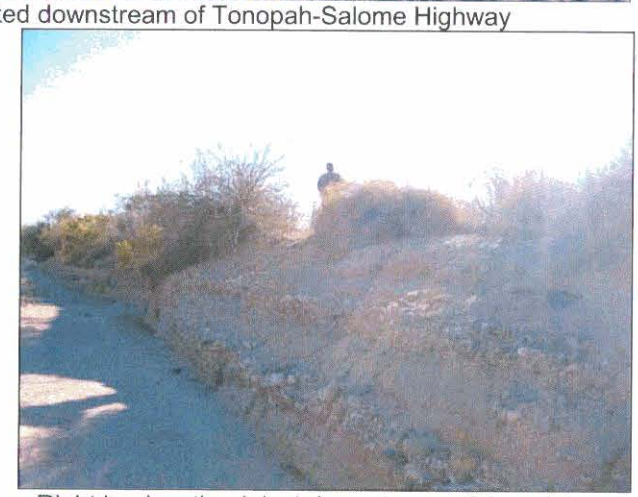

Right bank cutbank just downstream of the mining pit. View downstream.

Figure 2-18. Sand & gravel pit outflow channel

The double overhead utility line crossing is located immediately upstream of the northern sand and gravel operation. One set of poles on this alignment was located within the active channel. Field investigation of this site determined that the pole-set had no adverse impact on the active channel, although the channel has significant impacts on the poles, as described later in this chapter. Field photos of the structures in Reach 3 are shown in Figure 2-19.

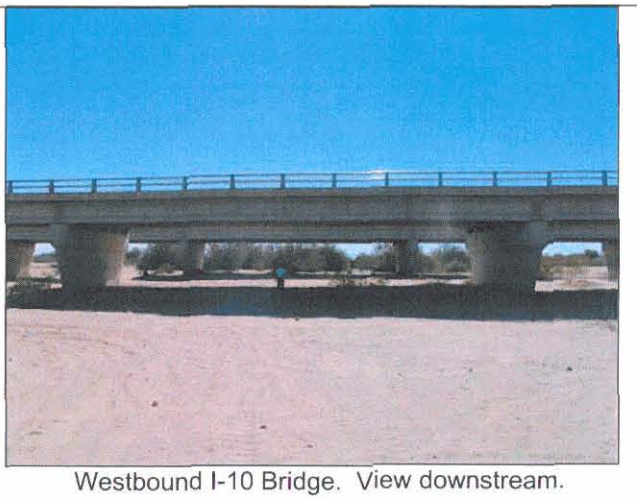

Westbound I-10 Bridge. View downstream.

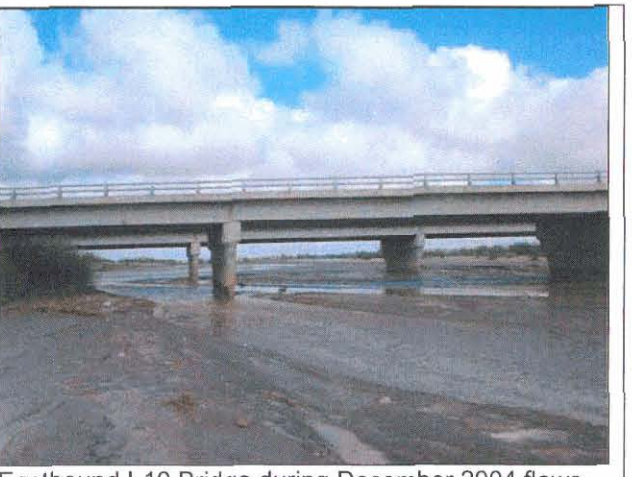

Eastbound I-10 Bridge during December 2004 flows. View upstream.

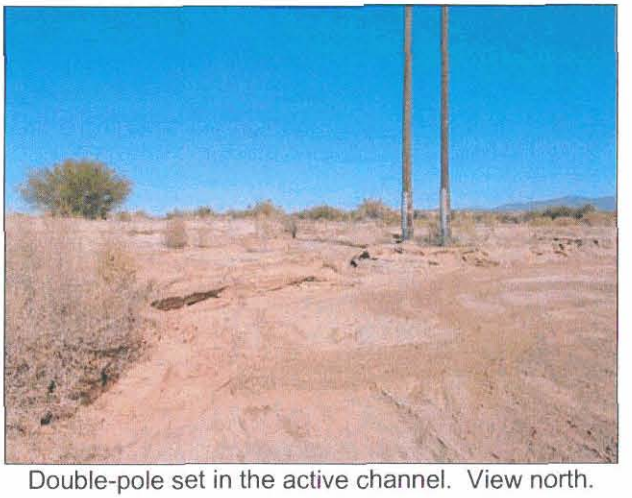

Double-pole set in the active channel. View north.

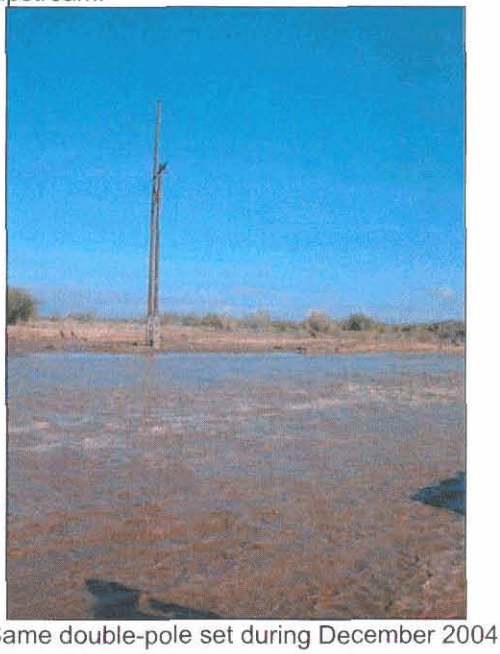

Same double-pole set during December 2004 flows. View west.

Figure 2-19. Reach 3 active channel field photos.

2.3.4 Hassayampa River Reach 4: Jackrabbit Wash to Wagner/Daggs Wash

Reach 4 is the longest reach in the study area. It begins upstream of the Daggs Wash/Wagner Wash confluence and extends downstream to the Jackrabbit Wash confluence. At the time of the field investigation, Reach 4 was the least disturbed reach in the study area, with no engineered structures or modifications to the active channel.

2.3.4.1 Channel Width, Pattern, and Sinuosity

The channel width in Reach 4 ranges from just under 100 feet to 460 feet. The channel pattern is braided, with only two small single-channel subreaches. The braided stream pattern complicates measurement of sinuosity, but it was estimated at 1.06.

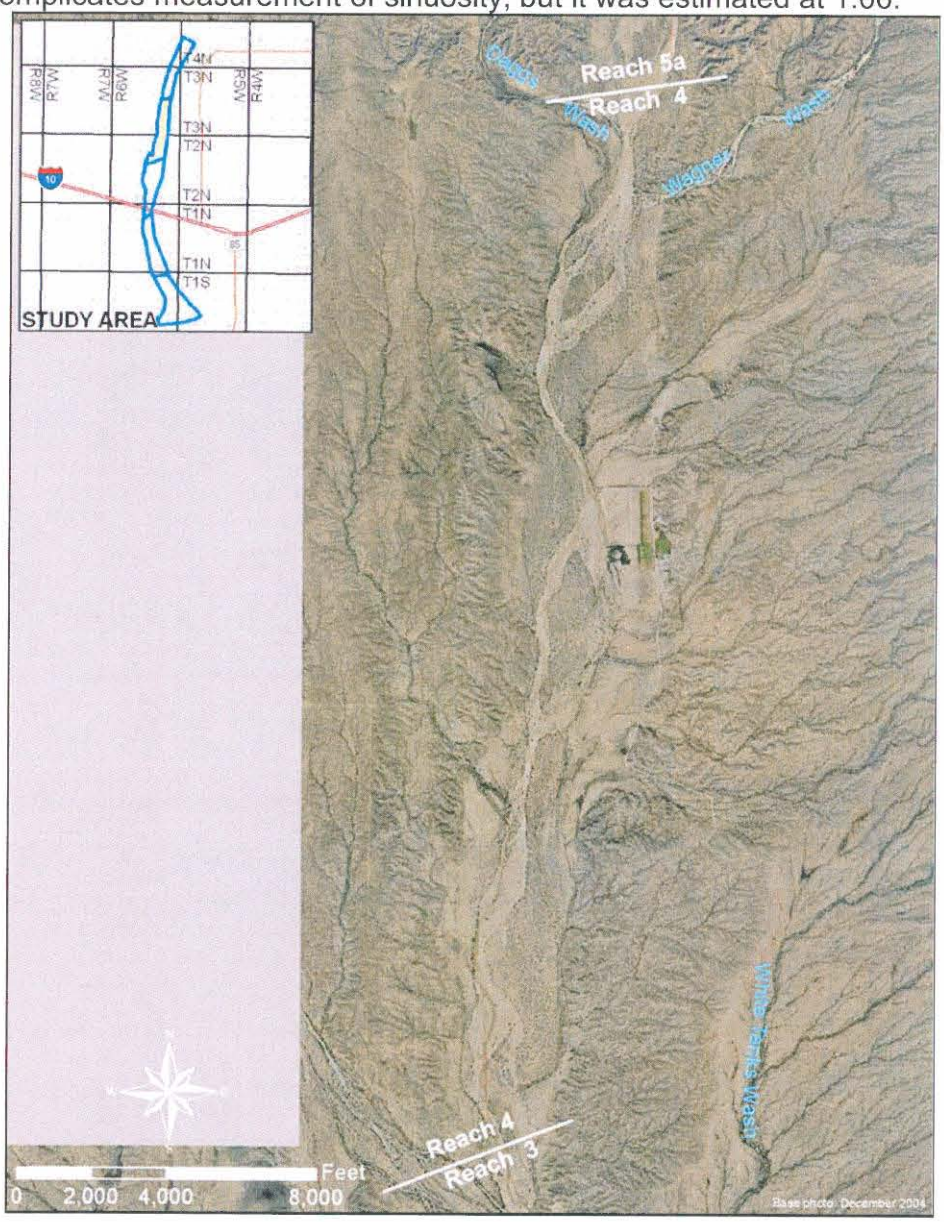

Figure 2-20. Reach 4 photograph showing channel pattern and features.

Two major tributaries enter the Hassayampa River in Reach 4 within 500 feet of one another. Wagner Wash joins the Hassayampa River from the east and Daggs Wash flows in from the west. Both field and aerial photograph evidence indicates that the sediment influx from these tributaries effectively controls the active channel position in a similar manner to that described for the Jackrabbit Wash confluence in Reach 3. Although the combined drainage area of these tributaries is significantly less (75 mi^2) than that of Jackrabbit Wash (366 mi^2), apparently the sediment supply is sufficient to narrow and constrain the active channel of the Hassayampa River. Figure 2-21 is a set of three historical aerial photos showing the consistency of the active channel position at the Daggs Wash/Wagner Wash confluence area. Note the white arrows indicating the consistent lateral position of the active channel at the confluence area.

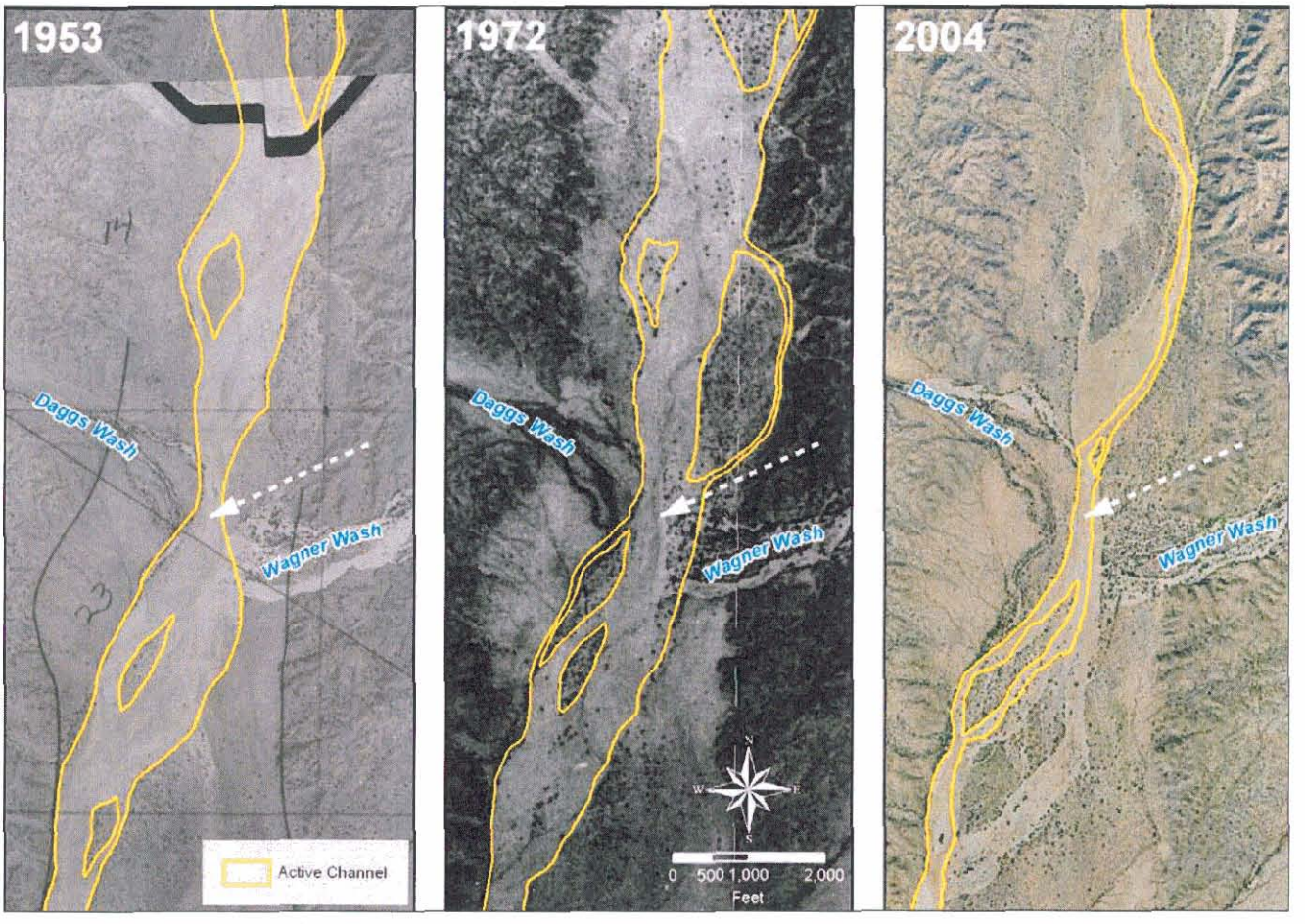

Figure 2-21. Reach 4 Wagner Wash/Daggs Wash confluence

2.3.4.2 Vegetation

Channel vegetation is sparse in Reach 4 and consisting of desert dicoria. Bank vegetation density varied throughout the reach from no vegetation on cutbanks to dense snakeweed, palo verde, creosote, and desert broom on less recently disturbed banks. More banks in Reach 4 have dense vegetation than in any of the downstream reaches, except for the portion of Reach below the irrigation tailwater outfall. Figure 2-22 shows typical examples of channel and bank vegetation in Reach 4.

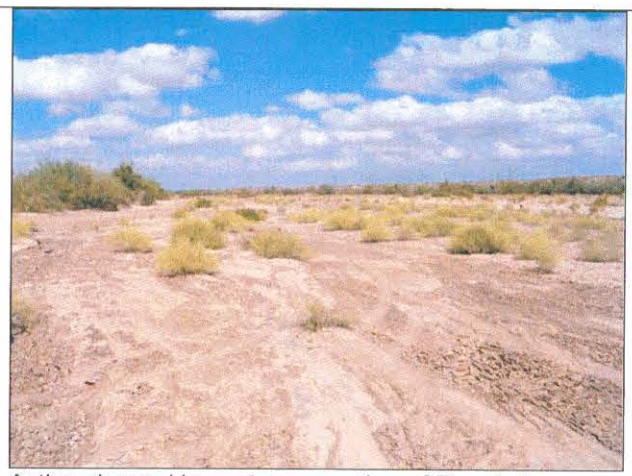

Active channel in upstream portion of Reach 4. View downstream.

Active channel in downstream portion of Reach 4. View upstream.

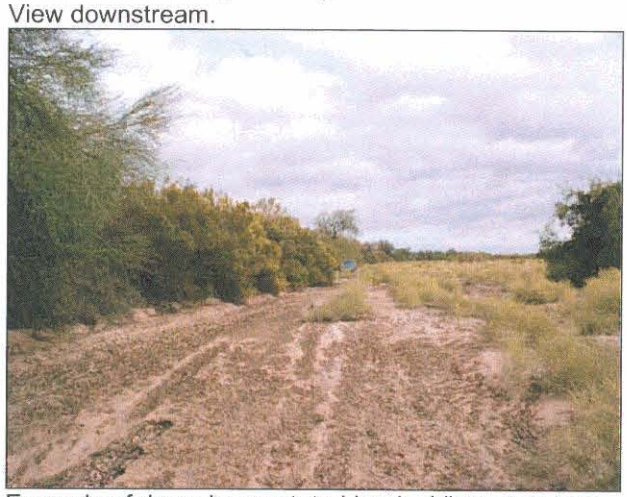

Example of densely vegetated bank. View upstream.

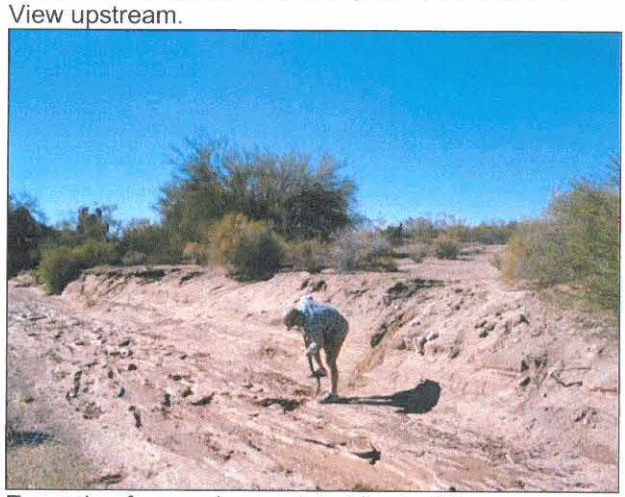

Example of sparsely vegetated bank. View downstream.

Figure 2-22. Reach 4 channel and bank vegetation

2.3.4.3 Cutbanks

Vertical cutbanks occur throughout Reach 4 on both banks and are typically between two and four feet in height. Reach 4 cutbank locations are shown in Figure 2-23. The hatched lines define the extent of the cutbanks and the numeric identifiers represent the bank heights in feet. Bedrock crops out along a 500-foot section of the right bank approximately 1.5 miles downstream from the Wagner Wash confluence. This is one of the two locations of exposed bedrock within the entire Hassayampa River study area. The active channel abuts the bedrock outcrop, which provides lateral erosion control for the right bank. Field photos are shown in Figure 2-24.

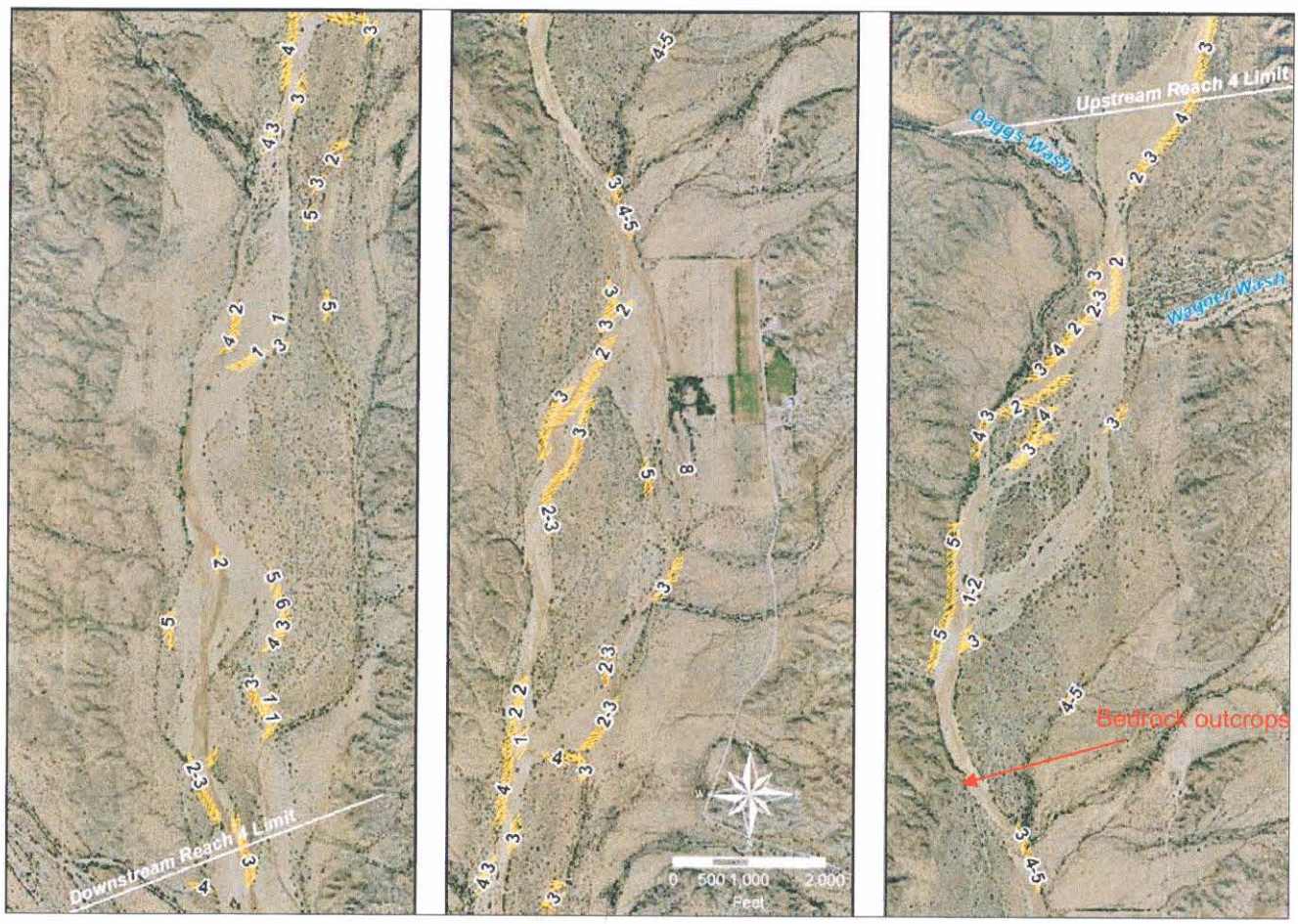

Figure 2-23. Reach 4 cutbank locations

Typical active channel cutbank. View west.

Left bank cutbank. View downstream.

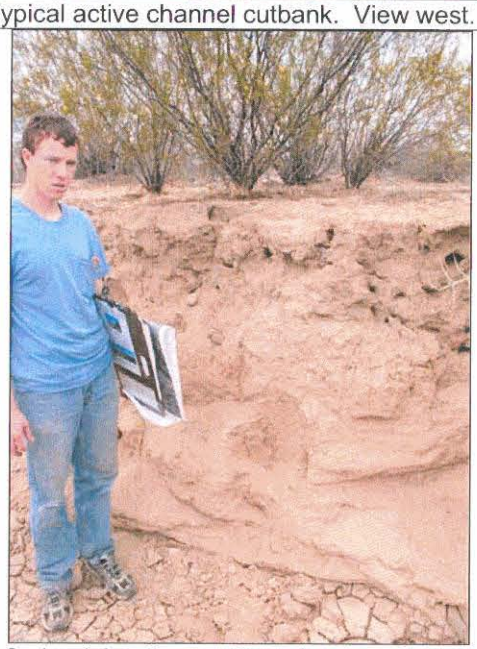

Cutbank in tributary deposit. View east.

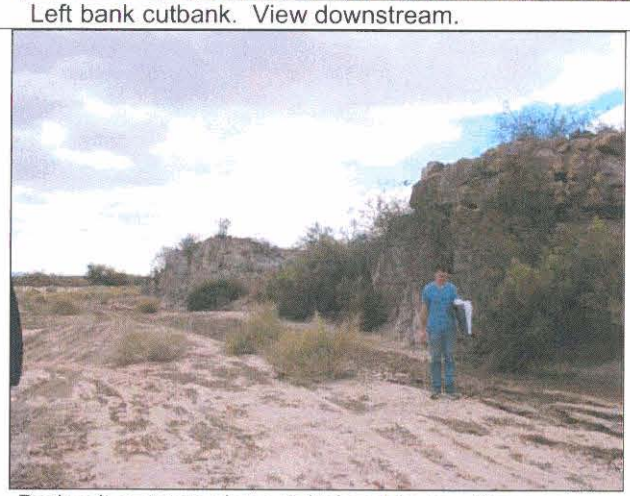

Bedrock outcrop along right bank below Wagner Wash confluence. View downstream.

Figure 2-24. Reach 4 cutbank field photos

2.3.4.4 Structure Impacts

No significant manmade structures were observed in Reach 4.

2.3.5 Hassayampa River Reach 5: Wagner/Daggs Wash to CAP Siphon

Reach 5 extends from the CAP siphon to the Daggs Wash confluence. As discussed in Chapter 1, Reach 5 was divided into two subreaches to facilitate map production. In this Chapter, reaches 5a and 5b are combined and discussed together.

2.3.5.1 Channel Width, Pattern, and Sinuosity

Channel width in Reach 5 varies from about 100 feet at the downstream limit to 460 feet upstream of the CAP siphon. The Reach 5 channel pattern alternates between a single and braided channel. Sinuosity in Reach 5 was estimated at 1.15, the highest of the five Hassayampa River subreaches.

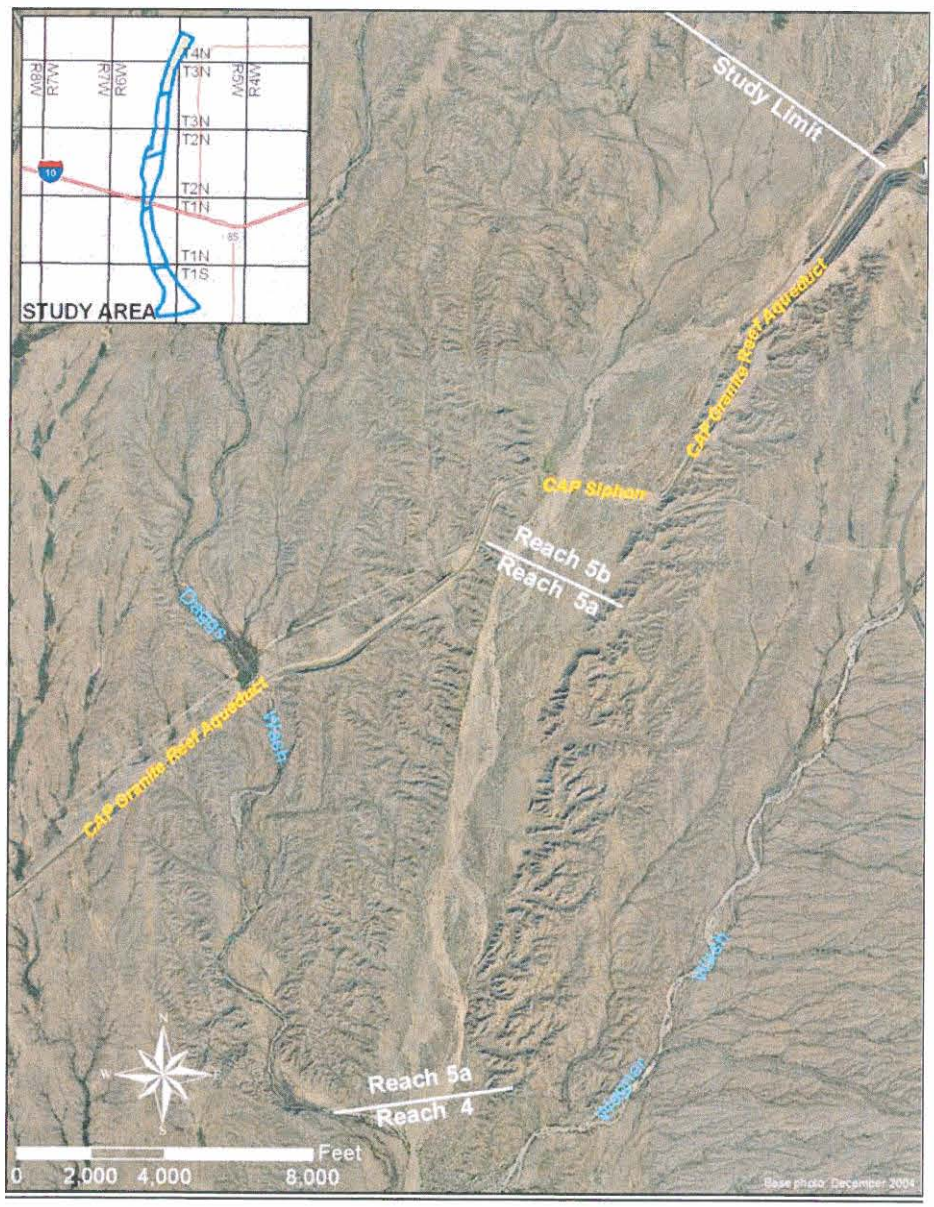

Figure 2-25. Reach 5 photograph showing channel pattern and features.

2.3.5.2 Vegetation

Channel vegetation in Reach 5 is consistent with that found in the rest of the study area and is composed of sparsely distributed desert dicoria. Bank vegetation is also consistent with vegetation found in most of the downstream reaches, varying from dense thickets to no vegetation present. When present, bank vegetation consists primarily of desert broom, palo verde, snakeweed, with occasional creosote. Figure 2-26 shows field photos of typical channel and bank vegetation in Reach 5.

Active channel near the upstream study limit. View downstream.

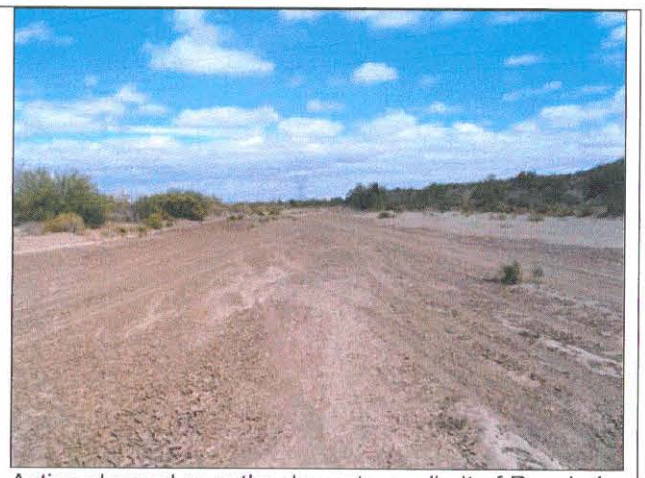

Active channel near the downstream limit of Reach 4. View upstream.

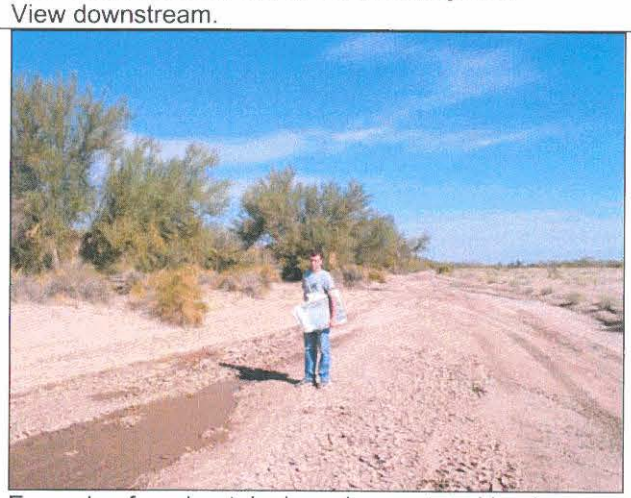

Example of moderately densely vegetated bank. View upstream.

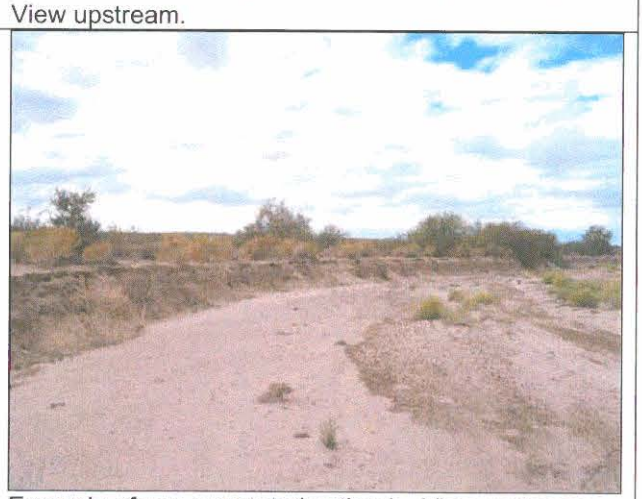

Example of non-vegetated cutbank. View upstream.

Figure 2-26. Reach 5 channel and bank vegetation

2.3.5.3 Cutbanks

Cutbanks were more frequent within the upper half of Reach 5 than the lower half, and were typically between two and five feet in height. Most of the channel banks in the lower half of Reach 5 were sloped at 3:1 or greater, suggesting more lateral stability (or at least less recent lateral erosion) of the active channel. Typical cutbank heights in the lower half of Reach 5 are two to four feet. Cutbank locations are shown in Figure 2-27. The hatched lines define the extent of the cutbanks and the numeric identifiers represent the bank heights in feet. Figure 2-28 shows field photos from Reach 5.

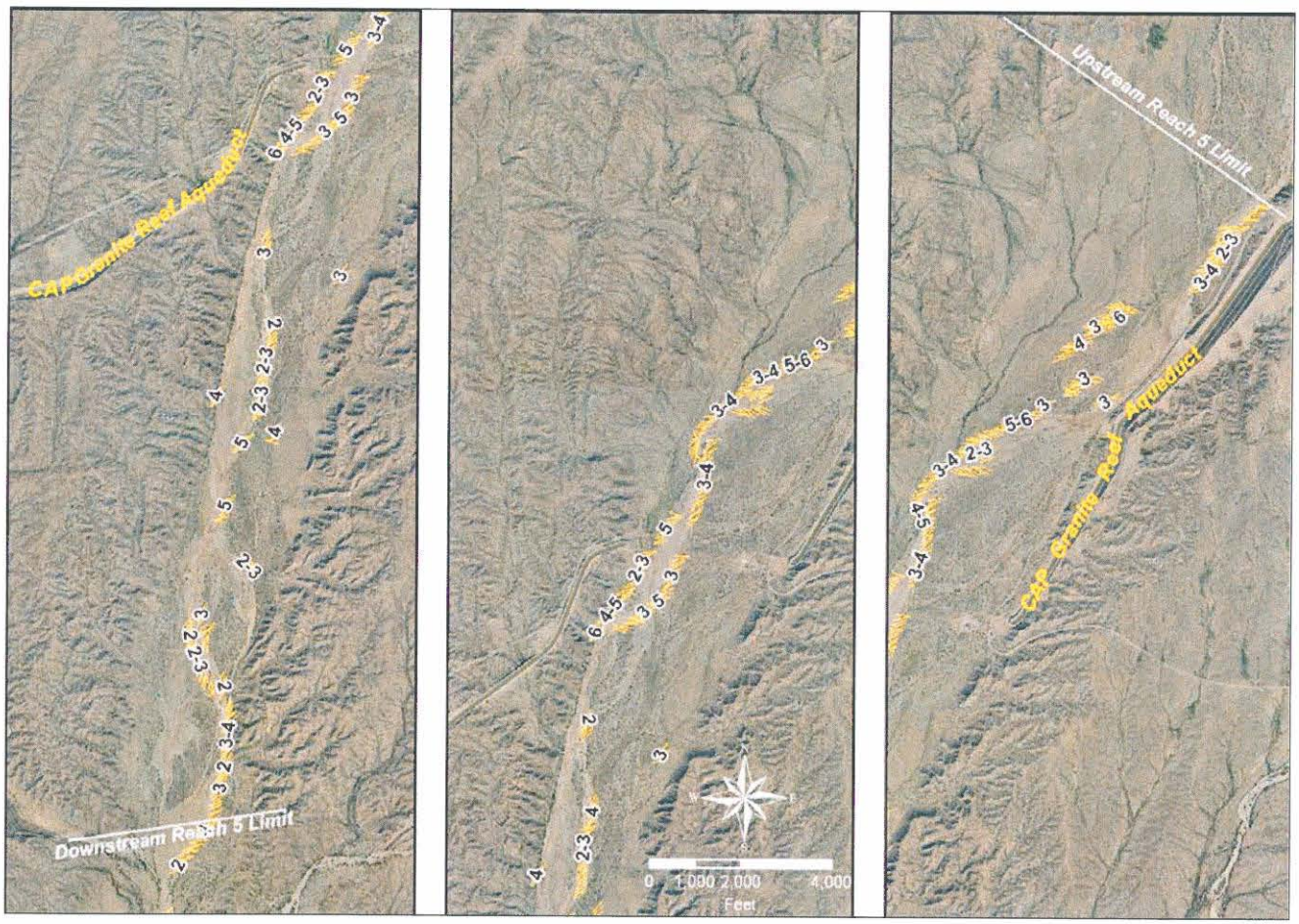

Figure 2-27. Reach 5 cutbank locations

Left bank cutbank in the lower portion of Reach 5. View downstream.

Right bank cutbank in mid-Reach 5. View upstream.

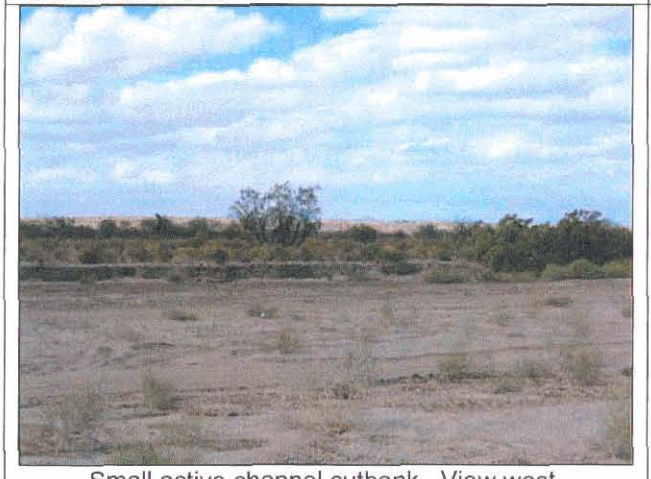

Small active channel cutbank. View west.

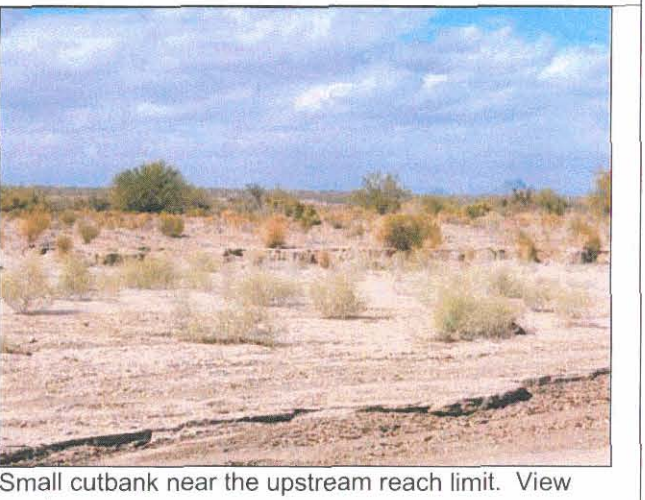

Small cutbank near the upstream reach limit. View west.

Figure 2-28. Reach 5 cutbank field photos

2.3.5.4 Structure Impacts

The following four structures were observed in Reach 5:

- CAP Canal
- CAP Siphon
- Two Overhead High Tension Power Line Alignments

Each of these structures was investigated to determine their impact on the active channel. The CAP canal alignment located east of the active channel, upstream of the siphon crossing, abuts the active channel and is aligned nearly parallel to the active channel. Much of the canal from the pump house to the siphon crossing was constructed on the slope of the Pleistocene terrace, and therefore does not directly affect the active channel. However, at the time of the field investigation, a 2,400 foot segment of canal directly abuts the active channel. The canal embankment is protected by recently constructed soil cement bank protection designed to stop erosion of the canal. The soil cement embankment is discussed in more in Section 2.6 of this chapter.

The siphon crossing itself was investigated and determined to have no adverse impact on the active channel because it is buried well below the active channel bed. Although significant disturbance of the active channel undoubtedly occurred during construction of the CAP siphon crossing, the field investigation determined the channel has recovered to a more natural condition.

The overhead power line crossings were located just upstream of the Reach 5 downstream limit. The northernmost alignment had one tower located directly in the path of the active channel. No evidence of adverse impacts on the active channel by the tower was found. The southernmost alignment had five towers located within the Holocene corridor; however, none were directly in the active channel corridor. Figure 2-29 shows field photos of structures in Reach 5.

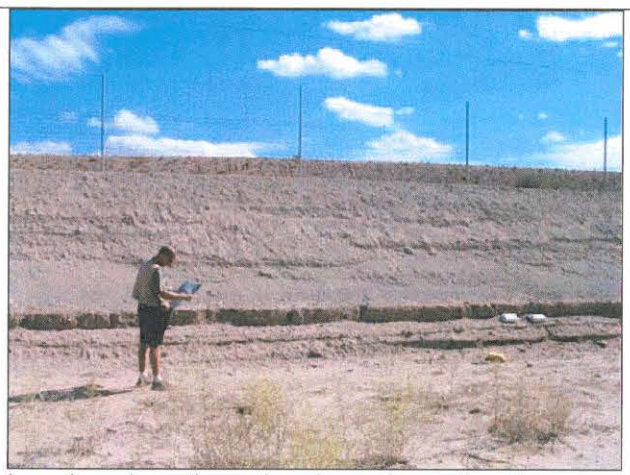

Location where the active channel was directly adjacent to the CAP canal embankment. View east.

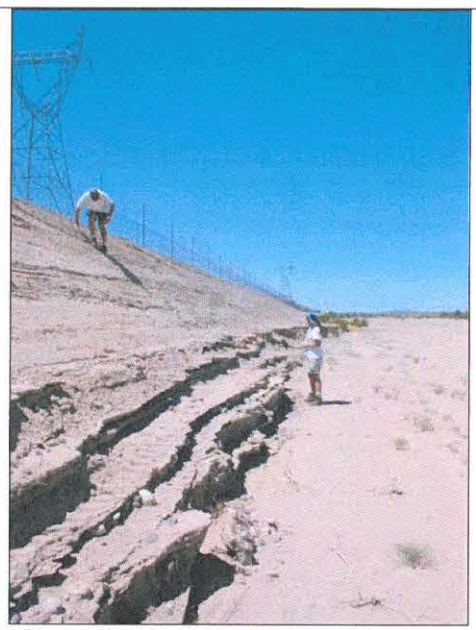

CAP canal embankment. View downstream.

Active channel at the CAP siphon crossing. View downstream.

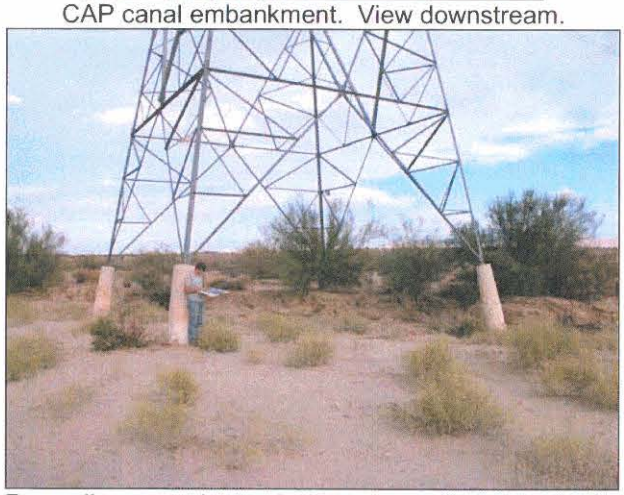

Power line tower located within the active channel. View across channel.

Figure 2-29. Reach 5 active channel field photos

2.4 Floodplain Conditions

For the purposes of the field reconnaissance report, the floodplain is defined as any area within the modern geologic floodplain[3] that is not part of the active channel, as defined in Section 2.3 of this chapter. The floodplain includes low and high terraces, deltaic and other tributary deposits, and disturbed areas outside the active channel. The defining characteristics of the floodplains are that they are not frequently inundated, and that they are typically subject to sediment deposition rather than to erosion. As stated above, the active channel comprises approximately 6% of the geologic floodplain, leaving the remaining 94% of the modern geologic floodplain as floodplain. The floodplain was divided into six geologic units, which were mapped and described in detail, as discussed in Chapter 3.

The floodplain descriptions presented below are segregated by reach. The following floodplain characteristics were observed and documented during the field investigations, with a brief explanation as to their significance:

1. Floodplain Width – Floodplain width is defined as the width of the modern geologic floodplain measured perpendicular to the primary flow direction of the river. Changes in floodplain width often indicate the presence of lateral constraints on the active channel corridor. Wider floodplain inundation limits allow for greater active channel migration, but may also indicate subtle changes in slope, which result in channel pattern changes.

2. Surface-Type Distribution – Different floodplain surfaces serve different functions within the river system. Basic characteristics, such as topographic position (elevation relative to the channel or to other surfaces), lateral position within the floodplain, sediment composition, vegetative cover suites, and relative areal extent, provide evidence as to the surface function. Detailed descriptions of floodplain geomorphic surfaces are provided in Chapter 3. For the purpose of the field reconnaissance described below, the surfaces were segregated into (1) low terraces and bars, (2) high terraces, and (3) tributary terraces. The areal distribution of the surfaces was calculated to provide insight into the relative stability of the reach. For example, if a particular reach contains a relatively high percent of tributary terraces in comparison with floodplain deposits, this may indicate that tributary sediment influx rate is greater than the main stem transport rate, indicating that the tributary deposits provide some degree of lateral control. Conversely, if a reach has a high percent of low terrace and bar deposits, it indicates that frequent lateral migration and/or avulsions will occur.

3. Geomorphic Features – Geomorphic features, such as headcuts and avulsion channels, observed on the floodplain provide insight to channel and floodplain processes that have occurred in the past. Headcuts on the floodplain indicate recent degradation of the active channel, formation of incipient avulsive flow paths, changes in active channel slope, concentration points for overland or

[3] The modern geologic floodplain includes Holocene-aged (~10,000 years before present) surfaces adjacent to the main channel and within the river valley, as defined by the margins of the high Pleistocene-aged (~2,000,000 years before present) terraces.

tributary flow in the floodplain, and/or recent deposition of tributary sediments. Avulsive flow paths in the floodplain indicate areas of potential future active channel alignments, frequent or past inundation of the floodplain, and general surficial stability conditions. Avulsive channels can be recognized in the field using surface topography, surficial sediment composition, high water marks, abandoned flood channels, and vegetative characteristics.

4. Vegetation – Floodplain vegetation provides information about the history and relative stability of the surface, such as the relative flood inundation frequency, history of manmade disturbances to the surface, type of soil comprising the surface, and the lateral limits of the surface. Vegetation type, density, and maturity vary consistently among the geomorphic surfaces observed within the study area. In this chapter, floodplain vegetation is described for the following three surfaces: low terrace, high terrace, and tributary terrace.

5. Structure Impacts – Manmade structures in a floodplain can potentially have an affect on the form and function of the surface. Structures may interfere with natural flow patterns during floods, causing changes in floodplain conditions. Impacts of the river on the structures are discussed in Section 2.6.

2.4.1 Hassayampa River Reach 1: Gila River to SPRR Bridge

The morphology and characteristics of Reach 1 differ from the rest of the Hassayampa River reaches. In addition to the levees and historical channelization, a large portion of the floodplain in Reach 1 has been graded, leveled, and modified by agriculture for at least seven decades. Even prior to agricultural modification, the floodplain in Reach 1 differed from the rest of the LHWCMP study area because it was the Hassayampa River delta within the Gila River geologic floodplain and because it was not confined by Pleistocene terraces. Because of these differences, the discussion of the Reach 1 floodplain was divided into the following two subreaches:

- Subreach 1A - SPRR Bridge to the Gila River
- Subreach 1B - Upstream limit of Reach 1 limit to SPRR Bridge

2.4.1.1 Floodplain Width

Subreach 1A

The Reach 1 floodplain downstream of the SPRR Bridge is essentially unconfined east of the Hassayampa River. None of the natural features that define the floodplain or its margins in the rest of LHWCMP study area, such as older river terraces or bedrock, exist east of Reach 1. Therefore, the floodplain width east of the river was not quantified.

West of Reach 1, a Late Tertiary-aged volcanic formation constrains the floodplain. The western floodplain width varies from over 7,500 feet near the Gila River confluence to less than 600 feet upstream of the Old US Highway 80 Bridge. The western floodplain between the Old US 80 Bridge and the SPRR Bridge was flanked by a Late Pleistocene surface which varied between three to five feet in height.

Subreach 1B

This relatively small, 3,200 foot-long subreach is characterized by a definable floodplain that is laterally constrained by older Pliocene[4], Pleistocene, or Tertiary[5] terraces. The floodplain width was fairly consistent in this reach at approximately 6,000 feet.

2.4.1.2 Surface-Type Distribution

The long history of agriculture combined with channelization of Reach 1 has resulted in the effective removal of nearly all the low terrace and bar deposits from the floodplain downstream of the Old US 80 Bridge. Therefore, high terraces and tributary terraces composed the majority of floodplain area in Reach 1. Table 2-1 lists the surface-type distribution.

Table 2-1. Reach 1 Surface-Type Distribution

Reach	Active Channel	Low Terrace & Bar	High Terrace	Tributary Terrace	Disturbed Areas
1	2%	7%	66%	22%	3%
2	5%	41%	14%	39%	1%
3	10%	21%	14%	48%	7%
4	7%	37%	15%	41%	0%
5	7%	41%	24%	26%	2%

2.4.1.3 Geomorphic Features

No headcuts or potential avulsion areas were identified in Reach 1, primarily because of the degree of historical agricultural use of the floodplain.

A Late Pleistocene (Ql) surface is mapped in the western floodplain downstream of the SPRR Bridge (See Chapter 3). Although the Ql surface is topographically low relative to the rest of the floodplain, no evidence of flood inundation was found. The lack of inundation of the Ql surface is probably due to the unconfined eastern floodplain that allows flooding to spread out across a large area, resulting in low flood depths. Well developed desert pavement and desert varnish were observed throughout the Ql surface.

2.4.1.4 General Vegetation Descriptions

Subreach 1A

The Hassayampa River active channel is channelized and protected by earthen levees downstream of the Old US 80 Bridge. The floodplain outside the levees has been farmed since the 1930's. Thus, no natural floodplain vegetation is present in Reach 1. Vegetation on the Ql surface was comprised exclusively of creosote. Figure 2-30 shows the location and Figure 2-31 shows field photos of the Ql surface in Reach 1.

Subreach 1B

Most of the floodplain east of the Hassayampa River was under cultivation at the time of

[4] Pliocene – geologic Epoch spanning 5.3 to 1.8 million years ago

[5] Tertiary – geologic Period spanning 65 to 1.8 million years ago

the field investigation, with the exception of a low terrace directly adjacent to the active channel. Vegetation on this terrace predominantly consisted of large tamarisk trees with intermittent desert broom.

The floodplain area west of the Hassayampa River in Subreach 1B was strikingly different than that to the east. No evidence of present or historical agricultural development was found on the west floodplain. Vegetation characteristics of this surface included sparsely distributed desert broom and snakeweed. Evidence of relatively frequent inundation included flotsam and flood debris scattered throughout the floodplain surface, and the lack of mature, established vegetation.

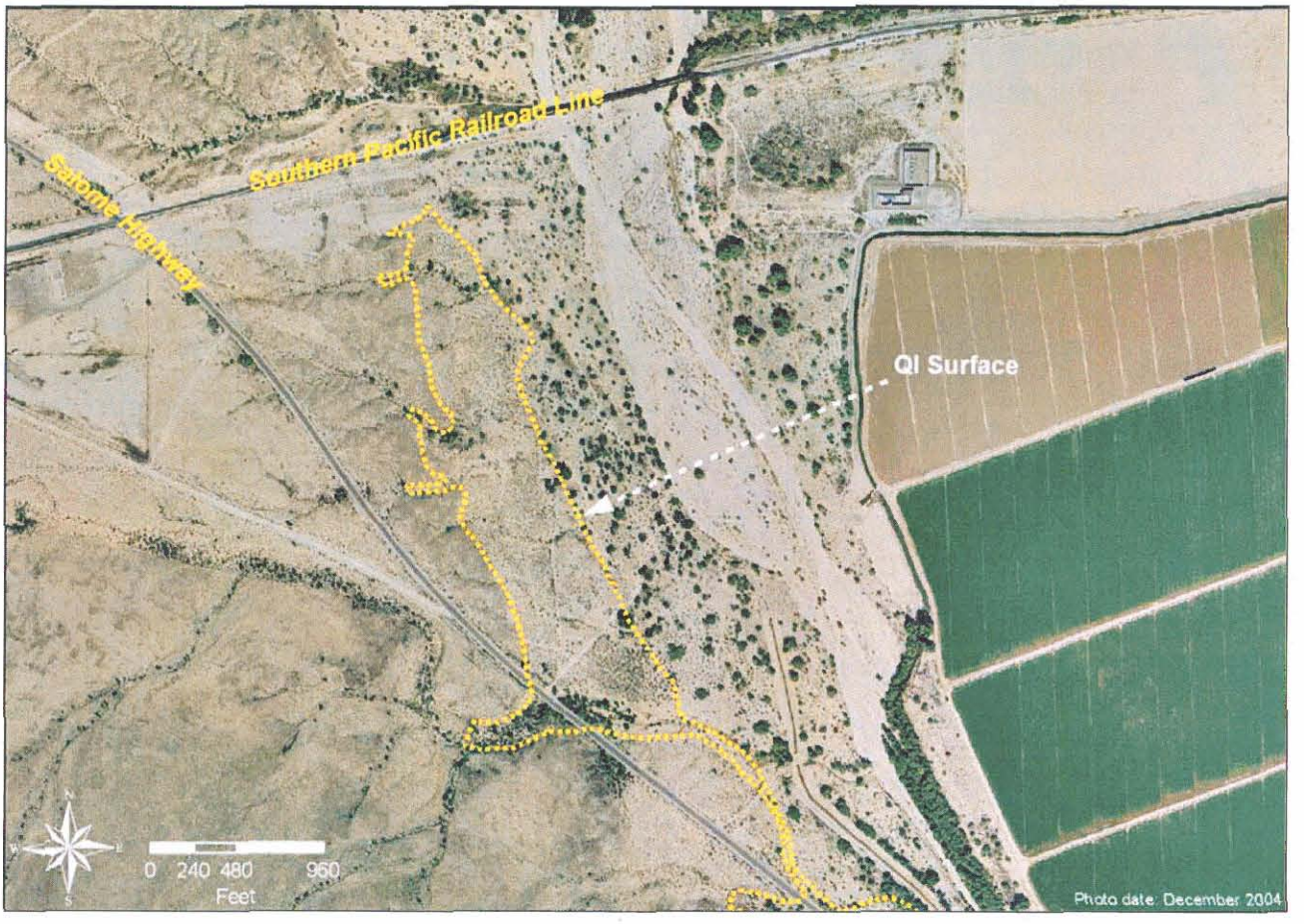

Figure 2-30. Reach 1 QI surface

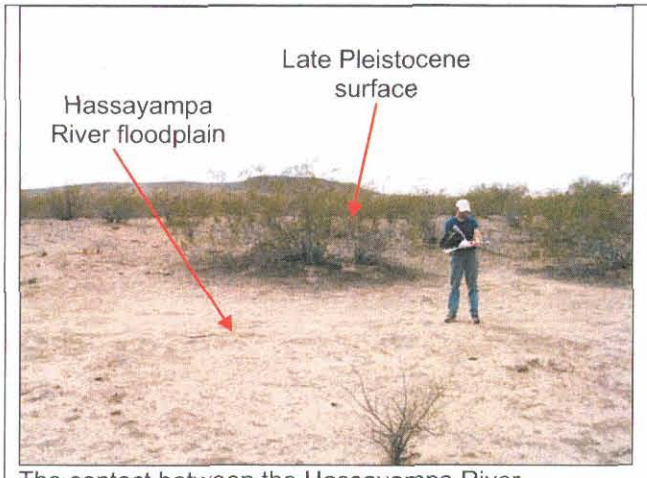

The contact between the Hassayampa River floodplain deposits and the Late Pleistocene surface. Note the minor topographic difference between the two surfaces. View westerly.

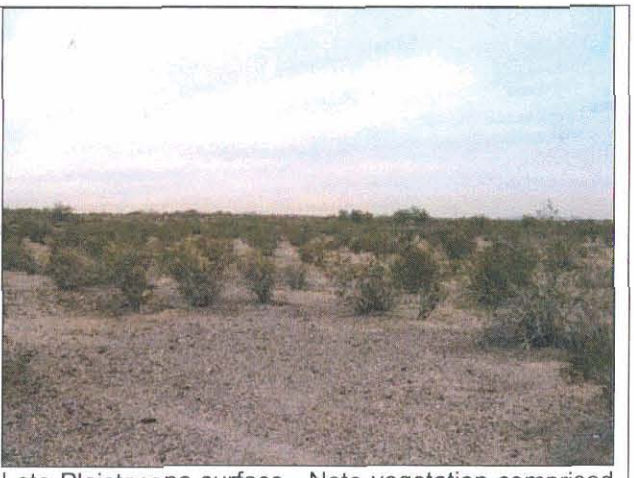

Late Pleistocene surface. Note vegetation comprised exclusively of creosote. View upstream.

Desert pavement on Late Pleistocene surface.

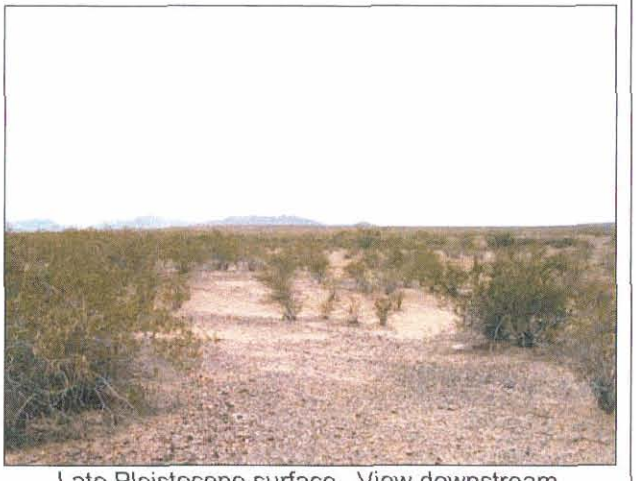

Late Pleistocene surface. View downstream.

Figure 2-31. Field photos of Late Pleistocene surface - Reach 1

2.4.1.5 Structure Impacts

Two earthen dikes were observed on the low terrace in the left floodplain (east) directly downstream of the Reach 1-Reach 2 boundary. The dikes are three to four feet high. A remnant of an irrigation canal is located near the low terrace/cultivated area contact. The dikes have had no obvious impact on the floodplain, due to their limited extent and alignment parallel to the channel.

Two additional earthen levees (or collection dikes) were observed in the right overbank just upstream of the SPRR Bridge (Figure 2-32). The purpose of these structures appears to be to direct overbank flow toward the bridge opening. Both dikes are tied into the Pleistocene terrace to the west. The upstream dike is between eight and ten feet high. The downstream dike is five to six feet high. With the exception of a breach in the upstream dike sometime between 1949 and 1953, field evidence suggests the structures have effectively served to direct flood flows toward the bridge opening.

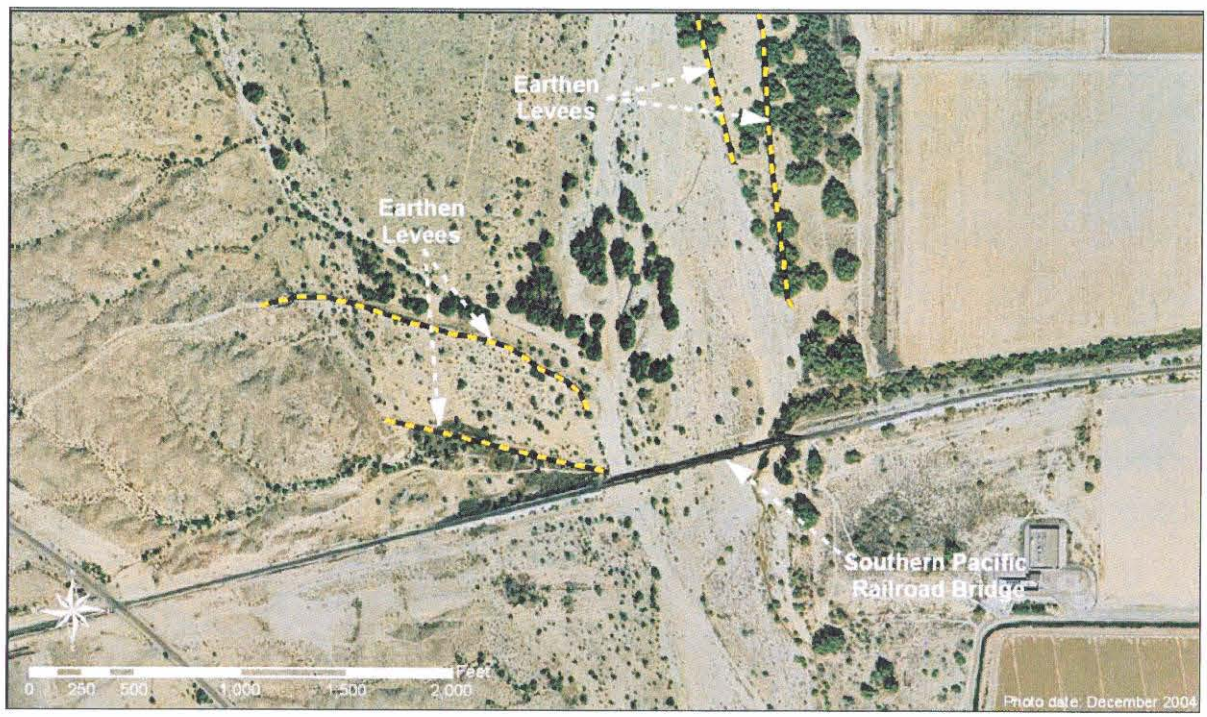

Figure 2-32. Levees upstream of SPRR Bridge

Other structures located in the floodplain of Reach 1 include the Old US 80 road alignment, the Arlington Canal and siphon, two rectangular water storage basins, and numerous canal laterals. During the field investigation construction of scour mitigation measures was underway in the channel at the Old US 80 Bridge. The two water storage basins are located in the eastern floodplain area outside the levees, and have had no observable impact on the floodplain. The basins' footprints equal a total of approximately six acres.

Figure 2-33 shows field photos of the floodplain areas in Reach 1 upstream of the SPRR Bridge and Figure 2-34 shows field photos of the floodplain areas downstream of the railroad bridge.

View southeast across cultivated fields.

Low floodplain terrace east of Hassayampa River active channel. View downstream.

Floodplain surface west of Hassayampa River active channel. View downstream.

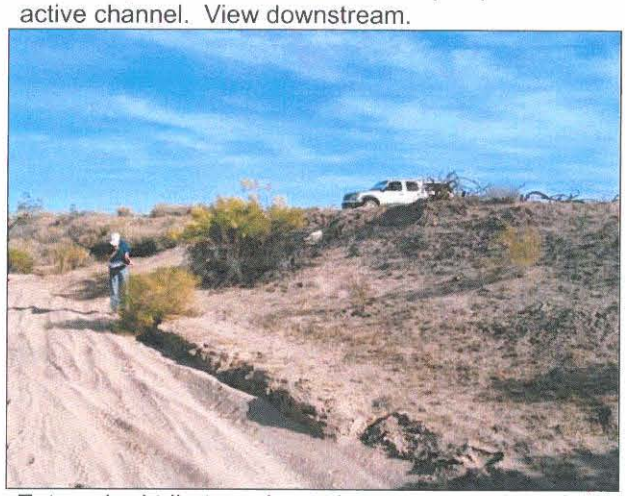

Entrenched tributary channel on western edge of the floodplain. View upstream.

Figure 2-33. Reach 1 floodplain field photos upstream of the SPRR Bridge

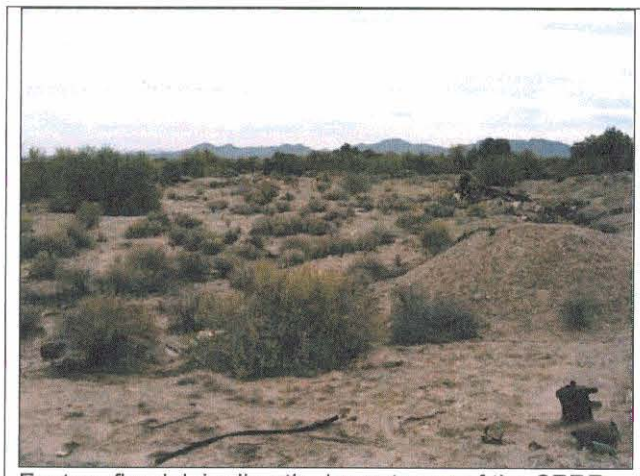

Eastern floodplain directly downstream of the SPRR Bridge. View downstream.

View of Buckeye Canal and cultivated fields in eastern floodplain area. View slightly upstream direction.

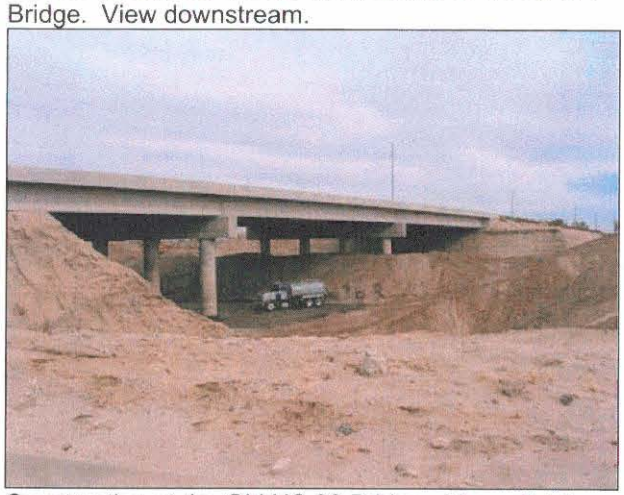

Construction at the Old US 80 Bridge. View slightly upstream.

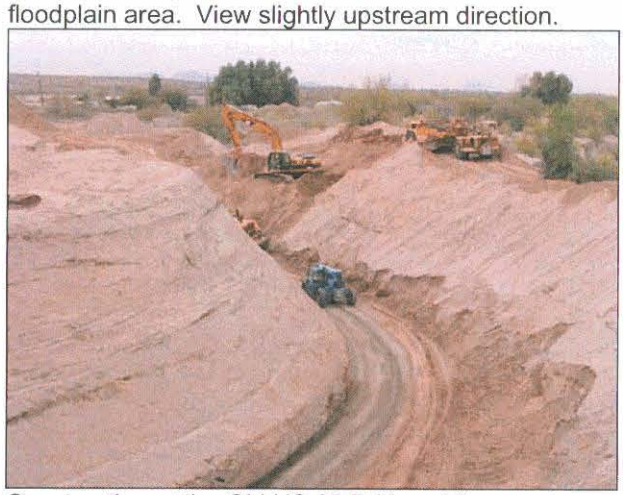

Construction at the Old US 80 Bridge. View upstream of active channel.

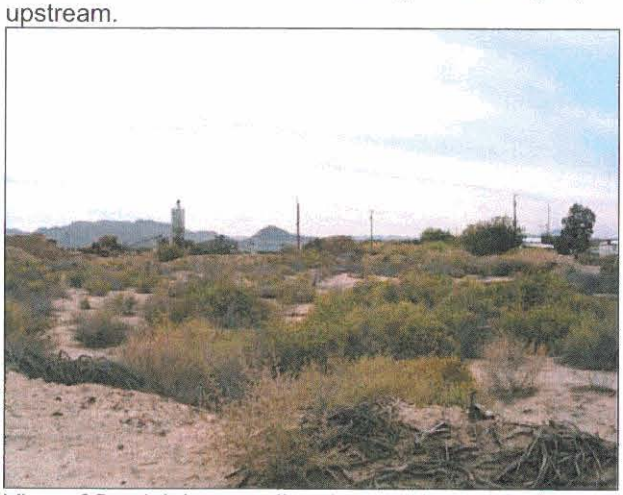

View of floodplain area directly upstream of Old US 80 Bridge with construction activity in background.

Cultivated fields in western floodplain area. View directly west.

Figure 2-34. Reach 1 floodplain field photos downstream of the SPRR Bridge

2.4.2 Hassayampa River Reach 2: SPRR Bridge to I-10 Bridge

2.4.2.1 Floodplain Width

The Holocene floodplain width in Reach 2 widened consistently in the downstream direction from just over 3,600 feet near the upstream reach limit to over 6,200 feet near the downstream reach limit.

2.4.2.2 Surface-Type Distribution

Although tributary terraces constitute a relatively large portion of the surface type (Table 2-2), no major tributary confluences were present in Reach 2. The Holocene floodplain in Reach 2 is laterally constrained by high Pleistocene-aged terraces. Dozens of small drainage channels dissect and drain these terraces and debouche onto the margins of Hassayampa River floodplain. Sediment transported by these drainages is deposited at the Pleistocene/Holocene contact, creating a nearly continuous zone of coalescing deposits. These deposits occur throughout the entire study area, but are significantly larger where the major tributaries join the Hassayampa River and form delta deposits. The high percent of low terrace and bar deposits relative to the high terrace deposits indicate that most of the floodplain is highly active and that frequent, future migration of the active channel should be expected.

Table 2-2. Reach 2 Surface-Type Distribution

Reach	Active Channel	Low Terrace & Bar	High Terrace	Tributary Terrace	Disturbed Areas
1	2%	7%	66%	22%	3%
2	5%	41%	14%	39%	1%
3	10%	21%	14%	48%	7%
4	7%	37%	15%	41%	0%
5	7%	41%	24%	26%	2%

2.4.2.3 Geomorphic Features

Few headcuts along floodplain flow paths were observed in Reach 2. Small clusters occurred in three areas, all of which were on tributary terraces. The first location is east of the active channel just downstream of the upper Reach 2 limit. The second location is near the reach midpoint west of the active channel. The third area was located just upstream of the Baseline Road crossing on the extreme western floodplain limit. Figure 2-35 shows the headcut locations (arrowheads point in the direction of headcut migration).

Several locations of potential avulsions were identified in Reach 2, based on evidence that suggests potential avulsion of the active channel onto a low terrace. Figure 2-36 illustrates these locations from upstream to downstream. The red arrows show the estimated flow path direction of the potential avulsion. Figure 2-37 shows field photos of both headcuts and potential avulsions in Reach 2.

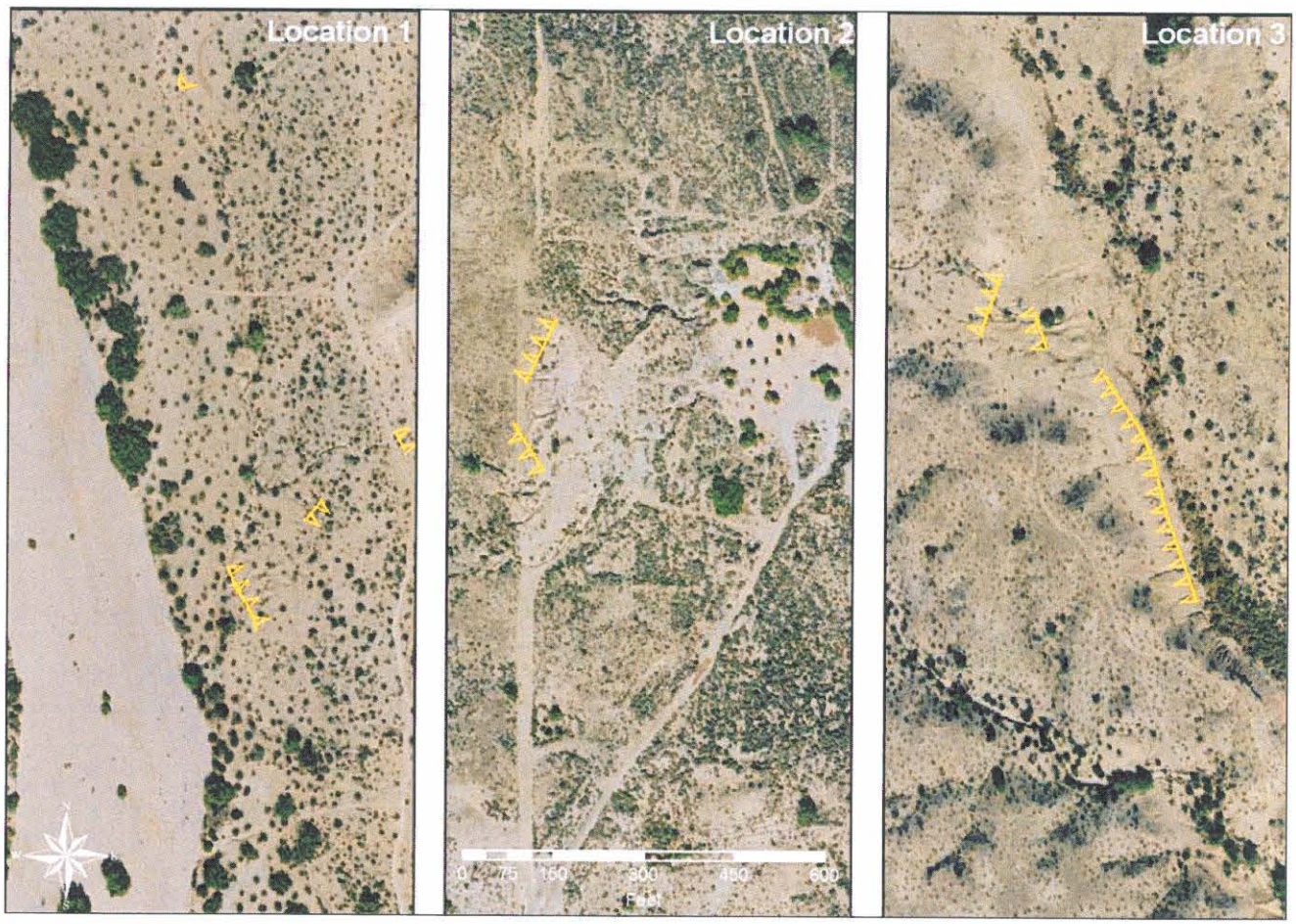

Figure 2-35. Locations of headcuts in Reach 2

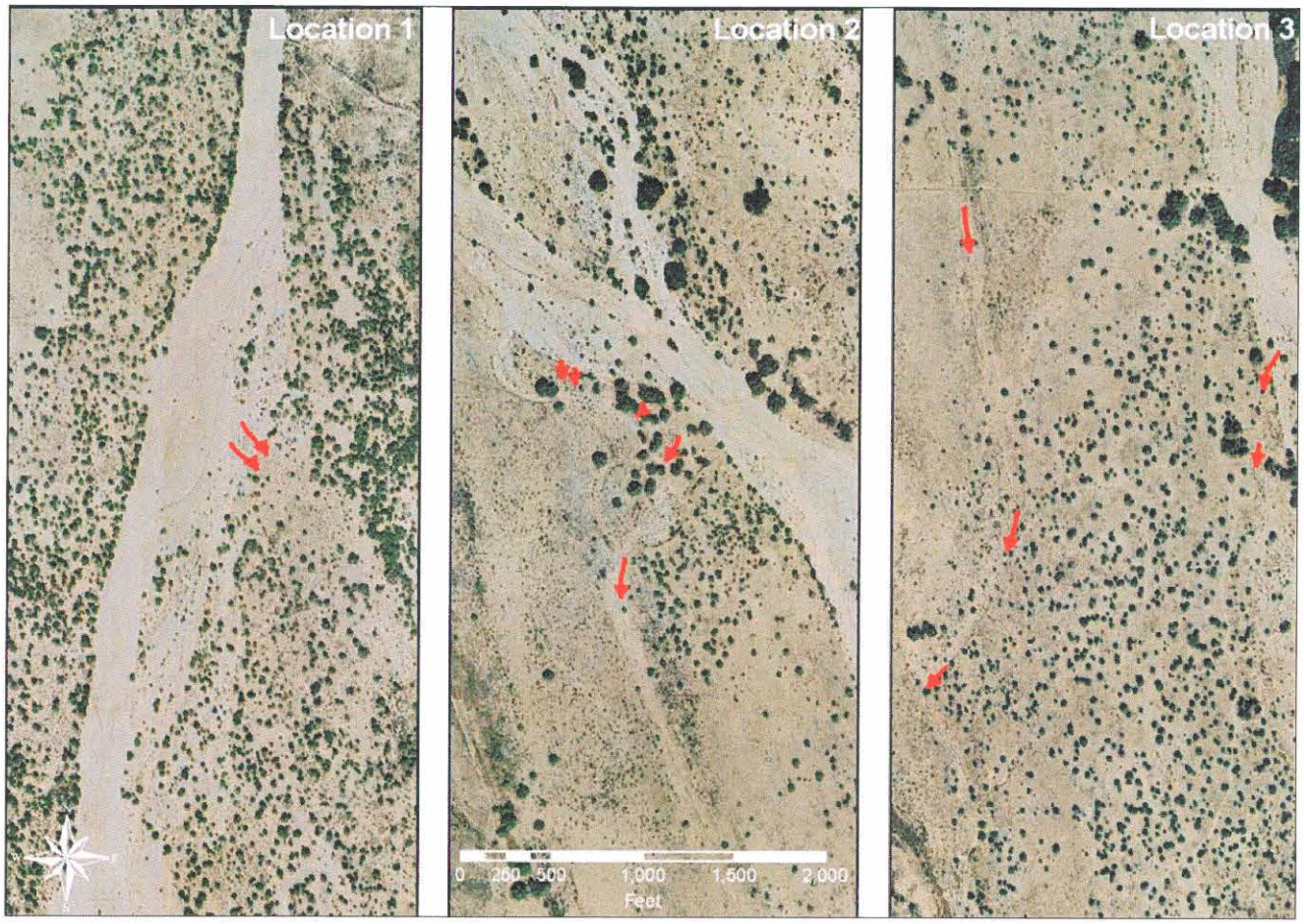

Figure 2-36. Locations of potential avulsions in Reach 2

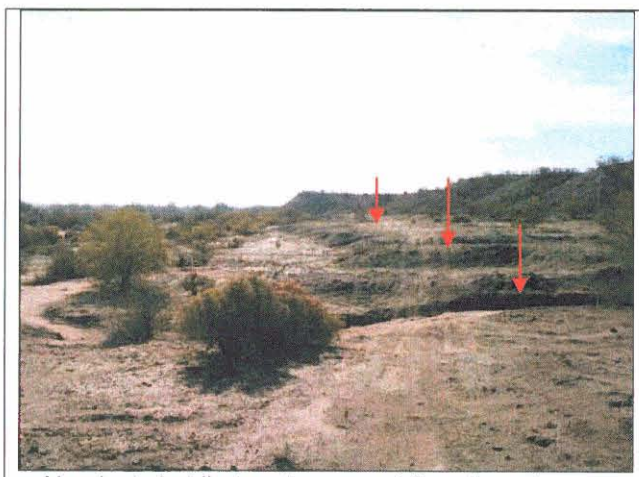

Headcuts in tributary terraces. View downstream.

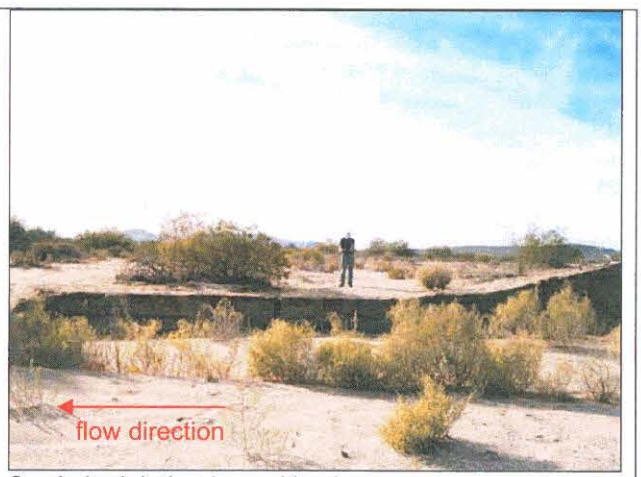

Swale in right bank resulting in a potential avulsion location. View south.

Figure 2-37. Photos of headcuts and potential avulsion locations in Reach 2

2.4.2.4 Vegetation

Floodplain vegetation in Reach 2 was substantially different than that found in Reach 1, and is more representative of natural floodplain vegetative suites in the study area. The vegetation descriptions below are segregated by geomorphic surface.

Low Terrace & Bars

The low terrace vegetation is consistent in Reach 2, except for an area east of the active channel upstream of Baseline Road, an area which appears to have been disturbed. Low terrace vegetation consists of large, mature tamarisk trees with an understory of sparsely distributed snakeweed and desert broom. A dense row of tamarisk grows along the left side of the floodplain for about one mile upstream of Baseline Road along a dike structure composed of buried piles of cut, chopped and discarded tamarisk. Tamarisk does not occur either in the channel or floodplain upstream of this location in the rest of the study area. The remainder of the low terrace surface in Reach 2 was characterized by sparse to moderately dense distributions of snakeweed, desert broom, and small palo verde and mesquite trees. There are also significant areas devoid of vegetation.

High Terrace

The high terrace comprises a small portion of the total floodplain area in Reach 2, and has been disturbed by agricultural development in the past, with most of the natural floodplain vegetation removed. In the disturbed areas, the dominant vegetation type was sage, which is consistent with observations in the rest of the LHWCMP study area where mass clearing occurred. This suggests that following active cultivation, sage is able to grow more quickly than other natural vegetation.

Tributary Terraces

Like the high terrace deposits, the tributary terraces in Reach 2 have been subject to historical agricultural development. Vegetation on undisturbed tributary terraces in Reach 2 was generally dominated by creosote with sparse cacti. Figure 2-38 shows typical floodplain vegetation for each geomorphic surface in Reach 2.

2.4.2.5 2.4.2.5 Structure Impacts

Two major structures are located in Reach 2. The Baseline Road crossing is located just upstream of the lower Reach 2 limit. The roadway crossed the channel and floodplain nearly perpendicular to the flow direction. Several small earthen levees have been constructed in the floodplain near the roadway crossing. Two levees are parallel to the roadway and located on the upstream and downstream faces. Another levee is located along the right overbank downstream of the roadway and is parallel to the flow direction. Another levee is oriented parallel to flow and runs along the left overbank upstream and downstream of the roadway. The levees are between four and eight feet high and are constructed of piled floodplain sediments. The levee parallel to the left overbank is composed of sediment and woody debris (mostly cut tamarisk). The levees may prevent small, frequent flows from leaving the active channel, but larger flows would likely erode them. Therefore, we conclude that neither the levees, nor the Baseline Road crossing itself have any adverse impacts on the floodplain.

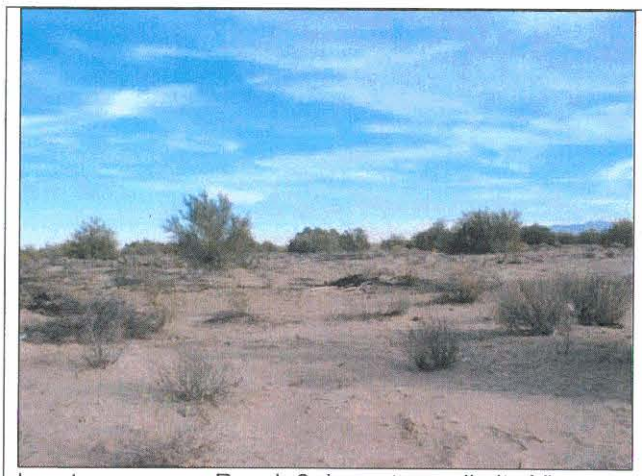

Low terrace near Reach 2 downstream limit. View north.

Typical low terrace vegetation suite in Reach 2. View north.

View of sage dominated high terrace surface. Historically, area was cultivated. View east.

High terrace. Note surface is disturbed and dominated by sage. View south.

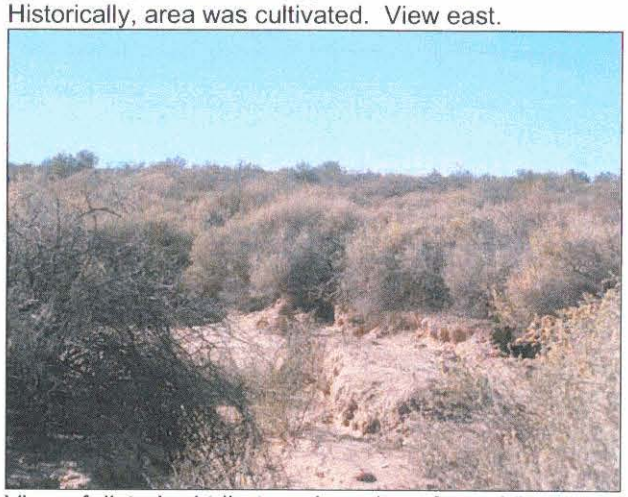

View of disturbed tributary deposit surface. View west.

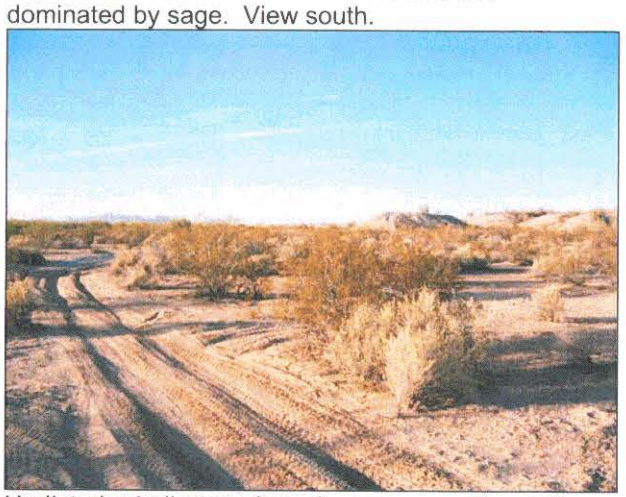

Undisturbed tributary deposit near upper Reach 2 study limit. View north.

Figure 2-38. Reach 2 floodplain vegetation

An overhead high tension power line is located approximately one mile from the upstream Reach 2 limit crossing the Hassayampa River at a 45 degrees angle. Three sets of towers are located in the floodplain. Of these sets, six individual towers are located within the Holocene floodplain. Observation of these towers indicates they have no discernable impact on the floodplain.

Two small, abandoned sand and gravel pits are found in Reach 2. The first pit is located about 500 feet from the downstream end of Reach 2. The second pit is located just over a mile from the downstream Reach 2 limit. Both pits are in the left overbank floodplain. Field evidence suggests that neither of the two pits is active, and no evidence was found to indicate the pits had been recently inundated by floods.

Figure 2-39 shows field photos of the structures located in the Reach 2 floodplain.

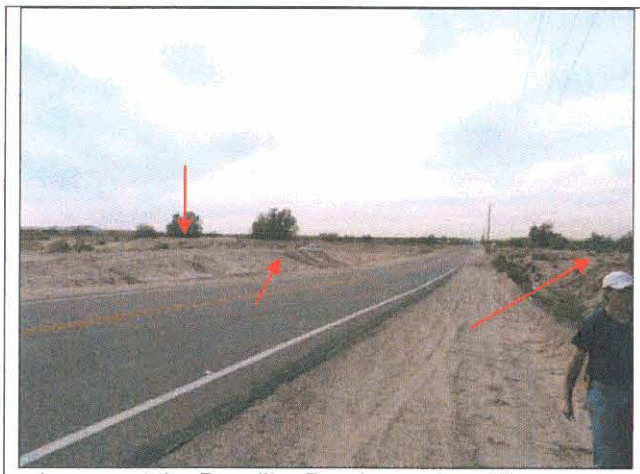

Levees at the Baseline Road crossing. View west.

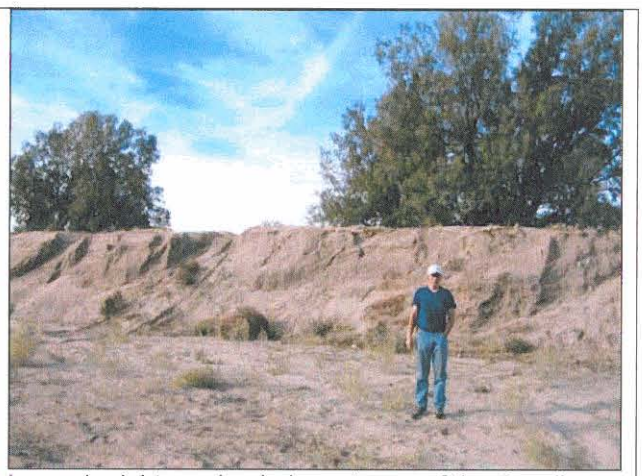

Levee in right overbank downstream of the Baseline Road crossing. View southwest.

Power line towers in the far right overbank floodplain. View northeast.

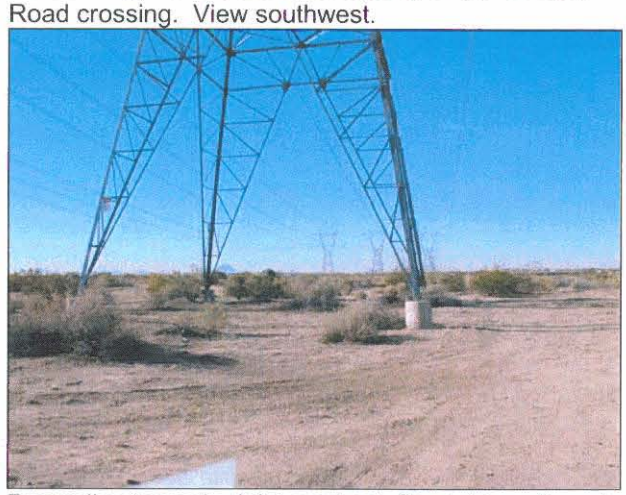

Power line tower in right overbank floodplain adjacent to the active channel. View southwest.

Figure 2-39. Photos of structures in the Reach 2 floodplain

2.4.3 Hassayampa River Reach 3: I-10 Bridge to Jackrabbit Wash

2.4.3.1 Floodplain Width

The Holocene floodplain width in Reach 3 narrows in the downstream direction, in contrast to the trend in Reach 2, up to the I-10 Bridges, after which the floodplain widens. The floodplain width is over 3,000 feet near the upper limit of Reach 3 and narrows to 1,600 feet at the Buckeye FRS #1 outlet channel, just upstream of the I-10 crossing. Directly downstream of I-10 the floodplain immediately widens to 4,500 feet.

2.4.3.2 Surface-Type Distribution

Tributary terraces constituted the largest area by geomorphic surface in Reach 3, primarily due to Jackrabbit Wash delta deposits. Table 2-3 lists the surface distributions for Reach 3.

Table 2-3. Reach 3 Surface-Type Distribution

Reach	Active Channel	Low Terrace & Bar	High Terrace	Tributary Terrace	Disturbed Areas
1	2%	7%	66%	22%	3%
2	5%	41%	14%	39%	1%
3	10%	21%	14%	48%	7%
4	7%	37%	15%	41%	0%
5	7%	41%	24%	26%	2%

The Jackrabbit Wash delta constitutes 20% of the Reach 3 floodplain. As discussed previously, the sediment supply rate from Jackrabbit Wash exceeds the Hassayampa River sediment transport rate, constraining the Hassayampa channel and floodplain. Another significant tributary deposit is located along the right bank downstream of I-10, where several small tributaries coalesce at the Hassayampa River. Historical aerial photo evidence indicates that although the sediment influx at this location has been significantly less than at the Jackrabbit Wash delta, it has been sufficient to provide lateral control of the Hassayampa River. Figure 2-40 shows both the Jackrabbit Wash delta and the tributary deposit downstream of I-10. The Hassayampa River low terrace and high terrace floodplain deposits in Reach 3 varied only 6% by area, indicating that active channel processes have been confined to a relatively narrow corridor.

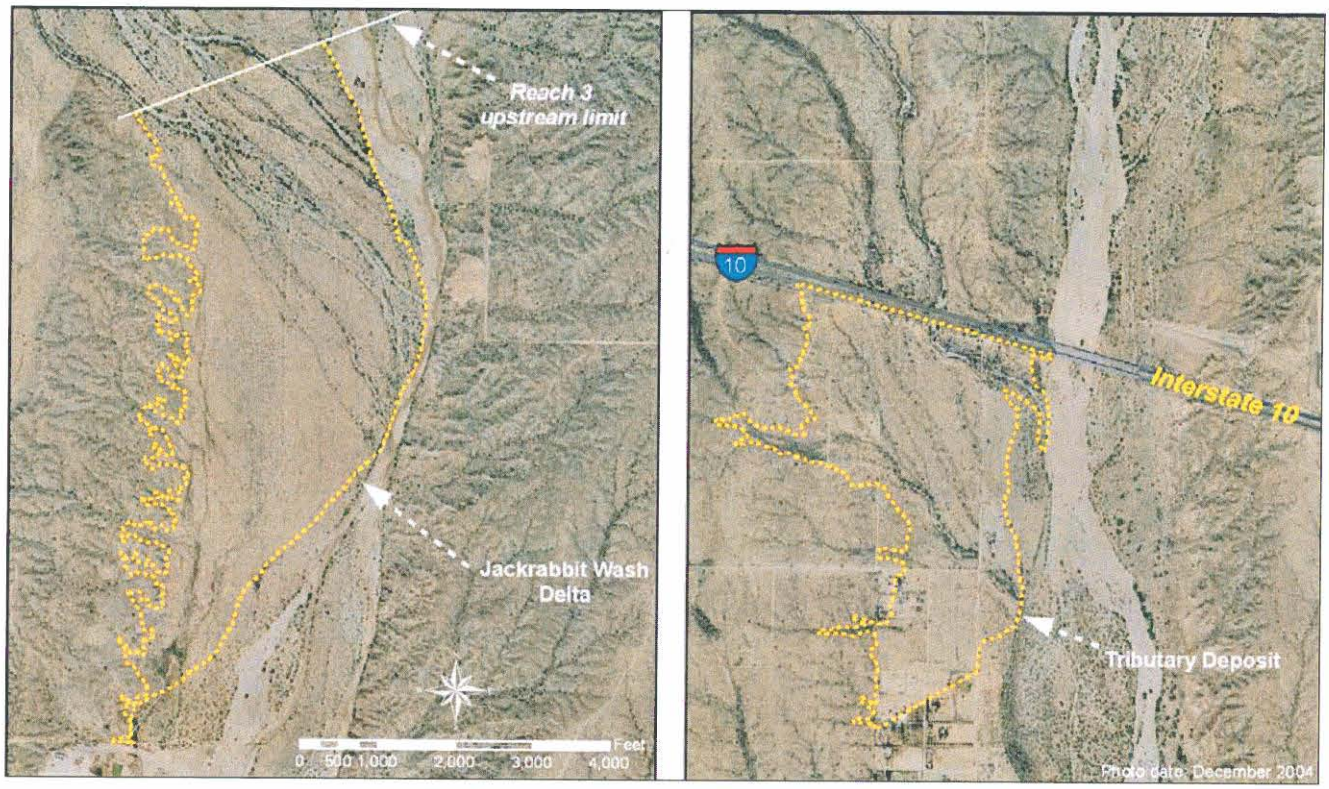

Figure 2-40. Reach 3 tributary terraces

2.4.3.3 Geomorphic Features

More floodplain headcuts occur in Reach 3 than Reach 2, and all were located downstream of the Jackrabbit Wash delta. The majority of headcuts were confined to tributary terraces along the margins of the Holocene floodplain, but a few were observed in the floodplain. Figure 2-41 shows the location of the headcuts in Reach 3. The arrows point in the headcut migration direction.

The potential avulsions identified in Reach 3 were confined to a relatively small area downstream of the Jackrabbit Wash delta and upstream of the I-10 crossing. All of the potential avulsions were found to be within the low terrace & bars surfaces. Figure 2-42 illustrates the potential avulsion areas. The red arrows point in the direction the avulsion would occur. Figure 2-43 shows field photos of both headcuts and potential avulsions.

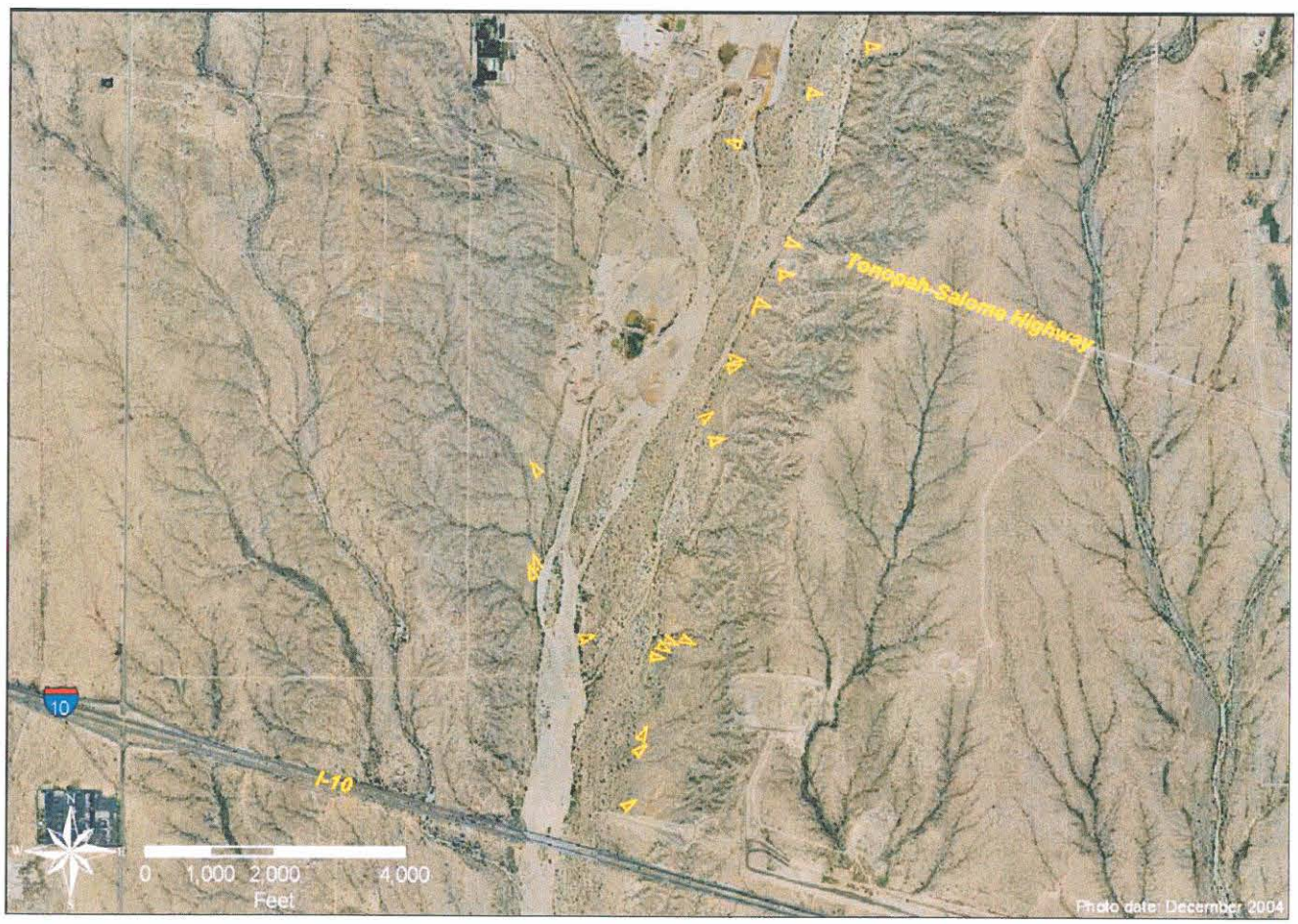

Figure 2-41. Locations of headcuts in Reach 3

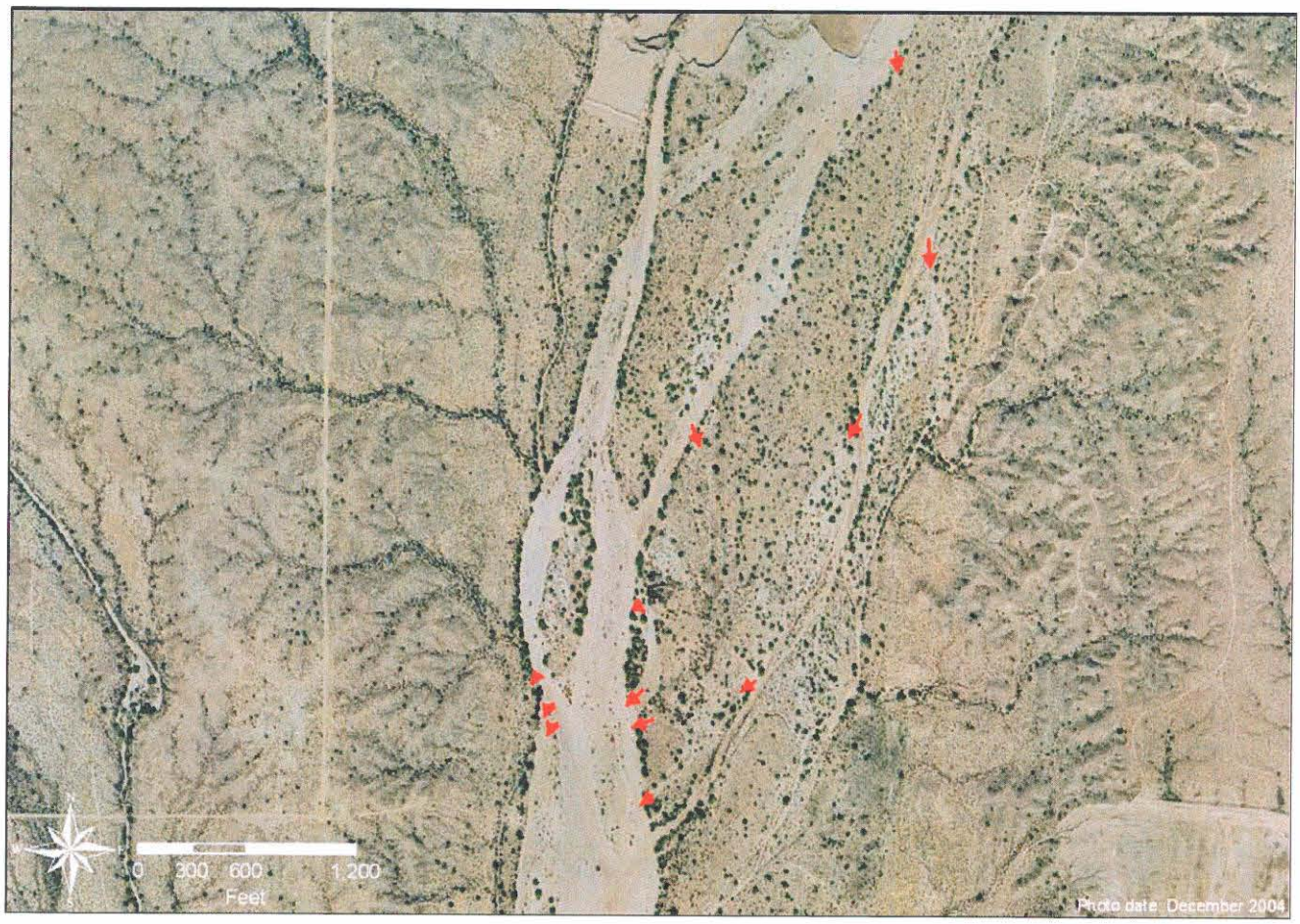

Figure 2-42. Locations of potential avulsion in Reach 3

Headcuts in a tributary deposit. View west.

A swale in the right bank indicates a potential avulsion location. View downstream.

Figure 2-43. Photos of headcuts and a potential avulsion location in Reach 3

Rather than agricultural development as in Reach 2, sand and gravel mining has been the major contributor to disturbance of the floodplain in Reach 3. Two large mines are located in the right overbank floodplain immediately upstream and downstream of the Tonopah-Salome Highway. The pits impact both the low and high floodplain terraces in addition to tributary terraces on the margin of the Holocene floodplain. The other location of floodplain disturbance is a small agricultural area in the far-right floodplain downstream of I-10. Historical aerial photos indicate this area has been developed since at least 1964. Figure 2-44 shows these disturbed floodplain areas.

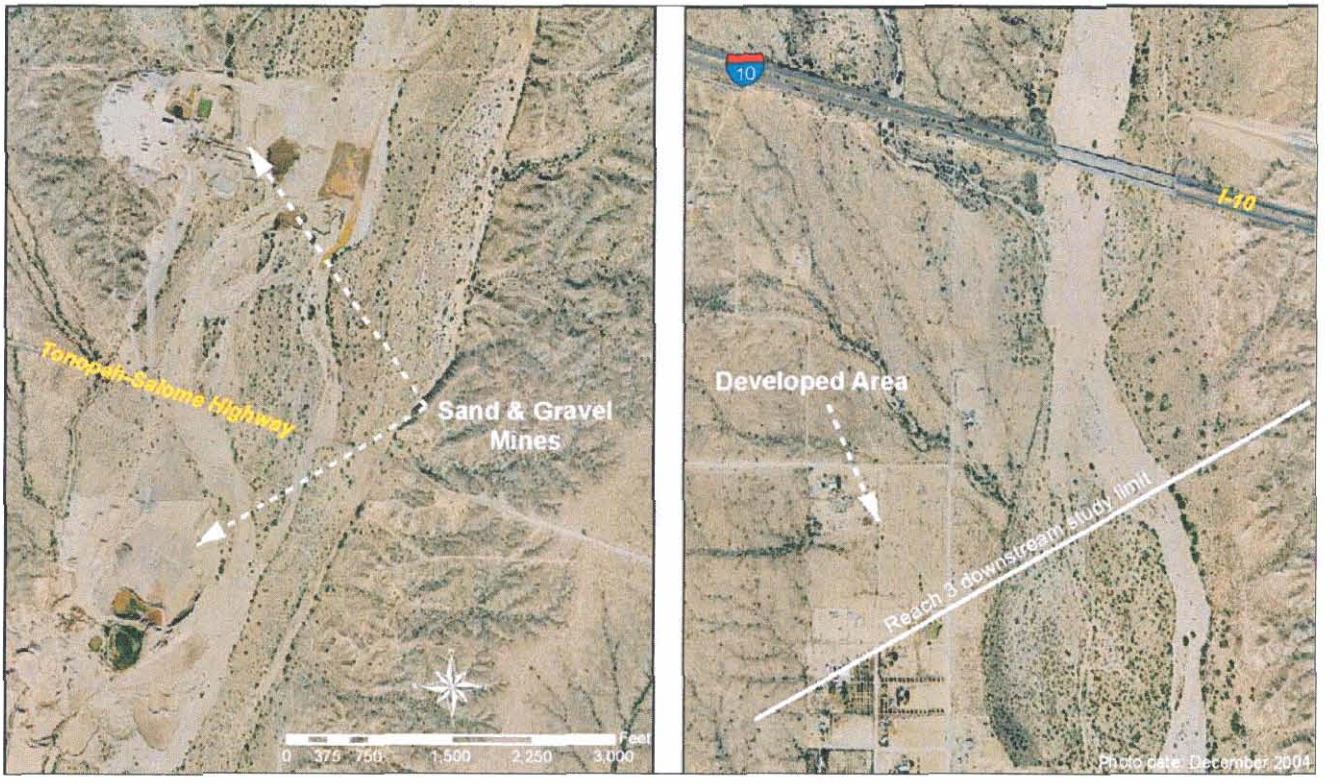

Figure 2-44. Reach 3 disturbed floodplain areas

2.4.3.4 Vegetation

Aside from the disturbed areas, floodplain vegetation is similar to that found on other floodplain surfaces in the study reach. Vegetation on the low terraces is dominated by low brush species (snakeweed, desert broom, and rabbit brush) with numerous immature palo verde trees. The high terrace vegetation is more variable than on the low terrace, but generally includes rabbit brush, Bermuda grasses, larger more mature palo verde and mesquite trees, creosote, and a variety of cacti species including saguaro, cholla, and prickly-pear. Excluding the Jackrabbit Wash delta, vegetation on the tributary terraces is composed almost exclusively of creosote with occasional saguaro cacti. The Jackrabbit Wash delta vegetation was dominated by creosote, but also includes palo verde trees. Figure 2-45 shows field photographs of the floodplain vegetation.

Low terrace upstream of the I-10 crossing. View downstream.

Low terrace just south of the Tonopah-Salome Highway crossing. View south.

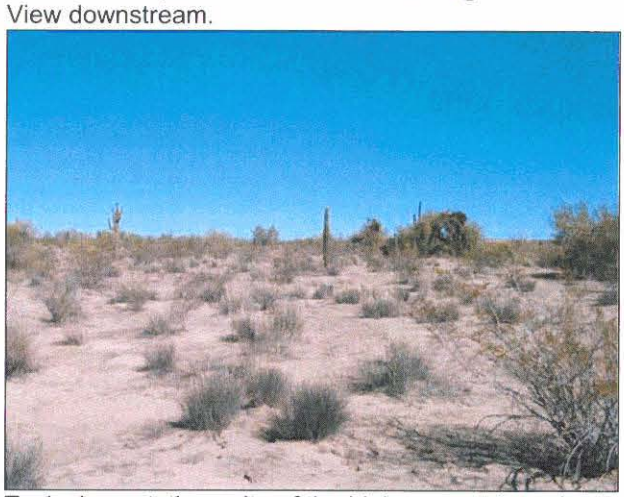

Typical vegetation suite of the high terrace deposits. View north.

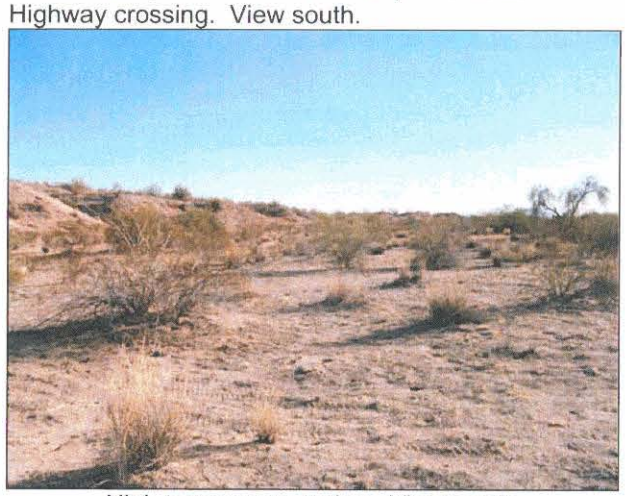

High terrace vegetation. View south.

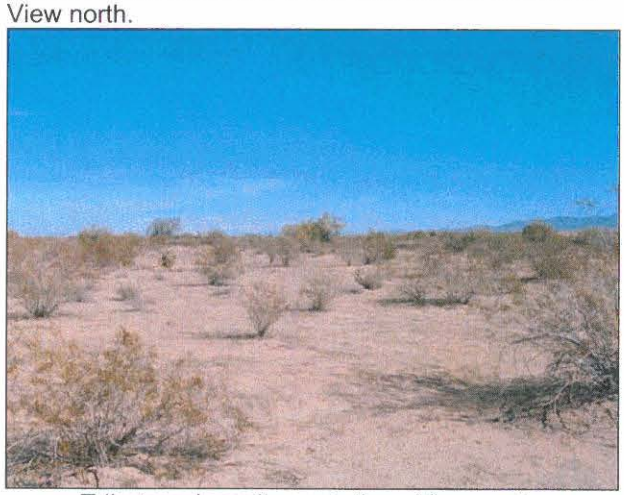

Tributary deposit vegetation. View north.

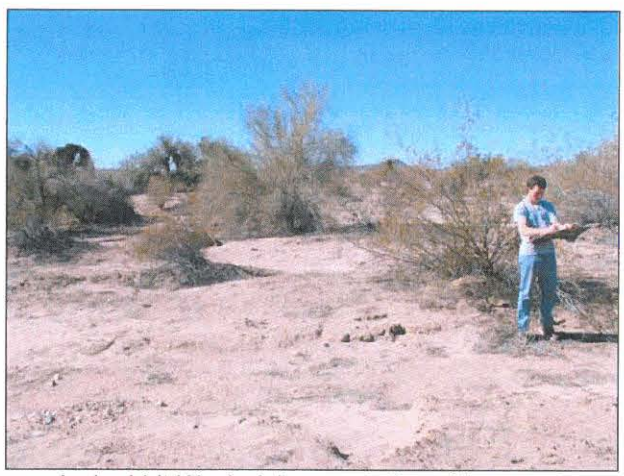

Jackrabbit Wash delta vegetation. View west.

Figure 2-45. Reach 3 floodplain vegetation

2.4.3.5 Structure Impacts

The structures located within the Reach 3 floodplain include the 1-10 bridges, the Buckeye FRS #1 outlet channel, the Tonopah-Salome Highway at-grade crossing, the two large sand and gravel mining operations, and the double-pole overhead utility line crossing north of the upstream mine. Figure 2-46 shows photos of these structures taken during the field investigations.

The I-10 bridges are nearly equal in length (~1,200 feet) and span just over half the Holocene floodplain width. Although no direct evidence of adverse impacts to the floodplain by the bridges or roadways was observed during the field investigations, it should be noted that the bridges only span the active channel and low terrace, resulting in flow discontinuity with the high terrace and flow contraction over the active channel. Future high magnitude floods will be forced through the bridges, potentially resulting in lateral erosion of the high terrace downstream.

The Buckeye FRS #1 outlet channel is oriented parallel to, and approximately 600 feet upstream of, the I-10 alignment. The outlet channel primarily impacts a tributary deposit surface. The construction of the channel created a break in the drainage pattern of tributary channels which were oriented to the southwest. Flow from these tributary channels is now intercepted and concentrated by the outlet channel embankment, resulting in entrenched channels parallel to the embankment to convey the intercepted runoff.

The floodplain conditions both upstream and downstream of the Tonopah-Salome crossing were observed over the entire floodplain width. No evidence of adverse impacts was found.

The sand and gravel mines in Reach 3 directly impacted both the active channel and floodplain as described in Section 2.3.4.4. At the time of the field investigations, a footprint of approximately 113 acres of floodplain had been excavated. Aside from these direct impacts, the pits will also greatly influence the horizontal and vertical distribution of flood and erosion hazards in this reach in the future.

The power line crossing upstream of the sand and gravel mine was inspected for potential impacts on the floodplain. Four sets of poles are located within the floodplain area. Each were observed and found to have no adverse impact on the floodplain.

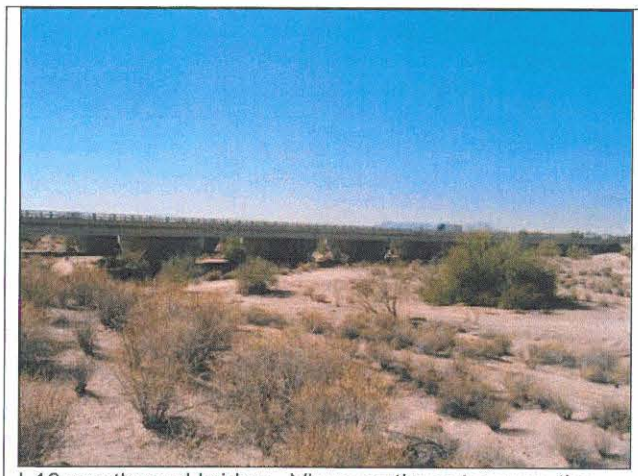

I-10 westbound bridge. View southwest across the floodplain.

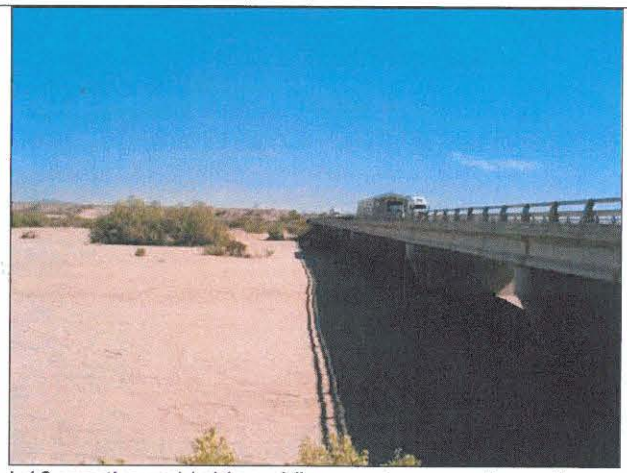

I-10 westbound bridge. View east across the active channel and distant floodplain.

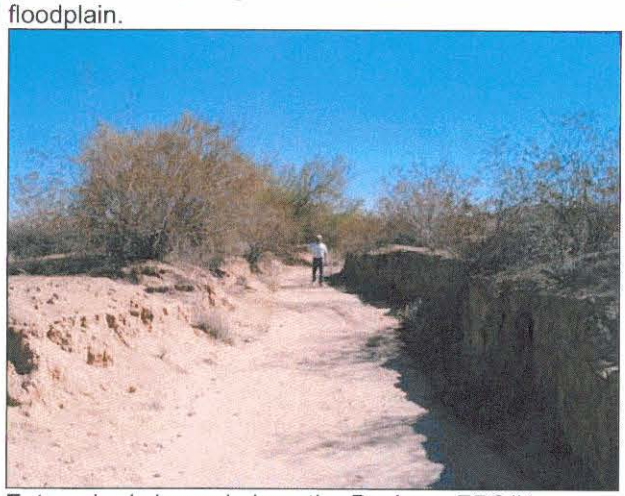

Entrenched channel along the Buckeye FRS#1 outflow channel embankment. View east.

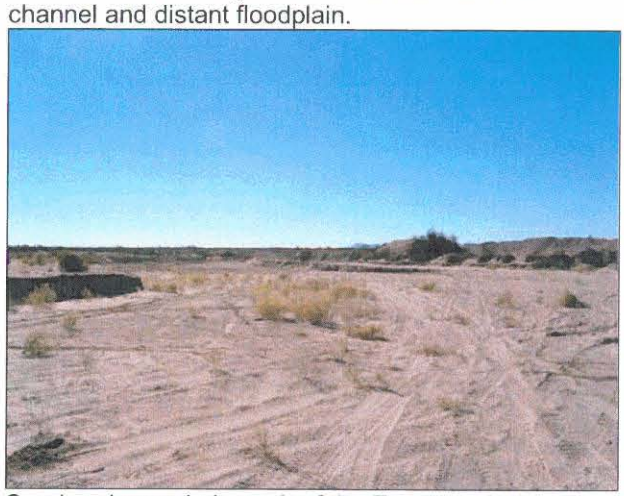

Sand and gravel pit south of the Tonopah-Salome Highway crossing. View south.

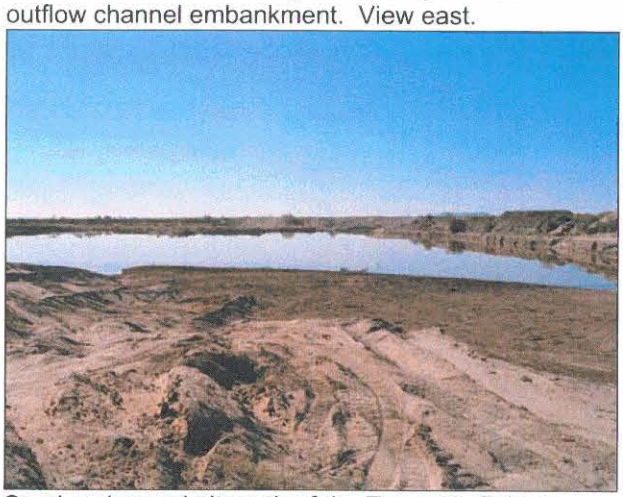

Sand and gravel pit north of the Tonopah-Salome Highway crossing. View south.

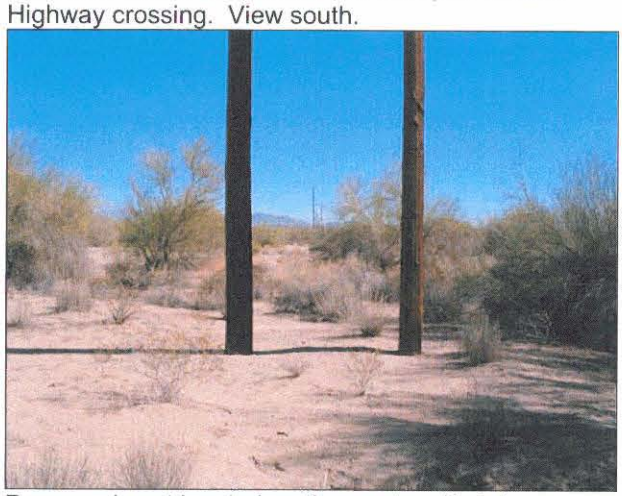

Power pole set located on the western high terrace surface. View east along the alignment.

Figure 2-46. Reach 3 floodplain structure field photos

2.4.4 Hassayampa River Reach 4: Jackrabbit Wash to Wagner/Daggs Wash

2.4.4.1 Floodplain Width

The floodplain width in Reach 4 is narrowest (2,900 feet) just downstream of the Daggs Wash/Wagner Wash confluence and widest (4,500 feet) near the midpoint of Reach 4.

2.4.4.2 Surface-Type Distribution

The presence of two major tributary confluences in Reach 4 contributes to a proportionately large distribution of tributary terrace surfaces. Additionally, most of Reach 4 is located upstream of White Tanks Wash, which collects most of the flow and sediment from the White Tank Mountain piedmont and conveys it into the Buckeye FRS #1 and away from the river. Without White Tanks Wash serving as a collector channel, the distributary piedmont channels feed directly into the Hassayampa River, creating larger tributary terraces on the Holocene floodplain margins, as illustrated in Figure 2-47. The surface-type distribution for Reach 4 is listed in Table 2-4.

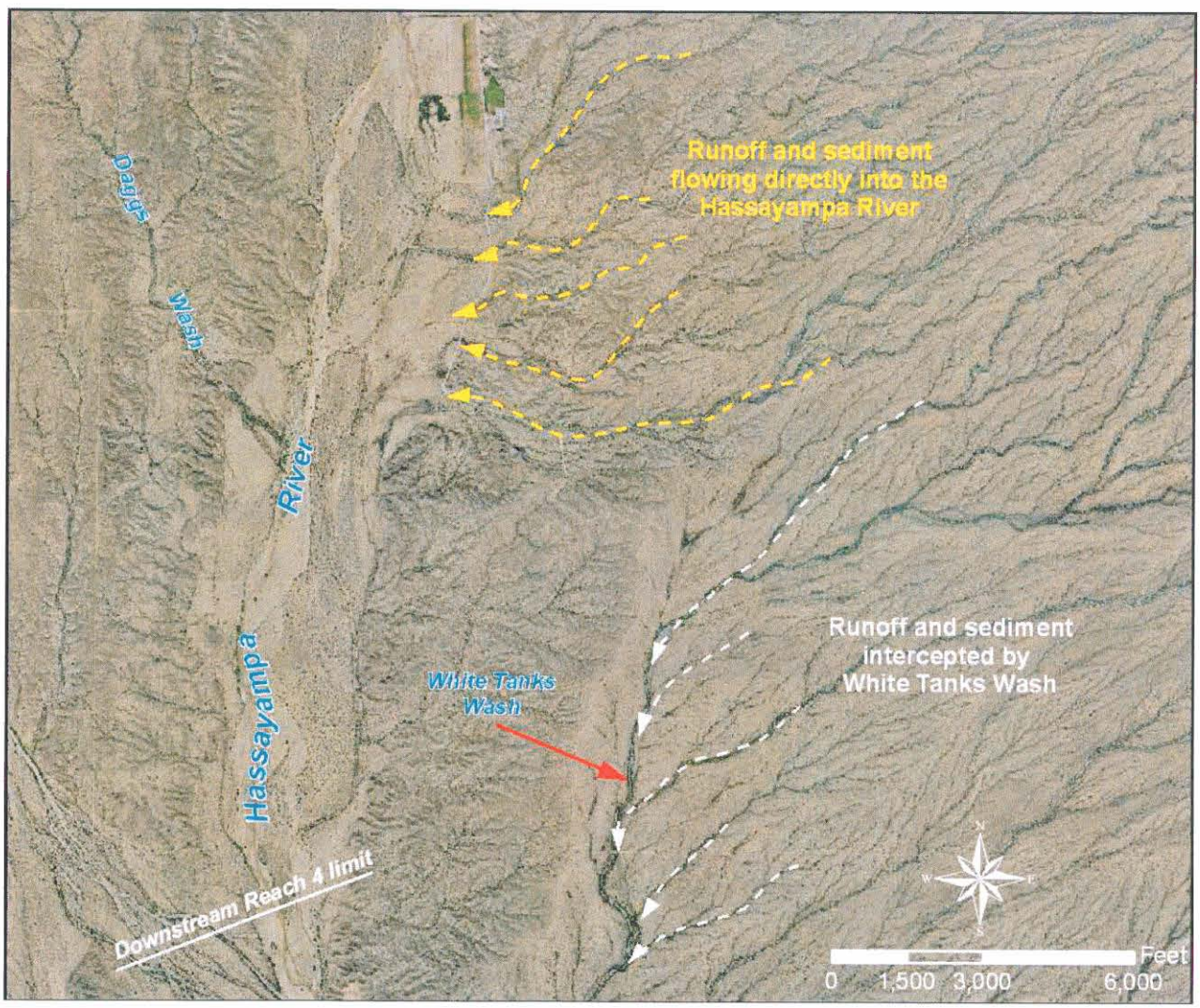

Figure 2-47. Runoff and sediment intercepted by White Tanks Wash

Table 2-4. Reach 4 Surface-Type Distribution					
Reach	Active Channel	Low Terrace & Bar	High Terrace	Tributary Terrace	Disturbed Areas
1	2%	7%	66%	22%	3%
2	5%	41%	14%	39%	1%
3	10%	21%	14%	48%	7%
4	7%	37%	15%	41%	0%
5	7%	41%	24%	26%	2%

The higher percentage of low terrace and bar deposits as compared with the high terrace deposits suggests the floodplain in Reach 4 has been dynamic and that the active channel has likely experienced significant lateral migration within recent geologic history.

2.4.4.3 Geomorphic Features

Floodplain headcuts are concentrated in the lower half of Reach 4 along the contacts of the tributary terraces and the Hassayampa River terraces, consistent with observations described for the downstream reaches. The presence of headcuts along the tributary terrace margins suggests the possibility that the Hassayampa River floodplain corridor has been degrading over recent geologic time.

Evidence for potential avulsions is found throughout Reach 4, but is concentrated in the upper and lower ends of the reach. Unlike the downstream reaches, a large number of potential avulsion locations were present at the high terrace margins, suggesting the possibility of greater lateral migration of the active channel. Figure 2-48 and Figure 2-49 show the locations of headcuts and potential avulsion locations as identified during the field investigations. Field photos of these features are shown in Figure 2-50.

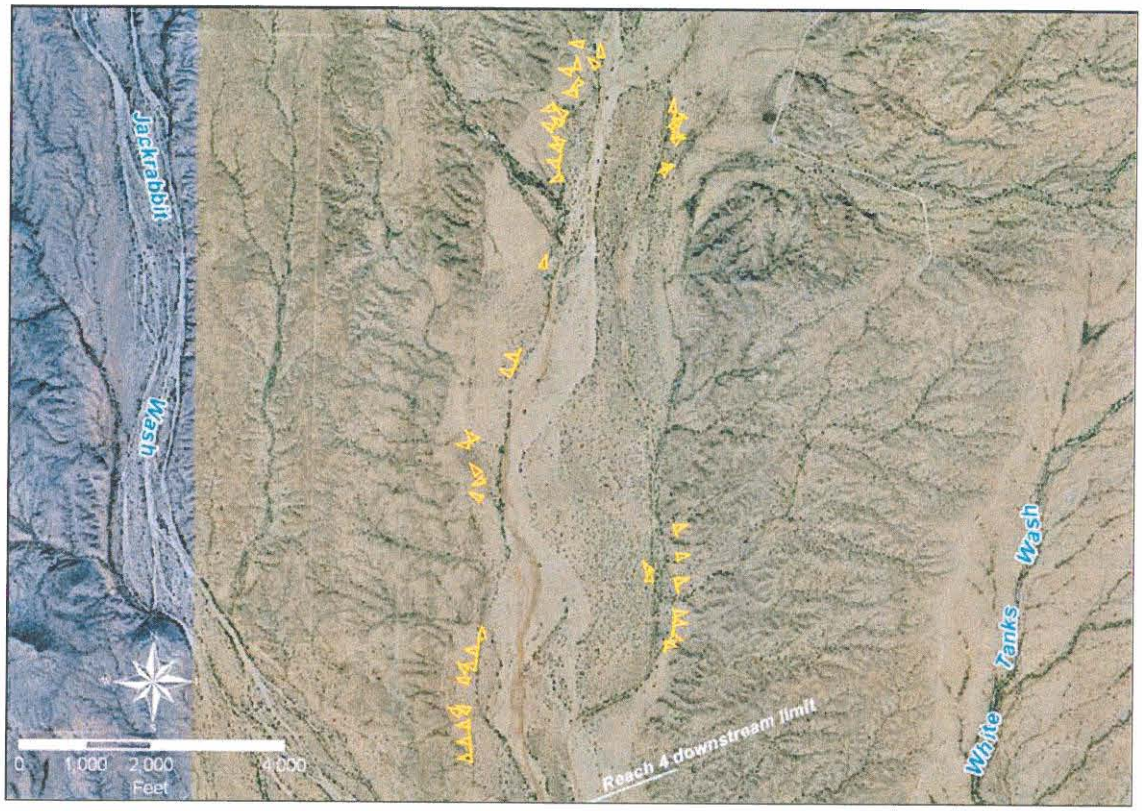

Figure 2-48. Reach 4 headcut locations

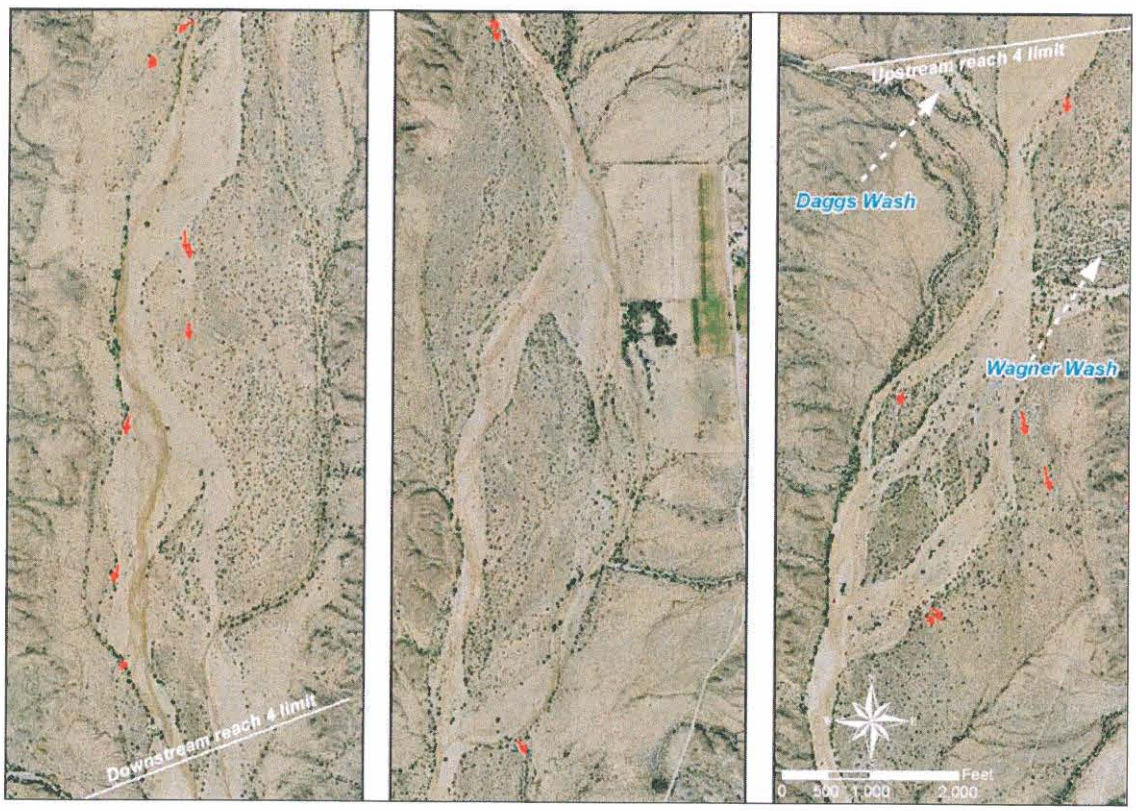

Figure 2-49. Reach 4 potential avulsion locations

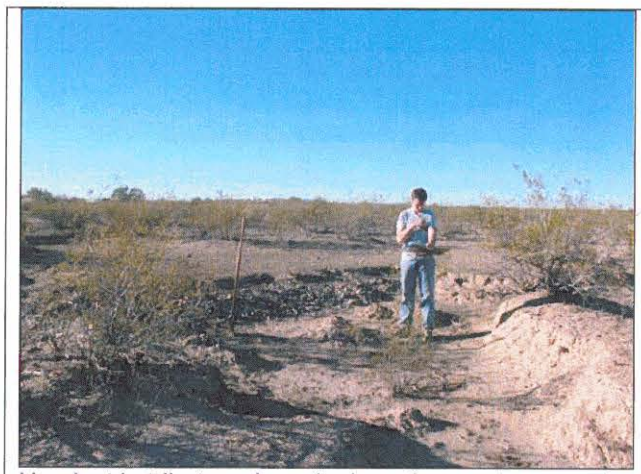

Headcut in tributary deposit along the western margin of the Holocene floodplain. View west.

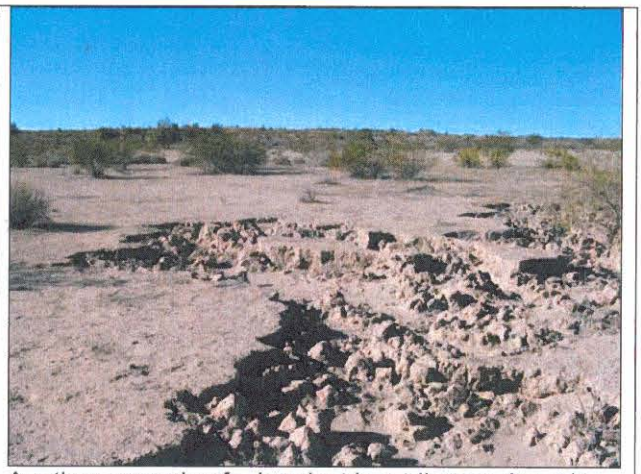

Another example of a headcut in a tributary deposit. View west.

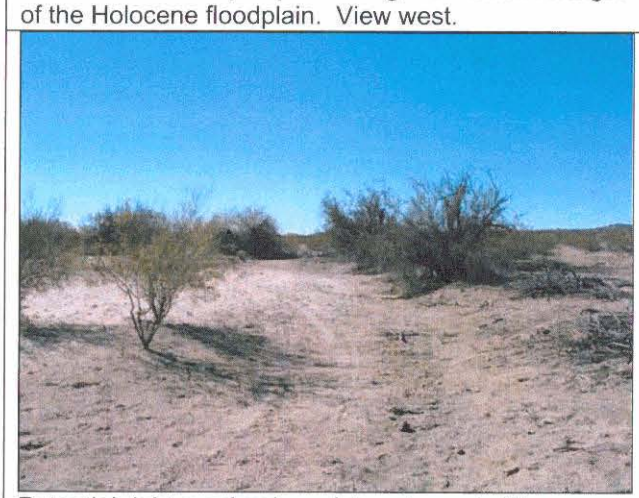

Potential right overbank avulsion channel. View downstream.

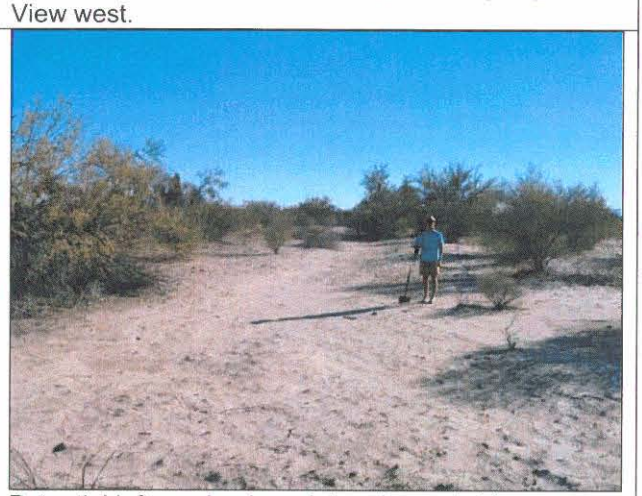

Potential left overbank avulsion channel. View downstream.

Figure 2-50. Reach 4 geomorphic feature field photos

2.4.4.4 Vegetation

Aside from a 65-acre agricultural area in the eastern floodplain near the middle of Reach 4, the floodplain is relatively undisturbed. Floodplain vegetation suites and densities are consistent with those found in undisturbed downstream reaches. Low terrace and bar vegetation is dominated by sparse low brush species (snakeweed, desert broom, and rabbit brush). The low terrace and bar surfaces frequently contain small, immature palo verde trees. Flotsam and flood debris are found on these surfaces, suggesting relatively frequent inundation. High terrace vegetation consists of large, mature palo verde and mesquite trees, creosote, Bermuda grasses, and a variety of cacti. Tributary terrace vegetation is almost exclusively comprised of creosote. Figure 2-51 shows typical examples of floodplain vegetation in Reach 4.

Typical Reach 4 bar deposit. Note lack of vegetation and abundance of flotsam debris. View east.

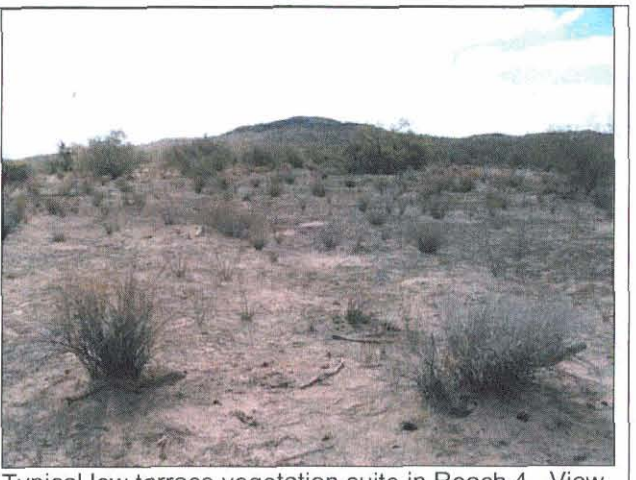

Typical low terrace vegetation suite in Reach 4. View northeast.

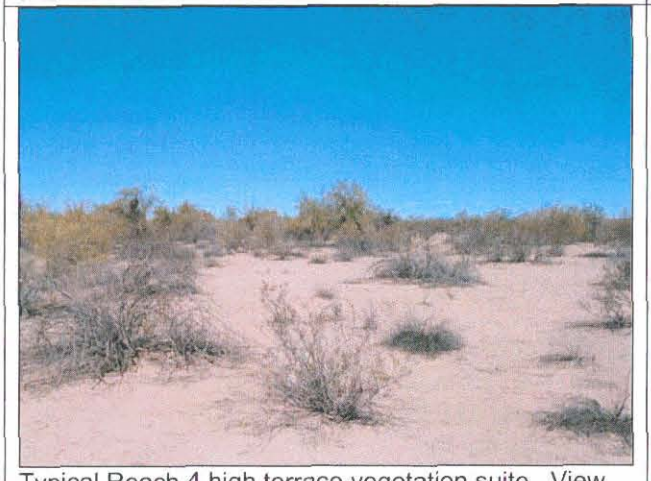

Typical Reach 4 high terrace vegetation suite. View north.

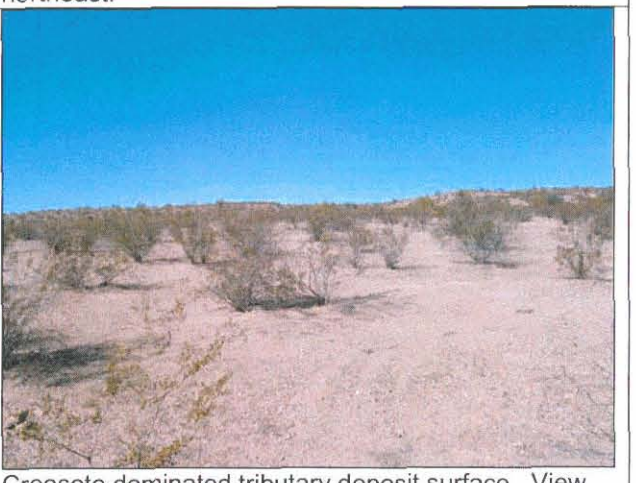

Creosote dominated tributary deposit surface. View west.

Figure 2-51. Reach 4 floodplain vegetation

2.4.4.5 Structure Impacts

No significant structures exist within the floodplain of Reach 4.

2.4.5 Hassayampa River Reach 5: Wagner/Daggs Wash to CAP Siphon

2.4.5.1 Floodplain Width

Reach 5 had the widest floodplain of the study area, with a width of about 6,000 feet or 1.1 miles at the upstream end of the Reach. The narrowest floodplain in Reach 5 was just over 2,400 feet, and was located approximately one mile above the downstream reach limit. Although other reaches had variable floodplain widths, only Reach 5 decreased by more than half.

2.4.5.2 Surface-Type Distribution

The wide floodplain area in Reach 5 was composed primarily of high terrace and tributary terrace surfaces. As the floodplain narrowed in the downstream direction, the

high terraces and tributary terraces became less dominant and were generally constrained to the margins of the Holocene floodplain, which is consistent with reaches downstream. The breakdown of surface-type in Reach 5 is listed in Table 2-5.

Table 2-5. Reach 5 Surface-Type Distribution

Reach	Active Channel	Low Terrace & Bar	High Terrace	Tributary Terrace	Disturbed Areas
1	2%	7%	66%	22%	3%
2	5%	41%	14%	39%	1%
3	10%	21%	14%	48%	7%
4	7%	37%	15%	41%	0%
5	7%	41%	24%	26%	2%

The high percentage of low terrace and bar deposits suggests that active river processes have occurred within a large portion of the floodplain within recent geologic time. This also suggests the possibility that the active channel has not been laterally stable recently.

2.4.5.3 Geomorphic Features

Floodplain headcuts occur less frequently in Reach 5 than in other reaches, most of the headcuts in Reach 5 are not associated with tributary terraces, as was seen consistently downstream (Figure 2-52). In Reach 5, headcuts were most frequently observed in areas with avulsive breakout channels that had become entrenched in the floodplain surfaces. These headcuts were generally localized and had limited extent (Figure 2-53). More long-term headcut processes were also observed on a more broad scale across the wide, high terrace surface in the upper reach. Aerial photos and field evidence suggest that these headcuts represent formation of an integrated drainage network on the surface itself. As the headcut process migrates upstream, the channels may eventually reconnect with the active channel, resulting in the potential of a major avulsion across this surface (Figure 2-54).

Many potential avulsion locations were observed and documented in Reach 5. An approximately equal number of avulsions occur on the low and high terraces (Figure 2-55).

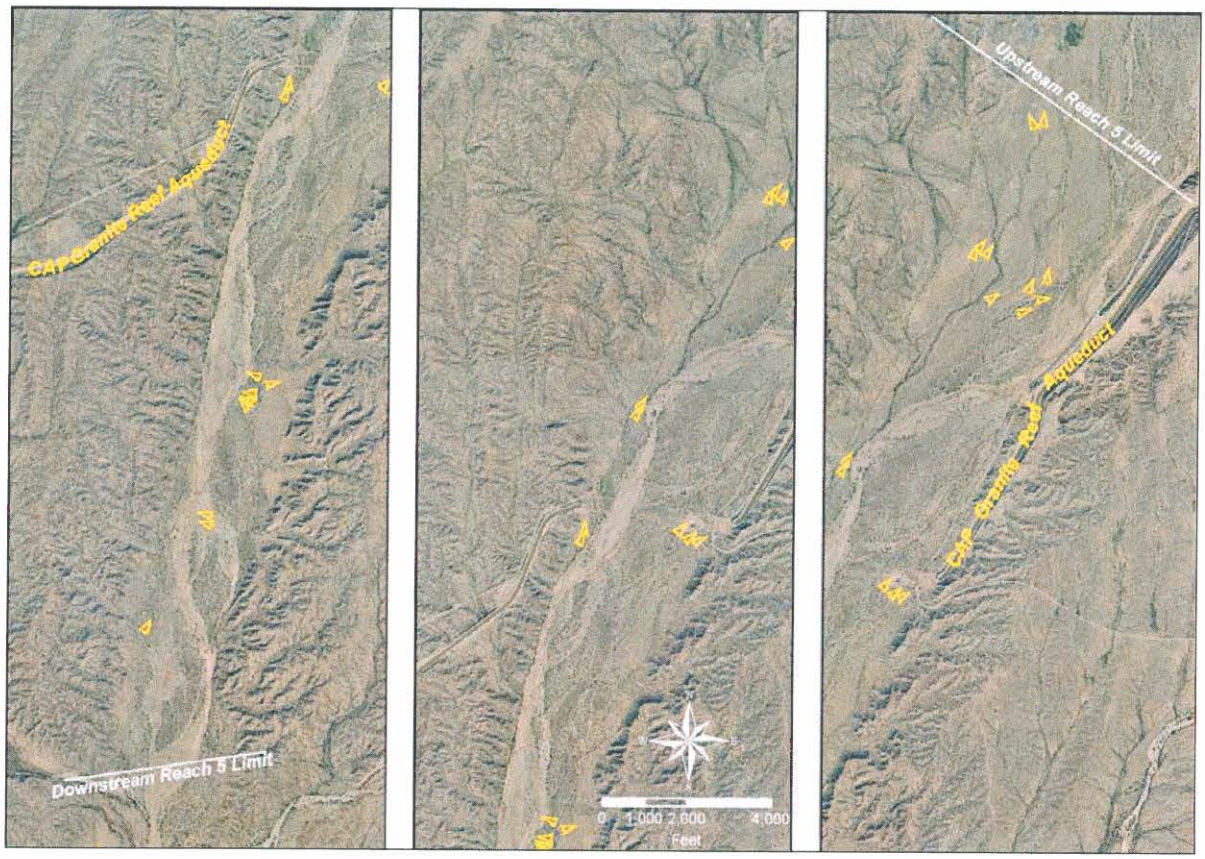

Figure 2-52. Reach 5 headcut locations

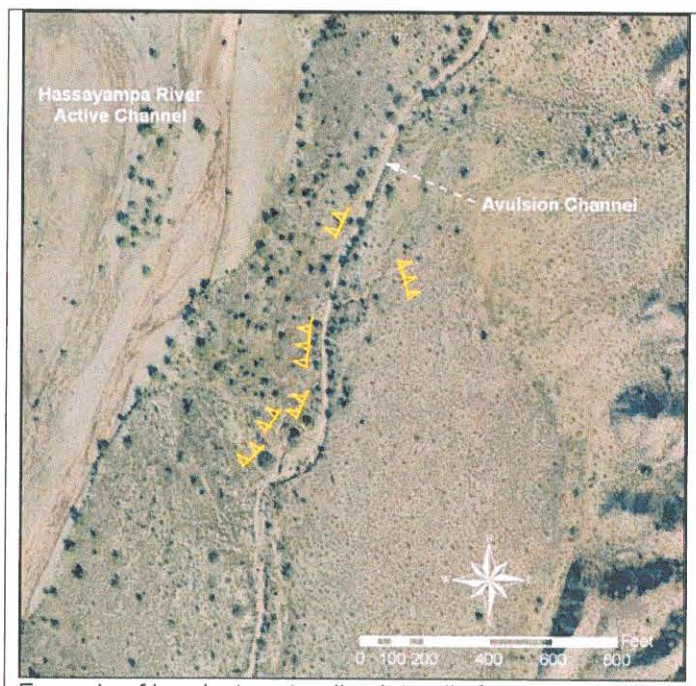

Example of headcuts extending laterally from an avulsion channel. Yellow arrows show headcut location and migration direction.

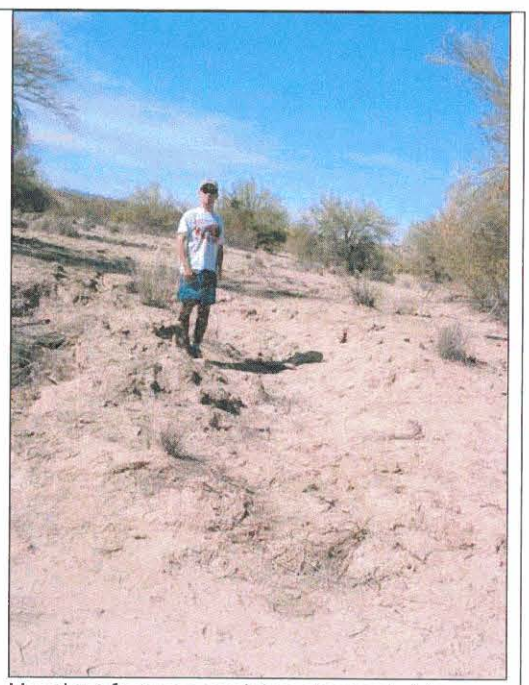

Headcut from an avulsion channel. View northwest.

Figure 2-53. Example of headcuts originating from avulsion channels

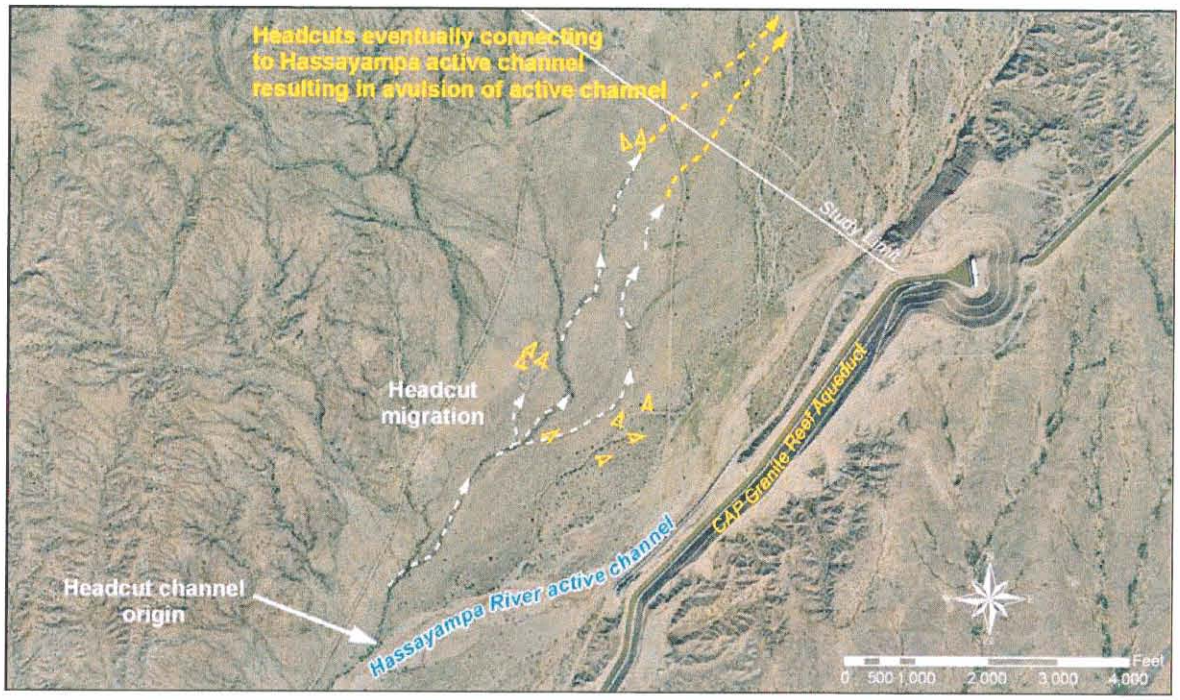

Figure 2-54. Example of long-term headcut migration

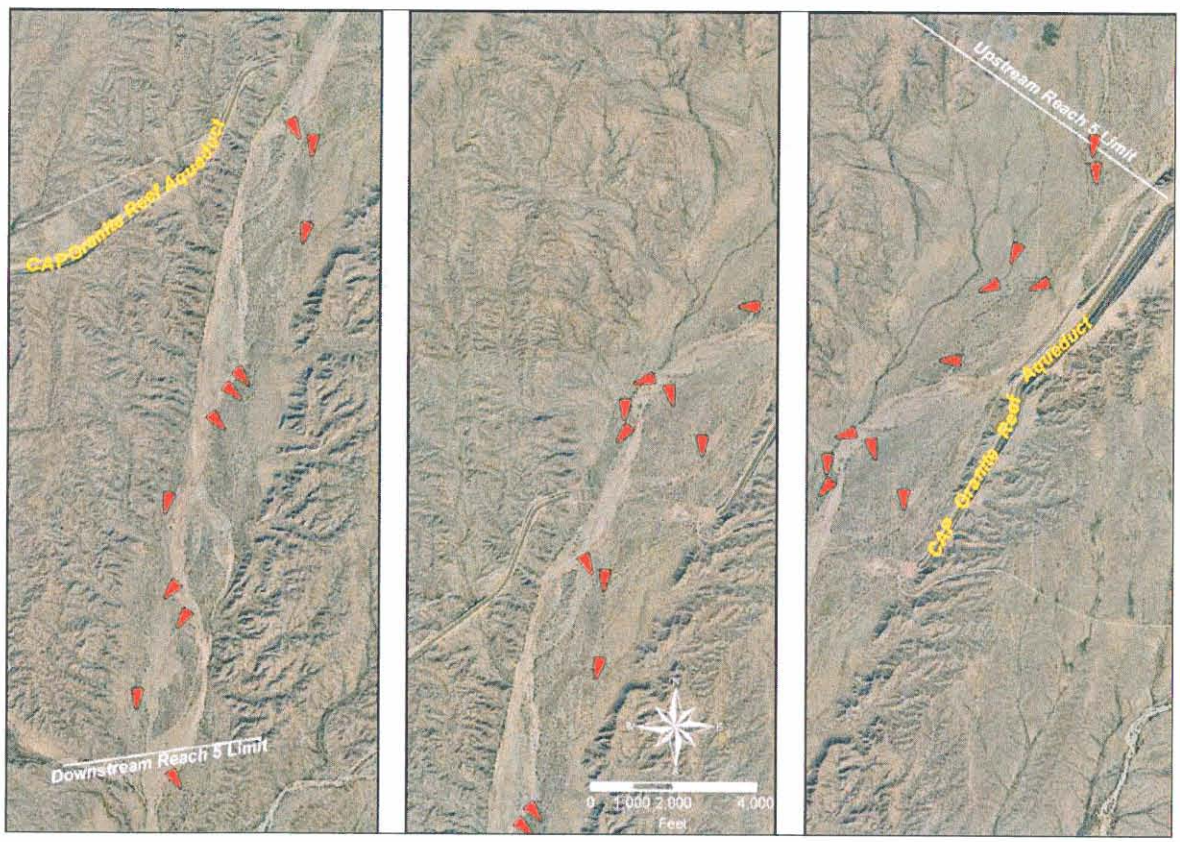

Figure 2-55. Reach 5 potential avulsion locations

2.4.5.4 Vegetation

Like Reach 4, very little historical disturbance of the floodplain has occurred in Reach 5, except at the CAP siphon crossing and at an inactive sand and gravel mine in the far northeast corner of the study area. The vegetation suite comprising the low terrace and bar surfaces is consistent with vegetation found in the downstream reaches. Bar vegetation consists of low brush species, generally desert broom and snakeweed, and consistently lacks trees of any size. The low terrace surface vegetation is similar to that found on the bar surface but usually contains small, immature palo verde trees. The high terrace vegetation in the downstream half of Reach 5 is consistent with high terrace vegetation downstream and generally contains a suite of large, mature palo verde and mesquite trees, creosote, Bermuda grasses, and a variety of cacti. The large area of high terrace surfaces in the upstream half of the study area had dramatically different vegetative cover compared to other high terrace surfaces, in that very few trees were present and vegetation was sparser. The dominant species were small (< 3 ft) creosote bushes and Bermuda grass (Figure 2-56).

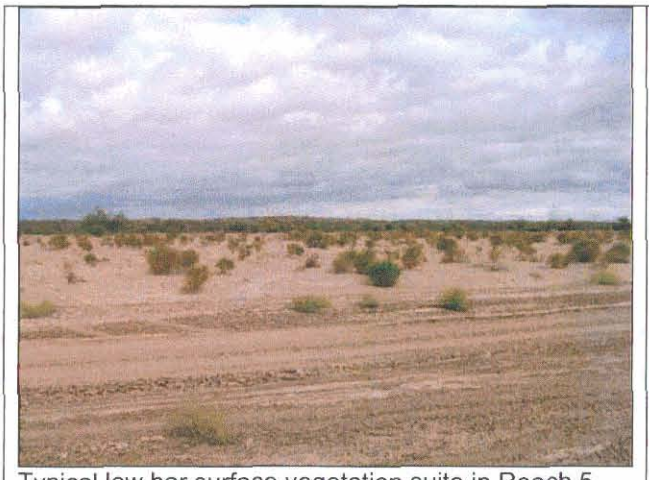

Typical low bar surface vegetation suite in Reach 5. View northwest.

Low terrace vegetation. View northeast.

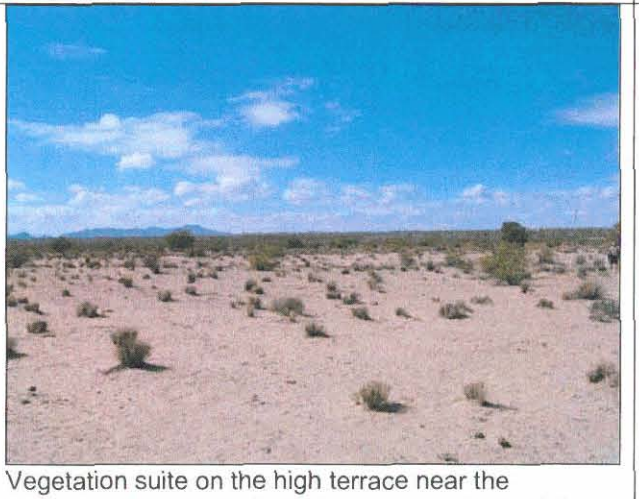

Vegetation suite on the high terrace near the upstream study limit. Note the sparse nature of the vegetation and the lack of trees. View west.

Typical vegetation populating the tributary terraces in Reach 5. View northeast.

Figure 2-56. Vegetative cover on Reach 5 floodplain surfaces.

2.4.5.5 Structure Impacts

Two structures were identified in the Reach 5 floodplain, the CAP siphon and an inactive sand and gravel mine. Significant disturbance of the floodplain probably occurred during the construction of the CAP siphon crossing. However, the field observations indicate that the disturbed areas recovered and native vegetation has reestablished itself. Aside from a small portion of the siphon pipe that had been excavated for inspection and repair, no field evidence was found indicating the buried structure had an adverse impact on the floodplain. At the time of the field investigations, the excavation footprint area was approximately 0.7 acres. The CAP siphon excavation is now closed and reburied. Figure 2-57 shows this area in both map view and via field photo.

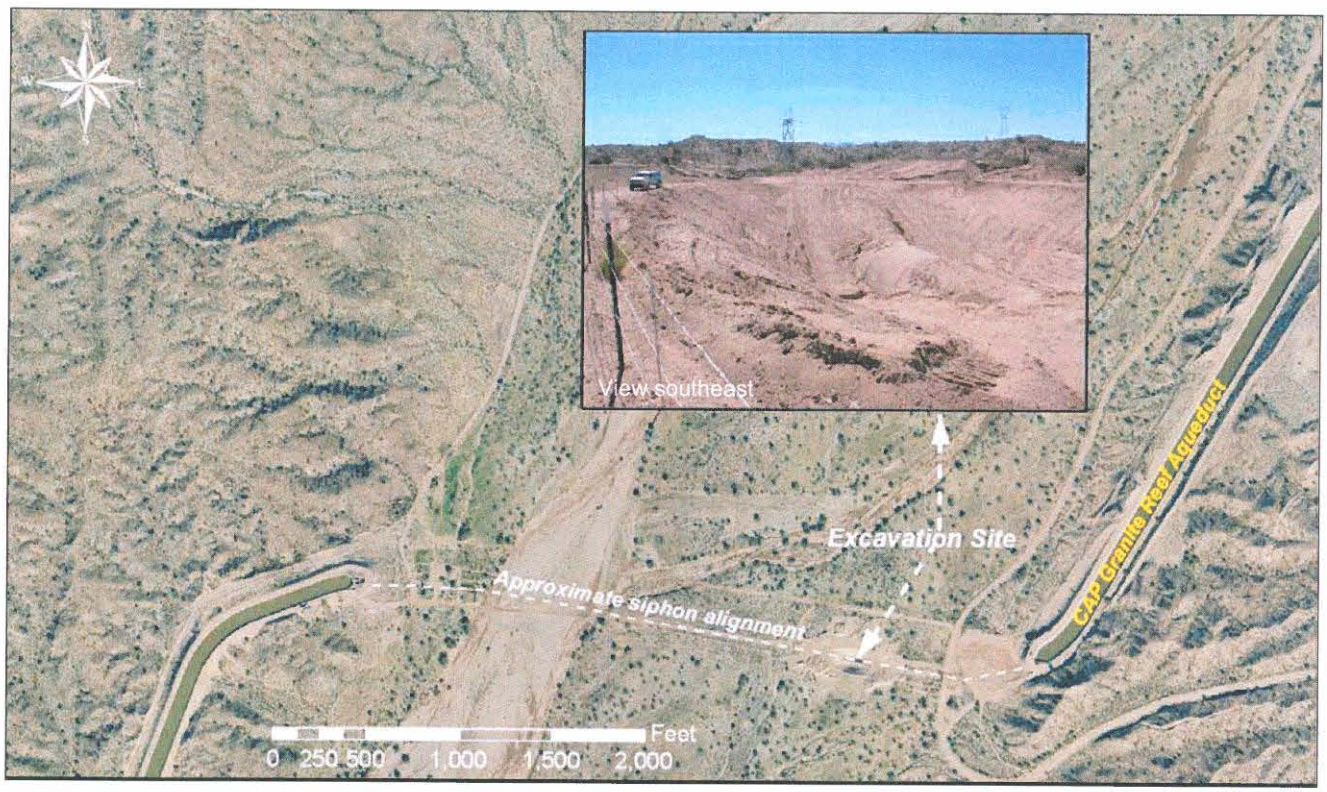

Figure 2-57. CAP siphon excavated area

The large, inactive sand and gravel mine is located in the far western Holocene floodplain. The pit comprised a footprint area of approximately 131 acres, which was contained entirely within a tributary deposit surface. Given the present position of the active channel, it is unlikely this pit will pose any immediate adverse impact, even during large magnitude floods. However, if a future avulsion of the active channel occurs across the high terrace surface as described previously and illustrated in Figure 2-54, the pit will likely pose a potential risk to the stability of the floodplain. Currently, an application to re-activate and expand the mine is pending at the District. The proposed expansion into the floodway and erosion hazard zone would likely have a significant impact on the floodplain stability. Figure 2-58 shows the existing pit location.

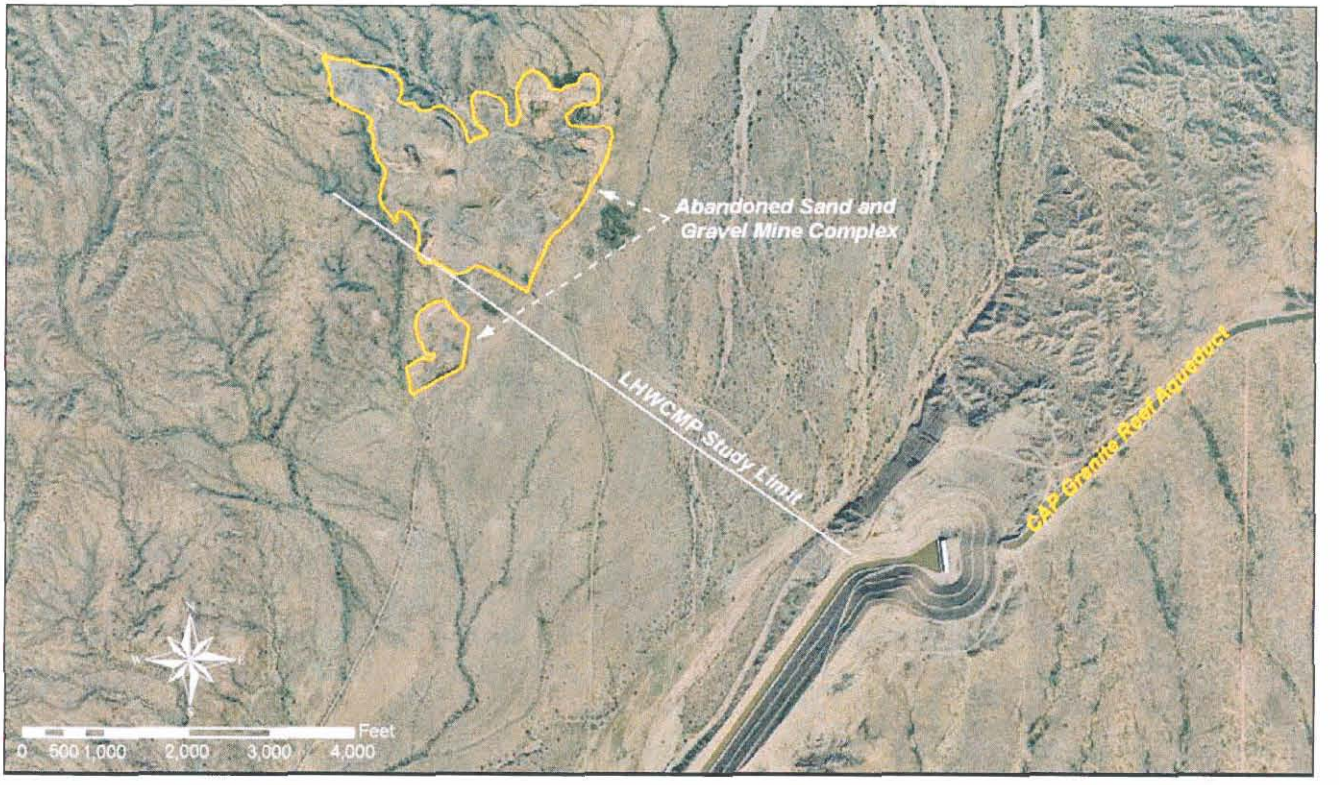

Figure 2-58. Reach 5 sand and gravel mine complex

2.5 Historical Flood Evidence

Evidence left by previous floods not only aids in understanding the magnitude of the specific event, but also provides insight into the channel processes that occur during large floods. During the field investigations, evidence of historical floods was identified and documented. Large magnitude floods are by nature self-censoring. That is, large floods often remove evidence and "overwrite" the records of previous floods. In this sense, flood evidence observed in the field may relate only to the last, largest event and generally is not a continuous record of flood history. By combining field evidence with historical aerial photography, the potential flood impacts can be better understood.

2.5.1 Avulsions

An avulsion is a sudden relocation of the active channel from one part of the floodplain to another. Avulsions are responsible for some of the most significant lateral channel movement on the large stream systems in central Arizona. It is therefore important to identify locations for potential future avulsions (as discussed previously in this chapter), in addition to attempting to understand the impact that avulsions have had on the system historically. Areas identified as potential future avulsions during the field investigations were discussed above. Locations of major historical avulsions were identified on the historical aerial photography and are discussed in Chapter 3.

2.5.2 Flotsam

Flotsam is commonly found on low terrace and bar deposits throughout the study area. Although not particularly informative in identifying individual flood events, because these

low surfaces are subject to relatively frequent inundation, the presence of flotsam was useful for quickly identifying these surfaces. Flotsam identified on the high terraces and Holocene floodplain margins provided information about the largest historical floods. The character of the flotsam discovered on these surfaces indicated that it was placed during the flood caused by 1890 Walnut Grove Dam failure.[6] These 1890 flood deposits provided a minimum relative estimate of the lateral extent of that flood, which exceeds the current regulatory flood peak estimate, within the Holocene floodplain at the particular location where the flotsam was discovered. Often this flotsam was in the form of cut timber boards, sometimes smooth cut on both sides of the board, sometimes only on one side, and sometimes with embedded square nails. The 1890 flotsam was often found on recently-deposited, massive, medium to fine-grained alluvial layers well above the computed 100-year water surface elevations. A map showing the location of flotsam deposits, in addition to field photos are provided in Figure 2-59 and Figure 2-60.

2.5.3 Sediment Deposits

Although sediment deposition is common during floods, long-term preservation of these deposits is less common. Subsequent floods often rework these deposits and erase the depositional record. Long-term preservation can occur, however, under specific conditions such as low energy, slackwater areas, or on terrace surfaces that are inundated by only the largest magnitude floods. Both types of deposits were found in the LHWCMP study area during field investigations.

2.5.3.1 High Terrace Deposits

A unique flood deposit was found associated with the high terrace surfaces at multiple locations within the study area. The deposits were comprised of medium coarse sand, similar to the material found in the existing active channel. The deposits are unique due to their position relative to the active channel. In general, the high terraces are interpreted as the lateral limit of the floodplain, inundated only by extreme floods. The environment on the high terraces surfaces would be characterized by low energy and shallow depth, conducive to fine sediment transport and deposition. Coarser sediments are transported in the high energy environment of the main channel. An explanation for the presence of these medium sand deposits on the high terrace is that they were emplaced during the 1890 Walnut Grove Dam flood. The 1890 flood was by far the largest in the record and possibly the largest in geologic history. Only a flood with the magnitude of the Walnut Grove Dam event would have had the discharge and energy sufficient to inundate the high terrace surfaces to a depth conducive to the transport and deposition of the medium coarse sands. The vegetation characteristics of the high terrace surfaces were also unique compared to that found on other high terraces in the study reach in that they were dominated by Bermuda grasses. The soil profiles on several high terraces were examined in more detail, as described in Chapter 3. Figure 2-61 shows the locations of several high terrace deposits in the upper study reach. Figure 2-62 shows field photos of one of these surfaces including a soil profile clearly illustrating the thickness of the medium coarse sand deposit.

[6] A discussion of the Walnut Grove Dam failure flood is provided in the LHWCMP Hydrology Report Appendix.

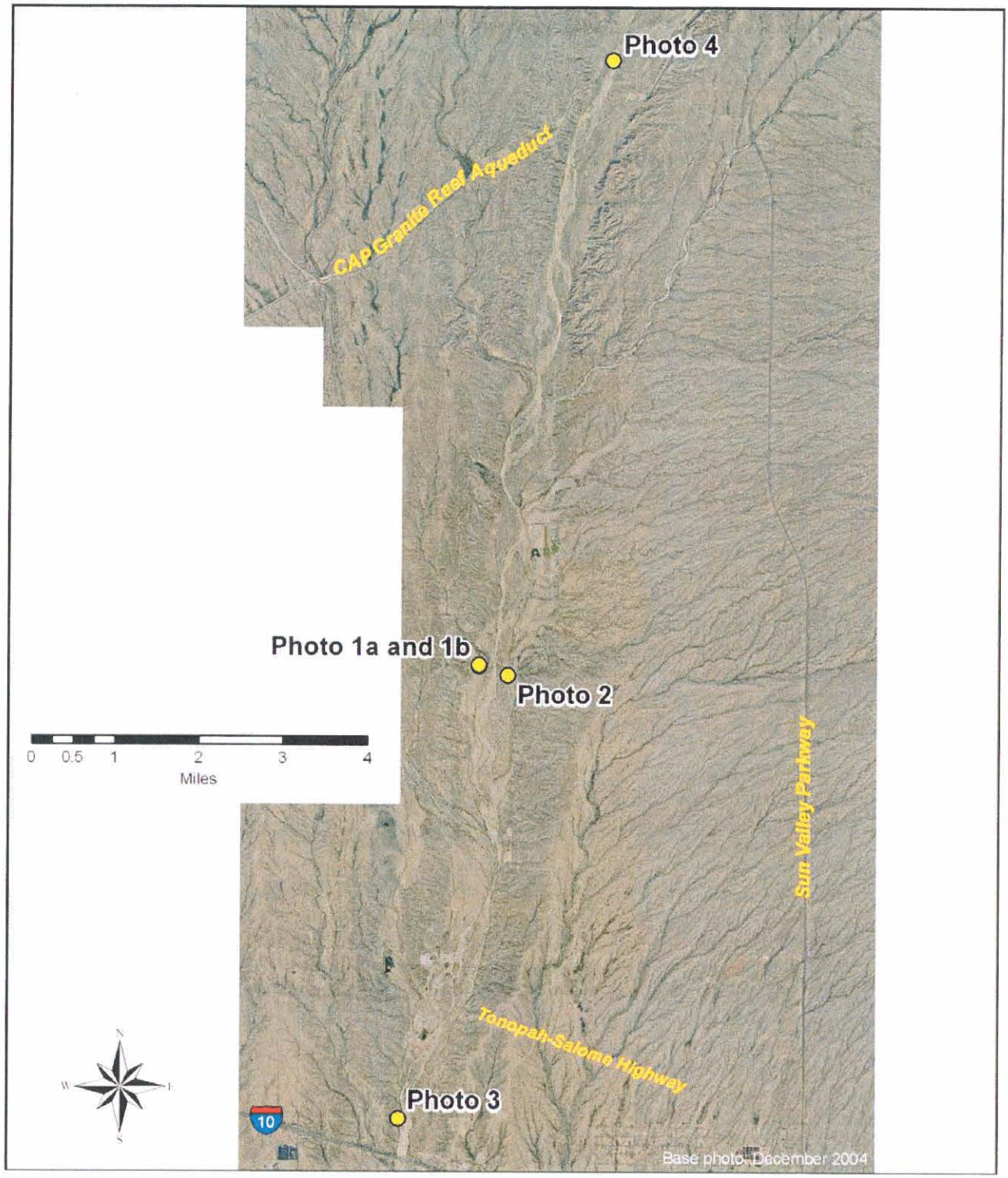

Figure 2-59. High terrace flotsam locations

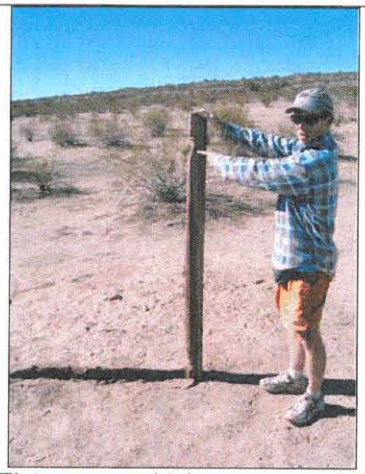

Photo 1a. Flotsam on a high terrace surface; possibly deposited by the 1890 Walnut Grove Dam flood. Ted's pointing to notches cut in the board.

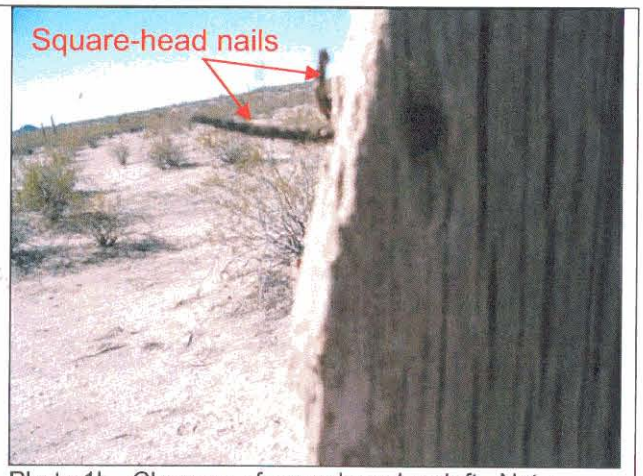

Photo 1b. Close-up of same board as left. Note rusty, square nails protruding.

Photo 2. Another cut board found on a high terrace surface, possibly from the 1890 Walnut Grove Dam flood.

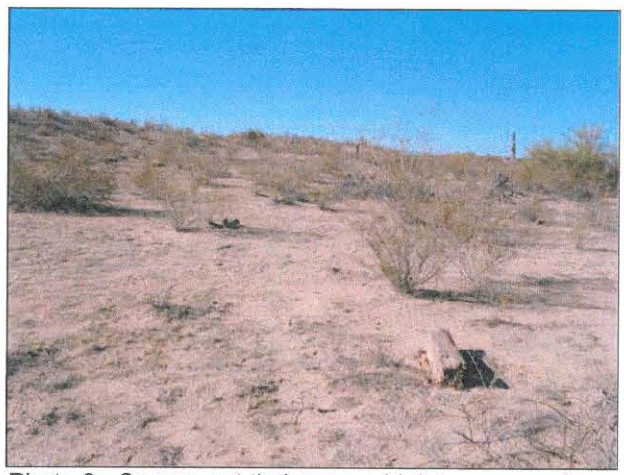

Photo 3. Square-cut timber on a high terrace surface.

Photo 4. Flotsam pile on high terrace surface.

Figure 2-60. Field photos of flotsam on high terrace surfaces

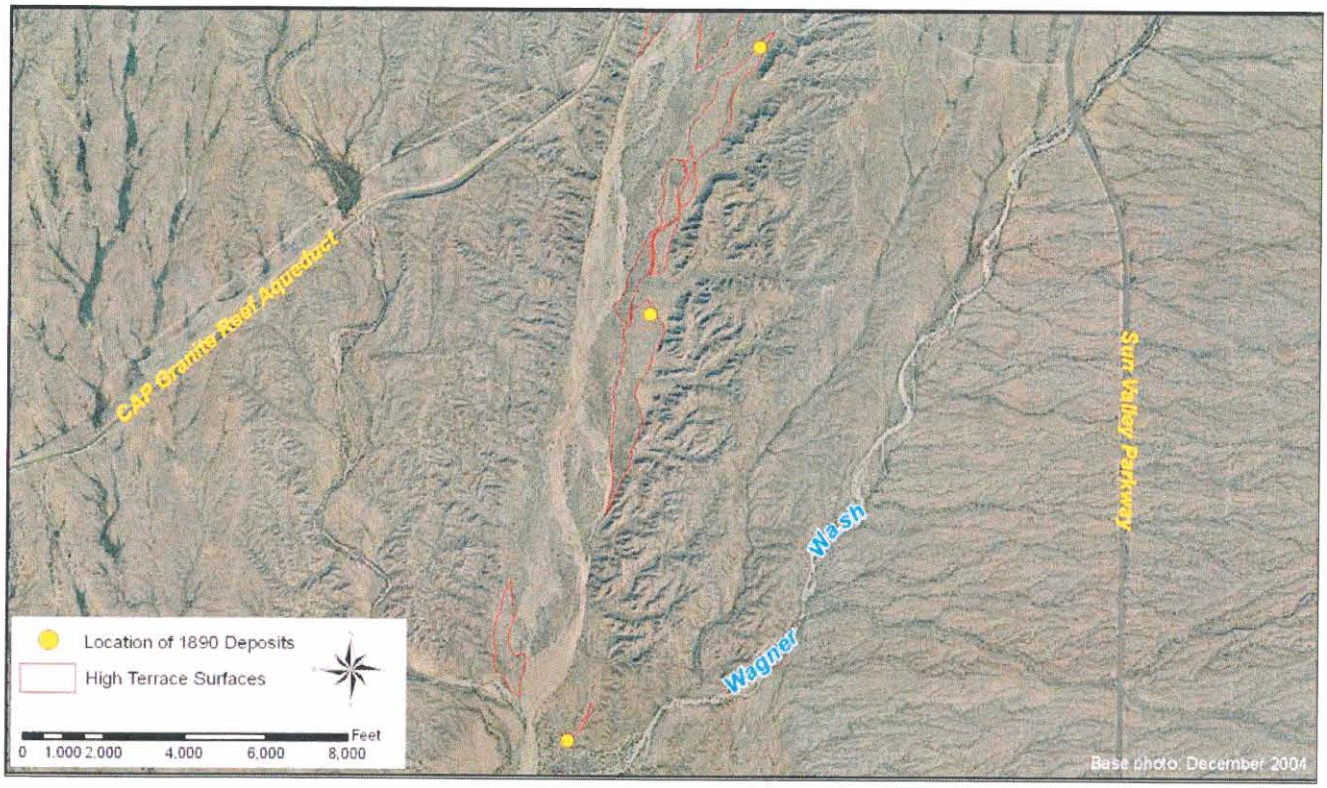

Figure 2-61. Locations of 1890 flood deposits

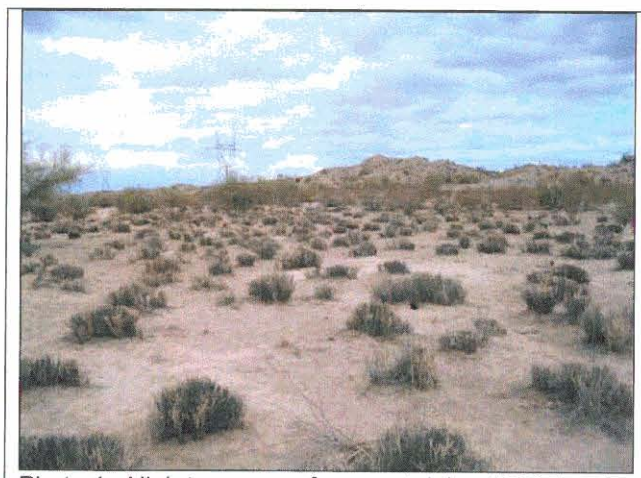

Photo 1. High terrace surface containing 1890 flood deposits. Note dominance of Bermuda grasses. View north.

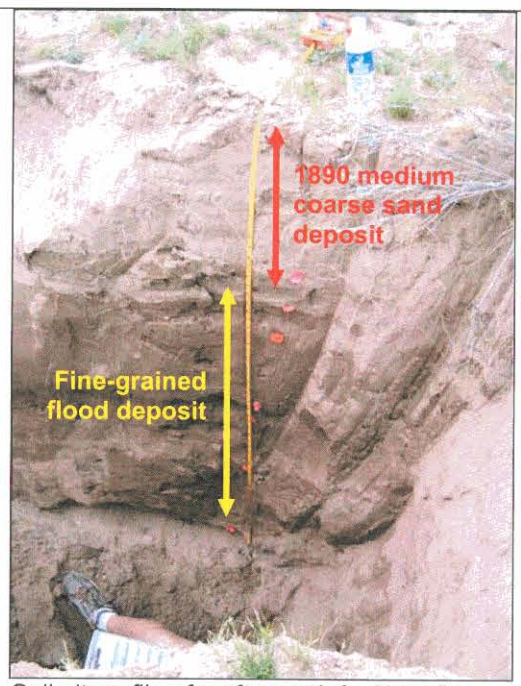

Soil pit profile of surface at left. Note fine grained flood deposits underlying the 1890 medium sand deposit.

Figure 2-62. Field photos of 1890 high terrace deposit

2.5.3.2 Slackwater Deposits

Slackwater deposits were identified frequently along the Holocene floodplain margins. The Pleistocene terrace/Hassayampa River contact was frequently characterized by small embayments at the mouths of tributaries. During large flood events these embayments create a low-energy slackwater environment in which suspended sediments drop out and accumulate (hence, the name slackwater deposit). Although these deposits were not analyzed in detail, their regional context with respect to the entire width of the Holocene floodplain suggests they are associated with the 1890 Walnut Grove Dam flood. Figure 2-63 shows a map view of a few of the locations in which slackwater deposits were found and a field photo of a typical deposit.

Figure 2-63. Typical locations of slackwater deposits

2.6 Structures Investigation

Previous discussions of structures were focused on impacts of the structures on the active channel and floodplain areas. This section addresses conditions at the structures themselves, as documented during the field investigations, and any visible impacts on the structures by channel and floodplain processes observed in the field. The location, dimensions, and general conditions of the structures were documented in structure impacts forms. This analysis does not include hydraulic computation of scour potential. Only field evidence of on-going scour is discussed. Examples of field forms are provided in Appendix 5.1.

The discussion of structure impacts is organized by structure type and by reach. The primary types of structures that were documented include the following:

- Bank Protection

- Bridges
- Levees
- At-Grade Roadway Crossings
- Irrigation and Siphon Crossings
- Power Line Towers and Poles

Reaches without structures are omitted from the discussion in this section.

2.6.1 Bank Protection

2.6.1.1 Reach 5

The only engineered bank protection found outside of bridge abutments within the LHWCMP study area was found along the CAP Granite Reef Aqueduct canal in Reach 5. At the time of the field investigations, approximately 2,900 linear feet of canal embankment was protected by soil cement, and the active channel was directly adjacent to the embankment for the entire length of the stabilization. It is noted that the bank protection was added some time after original construction of the CAP canal in response to lateral erosion during relatively small floods that move the active channel toward the canal alignment. The field observations of the bank protection were recorded in July and October of 2004. During each of the field visits it was noted that the toe of the bank protection was exposed in places and appeared to have been slightly trimmed by erosion. The toe of the soil cement is cut to vertical at the base and a series of lateral shelves are visible at a height of between four and five feet above the channel invert. Evidence indicating slight undermining of the bank toe was also found. Figure 2-64 shows a map view of this structure and Figure 2-65 shows field photos.

Figure 2-64. CAP canal bank stabilization

CAP canal bank stabilization. Note cutbank along toe. View downstream.

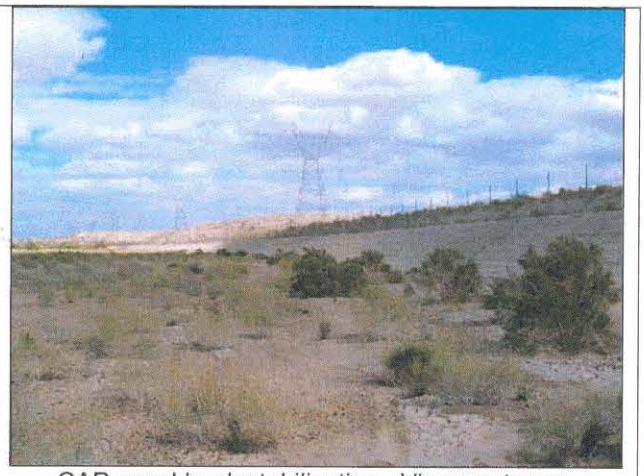

CAP canal bank stabilization. View upstream.

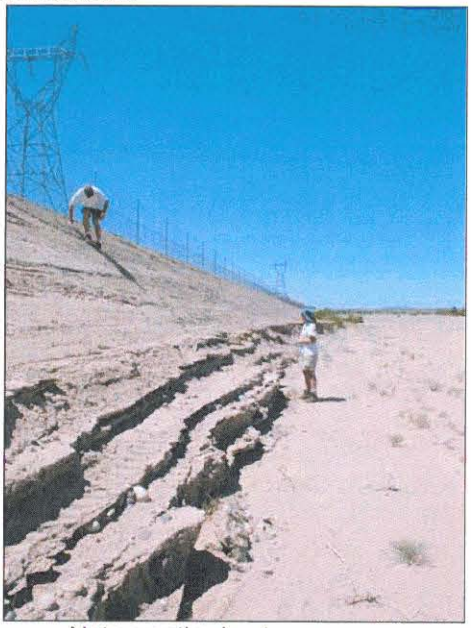

Note weathering terraces along toe of structure. View downstream.

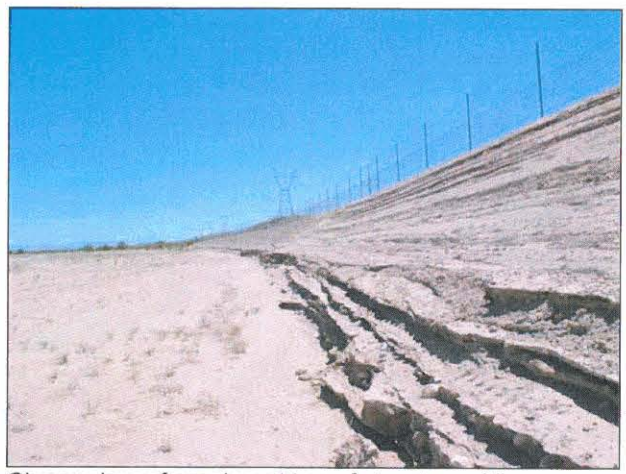

Closer view of erosion at toe of structure. View upstream.

Figure 2-65. Field photos of CAP canal bank stabilization

2.6.2 Bridges

2.6.2.1 Reach 1

Two bridges are located in Reach 1; the Old US Highway 80 Bridge and the SPRR Bridge. The condition of the bridge piers in addition to the abutments was documented in the field.

Old US Highway 80

As mentioned previously in this chapter, construction activity was occurring at the Old US 80 Bridge during the field investigation, restricting access to the bridge and limiting

the information collected as to the condition of the bridge piers and abutments. Field photos taken from the bridge deck are shown in Figure 2-66. At the completion of the construction work, the bridge section is fully lined. Therefore, scour impacts on the bridge are presumably mitigated. HEC-RAS modeling performed for the LHWCMP, summarized the Hydraulics Report, indicates that some flow may bypass the bridge via the floodplain.

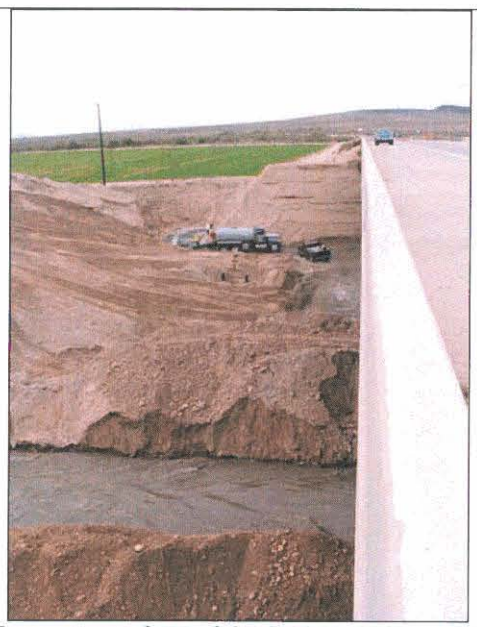

Downstream face of the bridge. View west.

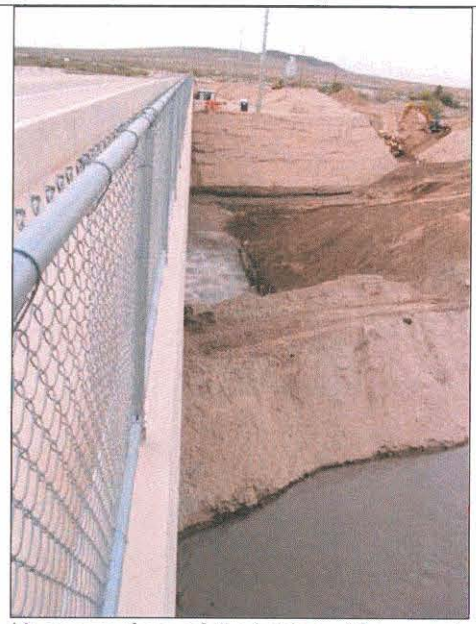

Upstream face of the bridge. View west.

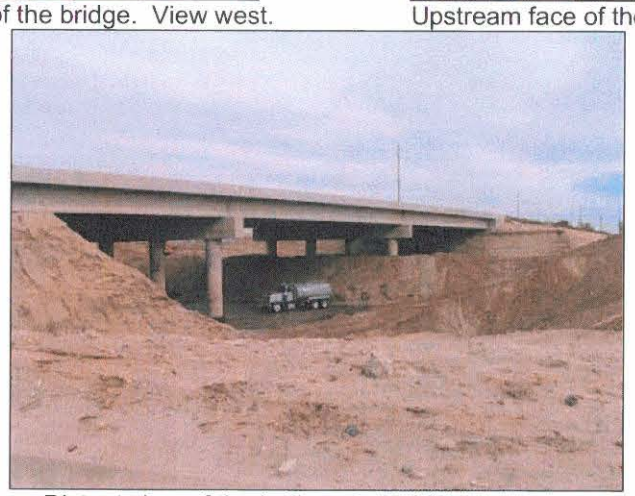

Distant view of the bridge piers. View northeast.

Figure 2-66. Field photos of the Old US Highway 80 Bridge

SPRR Bridge

The railroad bridge is supported by 12 piers (numbered river left to river right) spaced at approximately 80 feet. The upstream and downstream face of each pier was observed and photographed. Evidence of scour between one and three feet deep was observed at the upstream face of three piers. No scour was observed at the downstream face of the piers. A four foot high cutbank was observed at a distance of approximately 10 feet from pier 12. Aside from the cutbank, no evidence of erosion was found at the west

abutment. Unlike the west abutment, the east abutment was comprised of a set of three wooden trestles. No evidence of instability due to erosion was found on the east abutment. The active channel was located between piers 10 and 12 (numbered from river left to river right). Field photos of the structure are found in Figure 2-67.

2.6.2.2 Reach 3

The I-10 Bridges are located in Reach 3 and were observed and documented in the same manner as the SPRR Bridge. Each I-10 Bridge is supported by 14 piers spaced approximately 75 feet apart. No evidence of scour was found at any of the 28 piers. Flood high water mark evidence (likely from the October 2000 flood) was observed on many of the eastbound bridge piers. The height from the channel bed to the high water marks varied between one and three feet. Both the east and west bridge abutments were protected with a rock and rail system comprised of rounded rock riprap held in place by I-beam rails and chain fencing. A 20 foot x 20 foot (approx.) scour hole was observed along the base of the upstream east abutment bank protection. Scour was also observed at the toe of the abutment bank protection beneath the bridges. Large, angular rock had been dumped into the hole, probably as scour mitigation. Evidence of erosion was also observed along the toe of the west abutment at a two- to three-foot high cutbank encroaching on the bank protection. No evidence of scour was observed on the downstream face of either the east or west abutment. The active channel is split and is located between piers seven and nine and pier 12 and the west abutment (numbered from river left to river right). Figure 2-68 shows field photos of the bridges.

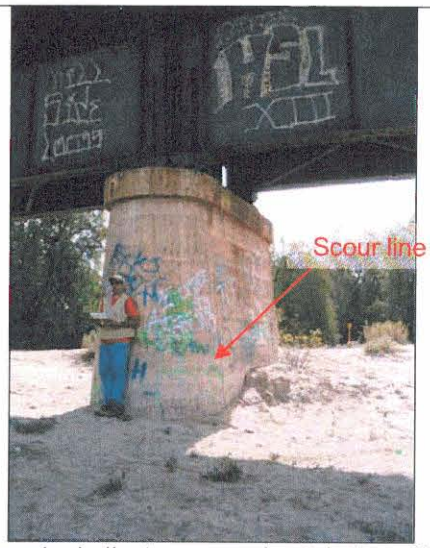

Stain on pier indicates approximately three feet of recent scour. View downstream.

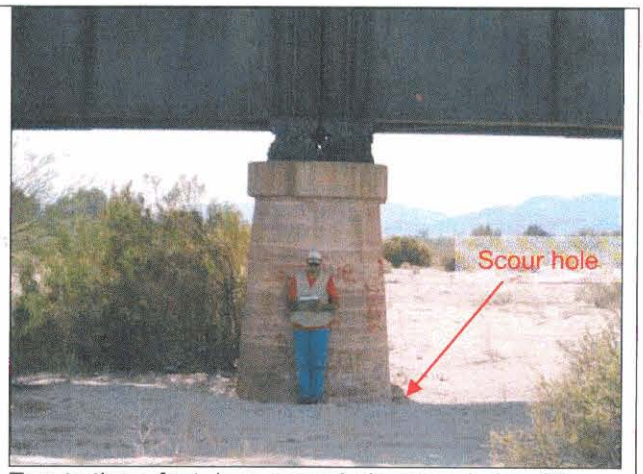

Two to three foot deep scour hole around pier. View downstream.

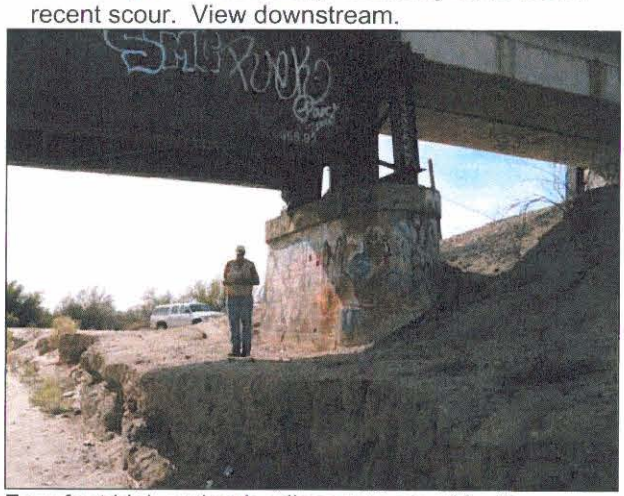

Four foot high cutbank adjacent to pier 12. View downstream.

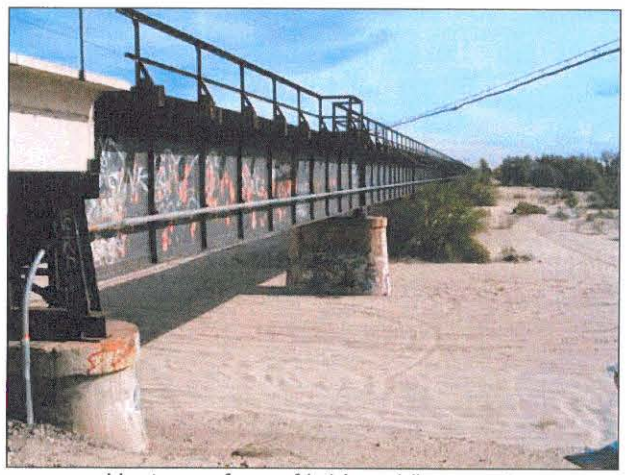

Upstream face of bridge. View west.

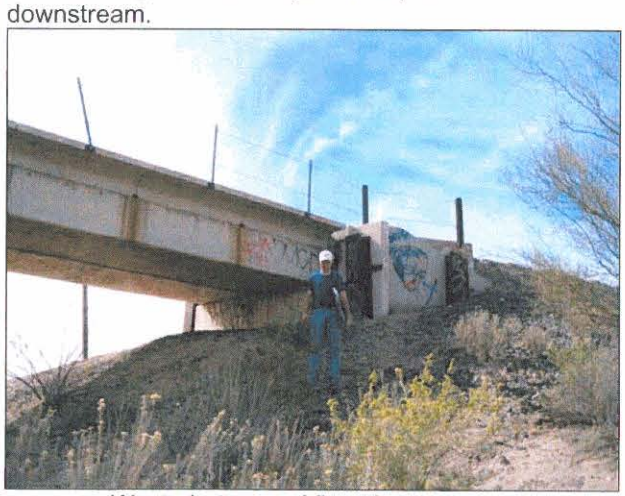

West abutment. View downstream.

East abutment. View downstream.

Figure 2-67. Field photos of railroad bridge

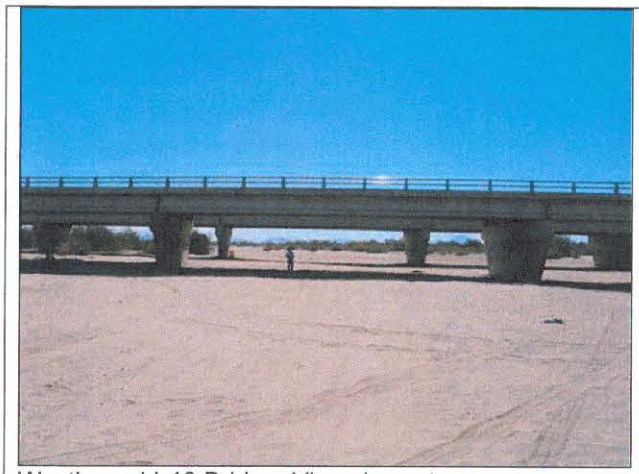

Westbound I-10 Bridge. View downstream.

High water mark evidence on pier. View downstream.

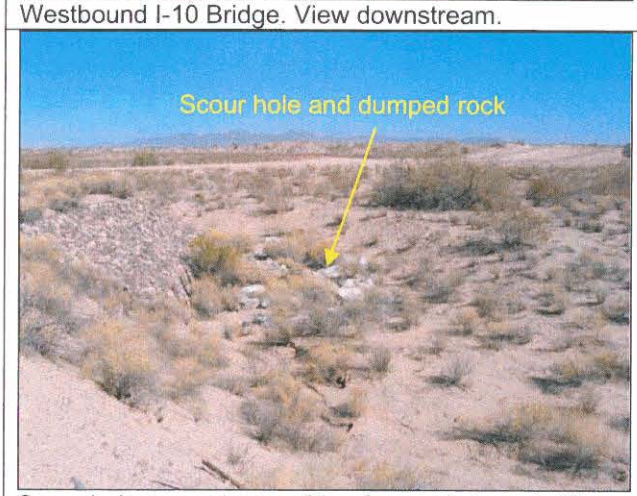

Scour hole on upstream side of east abutment. View upstream.

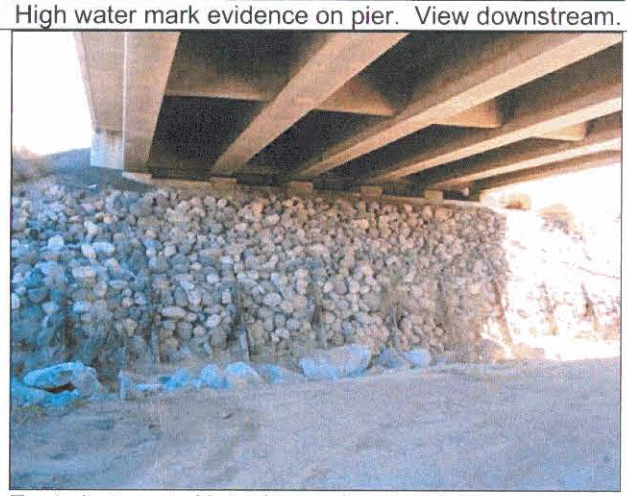

East abutment. Note dumped rock at the toe. View east.

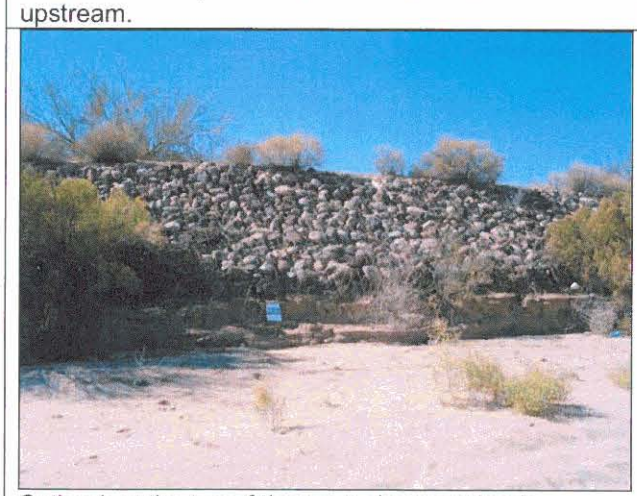

Cutbank at the toe of the west abutment bank protection upstream of the bridges. View west.

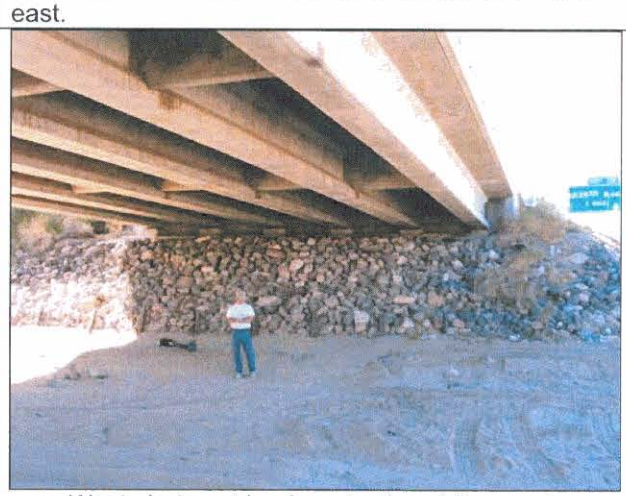

West abutment bank protection. View west.

Figure 2-68. Field photos of the Interstate 10 Bridges

2.6.3 Levees

2.6.3.1 Reach 1

The banks of the levees in the channelized portion of Reach 1 below the Old US 80 Bridge were observed during the field investigations. No engineered bank protection was in place. Vegetation varied from moderately dense to sparse. No evidence of bank instability was observed. The single (left bank) levee upstream of the Old US 80 Bridge was being actively eroded as evidenced by a 10-foot vertical cutbank shown in Figure 2-69.

The two right bank levees immediately upstream of the SPRR Bridge appeared to have been constructed to divert flood flows away from the railroad embankment. The upstream levee has been in place since at least 1949. 1953 aerial photos show a breach in the upstream levee (possibly the August 1951 flood), the likely cause for the construction of the secondary, downstream levee (Figure 2-70). The banks of these structures were earthen and not reinforced by engineered bank protection.

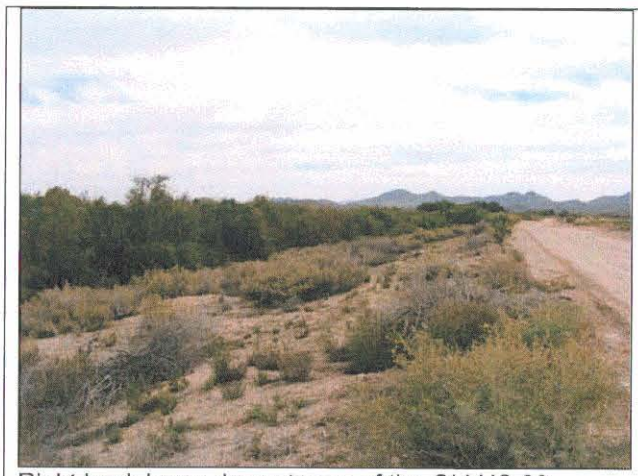

Right bank levee downstream of the Old US 80 Bridge. View downstream.

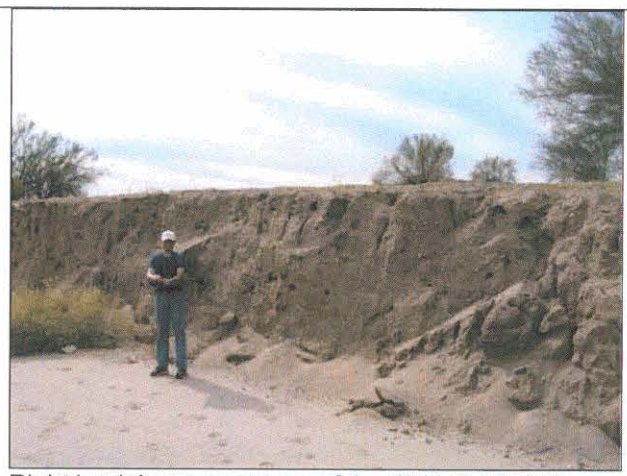

Right bank levee upstream of the Old US 80 Bridge. Note unstable, vertical cutbank View southwest.

Figure 2-69. Field photos of Reach 1 levees

2.6.3.2 Reach 2

The series of levees located at the Baseline Road at-grade crossing appeared to be temporary structures that are composed of uncompacted materials obtained from the active channel. It is likely that these structures are merely the result of road maintenance practices following floods.

A 2,600-foot long, 5-foot high levee in the left overbank approximately 1.2 miles upstream of the Baseline Road crossing apparently was constructed to protect the adjacent agriculture fields. The levee was earthen and no bank protection was present (Figure 2-71).

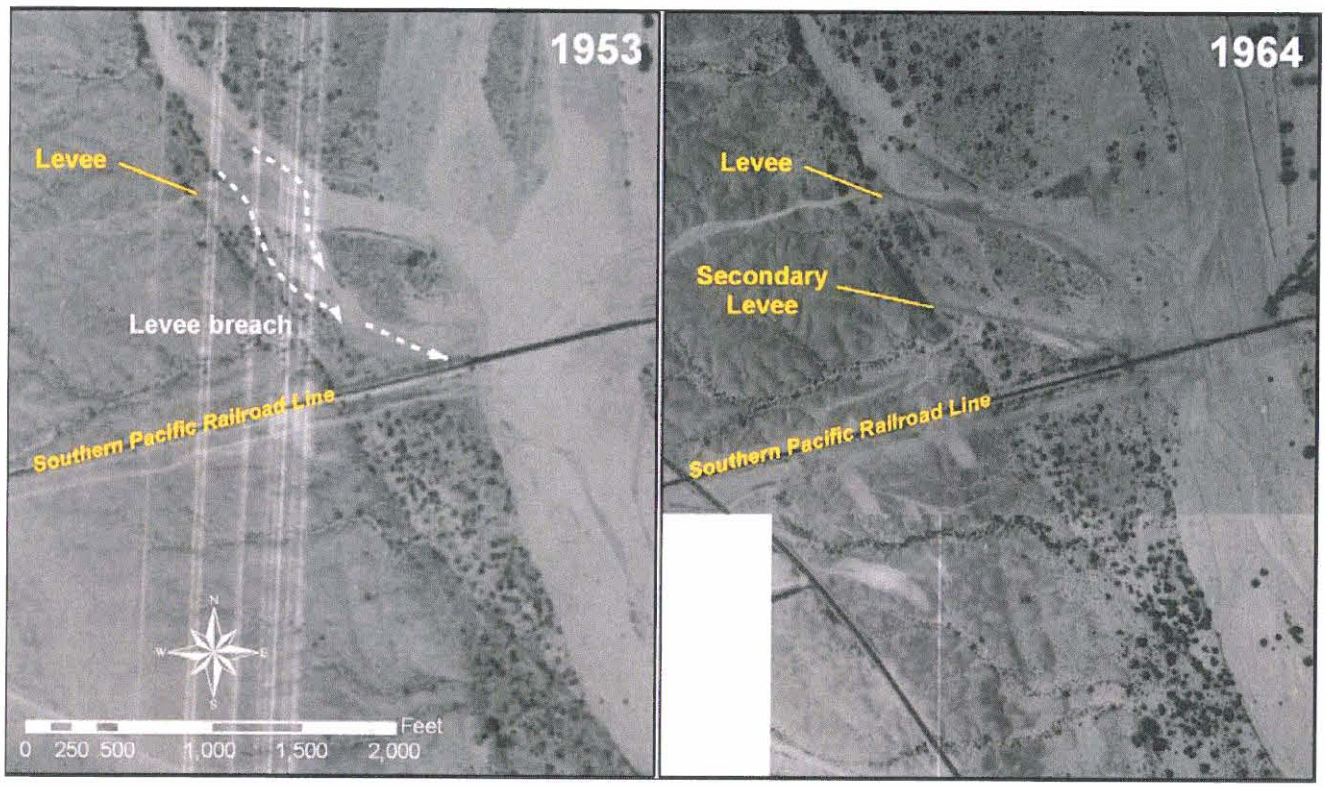

Figure 2-70. Levees upstream of railroad bridge

Figure 2-71. Reach 2 levee

2.6.3.3 Reach 4

A small 900 foot long levee was observed in Reach 4 in the far eastern floodplain, two miles downstream of the Wagner Wash confluence. The five foot high levee was earthen in composition, and appears to have been constructed to protect the adjacent agricultural fields (Figure 2-72).

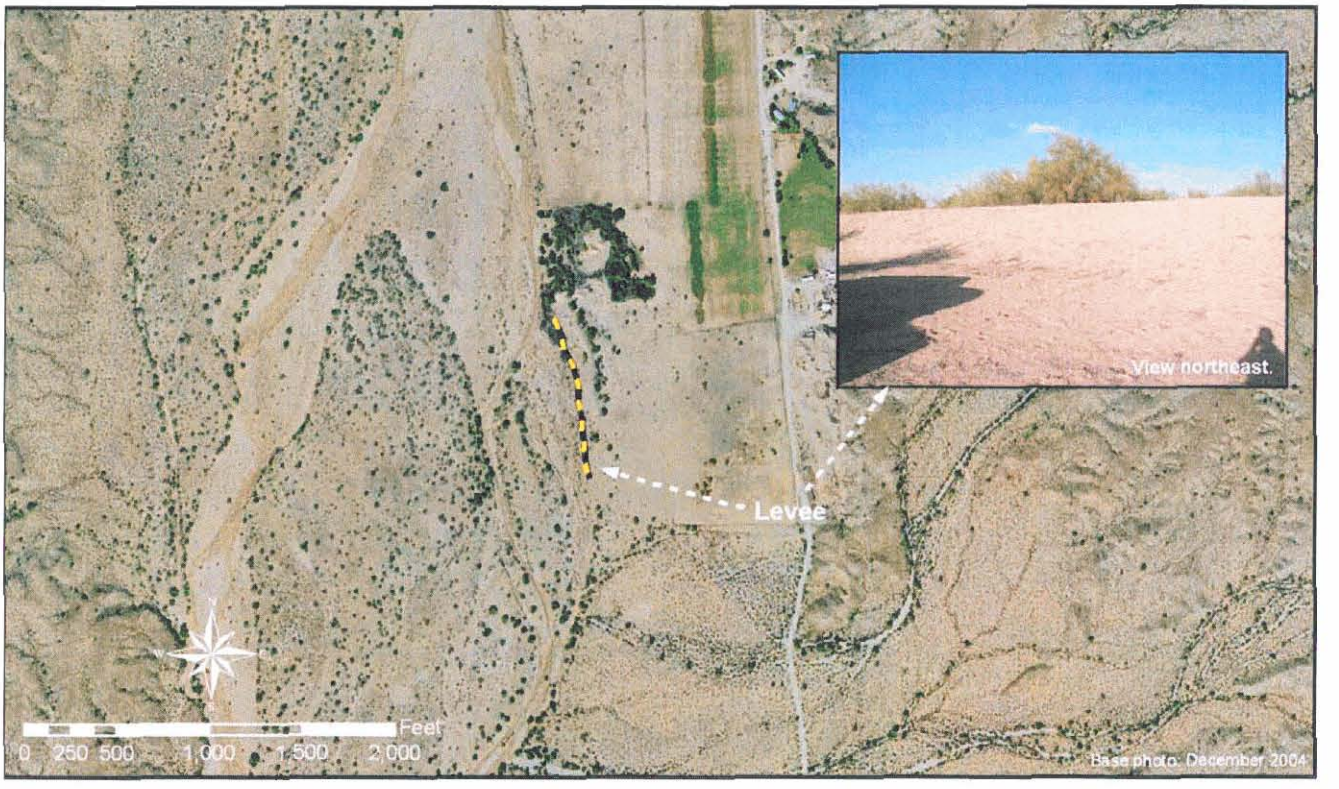

Figure 2-72. Reach 4 levee

2.6.4 At-Grade Road Crossings

2.6.4.1 Reach 2

Baseline Road is one of only two at-grade road crossings in the LHWCMP study area, and is the only paved one. Field observations of the crossing, both within the active channel and floodplain areas, indicated the structure is well-maintained with no evidence of existing or potential erosion from the Hassayampa River (Figure 2-11), although road damage should be expected during significant floods.

2.6.4.2 Reach 3

The Tonopah-Salome Highway at-grade road crossing is located in Reach 3. At the time of the field investigations the crossing was a graded, gravel road and no evidence of erosion was found. Subsequent visits to the site following the December 2004 floods revealed the impermanent nature of the crossing. Severe erosion of the crossing had occurred at multiple locations within the Hassayampa River floodplain. Similar erosion should be expected during future flow events (Figure 2-16).

2.6.5 Irrigation and Siphon Crossings

2.6.5.1 Reach 1

The Arlington Canal siphon crossing, located 3,000 feet upstream of the Gila River confluence, has been in place since at least 1934. Both the inlet and outlet of this structure were observed and showed no field evidence of adverse impacts from the Hassayampa River (Figure 2-73).

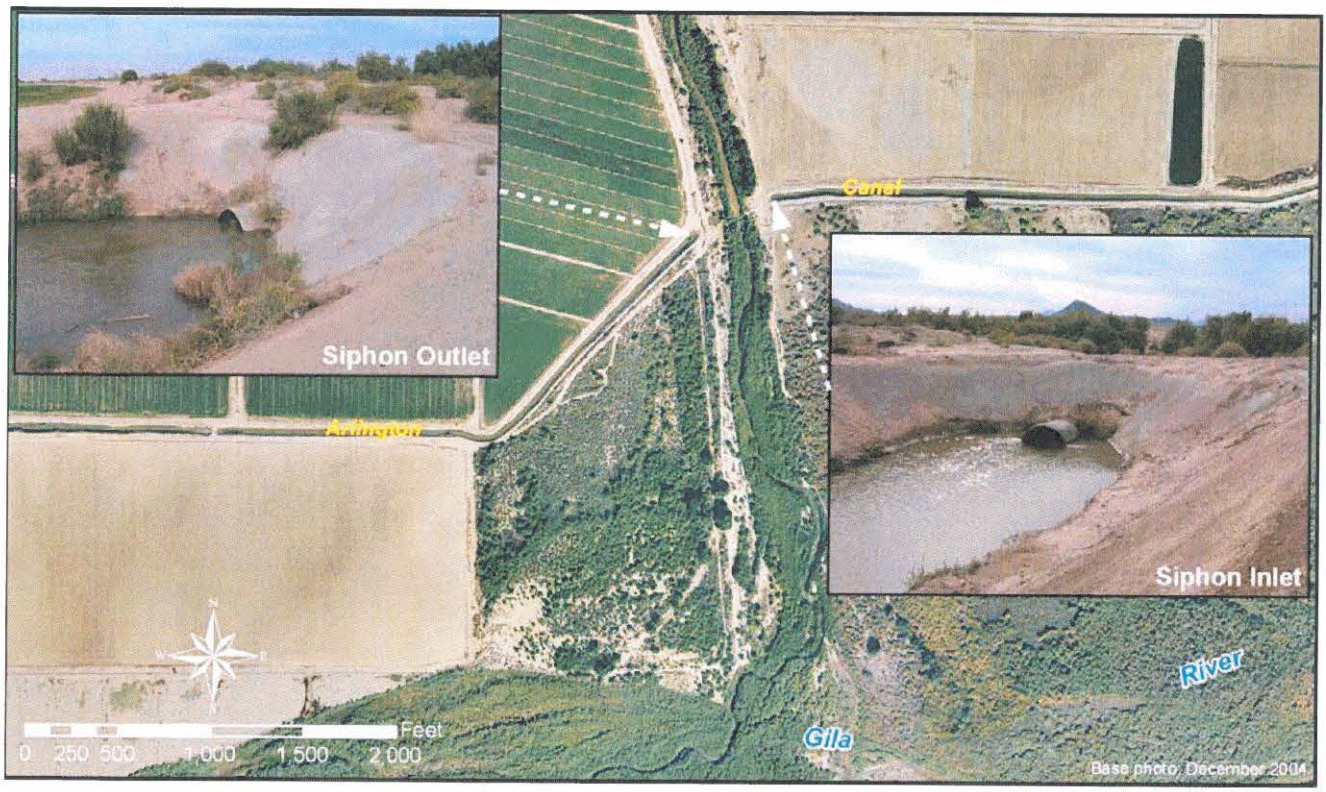

Figure 2-73. Arlington Canal siphon

2.6.5.2 Reach 2

Historical evidence of a siphon or surface canal known to have crossed the main channel during the historic period is completely lacking, except for some structures that are now partially buried in the floodplain on the west side of the river. Presumably, these features were obliterated by floods, as was recounted in the historical records and by local residents.

2.6.5.3 Reach 5

The CAP Granite Reef Aqueduct siphon extends the entire width of the Holocene Floodplain. The siphon inlet and outlet structures are located on the Pleistocene terrace, thus are outside direct effects of flooding on the Hassayampa River. The condition of the buried pipe that spans the floodplain was not possible to ascertain, however, it is actively maintained by the Central Arizona Project.

2.6.6 Power Line Towers and Poles

2.6.6.1 Reach 2

No evidence of active scour was observed around the power poles of the single-pole overhead utility alignment located just upstream of Baseline Road (Figure 2-74).

Pole in right overbank. View downstream.

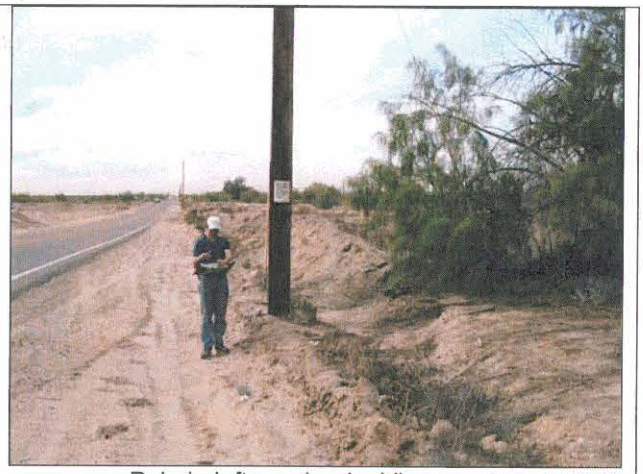

Pole in left overbank. View west.

Figure 2-74. Field photos of power poles at Baseline Road

As discussed in Sections 2.3.2.4 and 2.4.2.5, the high tension power line towers in the alignment that crosses the Hassayampa River in Reach 2 are not located directly in the active channel. However, lateral migration of the active channel is rapidly approaching the set of three towers located in the right overbank. A vertical cutbank on the outside of the bend has progressively moved toward the power poles over the past several years, despite a lack of significant floods. At the time of the field investigation, the northern-most tower was approximately 212 feet from the cutbank. Analysis of the distance between the tower and the cutbank, using orthophotography from 2001, 2003, and 2004, yielded the distance estimates summarized in Table 2-6.

Table 2-6. Reach 2 - cutbank erosion distance

Photo Year	Distance from Tower to Cutbank (feet)
2001	285
2003	280
2004	212

Although the data shown in Table 2-6 are limited, they indicate an erosion rate of about 18 feet/year. At this rate, the cutbank would reach the north tower by 2017. Historical evidence from other reaches indicates that a single large flood could easily erode the cutbank well past the existing 212 foot buffer. No evidence of scour from overbank flows was observed at the base of the tower pylons (Figure 2-75).

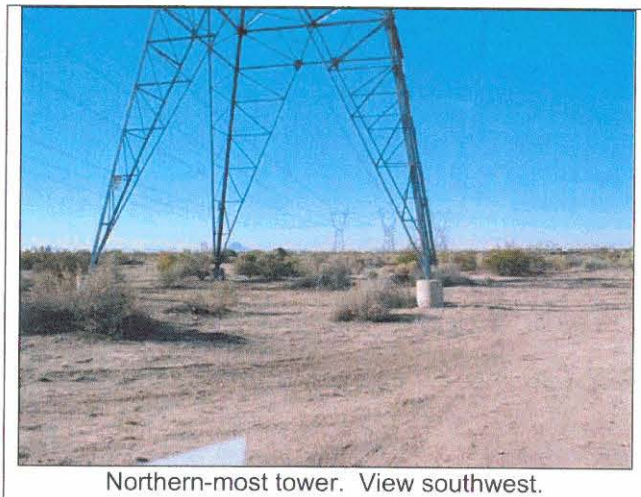

Northern-most tower. View southwest.

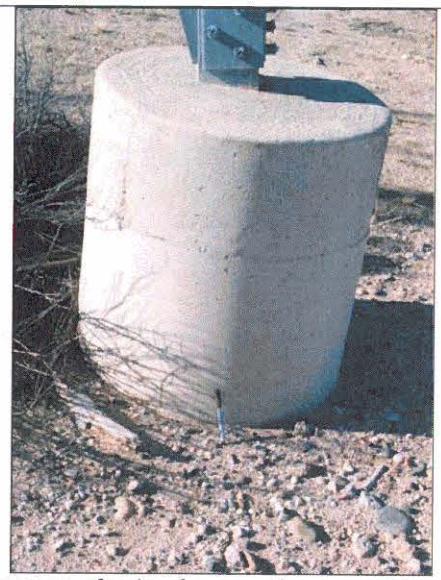

Close-up of pylon from northern-most tower.

Figure 2-75. Field photos of power line towers in Reach 2

2.6.6.2 Reach 3

During the initial (June 2004) field visits, as well as during subsequent field trips prior to December 2004, headcuts were observed approaching, then reaching, and then passing the double-pole overhead utility alignment located north of the Tonopah-Salome Highway. The site was visited during the December 2004 floods to view the progress of the erosion and it was found that sediment deposition had filled the sand and gravel pit downstream that initiated the headcut, and had buried the headcut itself. After the flood, the poles appeared no longer threatened (Figure 2-76).

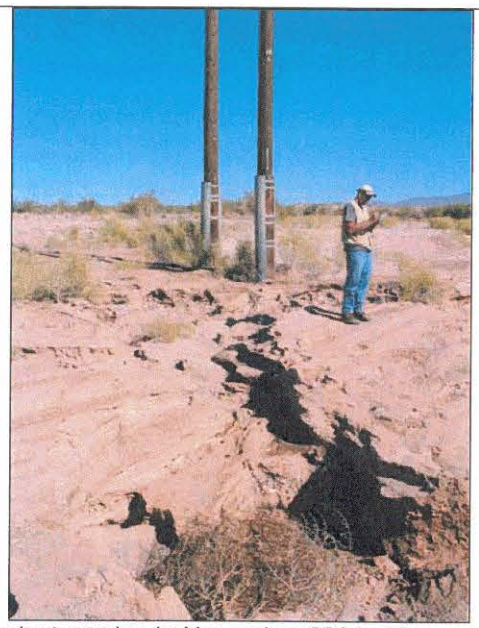

Headcut erosion in November 2004. View north.

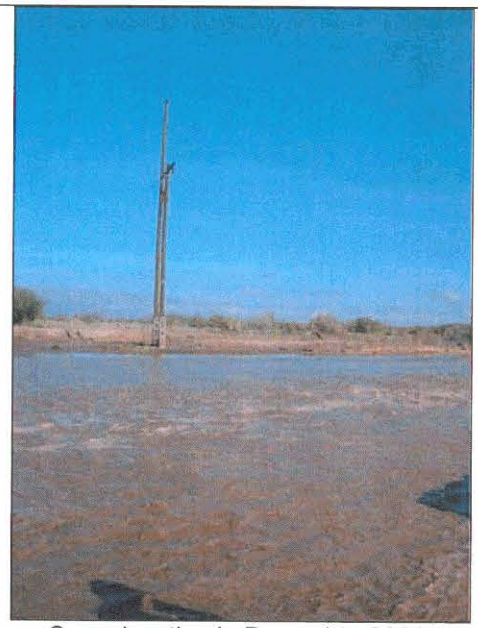

Same location in December 2004.

Figure 2-76. Reach 3 power pole alignment

2.6.6.3 Reach 5

The two power line alignments in Reach 5 are located just upstream of the Wagner Wash confluence. Each alignment contains multiple towers within the Hassayampa River floodplain, with one tower located directly in the active channel. Each tower within the floodplain was observed to assess the condition of the pylons and determine if erosion had occurred at the base of the towers.

Southern Alignment

The southern double-pole alignment had four towers in the floodplain, with the eastern-most set located on a low terrace surface and the western-most set on a low bar surface. Seven of the pylons on the eastern set appeared to have experienced no recent erosion. An avulsion channel located just east of the towers recently migrated toward one of the pylons, eroding about two feet of sediment from the base of the pylons (Figure 2-77). The western tower set was located on a frequently inundated surface as evidenced by an abundance of flotsam, some of which had accumulated on the pylons (Figure 2-77). Several of the pylons showed evidence of recent erosion at the base. Geomorphic evidence upstream suggests that a potential avulsion of the active channel onto the low bar surface was possible, and would result in more substantial erosion around the base of the towers in the future.

Eastern tower set. View downstream.

Southern tower of eastern set. View downstream.

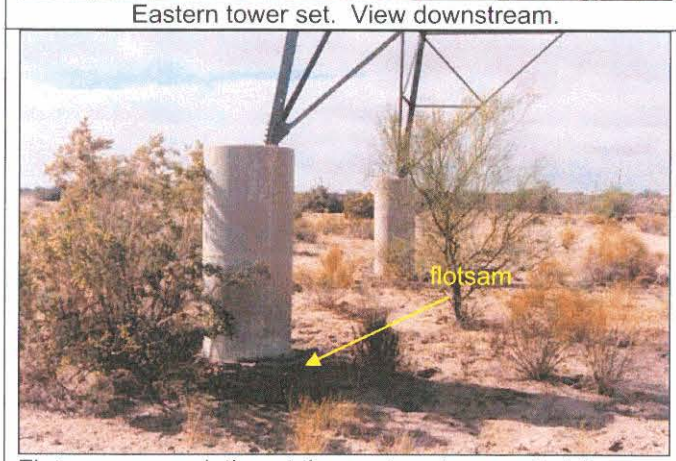

Flotsam accumulation at the western tower set. View downstream.

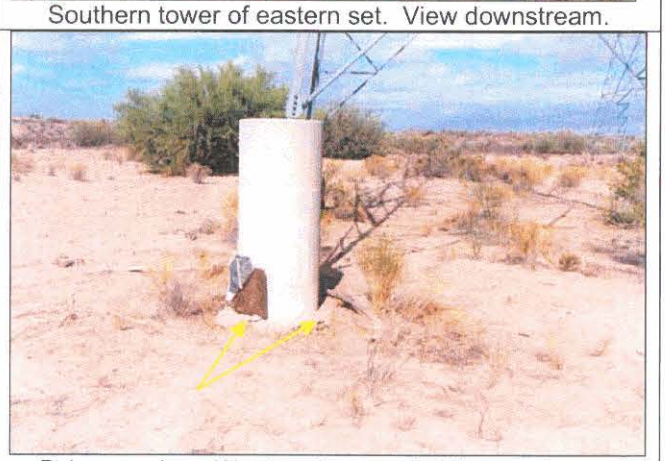

Pylon erosion. Western tower set. View upstream.

Figure 2-77. Reach 5 field photos of the southern power line alignment towers

Northern Alignment

The northern tower alignment has three towers in the floodplain. Two towers are located on low terrace surfaces on either side of the active channel, and the third is in the active channel itself. The eastern tower was approximately 20 feet from an avulsion channel. None of the pylons at the eastern tower show evidence of recent erosion. However, lateral migration of the avulsion channel could undermine the pylons in the future. The western tower is also directly adjacent to an avulsion channel. Staining on one of the three pylons suggests recent removal of approximately one foot of sediment. The third tower has three pylons located directly in the active channel. The three pylons in the channel show evidence of recent erosion. The distance from the ground surface to the top of each pylon was measured. The three pylons in the channel measured 7.6 feet, 6.7 feet, and 5.7 feet, while the pylon on the terrace measured four feet, indicating erosion of several feet from the base of the pylons in the channel (Figure 2-78).

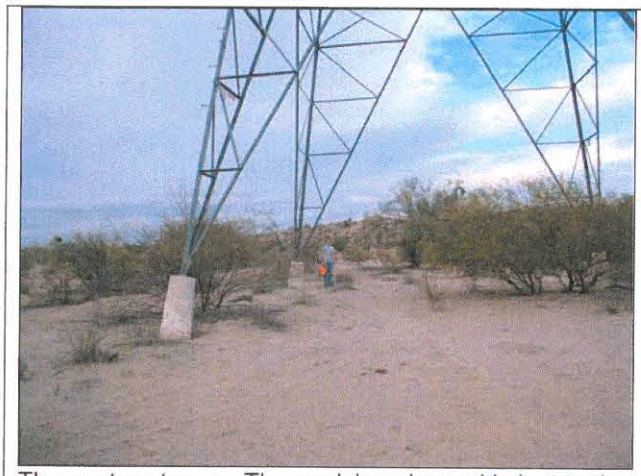

The eastern tower. The avulsion channel is just to the right out of the photo. View northeast.

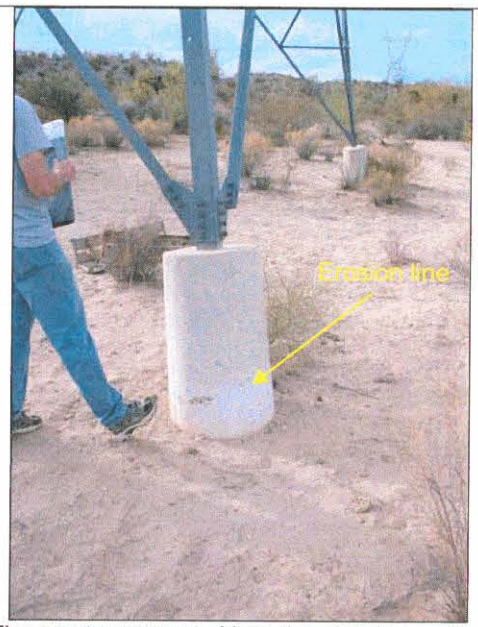

The western tower. Note the staining on the nearest pylon. View northwest.

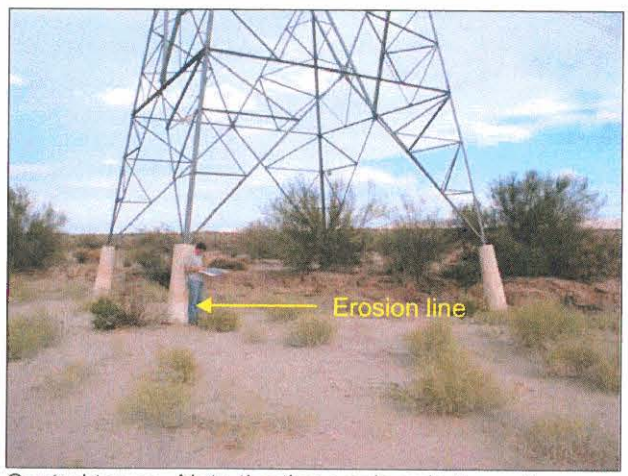

Central tower. Note the three pylons in the active channel and the staining indicating recent erosion. View east.

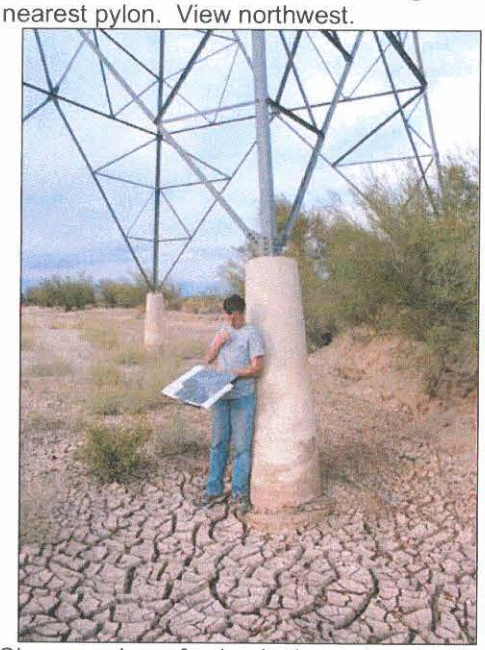

Close-up view of pylon in the active channel. View upstream.

Figure 2-78. Reach 5 field photos of the northern power line alignment towers

2.7 Sediment Data

Characteristics of channel and floodplain sediment were used in both the geomorphic and soil profile analyses. During the field investigations, surficial sediment data, such as relative firmness, composition, color, and general texture were used to characterize and identify differing geomorphic surfaces. During the soil pit analysis, specific properties of individual soil profiles were characterized to interpret the flood inundation history, relative age, and geomorphic surface. The soil pit analyses are presented in Chapter 3. General sediment characteristics that were observed during the field investigations and which are applicable to the entire study area are discussed here.

2.7.1 Channel Bed Sediments

Active channel bed sediment characteristics were consistent throughout the entire LHWCMP study area. Sieve analysis from the 19 sediment samples collected for the LHWCMP sediment transport analysis (Chapter 5) yielded a d_{50} value of 0.5mm which falls directly between a coarse sand and a medium sand. Gravel was frequently observed on the surface of the channel bed, and was visually estimated at about 5 to 10 percent of the total distribution. The percentage of gravel was consistently less below the surface layer. An early hypothesis that channel sediment size would increase immediately downstream of major tributaries due to coarser loads in the steeper tributaries was not supported by the field or laboratory analyses. However, the percentage of gravel in the channel banks did increase downstream of the tributaries. Figure 2-79 shows bed sediment photos from various locations.

2.7.2 Channel Bank Sediments

In most of the study area, channel banks are cut into the low terrace surfaces. However, where the channel banks are cut into high terrace surfaces, tributary terrace surfaces, and Pleistocene terrace surfaces, the bank sediments and characteristics are significantly different. Some bank features observed in older and higher terrace cuts provided information as to the general stability of the banks and their susceptibility to lateral erosion. These characteristics included sedimentary texture, cohesiveness, and calcium carbonate ($CaCO_3$) accumulation. Each of these bank types observed in the field are described below. Cohesiveness was measured using a shear vane that measures relative shear strength in tenths of 1 kg/cm^2. Field photos of each bank type are shown following the descriptions.

2.7.2.1 Low Terrace Banks

Most of the active channel banks in the study area are cut into low terrace surfaces. The low terrace banks were generally composed of fine grained, loamy sands with less than 10 percent gravel (Figure 2-80). Cohesiveness was generally low, with shear vane readings from 0 to 0.3 kg/cm^2. Vertical cutbanks were common. Calcium carbonate accumulation was undetectable using hydrochloric acid (HCL). Low terrace channel banks were erodible and unstable, and thus are considered highly susceptible to lateral erosion.

Channel bed sediment just downstream of the I-10 Bridges. Note the gravel in the undisturbed area, and the lack of gravel in the disturbed sediment taken from below the surface.

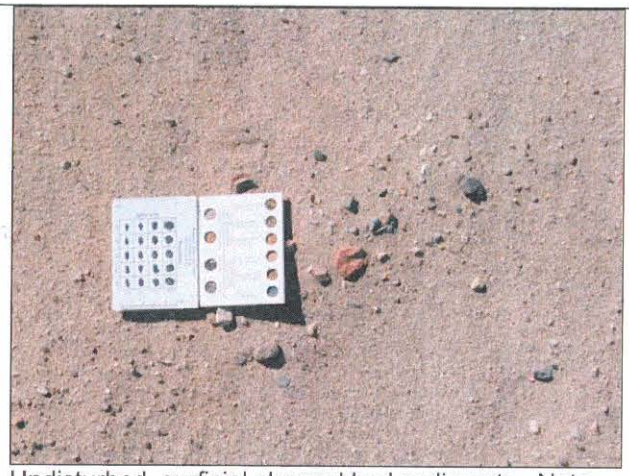

Undisturbed, surficial channel bed sediments. Note the gravels. Photo taken downstream of the I-10 bridge.

Profile of channel bed sediments. Note lack of gravel in the deposit. Photo taken near the upstream study limit.

Channel sediments at the Jackrabbit Wash confluence.

Figure 2-79. Field photos of channel bed sediments

Typical low terrace channel bank.

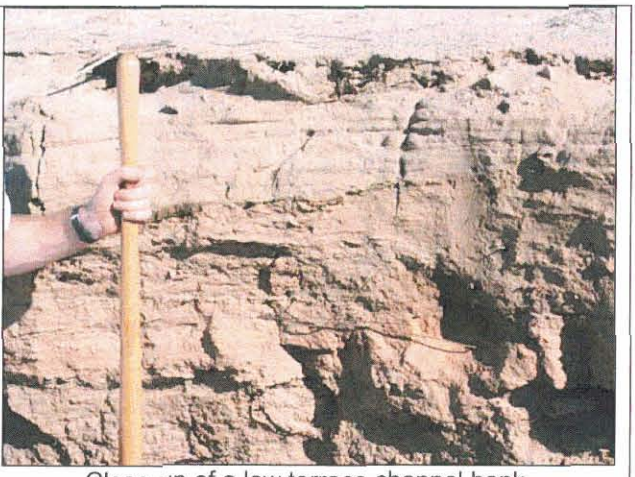

Close-up of a low terrace channel bank.

Figure 2-80. Low terrace channel bank sediments

2.7.2.2 High Terrace Banks

Channel banks cut into the high terrace surfaces were the second-most common after the low terrace banks. High terrace bank sediments were generally finer than the low terrace sediments and were composed of silty loam with less than 10 percent gravel. Cohesiveness was generally low, with shear vane readings of 0.3 to 0.55 kg/cm^2. Vertical cutbanks were frequent. Calcium carbonate was commonly detectable with HCL, but was finely disseminated. Like low terrace banks, high terrace channel banks are erodible and unstable, and thus are considered highly susceptible to lateral erosion (Figure 2-81).

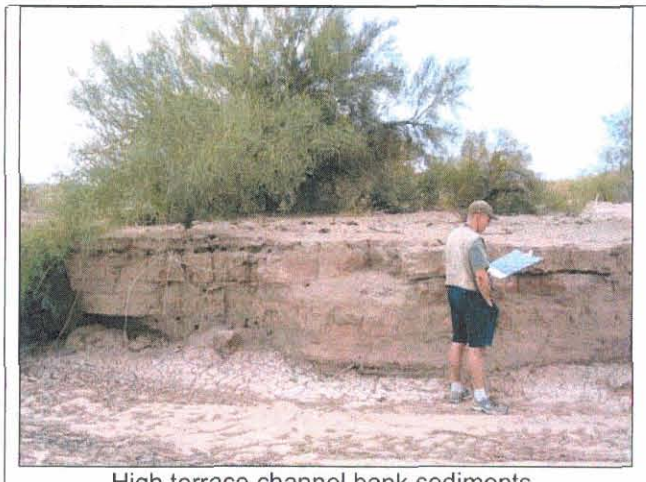

High terrace channel bank sediments.

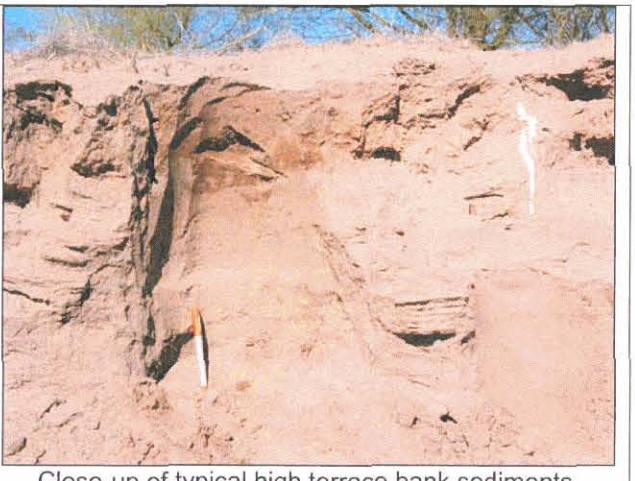

Close-up of typical high terrace bank sediments.

Figure 2-81. High terrace channel bank sediments

2.7.2.3 Tributary Terrace Banks

Locations in which the active channel was directly adjacent to a tributary terrace are less common than cuts into the high terraces. The tributary terrace channel bank sediments were very different than the floodplain terraces. The sediment matrix generally consisted of loam and loamy sands, but the percent of gravel was significantly

higher than the floodplain terraces, and ranged from 15 to 50 percent. Cohesiveness was also much higher, with shear vane readings of at 0.5 to 0.8 kg/cm^2. The higher cohesiveness was due to $CaCO_3$ cementation, which was commonly estimated at Stage I+. The soil structure of the tributary terrace sediments was blockier than sediments on the floodplain banks, indicating accumulation of fine-grained sediments, chemical weathering, and a much older age. Both vertical and overhanging cutbanks were very common. The tributary terrace channel banks were significantly more stable than the floodplain terrace banks, but cannot be considered erosion resistant. The banks are susceptible to erosion (Figure 2-82).

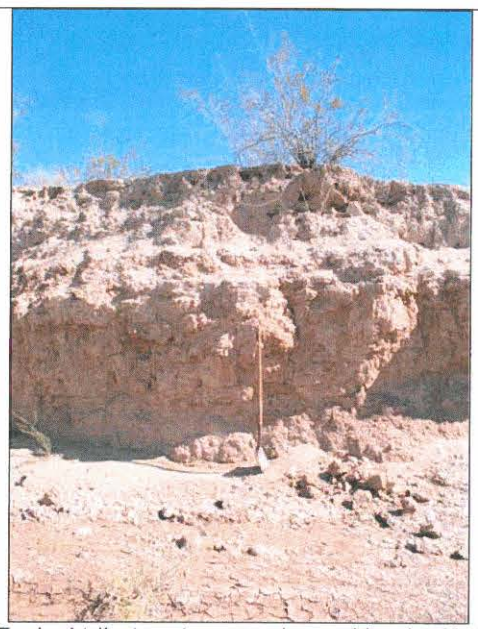

Typical tributary terrace channel bank. Note more blocky structure and lighter color than low and high terrace sediments.

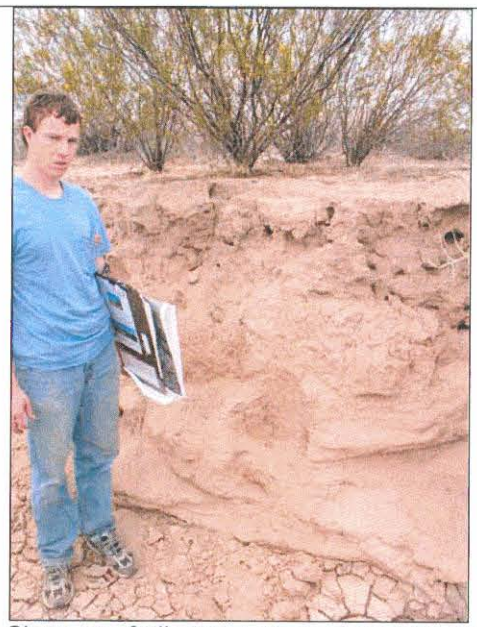

Close-up of tributary terrace channel bank sediments.

Figure 2-82. Tributary terrace channel bank sediments

2.7.2.4 Pleistocene Terrace Banks

Pleistocene terraces flanking the active channel were uncommon in the study area. The most prominent location where the active channel cuts a Pleistocene terrace was opposite the Jackrabbit Wash delta. The sediments comprising the Pleistocene terrace banks were not analyzed in detail, although they had similar characteristics to other such surfaces described on other river systems in central Arizona. These characteristics included very blocky soil structure, stage III to IV+ $CaCO_3$ development, and disseminated gravels. Undercutting and mass wasting seemed to be the dominant erosion process, both of which are facilitated by fluvial processes. The channel banks formed by Pleistocene terrace deposits are considered moderately stable. Elsewhere, average erosion rates for Pleistocene surfaces have been estimated at less than one foot per year. Given the relative resistivity of the banks opposite the Pleistocene terrace banks, the active channel probably tends to preferentially erode the younger surfaces (Figure 2-83).

Pleistocene terrace channel bank. Note large gravels on the surface.

Close-up of Pleistocene terrace channel bank sediments. Note very blocky structure and disseminated gravels.

Figure 2-83. Pleistocene terrace channel bank sediments

2.7.3 Floodplain Sediments

Floodplain sediments vary consistently by geomorphic surface in the study area. The soil pit analysis (Chapter 3) provides detailed descriptions of floodplain sediment from locations throughout the study area.

2.8 Field Evidence of Vertical Channel Change

Evidence of historical degradation or aggradation and points of natural grade control is generally lacking in the study area. Only the following types of information were identified during the field reconnaissance and are discussed below:

- Headcuts and Tailcuts Near Sand and Gravel Mines
- Headcuts on Floodplain and Tributary Terraces
- Long-Term Degradation in Reach 1
- Evidence of Aggradation
- Natural Grade Control

More detailed discussion of vertical channel changes is provided in Chapter 4

2.8.1 Headcuts and Tailcuts near Sand and Gravel Mines

Headcuts were observed upstream of the in-stream excavations near the Tonopah-Salome Highway. Where the pits had captured an active channel braid, the headcuts extended to the full depth of the pit, and became progressively deeper and longer with each small flow event. At one point, the headcut upstream of the 10-foot deep Pioneer Sand excavation (upstream of the Tonopah-Salome Highway) migrated nearly 0.5 miles

upstream along a sinuous headcut path (Figure 2-84). The banks of the headcut channel were vertical. The headcut channel itself was terraced, reflecting progressive deepening of the channel by subsequent flows. Shallower, less well-defined headcuts were observed upstream of the Hanson excavation located downstream of the Tonopah-Salome Highway After the December 2004 flood, the headcuts (and the in-channel pits) were buried by flood sedimentation.

Several aspects of the field observations deserve special note. First, in contrast to some of the engineering literature, the headcut depth was **not** limited to half the pit depth. Low inflow rates, pit length, and high infiltration rates probably were all factors that reduced ponding depths and resulted in the observed depth of the headcut. Second, the upstream length of the head extended well upstream of the length that would be predicted using the ADOT methodology (See Chapter 5 headcut modeling discussion). The extended length of the headcut was probably due to the highly mobile fine-grained bed sediment, the depth of the headcut, and the location of the mine in the low flow channel. Third, the headcut channel did not follow a direct upstream path, but rather had significant sinuosity which created meanders that were sometimes perpendicular to the valley alignment. The non-linear headcut path has implications for assessing off-site impacts for in-stream mines, since mine engineers typically assume that the headcut will take a linear path in the most direct upstream direction. Fourth, the headcut channel had a specific morphology of deep-narrow at the pit lip, which graded to wide-shallow at the upstream limit. Unfortunately, no systematic measurements of the channel geometry were made during the field visits.

Tailcutting tends to be more subtle than headcutting and thus more difficult to document in the field. However, distinct tailcut erosion was observed in the outlet channel for the Hanson pit (Figure 2-85). Along this outlet channel, which followed a pre-mining natural braid, channel bank and bank vegetation characteristics indicated that the channel had degraded by up to five feet, leaving vertical cut banks, perched vegetation, a perched floodplain, and a terraced channel. Tailcutting from the Pioneer Sand excavation appeared to have merged with headcutting from the Hanson operation in the vicinity of the Tonopah-Salome Highway during the December 2004 flood, generally lowering the bed elevation and damaging the at-grade road crossing.

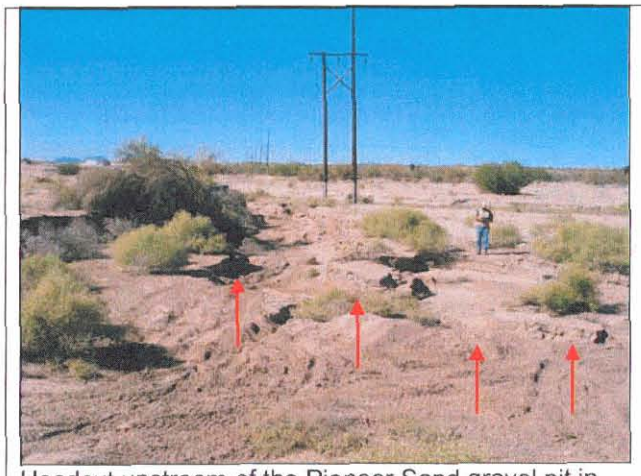

Headcut upstream of the Pioneer Sand gravel pit in November 2004. The arrows indicate the location of the headcut face. View downstream.

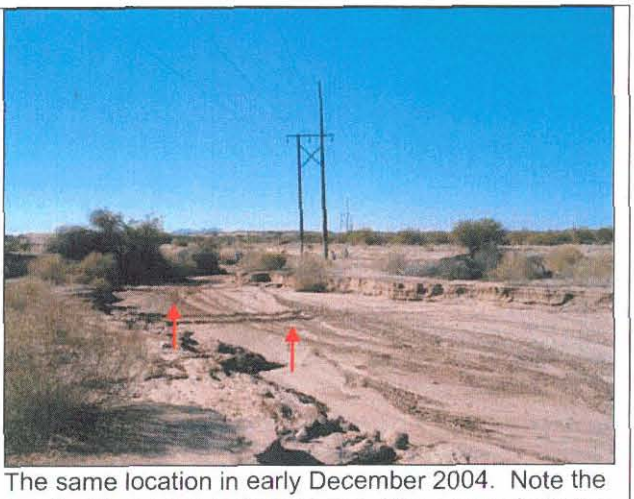

The same location in early December 2004. Note the headcut has migrated upstream. The arrows indicate the November 2004 location of the headcut. View downstream.

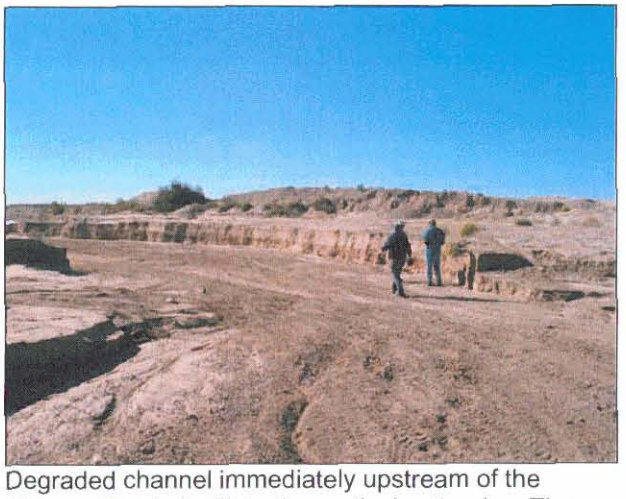

Degraded channel immediately upstream of the Pioneer Sand pit. Note the vertical cutbanks. The photo is early December 2004. View downstream.

Upstream view of the channel shown in the first two photos in this figure. Photo is during the winter flows on December 31, 2004. The arrows indicate the approximate location of the headcut shown in the first photo. The headcut has migrated a significant distance upstream.

Figure 2-84. Headcut upstream of the Pioneer Sand gravel pit.

Tailcut channel downstream of the Hansen pit. Note vertical cutbanks. View upstream toward pit.

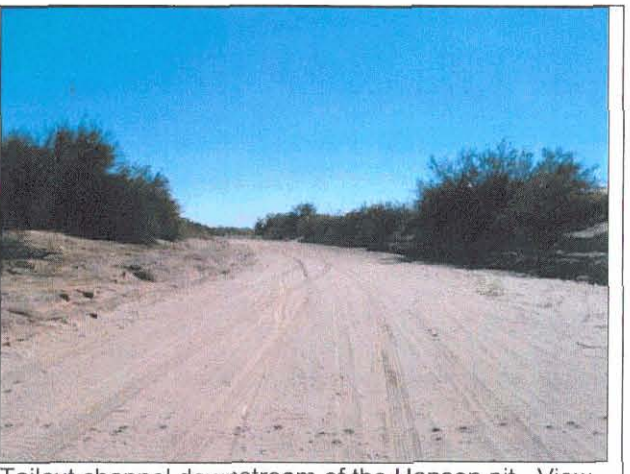

Tailcut channel downstream of the Hansen pit. View downstream.

Figure 2-85. Tailcut channel downstream of the Hansen gravel pit.

2.8.2 Headcuts on Floodplain and Tributary Terraces

Small headcuts occur on floodplain channels and at the margins of tributary terraces, as described in Section 2.4 of this Chapter. The overbank headcuts do not appear to be related to long-term degradation of the Hassayampa River. Instead, they appear to be mechanisms of lateral erosion (avulsion by formation of overbank flow paths) and processes related to integration of incipient internal drainage networks on the broad floodplain surfaces. The headcuts at the tributary margins may be related to net degradation of the Hassayampa River during geologic time (~2 million years), well outside the engineering time scale of concern for this study.

2.8.3 Long-Term Degradation in Reach 1

There is some evidence of vertical channel change in Reach 1 of the Hassayampa River. First, anecdotal accounts provided by long-term residents and stakeholders indicate that Reach 1 aggraded during the period after construction of Gillespie Dam (ca 1921). Similarly, residents claim that following the failure of Gillespie Dam in the 1993 flood on the Gila River, the bed of Reach 1 has been degrading. Second, the height of the Reach 1 floodplain above the existing channel bed supports the hypothesis that the main channel has experienced net degradation over the past 100 years. Third, field observations at the Naramore Road alignment crossing indicate that some progressive scour is occurring, which has lowered the downstream side of the dip section (Figure 2-86). Fourth, extreme cutbank heights in the confluence area within the portion of Reach 1 inside the Gila River floodplain indicate very recent degradation of the Hassayampa River main channel (Figure 2-87). Finally, discharge of sediment-free irrigation tailwater into the river is consistent with the occurrence of long-term scour, especially where the banks are lined with dense vegetation that reduces the chance of bank erosion.

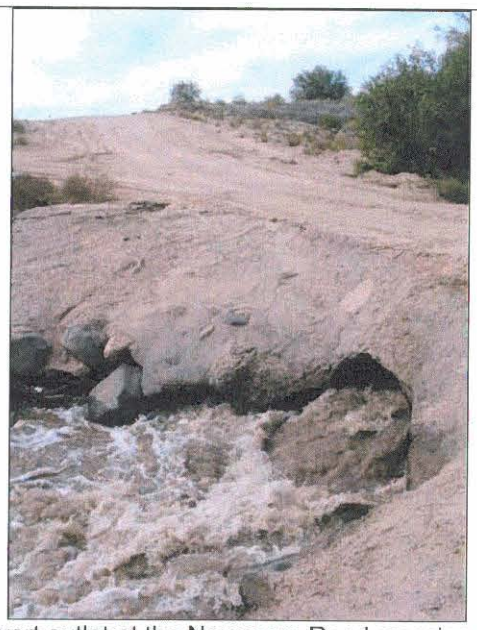

Culvert outlet at the Naramore Road crossing. View upstream.

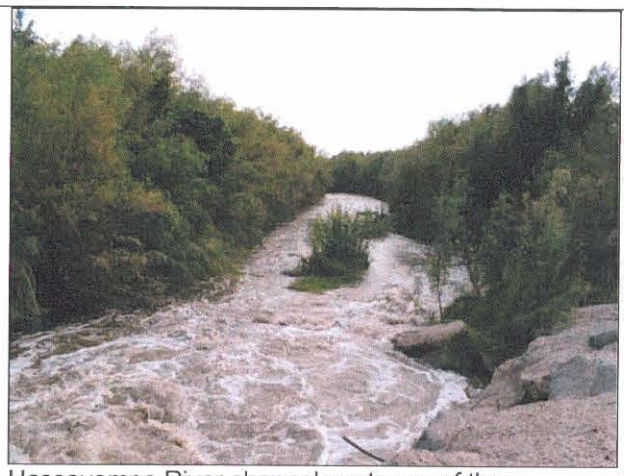

Hassayampa River channel upstream of the Naramore Road crossing. View upstream.

Figure 2-86. Hassayampa River at the Naramore Road crossing.

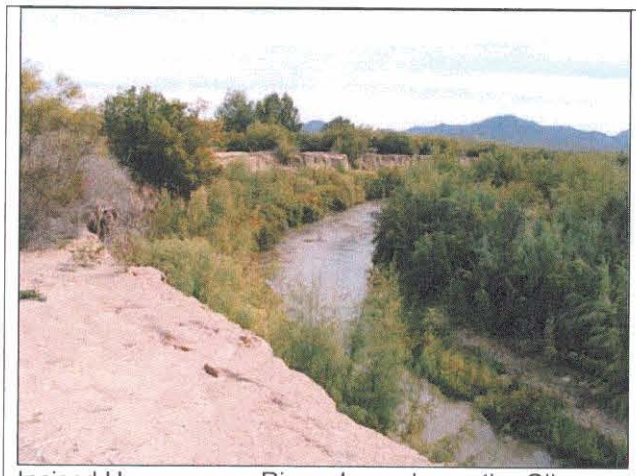

Incised Hassayampa River channel near the Gila River confluence. Note the high, vertical left cutbank. View downstream.

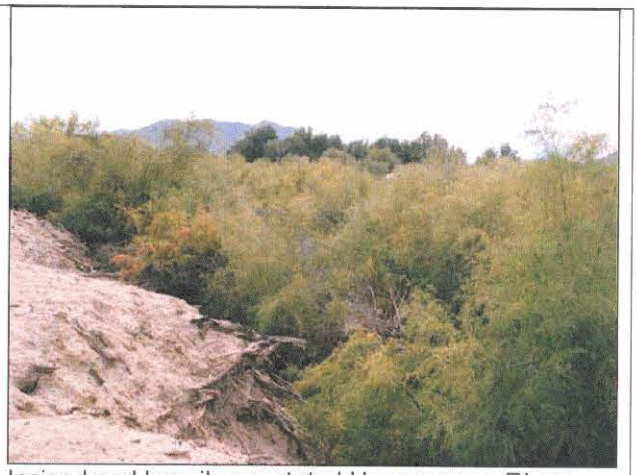

Incised and heavily vegetated Hassayampa River channel immediately downstream of the Arlington Canal. View downstream.

Figure 2-87. Photos of incised Hassayampa River near the Gila River confluence.

2.8.4 Evidence of Aggradation

Aggradation is best identified by comparison of historical topographic data and evaluation of the longitudinal profile, as is presented in Chapter 5 of this report. Field evidence of aggradation typically includes the following:

- Highly Braiding Channel Pattern
- Low Bank Heights
- Avulsive Channel Evolution
- Frequent Channel Movement

- Main Channel Elevations at or above Floodplain Elevations
- Mounding of the Active Channel (higher at channel center than margin)
- Lack of Distinct Stream Terraces Within the Geologic Floodplain
- Buried Floodplain Vegetation
- Buried Manmade Structures
- Loss of Hydraulic Capacity in Channels or at Bridges

With the exception of the loss of capacity at manmade structures, all of the characteristics commonly associated with aggradation were observed in the LHWCMP study area (See Sections 2.3 and 2.4). Furthermore, the terrace interpreted as the 1891 dam failure flood deposit was not buried and remains perched well above the 100-year floodplain. Therefore, we interpret the field evidence to suggest that while aggradation may have occurred in the study reach during much of the Holocene, the rate of aggradation has not been significant enough to impact manmade structures within an engineering time scale.

2.8.5 Natural Grade Control

No evidence of natural grade control was observed during the field reconnaissance. Bedrock may once have existed (and may still) beneath portions of Reach 1 where lava flows extend beneath the existing channel alignment, but no evidence of such outcrops were observed in the field. Other mechanisms of natural grade control, such as formation of cobble riffles or armoring, appear to be very unlikely for the Hassayampa River due to the fine-grained sediment distribution in the geologic floodplain.

2.9 Summary

The discussions in this chapter demonstrate the types of characteristics observed and recorded in the field and their relevance to the assessment of river behavior for the Lower Hassayampa River Watercourse Master Plan. The following key observations and conclusions were derived from the field reconnaissance:

- The Hassayampa River is subject to extreme rates of lateral erosion that includes rapid bank erosion, avulsive channel movement, braiding, and channel migration.

- The entire river valley between the Pleistocene-aged terraces is subject to some degree of lateral erosion hazard.

- No natural permanent barriers to lateral or vertical erosion exist along the Hassayampa River, except for a small area of bedrock outcrop on the west margin of the geologic floodplain in Reach 4.

- Avulsion appears to be a significant component of the lateral erosion history in the study reach. The wide, flat floodplain is composed of highly erosive fine-grained sediment that is vulnerable to scour wherever overbank flow concentrates, which leads for the formation of avulsive flow paths. Field evidence of recent or incipient avulsions was observed in Reaches 2, 3, 4, and 5.

- The Pleistocene-aged terraces that bound the modern geologic floodplain are

significantly more resistant to erosion that the Holocene-aged alluvium in the geologic floodplain, and therefore may provide some type of physical constraint on long-term lateral erosion.

- The Walnut Grove Dam failure flood left features such as terraces, flood deposits, and flotsam that are still visible in the landscape and apparently have not been modified by any floods in the past 115 years.

- Most of the LHWCMP is relatively undisturbed by human impacts, except in Reach 1 downstream of the SPRR Bridge.

- The few manmade structures in the floodplain have had little known impact on the Hassayampa River.

- The Hassayampa River has had relatively minor impact on structures constructed in the floodplain, except for those that attempt to cross the river at the surface (at-grade roads, canals), which get completely destroyed during moderate to large floods. Buried utilities and wide bridges have not been significantly impacted thus far. Field evidence suggests that overhead utility poles may experience scour and erosion problems in the future.

The information collected during the field investigations and introduced in this chapter was used in the subsequent Geomorphic Analysis (Chapter 3), Bed Elevation Analysis (Chapter 4), Sediment Transport Analysis (Chapter 5), Lateral Migration Analysis (Chapter 6), and the Sediment Trend Analysis (Chapter 7).

CHAPTER 3 - GEOMORPHIC ANALYSIS REPORT

3.1 Purpose

The purpose of the geomorphic analysis was to describe, interpret, and summarize the present and historical geomorphology of the Lower Hassayampa River through the following types of analyses presented in this chapter:

- Stream Classification
- Geomorphic Mapping
- Geomorphic Surface Age Analysis
- Empirical Geomorphic Relationship Evaluation

The geomorphic analysis builds on field data and interpretations presented in Chapter 2 of this report.

3.2 Stream Classification

The primary objective of stream classification is to match measurable stream characteristics with expected river responses. The following two classification systems were applied to the Lower Hassayampa River:

- Brice Classification System
- Rosgen Stream Classification System.

Data for the stream classification were obtained from field investigations, topographic mapping, aerial photographs, and published reports. Only the channel characteristics required to perform the stream classification are presented here. More detailed discussions of specific channel characteristics and specific reaches were provided in Chapter 2 of this report.

3.2.1 Brice Classification System

The Brice Classification System was developed primarily for the evaluation of stream stability near roadways and bridge structures, but is not limited to highway design applications. The Brice Classification System uses readily identified stream characteristics to make subjective predictions of lateral stability (FHWA, 1991; Brice and Blodgett, 1978). Use of the Brice Classification System is appropriate for the LHWCMP since one of the primary objectives is to assess stream stability and the potential for lateral migration.

The Brice Classification System assigns relative erosion potential classifications based on 13 stream characteristics summarized in Table 3-1. These classifications can be used to prepare a subjective, relative assessment of the potential for lateral migration. Where high or moderate potential for lateral migration is identified, more detailed analysis of lateral erosion potential is warranted.

Table 3-1. Brice Stream Classification System	
Stream Characteristic	**Lower Hassayampa River**
Stream Size	Medium *Average active channel width = 280 feet*
Flow Habit	Ephemeral
Bed & Bank Material	d_{50} = 0.5mm Stratified, non-cohesive bank material
Valley Setting	Low relief valley (< 100 feet)
Floodplain	Narrow (2-10 x channel width) *Average floodplain width = 2,504 feet*
Natural Levees	Few or no levees
Apparent Incision	Slightly incised channels
Channel Boundaries/Bank Materials	Alluvial channel boundaries *Isolated bedrock in two places*
Bank Vegetative Cover	< 50%
Sinuosity (S)	Sinuous (1.06-1.25) *Average sinuosity = 1.07*
Braiding	Locally braided (5-35%)
Anabranching	Locally anabranched
Width Variability/Bar Development	Random Variation

Each of the Brice classification system categories are discussed briefly below. More detailed descriptions of the geomorphic characteristics of the study area are provided later in this chapter.

1. Stream Size - The magnitude of lateral erosion generally increases with stream size. The Lower Hassayampa River is a medium channel and hence has a moderate potential for lateral channel movement based on its size alone.
2. Flow Habit - Perennial streams tend to experience more frequent erosion than ephemeral streams in equivalent climates. However, in arid regions where flash floods and unstable bank materials can cause significant lateral erosion, ephemeral streams are often highly erosive. The Lower Hassayampa River is ephemeral and experiences flash floods, and thus may be subject to rapid rates of lateral movement and long-term fluctuations in bed elevation.
3. Bed and Bank Material - The bed sediment distributions were consistently found to consist of poorly consolidated, layered, medium coarse sands. Bed and bank material size varied slightly depending on the geomorphic surface into which the bank was cut and only slightly with depth. Layered bank sediments were observed to increase vulnerability to scour and bank erosion to the potential for selective erosion of less resistant layers.
4. Valley Setting - Channel reaches with low valley relief (< 100 ft) typically have more erosion-prone banks than streams in valleys with high relief. The Lower Hassayampa River Valley is characterized by low relief and is entrenched between 30 to 50-foot high Pleistocene-aged terraces in most of the study area.
5. Floodplains - Channels with narrow floodplains (2-10 times channel width) typically experience less channel movement than channels with wide floodplains (>10 times channel width). The Lower Hassayampa River floodplain is on the boundary between narrow and wide. The average floodplain width is just under 10 times the average channel width. This condition suggests that moderate channel movement should be expected within the floodplain areas.

6. Natural Levees - Streams with natural levees tend to have low rates of lateral migration. The Lower Hassayampa River has few to no natural levees, thus would have a higher rate of lateral erosion than a stream with natural levees.
7. Apparent Incision - Streams with vertical cut banks are generally unstable. The Lower Hassayampa River has cutbanks throughout the study area with an average cutbank height of three to four feet. All of these banks are subject to erosion, some at greater rates than others. The rate of erosion will be greater along internal cutbanks than along the Pleistocene terraces. The Pleistocene terraces are subject to erosion by undercutting of the least consolidated of the stratified materials, or by mass wasting.
8. Channel Boundaries and Bank Materials - Alluvial streams are more susceptible to lateral erosion than non-alluvial streams. The Lower Hassayampa River Holocene floodplain is primarily composed of alluvial sediments. Bedrock is exposed in the bank at a few isolated locations upstream of Reach 1, and in the bed and bank at one location within Reach 1. Non-bedrock areas are susceptible to lateral erosion.
9. Vegetation - Streams that lack adequate vegetative cover along banks tend to be more susceptible to erosion than streams with densely vegetated banks. Dense, woody vegetation may also slow flood velocities against the banks, as well as redirect flow away from the banks. Roots can also stabilize the soils in the banks, by providing a structure that tends to hold bank materials together. Deeper and denser root networks provide greater stability than shallow, less dense roots which tend to be undercut. The Lower Hassayampa River generally has less than 50 percent bank vegetation within the study area. Few areas have dense enough bank vegetation to significantly reduce lateral erosion. Where bank vegetation exists, it tends to be shallow rooted, non-woody species.
10. Sinuosity – Sinuosity is the ratio of the valley length to the stream length. Straight streams in an alluvial valley are generally unstable if they remain straight for any significant length of time. Straight streams may also indicate entrenchment which reduces the potential for lateral erosion. Under natural conditions, a river may change its sinuosity to balance the energy between stream power and sediment load. The Lower Hassayampa River has an average sinuosity of 1.07, thus is considered sinuous and susceptible to lateral erosion.
11. Degree of Braiding - Braided streams tend to be laterally unstable. The Lower Hassayampa River alternates between a braided channel pattern and a straight channel pattern, often within a single reach. Areas with a braided pattern are thus likely to experience more rapid rates of lateral erosion that straight reaches.
12. Degree of Anabranching - The Lower Hassayampa River is anabranching locally, generally caused by an avulsion channel that has flanked the floodplain, resulting in an island feature. Anabranching streams are indicative of high rates of lateral erosion.
13. Variability of Width and Development of Bars - Streams with relatively uniform width and narrow, regular point bars tend to have slow lateral migration rates. The Lower Hassayampa River has irregular channel widths, irregular point bars, and is subject to rapid lateral migration.

According to the Brice classification scheme, the Lower Hassayampa River exhibits many characteristics that indicate it will frequently be subject to high rates of lateral

erosion. These broad stream characteristics indicate potential for frequent bank erosion and rapid lateral channel movement within the study area.

3.2.2 Rosgen Classification System

The Rosgen Classification System (Rosgen, 1996) is based on measurable channel characteristics observed on streams located primarily in the western mountain region of the United States, although the classification system is now used in many parts of North America. The Rosgen (1996) Classification System was applied to the study area because it has many adherents among State and Federal agencies in the western United States. The field survey techniques used for the study reach incorporated procedures recommended by Rosgen (1996) for obtaining channel sections, pool and riffle spacing, bankfull elevations, entrenchment ratio, slope, meander geometry, bank characteristics, and bed sediment distribution. The summary of the Rosgen classification data is listed in Table 3-2.

Table 3-2. Rosgen classification data

Lower Hassayampa River	Reach #				
	1	2	3	4	5
Entrenchment ratio	< 1.4	6.5	N/A	N/A	3.6
Width/Depth Ratio	< 12	202	321	435	580
Sinuosity	1.00	1.08	1.05	1.06	1.15
Channel Slope	0.0044	0.0041	0.0043	0.0042	0.0043
Channel Materials (d_{50})	0.5mm	0.5mm	0.5mm	0.5mm	0.5mm
Channel Pattern	Straight	Straight	Braided	Braided	Straight
Rosgen Classification	G5	D5	D5	D5	D5

Notes:
1. Sinuosity – measured on 2004 aerial photographs
2. Entrenchment ratio – Flood-prone width/bankfull width (data from HEC-RAS)
3. Width/Depth ratio – Q_2 flow width Q_2 flow depth (reach average data from HEC-RAS)
4. Channel slope – reach average of HEC-RAS S_o values
5. Channel materials – average from sieve analysis of all sediment samples

Stream classification data presented above indicate that the Lower Hassayampa River is a D5 stream in the undisturbed reaches and a G5 (gully) stream where it has been channelized and leveed. The Rosgen descriptions of D5 and G5 rivers are summarized below:

3.2.2.1 Rosgen D5 Stream (Reaches 2 to 5)

The following description of a Rosgen D5 braided stream is excerpted from *Applied River Morphology* (Rosgen, 1995):

> *The D5 stream types are multiple channel systems, described as braided streams found within broad alluvial valleys and on alluvial fans consisting of deposited sand-sized materials. The braided system consists of interconnected distributary channels formed in depositional environments. The D5 stream type occurs in gentle gradient, narrow, U-shaped glacial valleys consisting of glacio-lacustrine deposits, sand dunes (eolian); in very low relief alluvial valleys; and in glacial outwash areas and deltas. The D5 stream channels may be found in*

Valley Types III, V, VIII, IX, X, and XI[1]*. Channel bed materials are predominantly sand, with interspersed amounts of silt/clay materials on deltas and in varves of lacustrine depositional areas. The braided channel system is characterized by high bank erosion rates, excessive deposition occurring as both longitudinal and transverse bars, and annual shifts of the bed location. Bed morphology is characterized by a closely spaced series of rapids and scour pools formed by convergence/ divergence processes that are very unstable. The channels generally are of the same gradient as their parent valley. A combination of adverse conditions are responsible for channel braiding, including high sediment supply, high bank erodibility, moderately steep gradients, and very flashy runoff conditions which can vary rapidly from a base flow to an overbank flow on a frequent basis. Characteristic width/depth ratios are very high, exceeding values of 40 to 50 with values of 400 or larger often noted. D5 channel gradients are generally less than 2%, however, D5 types can also develop within alluvial fans which have slopes of 2% to 4% (D5b). Observations have been made of braided streams on alluvial fans with slopes greater than 4% (D5a). The D5 is a very high sediment supply system, and typically produces high bedload sediment yields.* *(Emphasis added.)*

The primary differences between the Reaches 2 to 5 in the Lower Hassayampa River and Rosgen's D5 category, as described above, include the following:

- Braided channel pattern – The Lower Hassayampa River is not strongly braided when examined at specific cross sections. While overall the character of the river is braided, there are many single channel sections and a limited number of mid-channel longitudinal bars typical of most braided streams. The channel cross section varies from reach to reach and within individual reaches. The pattern variability is as much a function of lateral constraints such as tributary terraces, as it is sediment supply and slope.
- Bed morphology – The Lower Hassayampa River maintains a nearly consistent bed slope throughout the study area. Although channel width is quite variable, channel bed morphology is relatively consistent. Pool/riffle sequences that Rosgen describes as the dominant bed morphology are not found in the Hassayampa River. The lack of pool/riffle sequences may be a function of the homogeneous bed load material that lacks significant amounts of cobbles and thus is not conducive to the formation of riffles.

3.2.2.2 Rosgen G5 Stream (Reach 1)

Application of the Rosgen Classification System to Reach 1 is problematic because of the level of human impacts that have been imposed on Reach 1 over the past 100 years. However, the G5 category best meets the Rosgen criteria for Reach 1, despite differences in some categories. The following description of a Rosgen G5 stream type is excerpted from *Applied River Morphology* (Rosgen, 1995):

[1] These valley types encompass the range of valley types found in the study area.

The G5 stream type is an entrenched, moderately steep, step/pool channel deeply incised in sandy materials. Channel sinuosities are relatively low, as are width/depth ratios. These "sandy gully" stream types transport great amounts of sediment due to the ease of particle detachment and fluvial entrainment. The G5 stream channels are generally in a degradation mode derived from near continuous channel adjustments, due to excessive bank erosion. Bedload transport rates can easily exceed 50% of total load; with active, extensive consistent channel erosion more typical than not. Exceptions may occur where very dense woody vegetation helps stabilize the toe of the stream bank slopes. The G5 stream type is similar to A5 channels except G5 channel gradients are less than 4% and tend to be more sinuous with somewhat higher width/depth ratios, due to the gentler channel slopes. The "slope continuum" concept is applied for the "gully" stream types if the observed reach exhibits slopes less then 2%. The lower gradient gully reaches are generally observed developing within a previously meandering, low gradient system with floodplains such as a C5 situated in wide alluvial valleys. These stream types are very sensitive to disturbance and to make significant adverse channel adjustments to changes in flow regime and sediment supply form the watershed.

The primary differences between the Reach 1 characteristics and Rosgen's G5 category, as described above, include the following:

- G5 streams typically have more sinuosity and a step/pool pattern. The channel in Reach 1 is straight and generally has few slope breaks.
- Reach 1 was probably much more braided (D5), given its previous position on the Hassayampa River confluence delta, rather than a meandering valley bottom stream theorized by Rosgen.

In general, the Rosgen system performs poorly for streams that are highly modified by human activities, which have included straightening, construction of levees, discharge of irrigation tailwater, and possible base level modifications in response to a dam failure.

3.3 Geomorphic Mapping

Analysis of a fluvial system's geomorphology is critical in understanding historical channel behavior. Geomorphic mapping was conducted for the LHWCMP study area to identify geologically recent active channel movement, historical active channel locations, and areas of historical lateral channel stability. Information describing the age of geomorphic surfaces adjacent to the stream corridor can be used to document the areas that have been subject to erosion and deposition over the past several hundred to several hundred thousand years. The techniques used to estimate the ages of geomorphic surfaces and conclusions regarding the lateral stability of Hassayampa River drawn from these estimates are described below.

3.3.1 Geomorphic Mapping and Lateral Stability

When a stream channel moves because of channel incision or lateral migration, the abandoned area may continue to be periodically inundated by floods. Flooding of the abandoned area continues until further channel incision (degradation) and/or floodplain aggradation leaves the abandoned surface above the flood-water level. Analysis of the sediment characteristics of the floodplain indicates the type of flood inundation that occurs. Active channels typically have coarser sediments such as sand, gravel and cobbles. Floodplain areas outside the main channel typically are composed of finer sediments such as sand, silt, and clay. After a stream channel moves, fine-grained sediments will be deposited over the generally coarser streambed alluvium originally left by the relocated stream.

Later, when the surfaces once subject to overbank flooding are no longer subject to inundation and sediment deposition, soil development processes modify the alluvium in the first few feet below the surface. The extent of soil development observed in the soil profile on abandoned floodplain surfaces can be used to estimate the period of time since that surface was subject to active channel processes. This period of inactivity (or soil development) defines the period of channel stability (lack of erosion and deposition) for that portion of the stream corridor, and can be used to estimate minimum rates of channel change due to lateral migration.

The following types of information can be gained from geomorphic mapping of alluvial surfaces adjacent to a stream:

- Geologic context. Geomorphic mapping provides a geologic context for expected channel change. Geologic information extends the period of record thousands to millions of years beyond the historical record. The types, rates, and scale of future channel change can then be predicted from evidence of the types, rates, and scale of channel change preserved in the geologic record.

  As shown in Figure 3-1, a minimum rate of lateral erosion for any surface can be estimated (X/Z), where X represents the width of a geomorphic surface within the river corridor, and Z represents the difference in age between two geomorphic surfaces. In addition, the total magnitude of lateral migration and vertical change can be estimated by mapping the geomorphic surfaces at a given location.

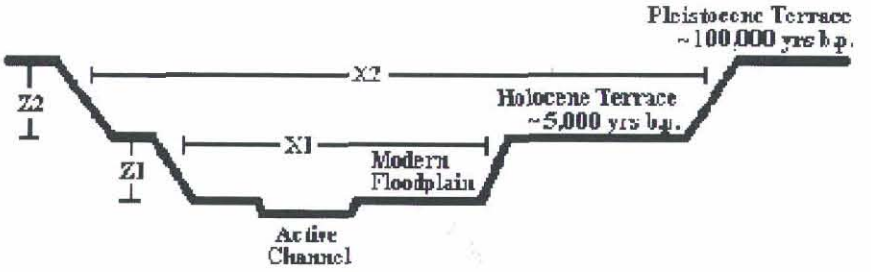

Figure 3-1. Idealized Sketch of Riverine Terraces and Ages.

- Modern anomalies. Estimated historical rates of lateral and vertical channel change (Chapter 4) can be compared to geologic information derived from mapping of geomorphic surfaces to determine if the rate of change has accelerated or slowed in modern times. If the historical rate of change is significantly different than the long-term geological rate of change, an investigation of potential human impacts on the rate of change may be warranted.

- Limits of channel change. The limits (magnitude) of channel processes preserved in the geologic record may indicate physical boundaries for future channel movement. At minimum, geologic evidence of no change on a geomorphic surface over long periods of time indicates a low probability of future change on that surface, unless a clear cause for future change can be identified.

- Channel processes. Geologic information can often provide a record of the types of stream and geomorphic processes active in a stream reach that have been obscured by historical or human interference. For example, soil data can be used to identify currently single channel reaches that are or were subject to avulsions, or that formerly had a braided channel pattern.

- Flood hazards. Geologic information can be readily used to identify surfaces subject to frequent flood inundation and sediment deposition, as well as surfaces that have not been affected by flooding for thousands to millions of years. If soil characteristics have developed, then that surface has not been subject to significant flood inundation or deposition by the active stream over the amount of time necessary to produce those soil characteristics. If a surface has not been inundated for a long period of time, the implication is that a human structure erected on that surface is less likely to be harmed during the inevitable flood events than a structure built on a surface whose surficial characteristics indicate that it is frequently flooded.

3.3.2 Methodology

The geomorphic analysis for this study was conducted using both field and desktop methods. Geomorphic surfaces comprising the Holocene floodplain were initially mapped using the following data sources:

- Previous Geologic Mapping

- Aerial Photography
- Topographic Data

The initial mapping was then tested and confirmed using field data and the results of the soil pit analyses. Field evidence was described in detail in Chapter 2, and included such information as relative topographic position, surficial characteristics, drainage pattern, fluvial channel and floodplain features, sediment size, vegetative suites, and evidence of surficial age.

3.3.2.1 Previous Geologic Mapping

The Arizona Geological Survey (AZGS) published surficial geologic mapping for a portion of the White Tank Mountains in November of 1991. The mapping scale was 1:24,000 and limited to the following USGS quadrangle extents: Daggs Tank, White Tank Mountains NE, McMicken Dam, Wagner Wash Well, White Tank Mountains, Waddell, Buckeye NW, Valencia, and Perryville. The AZGS maps depict the general ages and distribution of the Quaternary geomorphic surfaces adjacent to the White Tank Mountains. Three of these maps (Daggs Tank, Wagner Wash Well, and Buckeye NW) were reviewed and revised by AZGS in 2004 as part of the general geologic map revisions. Additional geologic maps relevant to the Hassayampa River drafted in 2004 included the Vulture Mine and Wickenburg SW quadrangles.

The revised AZGS surficial geology maps segregate the Hassayampa River valley deposits into five primary geomorphic units described below[2] in order from the youngest to the oldest:

> *Qycr – Active River Channel Deposits*
> *Moderately to poorly sorted sand, gravel and minor silt in active channels of the Hassayampa River. Gravel includes subangular to well-rounded clasts.*
>
> *Qy_2r – Late Holocene to Modern Floodplain Deposits*
> *Sand, silt, and gravel deposits associated with slightly higher terraces along the Hassayampa River. Terrace surfaces are smooth and are less than 3 m above the active channel. Terrace surfaces are covered with fine-grained floodplain deposits, but relict gravel bars and lenses are common.*
>
> *Qi_2r – Middle to Late Pleistocene River Deposits*
> *Older terrace deposits of very limited extent found in a few places along the Hassayampa River. Deposits are gravelly with some sand, silt, and clay. Soil development is moderate with some clay accumulation where terrace surfaces are well preserved. Terrace surfaces typically are less than 10 m above the active river channel.*
>
> *Qi_1r – Middle Pleistocene River Deposits*
> *Deposits associated with a set of high terraces along the Hassayampa River. Terraces are fairly flat or slope gently toward the river, but terrace surfaces are*

[2] Descriptions from: Ferguson, C.A., J.E. Spencer, P.A. Pearthree, A. Youberg, and J.J. Field, 2004, *Geologic Map of the Wagner Wash Well 7.5' Quadrangle, Maricopa County, Arizona*: Arizona Geological Survey Digital Geologic Map 38 (DGM-38), 7p., 1 sheet, scale 1:24,000.

dissected by tributary drainage. Deposits are quite gravelly at the surface but limited exposures indicate that they also contain sand and silt. Qi_1r terrace surfaces range from about 10 to 20 m above the active river channel.

Qor – Early Pleistocene River Deposits
Deposits associated with the high terraces along the Hassayampa River that record the maximum aggradation of the river. Terrace surfaces are fairly flat or broadly rounded, but all terrace surfaces are moderately to deeply dissected by tributary drainages and the river and have been substantially modified by erosion. Exposures are poor, but well-rounded gravel is evident at the surface. Terrace surfaces are also covered with litter from underlying petrocalcic soil horizons. Qor terrace surfaces are more extensive than any of the younger Pleistocene terraces (Qi_1r). Terrace surfaces range from about 20 to 30 m above the active river channel.

QTsr – Pliocene to early Pleistocene river deposits
A moderately thick sequence of old Hassayampa River deposits that underlies the Qor terrace/fan deposits. These deposits consist of river sand, gravel and silt with a substantial component of tributary sand and gravel. Local zones of substantial carbonate accumulation may represent moderately to strongly developed buried soils.

The Qycr and Qy_2r units described above represent the Hassayampa River Holocene floodplain. At a scale of 1:24,000 it is difficult to map the Holocene geomorphology in greater detail than is shown on the AZGS maps. The geomorphic analysis conducted for the LHWCMP study divided the Holocene floodplain into five distinct units which are described later in this chapter.

3.3.2.2 Aerial Photography

2004 color and 2003 black and white digital orthophotography provided the foundation for the geomorphic analysis. Initial geomorphic units were distinguished and delineated from the digital photography and later refined by field investigation and verification. Additional interpretation of specific surfaces was done using 2002 black & white stereo aerial photograph prints.

3.3.2.3 Field Investigation

Geomorphic interpretations and delineations made using aerial photography were verified in the field using the field methods described in detail in Chapter 2, and the soil analysis techniques discussed below.

3.3.3 Geomorphic Units

Throughout much of the study reach the Hassayampa River corridor is flanked by high (20 to 90 ft) Pleistocene terraces described by the AZGS as Qor and QTsr units. The relatively high relief of these terraces from the active river corridor suggests the Hassayampa River has been generally constrained within these surfaces at least throughout the Holocene (10,000 yrs B.P.). The Holocene river corridor was the

primary focus of the River Behavior Analysis. Therefore, the geomorphic mapping investigation focused on the surfaces within the Holocene floodplain.

The following seven geomorphic units were interpreted and described in the geomorphic analysis, and were distinguished based on their geomorphic function in the fluvial system:

- Active Channel Deposits
- Bar Deposits
- Terrace Deposits (Low, High, & Unidentified)
- Tributary Deposits
- Disturbed Areas

Each of the units is described below. The descriptions are based on the results of the field investigation and aerial photograph interpretation.

3.3.3.1 Active Channel Deposits

Qac – Active Channel

The Qac unit is found in the primary low-flow channel and channel braids. The Qac width varies from approximately 900 feet at the sand and gravel mine upstream of the Tonopah-Salome Highway to about 100 feet in Reach 4. Vegetation is generally very sparse to absent and varies in density by season. When present, vegetation consists almost exclusively of desert dicoria. Throughout the photographic record, the active channel varied in areal extent and lateral position. Flooding occurs most frequently within the active channel area, which also serves as the primary sediment transport corridor. The active channel is the topographically lowest feature within the Holocene floodplain and is the primary conveyance for both high and low frequency flows. Active channel sediment consists of moderately- to poorly-sorted medium-coarse sand, with less than five percent gravel. The Qac unit corresponds to a portion of the AZGS Qycr unit. The Qac unit comprises 6% of the Holocene floodplain.

Figure 3-2. Field photographs of active channel surfaces.

3.3.3.2 Bar Deposits

Qy_2a – Active Bar Deposits

Active bar deposits occur both within and adjacent to the active channel banks. Several avulsion channels with characteristics similar to the active bar deposits were also mapped as Qy_2a surfaces. Qy_2a surfaces are fluvially sculpted and often contain fresh flotsam. The Qy_2a bars are typically less than three feet above the active channel bed. Avulsion channels range between one and four feet above the active channel. Vegetation is composed of grasses, snakeweed, and other low brush species, and vegetation density is sparse. The active bars serve as sediment storage areas and are utilized as active sediment transport material during high frequency flows. Sediment in the Qy_2a surfaces is generally very coarse sand with minor gravels, and usually somewhat coarser than active channel deposits. The Qy_2a unit corresponds to the AZGS Qycr unit. The Qy_2a unit comprises 8% of the total mapped Holocene floodplain.

Figure 3-3. Field photographs of active bar surfaces.

3.3.3.3 Terrace Deposits

Qy_2 – Low Terrace Deposits

Qy_2 terraces comprise the active floodplain which is inundated during relatively frequent floods. These surfaces comprise both lateral and in-channel island terraces and are typically between two to four feet above the active channel bed. The terrace surfaces are fluvially sculpted, littered with flotsam and are soft (not compacted). Surface texture is generally hummocky. Shallow, overbank flood channels are frequently observed on Qy_2 surfaces. Vegetation typically consists of snakeweed, grasses with immature Palo Verde, mesquite, and creosote bush often present. Cactus are consistently absent from Qy_2 terraces, probably because of the frequency of inundation. Vegetation density varies from sparse to dense. In major tributary confluence areas, vegetation was often significantly denser and larger in size. Qy_2 terraces function as floodplains and fine-grain sediment transport and deposition zones during floods. Qy_2 sediments are comprised of very fine to fine floodplain sands and silts often capping coarser sands at depths varying from several inches to more than a foot. The Qy_2 unit corresponds to the AZGS Qy_2r unit. The Qy_2 unit comprises about 20% of the mapped Holocene floodplain.

Figure 3-4. Field photographs of low terrace surfaces.

Qy_1 – High Terrace Deposit

These terraces generally contain mature, moderately dense to dense vegetation cover. They are subject to inundation during moderately frequent to infrequent flood events, and are primarily a depositional surface. They are subject to active lateral erosion when directly adjacent to the active channel. Qy_1 surfaces function as floodplain storage and deposition areas during high flows, providing attenuation and overbank storage. Qy_1 terraces sometimes occur as in-channel islands formed during large magnitude flood events due to avulsions that flank the surfaces. The surficial characteristics include the presence of cryptogamic soil, firm compacted alluvium, moderately dissected internal drainage pattern, and sediment buildup (or lack of deflation) around vegetation. Vegetation includes snakeweed, desert broom, Bermuda grasses, creosote, mature mesquite and Palo Verde, saguaro, and cholla. The Qy_1 unit corresponds to the AZGS Qy_2r unit. The Qy_1 unit comprises about 13 % of the mapped Holocene floodplain.

Figure 3-5. Field photograph of high terrace surface.

Qy – Unidentifiable Deposit

Qy deposits exhibited evidence of anthropogenic disturbance within the photographic record. The disturbance was generally the result of agricultural development. These

surfaces have typically been topographically modified and natural vegetation as been removed. The surfaces may function as floodplains during low frequency, high magnitude flood events providing overbank storage, flow attenuation, and sediment deposition. The Qy unit corresponds to the AZGS Qy_2r unit. The Qy unit comprises about 16 % of the mapped Holocene floodplain.

3.3.3.4 Tributary Deposits

Qt – Tributary Deposit

Qt surfaces represent the outer-limits of the Holocene geologic floodplain and generally formed lateral to the active channel corridor. The deposits are composed of features such as alluvial fans, fan terraces, or deltaic features which often provide some degree of lateral control of the active channel corridor movement. At multiple locations within the study reach, tributary sediment inflows have historically been greater in volume and frequency than the Hassayampa River transport capacity. Thus, tributary deposits effectively control the location of the Hassayampa River active channel location and provide a measure of lateral stability (e.g., Jackrabbit Wash delta). Field evidence suggests that tributary deposits can be eroded by large magnitude, low frequency flow events, but apparently re-form faster than they are removed by the main stem. Surface characteristics of the Qt surface include hummocky terrain, cryptogamic soil, firm sediments, and a surficial gravel lag deposit. The presence of gravel lag may suggest tributary deposits exclusively or very limited (non-recent) contribution by the main stem stream. Vegetation on the Qt surface include creosote bush (often exclusively), mesquite, Palo Verde, saguaro, and cholla. The Qt unit corresponds to the AZGS Qy_2r and Ql_2r units. The Qt unit comprises about 34 % of the mapped Holocene floodplain.

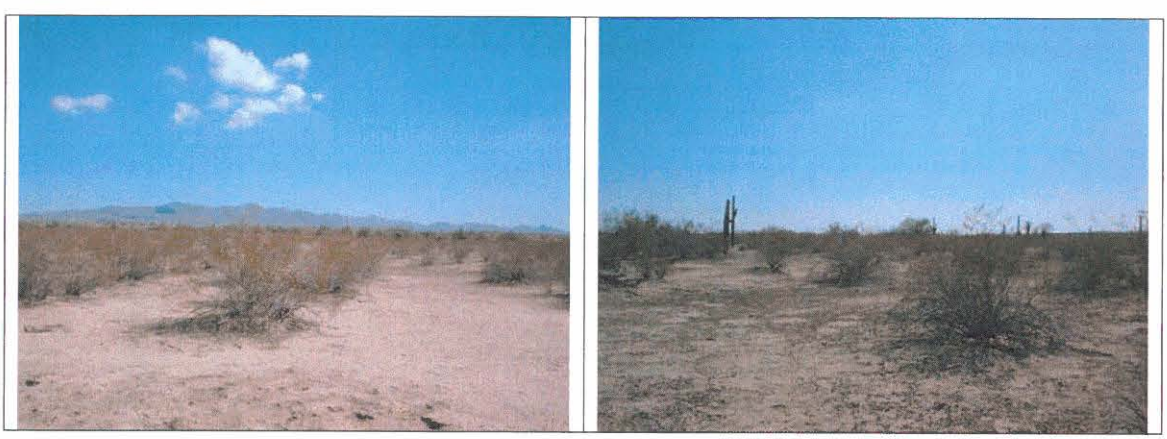

Figure 3-6. Field photographs of tributary deposit surfaces.

3.3.3.5 Disturbed Areas

d – Disturbed Areas

Areas mapped as disturbed are characterized by surficial disturbances that have occurred within the photographic record. Disturbance consisted of mining, construction of engineered structures, or channel improvements. An example is the channelization and levee construction subreach downstream of the Old U.S. Highway 80 Bridge. The d unit comprises about 3 % of the mapped Holocene floodplain.

3.4 Geomorphic Surface Age Analysis

Geomorphic surfaces identified and described in Section 3.3.3 were mapped based on surficial features observed in the field and interpreted from aerial photographs, supplemented by previous mapping by others. Soil profile descriptions were made to estimate the relative age of each of the surfaces described above, and to verify the interpretations made as part of the geomorphic mapping effort. Surface age estimates were based on the degree of soil development observed in soil profiles, in conjunction with the degree of development of the surficial features described above.

3.4.1.1 Soil Development

The physical characteristics of a landform or geomorphic surface give clues as to its depositional history, stability, and its flood potential. As a landform ceases to receive new deposits, its surface will begin to age. As it ages, the surface begins to develop distinctive physical and chemical characteristics indicative of its age. Clay and calcium carbonate accumulate in the soil, causing the soil to redden (clay) and become more cemented (carbonate) and resistant to erosion. Soil color also may change with time. Older desert soil horizons typically develop a more reddish color near the surface where minerals can be oxidized and a whitish color below the reddish horizons where calcium carbonate accumulates. The color change becomes greater over time, such that material that is tan or gray will become more red or white with increased soil age. The following major divisions within a soil are usually distinguished (Birkeland, 1984):

- O Horizon. The O horizon occurs and near at the ground surface, and consists of a surface accumulation of mainly organic matter.
- A Horizon. The A horizon occurs at or near the ground surface, and is the zone from which fine-grained or water-soluble material is transported. The A horizon often has higher organic content due to decay of surficial biotic matter.
- B Horizon. The B horizon occurs where fine-grained or water-soluble material accumulates from weathering of parent material or by translocation from the upper horizons. Clay (Bt) and carbonate (Bk) are the most common materials that are observed in arid region soils.
- K Horizon. The K horizon is a layer so impregnated with carbonate that its morphology is determined by the carbonate.
- C Horizon. The C horizon consists of slightly weathered to unweathered parent material.

O Horizon

No appreciable O horizons were observed in the soil pits in the study area due primarily to the very low vegetative density, aeolian and fluvial processes that tend to preserve bare soils, and the low moisture content.

A Horizon

The A horizons observed in the soil pits in the study area typically tended to be very thin or non-existent due to the arid climate, low precipitation and infiltration rates, the sparse surface vegetation, and slow rate of decay of biotic material. No appreciable

differences between the few, thin A horizons and the upper B horizon layers were observed.

B Horizon

Clay Accumulation

In Bt horizons, clay accumulation increases with time. In addition to the clay present initially in a deposit, clay forms over time from the chemical and physical weathering of the alluvium within a soil (pedogenic clay). Clay is also introduced into soils of desert regions as windblown dust (eolian clay). Aeolian and pedogenic clay is moved downward in a soil column by infiltrating rainfall or floodwater, and may be deposited as clay films on the faces of individual peds, in pores between soil grains, or as a bulk increase in clay content at a certain depth (Birkeland et al., 1991). Descriptions of the texture and clay films in soil layers allow for the detection of an increase in clay content. Given enough time, the increase in clay content or other soil constituents commonly causes the development of soil structure in the B horizon (Birkeland et al., 1991). The shape and size of the soil structure reflects the time since development began (soil age), the materials in which the structure developed, and the regional climate (Birkeland, 1984). The soil structure becomes more strongly developed with time.

In the study area, a loamy sand texture is characteristic of young (Holocene) soils and may vary to sandy or silty clay loams in Pleistocene soils. None of the soil profiles described for this study had strong Bt horizons or significant clay content, although the tributary terraces typically had more clay accumulation than any floodplain soil.

Calcium Carbonate

In Bk horizons, carbonate accumulates in soil profiles from aeolian sources and is driven into the profile by rainfall infiltration. In the desert soils of the Southwest, the amount of calcium carbonate ($CaCO_3$) in a soil layer can be used to estimate the period of time over which the carbonate accumulated. The degree of carbonate development is assigned a stage, with Stage I representing incipient (youngest) soil formation, and Stage VI representing maximum (oldest) accumulation of carbonate (Birkeland et al., 1991). The accumulation can be compared with other soils of known age and similar environment to estimate the soil age (Birkeland, 1984; Machette, 1985) and the age of the geomorphic surface. The degree of carbonate accumulation is measured by the reaction of the soil to the application of dilute hydrochloric acid (HCl), by the rind thickness which occurs on gravel clasts, or by the interval of maximum carbonate cementation. The gravel content of the soil must be considered when evaluating carbonate development, since carbonate accumulates more quickly in coarse alluvium than in fine alluvium. The most advanced stages of carbonate development often form very cohesive soils that may resemble bedrock in appearance and relative hardness. Advanced stages of $CaCO_3$ can provide resistance to lateral bank erosion.

In the study area, some carbonate accumulation was observed in some soil pit profiles, although no carbonate stage greater than I+ was observed in any soil pit, even in the older tributary terrace units. In addition, the native parent soils materials, like all soils in the western Maricopa County have high baseline levels of carbonate. The lack of strong Bk horizons is evidence of young geomorphic age.

C Horizon

The parent material comprising a C horizon in the LHWCMP study area is floodplain and channel alluvium deposited by the Hassayampa River. It is possible that a C horizon was present in the soil pits analyzed. However, given the young age of the soils within the geologic floodplain areas tested, there was insufficient soil development to distinguish parent materials from the soils above them.

3.4.1.2 Soil Pit Analyses

Twenty five locations within the LHWCMP study area were identified as candidates for a soil pit evaluation. The primary purpose of the soils analysis was to determine the relative age of the geomorphic surfaces within the Lower Hassayampa River geologic floodplain in an effort to interpret the extent of historical lateral migration. The secondary purposes of the soils analysis were to identify geomorphic surfaces based on their sedimentary composition, and to collect sediment samples for the sediment transport analysis (Chapter 5). Eleven of the pits were located in the overbank and floodplain areas, and the remaining 14 were located in the active channel. The selection criteria for each location varied, but were generally based on aerial photo interpretations, initial field observations, and geomorphic relationship uncertainties. Figure 3-7 shows a location map of the soil pits and their respective ID numbers.

The soil pit footprint dimensions were approximately 3 feet by 8 feet and the average depth was 6.6 feet. Soil characteristic information collected included: color, structure, percent gravel, moisture consistence, texture, presence of clay films, soil layer boundary type and clarity, presence and degree of development of $CaCO_3$, shear strength, and relative resistance. Table 3-3 summarizes the soil data collected for each soil pit. Detailed soil description sheets for each pit are attached in Appendix 5.2.

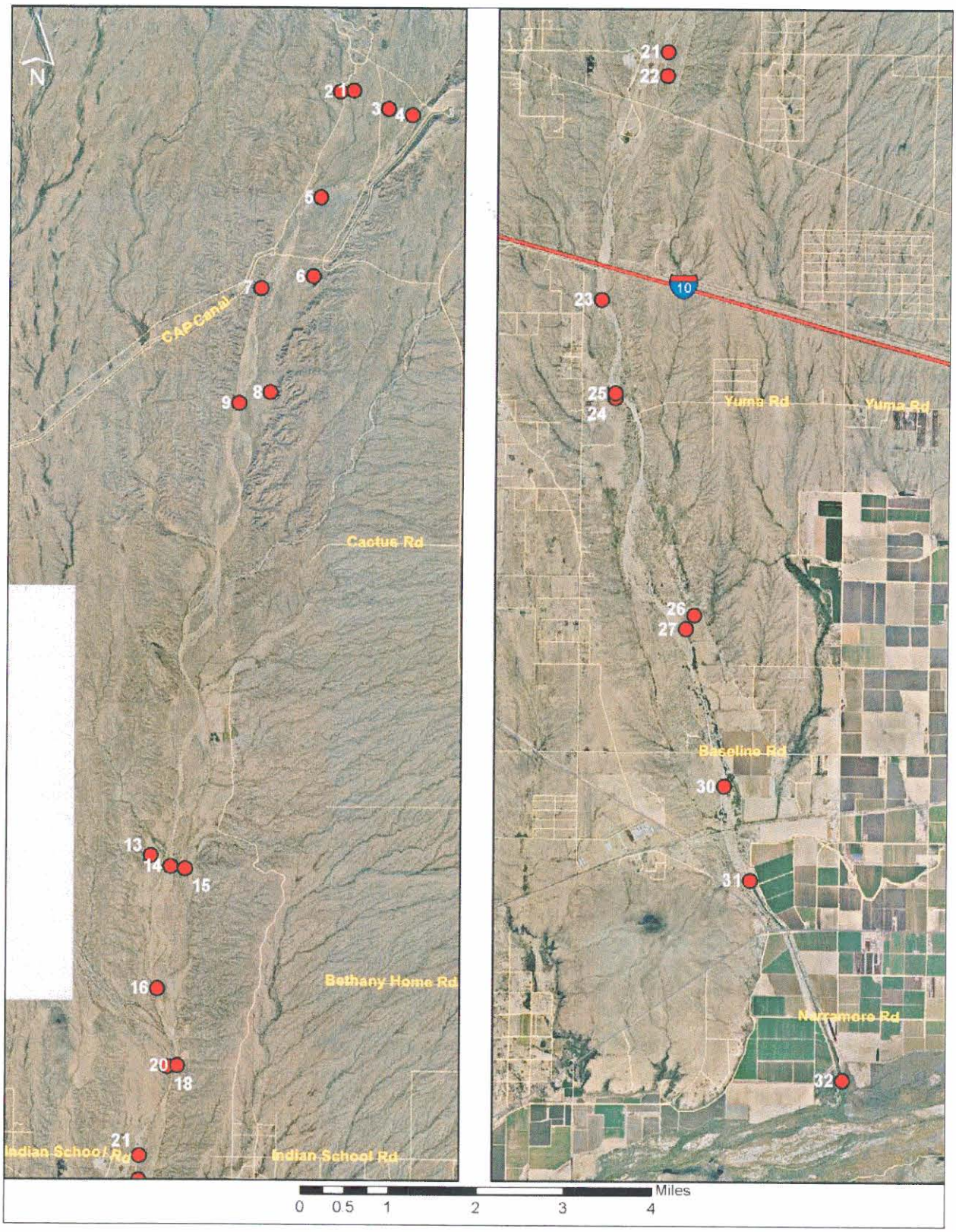

Figure 3-7. Soil pit location map

Table 3-3. Soil analysis summary

Pit ID	Surface	Purpose	Summary
1	Qy1	Determine depth to active channel deposits, if present. Verify the down-slope extent of the tributary deposits. Determine relative frequency of inundation, and depositional energy environment.	Sediments were composed of loose loamy sand and sand with minor traces of gravel. Minor traces of clay and $CaCO_3$. Brownish colors, no reddening. No evidence of geologic age.

Pre-excavation surface

Pit profile

Spoil material

Pit ID	Surface	Purpose	Summary
2	Qt	Determine the max lateral extent of Hassayampa River deposits and the inter-fingering relationship of Hassayampa deposits and the tributary deposits.	Sediments were composed of loamy sand. Higher gravel content than Pit 1. Very minor clay accumulation. Stage I+ $CaCO_3$ below 1.7ft from top of pit. Brownish colors, no reddening. Slightly older than Pit 1, but geologically young.

Pre-excavation surface

Pit profile

Spoil material

Pit ID	Surface	Purpose	Summary

Table 3-3. Soil analysis summary

3	Qy1	Determine the frequency of flood inundation and the depth to active channel deposits.	Sediments were composed of mostly loose sand. Minor (≤10%) gravel present in lower bottom 2 feet of pit profile. Very minor traces of clay. Stage I $CaCO_3$ development in lower 2 feet of profile. Brownish colors, no reddening. No active channel deposits present, all floodplain sediments. Geologically young surface.

Pre-excavation surface

Pit profile

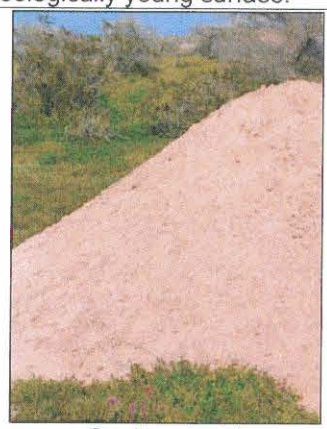
Spoil material

Pit ID	Surface	Purpose	Summary
6	Qy1	Determine the thickness of the 1890 flood deposit and the depth to active channel deposits.	Sediments were composed mostly of loamy sand. Sparse to no gravel content. Traces of clay in mid-layer. Brownish colors, no reddening. 1890 deposit approx 1.5 ft thick. Minor $CaCO_3$ accumulation in lower 4 feet of profile. Stage I+ $CaCO_3$ in bottom layer. Geologically young surface.

Pre-excavation surface

Pit profile

Spoil material

Pit ID	Surface	Purpose	Summary

Table 3-3. Soil analysis summary

8	Qy1	Determine if the surface sediments are from the 1890 deposit. Identify depositional history.	Sediments were composed of primarily loamy sand, with minor loam. Base profile is sand. Minor clay present in center of profile, no clay in upper and base of profile. Brownish colors, no reddening. Upper 3.5 feet of profile is 1890-like sediments. Basal layer (1.4 feet thick) is active channel sediments. Geologically young surface.

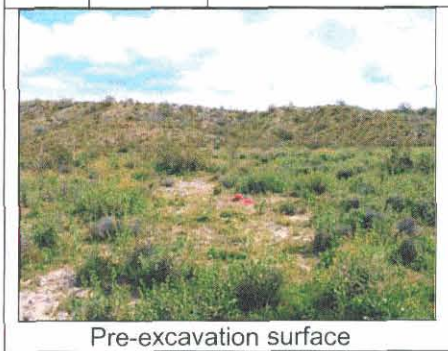
Pre-excavation surface

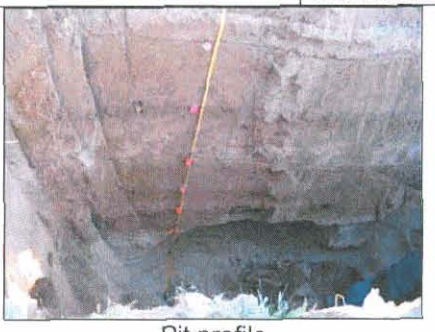
Pit profile

Spoil material

Pit ID	Surface	Purpose	Summary
13	Qt	Determine the relationship between the tributary deposits and Hassayampa deposits and identify deposition history.	Sediments were composed primarily of loam with minor clay loam. Traces of gravel (≤10%) present throughout the profile. Higher clay content than Hassayampa deposits. Stage 1+ $CaCO_3$ development throughout profile suggesting infrequent inundation. Slight reddening in color. No evidence of Hassayampa deposits in the profile.

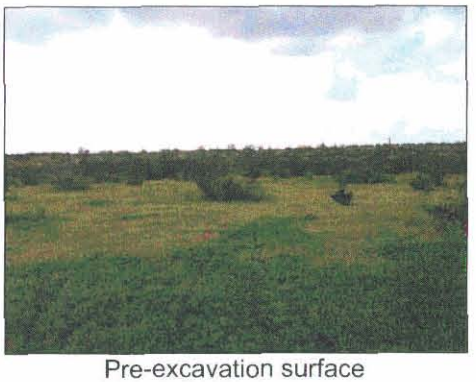
Pre-excavation surface

Pit profile

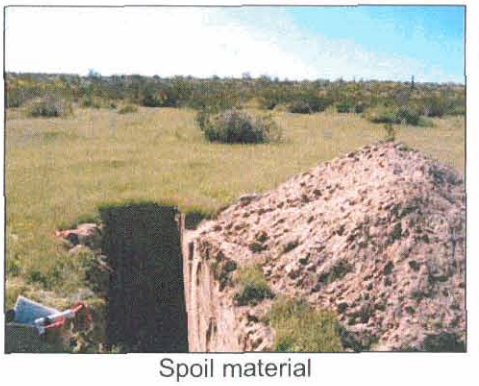
Spoil material

Pit ID	Surface	Purpose	Summary

Table 3-3. Soil analysis summary

15	Qy1	Confirm the age of the surface.	Sediments were composed of loamy sand with minor silty loam near base of profile. No clay present in profile except for very minor traces in lower 1.1 foot thick layer. Very minor traces of gravel scattered throughout profile. Basal 0.8 foot thick layer may be active channel deposit, all else is floodplain. Brownish colors, no reddening. Geologically young surface.

Pre-excavation surface

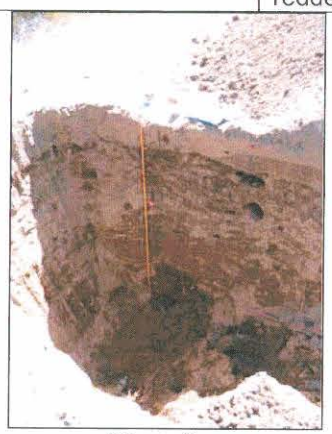
Pit profile

Spoil material

Pit ID	Surface	Purpose	Summary
18	Qy1	Determine the inundation frequency of the Jackrabbit Wash (JW) delta by the Hassayampa River (HR).	Sediments composed of alternating loamy sand and sand. Loamy sand is HR floodplain deposits, sand is JW deposits. Sand layers contain more gravel. No clay present in profile. Brownish colors, no reddening. Both had weak $CaCO_3$ development, but HR deposits had slightly higher accumulation of $CaCO_3$. No evidence of HR active channel. JW is dominant aggrading source. Geologically young surface.

Pre-excavation surface

Pit profile

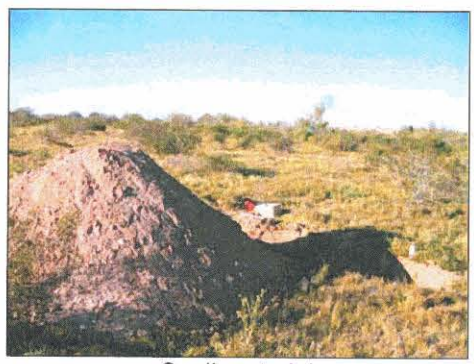
Spoil material

Pit ID	Surface	Purpose	Summary

Table 3-3. Soil analysis summary

22	Qy1	The surface is an island surrounded by active channels. Vegetation suggests the surface is inundated infrequently. Use soils to determine relative age.	Sediments were alternating loamy sand and sand suggesting near-channel floodplain processes. Gravel content was generally ≤10% with a few layers at 50%. Very minor traces of clay present in a few layers. All layers are brownish in color, no reddening. Minor traces of $CaCO_3$ accumulation, stage 1+ in lower 1 foot thick layer. All evidence suggests geologically young surface.

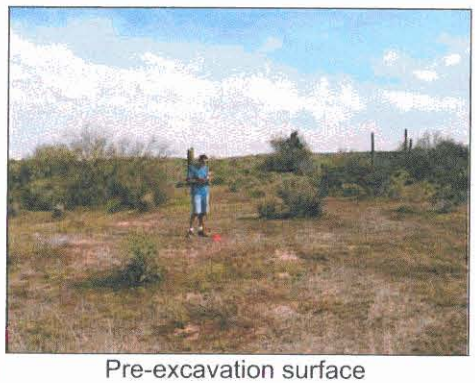
Pre-excavation surface

Pit profile

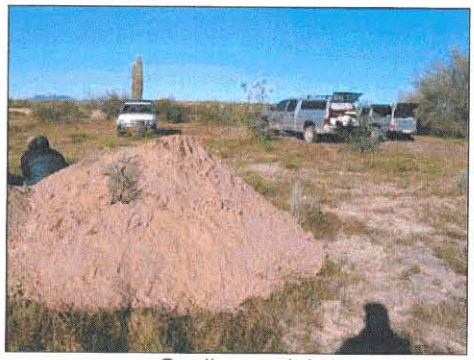
Spoil material

Pit ID	Surface	Purpose	Summary
24	Qy2	The surface forms a vertical cutbank adjacent to the active channel. Determine the inundation history of the surface and resistance to lateral erosion.	Sediments were alternating loamy sand and sand, with the lower profile more sandy. Gravel was ≤10% throughout the profile. No clay present. Brownish colors, no reddening. Very minor $CaCO_3$ accumulation throughout profile. Evidence suggests geologically young surface, historically frequent inundation. No resistance to lateral erosion.

Pre-excavation surface

Pit profile

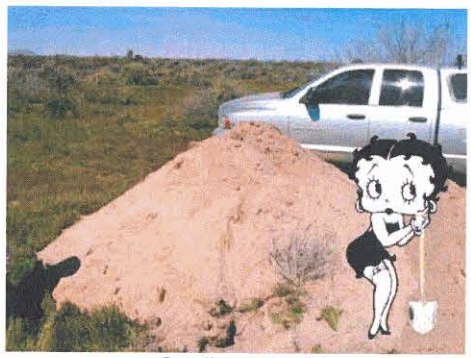
Spoil material

Pit ID	Surface	Purpose	Summary

Table 3-3. Soil analysis summary

26	Qt	Mapped by the AZGS an unknown. Determine inundation history and relative age.	Sediments were silty loam and loam, massive, no layering. Surface was agricultural use since at least the 1930s, thus sediments are highly disturbed. Gravel content was ≤10%. Moderate clay content and $CaCO_3$ accumulation (stage 1+), however, irrigation likely caused accelerated clay and $CaCO_3$ accumulation. Colors were brownish, no reddening. Degree of disturbance makes age estimate difficult. No evidence of recent inundation and floodplain deposition.

Pre-excavation surface

Pit profile *(camera lens partially closed)*

Spoil material *(camera lens partially closed)*

Pit ID	Surface	Purpose	Summary
In-Channel Pits	Qac	Sediment sampling for sieve analysis for sediment transport modeling.	Active channel sediments were consistent throughout the entire study reach. Sediments were composed of coarse sand, massive in structure. Gravel content was very low for most of the study reach. Gravel content increased slightly in reaches downstream of tributaries. Depth to reddish-clay rich layer varied from 1.5 feet to 3.5 feet.

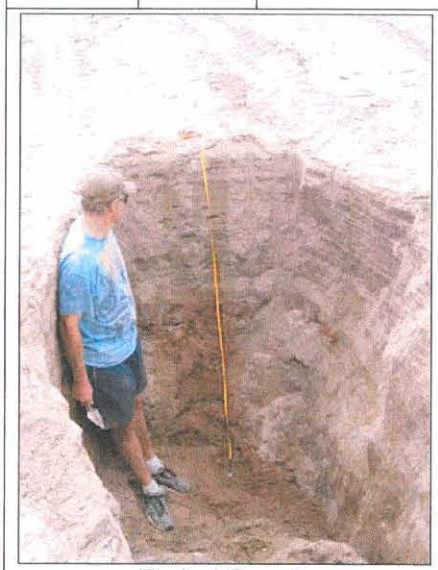

Typical Qac pit

Collecting sediment sample

Reddish layer in pit profile

3.4.2 Results

The results of the geomorphic mapping and soils analyses described above are shown in Figure 3-8 to Figure 3-13 and (Appendix 5.3). The following conclusions can be drawn from the geomorphic mapping:

- There is no evidence of surface stability within the geologic floodplain of the Lower Hassayampa River. Of the 11 soil pits that were excavated in the overbanks and floodplain, none indicated evidence of geologic age greater than 1,000 years, and most surfaces except the tributary terrace deposits have ages less than 100 years.

- Stratigraphic analysis of the alluvium examined in the soil pits indicates that the active channel of the Lower Hassayampa River actively migrates across the geologic floodplain within very recent geologic time.

- No evidence indicating erosion resistance in the soils that comprise the geomorphic surfaces in the geologic floodplain was found.

- Active channel processes occur across the entire river valley over time, without preference for one side or the other.

- Major tributary sediment supply has a significant local impact on channel morphology as well as the distribution of geomorphic surfaces within the geologic floodplain near the tributary confluence.

- The zone of influence of tributary sedimentation is relatively limited and does not appear to extend downstream of the confluences more than one mile.

- There appear to be significant changes in geomorphic surface distribution upstream of Reach 5, as well as at the Gila River confluence in Reach 1.

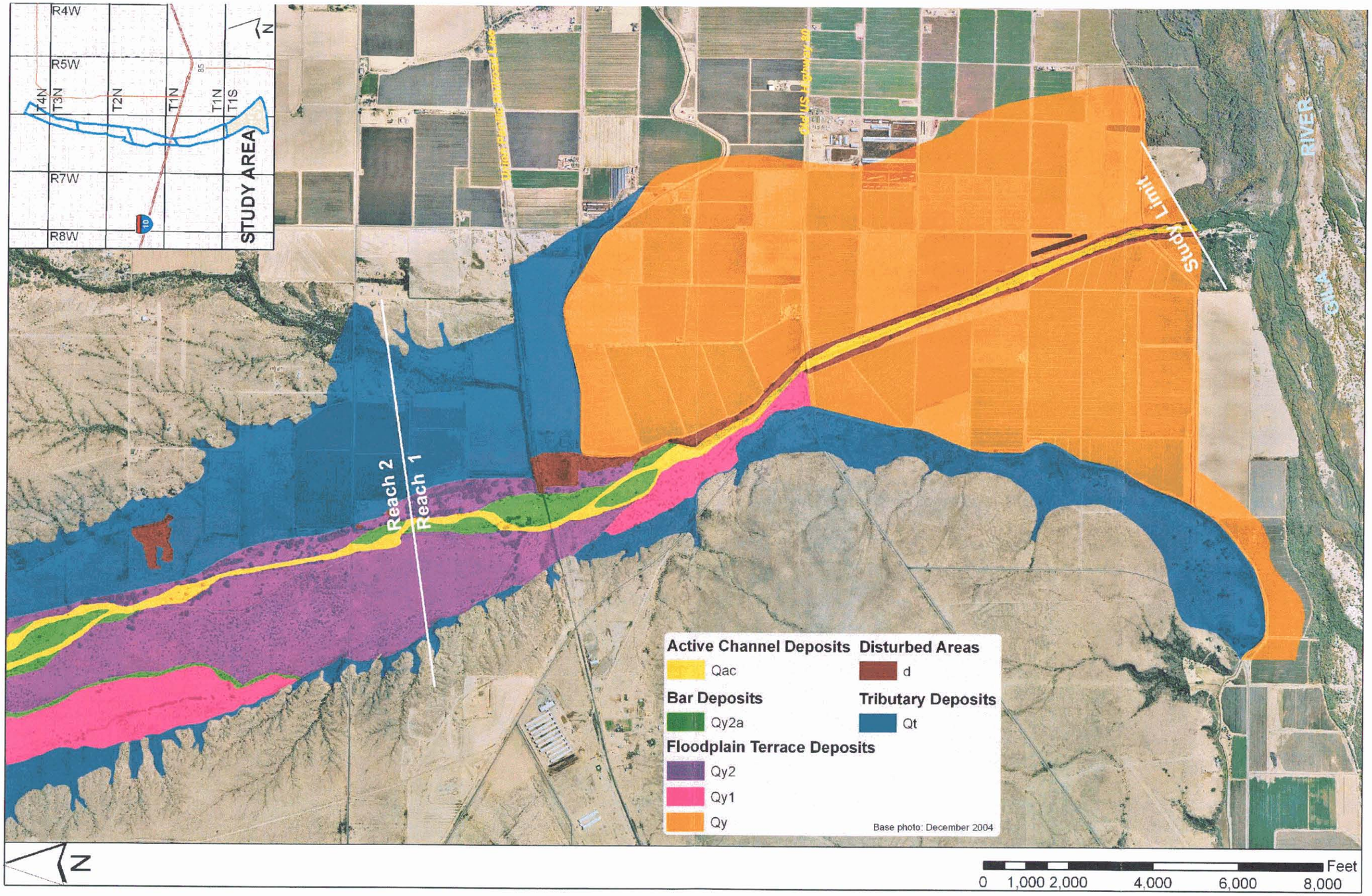

Figure 3-8. Reach 1 mapped geomorphology

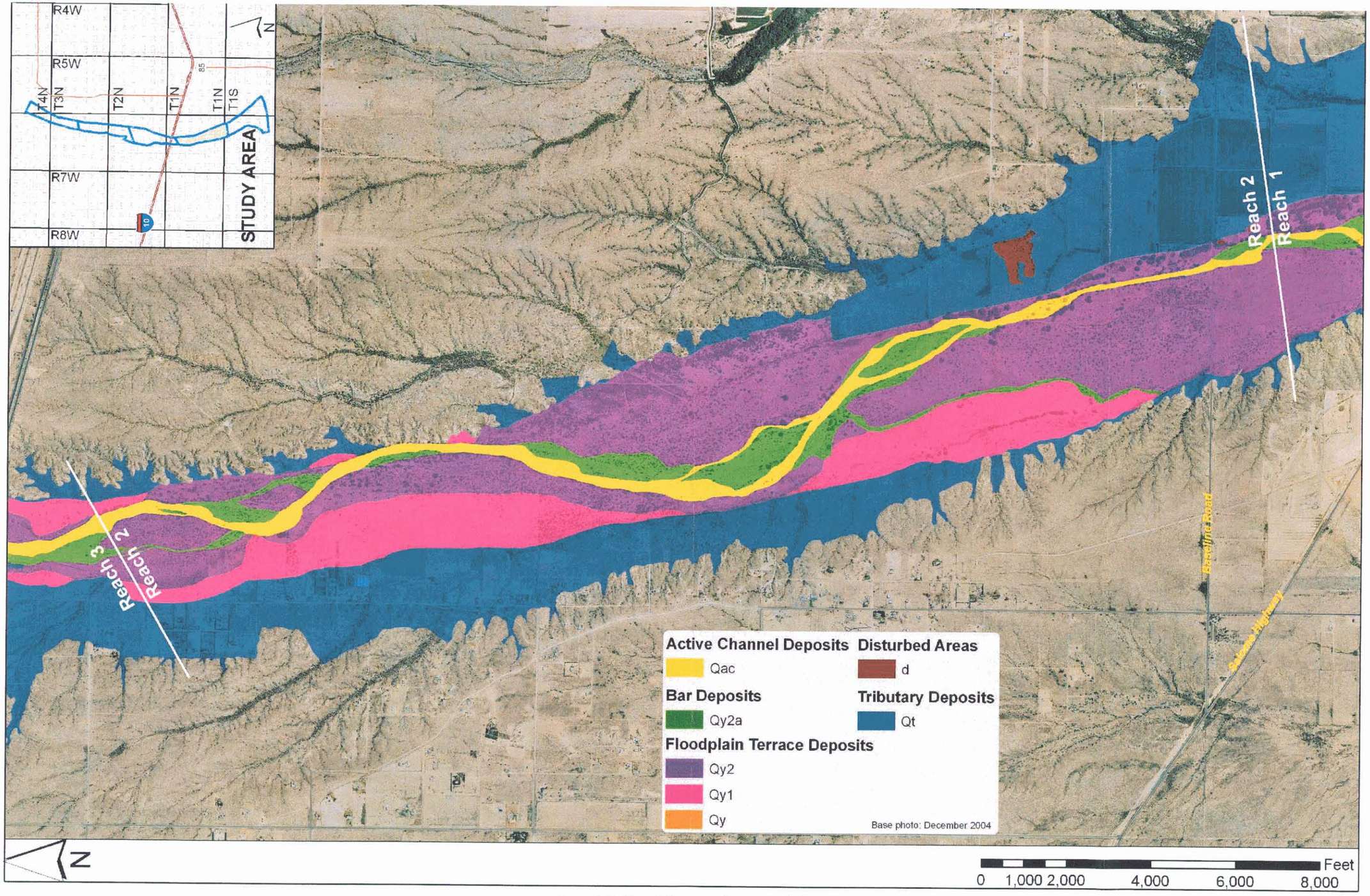

Figure 3-9. Reach 2 mapped geomorphology

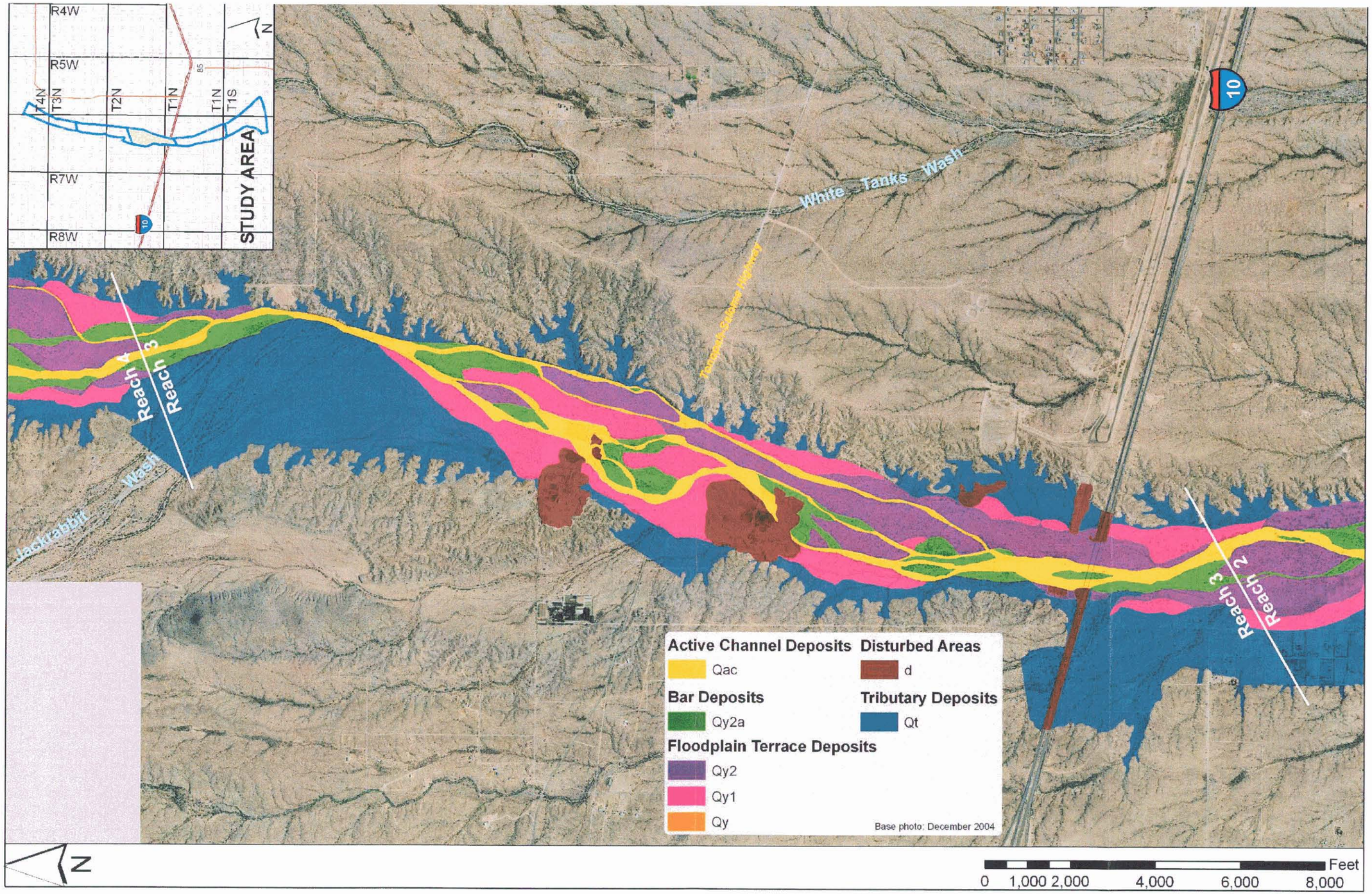

Figure 3-10. Reach 3 mapped geomorphology

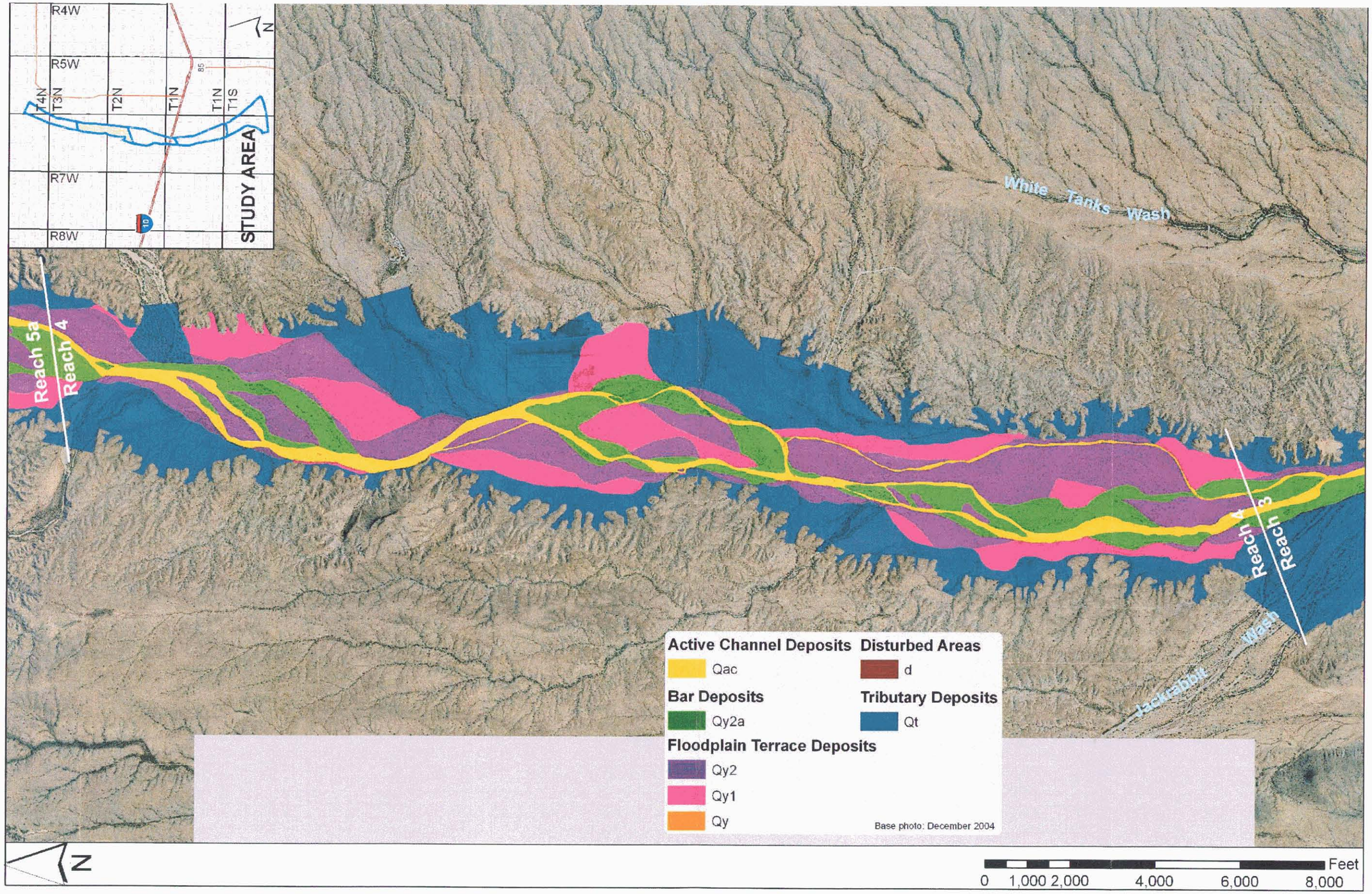

Figure 3-11. Reach 4 mapped geomorphology

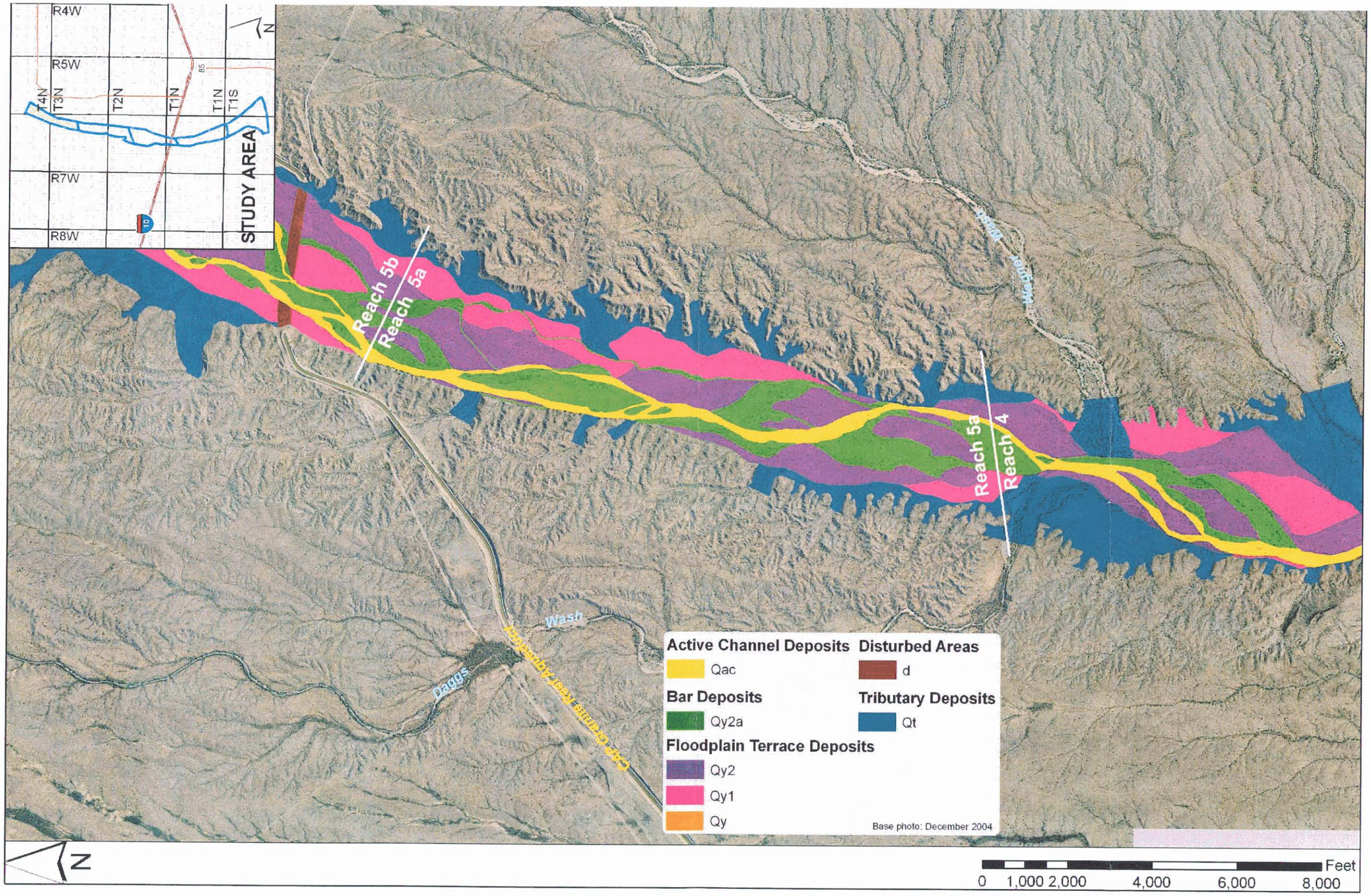

Figure 3-12. Reach 5a mapped geomorphology

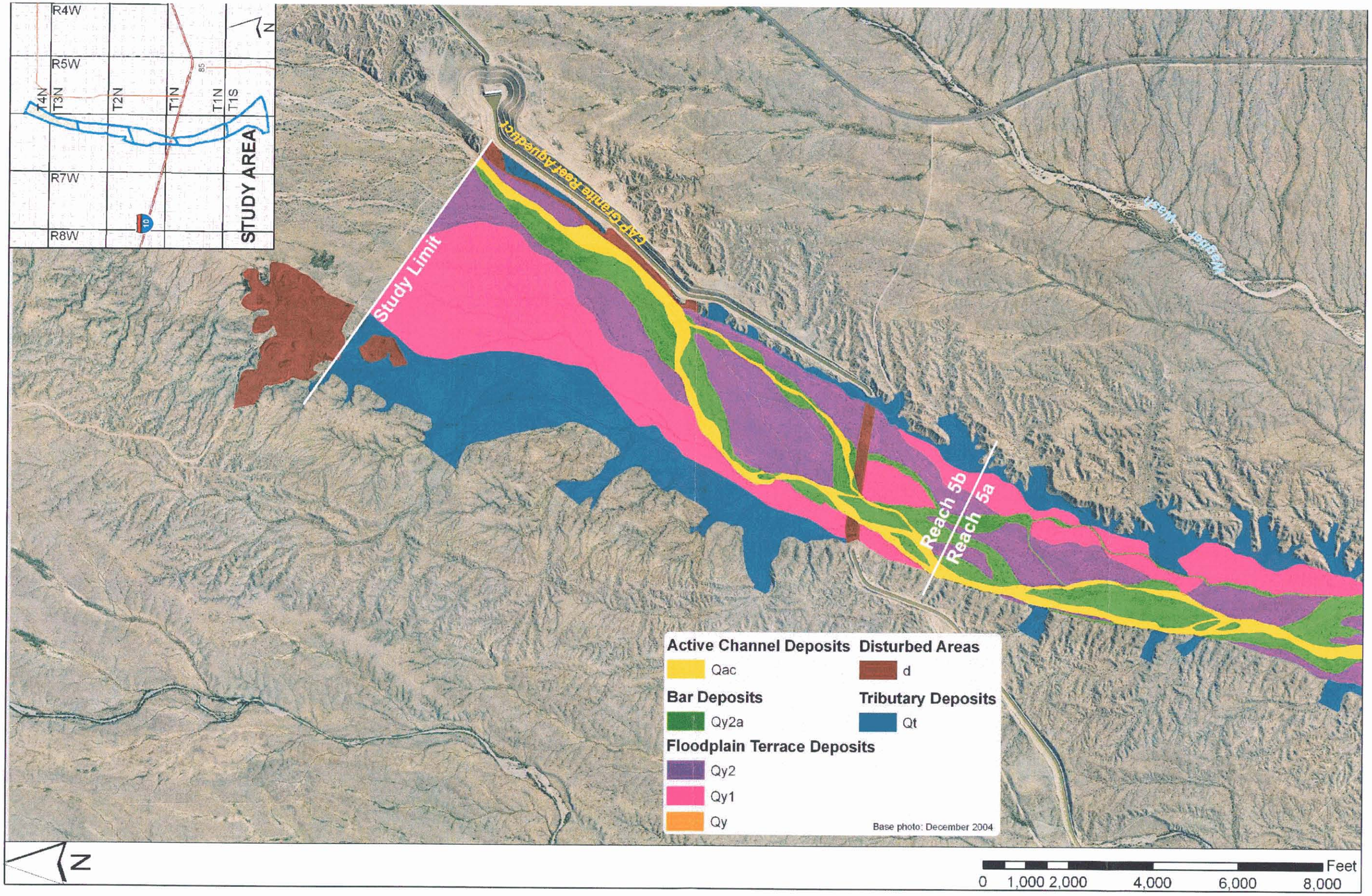

Figure 3-13. Reach 5b mapped geomorphology

3.5 Historical Analysis

Understanding the geomorphic history of a river system is critical when attempting to estimate future behavior. Aerial photography, topography, ground photography, flow records, engineering reports and studies, and anecdotal information provide clues to the river's past behavior and natural tendencies. For the Lower Hassayampa River, past river behavior was evaluated by delineating geomorphic surfaces on historical aerial photography, using the information gleaned from the mapping exercise described in Section 3.3. The following four primary functional surfaces were identified:

- Active Channel
- Bar Deposits
- Floodplain Terrace Deposits
- Tributary Deposits.

Historical avulsions were also identified and mapped using historical aerial photography. Identification and mapping of historical avulsions helps determine the magnitude of change that has occurred during a single flood event and provides a base from which future estimates of channel change can be made. Note that the historical geomorphic analysis was based on a 70-year photographic record (1934-2004) and that the geologic processes that govern river behavior generally occur over thousands to hundreds of thousands of years. Thus, the 70-year historical record is only a brief segment of time in a geologic context that must be supplemented by geomorphic interpretation of fluvial processes, as described elsewhere in this report. The 70-year photographic record is, however, an excellent means to identify human impacts on the river system.

3.5.1 Functional Surfaces

Segregating functional geomorphic surfaces helps describe past river behavior. By describing each geomorphic unit with respect to its function, the investigator can better understand the behavior as those surfaces change with time. The one important difference between mapping functional surfaces using historical, rather than recent aerial photography is that historical interpretations cannot be field verified. Figure 3-14 to Figure 3-37 show the historical geomorphic mapping by surface type for each year of photographic coverage.

3.5.1.1 Active Channel

The criteria for delineating the historical active channel surfaces were the same as was used to delineate the Qac unit described in Section 3.3. The interpreted function of the historical active channel surface was the primary conveyance area for high frequency flows and sediment transport. The active channels were also the topographically lowest feature within the Holocene floodplain. Side-by-side comparisons of the active channel delineations for the entire set of historical aerial photos shows the lateral migration history of the river within the study area. Quantitative analysis of these channel changes is presented in Chapter 6 (Lateral Migration Analysis).

3.5.1.2 Bar Deposits

Historical bar deposits function as sediment storage areas during high frequency flows and conveyance areas during low frequency flows. Bars mapped in this exercise include both island bars which were entirely surrounded by active channels, and lateral bars found on the margins of the active channels. Comparing the surface area of these features, in addition to their geographic distributions throughout the photographic record, aided in an understanding of the general sediment transport characteristics of the system. This information was used in the overall lateral stability assessment of the study area.

3.5.1.3 Floodplain Terrace Deposits

For purposes of the historical functional surface analysis, the floodplain terraces were delineated as one general surface, because the primary characteristics used to differentiate the floodplain terraces (Qy_2, Qy_1, and Q_y) described in Section 3.3 were field based, and could not be distinguished solely from aerial photographs. Although the historical floodplain terraces served slightly different functions in the system, as do the present surfaces, delineating them based solely on aerial photography is not possible. The general function of the historical floodplain was to provide overbank flood and sediment storage, and attenuate flows during flood events. Like the bar deposits, measurable changes to the historical floodplain surfaces such as surface areas and geographic distribution, provided information as to the lateral migration history of the Holocene floodplain within the study area.

3.5.1.4 Tributary Deposits

The tributary deposit surface distribution remained the most consistent in terms of surface area and geographic distribution of all the geomorphic surfaces within the Holocene floodplain. As described Section 3.3, many of the tributary deposits within the study area provide a degree of lateral control of the active channel.

3.5.1.5 Functional Surface Mapping

Maps of functional surface by year of aerial photograph coverage are provided in Figure 3-14 to Figure 3-37 on the following pages. The maps are segregated by the four functional surface types described above.

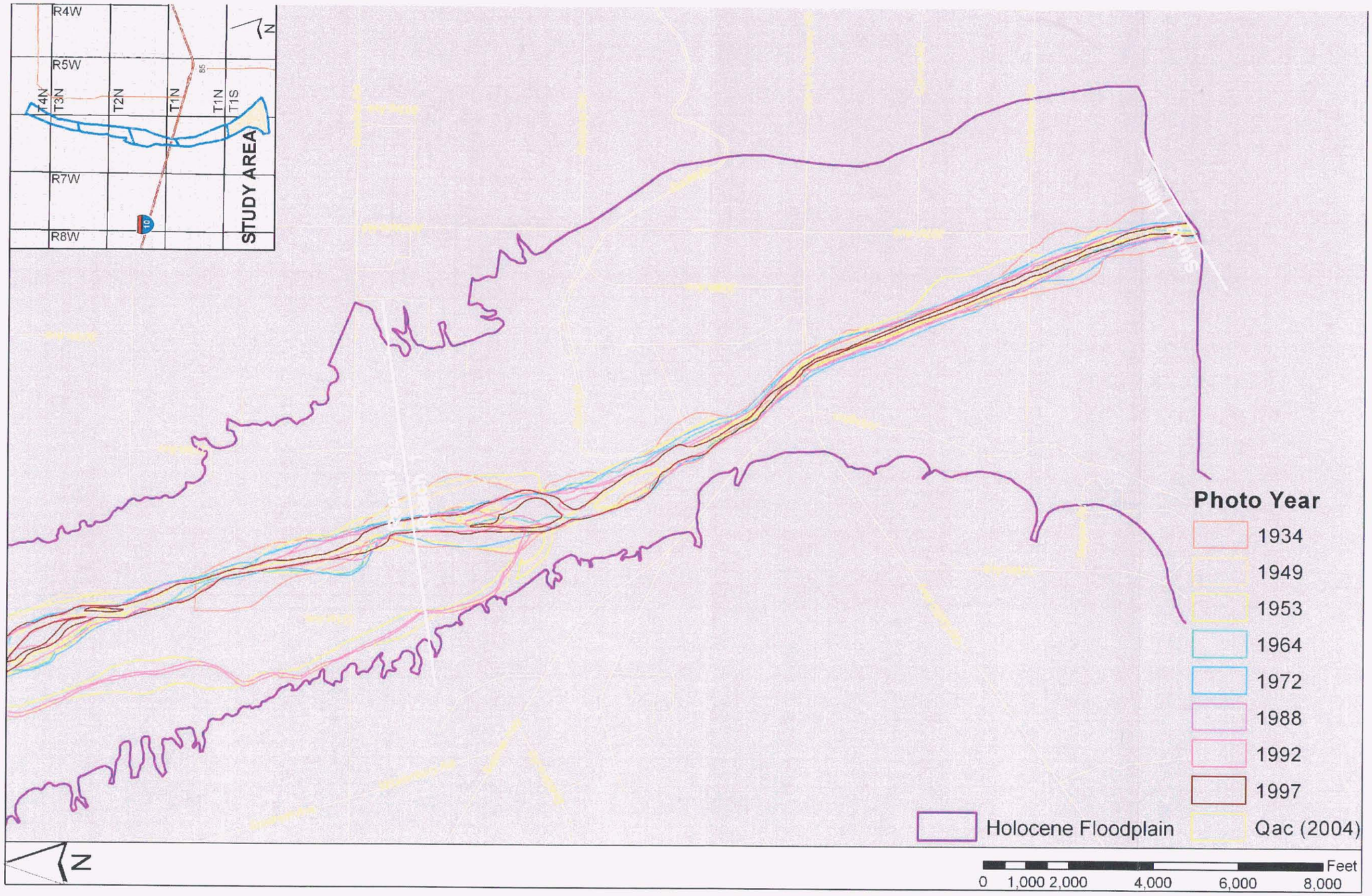

Figure 3-14. Reach 1 active channel surfaces

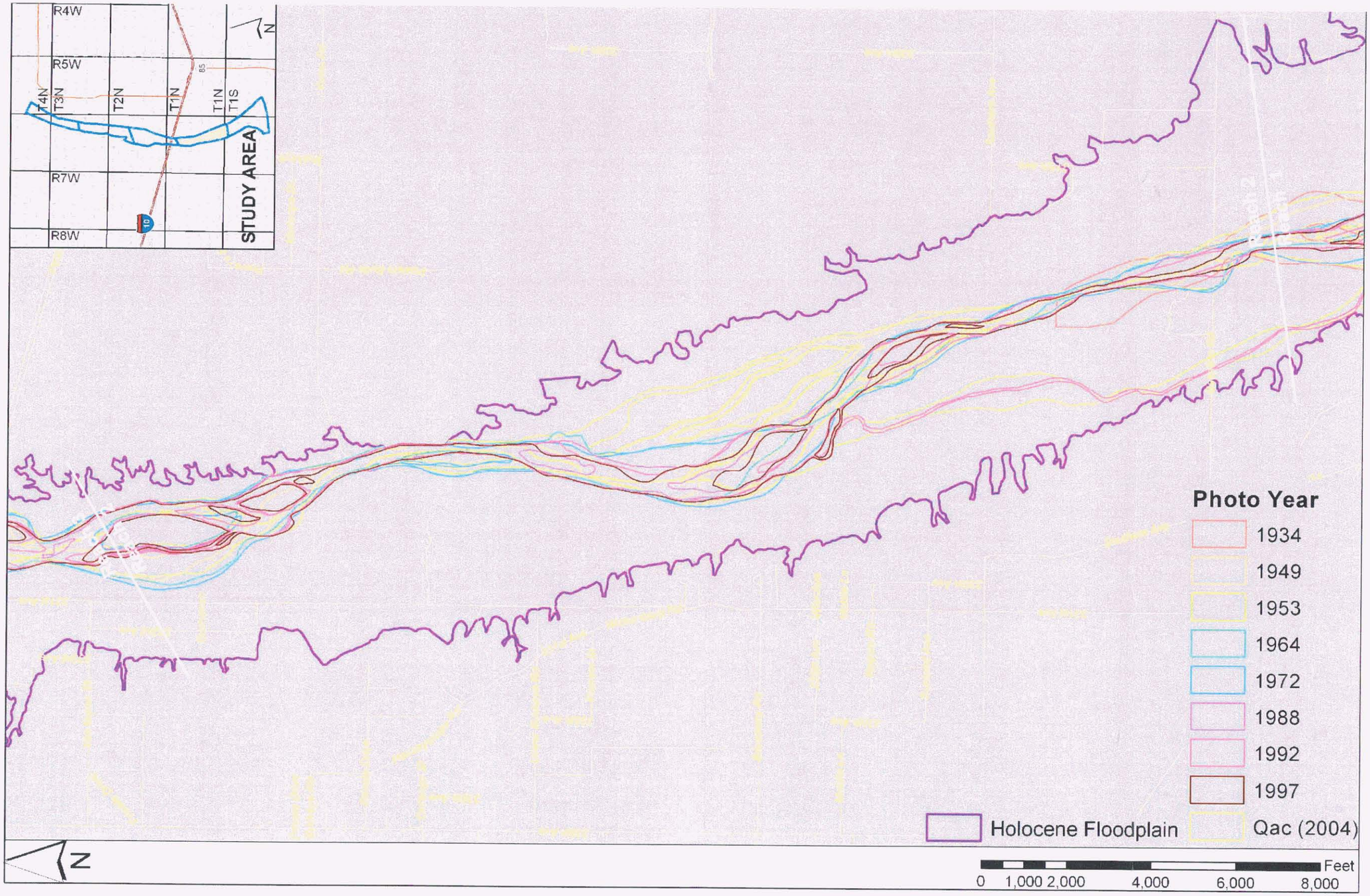

Figure 3-15. Reach 2 active channel surfaces

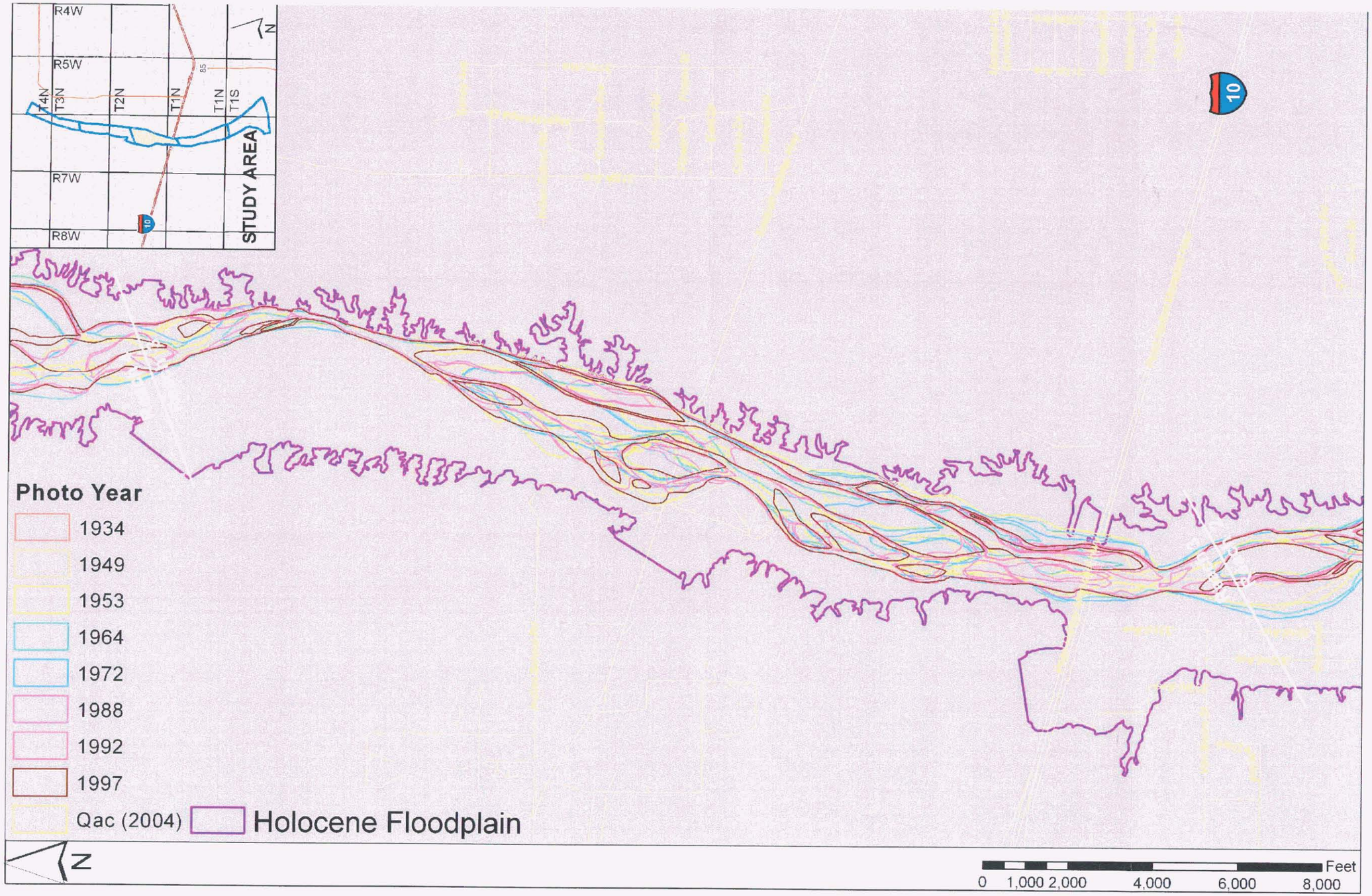

Figure 3-16. Reach 3 active channel surfaces

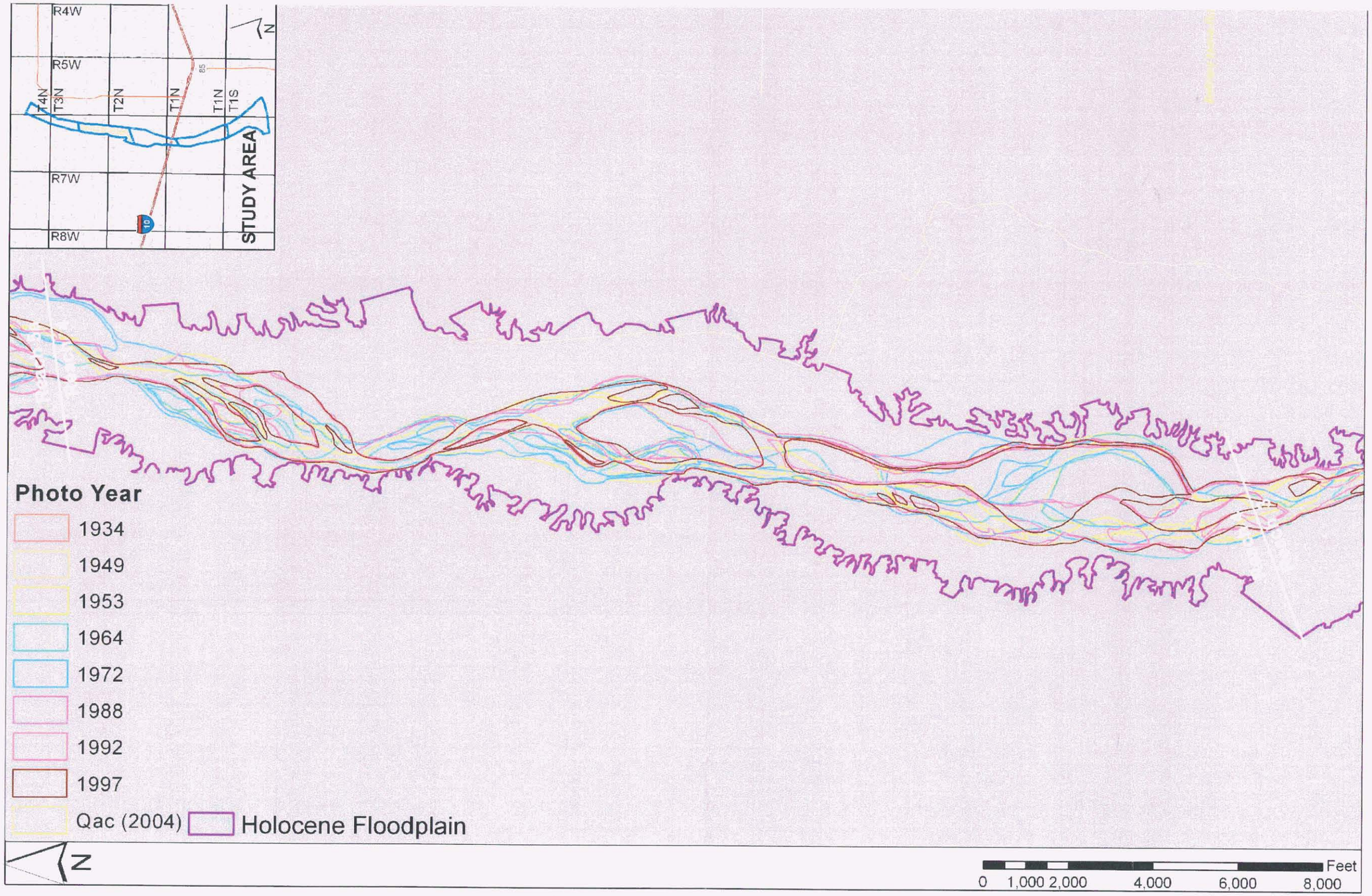

Figure 3-17. Reach 4 active channel surfaces

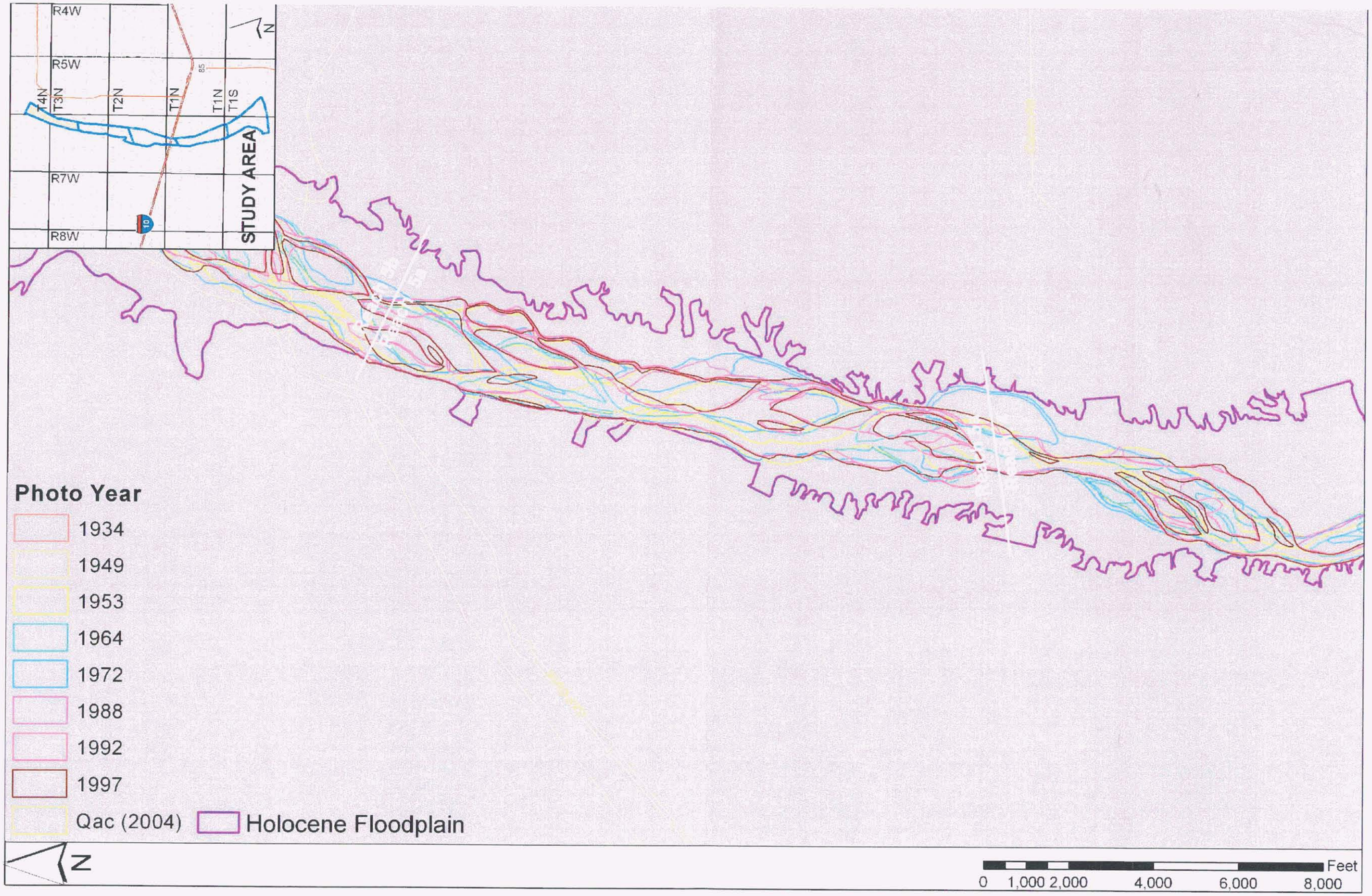

Figure 3-18. Reach 5a active channel surfaces

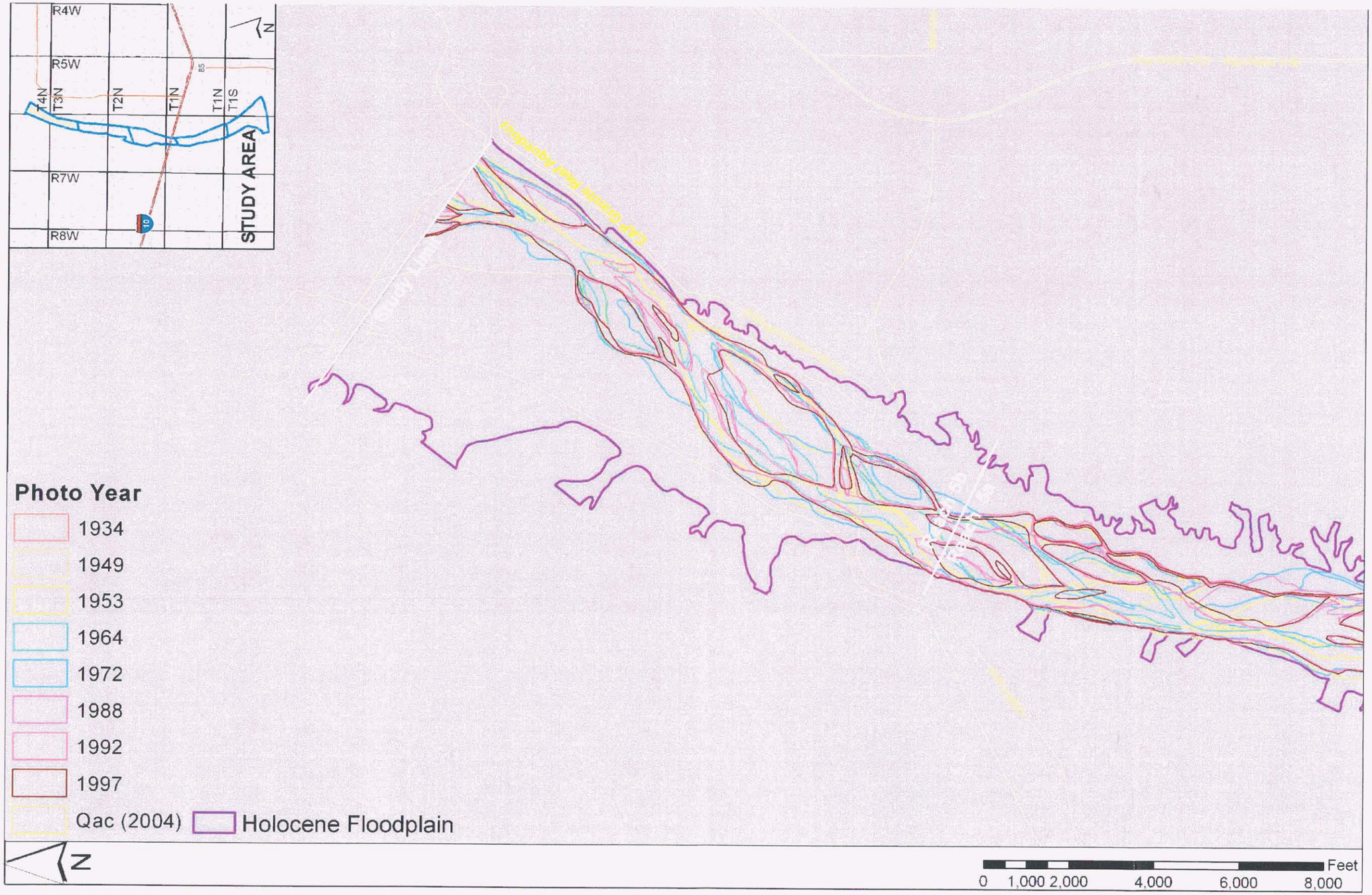

Figure 3-19. Reach 5b active channel surfaces

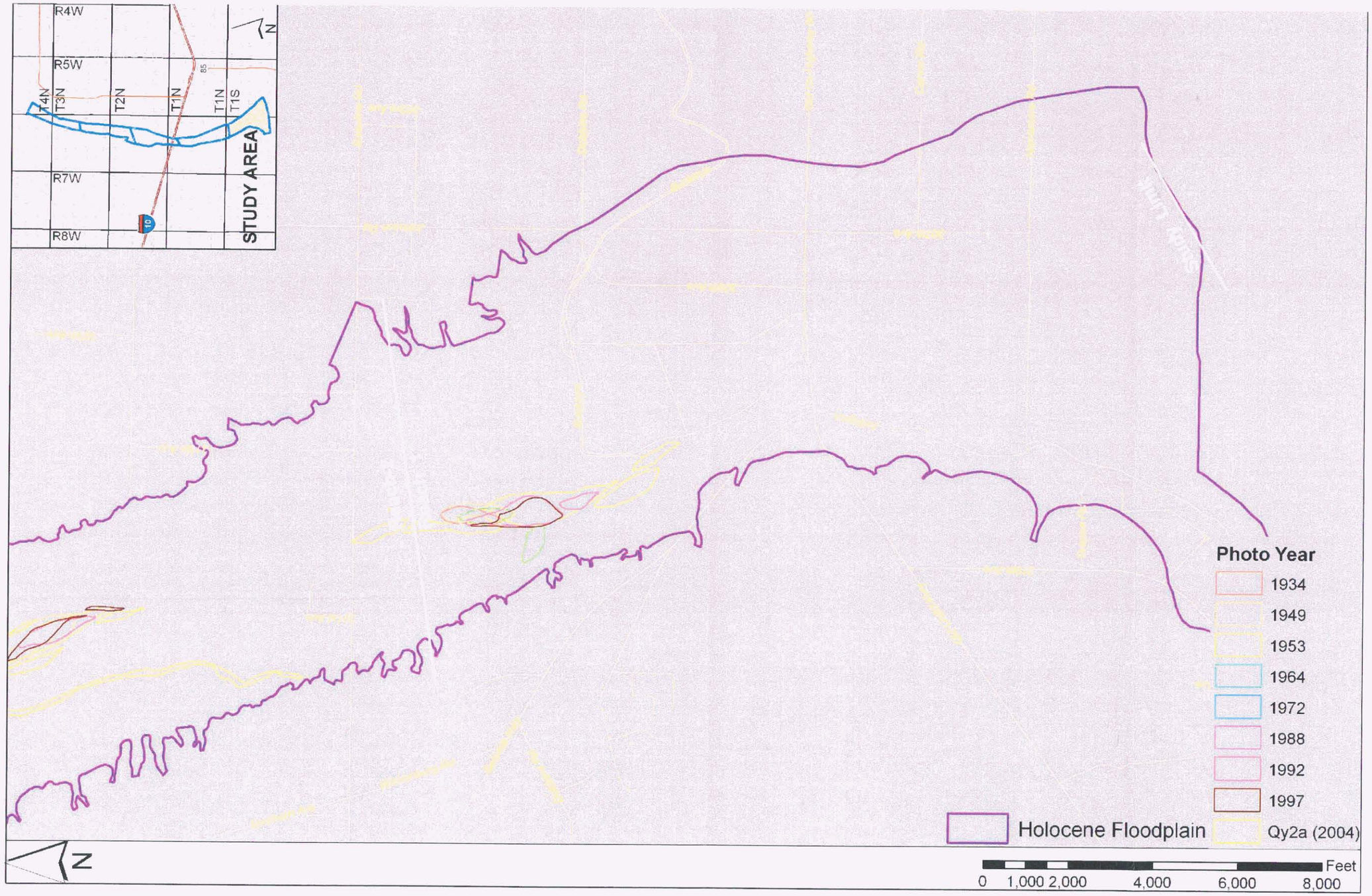

Figure 3-20. Reach 1 bar surfaces

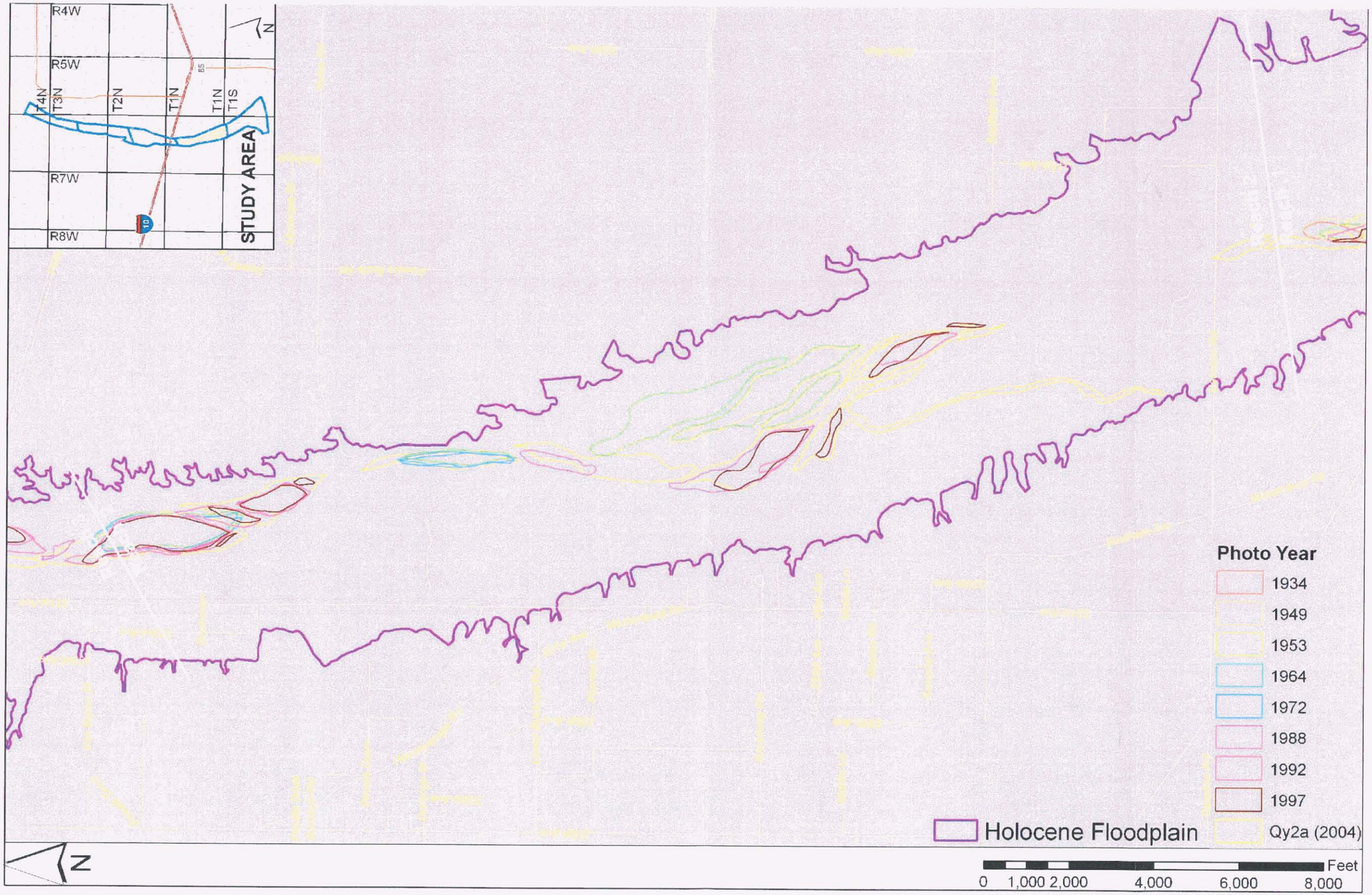

Figure 3-21. Reach 2 bar surfaces

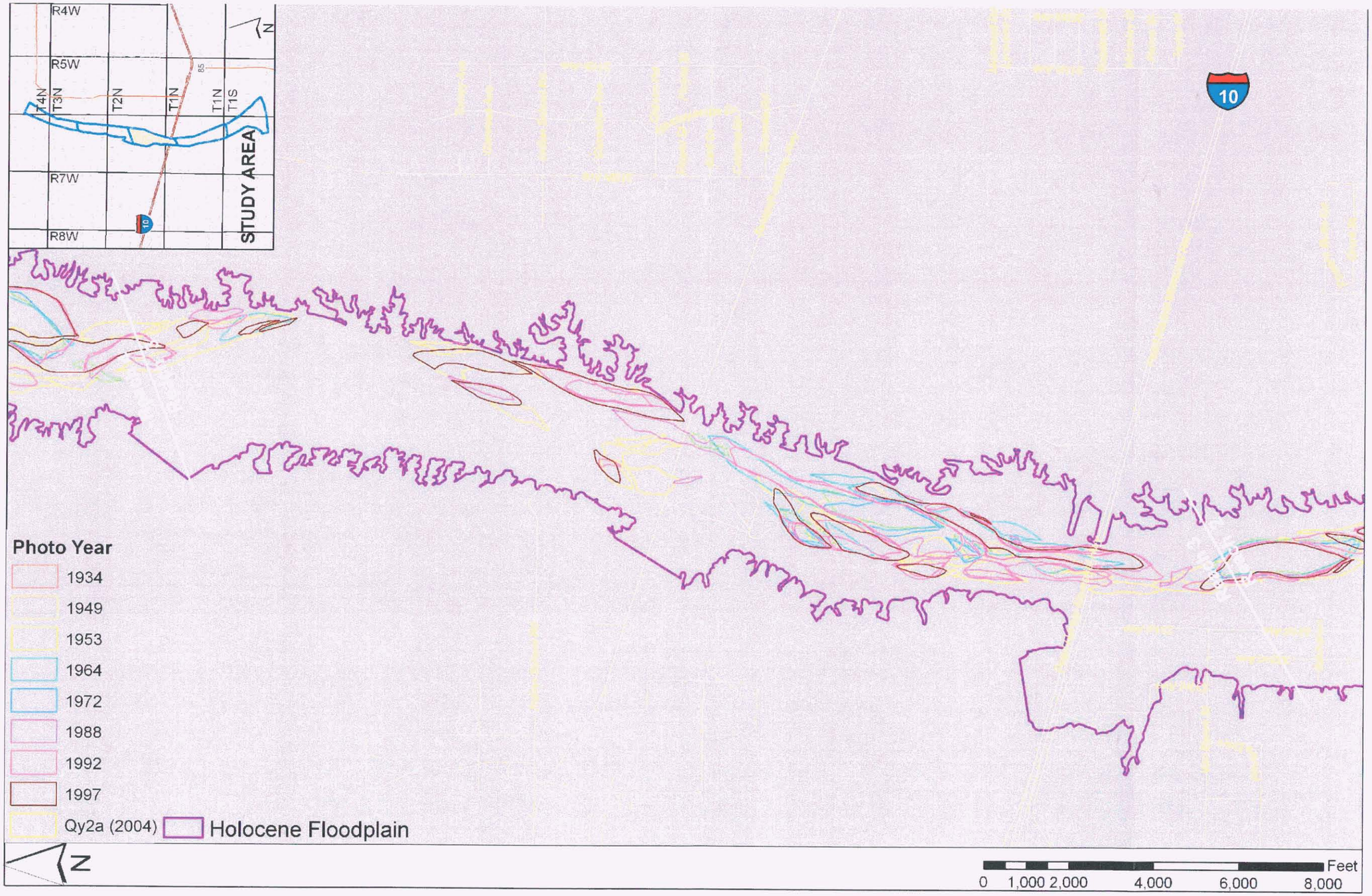

Figure 3-22. Reach 3 bar surfaces

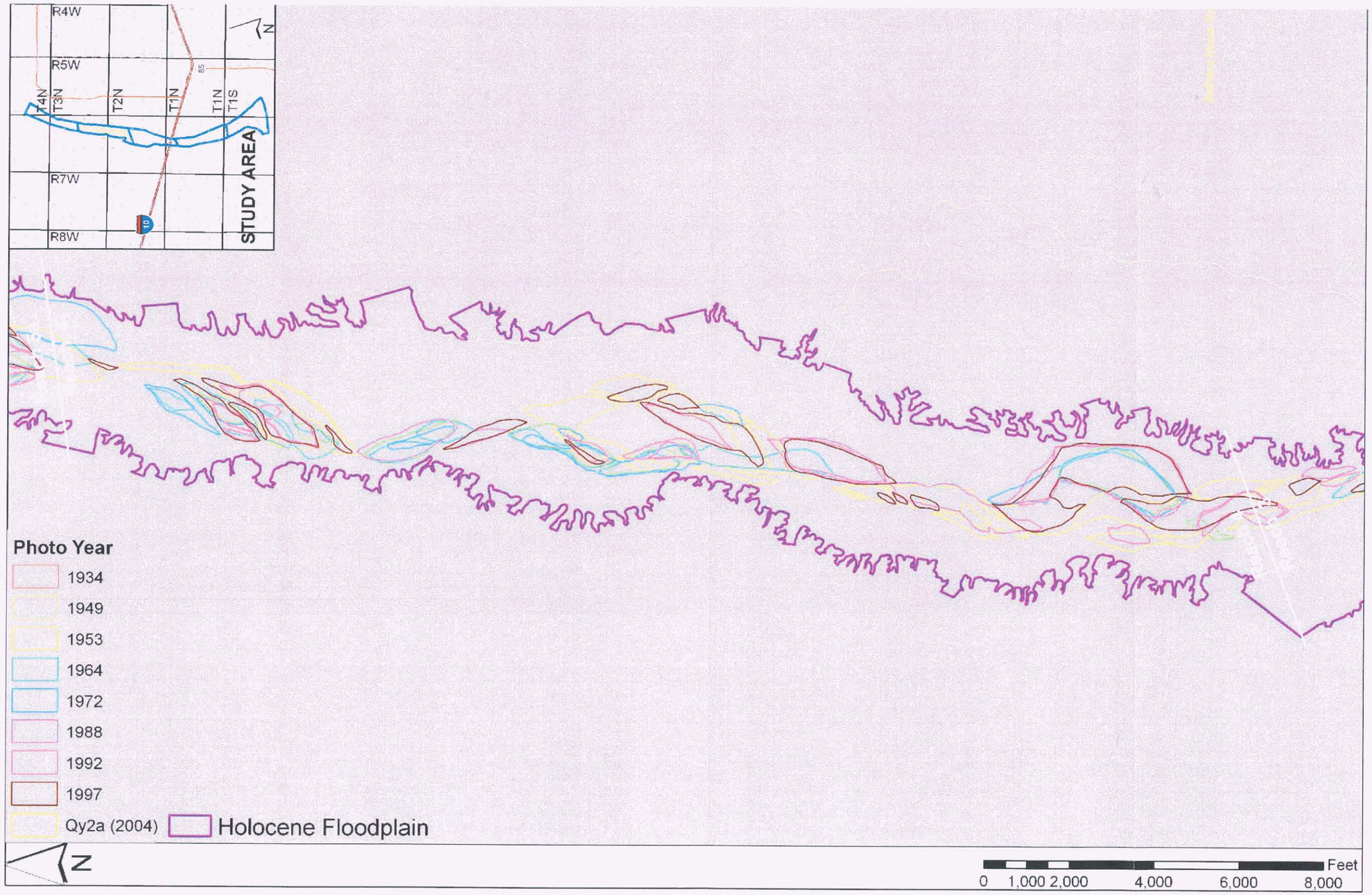

Figure 3-23. Reach 4 bar surfaces

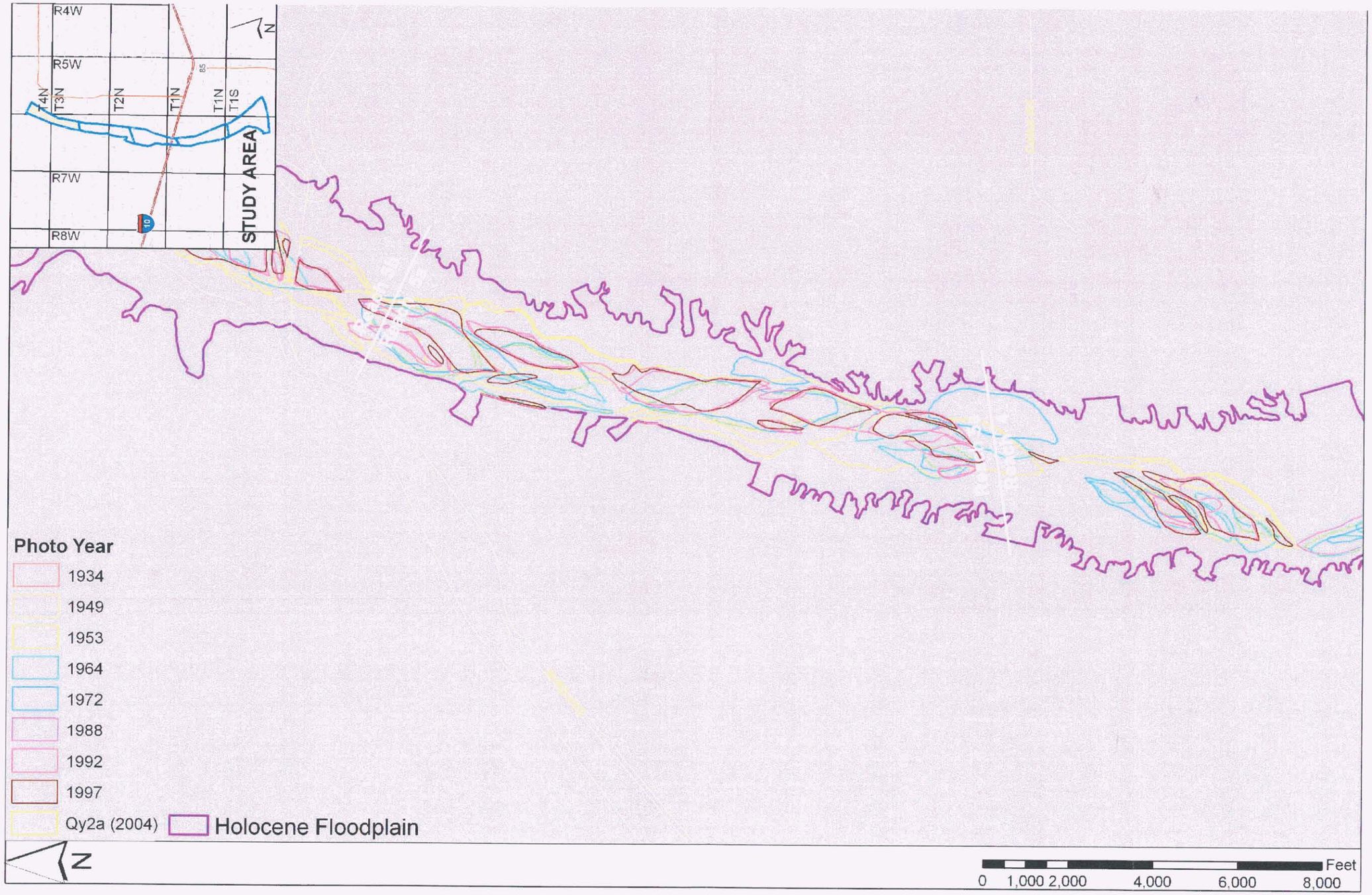

Figure 3-24. Reach 5a bar surfaces

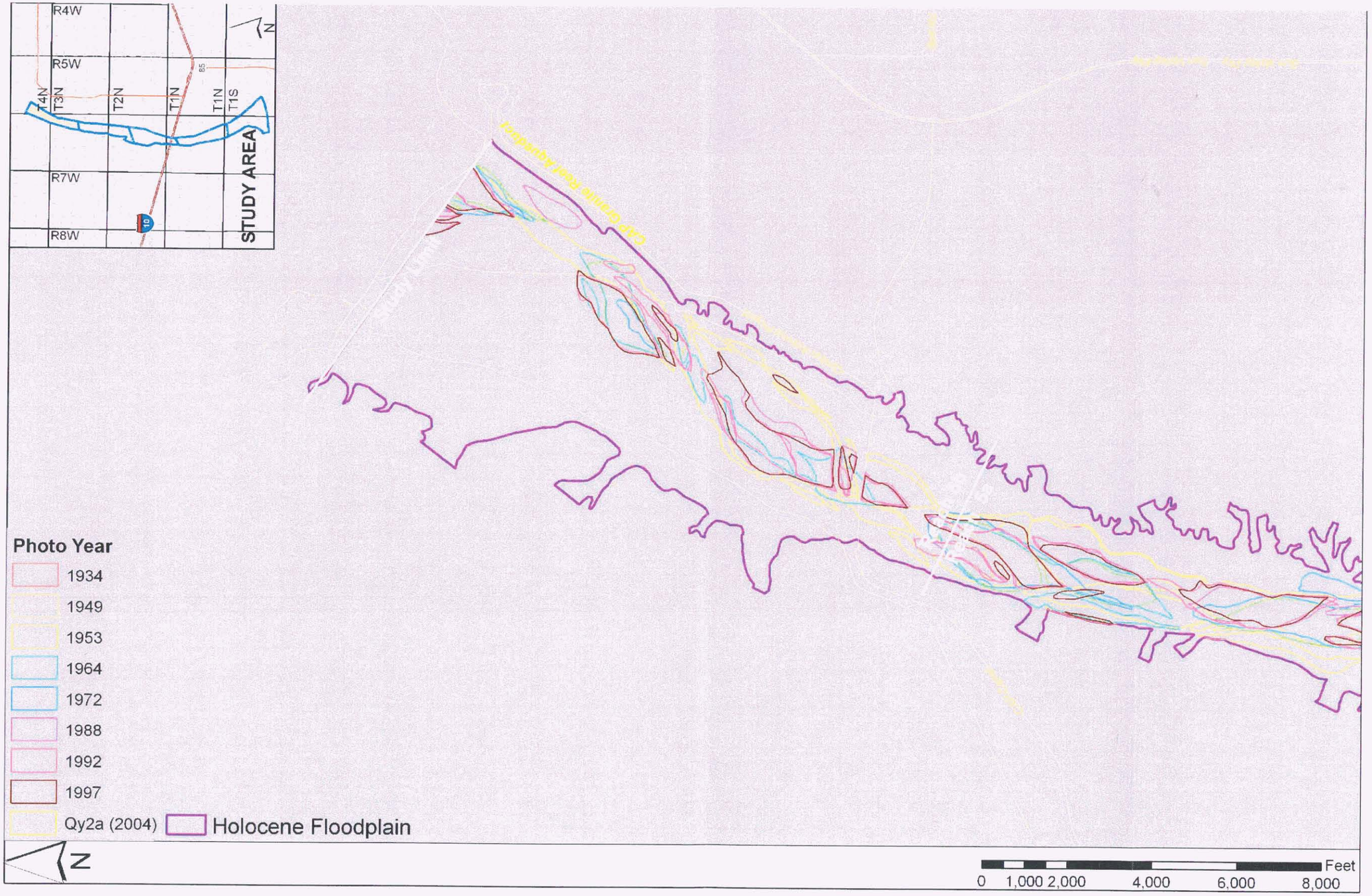

Figure 3-25. Reach 5b bar surfaces

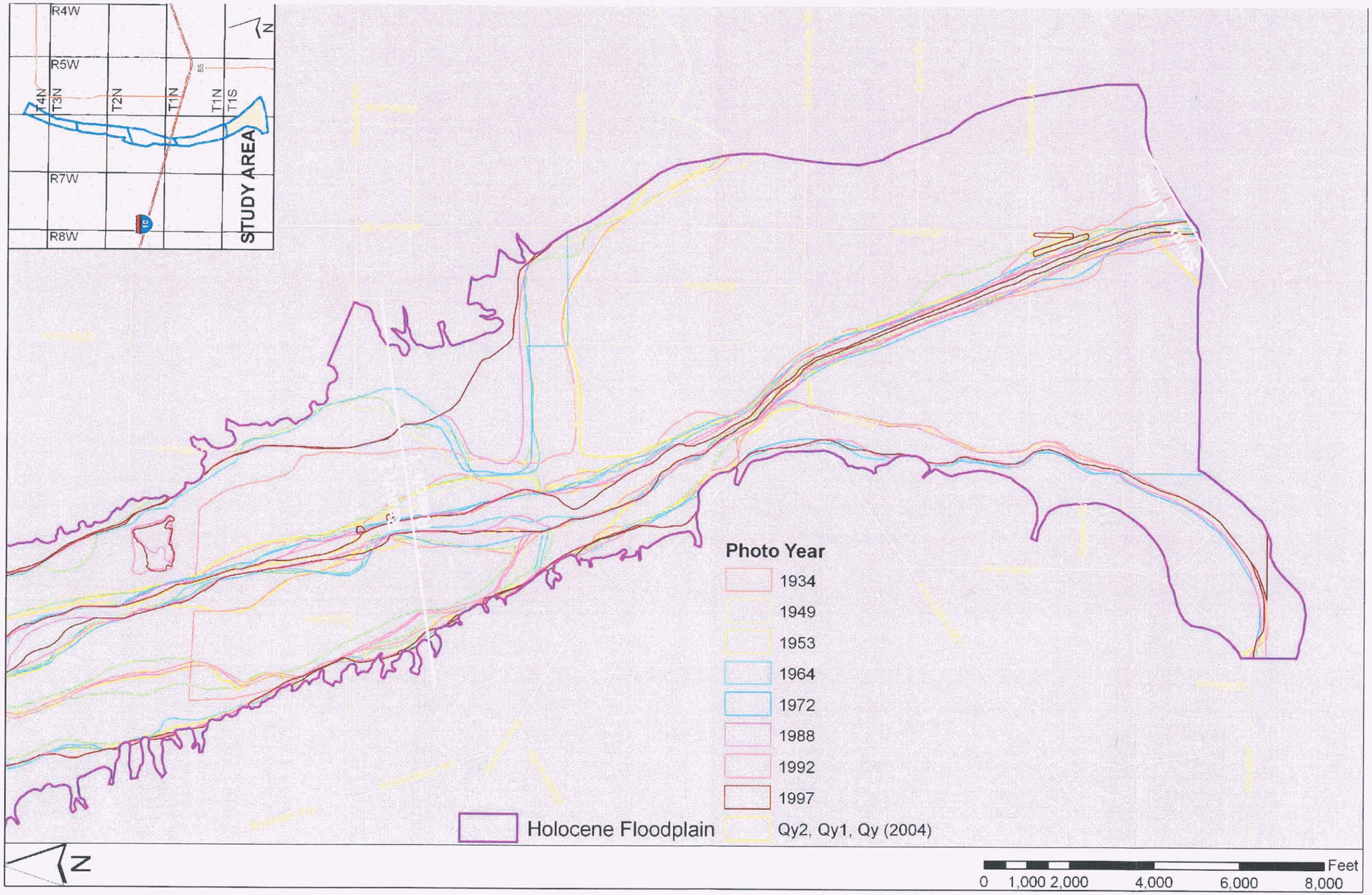

Figure 3-26. Reach 1 floodplain terrace surfaces

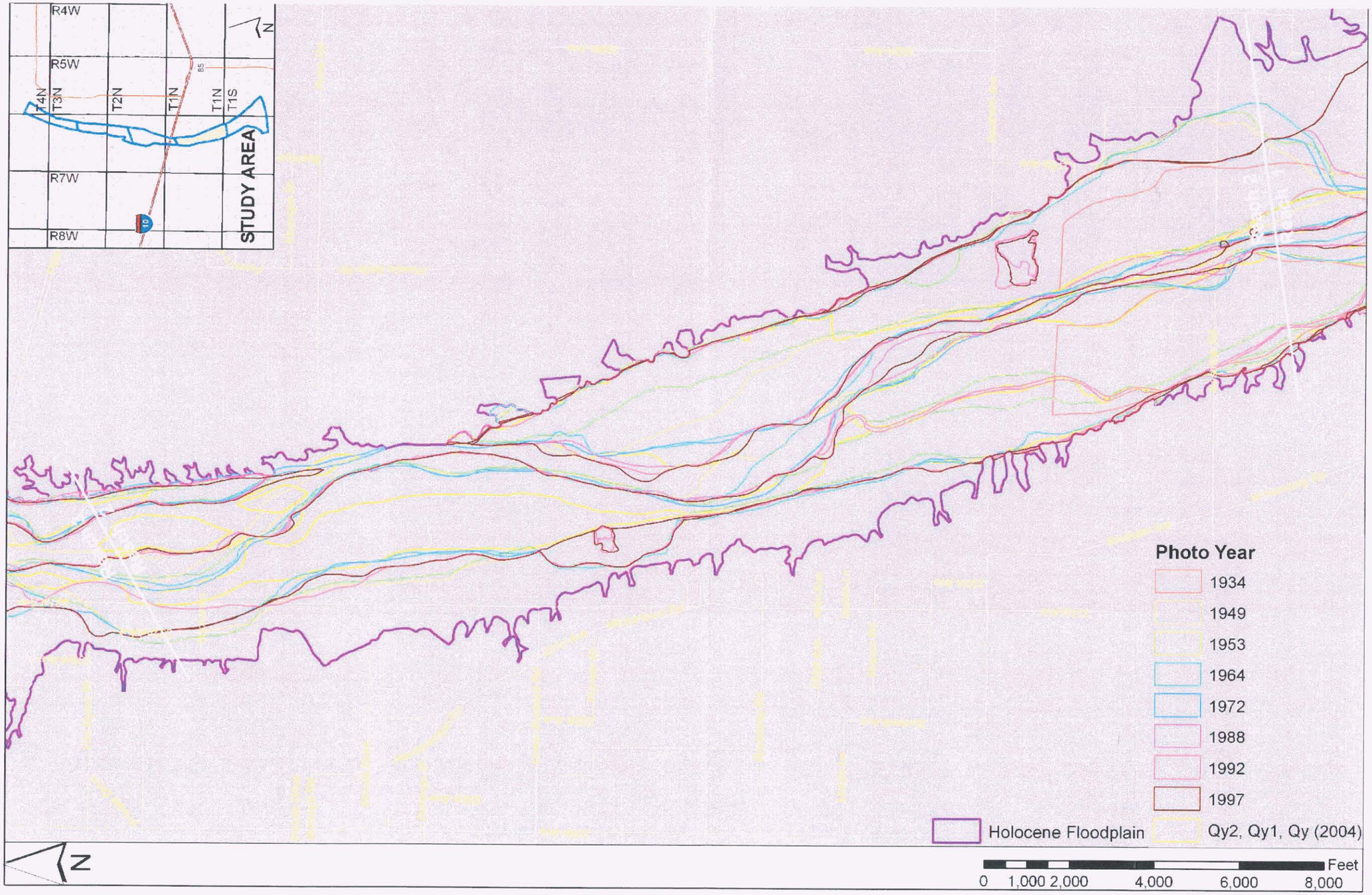

Figure 3-27. Reach 2 floodplain terrace surfaces

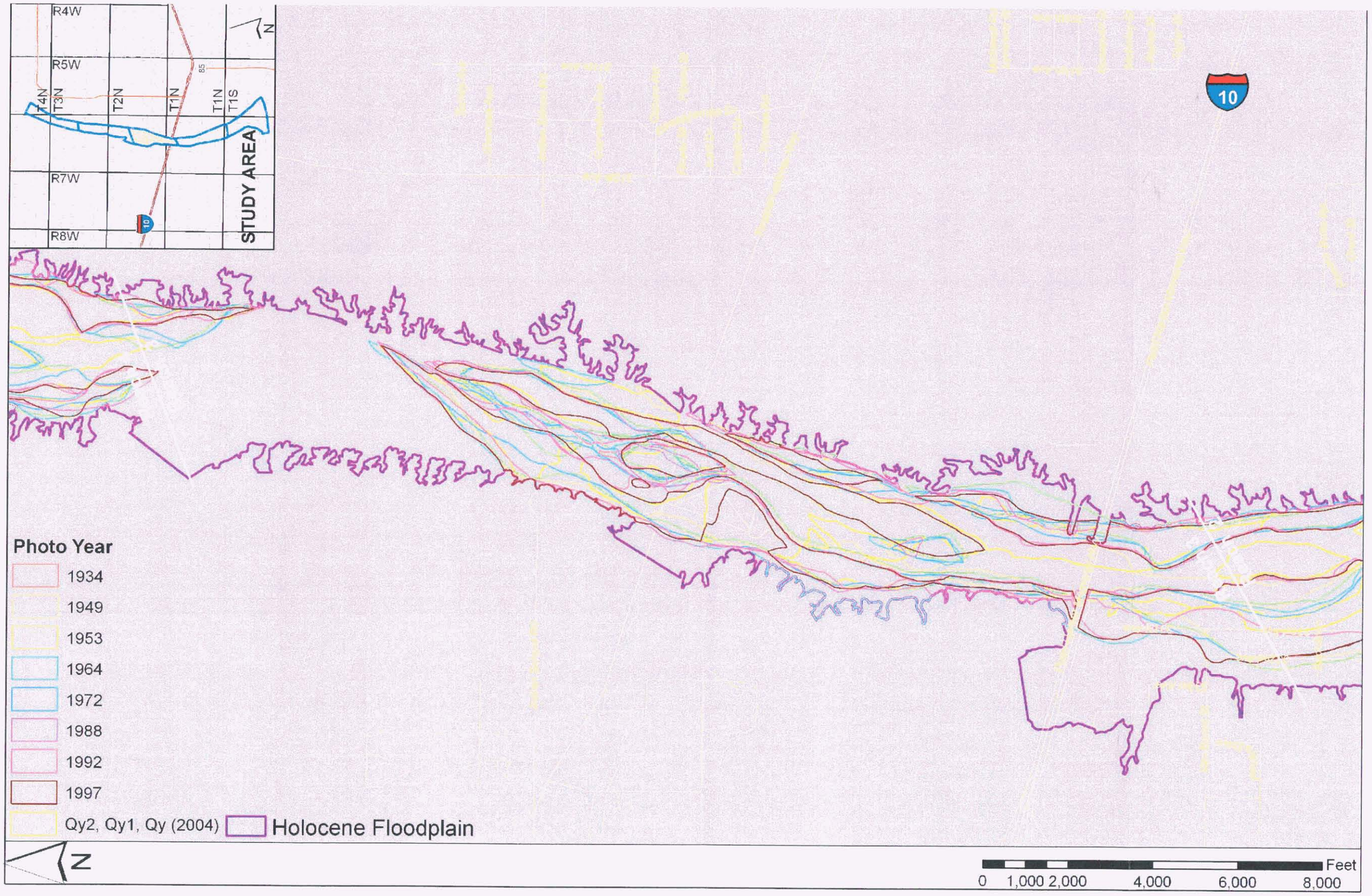

Figure 3-28. Reach 3 floodplain terrace surfaces

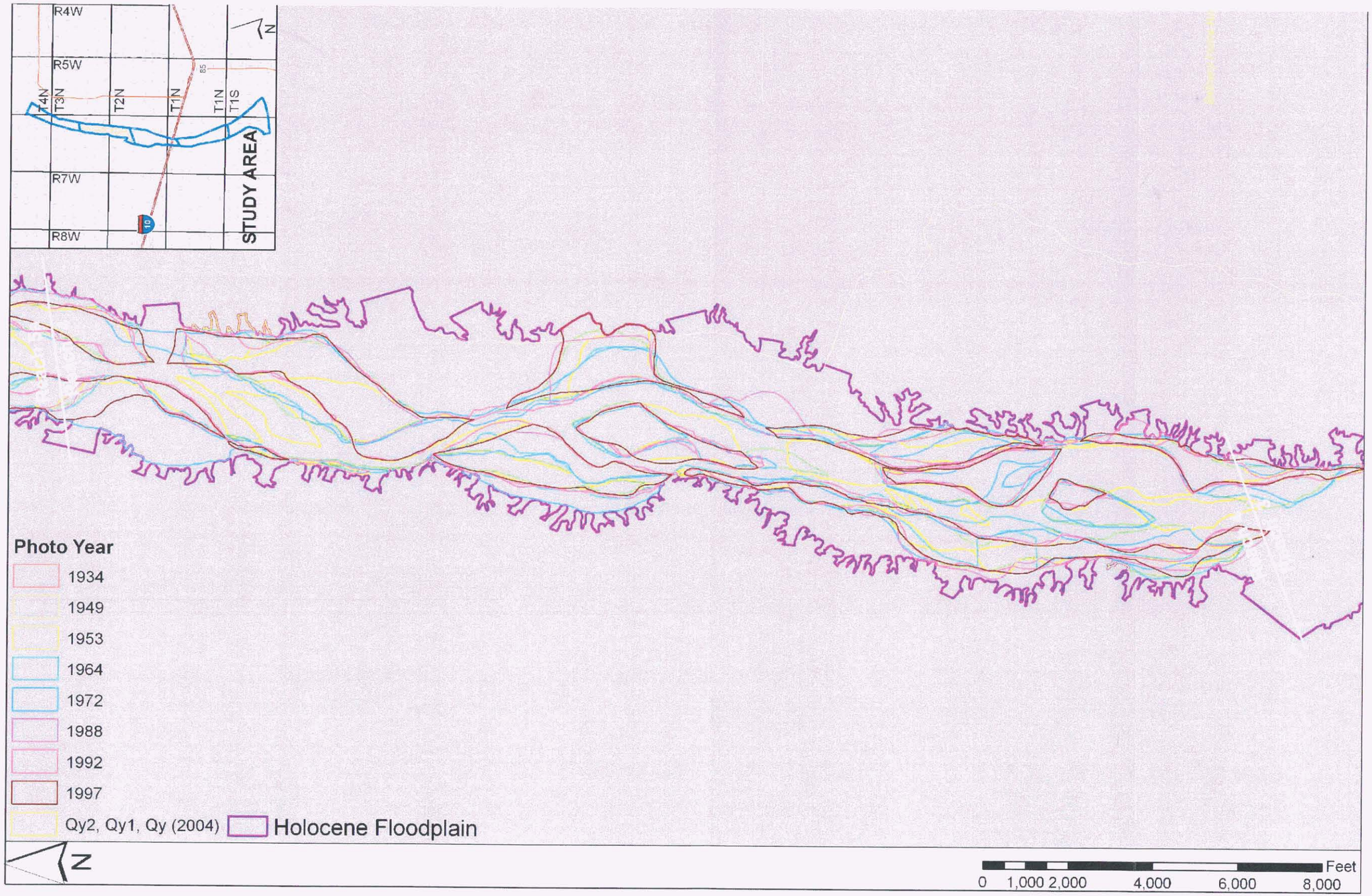

Figure 3-29. Reach 4 floodplain terrace surfaces

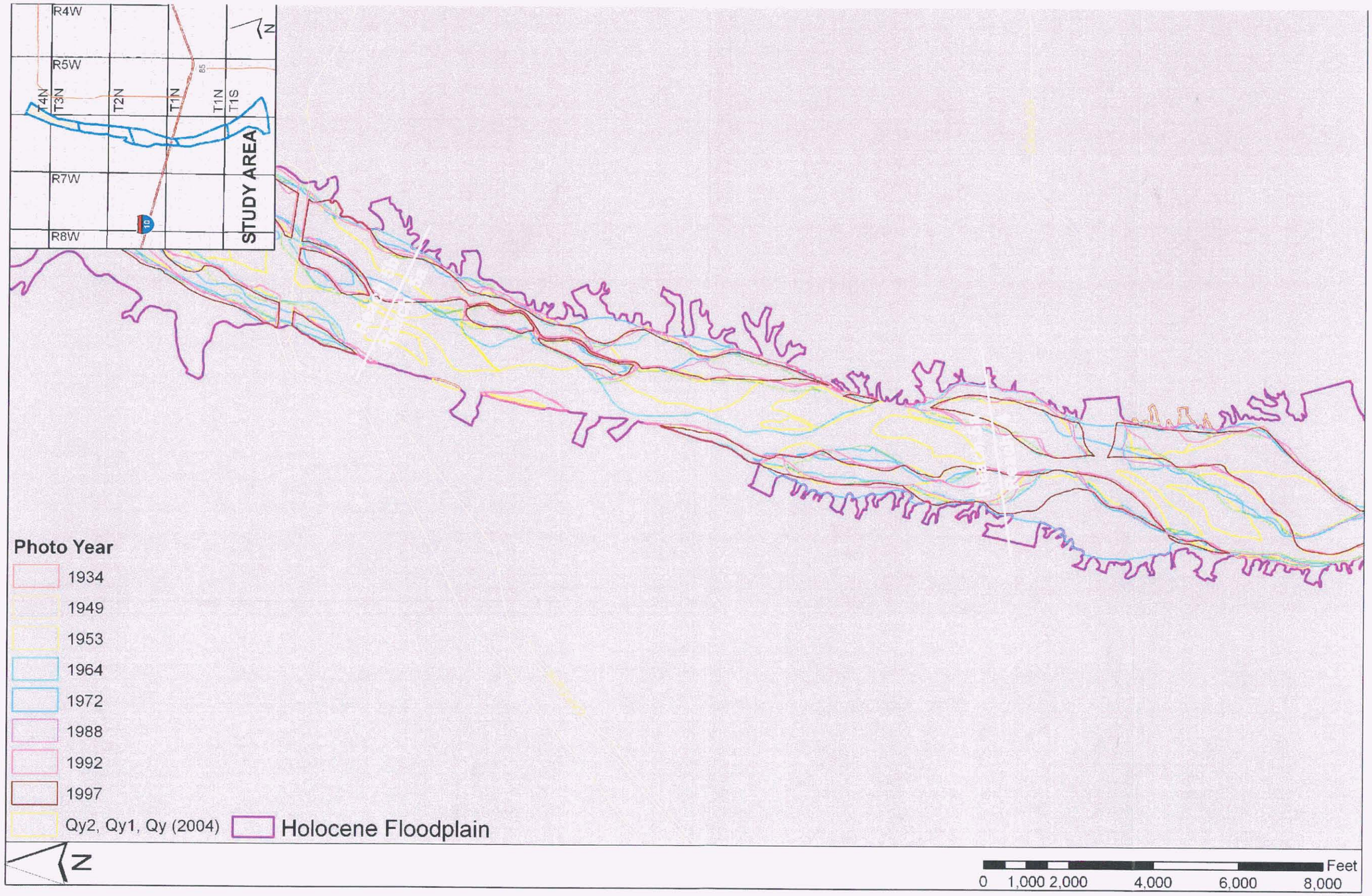

Figure 3-30. Reach 5a floodplain terrace surfaces

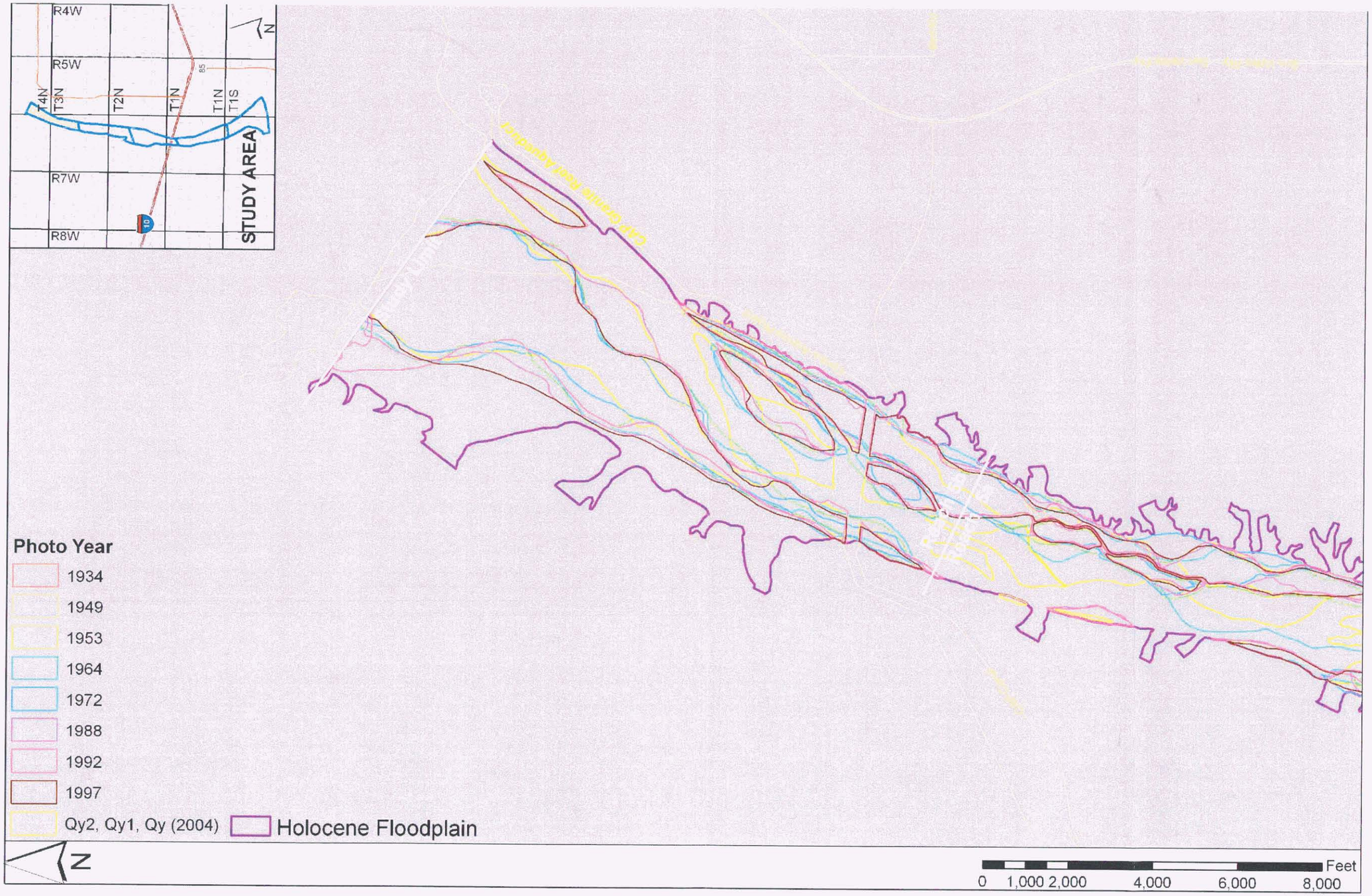

Figure 3-31. Reach 5b floodplain terrace surfaces

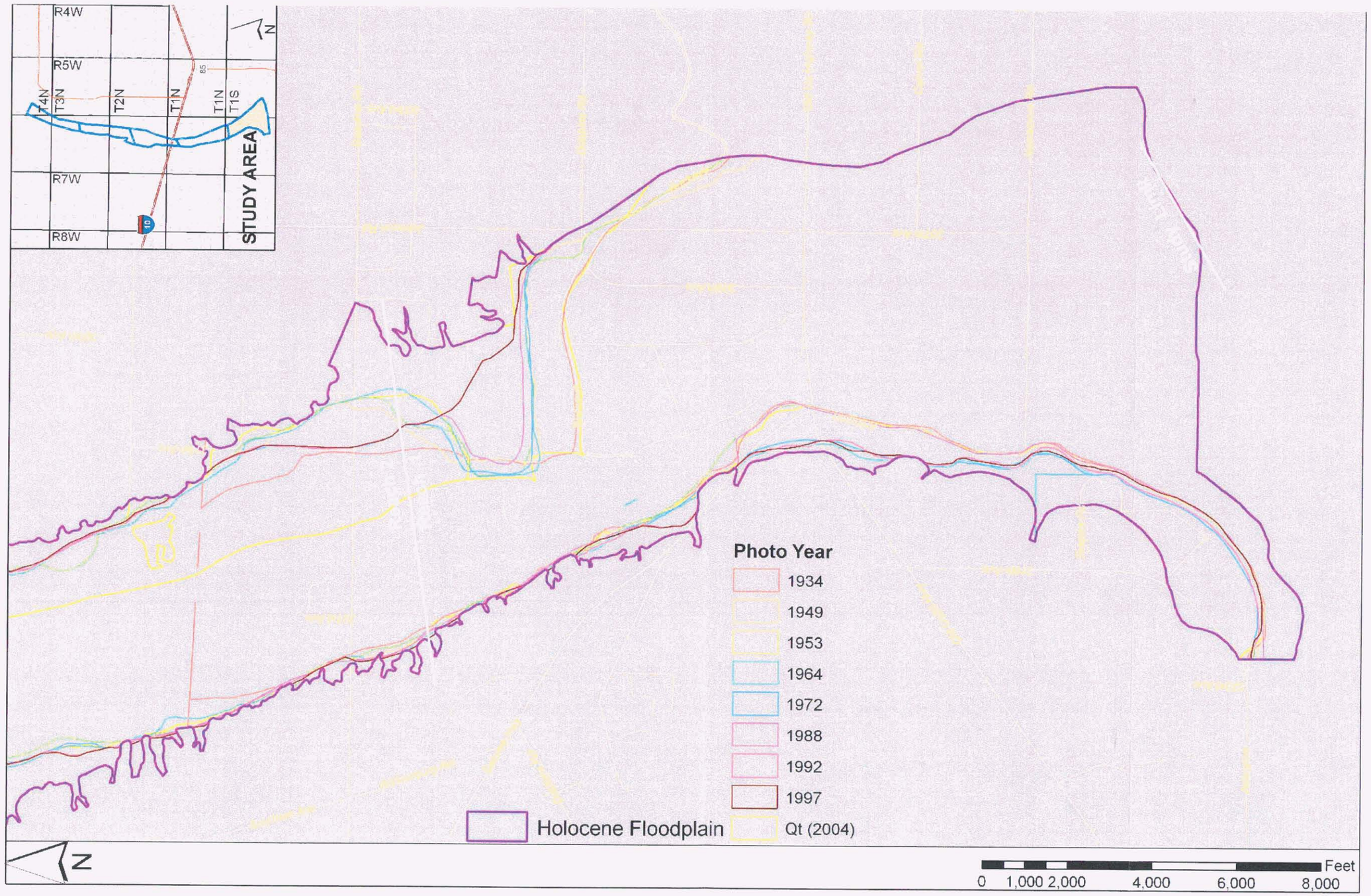

Figure 3-32. Reach 1 tributary deposit surfaces

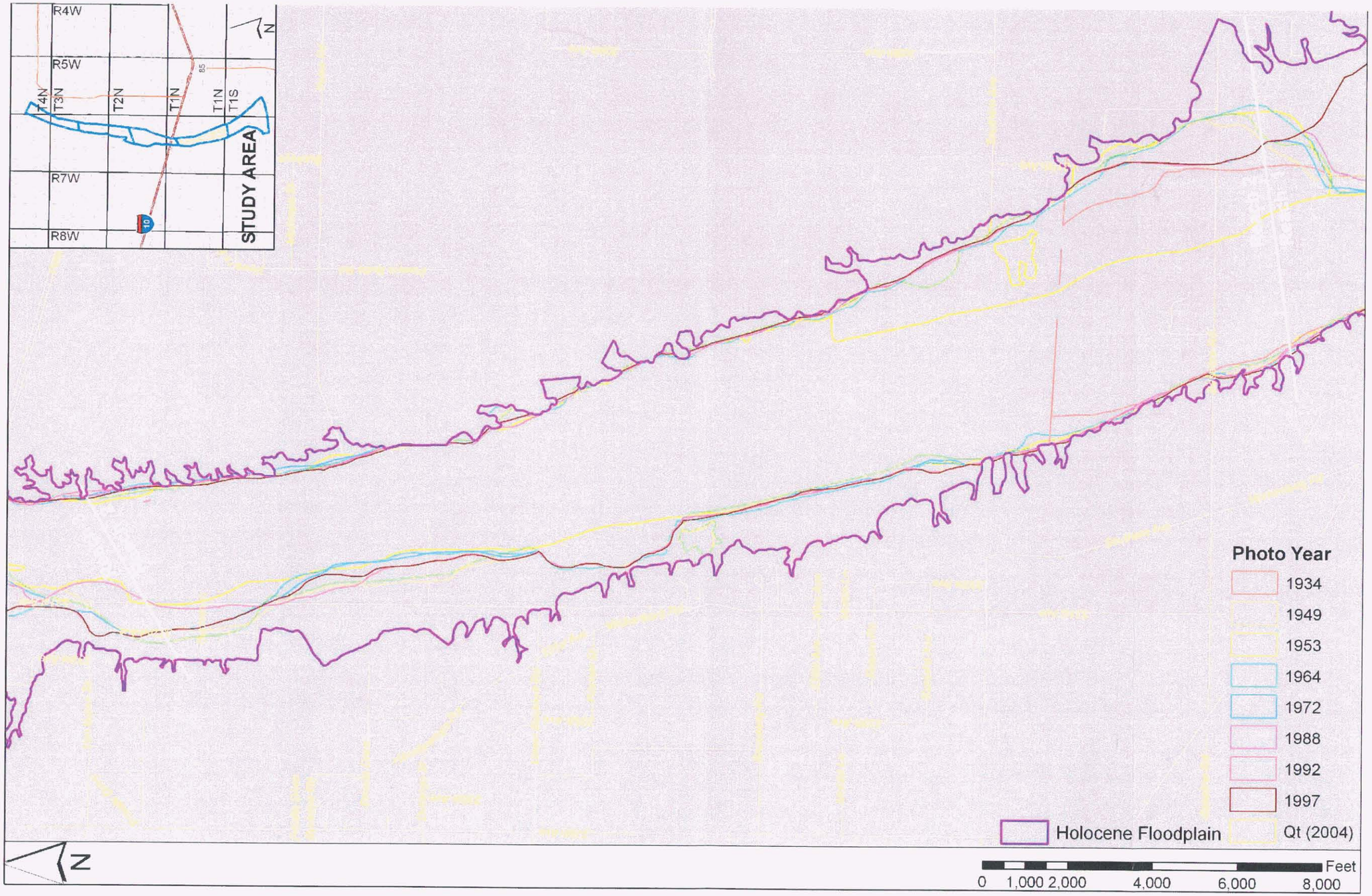

Figure 3-33. Reach 2 tributary deposit surfaces

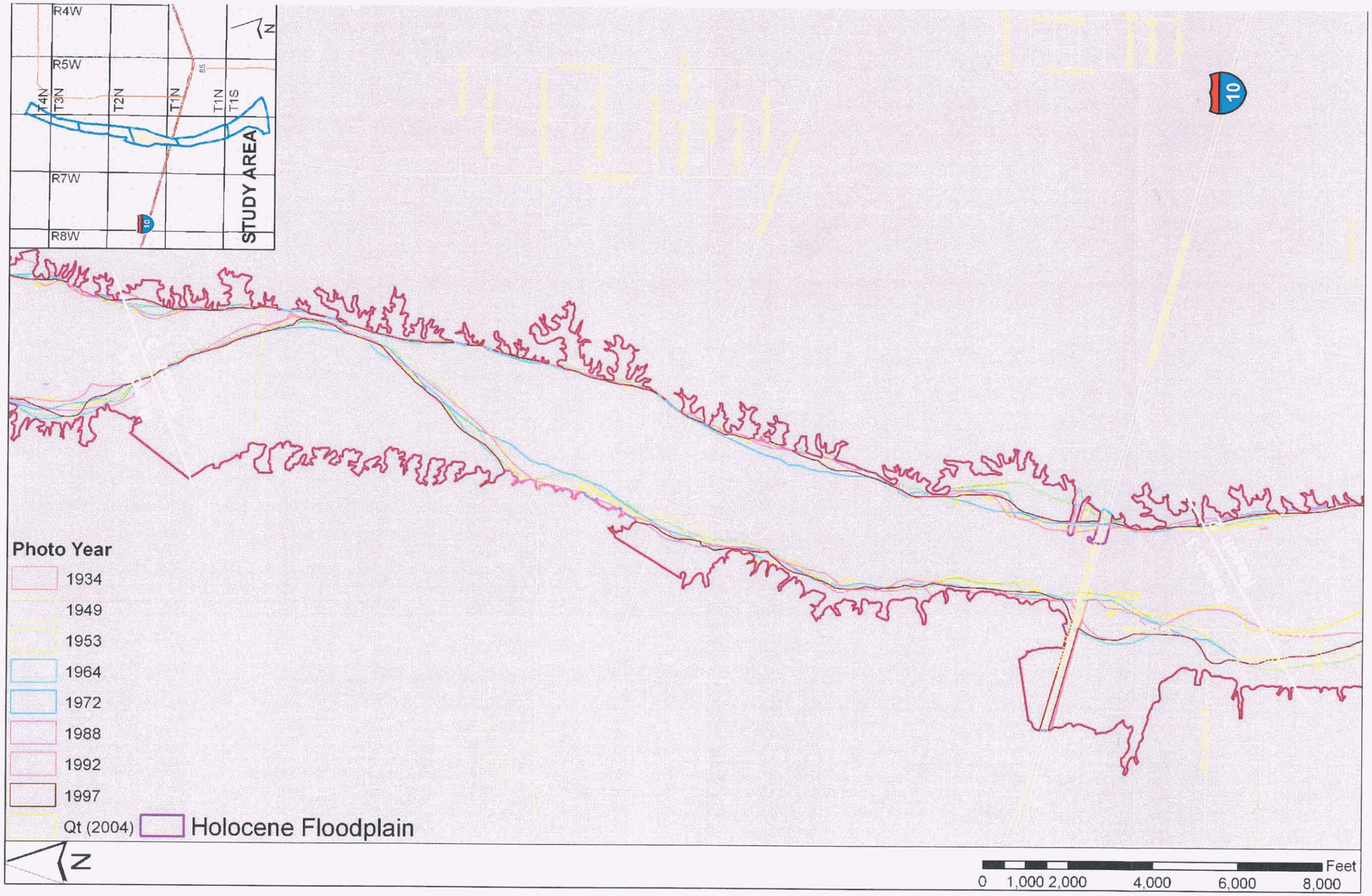

Figure 3-34. Reach 3 tributary deposit surfaces

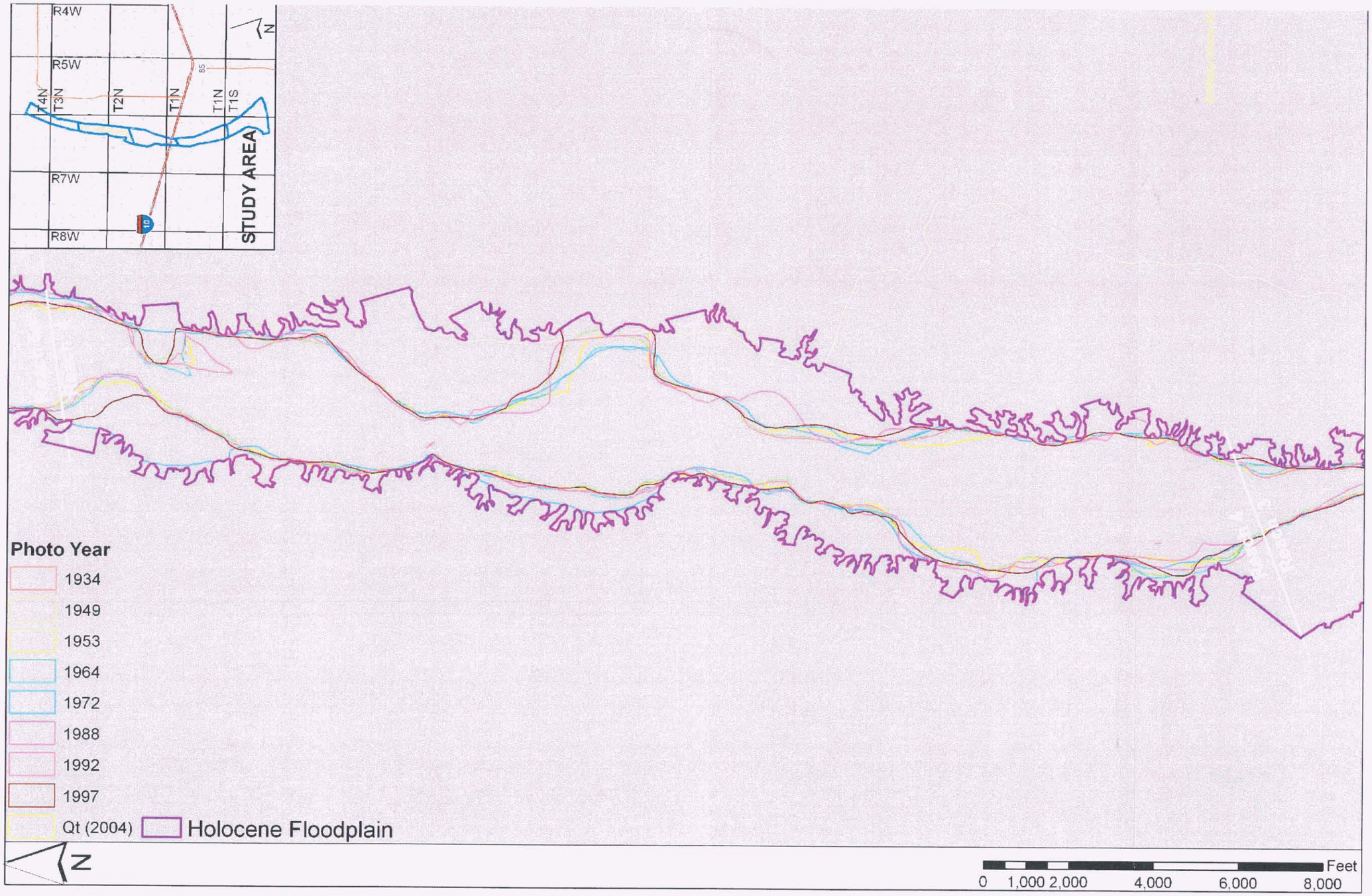

Figure 3-35. Reach 4 tributary deposit surfaces

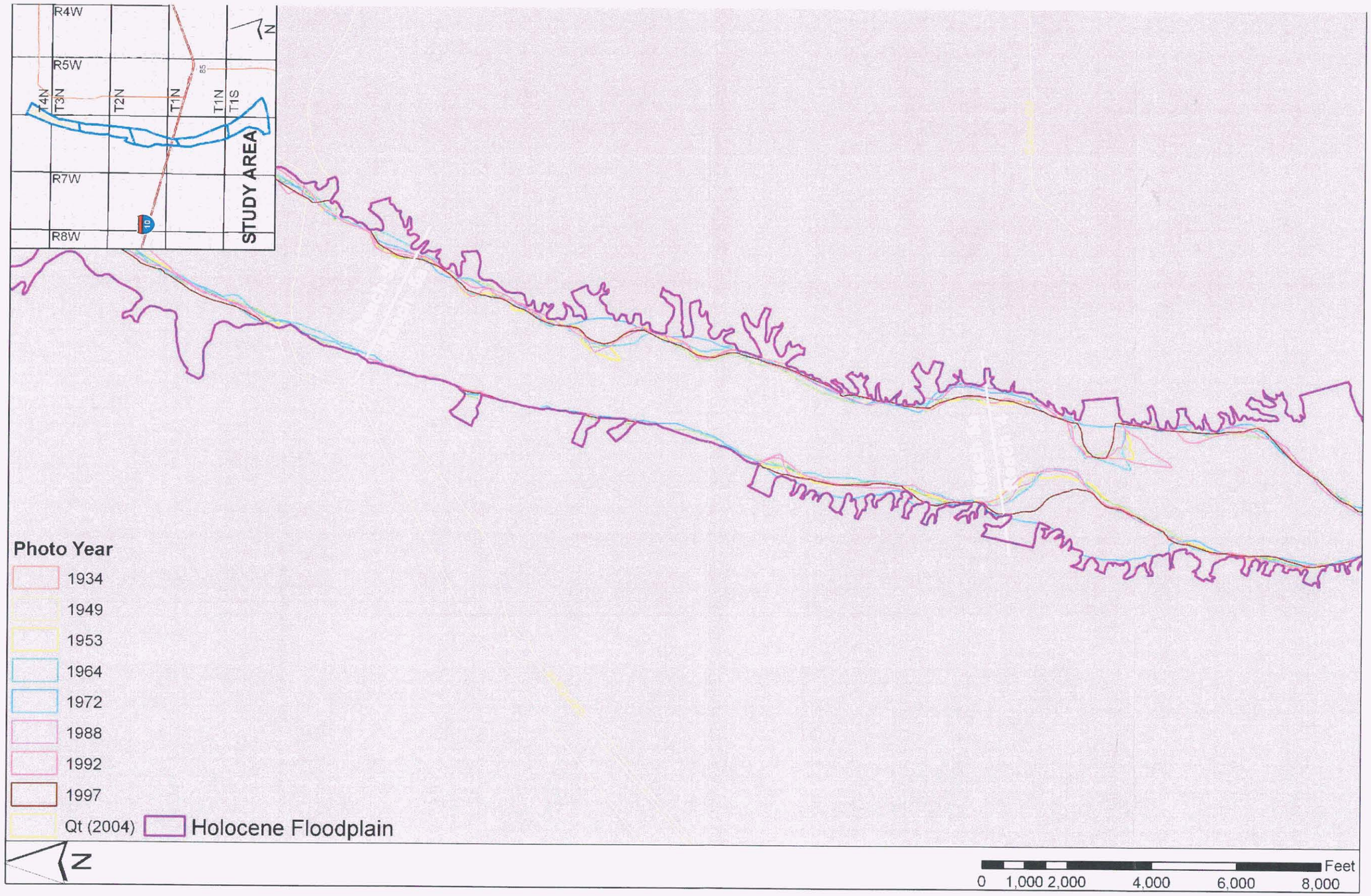

Figure 3-36. Reach 5a tributary deposit surfaces

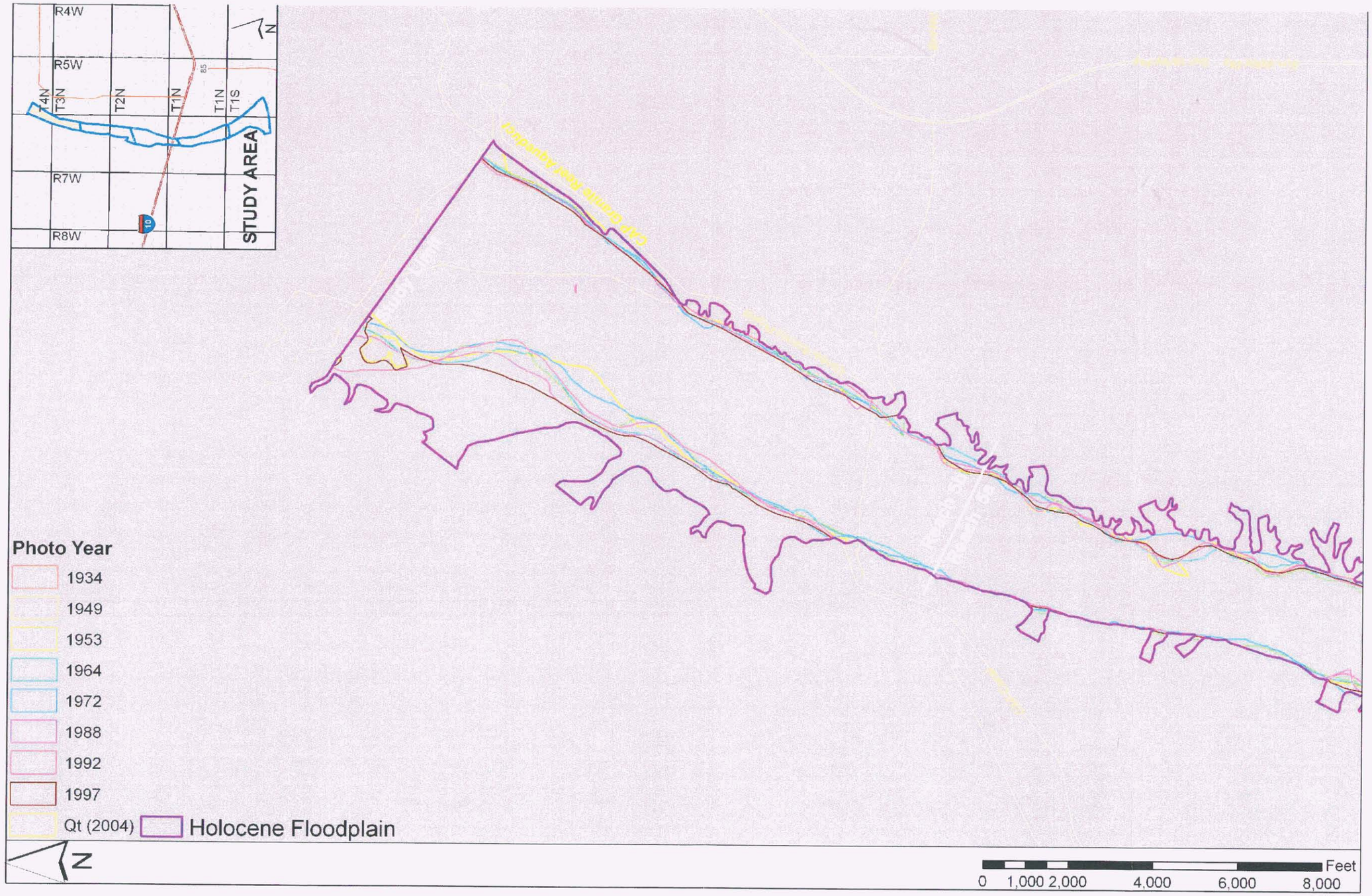

Figure 3-37. Reach 5b tributary deposit surfaces

3.5.2 Results

The 70-year photographic record indicates that the active channel varied in width and position within the Holocene floodplain. The active channel occupied a total of 28 percent of the Holocene floodplain area in just 70 years. The cumulative area occupied by bars and terraces is 33 percent, indicating that active river processes (active channel, bars, and terraces) have impacted a total of 61 percent of the Holocene floodplain area within the past 70 years. The following observations and conclusions are made relative to the functional surface plots shown in Figure 3-14 to Figure 3-37:

- The relative stability of the low flow channel in Reach 1 is artificially imposed on the river by levees that have been maintained by the local farmers. However, it may be significant that, despite the high degree of movement documented in upstream reaches, the river has not overcome human efforts to constrain it.
- Differences between Reach 1 and the other study reaches are readily apparent from the functional surface analysis. There are essentially no bar deposits in Reach 1; it consists solely of the active channel and the (disturbed) floodplain.
- Extensive lateral movement of the active channel occurred in Reaches 2 to 5, except at the confluences of the major tributaries (Jackrabbit Wash, Wagner/ Daggs Wash), where almost no movement of the active channel occurred.
- A primary geomorphic flood response is expansion of active channel and bars. Future channel widening and avulsions should be expected.
- Tributary terraces have the most persistent landforms during the past 70 years, but the functional surface analysis indicates that the small tributary terrace deposits are readily eroded when the main stem active channel abuts them.
- The active channel, bar, and floodplain terrace all showed significant movement during the period of record, although the overall pattern was relatively consistent.
- The existing low flow and flood channel pattern is similar to the historical pattern. The flood channel pattern is merely a larger version of the low flow pattern.

3.5.3 Historical Avulsions

Avulsions are readily identified by comparing channel positions plotted on a series of historical aerial photographs. Identification of avulsions provides information about general channel behavior during floods. In some cases, the location of avulsions can be predicted from the characteristics of the floodplain and channel positions, as described in Chapter 1, though avulsions occur in areas with no readily observable signs. Because avulsive channel change is a major component of the erosion hazard, it is important to quantify the frequency and magnitude of avulsions to adequately understand the lateral stability of the system and define the erosion hazard corridor.

Locations of historical avulsions were identified in the aerial photography and are shown on the Figures on the following pages. Figure 3-38 shows an avulsion that occurred upstream of Baseline Road during the 1951 flood. The active channel split and occupied what was formerly a parallel tributary drainage channel. Figure 3-39 shows another avulsion that occurred just upstream of the Tonopah-Salome highway during the same flood event.

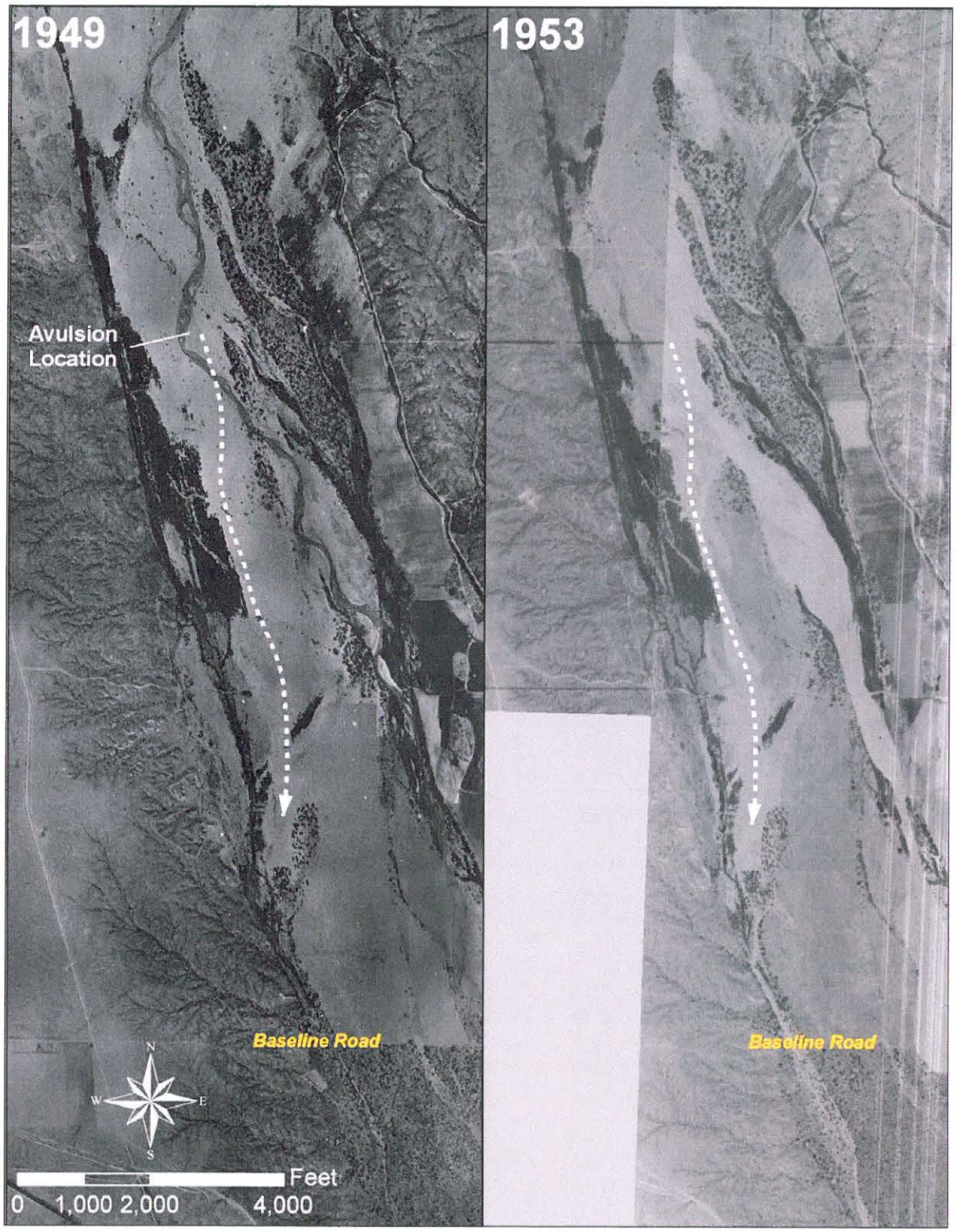

Figure 3-38. 1951 channel avulsion near Baseline Road

Figure 3-39. 1951 channel avulsion near Tonopah-Salome Highway

3.6 Empirical Geomorphic Analysis

Empirical methods were used to assess the stability and expected behavior of the Lower Hassayampa River. The expected channel dimensions and forms computed from empirical equations can be compared to observed river characteristics, and the differences interpreted as tendencies for future river change. The empirical analyses support the overall river behavior assessment, as well as erosion hazard zone delineation for the study reach.

3.6.1 Hydraulic Data

An important element of the empirical geomorphic analysis was the hydraulic data used in the various empirical geomorphic relationships. The HEC-RAS hydraulic model developed by WEST Consultants for the Lower Hassayampa WCMP was used as the base model for the empirical analyses. The WEST HEC-RAS model is described in the LHWCMP Hydraulics Report. However, to meet the project schedule and achieve objectives specific to the river behavior analysis, the WEST model was modified, as described below.

3.6.1.1 HEC-RAS Modifications

The WEST HEC-RAS model was used to generate hydraulic data for use in geomorphic assessments and channel stability studies. As described in the LHWCMP Hydraulics Report, the primary objective of the WEST HEC-RAS model was to evaluate the current effective Flood Insurance Study (FIS) floodplain delineation performed by Cella Barr Associates (CBA, 1989). The base WEST model was then modified for the empirical geomorphic analyses associated with the river behavior analysis. The following types of modifications were made to the WEST model:

- Discharge
- Bank Station Definition
- Ineffective Flow Areas

Discharge

For most geomorphic studies, a range of flow rates that include a variety of recurrence intervals are evaluated. Therefore, the parameterization of the HEC-RAS model must be applicable for the entire range of discharges that may occur in the study reach, not just the peak of the 100-year flood as is typical for a FIS HEC-RAS model. Where the model cannot be realistically modified for the full range of flows, the model should be optimized for flows approximating the bankfull discharge.

Four profiles were computed in the modified HEC-RAS model:

- The effective FIS discharge
- The "best-estimate" of the 50-year discharge
- The "best-estimate" of the 10-year discharge
- The "best-estimate" of the 2-year discharge

The frequency data used in the model were obtained from the effective FIS model and from the Hydrology Study for the LHWCMP (JEF, 2005).

Bank Station Definition

The WEST model bank stations were modified to reflect the location of the primary area of sediment movement within the river. When using hydraulic models, it is necessary to distinguish areas where sediment moves primarily as bed-material load (i.e., channels, subject to both scour and deposition) from areas where sediment moves primarily as wash load or suspended load (i.e., overbanks, primarily subject to deposition). If portions of the overbank areas are included in the channel, the channel velocity and hydraulic depth will be underestimated, resulting in low estimates of sediment transport capacity and/or erosion potential.

The bank station locations were selected by examination of recent color aerial photographs, detailed two-foot topography, and field observations. The banks were generally defined as the limits of the sandy-bottom channel (or channels in the case of multiple channel reaches). Bank locations were also associated with abrupt breaks in slope such as at the top of cutbanks. The bank locations were delineated in GIS and then transferred to the HEC-RAS model.

Ineffective Flow Areas.

The ineffective flow areas defined in the model should be appropriate for the full range of discharges. Ineffective flow limits were set at multiple levels for each cross section in order to model, as realistically as possible, the transfer of flow from one cross section to the next for each profile modeled. In some cases it was not possible to achieve a good balance for all profiles. In those cases, the 2-year and 10-year profiles were given priority.

Limitations

The following limitations to the HEC-RAS modeling effort are noted:

- The HEC-RAS model has multiple reaches downstream of the SPRR Bridge in Reach 1 to model overflows into the right overbank and outflows from the levee reach downstream of Old US 80. The hydraulic results and empirical equation results for Reach 1 were processed only for the main channel (i.e. Reach 1 in the HEC-RAS model).
- HEC-RAS is a one-dimensional, gradually varied flow model. It assumes a horizontal water surface, with no waves or superelevation on bends, and no sediment movement or bank erosion during the passage of the flood. There is uncertainty in the discharge estimate, the channel geometry, and the hydraulic modeling coefficients. The actual accuracy of the predicted water surface probably is not known within one foot. Results should be interpreted accordingly.

3.6.2 Hydraulic Geometry/Regime Equations

Regime equations and hydraulic geometry analyses attempt to relate measurable stream characteristics, such as sediment size, mean annual discharge or bankfull discharge, to equilibrium channel geometry characteristics such as stream width, channel depth, flow velocity or channel slope. Regime theory originated from studies of non-scouring and non-silting stable alluvial canals (cf. Kennedy, 1895), and has been extended to a wide variety of stream types (cf., Ackers & Charlton, 1971; Blench, 1951). Regime equations are typically based on discharge, sediment characteristics, and channel geometry. Hydraulic geometry analyses are theoretically similar to regime theory, but are based on empirical data gathered from natural streams or flumes and are typically based solely on discharge. Hydraulic geometry expresses the variation of channel characteristics with increasing discharge at a single section or along the length of a stream. The U.S. Geological Survey (cf., Leopold & Maddock, 1953) published the most widely used hydraulic geometry data.

Regime equation and hydraulic geometry analyses were applied to the Lower Hassayampa River study reaches to evaluate the following stream characteristics:

- Channel Pattern
- Channel Geometry
- Hydraulic Geometry

Lateral stability was evaluated by comparing predicted stream characteristics from one or more of these methodologies to the observed characteristics. These analyses assume that over the long-term the alluvial rivers will tend to erode their bed and banks, or adjust their slope or channel pattern to better match the expected characteristics. In addition, even though regime equations and hydraulic geometry relationships are empirically derived using data sets from very specific stream types (e.g., sand-bed rivers, canals, etc.), the data typically still have a large amount of scatter. The scatter in the original data limits the accuracy of the results. To increase the accuracy of the results, the equations selected for this study were based on data sets from streams which were the most similar to the study area characteristics. It is noted that ephemeral streams in central Arizona are unique, and therefore the results obtained by applying these equations must be interpreted cautiously. In general, the results are best interpreted as order-of-magnitude estimates of the direction of expected change, rather than precise predictions of the magnitude of future channel adjustments.

3.6.2.1 3.5.2.1 Data Sources

Stream characteristics and other data used in the analyses described below were obtained from the following sources described elsewhere in the LHWCMP project documentation:

- Recent Topographic Mapping – Hydraulics Report
- USGS Gauge Records – Hydrology Report
- Hydrologic Modeling – Hydrology Report

- Field Observations and Measurements – Chapter 2
- HEC-RAS Modeling – Hydraulics Report

3.6.2.2 3.5.2.2 Channel Pattern Relationships

Methodology

The slope of a stream has a strong influence on the channel pattern for a given discharge. Numerous researchers have used empirical data, flume studies, and theoretical relationships to establish a threshold slope that separates braided and meandering stream patterns. The following four slope-discharge relationships were selected for evaluation of the study reach:

- Lane Equation
- Ackers & Charlton Equation
- Leopold & Wolman Equation
- Henderson Equation

Lane Equations

Lane (1952) published empirical formulas to define the threshold slope for channel pattern, based on data from alluvial sand bed rivers. His equations leave an intermediate zone between the lines defined by the two slope equations where either pattern occurs. The Lane equations for channel pattern are:

$S_o > 0.010\ Q_m^{-0.25}$ (Braided channels)

$S_o < 0.001\ Q_m^{-0.25}$ (Meandering channels)

Where S_o = channel slope (ft./ft.), and

Q_m = mean annual discharge (cfs)

The mean annual discharge for the Lower Hassayampa River was estimated from USGS gauge records from the Hassayampa near Morristown station (Q_m = 25 cfs). The Hassayampa River near Arlington station was not used due to the frequent agricultural tailwater flows experienced at that station.

Ackers & Charlton Equations

The Ackers and Charlton (1971) equations are based on data obtained from flume studies. The results generally agree with the results of the Lane equations (MacBroom, 1981).

$S_o > 0.0015\ Q_m^{-0.12}$ (Straight channels)

$S_o < 0.0021\ Q_m^{-0.12}$ (Meandering channels)

Where S_o = channel slope (ft./ft.), and

Q_m = mean annual discharge (cfs)

The data sources were the same as for the Lane equation.

Leopold & Wolman Equations

The Leopold and Wolman equations (1957) were developed using data from rivers with coarse bed material (D50 > ¼ inch).

$S_o > 0.06\ Q_{maf}^{-0.44}$ (Braided channels)

$S_o < 0.06\ Q_{maf}^{-0.44}$ (Meandering channels)

Where S_o = channel slope (ft./ft.), and

Q_{maf} = mean annual flood (cfs)

The equations are based on bankfull discharge, which Leopold and Wolman determined to be equal to the mean annual flood. The mean annual flood has a recurrence interval of about 2.33 years (ADWR, 1985). The 2-year discharge was used in this analysis as an approximation of the mean annual flood. Leopold and Wolman found that straight channels could occur on all slopes, and that the occurrence of straight channels had poor correlation to bankfull discharge.

Henderson Equation

Henderson (1961) used Leopold's and Wolman's data, but added a variable describing the mean bed sediment diameter.

$S_o > 0.64\ D_{50}^{1.14}\ Q_{maf}^{-0.44}$ (Braided channels)

Where S_o = channel slope (ft./ft.), and

Q_{maf} = mean annual flood (cfs), and

D_{50} = mean sediment diameter (ft.)

Sediment diameter data were obtained from sieve analyses as described in Chapter 5.

Results

Application of the four channel pattern equations to the study area are shown in Table 3-4. The results vary by discharge because the energy slope was used in each equation instead of the bed slope. The measured bed slope for each reach is also shown. Computation using the energy slope allows one to assess how the channel pattern might adjust to a discharge higher than the mean annual flood. Given the flashy nature of floods on the Hassayampa River, full adjustment to higher discharges is not expected during a single flood, but the tendency toward adjustment in a particular direction is of interest to the stability assessment.

Field observations suggest that flow in the Lower Hassayampa River is often straight or slightly sinuous and becomes braided in some reaches, especially downstream of natural constrictions such as the confluence with major tributaries. As shown in Table 3-4, the channel pattern equations predict a variety of patterns. The equations for sand channels predict intermediate or straight channel pattern, while the gravel-bed equations predict a strongly braided pattern. Because the Hassayampa River is a predominantly sand-dominated system, the Lane and the Ackers & Charlton equations are probably the most appropriate. The observed pattern also varies along the study

reach. In fact, Reaches 2 through 5 vary in pattern within each reach. The observed pattern in those reaches is for a slightly sinuous straight channel at very low flows increasing in braided character with increasing flow rate up until about probably the 50-year level, when the river pattern begins to mimic the relatively straight valley pattern. At some locations, such as the Wagner-Daggs Wash and Jackrabbit Wash confluences, the river channel pattern is straight through the full range of flows.

Table 3-4. Channel Pattern Relationships: Threshold Slope for Braided Channels

Reach	Methodology - Channel Pattern				Observed Pattern	Observed Slope
	Lane	Ackers & Charlton	Leopold Wolman	Henderson		
FDS						
5	B52	S99	B100	B100	Braided	0.0043
4	I60	S95	B97	B100	Braided	0.0042
3	I74	S95	B95	B100	Braided	0.0043
2	I60	S98	B98	B100	Straight	0.0041
1	I63	S71	B76	B100	Straight	0.0044
10Yr						
5	I52	S76	B81	B100	Braided	0.0043
4	I52	S87	B94	B100	Braided	0.0042
3	I66	S93	B93	B100	Braided	0.0043
2	I57	S90	B93	B100	Straight	0.0041
1	I55	S73	B76	B100	Straight	0.0044
2Yr						
5	I51	S93	B94	B100	Braided	0.0043
4	I61	S87	B90	B100	Braided	0.0042
3	I61	S89	B98	B100	Braided	0.0043
2	I63	S97	B98	B100	Straight	0.0041
1	I53	S73	B76	B94	Straight	0.0044

Notes: S = Straight, I = Intermediate, B = Braided, M = Meandering, H=Shoaled

1. The subscript number after the pattern code (S, I, B, M, H) indicates the percent of sections predicted for the given pattern, e.g. B87 = 87% braided.
2. Channel patterns are not reported for the bridge reaches.

3.6.2.3 Channel Geometry Relationships

Methodology

Equations for stable channel geometry have been developed from streams that have been stable for long periods of time. These equations relate bankfull channel width, depth, and velocity to a specific discharge rate, such as the average annual flow or the dominant discharge. Several stable geometry equations were applied to the Lower Hassayampa River to assess the expected direction of future channel change.

Bray Equation #1

Bray (1979) developed equations for the geometry of alluvial gravel-bed rivers based on the 2-year discharge.

$W = 2.38\ Q_2^{0.527}$

$d = 0.266\ Q_2^{0.33}$

$V_m = 8.0\ d^{0.6}\ S_o^{\ 0.29}$

Where W = surface flow width (ft.)

Q_2 = 2-year discharge (cfs.)

d = flow depth (ft.)

V_m = mean channel velocity (ft./sec.)

S_o = channel slope (ft./ft.)

Bray Equation #2

Bray later modified his channel geometry relationships (Hey et. al., 1982) for gravel-bed rivers to include bankfull discharge and the bed material size.

W = 2.08 Qbf0.528 D50–0.07

$d = 0.256\ Q_{bf}^{0.331}\ D_{50}^{-0.025}$

$V_m = 1.87\ Q_{bf}^{0.14}\ D_{50}^{0.095}$

$S_o = 0.0965\ Q_{bf}^{-0.334}\ D_{50}^{0.586}$

Where W = surface flow width (ft.)

Q_{bf} = Bankfull discharge (cfs.)

D_{50} = medium bed sediment diameter (ft.)

d = flow depth (ft.)

V_m = mean channel velocity (ft./sec.)

S_o = channel slope (ft./ft.)

Hey Equation

Hey (1982) developed regime equations for gravel bed rivers in England that relate stable channel geometry to bankfull discharge and bedload transport rate.

$WP = 2.2\ Q_{bf}^{-0.54}\ D_{50}^{\ -0.05}$

$R = 0.161\ Q_{bf}^{0.41}\ D_{50}^{\ -0.15}$

$d_{max} = 0.252\ Q_{bf}^{0.38}\ D_{50}^{\ -0.16}$

$S_o = 0.679\ Q_{bf}^{-0.53}\ Q_s^{-0.13}\ D_{50}^{\ 0.97}$

Where WP = Wetted perimeter (m)

Q_{bf} = Bankfull discharge (m)

D50 = Median sediment diameter (m.)

R = Hydraulic radius (m)

d_{max} = Maximum channel depth (m)

S_o = Channel slope (m/m)

Q_s = Bedload sediment discharge (%)

However, because the results of the Hey equation for depth (dmax) were so much greater than was computed by the other equations used to compute stable depth, the Hey equation results were not included in the computation of the reach-average statistics shown in **Table 3-5**.

Parker Equation (Gravel Bed Rivers)

Parker (1979) examined gravel bed rivers to obtain his channel geometry equations. He found that, unlike the bed material in sand bed streams, the gravel and cobble bed material in coarse bedded streams is moved only during larger flows. He also noted that the banks of gravel bed streams tended to be more stable and straighter than streams with finer bed materials (MacBroom, 1981). Parker's equations use a dimensionless discharge parameter (Q*), as described below.

$$W_{bf} = 0.173\ Q^{*0.5}\ D_{50}$$

$$d = 0.010\ Q^{*0.415}\ D_{50}$$

$$S_e = 0.223\ Q^{*-0.410}$$

Where W_{bf} = bankfull width, width at top of bank (ft)

$Q^* = 0.039\ V_m\ d^{-1}\ D_{50} / ((\rho_s-1)/\rho)\ g\ d)^{1/2})$ (dimensionless)

D_{50} = mean sediment diameter (ft.)

d = average channel depth (ft)

S_e = energy slope (ft./ft.)

Ackers & Charlton Equation

The Ackers and Charlton (1971) equations were based on data from flume studies which used sand bed materials.

$$W = K_{ac}\ Q^{0.42}$$

Where W = surface channel width (ft.)

Q = discharge (cfs)

K_{ac} = a coefficient varying from 3.6 for straight channels to 7.2 for meandering channels

Lacey Equation

The Lacey equation (1929) was developed to describe the geometry of silt-laden canals in India. However, Bray reported (1979) that in gravel rivers in Canada, the Lacey equation was as accurate for predicting velocity as the Manning's equation.

$$V = 0.8Q^{0.167}$$

Where V = mean channel velocity (ft./sec.)

Q = discharge (cfs)

Chang Equation

Chang's (1988) gravel bed equations for channel geometry support the FLUVIAL-12 sediment transport model, which attempts to simulate channel change from sediment continuity data using minimum stream power concepts. Chang provides equations for channel width, depth, and slope.

$$S_o = 0.000442\ D_{50}^{1.15} / Q_{bf}^{0.42}$$

$$W = [1.905 + 0.249(\ln(0.001065\ D_{50}^{1.15} / (S_o\ Q_{bf}^{0.42}))^2]\ Q_{bf}^{0.47}$$

$$d = [0.2077 + 0.0418(\ln(0.000442\ D_{50}^{1.15} / (S_o\ Q_{bf}^{0.42})))]\ Q_{bf}^{0.42}$$

Where S_o = channel slope (ft./ft.)

D50 = median sediment diameter (mm.)

Q_{bf} = bankfull discharge (cfs)

W = channel width (ft)

d = average channel depth (ft)

In general, the Chang equation for slope performed poorly when applied to the study area. Some of the predicted channel geometry values were well outside the range of possibility (e.g., negative flow depths). Therefore, the results of the Chang equation are included in **Table 3-5**, but the predicted values were not used to obtain the average predicted values that were compared with existing reach characteristics.

Kellerhalls (1967) Equations

Kellerhalls developed equations for the equilibrium channel width and depth in gravel bed rivers. The Kellerhalls equations use the dominant discharge, which is also referred to as the channel-forming or effective discharge.

$$W = 1.8\ Q_{dd}^{0.5}$$

$$d = 0.166\ Q_{dd}^{0.4}\ K_n^{-0.12}$$

Where W = channel width (ft)

Q_{dd} = dominant discharge (cfs)

d = average channel depth (ft)

K_n = Nikuradse's sand grain roughness coefficient

However, because the results of the Kellerhalls equation for depth were so much greater than was computed by the other equations used to compute stable depth, the Kellerhalls equation results were not included in the computation of the reach-average statistics shown in **Table 3-5**.

Schumm Equation

Schumm (1961) preferred to examine the width/depth ratio of semi-arid streams, rather than either parameter separately. Schumm's equation is based on the percentage of fine-grained material in the channel banks.

$$F = 255\ M^{-1.08}$$

Where F = width/depth ratio

M = percentage of silt/clay in the bed.

The percentage of silt and clay in the bed material and banks was extracted from detailed SCS soils mapping of the study area (Camp, 1986). Application of the Schumm equation to streams with stratified bank materials is difficult. The results of the Schumm equation are consistent with the AMAFCA results, and are therefore reported on the same line in **Table 3-5** as the AMAFCA results.

AMAFCA Equations

The AMAFCA (1994) equations for width and equilibrium slope were developed from empirical and theoretical data for application to the arroyo systems of northern New Mexico.

$$W = 0.5\ F^{0.6}\ Fr^{-0.4}\ Q^{0.4}$$

$$S_o = 18.28\ n^2\ F^{0.133}\ Fr^{2.133}\ Q^{-0.133}$$

Where W = width of channel (ft.)

F = width/depth ratio

Fr = main channel Froude number

Q = discharge (cfs.)

S_o = channel slope (ft./ft.)

n = Manning's n value for channel

Moody & Odem Equations

Moody and Odem (1999) completed an investigation of bankfull channel geometry relationships on a variety of stream types in Arizona using Rosgen channel classification methods. Channel geometry relationships were defined for a number of regions in Arizona.

$$Q_{bf} = 52.334\ DA^{0.5766}$$

$$A = 11.428\ DA^{0.5291}$$

$TW = 12.301\ DA^{0.3756}$

$d = 0.9455\ DA^{0.1506}$

Where Q_{bf} = Bankfull discharge (cfs)

DA = Watershed drainage area (mi^2)

A = Section flow area at bankfull discharge (ft.)

TW = Flow width at bankfull discharge (ft.)

d = Average flow depth at bankfull discharge (ft.)

BUREC Equation

The Bureau of Reclamation (Lane and Carlson, 1953) developed relationships that describe stable channel dimensions for canals cut into coarse grained alluvium.

$d_{max} = (Q_{bf}/2 \tan \phi)^{0.5}$

$A = 2\ d_{max}^2 / \tan \phi$

$V_m = 1/n\ (d_{max} \cos \phi / (0.5\ \pi\ (1 - \cos \phi))^{0.667}\ S_e^{0.5}$

$TW = d_{max}\ \pi / \tan \phi$

Where d_{max} = Maximum depth of flow (ft.)

Q_{bf} = Bankfull discharge (cfs)

ϕ = Angle of repose of bank material

V_m = mean flow velocity (ft./sec.)

N = Mannings' n value

S_e = Energy slope (ft./ft.)

TW = Top width of flow (ft.)

The results for depth from the BUREC equations were much different than the results from the other equations, were not considered reasonable to the Lower Hassayampa River, and were not included in the reach-average estimates shown in **Table 3-5**.

Results

The results of applying the channel geometry equations to the Lower Hassayampa River are shown in **Table 3-5**. The 2- and 10-year discharges were substituted for the discharge variable used in the original channel geometry equations to examine the trend of potential adjustments in channel geometry at each flow rate. Predicted values of widths, depths, slopes and velocities from the channel geometry equations were compared to the measured values obtained from field data, topographic mapping and HEC-RAS models. The differences were interpreted as follows:

- Width. Where the predicted channel width is greater than the HEC-RAS modeled channel width, the channel is expected to erode its banks to achieve the greater width during future floods. Where the predicted channel width is less

than the HEC-RAS modeled channel width, the channel is assumed to have low potential for lateral movement due to channel widening, and is likely to experience deposition along at least one of the banks at the flow rates considered.

- Depth. Where the predicted channel depth is greater than the HEC-RAS modeled channel depth, the channel is expected to erode its bed (degrade) to achieve the equilibrium depth during future floods. Where predicted channel depth is less than the HEC-RAS modeled channel depth, the channel is expected to aggrade (deposit sediment) to reach the equilibrium state.

- Slope. Where the predicted slope is less than the existing slope, the channel is expected to decrease its slope (scour) to achieve a more stable form.

- Velocity. Where the predicted velocity is less than the HEC-RAS modeled velocity, floods will be more erosive than predicted by the channel geometry equations.

Geomorphic interpretations of the results shown in **Table 3-5** for the five project reaches include the following:

- Width/Depth Ratio. The Hassayampa River existing channel, and hence the probable equilibrium channel geometry, is wider and shallower than the streams used to development the regime and hydraulic geometry equations. The existing banks are wider than even the 100-year predicted channel widths.

- Slope. The predicted slopes are almost uniformly lower than the existing slopes by an order of magnitude, except for the slope predicted by the AMAFCA equation. Slope adjustment by an order of magnitude is not a reasonable expectation for the Hassayampa River, unless major watershed changes occur.

Table 3-5. Observed and Expected Channel Characteristics												
Equation	Channel Width (ft)			Flow Depth (ft)			Channel Slope (ft/ft)			Channel Velocity (ft/s)		
	FDS	10Yr	2Yr	FDS	10Yr	2Yr	FDS	10Yr	2Yr	FDS	10Yr	2Yr
Reach 5												
Bray - Equation #1	585	327	156	8.6	5.9	3.7	0.0010	0.0015	0.0024	6.8	5.8	4.8
Bray - Equation #2	812	454	215	9.5	6.6	4.2	0.0001	0.0001	0.0002	4.4	3.7	3.1
Hey	236	137	69	38.2	25.1	14.7	<0.0001	<0.0001	0.0001			
Ackers & Charlton/Lacey	288	182	101							4.6	3.8	3.0
Parker	1528	881	435	10.8	6.9	3.8	<0.0001	<0.0001	<0.0001			
Chang	1746	899	404	-8.5	-4.1	-1.7	<0.0001	<0.0001	<0.0001			
Kellerhalls	333	192	95	19.3	12.4	7.1	<0.0001	<0.0001	0.0001	5.3	4.7	4.1
AMAFCA/Schumm	874	668	375				0.0045	0.0042	0.0045			
Moody & Odem	159	159	159	5.3	5.3	5.3						
BUREC	113	77	44	30.1	20.5	11.7				15.9	11.8	8.8
Average	425	274	152	8.6	6.2	4.3	0.0008	0.0008	0.0010	5.3	4.5	3.8
HEC-RAS Data	1311	1140	733	3.4	2.0	1.2	0.0046	0.0043	0.0048	8.5	5.9	4.4
Expected Behavior	Fill	Fill	Fill	Scour	Scour	Scour	Scour	Scour	Scour	Erosion	Erosion	Erosion
Reach 4												
Bray - Equation #1	621	345	154	8.9	6.2	3.7	0.0010	0.0014	0.0024	6.9	5.9	4.8
Bray - Equation #2	862	478	213	9.9	6.8	4.1	0.0001	0.0001	0.0002	4.4	3.8	3.1
Hey	249	144	68	40.0	26.2	14.7	<0.0001	<0.0001	0.0001			
Ackers & Charlton/Lacey	303	190	100							4.7	3.9	3.0
Parker	1620	927	431	11.4	7.2	3.8	<0.0001	<0.0001	<0.0001			
Chang	1833	961	395	-8.9	-4.5	-1.7	<0.0001	<0.0001	<0.0001			
Kellerhalls	353	202	94	20.2	13.0	7.0	<0.0001	<0.0001	0.0001	5.4	4.8	4.1
AMAFCA/Schumm	765	582	306				0.0042	0.0045	0.0047			
Moody & Odem	161	161	161	5.3	5.3	5.3						
BUREC	121	79	44	32.4	21.2	11.8				15.5	12.0	8.5
Average	430	273	143	8.9	6.4	4.3	0.0008	0.0009	0.0011	5.3	4.6	3.7
HEC-RAS Data	1068	962	533	4.5	2.5	1.3	0.0043	0.0044	0.0049	9.4	6.5	4.5
Expected Behavior	Fill	Fill	Fill	Scour	Scour	Scour	Scour	Scour	Scour	Erosion	Erosion	Erosion
Reach 3												
Bray - Equation #1	751	346	153	10.1	6.2	3.7	0.0009	0.0014	0.0024	7.3	5.9	4.8
Bray - Equation #2	1042	480	211	11.1	6.9	4.1	0.0001	0.0001	0.0002	4.7	3.8	3.1
Hey	297	145	68	45.8	26.3	14.6	<0.0001	<0.0001	0.0001			
Ackers & Charlton/Lacey	353	190	99							4.9	3.9	3.0
Parker	1938	930	427	13.2	7.2	3.8	<0.0001	<0.0001	<0.0001			
Chang	2220	966	388	-10.7	-4.6	-1.6	<0.0001	<0.0001	<0.0001			
Kellerhalls	423	203	93	23.4	13.0	7.0	<0.0001	<0.0001	0.0001	5.6	4.8	4.1
AMAFCA/Schumm	800	550	287				0.0038	0.0043	0.0043			
Moody & Odem	180	180	180	5.9	5.9	5.9						
BUREC	143	81	45	38.1	21.5	11.9				16.0	11.8	8.1
Average	498	272	142	10.1	6.5	4.4	0.0007	0.0008	0.0010	5.6	4.6	3.7
HEC-RAS Data	1105	918	485	6.0	2.7	1.5	0.0040	0.0045	0.0046	10.4	6.6	4.6
Expected Behavior	Fill	Fill	Fill	Scour	Scour	Scour	Scour	Scour	Scour	Erosion	Erosion	Erosion

Table 3-5 Cont'												
Reach 2												
Bray - Equation #1	604	345	152	8.8	6.2	3.7	0.0010	0.0014	0.0024	6.9	5.9	4.8
Bray - Equation #2	839	478	210	9.7	6.8	4.1	0.0001	0.0001	0.0002	4.4	3.8	3.1
Hey	243	144	67	39.2	26.2	14.5	<0.0001	<0.0001	0.0001			
Ackers & Charlton/Lacey	296	190	99							4.6	3.9	3.0
Parker	1577	927	425	11.1	7.2	3.8	<0.0001	<0.0001	<0.0001			
Chang	1788	957	385	-8.7	-4.5	-1.6	<0.0001	<0.0001	<0.0001			
Kellerhalls	344	202	93	19.8	13.0	7.0	<0.0001	<0.0001	0.0001	5.3	4.8	4.1
AMAFCA/Schumm	527	427	229				0.0042	0.0046	0.0043			
Moody & Odem	181	181	181	6.0	6.0	6.0						
BUREC	122	82	44	32.7	21.8	11.8				14.5	11.4	8.2
Average	395	256	134	8.9	6.5	4.4	0.0008	0.0009	0.0010	5.3	4.6	3.7
HEC-RAS Data	680	640	338	5.8	3.1	1.7	0.0042	0.0043	0.0043	10.3	7.3	5.2
Expected Behavior	Fill	Fill	Fill	Scour	Scour	Scour	Scour	Scour	Scour	Erosion	Erosion	Erosion
Reach 1												
Bray - Equation #1	645	343	150	9.1	6.2	3.6	0.0009	0.0014	0.0024	7.0	5.9	4.8
Bray - Equation #2	896	475	208	10.1	6.8	4.1	0.0001	0.0001	0.0002	4.5	3.8	3.0
Hey	258	144	67	41.1	26.1	14.4	<0.0001	<0.0001	0.0001			
Ackers & Charlton/Lacey	312	189	98							4.7	3.9	3.0
Parker	1679	922	421	11.7	7.1	3.7	<0.0001	<0.0001	<0.0001			
Chang	1786	874	343	-8.2	-3.6	-0.8	<0.0001	<0.0001	<0.0001			
Kellerhalls	366	201	92	20.8	12.9	6.9	<0.0001	<0.0001	0.0001	5.4	4.8	4.1
AMAFCA/Schumm	392	311					0.0037	0.0040	0.0044			
Moody & Odem	181	181	181	6.0	6.0	6.0						
BUREC	158	109	71	42.2	29.1	19.1				10.9	7.8	5.2
Average	401	244	124	9.2	6.5	4.4	0.0007	0.0008	0.0010	5.4	4.6	3.7
HEC-RAS Data	512	457	304	10.5	6.5	4.1	0.0038	0.0041	0.0045	9.5	6.2	4.0
Expected Behavior	Fill	Fill	Fill	Fill	Equal	Scour	Scour	Scour	Scour	Erosion	Erosion	Erosion

The AMAFCA equation predicts slopes that are nearly equal to the existing channel slopes, and is considered a reasonable estimate of expected channel behavior. That is, no long-term slope adjustment is expected for existing conditions.

- Velocity. Predicted channel velocities are uniformly lower than the velocities estimated from HEC-RAS. This difference is interpreted to mean that the Hassayampa River is more erosive than average rivers, particularly given the high measured width/depth ratios.

- Reach 1. The predicted width, depth, slope and velocity for Reach 1, the most disturbed reach, is more in line with the measured values in Reach 1 than for any of the other (more natural) reaches considered.

Note that the stable geometry equations described above reflect the dimensions of channels which have been stable over long periods of time. The stable geometry equations suggest the nature of possible future channel adjustments to the Lower Hassayampa River. However, given the wide disparity between the observed and predicted channel geometry, these predictions should be viewed as less reliable than predictions based on observed (i.e., historical) channel changes.

3.6.3 Allowable Velocity

Allowable velocity criteria have long been used in channel design to estimate the velocity at which channel bed and bank sediments will begin to erode. A variety of allowable velocity data have been published by the US Army Corps of Engineers (1970, 1990, 1995) and the USDA Soil Conservation Service (1977), as well as by many other agencies.

3.6.3.1 3.5.3.1 Methodology

The following allowable velocity approaches were applied to the Lower Hassayampa River study reaches:

- Fortier & Scobey Table
- BUREC/Mavis & Laushey Equation
- Neill Equation
- USACOE Permissible Velocity Tables

3.6.3.2 3.5.3.2 Fortier & Scobey Table

Fortier and Scobey (1926) published one of the first tables of permissible velocity in 1926. Their data, based on records of seasoned stable canals, was later republished by a number of federal agencies and other organizations including the FHWA, ASCE, and Chow (MacBroom, 1981). The Fortier and Scobey data (Table 3-6) distinguish erosion hazards for clear water, silt-laden water, and water transporting sand and gravel (bedload). Their data presumably do not account for the stabilizing effect of bank vegetation. Further modifications to this method are described in Chow (1959) from Soviet researchers in 1936. These modifications include an adjustment to the

permissible velocity based on depth. An additional modification was proposed by Lane (1955) for sinuous channels.

Table 3-6. Fortier & Scobey Table of Permissible Canal Velocities (ft/s)

Bank Material	Clear Water	Silt-Laden	Sand/Gravel Bedload
Sandy Loam	1.75	2.50	2.00
Firm Loam	2.50	3.50	2.25
Fine Gravel	2.50	5.00	3.75
Stiff Clay	3.75	5.00	3.00
Coarse Gravel	4.00	5.50	6.50
Cobbles	5.00	5.50	6.50

3.6.3.3 3.5.3.3 BUREC/Mavis & Laushey Equation

The BUREC (1974) recommends that permissible velocity be estimated using a modification of the Mavis and Laushey equation (Jurnikis, 1971), which was developed by bridge engineers in Great Britain (MacBroom, 1981). The BUREC equation is a function of grain size, and is most applicable to bed material.

$$V_b = 0.64\ D^{(4/9)} \qquad \text{for } D < 6.0 \text{ mm}$$

$$V_b = 0.5\ D^{1/2} \qquad \text{for } D > 6.0 \text{ mm}$$

Where V_b = competent velocity (ft/sec)

D = particle diameter (mm)

3.6.3.4 3.5.3.4 Neill Equation

Neill (1975) developed equations that are a function of flow depth and grain size for permissible velocities on gravel and cobble bed streams, with a separate equation for cohesive soils.

$$V_b = 3.15\ d^{(1/3)}\ D^{(2/3)} \quad \text{(non-cohesive soils)}$$

$$V_b = 7.5\ d^{(1/6)}\ \tau_c^{1/2} \quad \text{(for cohesive soils)}$$

Where V_b = competent velocity (ft/sec)

d = flow depth (ft)

D = grain size (ft)

τ_c = *critical shear stress* (lb/ft^2)

3.6.3.5 3.5.3.5 USACOE Permissible Velocity

The Corps of Engineers (1970; 1995) has established suggested maximum velocities for design of non-scouring flood control channels of various bank materials, as shown in Table 3-7.

Table 3-7. Suggested Maximum Permissible Mean Channel Velocities (USACOE, 1995)	
Channel Material	Mean Velocity (ft/sec)
Fine Sand (0.075 – 0.45 mm)	2.0
Coarse Sand (2 – 5 mm)	4.0
Fine Gravel (5 - 20 mm)	6.0
Grass-Lined Banks (< 5% Slope, Sandy Silt, Bermuda Grass)	8.0
Poor Rock (Sedimentary)	10.0
Good Rock (Igneous or Metamorphic)	20.0

The Corps of Engineers (1990) has also developed criteria relating flow depth and velocity to the beginning of movement of granular bed materials and erosion of cohesive bank materials, as summarized in Table 3-8.

Table 3-8. Corps of Engineers Erosive Velocity Data					
Grain Size (mm)	Flow Depth (ft)	Velocity (ft/sec)	Cohesiveness	Flow Depth (ft)	Velocity (ft/sec)
1 (sand)	5 10	2.5 4.0	Very Soft	5 10	2.0 2.5
10 (gravel)	5 10	4.5 5.5	Average	5 10	3.5 4.0
100 (cobbles)	5 10	9.5 10.5	Very Stiff	5 10	5.5 6.0

3.6.3.6 3.5.3.6 Results

In general, the internal alluvial banks of the Lower Hassayampa River are composed of sand with generally sparse vegetation cover. The outer margins of the geologic floodplain tend to be cut into Pleistocene- or Tertiary-aged terraces capped with caliche and underlain by less resistant sand, and gravel. In some places the channel intersects and cuts these surfaces. No significant grass cover was observed anywhere in the field.

Table 3-9 shows reach-averaged velocities for the channel, left and right overbanks for five flood profiles. The reach-averaged data show that the Lower Hassayampa River is erosive for the full range of discharges within the main channel. Overbank velocities are generally below the erosive limits for sands for the 10-year and more frequent flows. Above the 10-year flow rate, overbank velocities become erosive. In addition, locally the maximum overbank velocities are erosive for sand-sized particles through the range of flow rates. Since many of the overbank areas are composed of finer-grained materials erosion of the overbank areas is expected during flows greater than about the 10-year flood.

Table 3-9. Flood Velocities						
Reach	Average Velocity (ft/s)			Maximum Velocity (ft/s)		
	Main Channel	Overbanks		Main Channel	Overbanks	
		Left	Right		Left	Right
FDS						
5	8.5	4.8	4.5	12.1	9.7	7.2
4	9.4	3.9	4.1	13.1	6.9	7.6
3	10.4	5.0	4.9	14.6	11.9	7.9
2	10.3	3.4	5.0	14.0	7.1	7.1
1	9.5	2.4	3.6	18.1	6.3	6.5
10 Yr						
5	5.9	3.1	2.6	9.2	6.0	5.5
4	6.5	1.9	2.7	9.6	4.2	6.0
3	6.6	3.0	2.6	11.2	5.3	5.2
2	7.3	1.6	2.0	10.2	4.9	4.7
1	6.2	1.4	2.5	11.0	2.5	8.0
2 Yr						
5	4.4	1.5	1.4	7.1	3.1	4.4
4	4.5	1.1	1.7	7.2	3.0	3.0
3	4.6	1.1	2.1	9.3	2.6	4.7
2	5.2	1.3	1.4	7.9	3.6	2.3
1	4.0	0.1	1.9	8.8	0.1	7.6

Table 3-10. Allowable Velocity Results							
Reach	**Fortier-Scobey**	**BUREC**	**Neill: Non-cohesive**		**Neill: Cohesive**		**USACOE**
			Erosive	**Velocity**	**Erosive**	**Velocity**	
FDS							
5	E100	E100	E100	0.3	S79	8.8	E97
4	E100	E100	E100	0.3	S87	10.3	E100
3	E100	E100	E100	0.3	S98	11.9	E98
2	E100	E100	E100	0.3	S97	12.2	E100
1	E98	E100	E100	0.4	S100	15.9	E86
10Yr							
5	E100	E100	E100	0.2	E52	5.9	E54
4	E100	E100	E100	0.3	S61	6.8	E65
3	E100	E100	E100	0.3	S67	7.1	E54
2	E100	E100	E100	0.3	S68	8.0	E82
1	E94	E100	E98	0.4	S90	11.1	E69
2Yr							
5	E99	E99	E100	0.2	S54	4.4	S90
4	E100	E100	E100	0.2	S53	4.6	S92
3	E100	E100	E100	0.2	S64	5.0	S84
2	E100	E100	E100	0.2	E57	5.5	S77
1	E88	E94	E94	0.3	S86	7.1	S92

Notes:
E = allowable velocity exceeded; erosion expected
S = allowable velocity not exceeded; erosion not expected
E100 = 100 % of sections in reach have indicated erosive trend, E87 = 87 % of sections in reach, etc.

The reach-averaged velocities estimated from the HEC-RAS models for the five flood profiles were compared to the allowable velocities determined by the methodologies described above, as shown in Table 3-10. Erosion (E) is expected where the allowable velocities are exceeded by the predicted HEC-RAS reach-averaged velocities. Where the allowable velocities are not exceeded, the channel is expected to be stable (S). The number listed after S or E in Table 3-10 indicates the percent of the cross sections within the reach which exhibit the S or E trend.

Most of the allowable velocity methodologies used indicate that the materials in the bed and banks of the Lower Hassayampa River are erodible. However, Neill's equation for cohesive soils predicts that the banks will be stable up to the 100-year event. Since cohesive soils are generally not present within the study area, the results of Neill's cohesive soil equation are not applicable for most of the reach. Comparison of HEC-RAS channel velocities with the USACOE and Fortier & Scobey erosive velocity thresholds indicate that the channel banks are probably erodible during flows as frequent as the 2-year event. This matches with observations of flooding and erosion that occurred during this study when relatively small discharges in the winter of 2004-05 were seen to have eroded channel banks and reworked channel bed sediments throughout the study reach.

3.6.4 Conclusions

Allowable velocity criteria provide general information on the likelihood of bank and channel erosion. However, accurate predictions of lateral stability based on allowable velocity criteria are difficult to achieve because of the effect of soil cohesiveness, vegetation, carbonate accumulations, and soil physics on erodibility. The range of allowable velocities indicated by the Neill equations illustrates the effect of cohesion on erodibility. Broadly interpreted, the allowable velocity data indicate that all of the channel banks in the study area will erode even in small floods if the banks are not cohesive, but will resist erosion if they are cohesive. Finally, the effects of bank vegetation (increase stability), stratified bank sediments (decrease stability), and other local variations ($CaCO_3$ content, piping, bed scour, etc.) create additional uncertainty for the reliability of allowable velocity predictions.

3.7 Summary

The geomorphic analyses summarized in this Chapter included stream classification methods, empirical equations, geomorphic mapping, and soils analysis. The results of these analysis included the following:

- Stream Classification. Both stream classification models (Brice and Rosgen) applied to the study area predict that the Lower Hassayampa River has a naturally braided pattern which tends to be laterally unstable and subject to high rates of lateral erosion.

- Functional Surface Analysis. Analysis of geomorphic surfaces over a 70-year photographic record indicates that active channel has varied in width and lateral position within the Holocene floodplain. The active channel has occupied a cumulative total of 28 percent of the Holocene floodplain, and the cumulative

area occupied by the bars and terraces is 33 percent. Active river processes (active channel, bars, and terraces) have occupied a cumulative total of 61 percent of the Holocene floodplain area within the past 70 years.

- Geomorphic Mapping. Four primary geomorphic units that comprise the Holocene floodplain were mapped. None of the units showed any evidence of significant geomorphic age, resistance to erosion, or geologic permanence.

- Avulsions. Historical evidence demonstrates that channel avulsions have occurred and should be expected to occur during future floods.

- Empirical Analysis. The empirical analyses demonstrated that the Lower Hassayampa River is significantly different in form than other river types and has a naturally wider, shallower, steeper channel that experiences high velocities and lateral erosion.

- Allowable Velocity. Computed velocities uniformly exceed the standard threshold of erosion throughout the study area. Lateral erosion should be expected during even the smallest floods.

CHAPTER 4 - BED ELEVATION ANALYSIS

4.1 Introduction

The purpose of the bed elevation change analysis was to document historical changes in bed elevation, and compare historical trends with the computational methods to predict future changes in bed elevation. The methods used for the LHWCMP bed elevation analyses included the following:

- Scour Equations
- Equilibrium Slope Analysis
- Armoring Analysis
- Historical Topography Comparison
- Longitudinal Profile Analysis
- Field Observations

The data and analyses used are described relative to the information they provide about the degree and extent of erosion hazards along the Lower Hassayampa River. The hydraulic data used in the engineering methods presented in this chapter were derived from the modified HEC-RAS model described in Section 3.5. The hydraulic data were processed through the equations described below using Excel spreadsheets and Visual Basic programming. The historic data were taken from available historic contour data sets collected for the project, including USGS quadrangles, previous floodplain studies, and mapping performed by the District in support of the LHWCMP.

4.2 Scour

Scour is defined as any lowering of the channel bed elevation that occurs as a result of flowing water. Scour can be caused by changes in the sediment transport capacity of a channel during the passage of a flood wave (general scour), by the formation of bed forms (dune, anti-dune, thalweg scour), by velocity currents around channel bends (bend scour), by local flow obstructions (local scour), or by progressive slope adjustments to watershed and watercourse changes (long-term scour). Scour is directly proportional to flow velocity and flow duration, and inversely proportional to sediment size, sediment supply, and flow depth. Scour during a design flow (a.k.a. single-event scour or short-term scour) is discussed in this Chapter as well as in Chapter 5 of this report. Long-term scour was evaluated using a variety of approaches and is discussed throughout this Chapter.

The objective of the scour analysis was to compute reach-averaged trends for use in predicting future regional channel change and order of magnitude relative trends in channel behavior between adjacent reaches. The LHWCMP scour analysis is not intended to generate design-level scour estimates at any point within the study reach. The scour estimates listed in this chapter are not appropriate for any design purpose. Site-specific scour analyses should be performed in support of any design study.

4.2.1 Methodology

Scour in the Lower Hassayampa River was estimated using procedures outlined in the Arizona Department of Water Resources Engineering Analysis of Fluvial Systems (ADWR, 1985; hereafter, "the ADWR Manual"). The ADWR scour equation is:

$$Z_t = SF\ (Z_{deg} + Z_{gs} + \tfrac{1}{2} Z_a + Z_{ls} + Z_{bs} + Z_{lft})$$

where:

Z_t = Design scour depth, excluding long-term degradation or aggradation (ft)

Z_{gs} = General scour depth (ft)

Z_a = Anti-dune trough depth (ft)

Z_{ls} = Local scour depth (ft)

Z_{bs} = Bend scour depth (ft)

Z_{lft} = Low-flow thalweg depth (ft)

Z_{deg}= Long-term degradation

SF = Safety factor (1.0 – 1.5)

General scour, Z_{gs}, is the component of scour that represents the mobile portion of the bed-material of the channel bottom. The discussion in the ADWR Manual relating to directs the reader to the Section 5.3.11 (Contraction Scour) or Section 5.3.14 (Evaluation of Gravel Mining Impacts). Contraction scour (ADWR Equations 5.19 to 5.24, p. 5-103) is estimated using the following equations:

$$Z_{gs} = Y_2 - Y'_2$$

where:

Z_{gs} = General scour depth (ft)

Y'_2 = Original (non-equilibrium) flow depth at the constriction (ft)

$$Y_2 = \left(\frac{q_{s2}}{a\, q_2^c}\right)^{\frac{1}{b-c}}$$

, the computed equilibrium flow depth (ft)

q_{s2} = $W_1/W_2\ q_{s1}$

q_{s1} = $a\ Y_1^b\ V_1^c$

q2 = $W_1/W_2\ q_1$

a, b, c = sediment transport coefficients from ADWR Table 5.6a

W_1 = active channel width at the upstream section

W_2 = active channel width at the constricted section

Y_1, V_1 = hydraulic depth (Y) and channel velocity (V) at upstream section

The discussion of sand and gravel mining impacts related to scour in the ADWR Manual relates to headcut formation and propagation upstream of in-stream mines and is not applicable to the reach-average general scour application for the LHWCMP river behavior analysis. Headcut scour from in-stream mining was evaluated separately and is discussed in Chapter 5 of this report. Other technical manuals describe alternative methods for estimating general scour such as using the maximum scour depth computed in a sediment routing model (e.g., HEC-6) or by using specific general scour equations (e.g. City of Tucson Manual). Several alternative methods were explored and resulted in similar, but slightly smaller (< 10%) general scour depth predictions.

Where Z_{gs} was determined to be negative, the general scour component was assumed to be zero prior to determining the reach average general scour value reported below.

Anti-dune trough depth, Za, is the component of scour caused by movement of dune shaped bed forms along the bottom of the channel. The anti-dune trough depth was estimated using the following equation:

$$Z_a = 0.0273\ V_m^2$$

where:

V_m = Average velocity of flow at design discharge (ft/sec)

The anti-dune trough depth is limited to a maximum of ½ the flow depth (since Z_a cannot be greater than flow depth, ADWR Manual p. 24). Anti-dunes have been observed on many sand bed streams in Arizona. Therefore, it was assumed that antidunes could form within the study reach.

Low-flow thalweg scour, Z_{lft}, occurs if a small channel forms to convey minor flows within the main channel of a stream. Normally, the low-flow thalweg component of scour is not considered for a natural channel, since the natural channel minimum elevation already reflects the elevation of the thalweg. The intent of the low-flow thalweg scour component is to address a feature that sometimes forms within large constructed channels (with bottom widths greater than the natural bankfull width) with a high width to depth ratio and with mobile bed sediments. The low-flow thalweg is best estimated from field evidence of the low flow channel depth. Lacking field evidence, the low-flow thalweg component of scour is typically assumed to be one to two feet. For the LHWCMP scour analysis, a thalweg depth of one foot was used based on direction from District staff in other watercourse master plan scour studies. Given that the Hassayampa River, in its existing condition, has a self-formed natural channel, and the concept of formation of a thalweg within a channelized section is not applicable, the assumed thalweg depth is conservative, but was added at the direction of District staff.

Bend scour, Z_{bs}, occurs on the outside of bends in a stream channel, and is caused by spiral transverse currents. Bend scour was estimated using the following equation:

$$Z_{bs} = 0.0685\ Y_{max}\ V_m^{0.8}\ Y_h^{-0.4}\ S_e^{-0.3}\ \{2.1\ [\sin^2(\alpha/2)/\cos\alpha]^{0.2} - 1\}$$

where:

Z_{bs} = Bend-scour component of total scour depth (ft), and

Y_{max} = Maximum depth of flow immediately upstream of the bend (ft)

V_m = Average velocity of flow immediately upstream of the bend (ft/sec)

Y_h = Hydraulic depth of flow immediately upstream of the bend (ft)

S_e = Energy slope immediately upstream of the bend (ft/ft)

α = Angle formed by the projection of the channel centerline from the point of curvature to a point which meets a line tangent to the outer bank of the channel (degrees)

r_c = radius of curvature along centerline of channel (ft)

T = channel topwidth (ft)

In past watercourse master plan studies, a reach-averaged bend angle was computed from the arccosine of the reciprocal of the sinuosity, to reflect a reach-averaged bend angle. However, for the LHWCMP, at the direction of the District, a maximum bend angle was used to reflect the potential for future channel alignment changes. Use of the maximum bend angle generates a more conservative scour estimate, and in fact, appears to be the major component of the total scour estimates. Given the high potential for channel alignment changes, and the presence of sharp bends in the existing channel, use of the maximum bend angle is reasonable.

Local scour, Z_{ls}, occurs where there is an abrupt change in the direction of flow caused by obstructions such as bridge piers, abutments, or other structures. However, since local scour at these structures will be limited just to the bridge section or structure site, the local scour component was not included in the estimate of the reach-average total scour for the adjacent study reach. Local (bridge) scour for the 100-year event was computed using the HEC-RAS hydraulic design modeling component, and default HEC-18 bridge scour equations. Local scour results are reported separately in Table 4-2.

Long-term scour, or aggradation and degradation, is best evaluated on undisturbed streams from historical evidence and field data. Historical evidence of long-term changes in channel bed elevation, as discussed later in this chapter, was found to be minimal in most of the study reach. Other approaches for estimating long-term scour include use of equilibrium slope equations (described later in this chapter) and sediment continuity (HEC-6, See Chapter 5) modeling, both of which have practical and theoretical limitations for ephemeral streams. For existing conditions, historical, field data, equilibrium slope equations, and HEC-6 modeling indicate that the long-term scour component, absent human impacts, is near zero or is aggrading. Therefore, a long-term scour estimate of zero was used for the scour computations summarized below.

The ADWR Manual states that the safety factor generally varies between 1.0 and 1.5, but should be selected based on risk, consequence of failure, incremental construction

cost, and regulatory factors. For the LHWCMP scour analysis, a safety factor of 1.3 was used at the direction of the District staff.

4.2.2 Discussion & Results

Scour estimates for the Lower Hassayampa River were summarized in Table 4-1. The following results were obtained:

- The total scour along the study reach is about five to six feet for the 2-year event, eight to ten feet for the 10-year event, and greater than 10 feet for the 100-year event.

- In general, the largest component of scour is bend scour. Given that the bend scour is limited to the outside of channel bends, the scour estimates listed in the first columns of Table 4-1 are conservative when applied to an entire reach, particularly since the maximum bend angle was used. However, given the potential for future channel movement within the stream corridor, and sharper than average bends within a reach, the reported bend scour estimates may not be conservative at some points within the reach. More detailed consideration of bend scour at specific points within the reach is prudent for future structure design, especially those with an extended design life.

- Antidune scour will be limited to areas where the bed sediments are fine enough for antidunes to form. Typically, antidune formation is limited to sand-bed channels. Since the Lower Hassayampa River is a sand-bed stream, antidune scour is likely to occur throughout the study reach, though the probability that antidunes would develop at the margins of a channel near a structure is limited.

- In Reach 1, large scour depths were computed due primarily to the constricted channel that creates large flow depths and high channel velocities.

- Local scour was estimated as zero for the study, since reach-averaged values for a local condition could not be justified. HEC-RAS bridge scour estimates are shown separately for each of the four bridges in the study reach.

- Scour estimates vary without any longitudinal trend in the study reach.

- Bridge scour (local scour) estimates are not reported in Table 4-1 because the scour impacts only the bridge section rather than the entire reach in which the bridge is located. Bridge scour results for the 100-year event are given in Table 4-2 and are illustrated in Figure 4-1 to Figure 4-4.

- Comparison of bridge scour estimates with I-10 Bridge as-built plans indicates that the bridge should be considered scour critical. As-built plans for the Union Pacific Railroad Bridge were not available, but given the estimated scour depths, it is likely that there are stability issues with the bridge. The Old US 80 Bridge section was recently lined with CSA as a scour countermeasure.

Table 4-1. Scour Estimates (ft)							
Reach	**Total Zt**	**General Zgs**	**Long-Term Zdeg**	**Antidune Zga**	**Bend Zbs**	**Local Zls**	**Thalweg Zlft**
FDS – 100-Year							
5.0	11.4	0.2	0.0	1.4	6.2	0.0	1.0
4.0	13.1	0.3	0.0	1.6	7.1	0.0	1.0
3.0	16.0	0.3	0.0	2.1	8.9	0.0	1.0
2.0	15.0	0.3	0.0	2.1	8.1	0.0	1.0
1.0	21.4	0.9	0.0	1.5	13.1	0.0	1.0
10Yr							
5.0	7.8	0.2	0.0	0.6	4.2	0.0	1.0
4.0	8.7	0.2	0.0	0.8	4.7	0.0	1.0
3.0	9.0	0.2	0.0	0.8	4.9	0.0	1.0
2.0	9.8	0.2	0.0	1.0	5.4	0.0	1.0
1.0	13.6	0.8	0.0	0.6	8.0	0.0	1.0
2Yr							
5.0	5.4	0.1	0.0	0.4	2.7	0.0	1.0
4.0	5.5	0.2	0.0	0.4	2.7	0.0	1.0
3.0	5.5	0.2	0.0	0.4	2.7	0.0	1.0
2.0	5.7	0.1	0.0	0.5	2.7	0.0	1.0
1.0	8.7	0.8	0.0	0.3	4.6	0.0	1.0

Notes:
1. Scour estimates are not intended for use in design of hydraulic structures.
2. A safety factor of 1.3 was applied to the scour equations.

Table 4-2. HEC-RAS 100-Year Bridge Scour Estimates (ft)				
Scour Component	**Bridge**			
	I-10 West	**I-10 East**	**UPRR**	**Old US 80**
Pier Scour	14.2	14.7	7.2 – 20.0	37.4
Contraction Scour	0.3	0.3	2.0	0
Total Scour	14.5	15.0	9.2 – 22.0	37.4
Foundation Depth	~10 ft	~ 10 ft	Unknown	Full CSA Lining

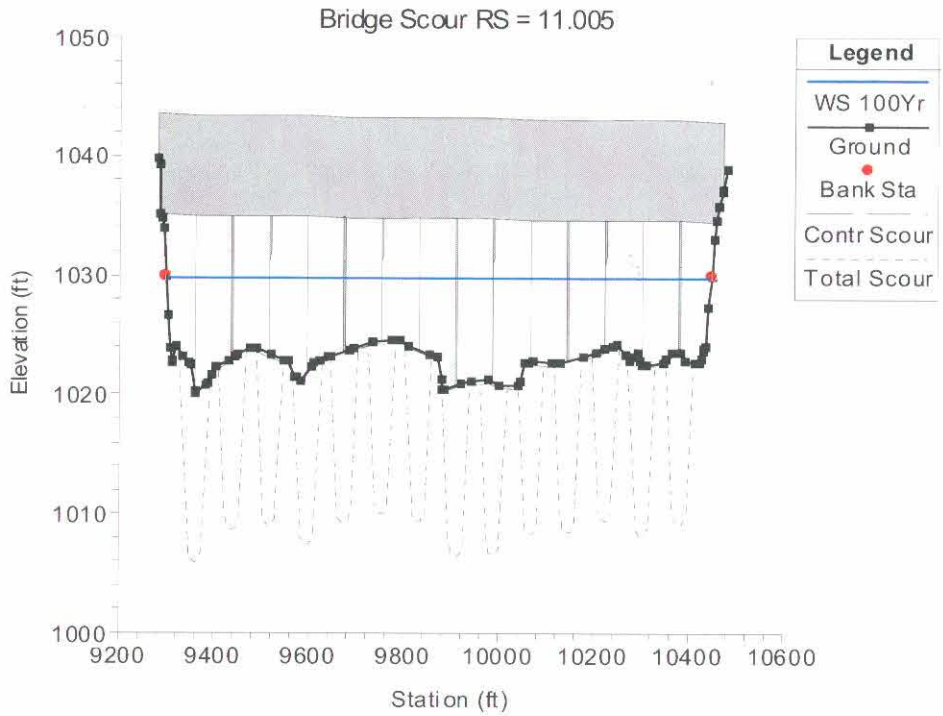

Figure 4-1. I-10 Westbound Bridge 100-year HEC-RAS bridge scour plot.

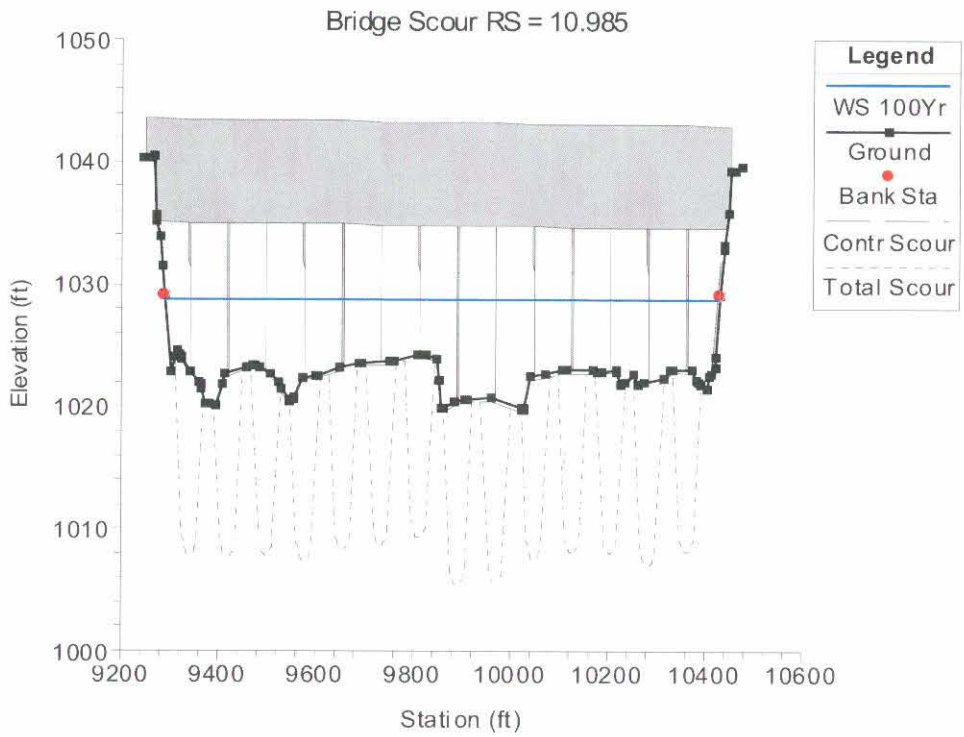

Figure 4-2. I-10 Eastbound Bridge 100-year HEC-RAS bridge scour plot.

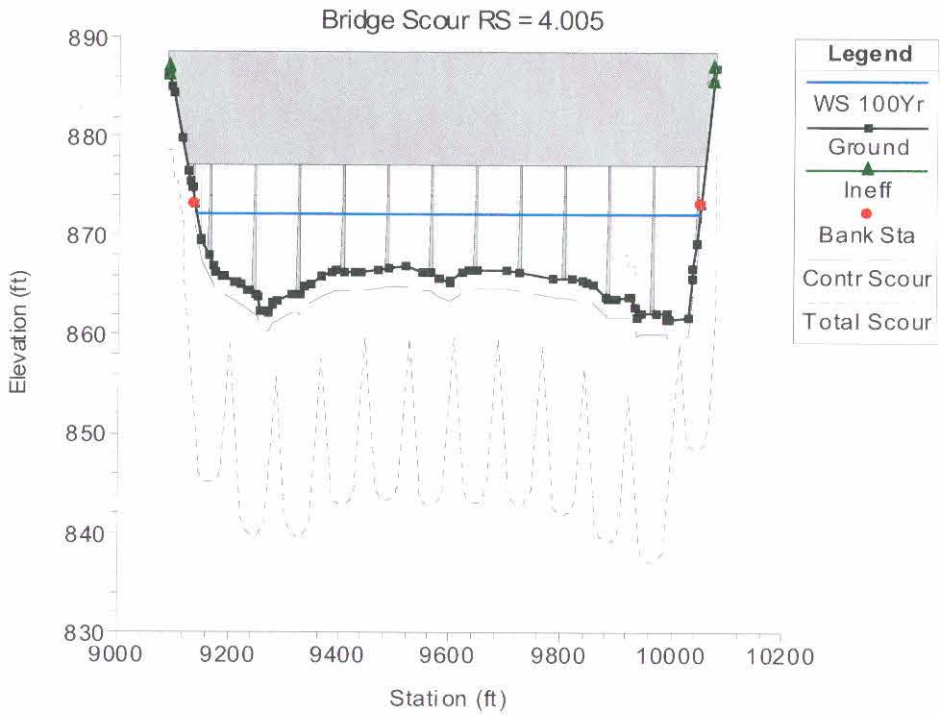

Figure 4-3. Union Pacific Railroad Bridge 100-year HEC-RAS bridge scour plot.

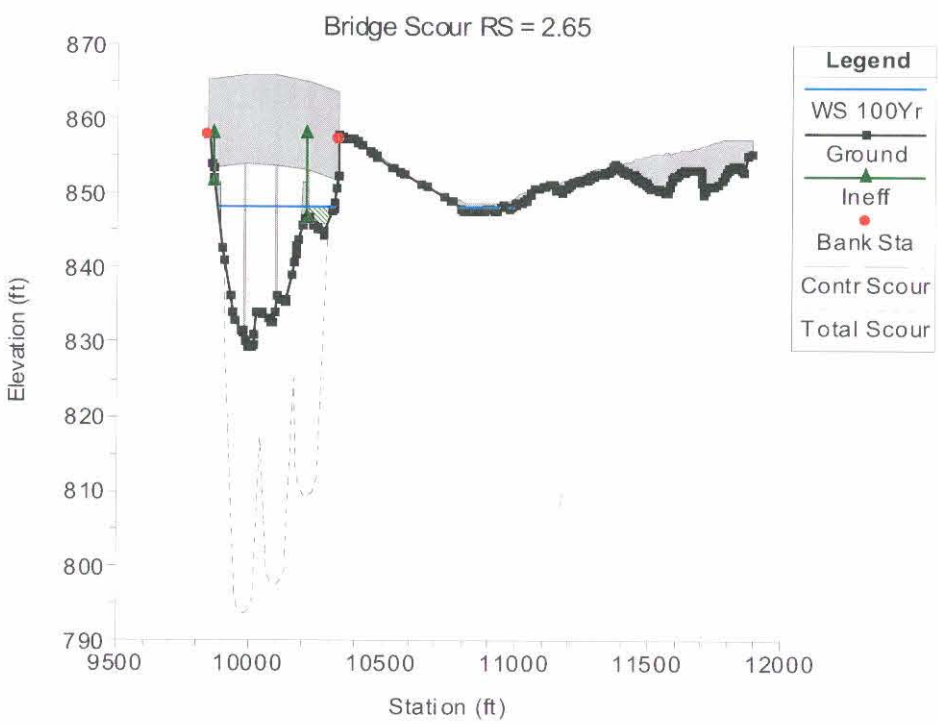

Figure 4-4. Old US 80 Bridge 100-year bridge scour plot.

4.2.3 Long-Term Scour

The long-term scour component is the progressive lowering of a stream bed that occurs over long time periods, rather than in response to a single flow event. Long-term scour was estimated from the following types of data:

- Field estimates of recent scour
- Interpretation of longitudinal profiles
- Interpretation of historical maps and photographs
- Interpretation of the ages of geomorphic surfaces
- Comparison of equilibrium and existing channel slopes

Field data were described in Chapter 2 (Section 2.8) of this report, and consisted of qualitative estimates of whether the channel had recently scoured or filled, and the depth of recent long-term scour. Longitudinal profiles are described in Section 4.6.2.1.3 of this report and were used to estimate whether the bed elevation had moved up or down during the period of record. Predictions of the magnitude of long-term degradation or aggradation can also be made by comparing the predicted equilibrium slope with the existing channel slope, as described in Section 4.3.

Geomorphic mapping of stream terraces, as described in Section 3.3 and 3.4 of Chapter 3, was used to establish the net channel bed adjustments over the past 10,000 to 2,000,000 years, as illustrated in Figure 3-1. Given that Pleistocene-aged terraces are up to 90 feet above the channel invert, the maximum net rate of degradation over the past 2,000,000 years is about 5×10^{-5} ft/year (< 1 inch/1000 years), using the reasoning illustrated in Figure 3-1. Similarly, given an average height of the Holocene floodplain of about six feet, the maximum net rate of long-term degradation in recent geologic time in the study reach is about 6×10^{-4} ft/yr (< 1 inch/century).

Clearly, a wide variety of types of evidence suggest that long-term scour has not been an important element for the existing condition of the study reach.

4.3 Equilibrium slope

Equilibrium slope[1] is defined as the slope which causes the channel's sediment transport capacity to equal the incoming sediment supply (ADWR, 1985). If the slope is too steep, channel velocities will be high and net erosion will occur. If the slope is too flat, channel velocities will be low and net deposition will occur. The equilibrium slope is the slope that the undisturbed, natural channel will tend towards over the long term. While there are philosophical and practical problems with applying equilibrium slope concepts to ephemeral streams with variable channel geometry and high flash flood potential, or streams where the natural hydrology has been altered by urbanization, equilibrium slope equations provide a useful order-of-magnitude assessment of the likelihood of vertical channel adjustments.

[1] Equilibrium slope is also referred to as stable slope or limiting slope.

4.3.1 Methodology

Reach-averaged data required for application of equilibrium slope equations to the study area were derived from the following sources:

- Hydraulic data - HEC-RAS modeling (Hydraulics Report)
- Hydrologic data - HEC-1 modeling and USGS gauge records (Hydrology Report)
- Topographic data – Floodplain delineation studies (Hydraulics Report)

Most equilibrium slope equations are based on the mean annual flood, the "channel-forming," or "bankfull" discharge. On many perennial alluvial streams, particularly in humid climates, the mean annual flood and the channel-forming and bankfull discharges are nearly equivalent. However, on ephemeral streams where flow events are rare, the channel-forming discharge is often difficult to determine. To account for the discrepancies in what flow rate is appropriate for equilibrium slope analyses, and to assess the trend of expected slope adjustments during floods, the 2- and 10-year peaks were used in the equilibrium slope equations to assess the expected slope adjustment over a range of discharges. The 2-year event approximates the mean annual flood calculated on a probability-weighted basis. The 10-year event better approximates bankfull conditions in the study reach. The following equilibrium slope equations were applied to the study reach:

- Arizona Department of Water Resources (ADWR) Equation
- Albuquerque Metropolitan Arroyo Flood Control Authority (AMAFCA) Equations

The BUREC (Pemberton and Lara, 1984) published a manual for computing scour and channel degradation downstream of dams or other structures that interrupt the natural sediment supply to the downstream channel. The BUREC manual describes the following approaches for estimating equilibrium slope:

- Schoklitsch Equation
- Meyer-Peter Muller Equation
- Shield's Diagram Method

The latter three equations listed above are zero bed sediment discharge (clear water) equations, and represent minimum slopes that would occur if sediment supply were disrupted, such as might occur downstream of a large in-stream sand and gravel mine. The BUREC equations do not apply for the existing conditions analysis.

4.3.2 ADWR Equation

The ADWR equation for equilibrium slope is described in Design Manual for Engineering Analysis of Fluvial Systems (ADWR, 1985). For streams with wide channels, such as the Hassayampa River, the ADWR equilibrium slope equation (Eq'n 5.11) reduces to the following:

$$S = \left(\frac{a}{q_s}\right)^{\frac{10}{3(b-c)}} q^{\frac{2(2c+3b)}{3(b-c)}} \left(\frac{n}{1.49}\right)^2$$

Where:

S	= equilibrium slope (ft/ft)
q_s	= unit sediment discharge (cfs/ft)
	= a $Y_h^b V^c$
Y_h	= hydraulic depth of channel (ft) = flow area/ top width
V	= mean channel velocity (ft/s)
q	= unit water discharge (cfs/ft)
n	= Manning's N value
a,b, c	= coefficients (ADWR Table 5.6a & 5.6b)

The coefficients a, b, and c are obtained from Tables 5.6a and 5.6b in the ADWR Manual. For the LHWCMP study reach, with a slope of 0.003 ft/ft, a d50 of 0.45 mm, and a gradation coefficient of 2.8, the following coefficient values were interpolated from Table 5.6a:

a	= 4.50×10^{-5}
b	= 0.264
c	= 3.87

Using these coefficient values and the HEC-RAS hydraulic data for the 10-year event, the equilibrium slope was computed from Equation 5.11.

The discussion of the equilibrium slope equation in the ADWR Manual includes the following guidelines, statements, and information relating to computation of equilibrium slope:

- Equilibrium slope equations are not appropriate for single event slope adjustment analyses.
- The analysis should begin with a study of historical bed profile changes. Historical trends should be traced to a cause, and if historical data indicate a trend, then begin with the method described. Historical bed profile data for the LHWCMP study reach were evaluated, as summarized in Section 4.6.3.
- The dominant discharge (Q5-Q10 for ephemeral streams) should be used, and limited to the bankfull discharge (i.e., no overbank flow). For the LHWCMP, the 2- and 10-year events were evaluated.
- If the width to depth ratio of the channel is greater than 10 (wide channel), the simplified method (Equation 5.11) should be used. Because the width/depth ratio is greater than 10 for the LHWCMP study reach, equation 5.11 was used.
- Identify pivot points from which equilibrium slope adjustments may occur. No such pivot points exist in the LHWCMP study reach. Temporary grade control may be provided by paved dip sections, but these crossings tend to be destroyed

in channel forming events and thus are unlikely to serve as reliable pivot points. Therefore, reach lengths were used to estimate adjustments.

- Identify stable bank height. Vertical bank heights up to seven feet were observed in the study reach, although bank heights were typically less than seven feet. There is no evidence to suggest that the observed vertical banks in the LHWCMP reach are in any way stable, nor is there evidence to suggest that higher vertical banks could not form if long-term degradation occurred.
- Watersheds considered in equilibrium may not require equilibrium slope analysis, unless proposed floodplain improvements alter the sediment supply or transport capacity (p. 5.73). For the Phase 1 LHWCMP, which is an existing condition assessment, no floodplain improvements or changes in sediment supply are proposed. Therefore, the ADWR methodology should predict no equilibrium slope adjustment.
- If Manning's n, channel geometry and total discharge are the same in each reach, the only independent variable is slope, and the equilibrium slope equation reduces to

  - $S_{eq} = S_{ex}\ (Q_s,\ \text{supply}/\ Q_s\ \text{reach})^z$

  In the case of the LHWCMP, upstream of Old US80, it is reasonable t assume that the channel forming Q, Manning's n, and channel geometry are the same. Therefore, no equilibrium slope adjustment is expected based on the ADWR methodology.

In addition, the following potential challenges in applying the results of the ADWR equilibrium slope method are noted:

- The method assumes sediment deficit or surplus will be met by slope adjustments, rather than width adjustments (historical data contract this assumption). Therefore, it will over-predict slope change if the channel has freedom to adjust laterally.
- The method neglects impact of excess sediment stored in, or derived from, the floodplain in subsequent downstream reaches.
- The method uses reach-average hydraulic variables. Therefore, either slope is iterated between each cross section (several thousand iterations needed) or averaged variables for each reach is used.
- The method assumes upstream (supply) reach is in equilibrium.

Finally, the ADWR Manual included the following word of caution, "due to complex interaction of variables, simplifying assumptions, the results can be very subjective and only useful in qualitative sense" (p. 5.74).

4.3.3 AMAFCA Equation

The AMAFCA (1994) equation for the maximum equilibrium slope is based on the sediment transport characteristics of the reach. The formulation of the AMAFCA equation is very similar to the ADWR equation, and thus the results are not surprisingly quite similar. The AMAFCA equilibrium slope equation is written as follows:

$$S_L = \left(\frac{a}{q_s}\right)^{\frac{10}{3(c-b)}} q^{\frac{2(2b+3c)}{3(c-b)}} \left(\frac{n}{1.49}\right)^2$$

Where S_L = channel slope (ft./ft.)

q_s = unit sediment transport (cfs/ft)

q = water discharge (cfs)

n = Manning's roughness

a, b, c = power function coefficients from sediment transport function

A simplified version of the AMAFCA Equation is written for wide, rectangular channels, similar to the study reach, based on the assumptions that steep, wide, rectangular alluvial streams flow at or close to critical depth and that sediment supply is transport limited.[2] These assumptions are valid for the LHWCMP reach in existing conditions.

$$S_s = 18.28\ n^2\ F^{0.133}\ F_r^{2.133}\ Q_{dd}^{-0.133}$$

Where S_s = Stable slope (ft/ft)

n = Manning's roughness value for the channel

F = Width/depth ratio of the channel

F_r = Froude number for the channel

Q_{dd}= Dominant discharge (cfs)

4.3.4 Schoklitsch Equation

The Schoklitsch (Shulits, 1935) equation is based on the concept of zero bedload transport.

$$S_L = K_s\ (D\ W_{bf}/Q)^{3/4}$$

Where S_L = Stable slope (ft/ft)

K_s = 0.00174

W_{bf} = Bankfull width (ft)

D = Mean bed sediment diameter (mm)

Q = Dominant discharge (cfs)

4.3.5 Meyer-Peter, Muller Equation

The Meyer-Peter, Muller (1948) equation is based on the incipient motion theory, or the point of initiation of sediment transport, for zero sediment inflow.

$$S_L = K_{mpm}\ (Q/Q_{bf})\ (n_s/D_{90}^{1/6})^{3/2}\ D / d$$

[2] Transport limited means that the sediment inflow equals or exceeds the reach transport capacity.

Where S_L = Stable slope (ft/ft)

K_{mpm} = 0.19

Q/Q_{bf} = Ratio of total flow to flow over the channel

Q_{bf} = Dominant discharge (cfs)

n_s = Manning's n for the stream bed

D_{90} = Bed sediment diameter for which 90 percent is smaller (mm)

D = Mean sediment diameter (mm)

d = Channel depth (ft)

4.3.6 Shields Diagram Method

The Shields diagram (1936) for determining the boundary condition for no sediment transport can be used to define an equation for stable slope.

$$R_* = U_* D / \upsilon$$

$$U_* = (S_L R g)^{1/2}$$

$$T_* = \tau_c / ((\gamma_s - \gamma_w) D)$$

Where S_L = Stable slope (ft/ft)

R_* = Boundary Reynold's number

U_* = Shear velocity = $(S_L R g)^{\wedge 0.5}$

D = Mean sediment diameter (mm)

υ = Kinematic viscosity of water (ft^2/sec)

R = Hydraulic radius for wide channels (ft)

g = Gravitational constant = 32.2 ft/sec^2

T_* = Dimensionless shear stress

τ_c = Critical shear stress (lb/ft^2)

γ_s, γ_w = Specific weight of sediment (lb/ft^3) and water (lb/ft^3)

4.3.7 Results

The results of the equilibrium slope computations are shown in Table 4-3 and Table 4-4. The Schoklitsch, Meyer-Peter Muller, and Shield's Diagram results represent minimum slopes for the specific condition of clear-water discharges. Therefore, the results from these four equations are probably not suitable for application to the uncontrolled natural Hassayampa River. However, if at some future date, sediment supplies were significantly reduced, such as in reaches downstream of large in-stream sand and gravel excavations, the channel slope might be expected to flatten significantly as suggested by the results of these equations.

For both sets of equations, long-term degradation (or aggradation) can be predicted by comparing the equilibrium slope and existing channel slopes for a given reach. If the predicted equilibrium slope is less than the existing channel slope, long-term degradation should be expected. Conversely, if the predicted equilibrium slope is greater than the existing channel slope, long-term aggradation should be expected. This comparison was done using the District's preferred ADWR equations as shown in Table 4-3. The extremely high magnitude of predicted aggradation is due to the long reach lengths. In reality, lacking controlled pivot points, and having the freedom to adjust laterally, a more muted response is expected. Where long-term degradation occurs, lateral instability usually occurs as a by-product due to undercutting the channel banks. Where long-term aggradation occurs, lateral instability occurs due to increased braiding and avulsions. While the magnitude of long-term degradation or aggradation cannot be reliably predicted using the equilibrium slope equation, the strength of the trend in either direction probably can be gauged. The strongest trends are predicted where the difference between the average equilibrium slope and the existing channel slope is greatest.

Table 4-3. ADWR Equilibrium Slope Results (ft)

Reach	Channel Slope	Equilibrium Slope	Reach Length	Long-Term Change
Q10				
5	0.00431	0.00465	33475.2	11.3
4	0.00410	0.00498	30518.4	26.8
3	0.00421	0.00477	27878.4	15.6
2	0.00421	0.00498	29462.4	22.6
1	0.00428	0.00442	22070.4	2.9
Q2				
5	0.00431	0.00502	33475.2	23.5
4	0.00410	0.00527	30518.4	35.7
3	0.00421	0.00477	27878.4	15.7
2	0.00421	0.00467	29462.4	13.5
1	0.00428	0.00487	22070.4	12.9

Table 4-4. Equilibrium Slope Analysis Results (Slope in ft/ft)									
Reach	Methodology - Stable Slope (ft/ft) (minimum slope equations)			Average (ft/ft)	Methodology - Stable Slope (ft/ft) (expected slope equations)		Average Slope (ft/ft)	Measured Slope (ft/ft)	Predicted Trend
	Schok-litsch	MPM	Shield		ADWR	AMAFCA			
10Yr									
5	0.00019	0.00026	0.00004	0.00016	0.00465	0.00423	0.004441	0.00431	Aggrade
4	0.00014	0.00017	0.00004	0.00012	0.00498	0.00451	0.004743	0.00410	Aggrade
3	0.00013	0.00017	0.00003	0.00011	0.00477	0.0043	0.004534	0.00421	Aggrade
2	0.00011	0.00014	0.00003	0.00009	0.00498	0.00458	0.00478	0.00421	Aggrade
1	0.00008	0.00014	0.00002	0.00008	0.00442	0.00403	0.004223	0.00428	Scour
2Yr									
5	0.00038	0.00029	0.00007	0.00025	0.00502	0.00453	0.004774	0.00431	Aggrade
4	0.00029	0.00027	0.00007	0.00021	0.00527	0.00467	0.004968	0.00410	Aggrade
3	0.00027	0.00025	0.00006	0.00019	0.00477	0.00434	0.004557	0.00421	Aggrade
2	0.00021	0.00021	0.00005	0.00016	0.00467	0.00432	0.004496	0.00421	Aggrade
1	0.00019	0.00027	0.00003	0.00016	0.00487	0.00437	0.004619	0.00428	Aggrade

4.3.8 Summary

In general, the ADWR and AMAFCA equilibrium slope equations suggest that long-term aggradation will occur in the study area, contrary to field observations and historical topographic data. The equations for zero sediment inflow predict equilibrium slopes at least an order of magnitude below the existing channel slope. The AMAFCA and ADWR equations predict a stable slope very similar to the measured slope throughout the study reach, which is consistent with historical data and field observations that suggest the river is in equilibrium in the existing condition. The three equilibrium slope equations that assume no sediment inflow (Schoklitsch, MPM, and Shield) predict very flat channel slopes and long-term scour, which serves as a warning that development guidelines should address sediment supply issues to assure channel stability.

The scour and deposition caused by the channel's adjustment to its equilibrium slope will be limited to a reach length sufficient for the channel to regain a sediment transport balance. In general, the (live-bed) equilibrium slope equations predict long-term aggradation, although the geologic, field and historical evidence do not support this conclusion. The actual magnitude of the expected bed elevation changes will be based on the sediment supply and the magnitude and frequency of the flows experienced in the future. Note that the AMAFCA and ADWR equations compute a stable slope similar to the observed existing slope. The ADWR and AMAFCA equations are most appropriate for analysis of the Hassayampa River, and that the channel is currently in an equilibrium state with its water and sediment supply. Given the relatively natural state of the Hassayampa River watershed, this result is not surprising.

4.4 Armoring

When the channel sediment transport capacity exceeds the upstream sediment supply, the balance of the sediment load may be eroded from the channel bed, causing the channel to degrade. Because fine sediments can be transported at more frequent lower discharges and velocities than coarse sediments, which may require large floods to be moved, fine sediment tends to be preferentially removed from the channel bed. Selective removal of fine sediments causes channel bed material to become progressively coarser over time, as long as the upstream sediment supply is limited. If this process continues over a long period, it ultimately creates a surficial layer of coarse channel sediments, called an armor layer, that the stream is incapable of transporting (Yang, 1996).

4.4.1 Methodology

The BUREC (Pemberton and Lara, 1984) recommends the following methodologies for estimating the minimum sediment size and depth of scour required to form an armor layer for a given flow rate:

- Meyer-Peter, Muller Bedload Transport Function
- Competent Bottom Velocity
- Shields Diagram
- Yang Incipient Motion

Each of these methodologies was applied to the study reach.

4.4.2 Meyer-Peter, Muller Bedload Transport Function

The Meyer-Peter, Muller (1948) bedload sediment transport function for the beginning of transport of individual grain sizes can be used to estimate the non-transportable sediment size.

$$D_c = d\ S\ /\ (K_{mpm}\ (n/D_{90}^{(1/6)})^{3/2})$$

Where D_c = Non-transportable sediment diameter (mm)

d = Average flow depth (ft)

S = Energy slope (ft/ft)

$K_{mpm} = 0.19$

n = Manning's n for the stream bed

D_{90} = Particle size for which 90% of the bed material is finer (mm)

4.4.3 Competent Bottom Velocity

This methodology is based on the work of Mavis and Lushey (1948), who developed an equation for the beginning of sediment movement on a stream bed.

$$D_c = 1.88\ V_m^2$$

Where D_c = Armor size (mm)

V_m = Average channel velocity (ft/s)

4.4.4 Shields Diagram

The Shields (1936) diagram is a standard method used to define the initiation of motion for various channel bed sediment sizes. The method uses an iterative process to compute dimensionless shear stress (T*) and the armor diagram from the Shields diagram.

$$T_* = \tau_c\ /\ ((\gamma_s - \gamma_w)\ D_c)$$

Where T_* = Dimensionless shear stress

D_c = Armor size (mm)

τ_c = Critical shear stress (lb/ft^2)

γ_s = Specific weight of water = 62.4 lb/ft^3

γ_w = Specific weight of sediment = 165 lb/ft^3

Note that for gravel sediment sizes and turbulence levels typical in natural streams:

T_* = 0.05 for sediment sizes greater than 1 mm and Boundary

Reynold's Number (R_*) > 500

4.4.5 Yang Incipient Motion

Yang (1973) developed a relationship between dimensionless critical velocity (V_{cr}/w, where w = fall velocity, ft/s) and shear velocity Reynold's number R* at incipient motion. Under natural stream conditions for sediment sizes greater than 2 mm, Yang's equation can be written as follows:

$$D_c = 0.00659\ V_{cr}^2 \qquad \text{(For D > 2 mm)}$$

Where D_c = Armor size (ft)

V_{cr} = Critical average velocity at incipient motion (ft/s)

4.4.6 Depth to Armor Equation

Once the size of material (D_c) that will form an armor layer is estimated from one or more of the equations listed above, the depth of scour required to form a stable armor layer can be estimated from the sediment distribution of the channel bed material. The equation for the depth to armor is the following:

$$Y_d = y_a\ (1/\Delta p - 1)$$

Where Y_d = Depth from original streambed to the bottom of the armor layer (ft)

y_a = Thickness of the armor layer (ft)

Δp = Decimal percentage of the bed material larger than the armor size

4.4.7 Results

The results of the application of the BUREC methodologies to the study area are summarized in Table 4-5. Channel sediment size distribution data for the study reach (Chapter 5) were compared with the critical armoring sediment diameter. As can be seen from the data in Table 4-5, there is not sufficient large gravel in the Lower Hassayampa River to form an armor layer for even the smallest flood discharges.

Table 4-5. Armoring Analysis Results								
Reach	Methodology - Critical Armor Diameter (mm)				Average Critical Diam. (mm)	Field D50 (mm)	Armor Layer Likely?	Depth to Armor (ft)
	MPM	CBV	Yang	Shield				
FDS								
5	22.5	140.2	149.8	50.3	91	0.5	No	N/A
4	26.2	171.2	182.9	63.6	111	0.5	No	N/A
3	30.5	212.2	226.7	77.0	137	0.5	No	N/A
2	29.6	203.4	217.4	80.4	133	0.5	No	N/A
1	26.9	189.7	202.7	129.1	137	0.5	No	N/A
10Yr								
5	13.2	71.4	76.3	28.9	47	0.5	No	N/A
4	14.8	83.8	89.6	34.8	56	0.5	No	N/A
3	15.4	86.1	92.0	37.3	58	0.5	No	N/A
2	16.7	103.0	110.0	44.8	69	0.5	No	N/A
1	14.1	79.4	84.9	82.0	65	0.5	No	N/A
2Yr								
5	8.9	39.7	42.4	18.8	27	0.5	No	N/A
4	8.8	40.3	43.1	19.9	28	0.5	No	N/A
3	9.4	43.6	46.6	22.4	30	0.5	No	N/A
2	10.5	52.7	56.3	24.6	36	0.5	No	N/A
1	7.7	36.0	38.5	45.0	32	0.5	No	N/A

MPM = Meyer-Peter, Muller Yang = Yang's incipient motion
CBV = Competent Bottom Velocity Shield = Shield Method

4.4.8 Conclusions

The following conclusions can be drawn from the armoring analysis results summarized in Table 4-5:

- The channel bed scour depth is not limited by armoring during floods.
- The channel bed material is mobile, and will be transported during even small flows. This conclusion is supported by field observations of highly sediment-laden flows even during very low discharges.
- Sediments observed in the gravel pits were not significantly more coarse-grained than the material exposed on the surface. That is, effective armor layers were not observed in the field at gravel pits.
- The Lower Hassayampa River historically has adjusted its geometry predominantly by horizontal adjustments of its main channel. Vertical scour has been limited to a few feet, according to field observations of exposures of channel alluvium in gravel pits and soil pits.

4.5 Comparison of Armoring, Scour, and Equilibrium Slope

Channel degradation can be prevented by armoring of the channel bed, by achieving a non-scouring stable slope, or by physical barriers to scour such as bedrock or artificial grade control. A comparison of the armoring, scour and equilibrium slope estimates described in the previous sections of this chapter is provided in Table 4-6. Obviously, given the results in Table 4-5, armoring will not limit scour, either single-event or long-term scour.

The possible slope adjustment, or depth of long-term scour caused as the channel adjusts to stable slope, was estimated by multiplying the difference in the predicted (regime) and existing channel slopes by arbitrary reach lengths of 1,000 or 5,000 feet. The latter two distances were selected to test the possible bed elevation adjustment for illustrative purposes. The distances are intended to illustrate the order of magnitude of vertical change possible due to slope adjustments, rather than a specific prediction of long-term scour at any specific point in the study reach. Actually, long-term changes will depend on a variety of site-specific variables.

The AMAFCA equilibrium slope was used in Table 4-6 for reasons discussed in Section 4.3. Use of the average equilibrium slope resulted in slope adjustment predictions of over 10 feet for reach lengths of 5,000 feet, which is well beyond the geologic estimate of long-term scour based on Holocene floodplain elevations.

Table 4-6. Comparison of Armoring, Scour, and Equilibrium Slope Estimates

1	2	3	4		5	
Reach	Depth to Armor (ft)	Scour Depth (ft)	Stable Slope		Slope Adjustments	
			Average ADWR-AMAFCA	Actual	1000 ft.	5000 ft.
10 Yr						
5	> 20 ft	4.3	0.004441	0.0043	0.1	0.7
4	> 20 ft	3.3	0.004743	0.0042	0.5	2.7
3	> 20 ft	2.9	0.004534	0.0043	0.2	1.2
2	> 20 ft	4.2	0.00478	0.0041	0.7	3.4
1	> 20 ft	3.3	0.004223	0.0044	-0.2	-0.9
2 Yr						
5	> 20 ft	3.0	0.004774	0.0043	0.5	2.4
4	> 20 ft	2.2	0.004968	0.0042	0.8	3.8
3	> 20 ft	2.0	0.004557	0.0043	0.3	1.3
2	> 20 ft	2.7	0.004496	0.0041	0.4	2.0
1	> 20 ft	2.2	0.004619	0.0044	0.2	1.1

Notes: No = scour not limited by armoring
Yes = scour limited by formation of armor layer
Yes* = scour limited by formation of armor layer for long reaches but not shorter reaches
N/A = not applicable, aggradation is predicted (no long-term scour)
Armor v. Scour: compare column 3 to 1, i.e. will scour be limited by armoring?
Armor v. Slope: compare column 5 to 1, i.e. will long-term scour be limited by armoring?

As shown in Table 4-6, armoring generally will not prevent long-term degradation (last column) on the Hassayampa River because armoring will not occur. Short-term or

single event scour similarly will not be prevented by armoring during any event.

4.5.1 Conclusion

The engineering analyses described in the preceding sections predict that scour is likely during floods, as well as potential long-term scour, particularly if the sediment supply is reduced from the existing condition. Armoring will not limit scour or degradation.

4.6 Bed Change Analysis

A comparison of historical topographic data was made to examine and quantify historic changes in bed elevation in the study reach.

4.6.1 Data Sources

Historical topographic data spanning the period from 1957 through 2004 were used to assess bed change along the Lower Hassayampa River. Five primary sources of historical topography were used, as listed in Table 4-7.

Table 4-7. Sources of historical topography

Topography Year	Contour Interval	Datum	Source	Format	NAVD88 to NGVD29 Conversion Factor
1957-1962	20-40 ft	NGVD29	USGS DRG quadrangle maps	Raster	-
1966	5 ft	NGVD29	Williams & Ellis FPS (FCDMC)	Raster	-
1988	4 ft	NGVD29	Cella Barr FIS (FCDMC)	Digital (HEC-2)	-
2000	10 ft	NAVD88	FCDMC county-wide	Digital (GIS)	2
2002-2004	2 ft	NAVD88	Multiple FCDMC projects	Digital (GIS)	2

Since three of the five data sets used in the analysis predate 1991, the year the National Geodetic Survey converted to the NAVD88 vertical datum, NGVD29 was used as the base vertical projection. To consistently compare elevations between data sets, the 2000 and 2002-2004 topography was converted to the NGVD29 datum using the National Geodetic Survey's VERTCON software. The conversion value varied slightly (1.98 ft to 2.08 ft) within the study area. Since the resolution of the raster topographic data sets was to the whole foot, the digital sets were rounded to the whole foot for the analysis, which made the variance in the VERTCON conversion values insignificant. Thus, a rounded value of 2 was used to convert the NAVD88 elevations to NGVD29.

4.6.2 Cross Section Profile Analysis

A common set of geographic locations is required to compare historical elevations. For this analysis, specific 1988 Cella Barr FIS cross-section alignments were chosen as the comparison points. Cross-section profiles for the 2000 and 2002-2004 topography were generated digitally using ArcGIS tools. The Cella Barr FIS HEC-2 input file was used to obtain cross-section data for the 1988 topography. The District provided the 1966 Williams and Ellis Floodplain Study (FPS) work maps in a scanned, digital format, which

were then semi-rectified. Cross-section profiles for both the USGS DRGs and the 1966 work maps were manually generated using ArcGIS. Cross-section profiles were created for each set of historical topography, and they were plotted for comparison, as shown in Figure 4-5 to Figure 4-37. The plots are labeled by cross-section station ID, using the 1988 Cella Barr FIS section numbering. Each of the 34 cross section plots includes an aerial photo to identify the cross-section location.

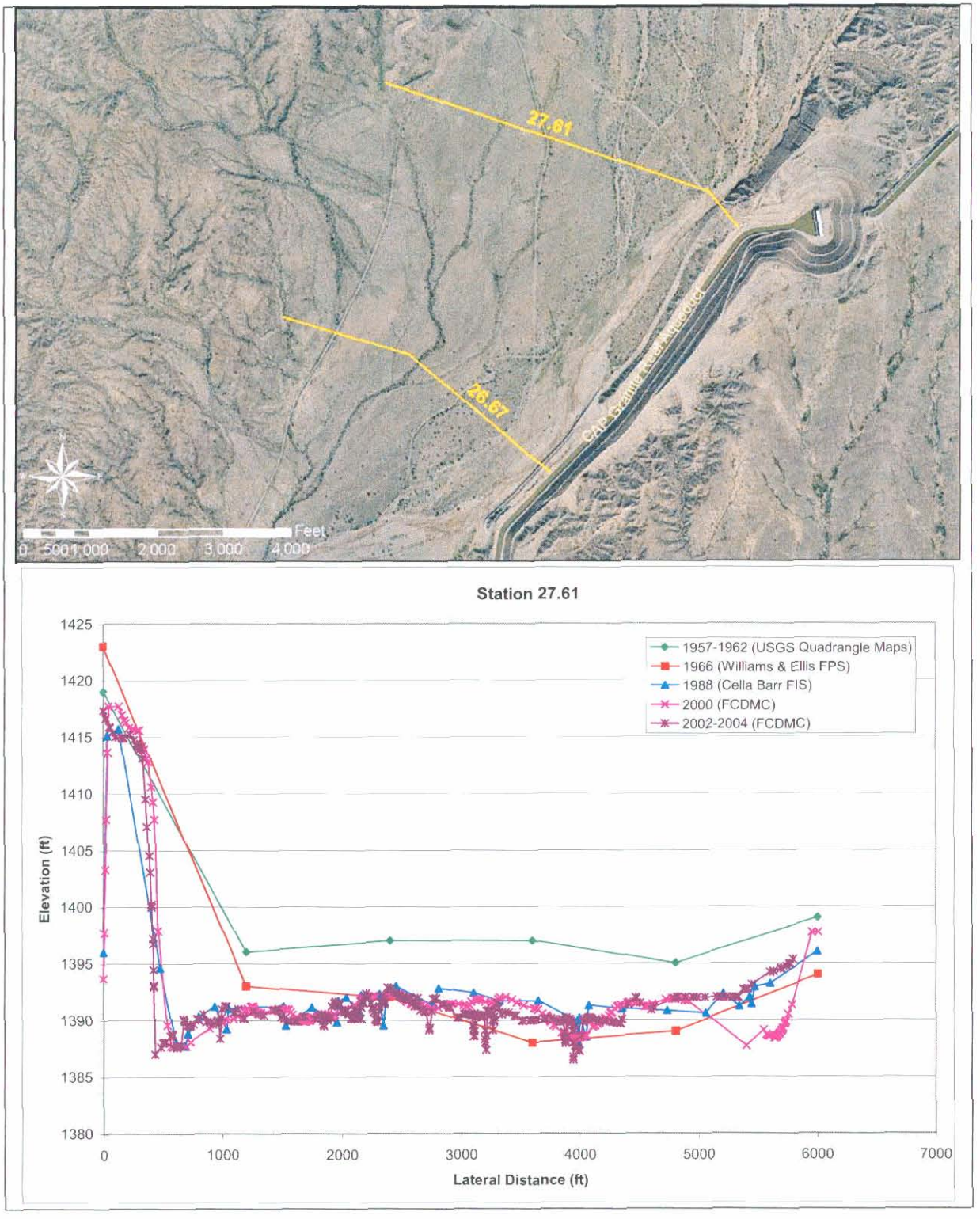

Figure 4-5. Cross-Section 27.61 Profile Comparison

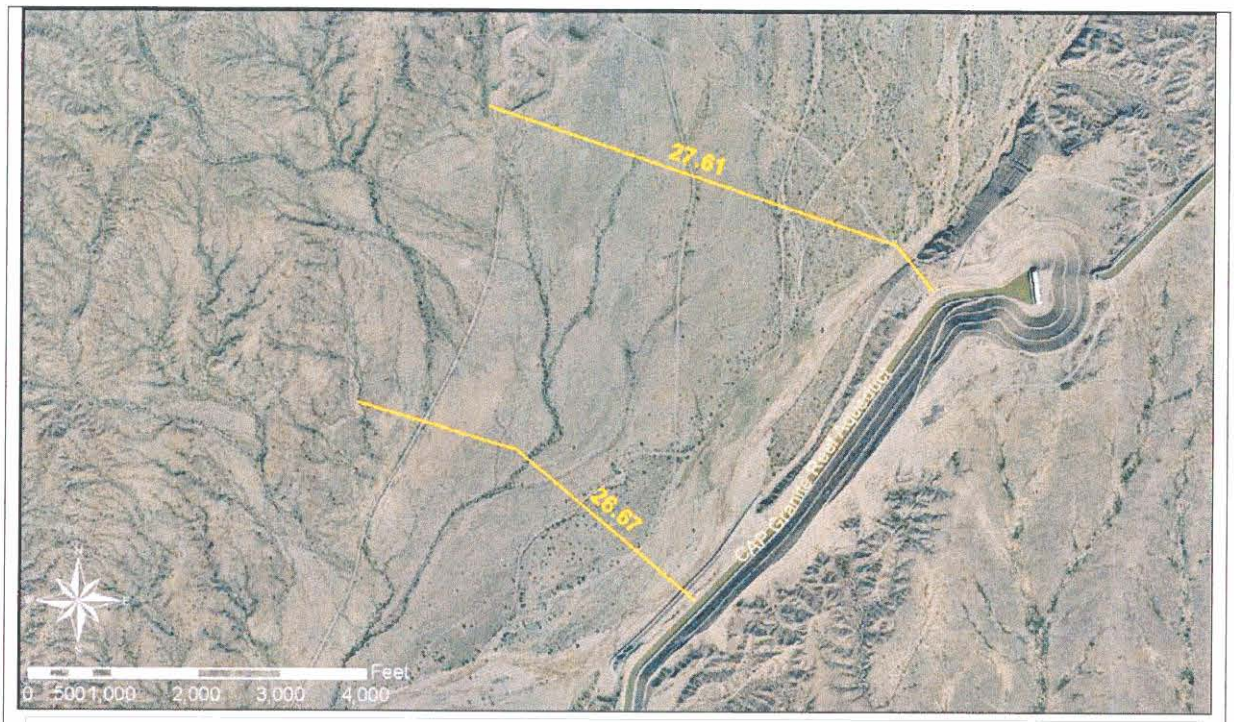

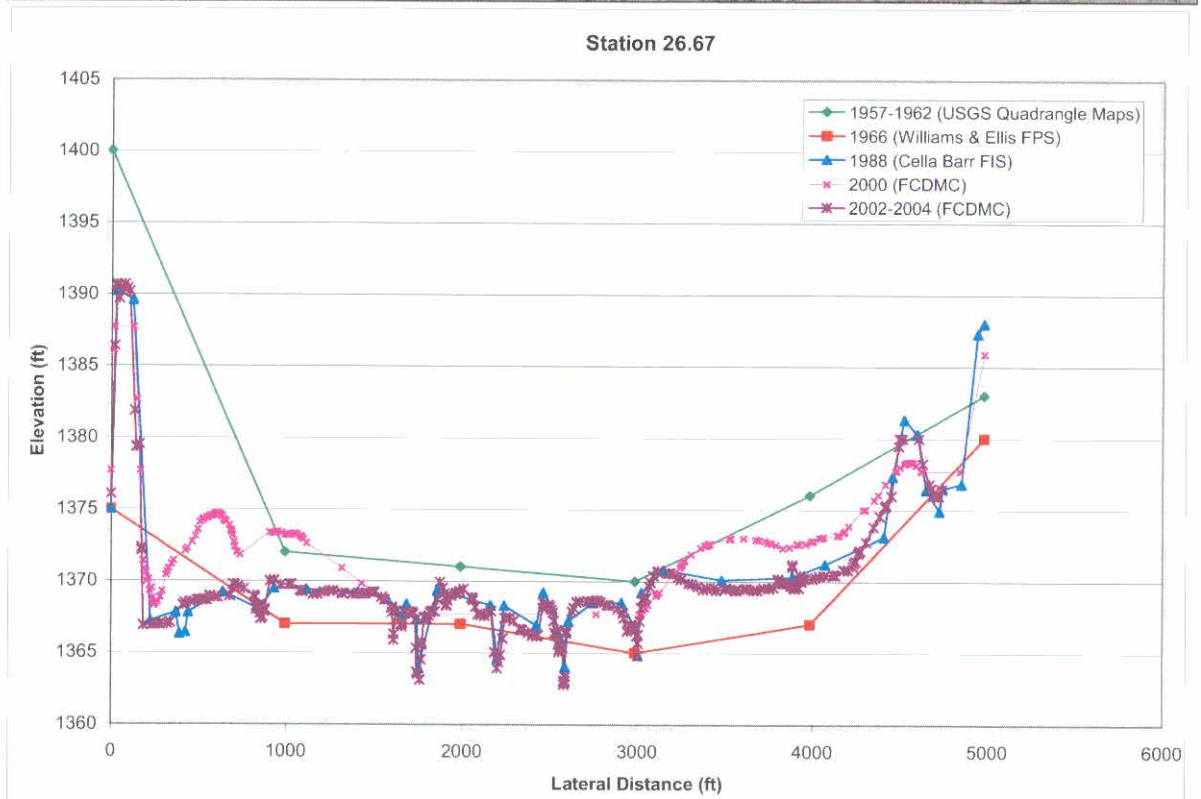

Figure 4-6. Cross-Section 26.67 Profile Comparison

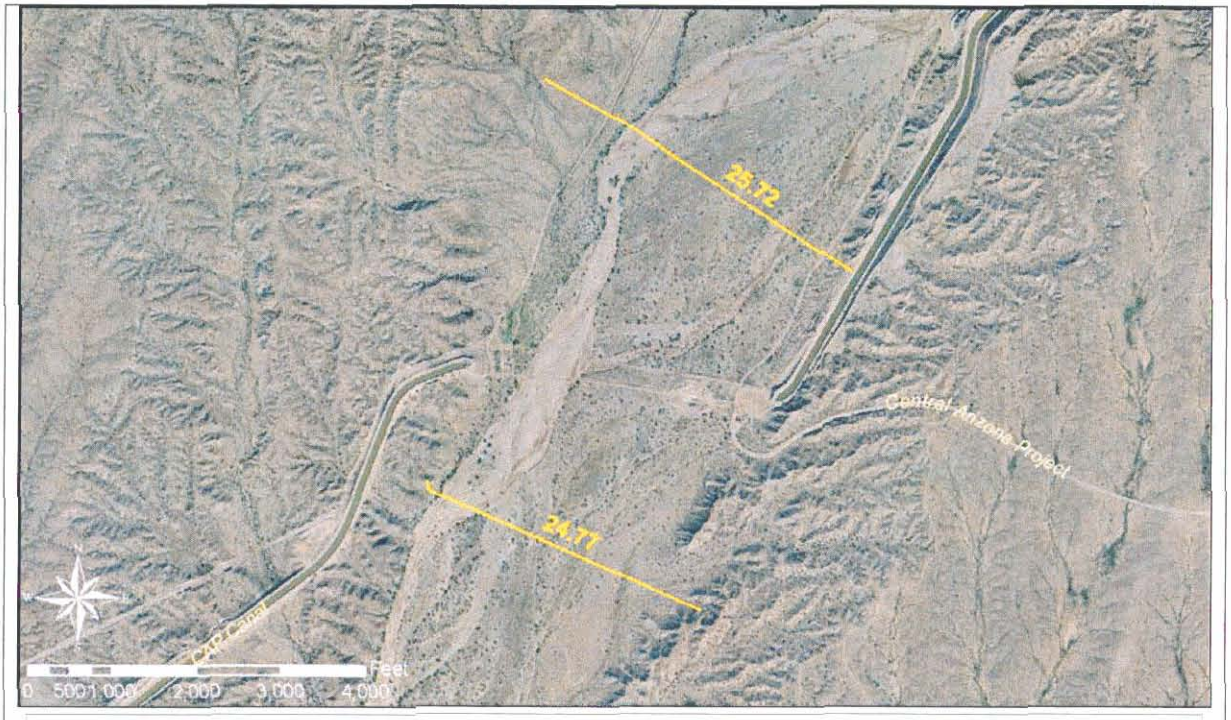

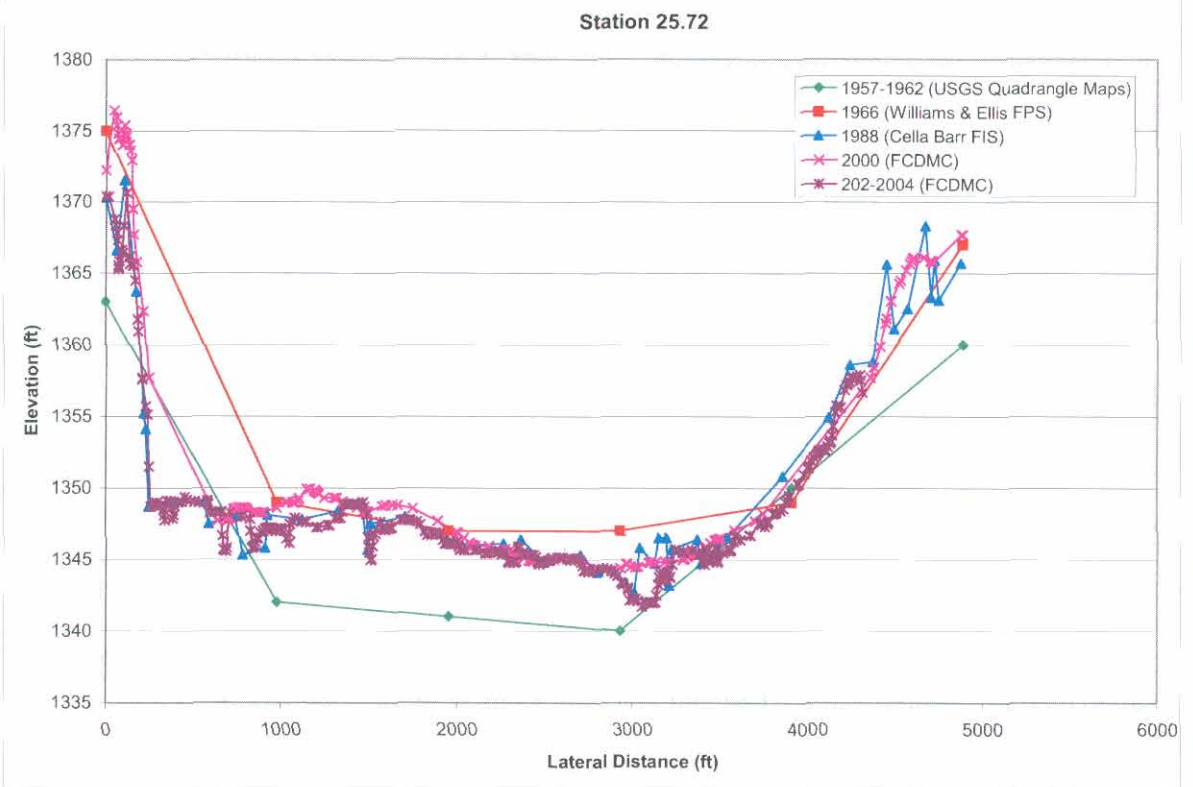

Figure 4-7. Cross-Section 25.72 Profile Comparison

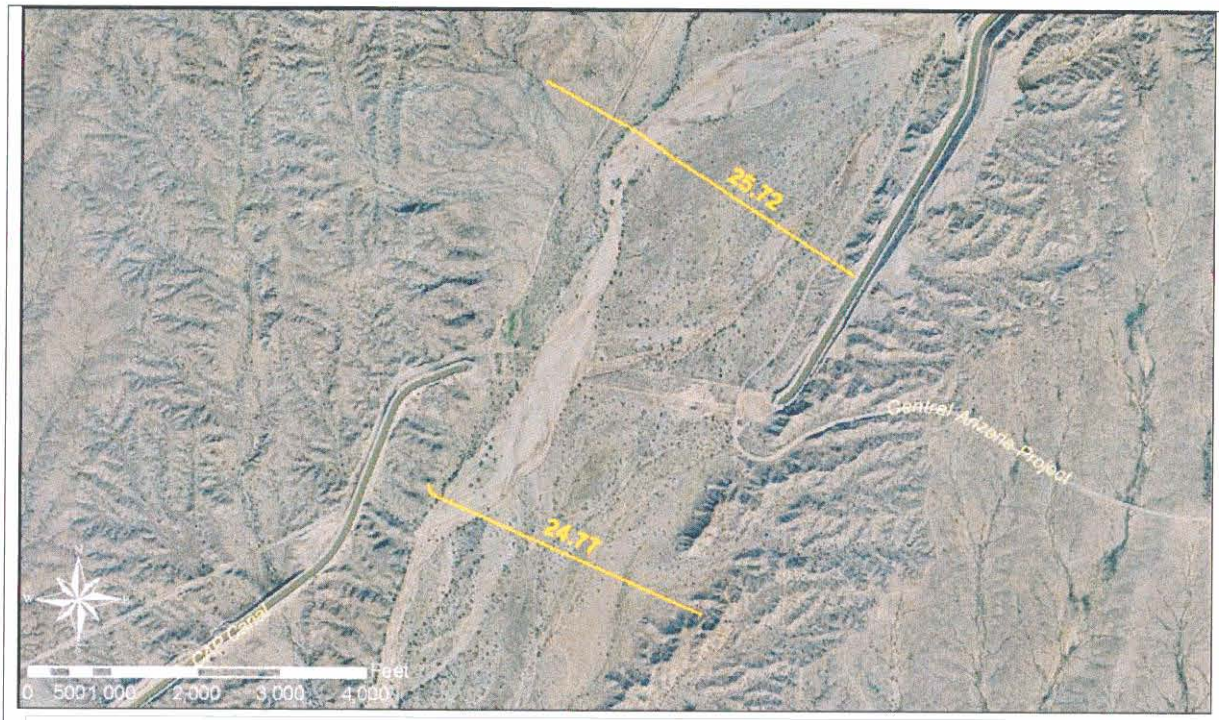

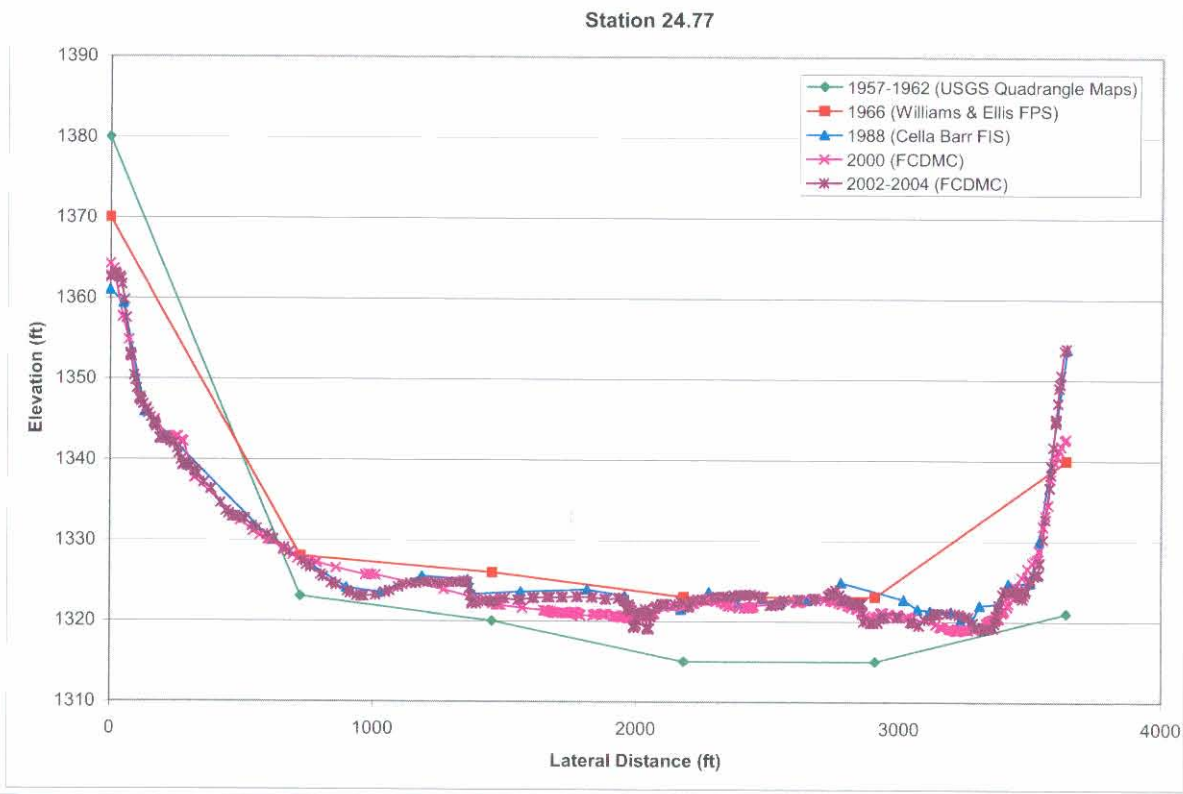

Figure 4-8. Cross-Section 24.77 Profile Comparison

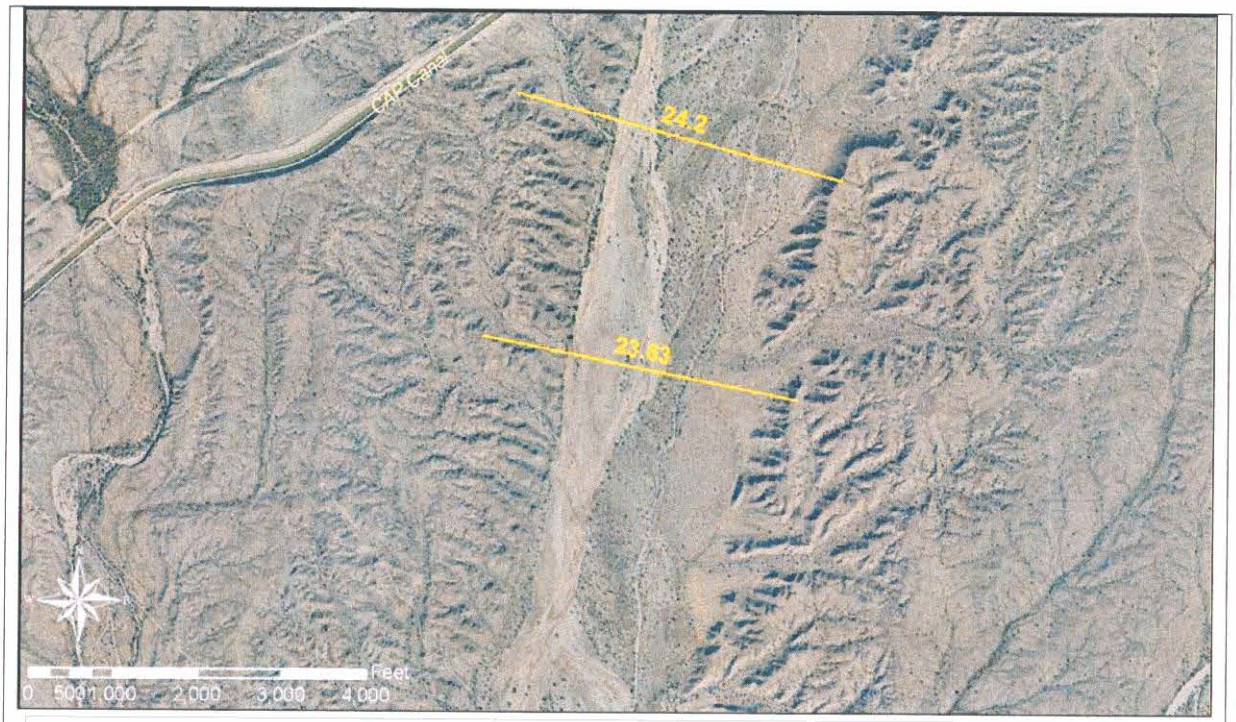

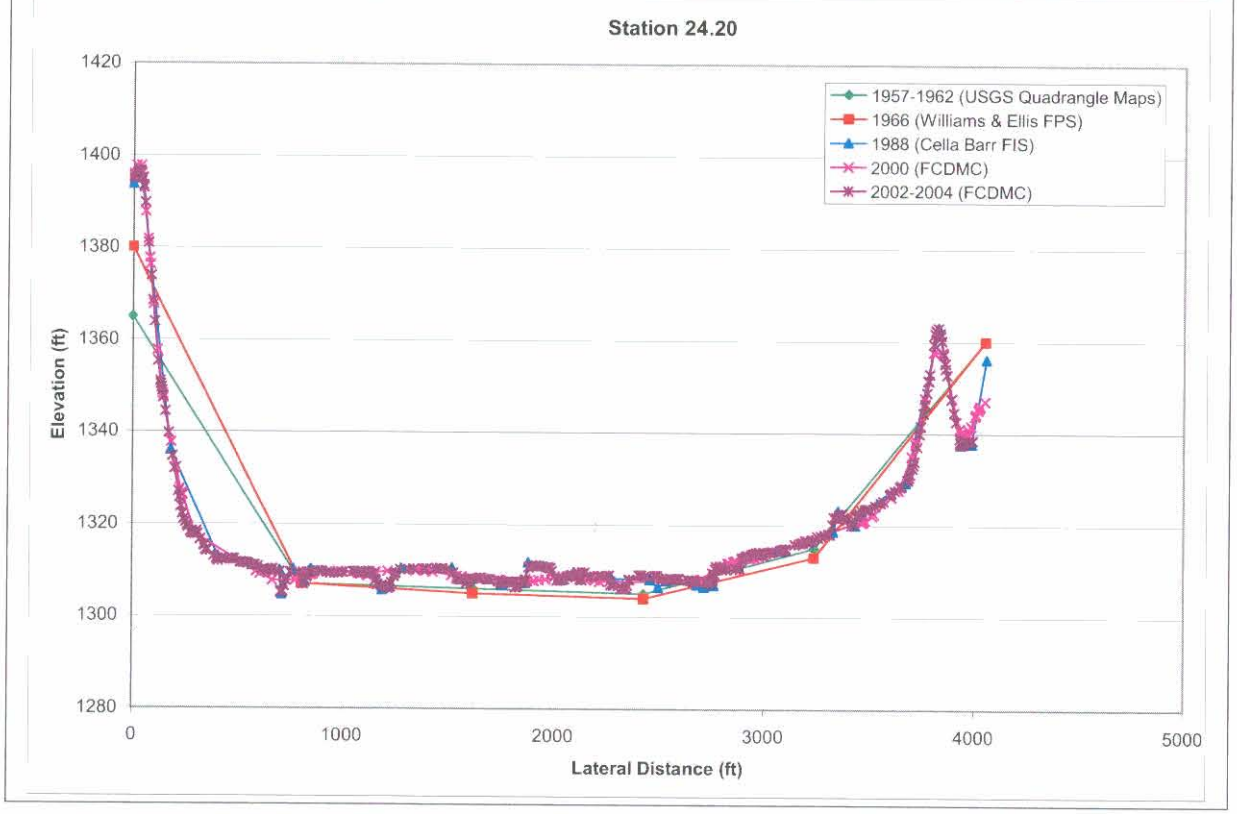

Figure 4-9. Cross-Section 24.20 Profile Comparison

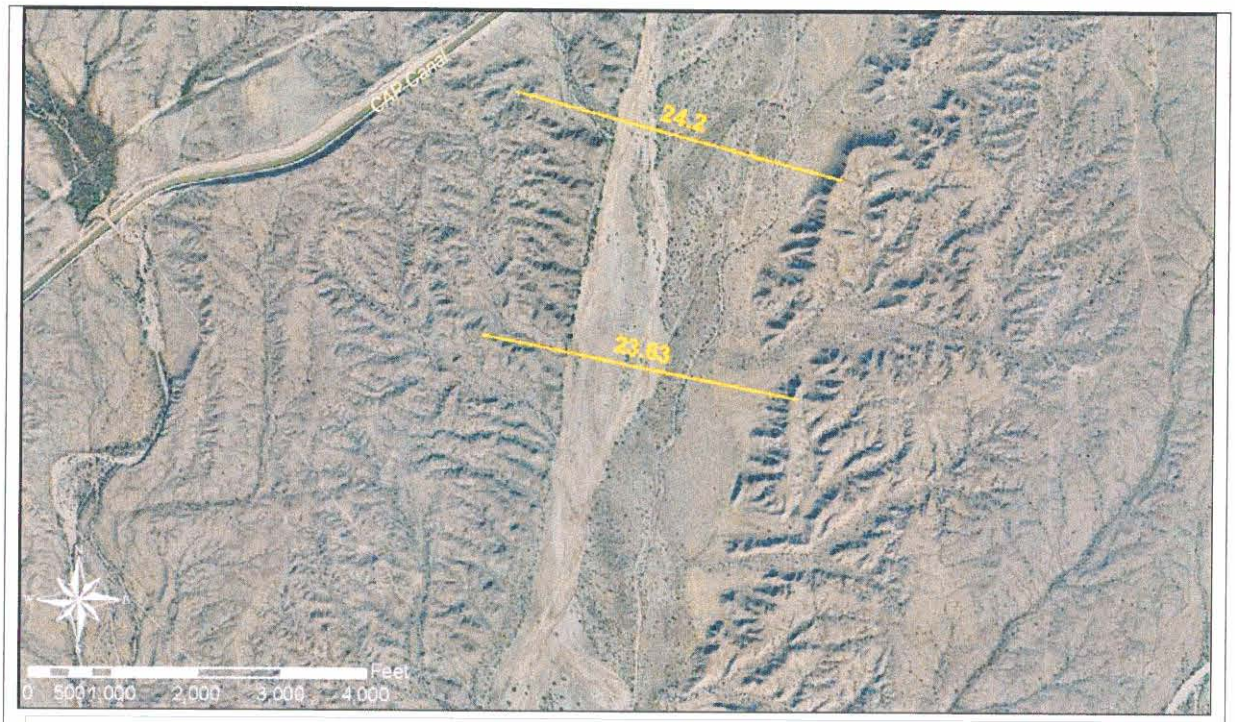

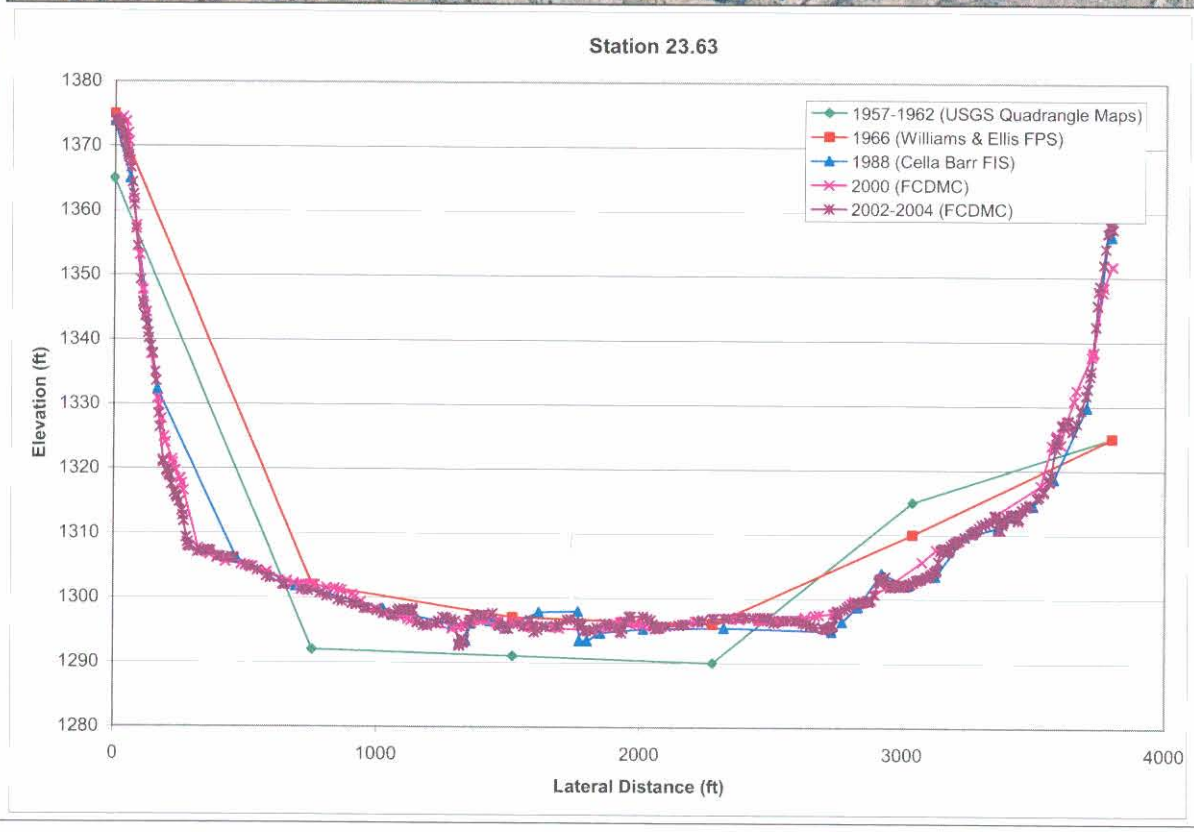

Figure 4-10. Cross-Section 23.63 Profile Comparison

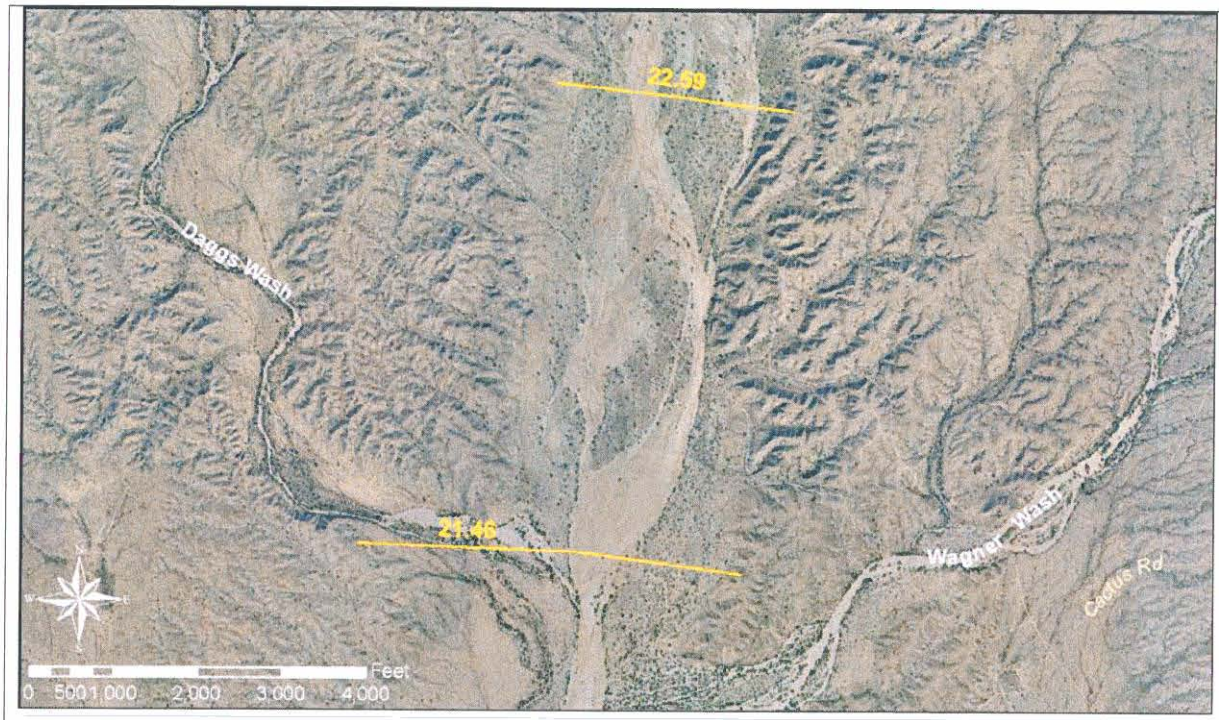

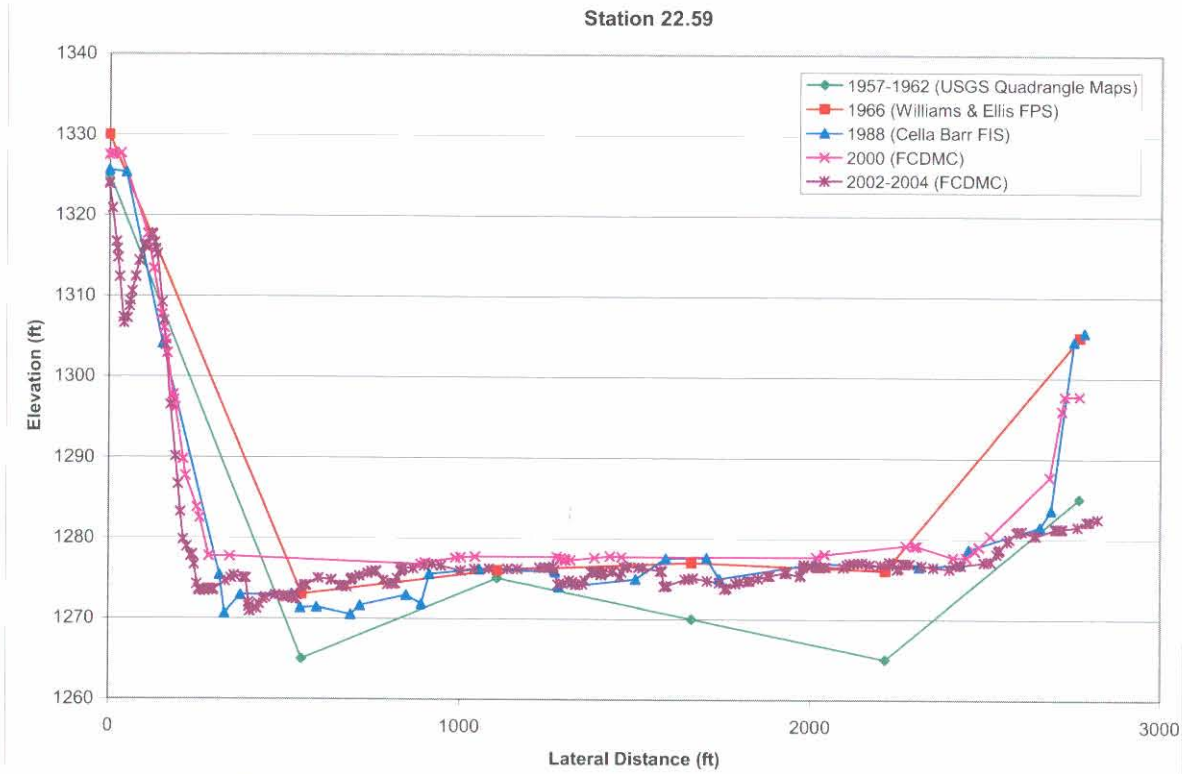

Figure 4-11. Cross-Section 22.59 Profile Comparison

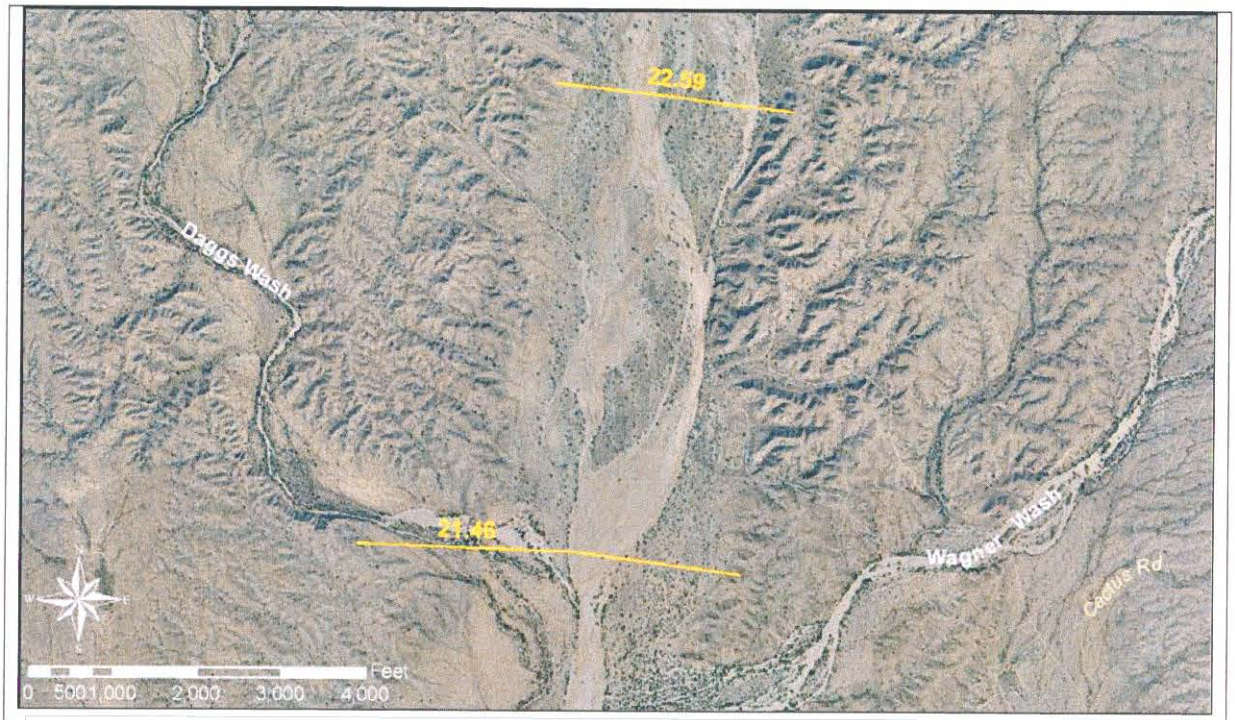

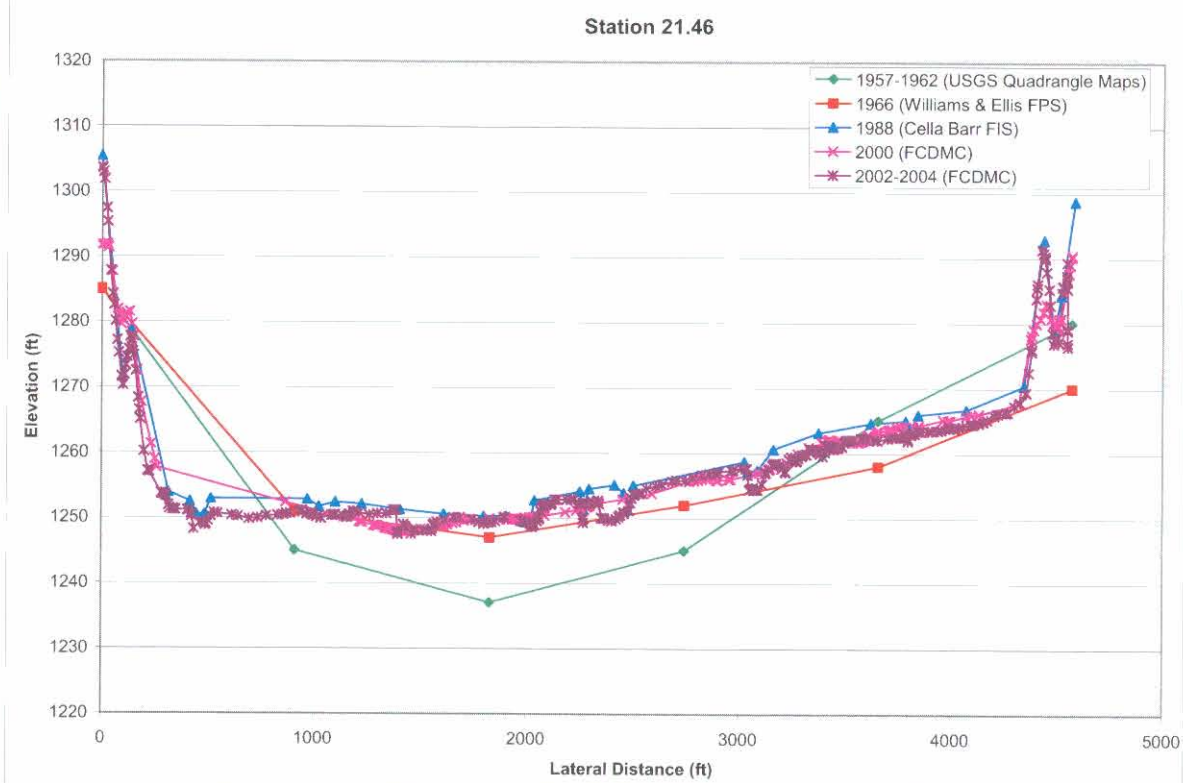

Figure 4-12. Cross-Section 21.46 Profile Comparison

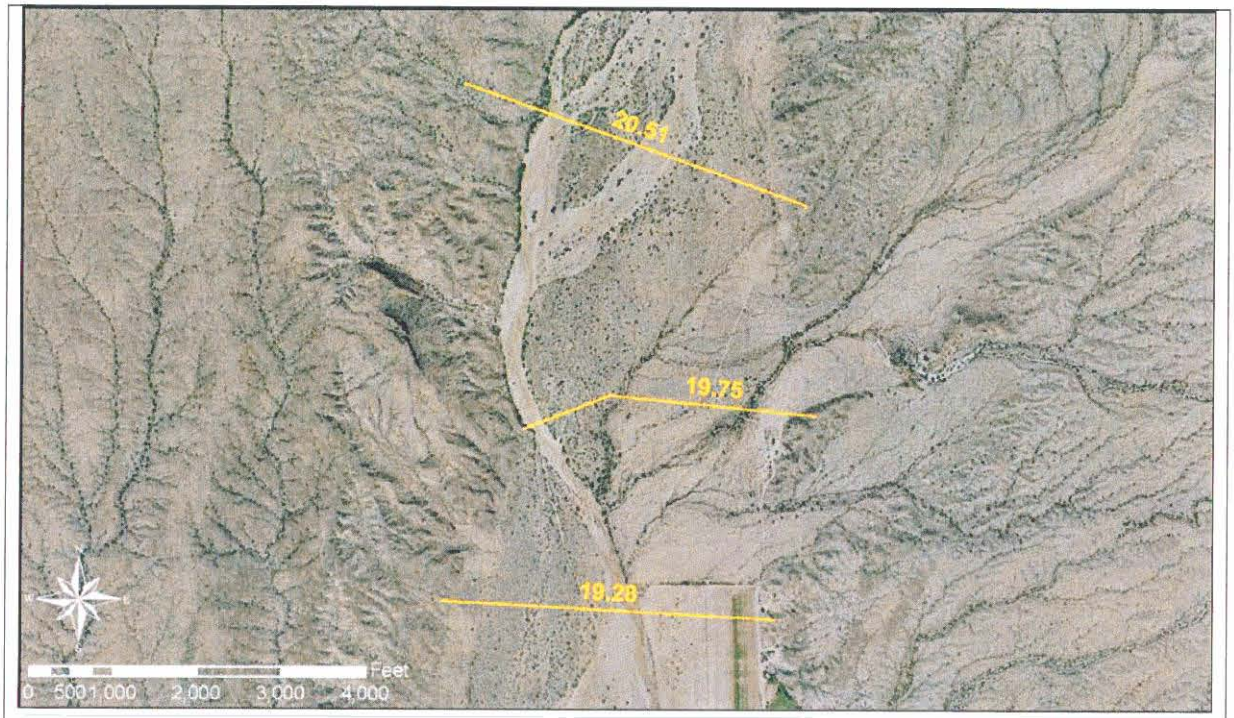

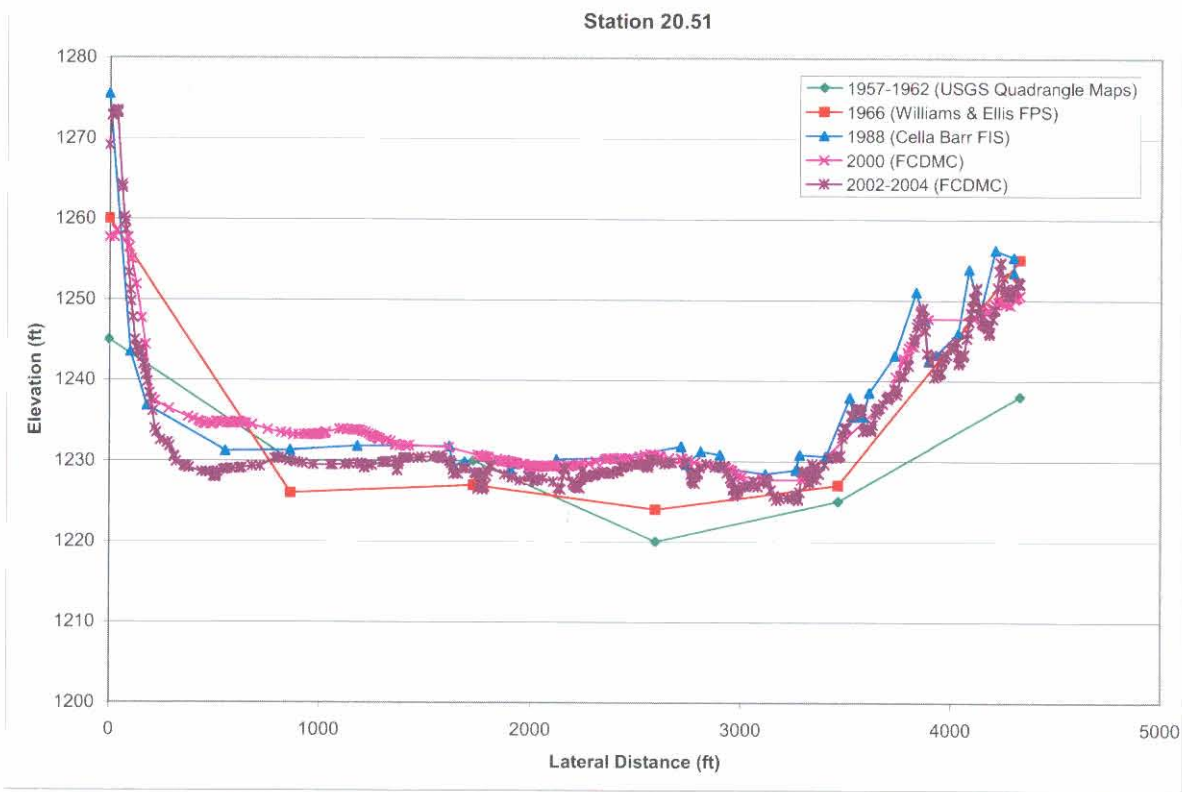

Figure 4-13. Cross-Section 20.51 Profile Comparison

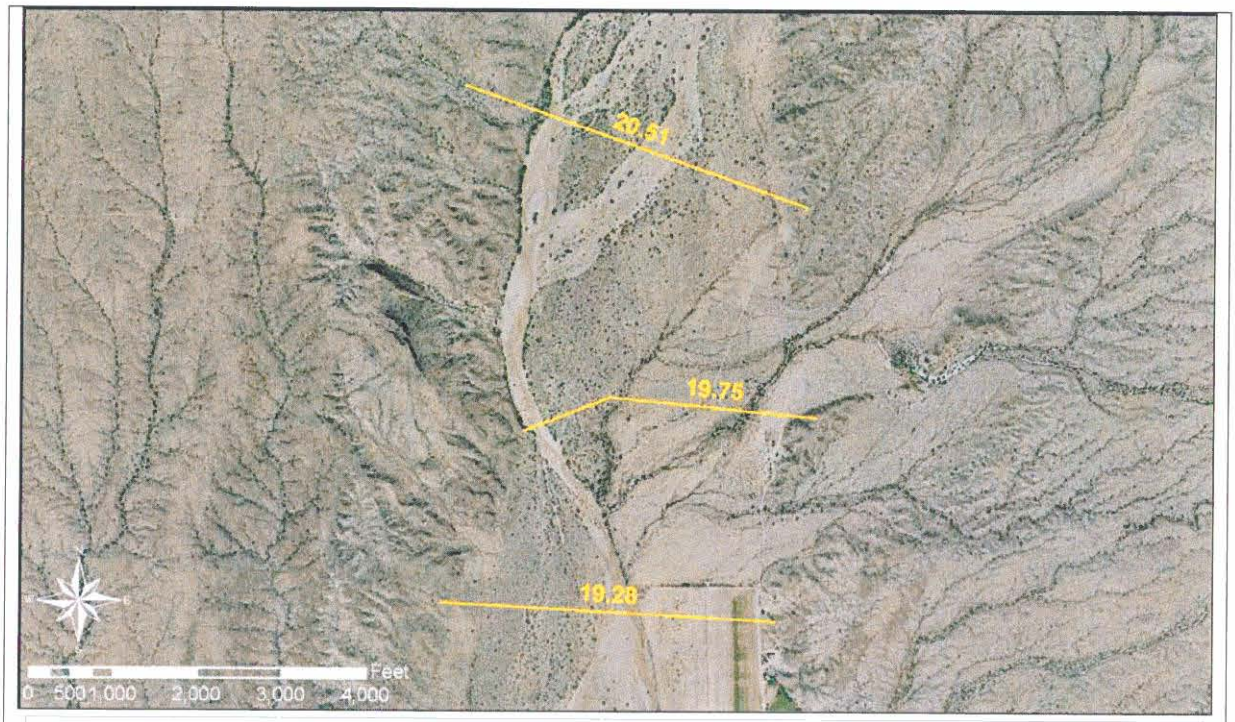

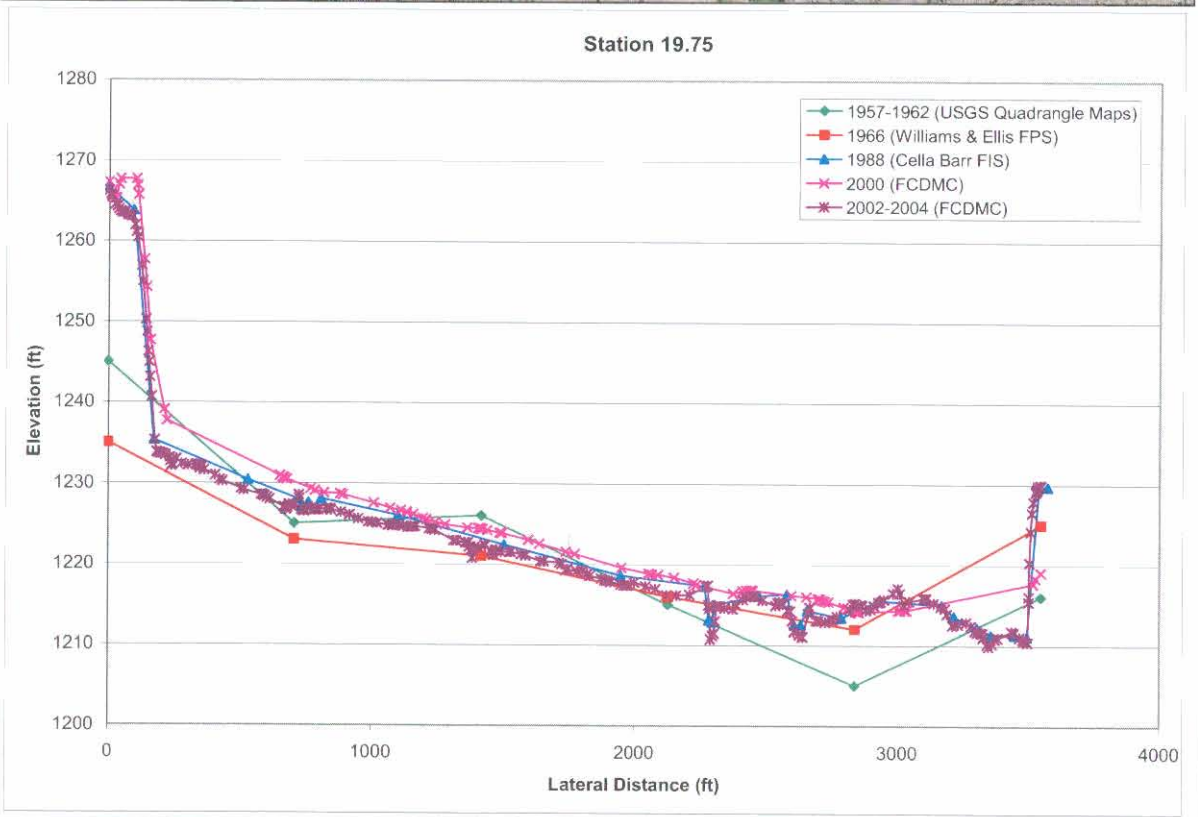

Figure 4-14. Cross-Section 19.75 Profile Comparison

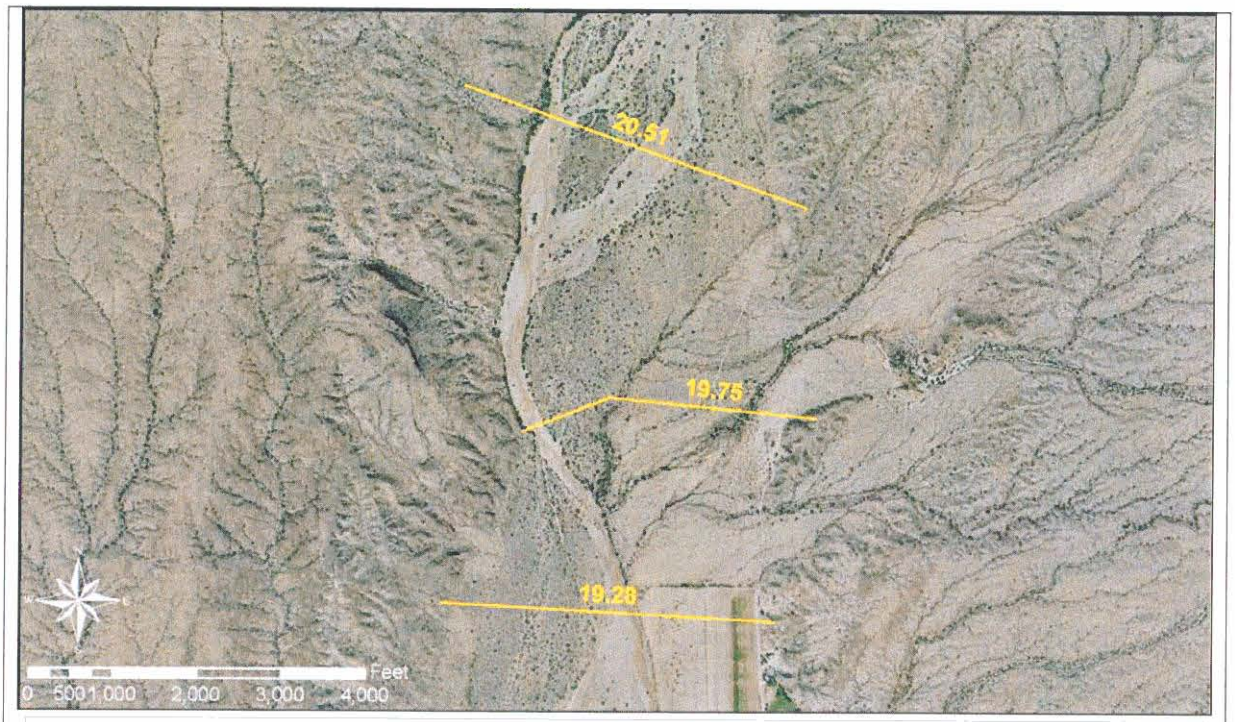

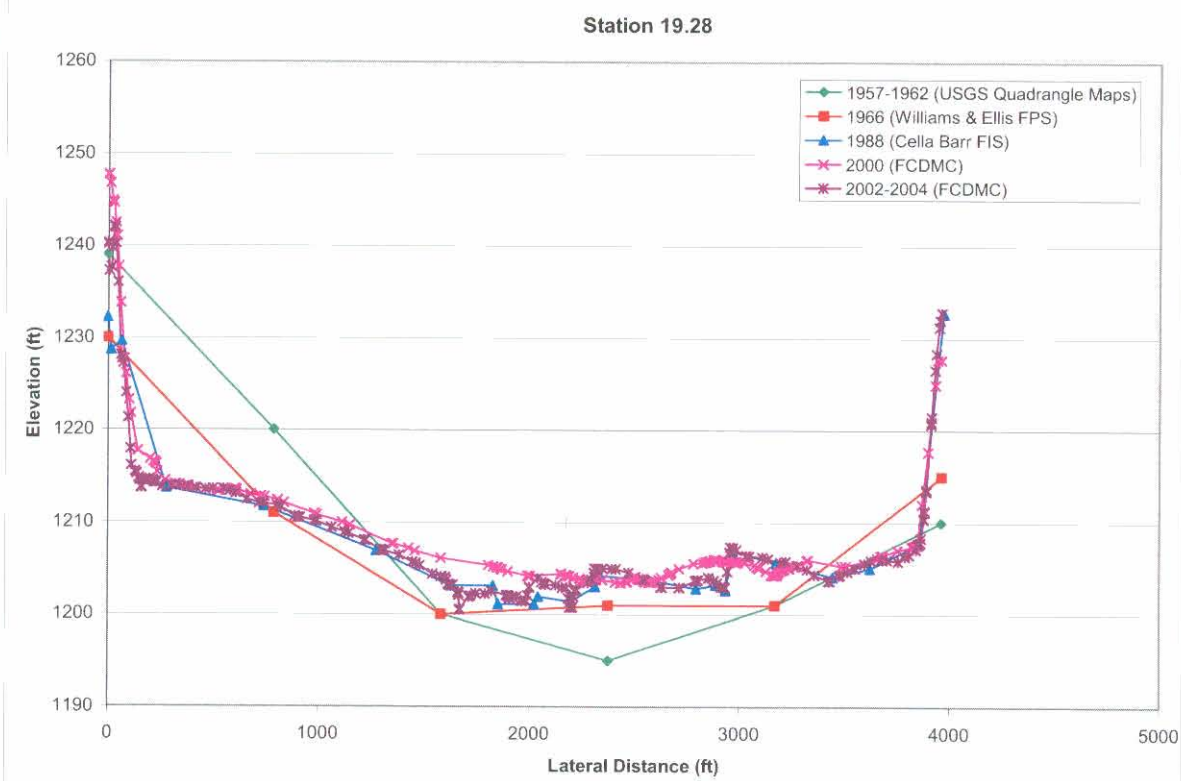

Figure 4-15. Cross-Section 19.28 Profile Comparison

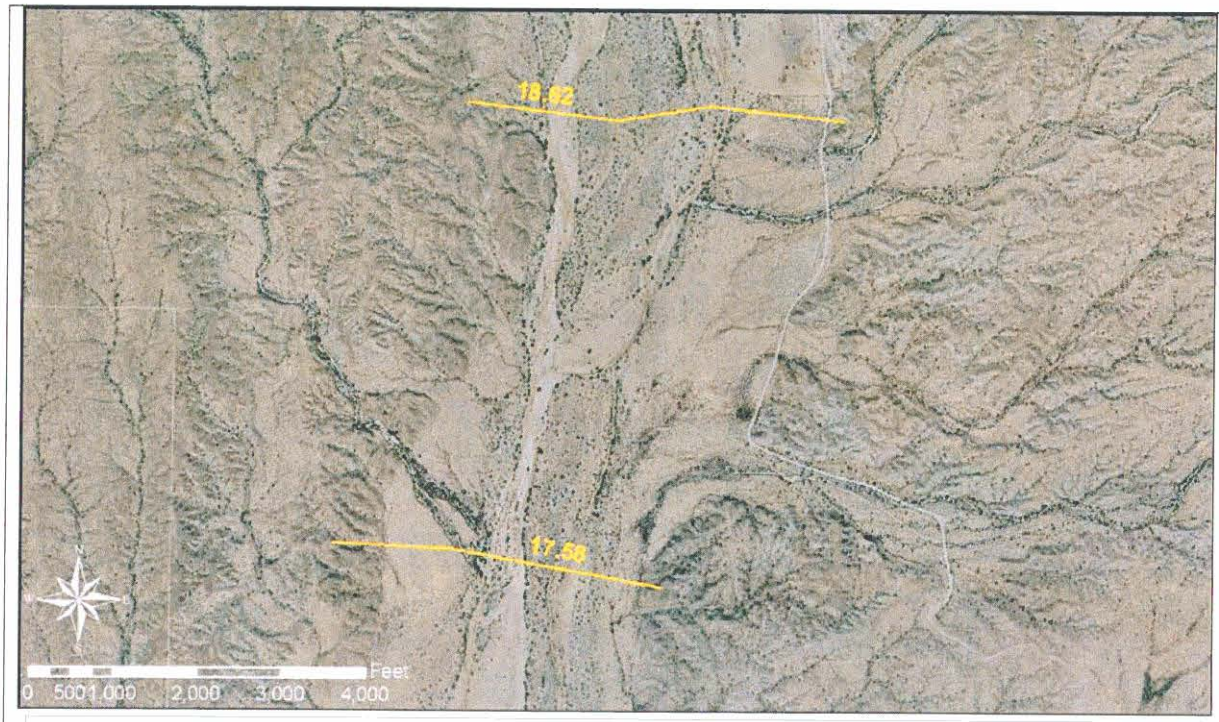

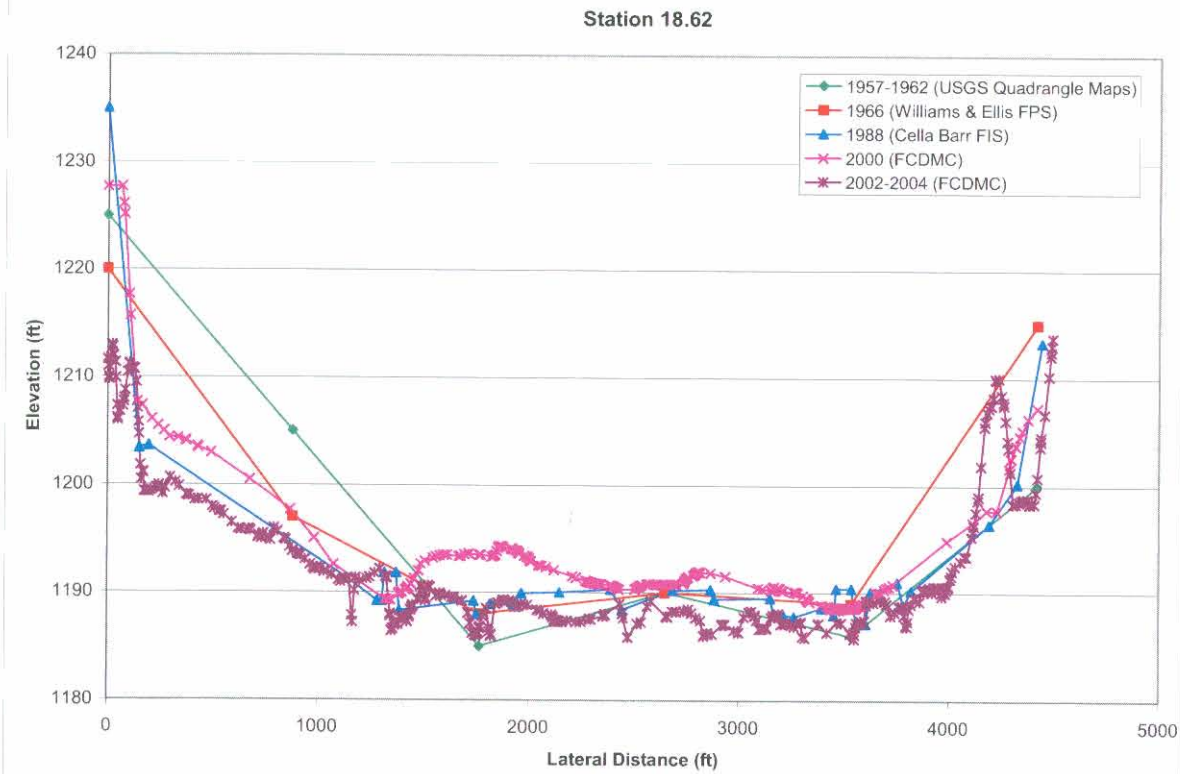

Figure 4-16. Cross-Section 18.62 Profile Comparison

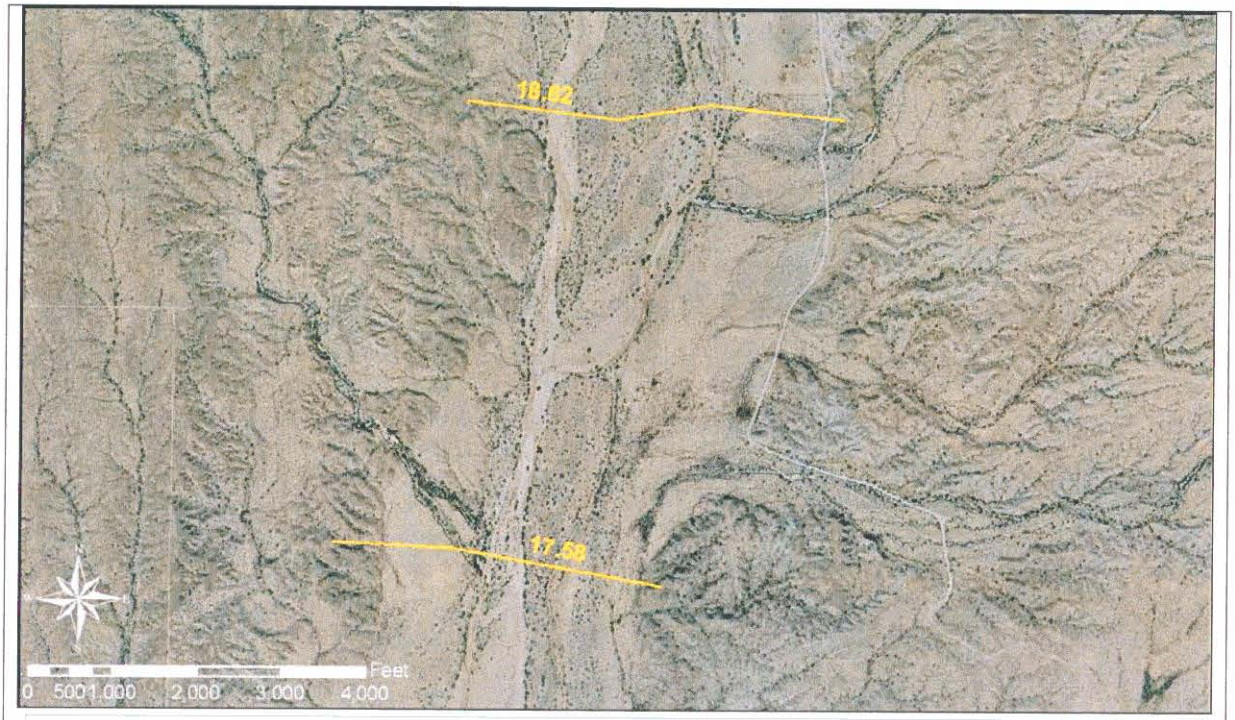

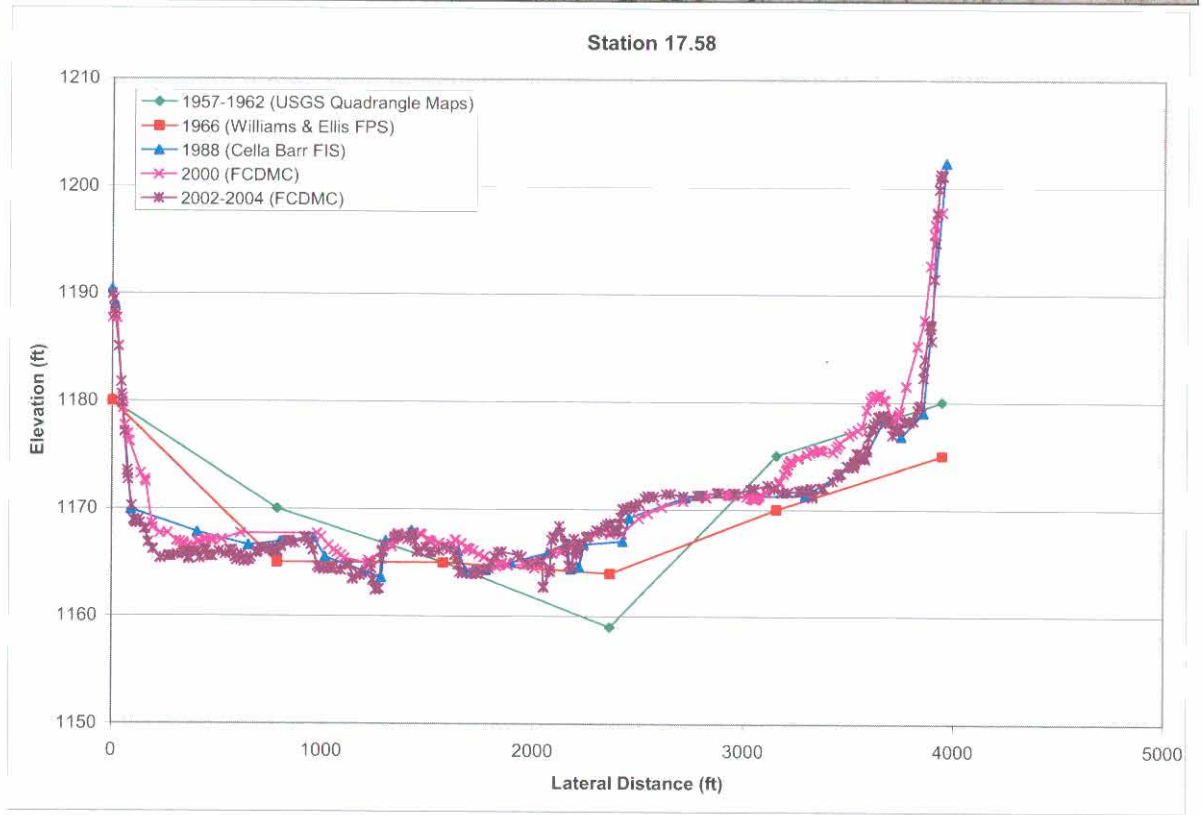

Figure 4-17. Cross-Section 17.58 Profile Comparison

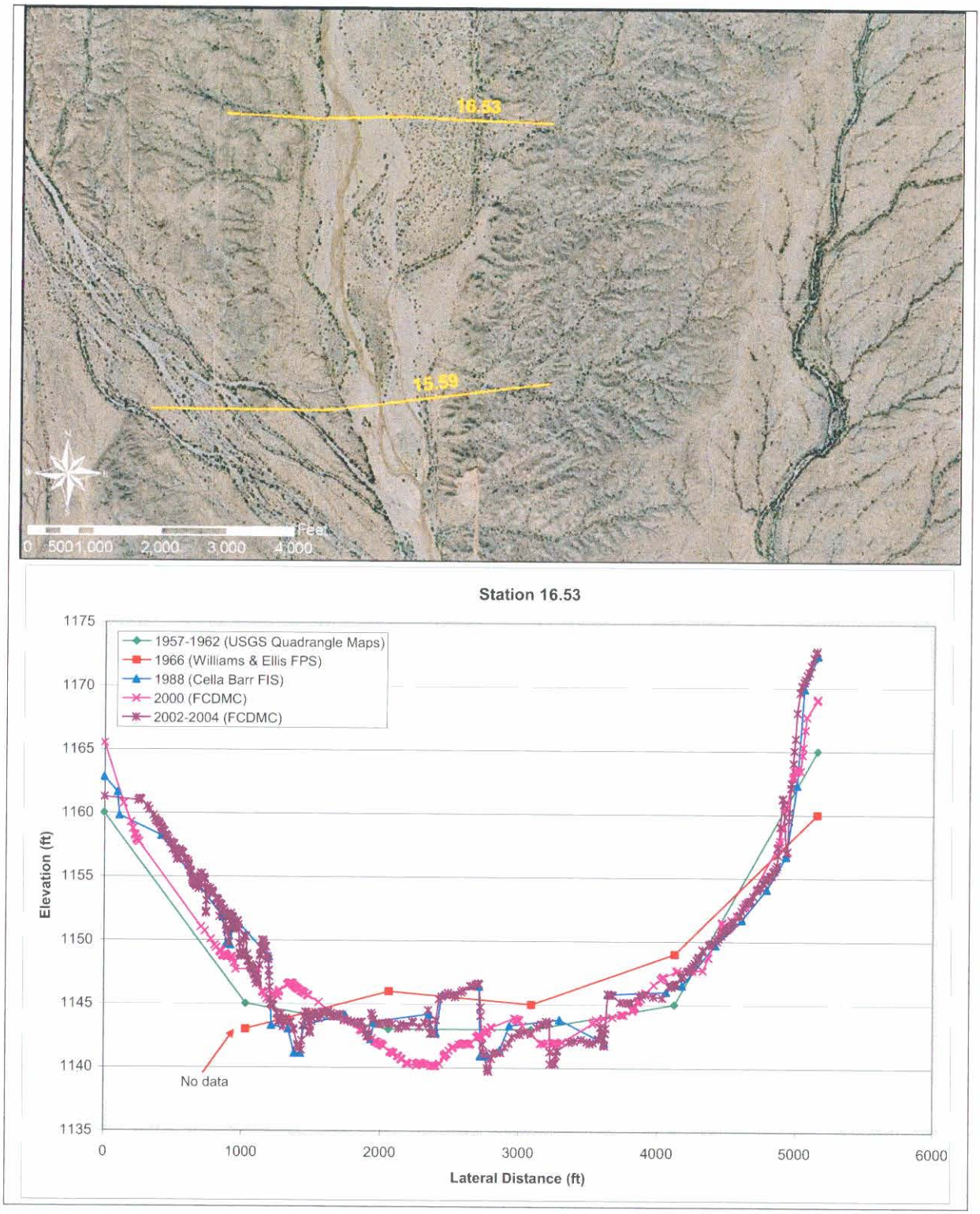

Figure 4-18. Cross-Section 16.53 Profile Comparison

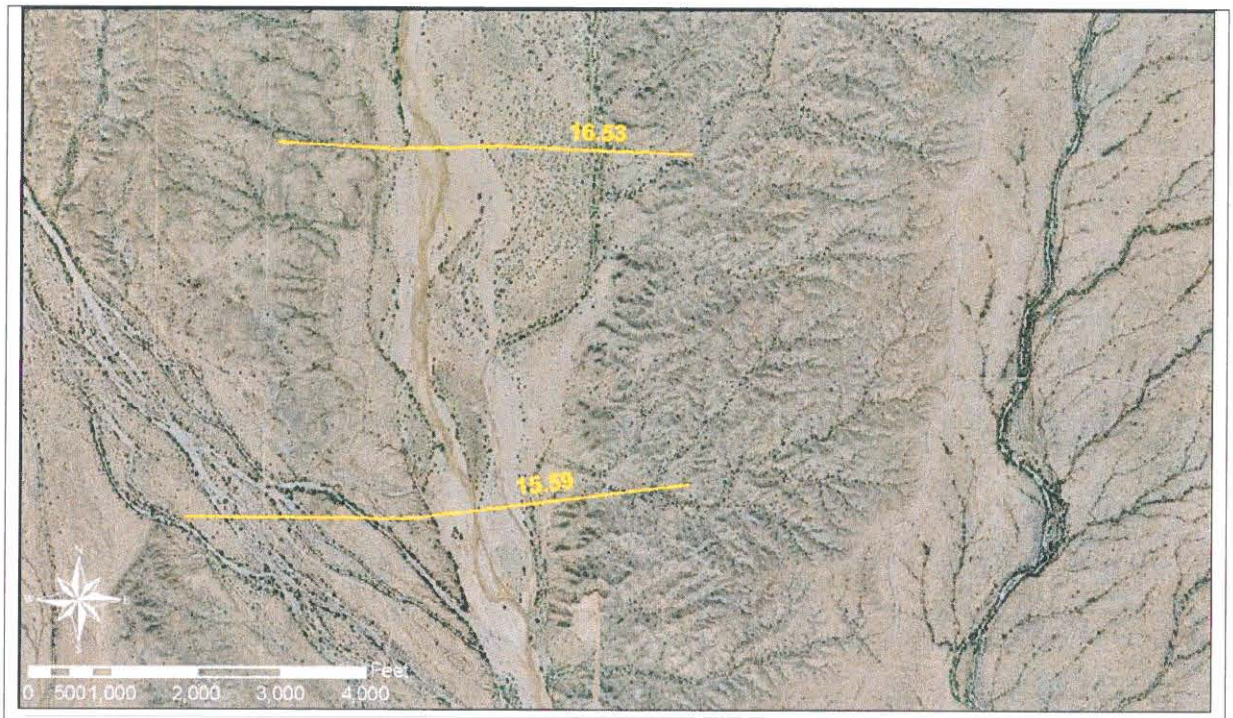

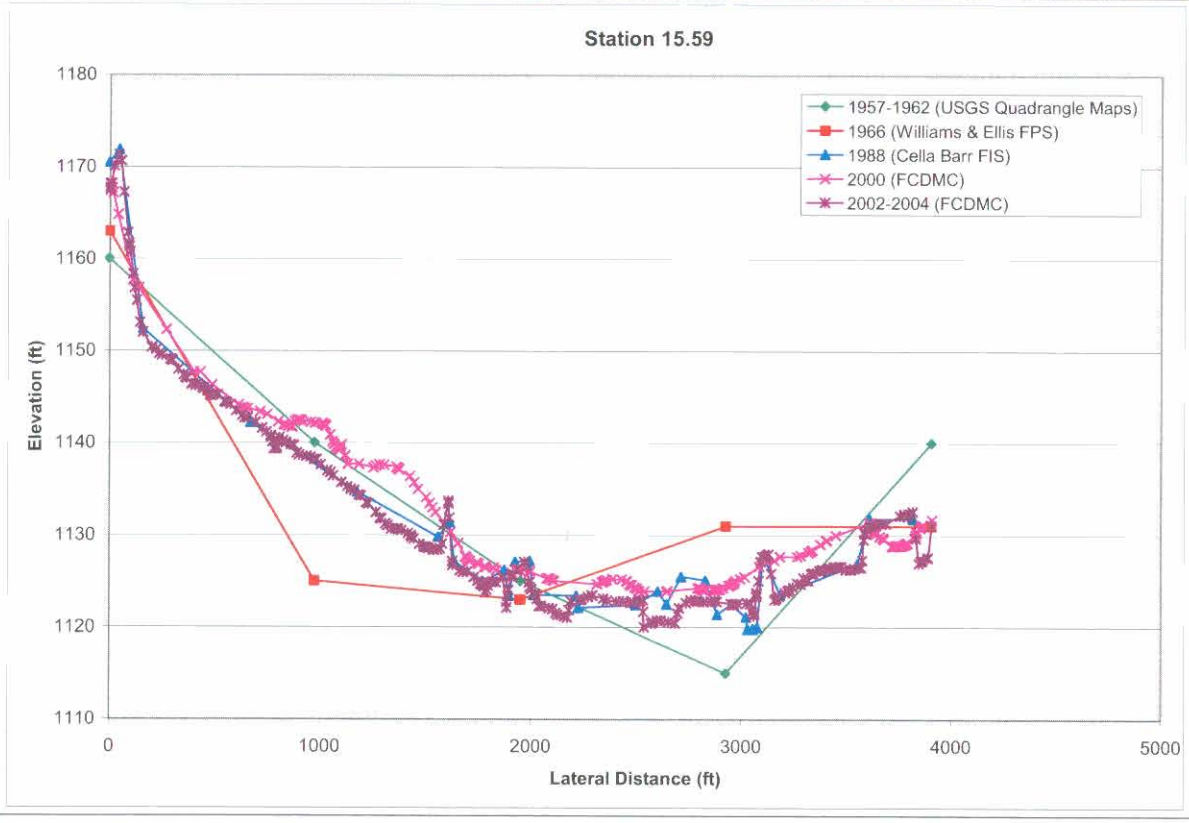

Figure 4-19. Cross-Section 15.59 Profile Comparison

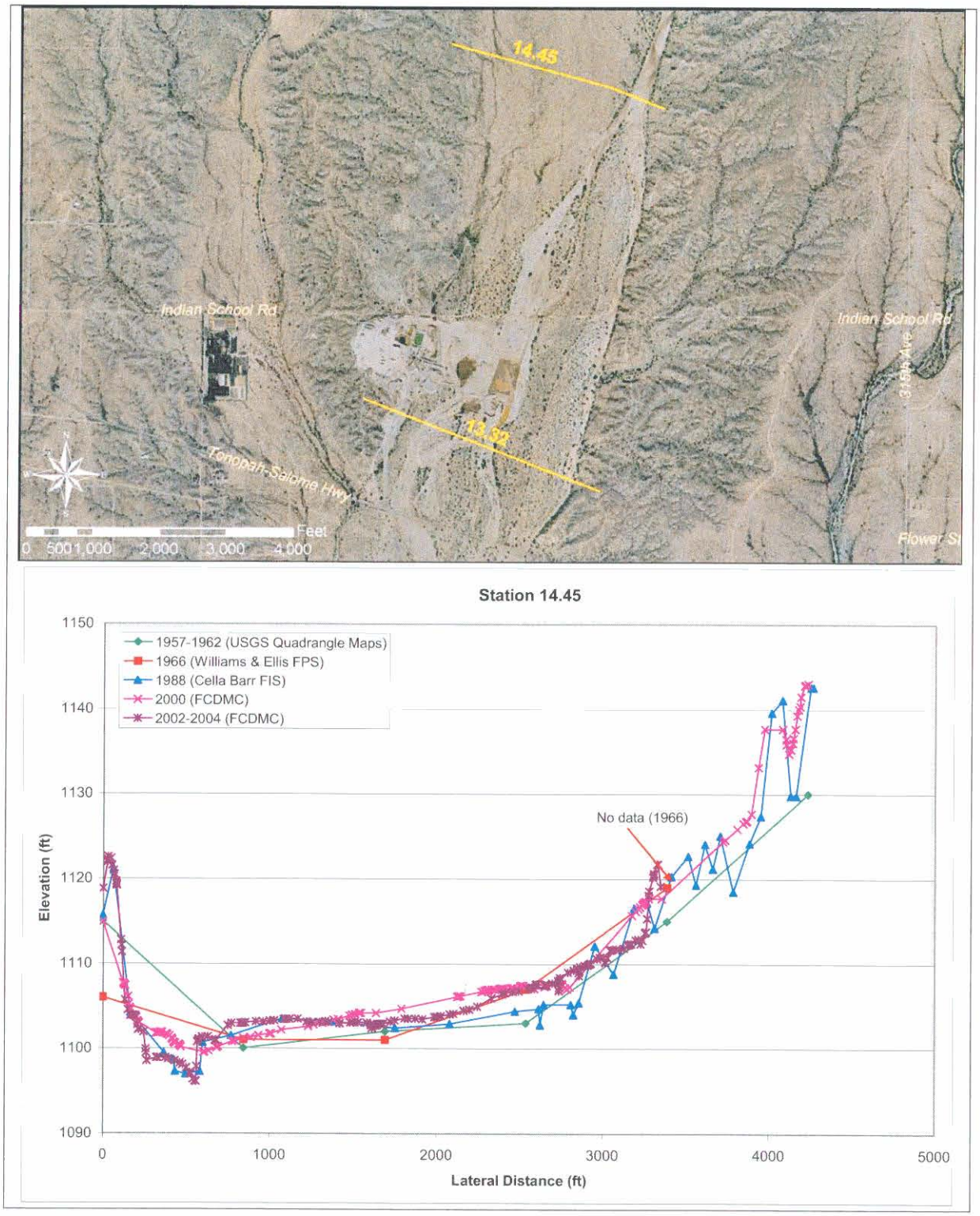

Figure 4-20. Cross-Section 14.45 Profile Comparison

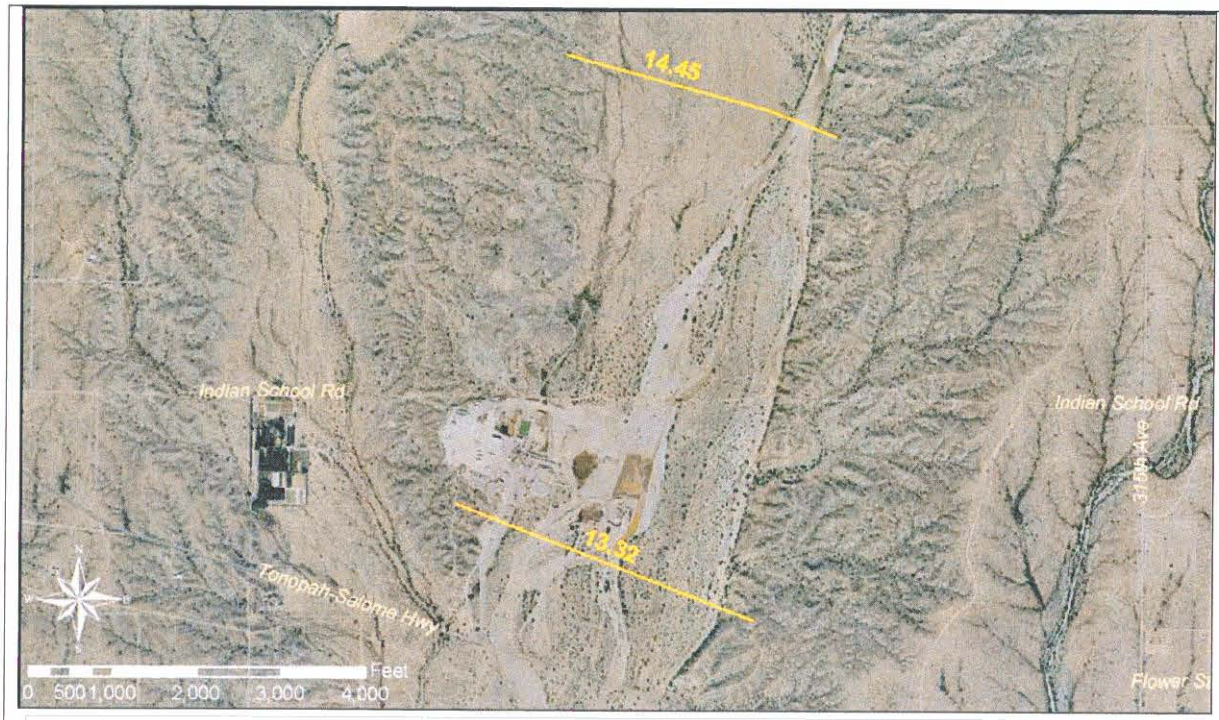

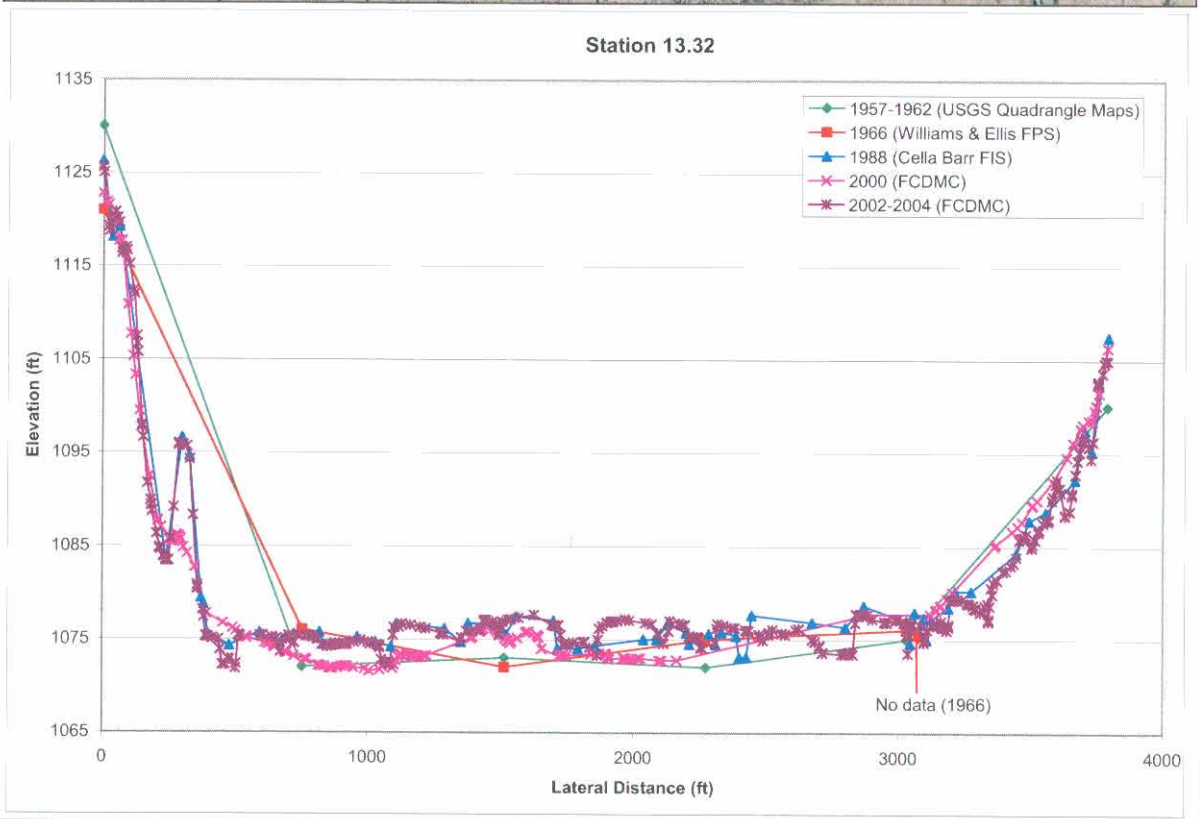

Figure 4-21. Cross-Section 13.32 Profile Comparison

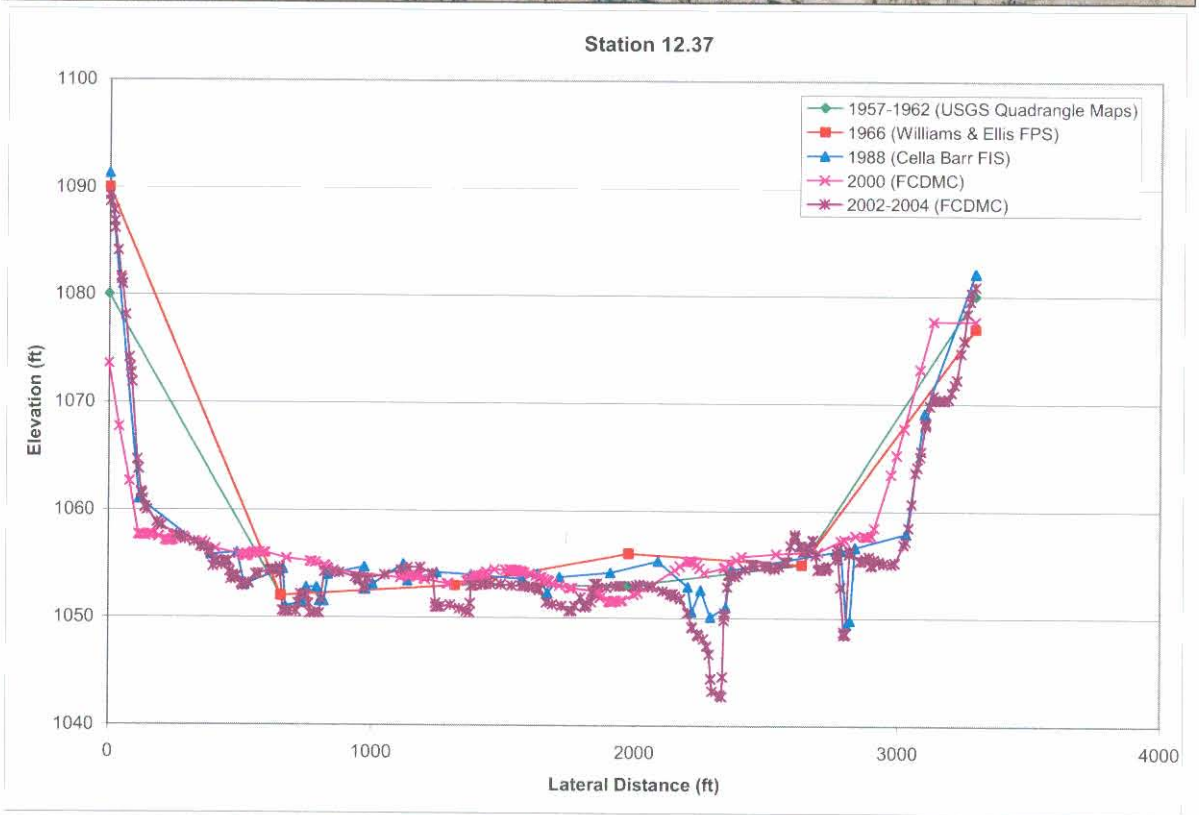

Figure 4-22. Cross-Section 12.37 Profile Comparison

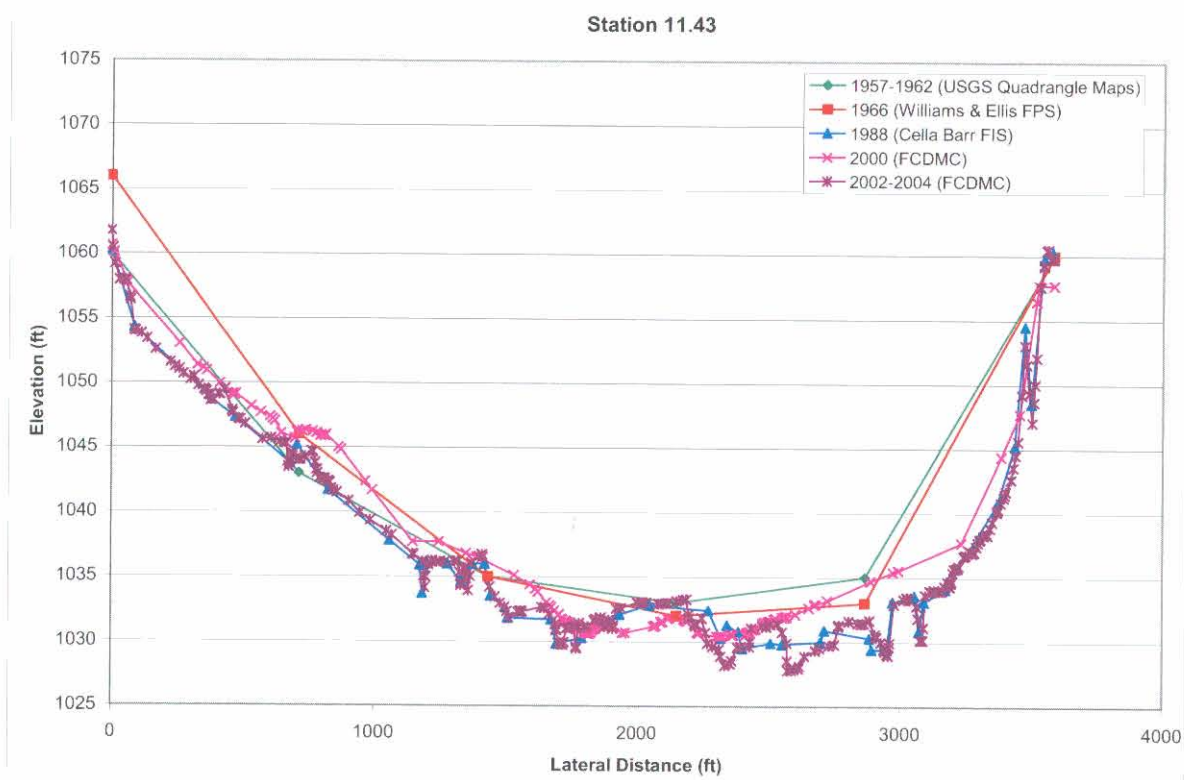

Figure 4-23. Cross-Section 11.43 Profile Comparison

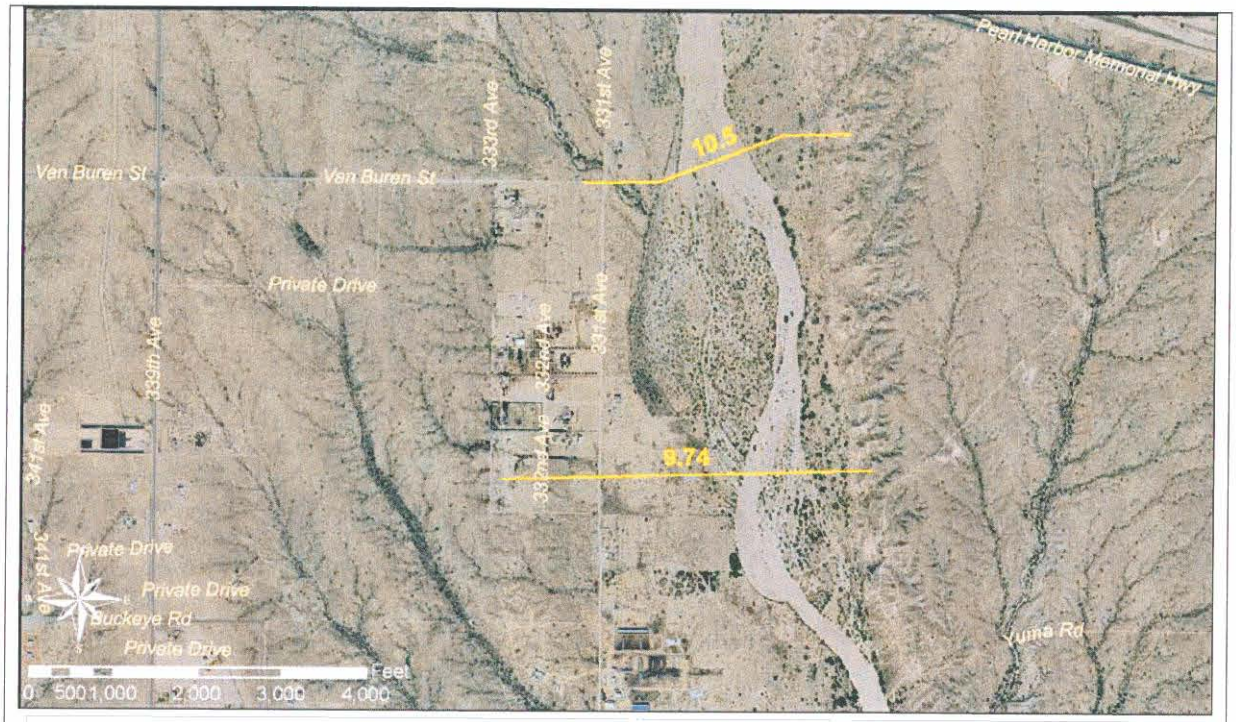

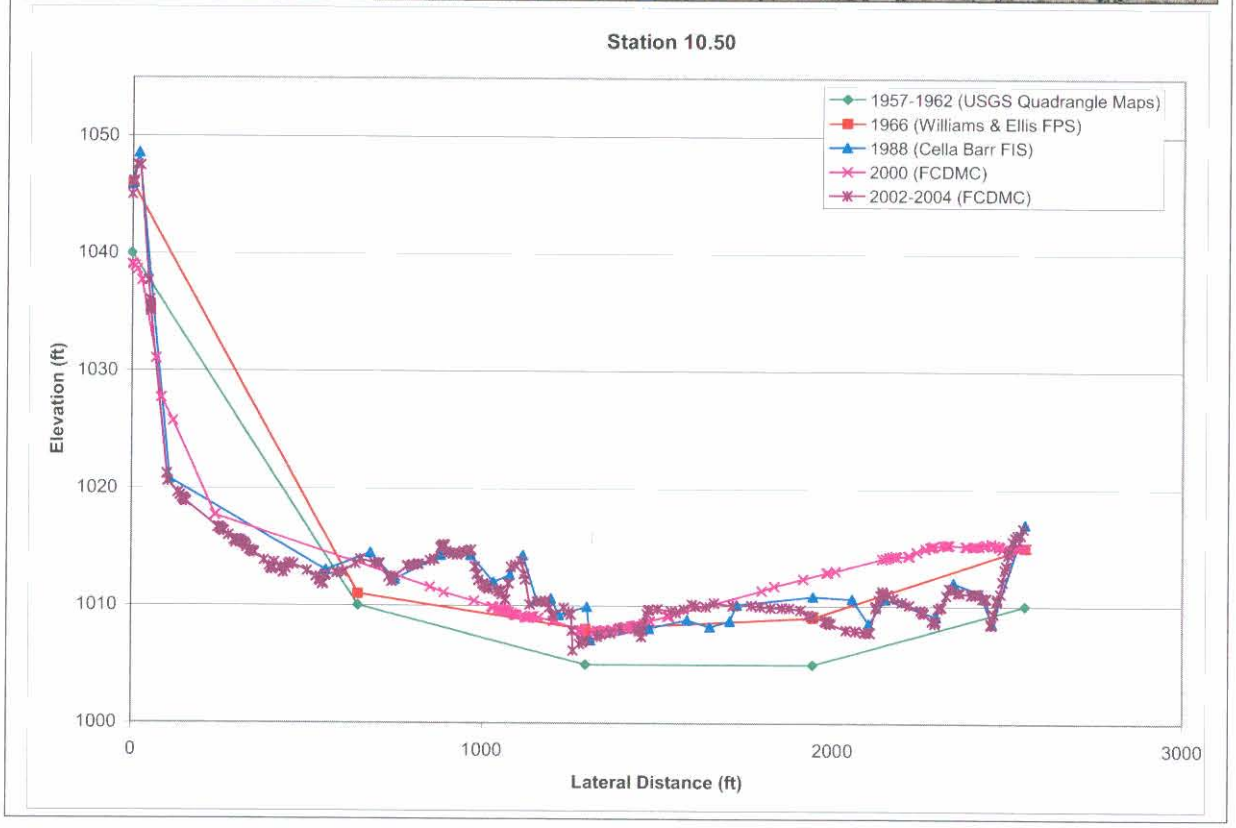

Figure 4-24. Cross-Section 10.50 Profile Comparison

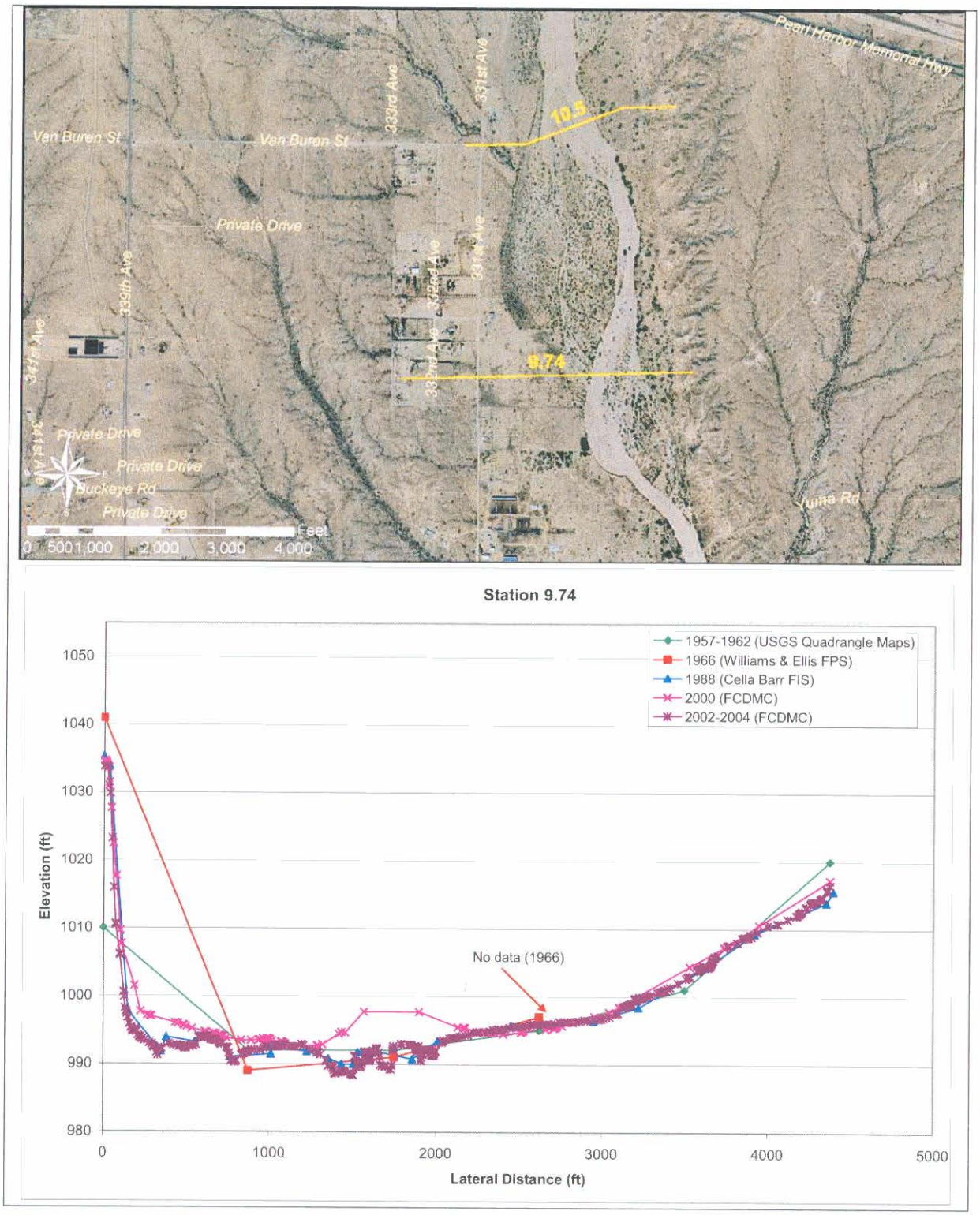

Figure 4-25. Cross-Section 9.74 Profile Comparison

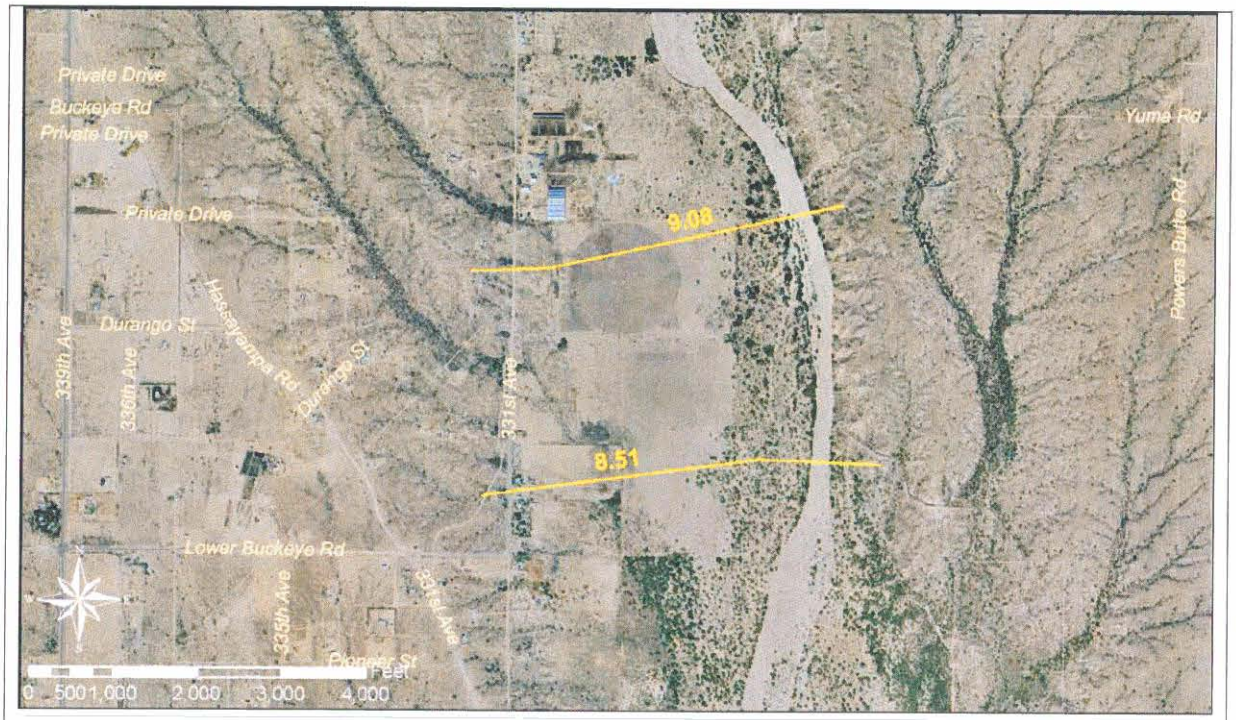

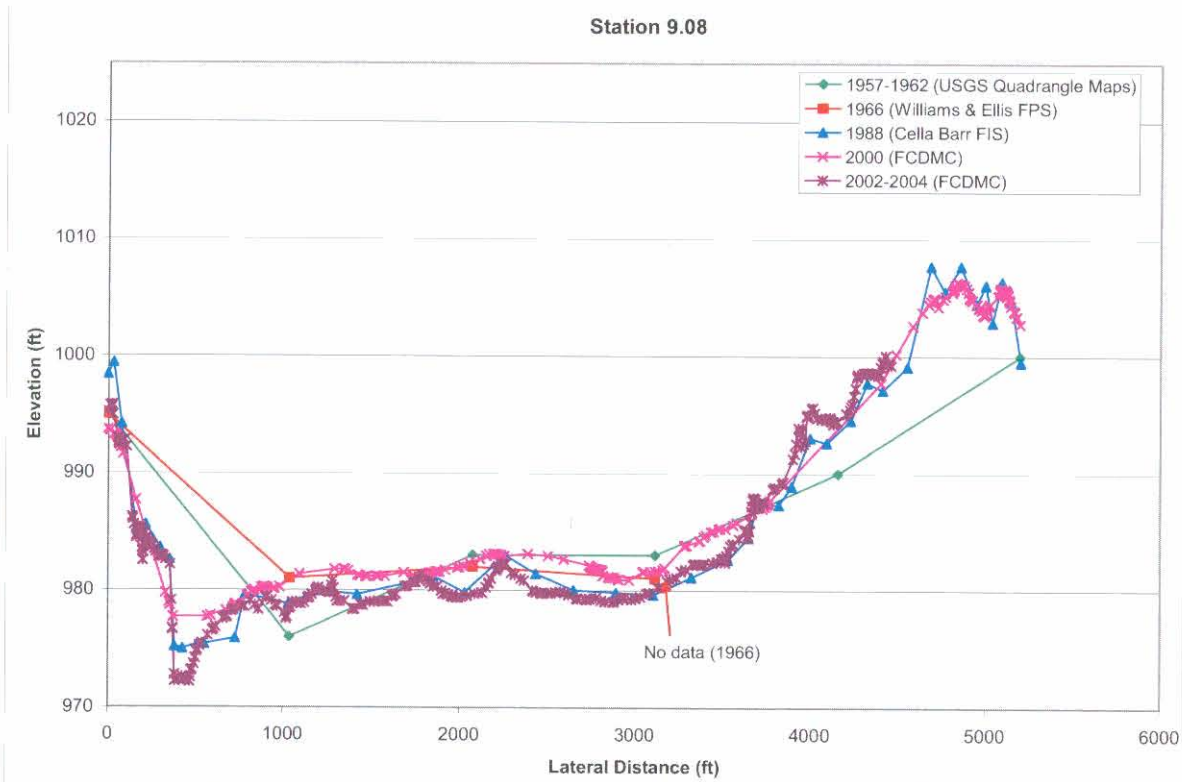

Figure 4-26. Cross-Section 9.08 Profile Comparison

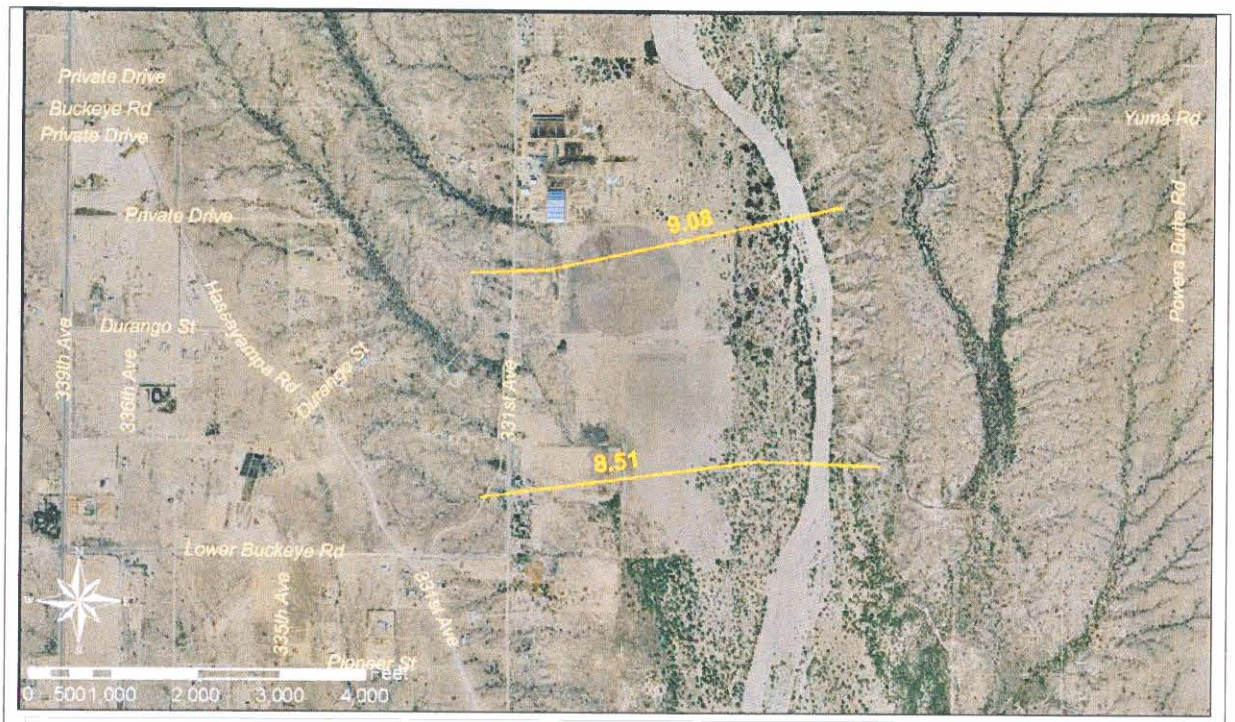

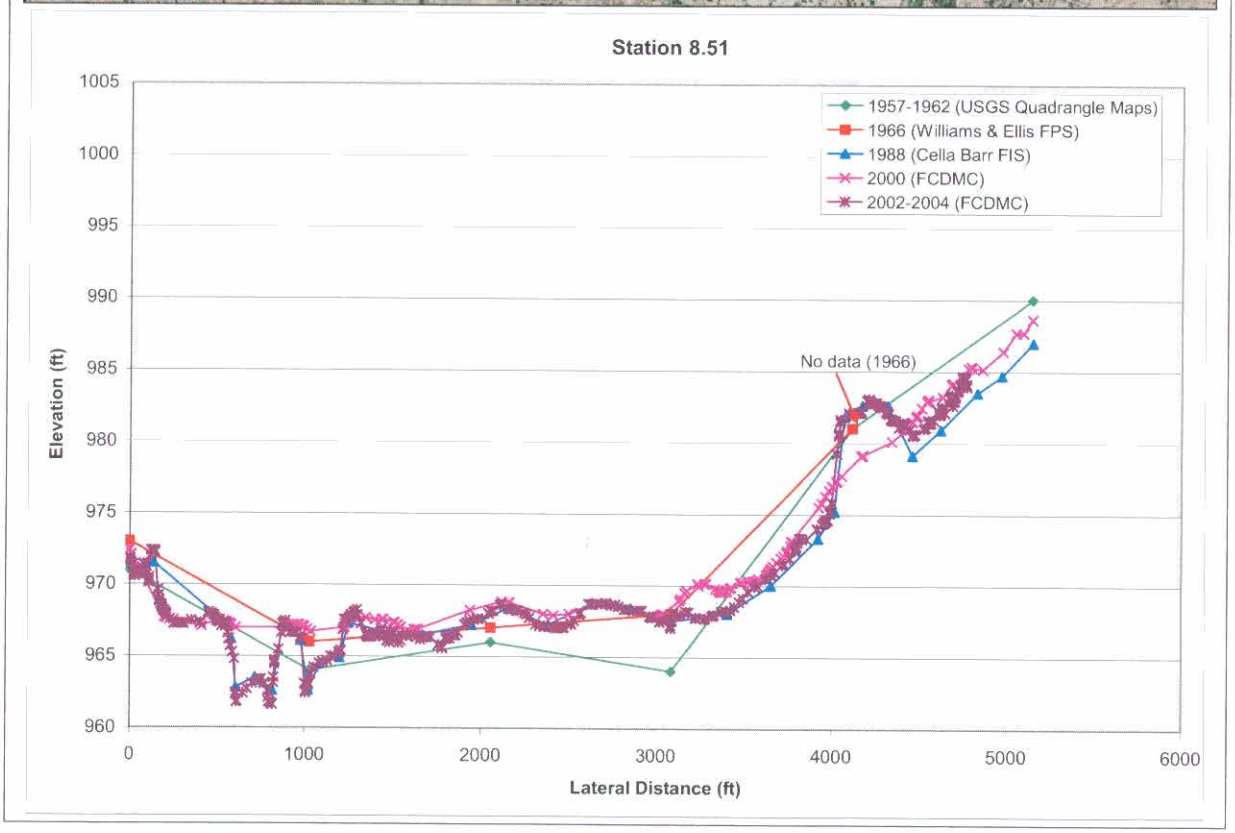

Figure 4-27. Cross-Section 8.51 Profile Comparison

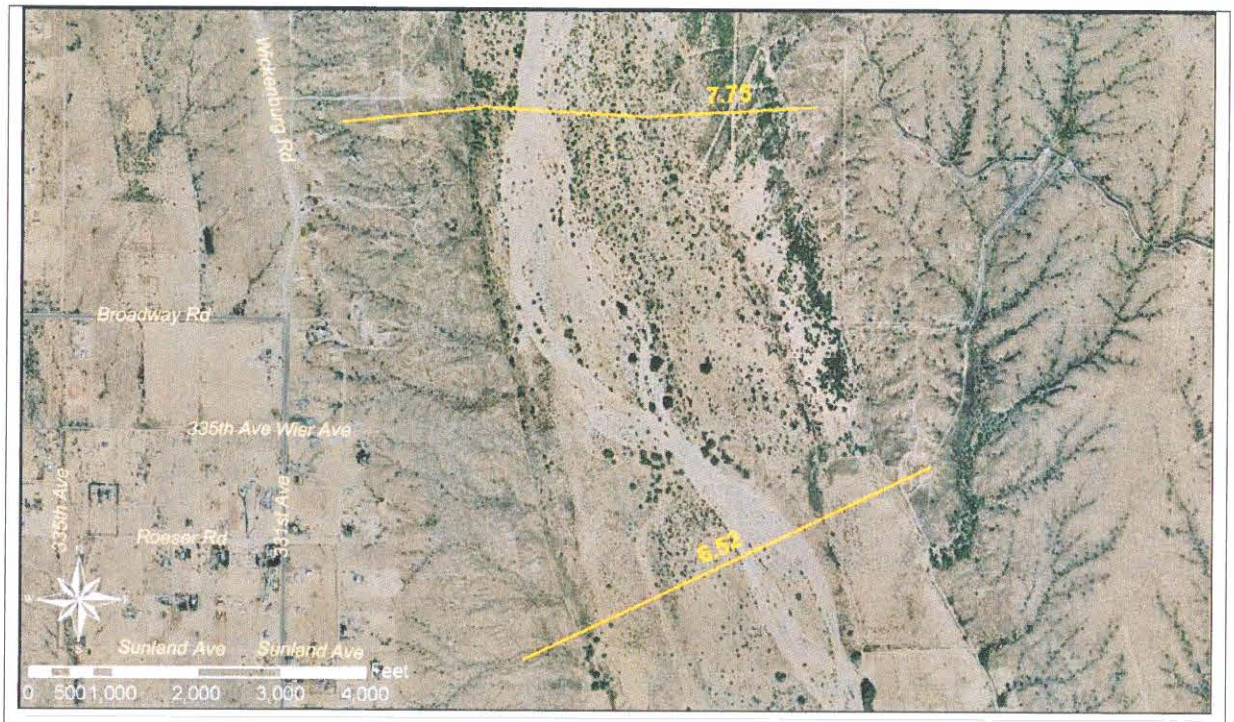

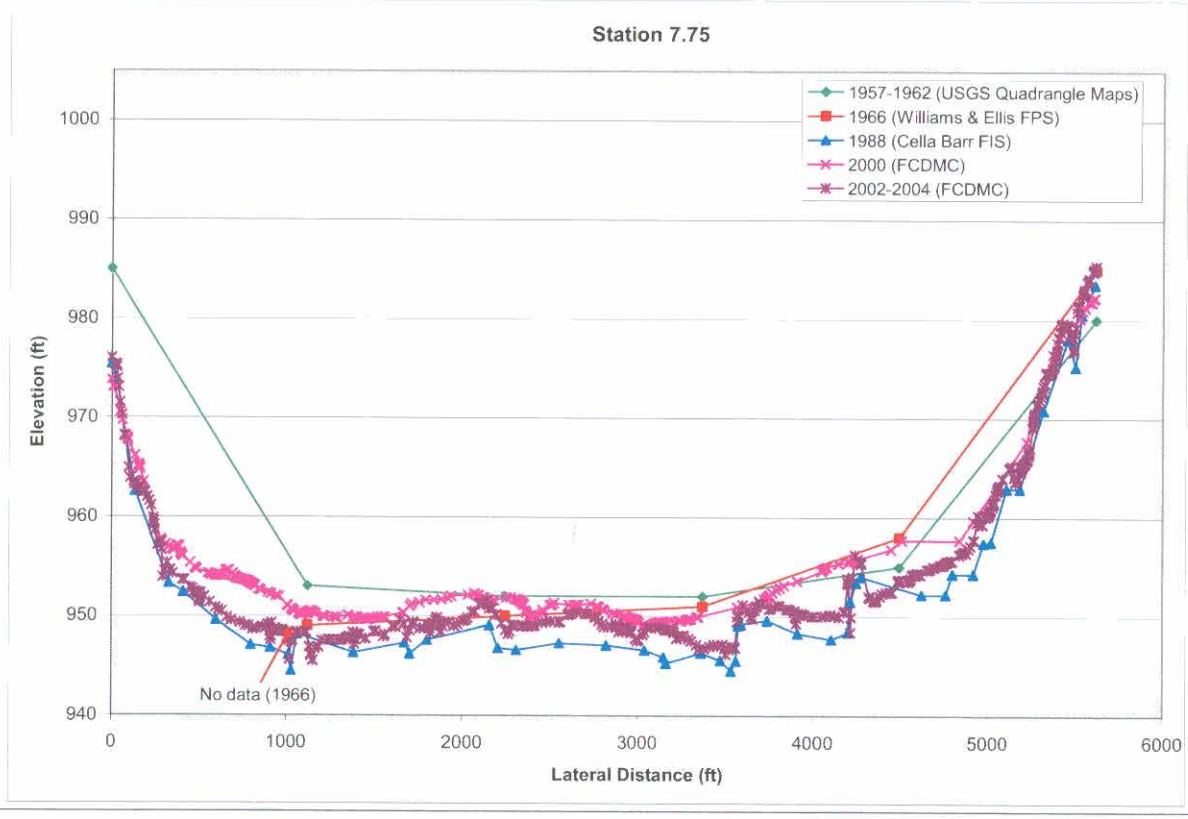

Figure 4-28. Cross-Section 7.75 Profile Comparison

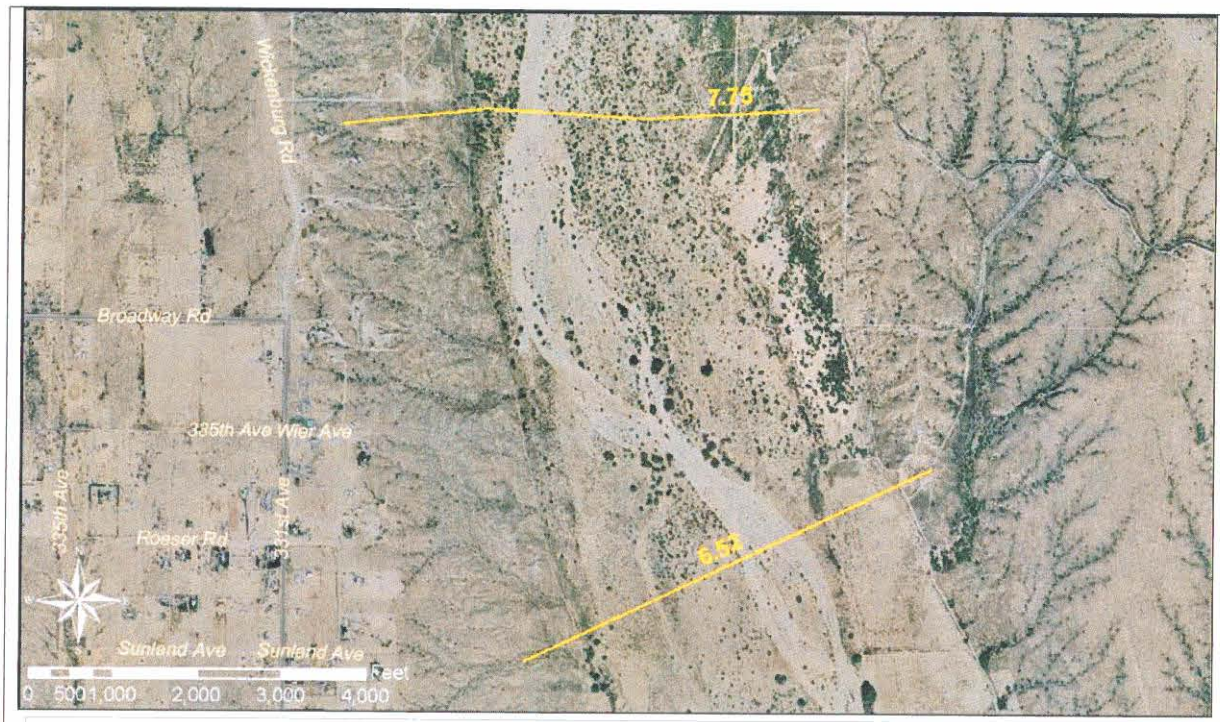

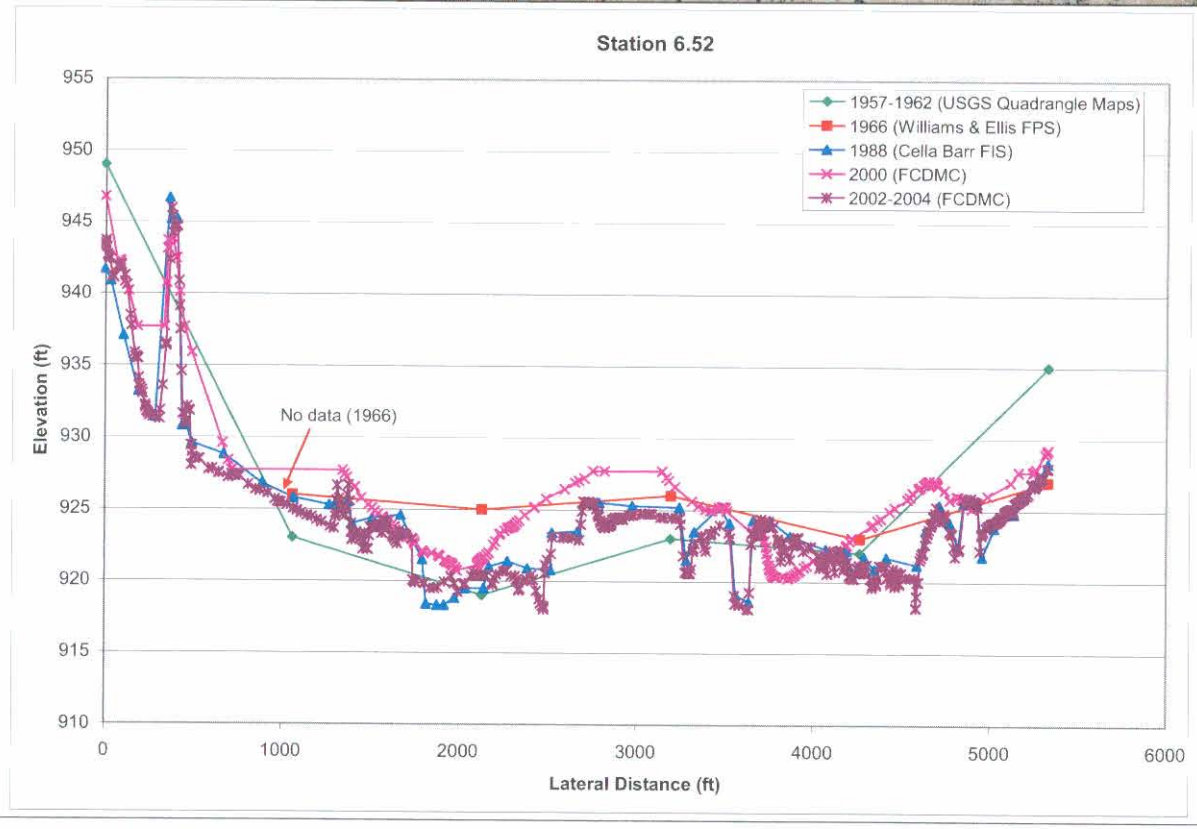

Figure 4-29. Cross-Section 6.52 Profile Comparison

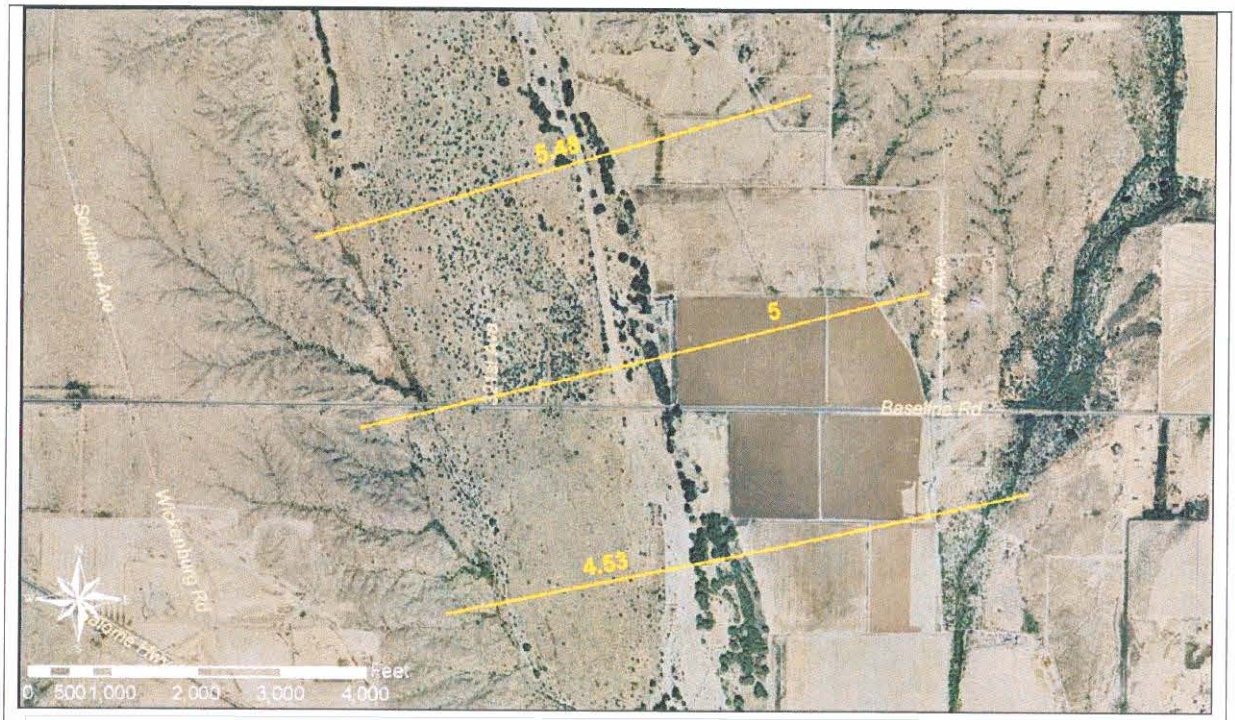

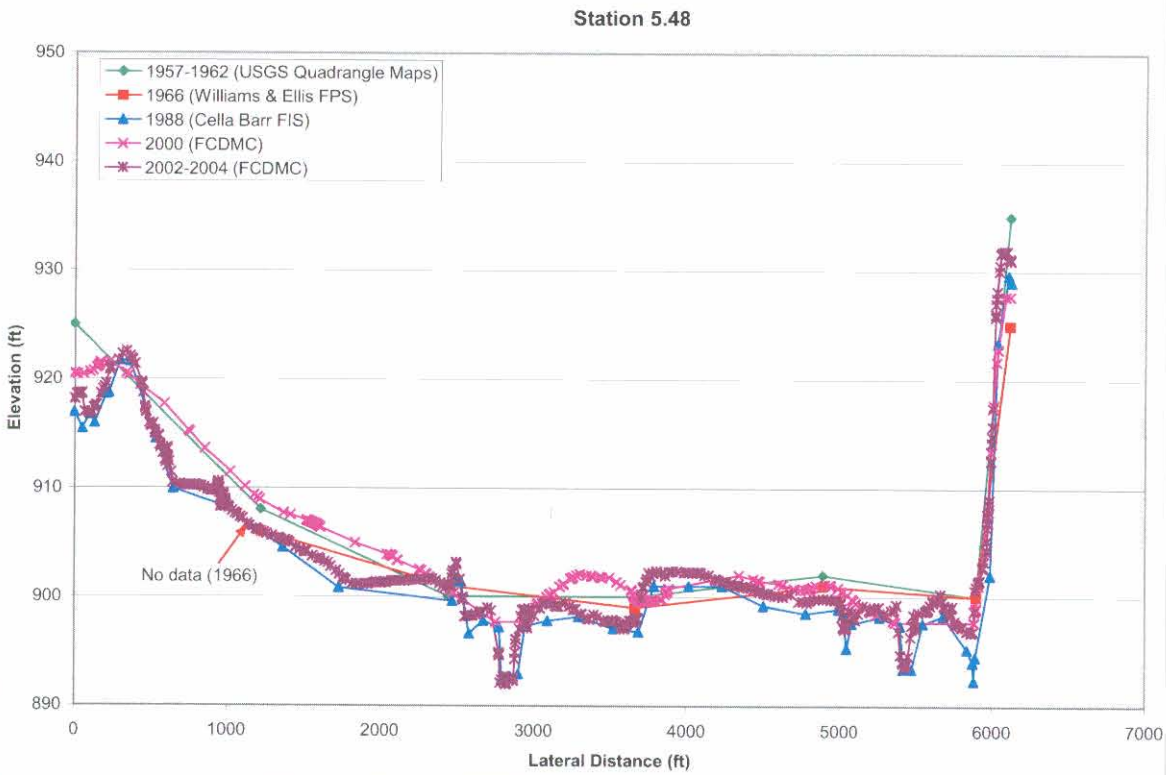

Figure 4-30. Cross-Section 5.48 Profile Comparison

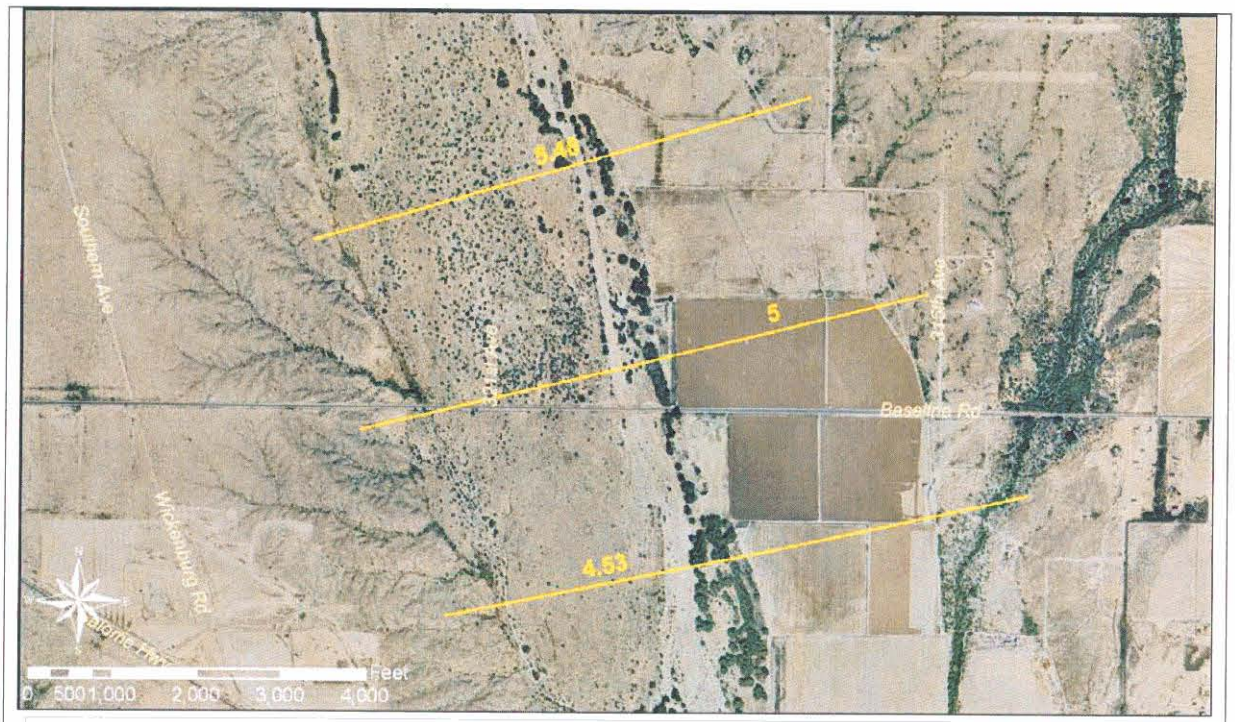

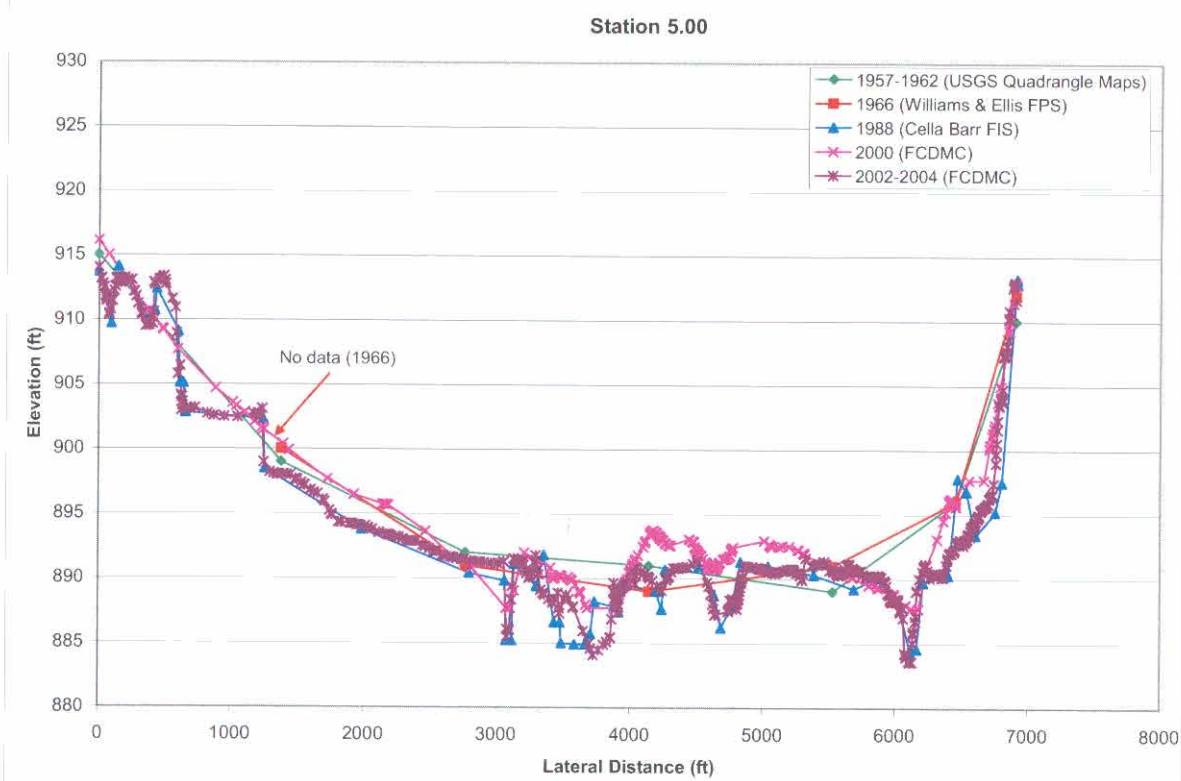

Figure 4-31. Cross-Section 5.00 Profile Comparison

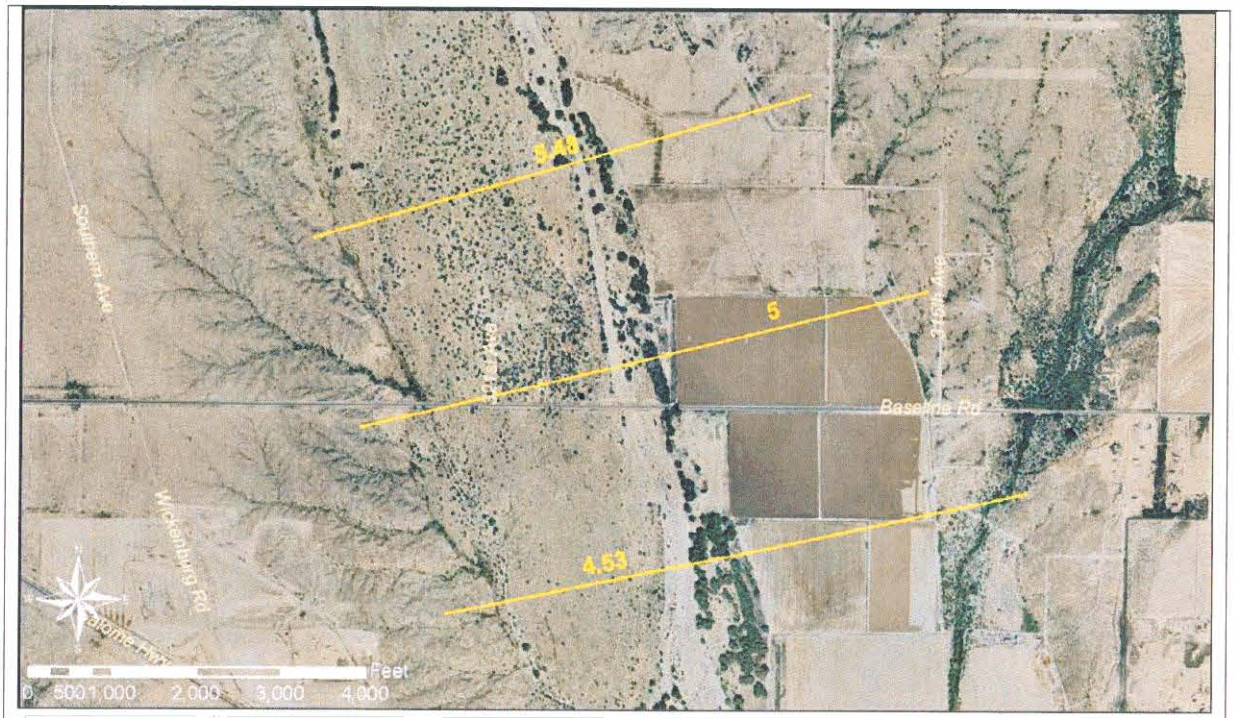

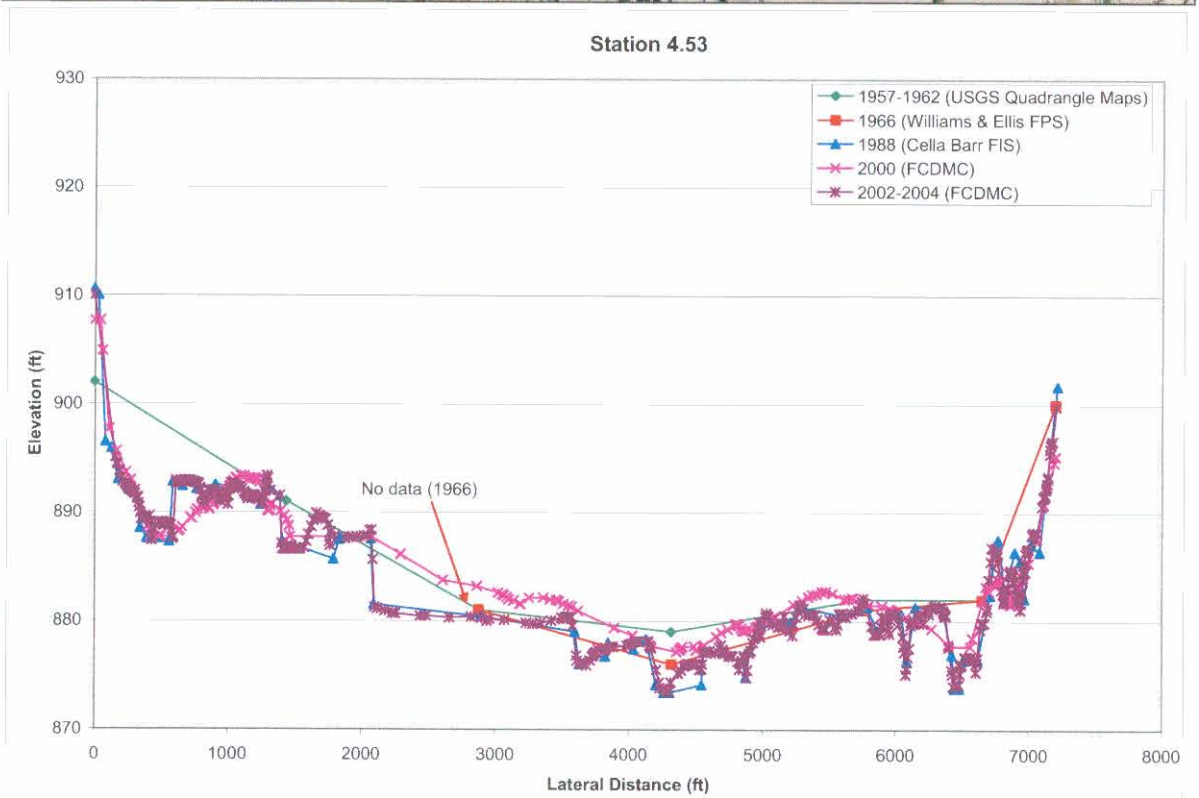

Figure 4-32. Cross-Section 4.53 Profile Comparison

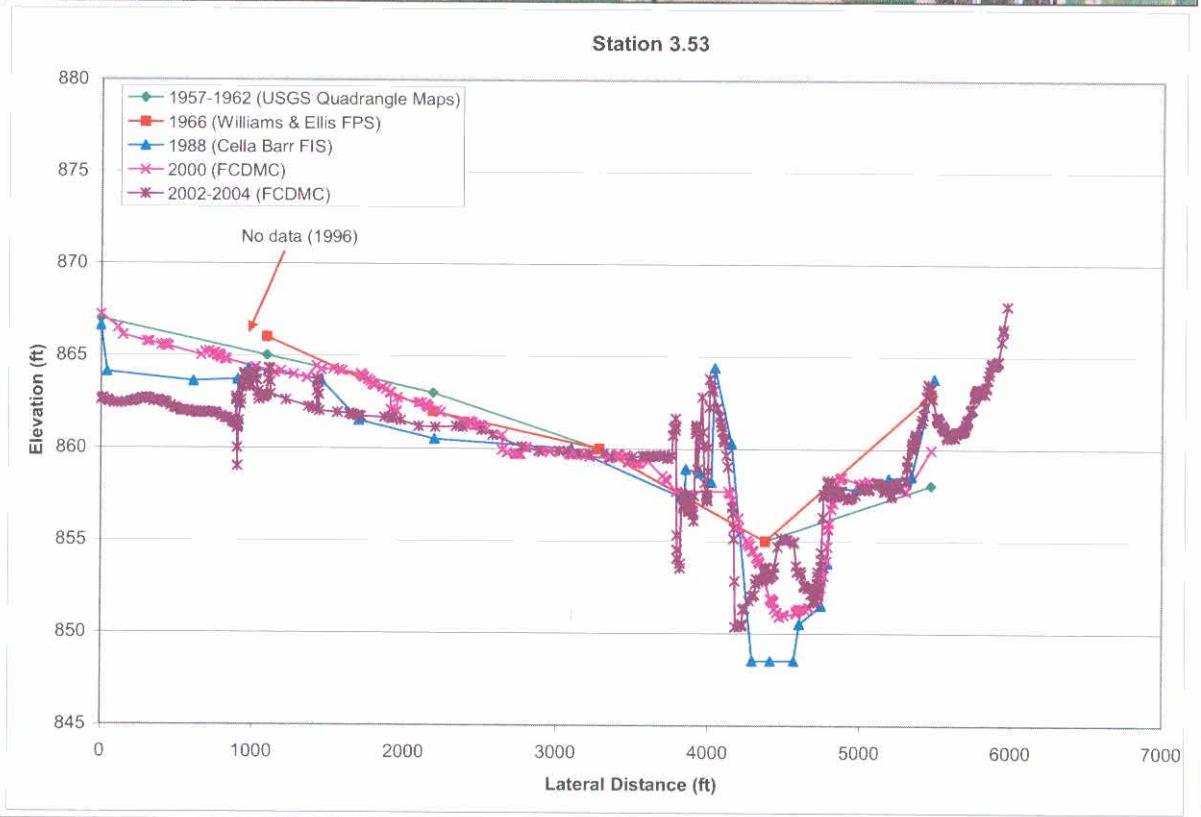

Figure 4-33. Cross-Section 3.53 Profile Comparison

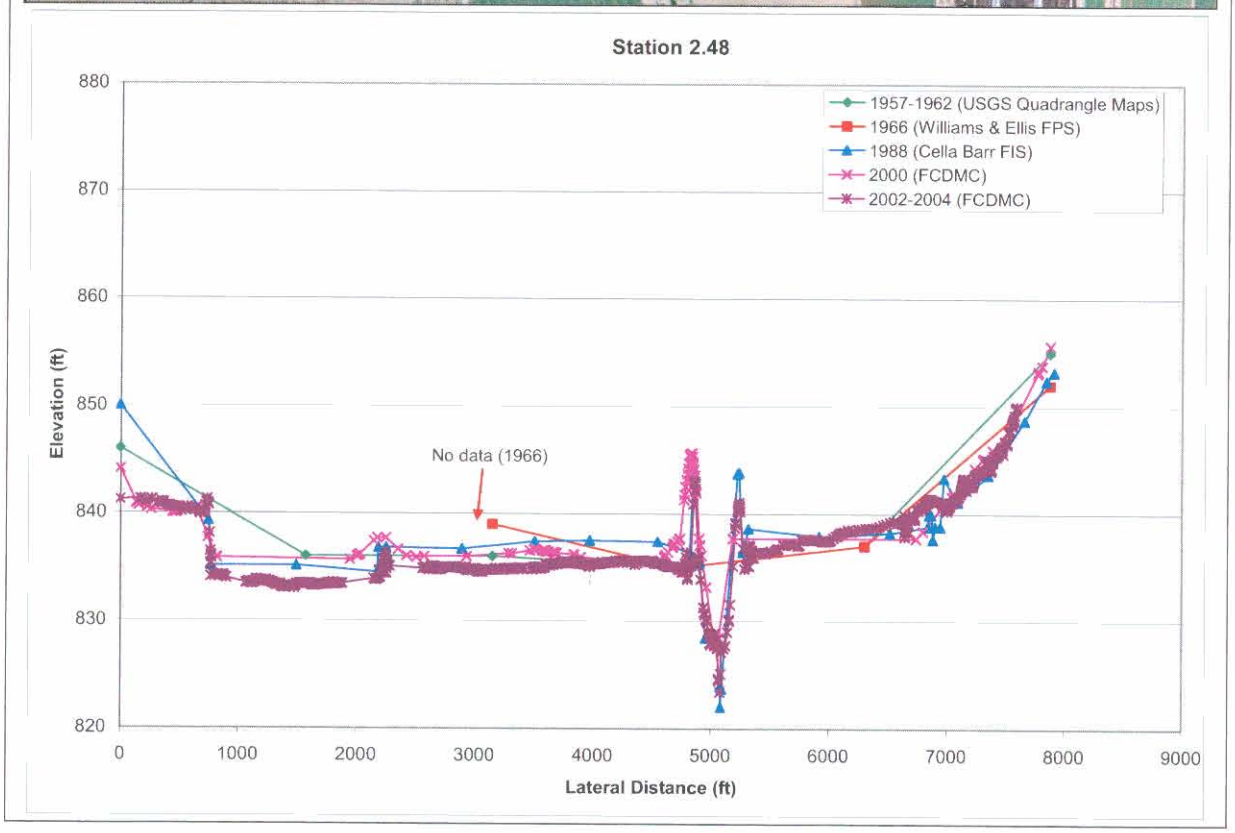

Figure 4-34. Cross-Section 2.48 Profile Comparison

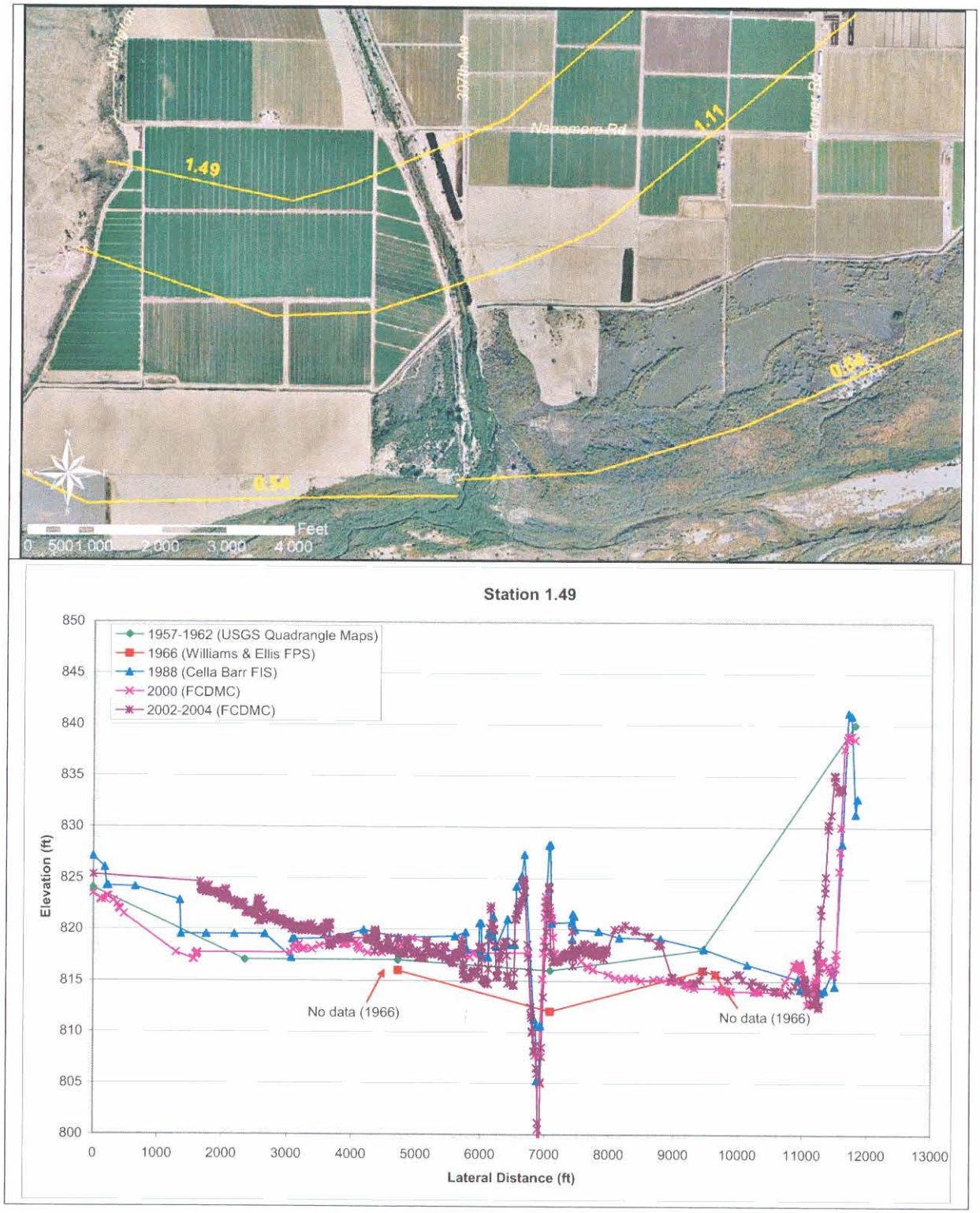

Figure 4-35. Cross-Section 1.49 Profile Comparison

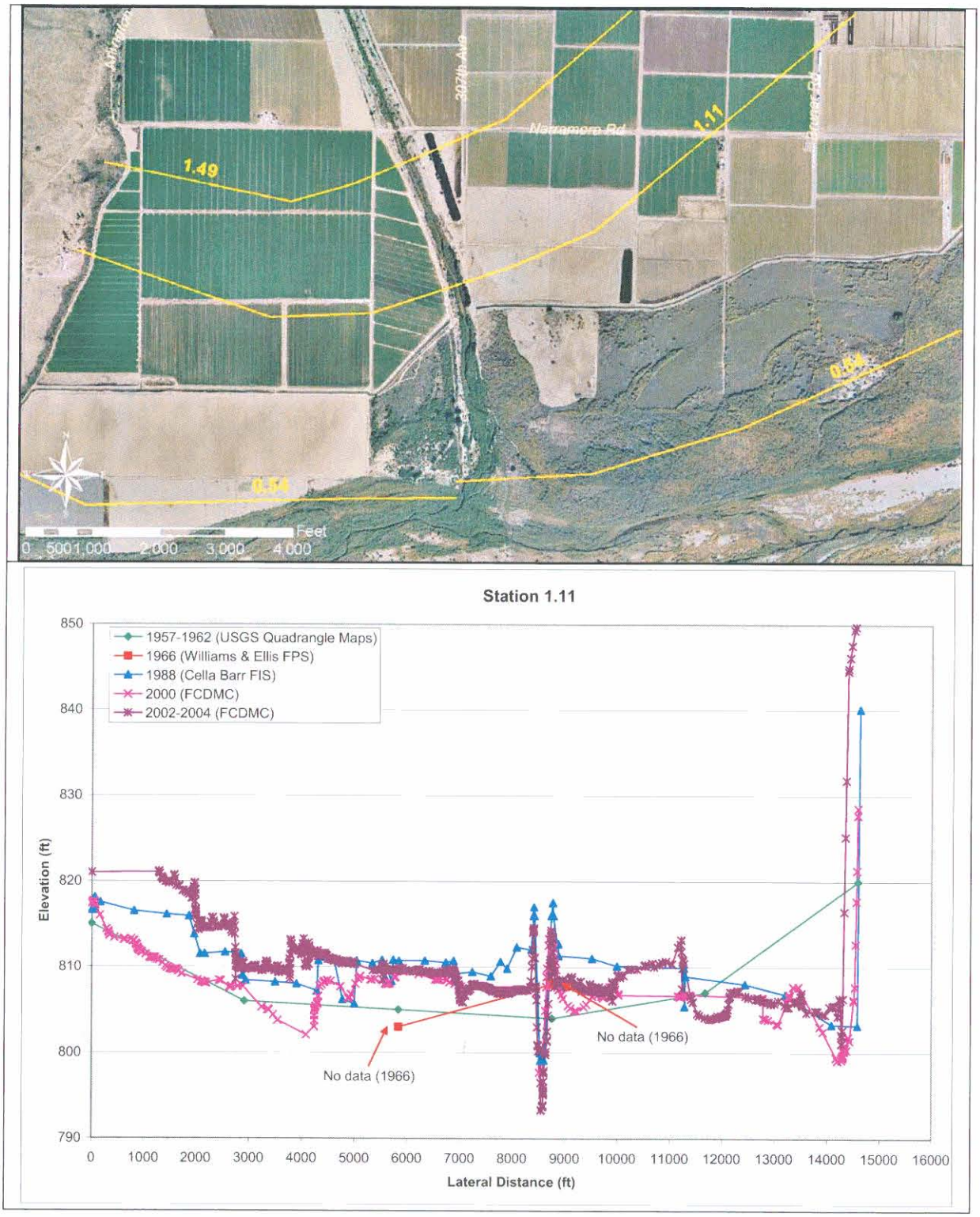

Figure 4-36. Cross-Section 1.11 Profile Comparison

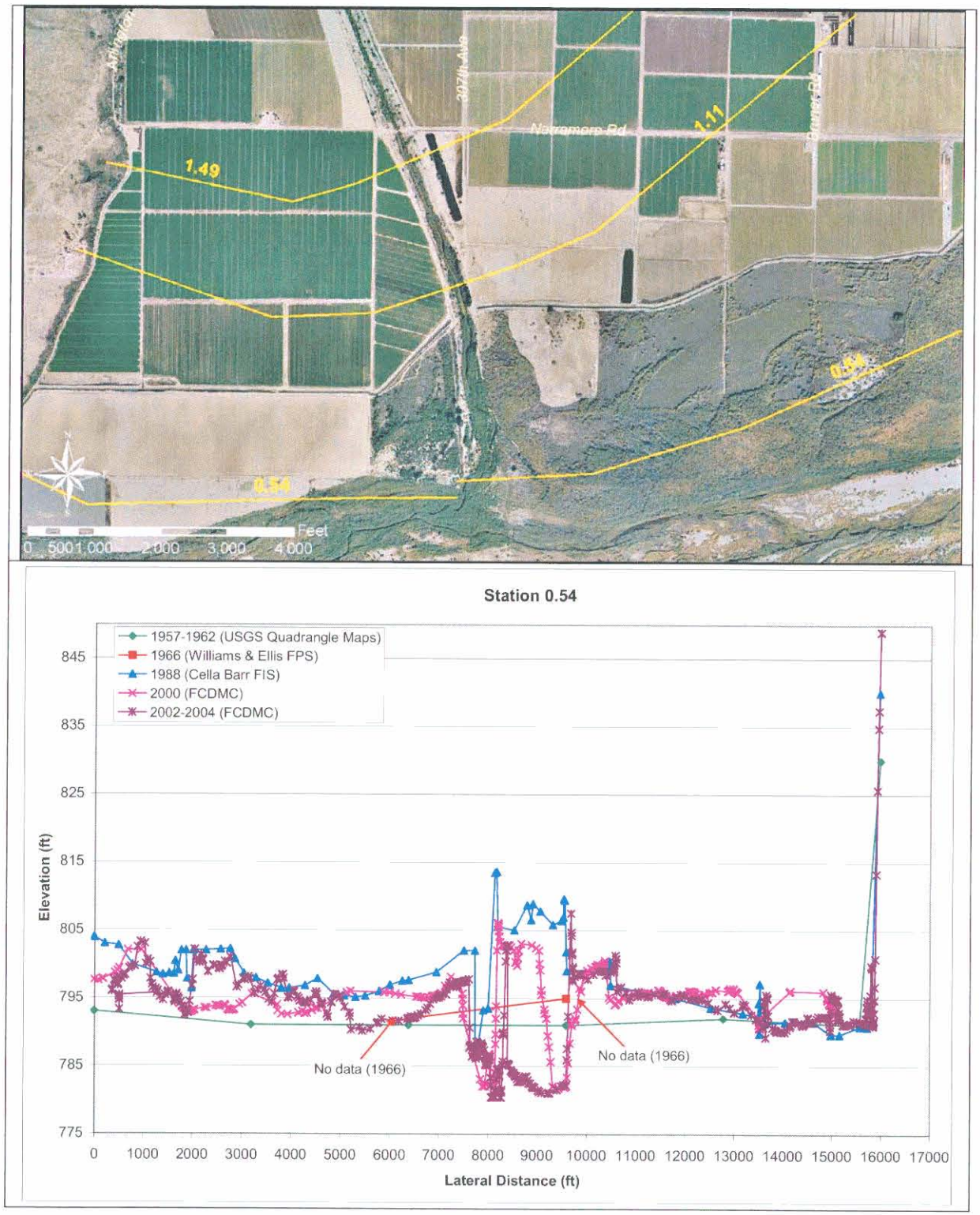

Figure 4-37. Cross-Section 0.54 Profile Comparison

4.6.2.1 Interpretation

The cross-section profile plots were examined to identify changes in floodplain elevation and cross-sectional area for the period of record, and to identify potential long-term trends in channel and floodplain morphology. The cross section plot comparisons can be used to identify trends in aggradation, degradation and lateral channel movement.

The most significant differences in channel and floodplain elevation visible in Figure 4-5to Figure 4-37 are between the 1957/1962 data set, the 1966 data set, and the remaining topographic data. The 1957/1962 data were taken from USGS quadrangle maps with contour intervals of 20 or 40 feet. Therefore, any elevation differences less than 20 feet between the USGS data and the other topographic data sets are well below the map accuracy, and cannot be relied on as actual elevation changes. In all cases, the elevation differences shown in Figure 4-5to Figure 4-37 are less than 20 feet, and are typically less than 10 feet. Similarly, the contour interval of the 1966 data is five feet. Without exception, the cross section plots depict elevation changes from 1966 to 1988 less than 5 feet. Therefore, any apparent trends of aggradation or degradation indicated by the 1957/1962 and 1966 data sets were disregarded in favor of more reliable data such as historical data, field observations, or geomorphic landform interpretations. However, the lower resolution USGS data sets were plotted for informational purposes and illustrate broader trends of elevation changes.

The data from 2000 topographic mapping indicated anomalous trends. The 2000 data consistently plot at a higher elevation than both the 1988 and 2002-2004 data (e.g., Sections 26.67, 20.51, 18.62, 16.53). This trend suggests that between 1988 and 2000 the channel and floodplain aggraded between 2 to 6 feet, then degraded back to its pre-2000 elevations with no net change in channel elevation or position, a rather unlikely scenario. In general, the apparent elevation changes shown by the 2000 data plots are less than the half of the 10-foot contour interval of the 2000 data. Therefore, any elevations less than five feet indicated by comparing pre- and post-2000 data fall within the potential margin of interpretational error and are not reliable indicators of actual channel change.

The lateral resolution of the 1957/1962 and 1966 data sets is also suspect. Many of the cross section plots indicated major changes in the Pleistocene terrace scarp location that would indicate significant lateral erosion of that surface (e.g., Sections 27.61, 21.46, 16.53, 13.32). However, the analysis of semi-rectified historical aerial photographs described in Chapter 3 conclusively proves that such lateral erosion of the Pleistocene terraces that bound the Hassayampa River geologic floodplain has not occurred. Rather, it is likely that the lower-resolution older topography was unable to pick up landscape detail at the terrace-floodplain boundary and is not reflective of geomorphic changes to the floodplain margins.

4.6.2.1.1 Aggradation Trends

The variance between the most reliable topographic data sets, 1988 and 2004, is relatively minor. Localized aggradation within the channel and floodplain is evident when comparing the 1988 to 2004 data, specifically at cross sections 22.59, 14.45,

7.75, and 5.48. However, evaluation of the cross sections adjacent to those showing aggradation indicates no longitudinally persistent pattern of aggradation. This localized condition is probably due to low-flow channel splits and avulsions where the former channel becomes a low bar or terrace. Most of the elevation changes are less than four feet, within the margin of error for the 1988 data, and very near the margin of error for the 2002-2004 data.

4.6.2.1.2 Degradation Trends

The most recent topographic data sets also indicate several locations of channel degradation (e.g., Sections 20.51, 18.62, 12.37, 11.43, and 9.08). Lower bed elevation values at these sections range from two feet to eight feet, with the largest occurring at Section 12.37. As with aggrading Sections, the degradation appears to be localized and is not continuous over any significant reach length. Section 12.37 is located downstream of the in-stream sand and gravel mine near the Tonopah-Salome Highway crossing. The eight foot change in bed elevation reflects excavation of the pit between 1988 and 2004, and tailcut erosion. A split channel that formed between 2000 and 2004 is also shown to the right of the main channel in the cross-section profile plot. This channel formation represents a localized condition due to in-stream mining and is not indicative of active channel degradation on a larger scale.

4.6.2.1.3 Lateral Channel Movement

The topographic cross section comparisons indicate surprisingly little lateral migration during the period of record, in direct contrast to the significant changes in lateral channel position documented in Chapter 3. The apparent lack of lateral movement is due in part to the low resolution of the older topographic data sets, and in part due to the relatively minor floods that occurred between 1988 and 2004, but mostly to the horizontal scale of cross section plots (> 1"=1,000'). Lateral channel movement is seen at several of the cross section plots. New channels were cut and widened at Sections 14.45, 13.32, 9.08, and 6.52. Net lateral movement is also shown at Section 10.50.

4.6.3 Longitudinal Profile Analysis

A longitudinal profile is a plot of the channel elevation versus distance along the stream bed. Analysis of the longitudinal profile can be used to identify slope irregularities, over-steepened or flat reaches, headcuts, and areas of natural grade control. Interpretation of the longitudinal profile also provides information on the expected lateral stability of the stream. Reaches with lower slopes than upstream reaches will tend to experience net deposition (aggradation) and bank erosion associated with braiding and avulsions. Reaches with steeper slopes than upstream reaches will tend to experience net degradation and bank erosion associated with undercutting and scour. Comparison of historical profiles with modern profiles can be used to indicate where degradation and aggradation have occurred in the recent past, and where future adjustments of channel geometry are most likely to occur. A longitudinal profile analysis was performed on the Lower Hassayampa River within the study area.

4.6.3.1 Data Sources

Topographic data used in the longitudinal profile analysis consisted of the same data

sources described in Section 4.6.2 (Table 4-7). The minimum elevation at each cross-section was extracted to represent the lowest bed elevation, or channel thalweg, for each time period represented by topographic data. The river distance, or thalweg length, was computed using the reach length values from the 1988 Cella Barr FIS hydraulic model. Figure 4-39 shows the longitudinal profile plot for the entire study area and Figure 4-40 through Figure 4-44 show the results of the longitudinal profile analysis by reach.

4.6.3.2 Geomorphic Setting

The longitudinal profile in Figure 4-38 extends from the Gila River confluence to Wickenburg, approximately 30 miles upstream of the LHWCMP study reach, and shows the regional geomorphic context of the profiles depicted in the following Sections. Within in the LHWCMP study reach (downstream of RM 30), the profile is extremely uniform, which is an indication of long-term equilibrium. A slight convex bulge in the profile upstream of the study reach between RM 32 and RM 45 indicates net sediment deposition where the profile slope flattens. Deposition upstream of the study reach is probably due to high transport rates through the Vulture Mountain canyon reach dropping out of transport as river enters the wider, alluvial section. This depositional area represents a significant sediment supply reservoir for the study reach.

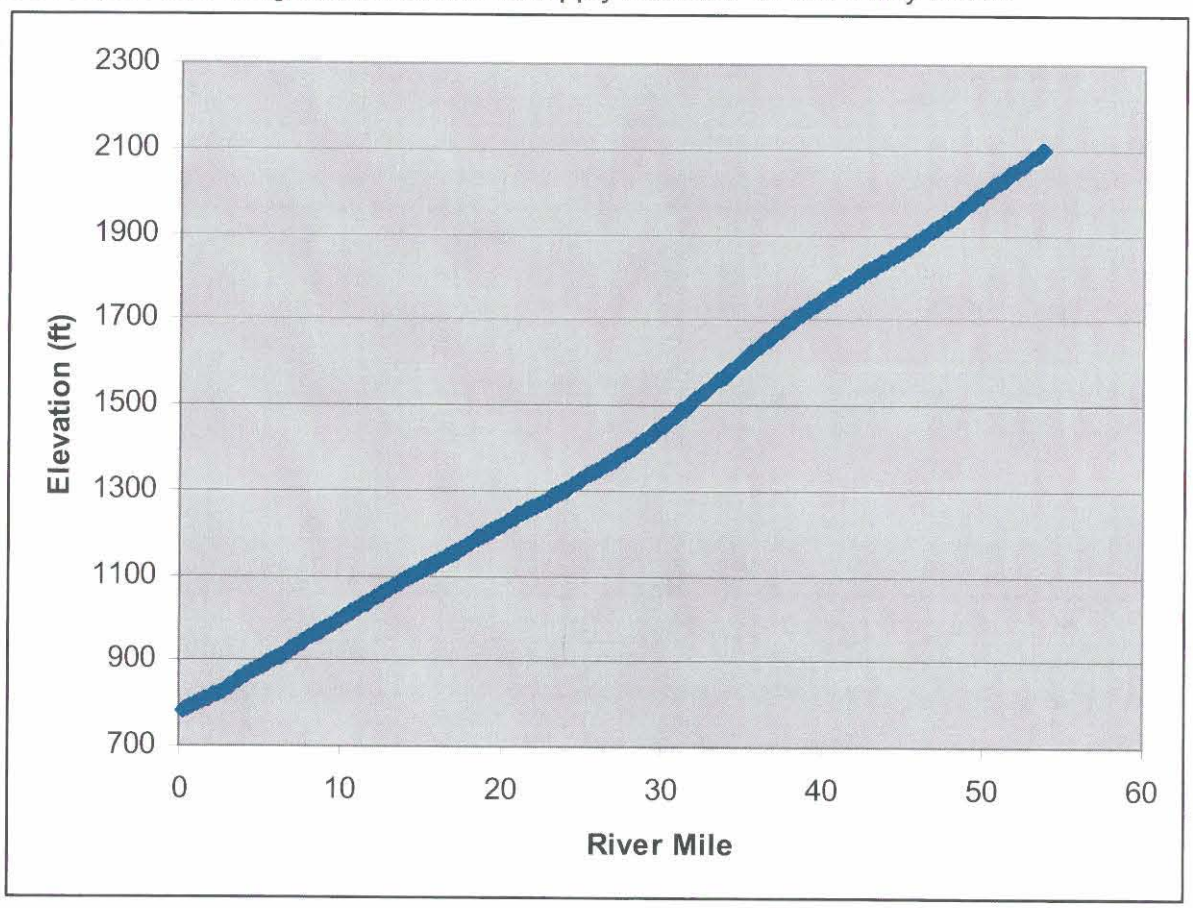

Figure 4-38. Longitudinal Profile of Hassayampa River - Gila River Confluence to Wickenburg

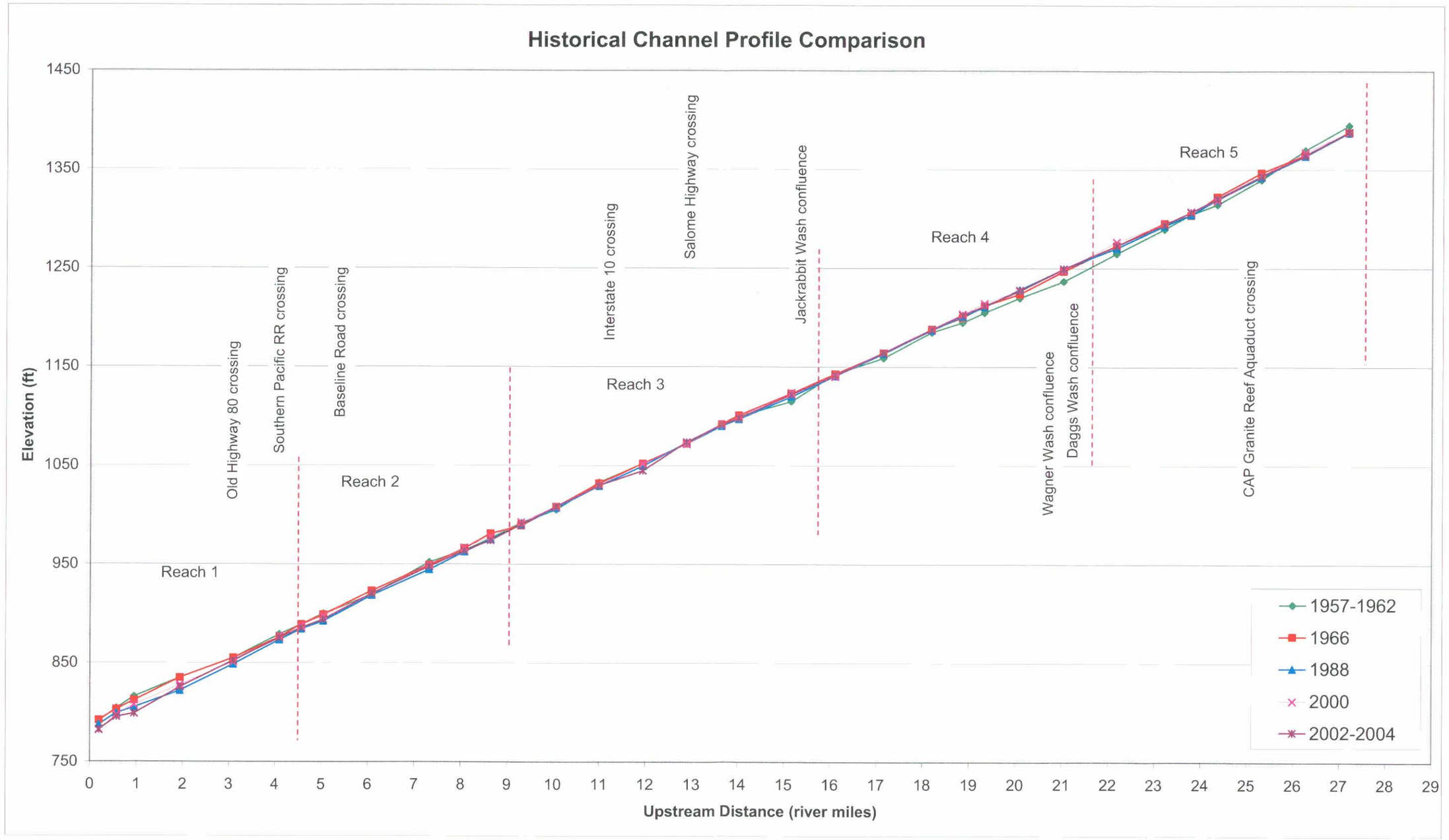

Figure 4-39. Historical Longitudinal Profile Plot

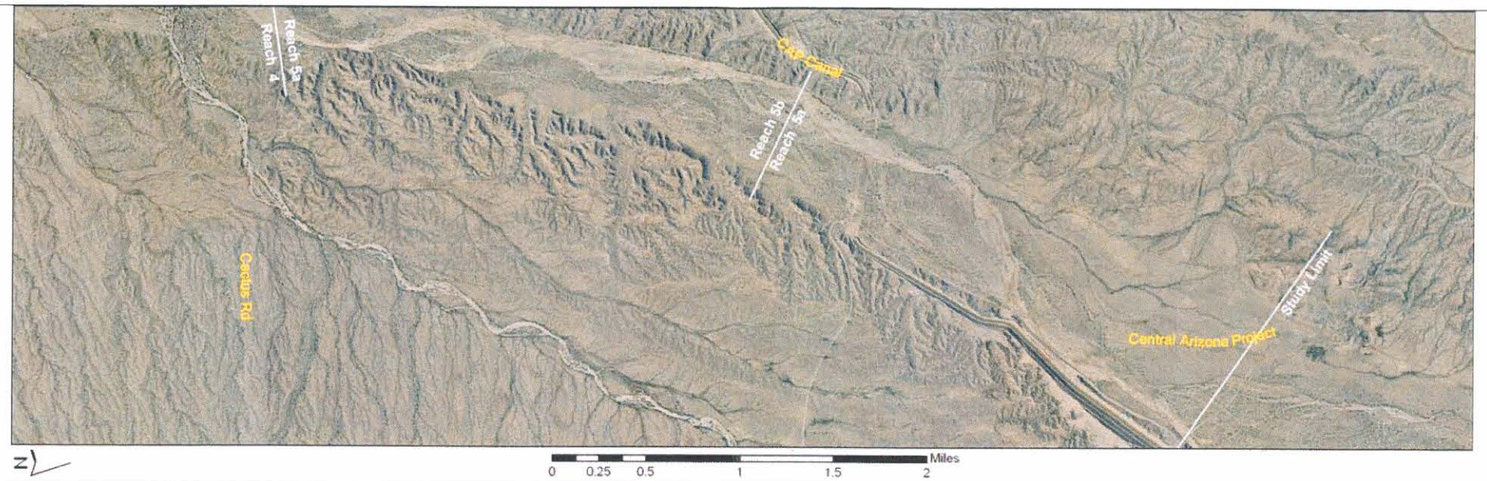

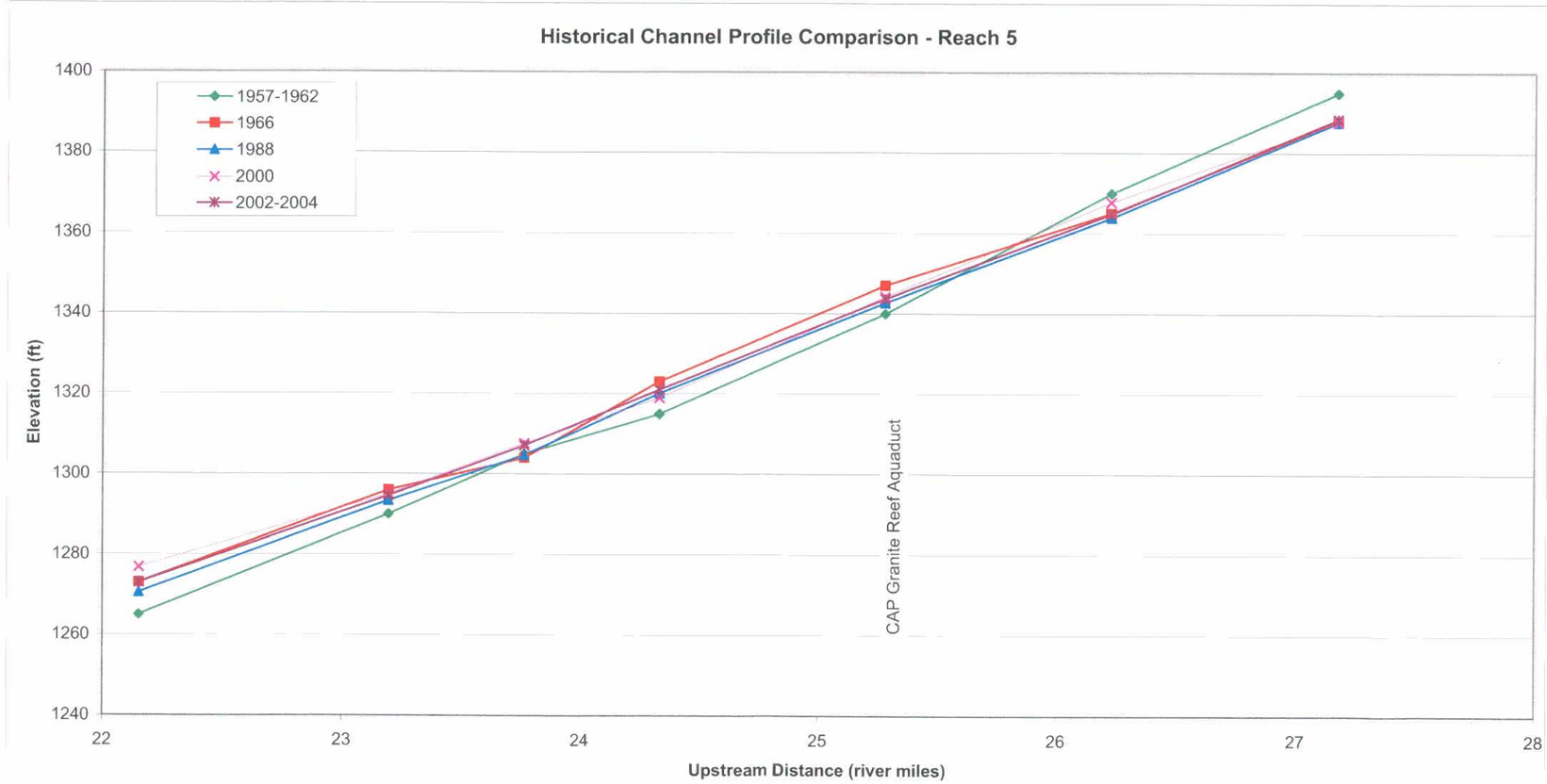

Figure 4-40. Reach 5 Longitudinal Profile

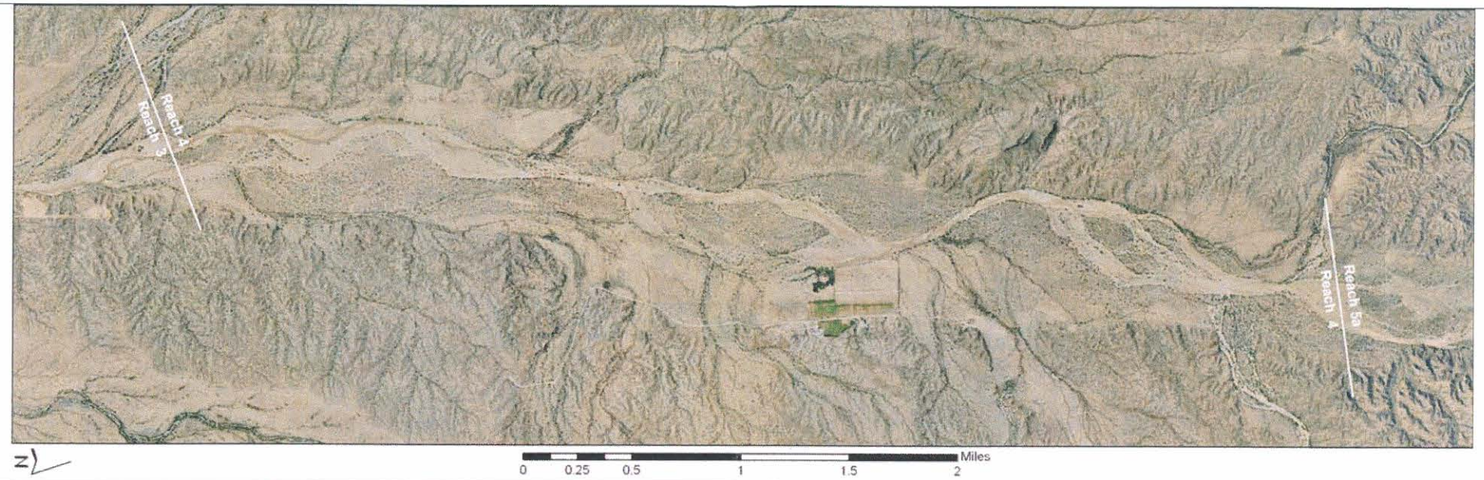

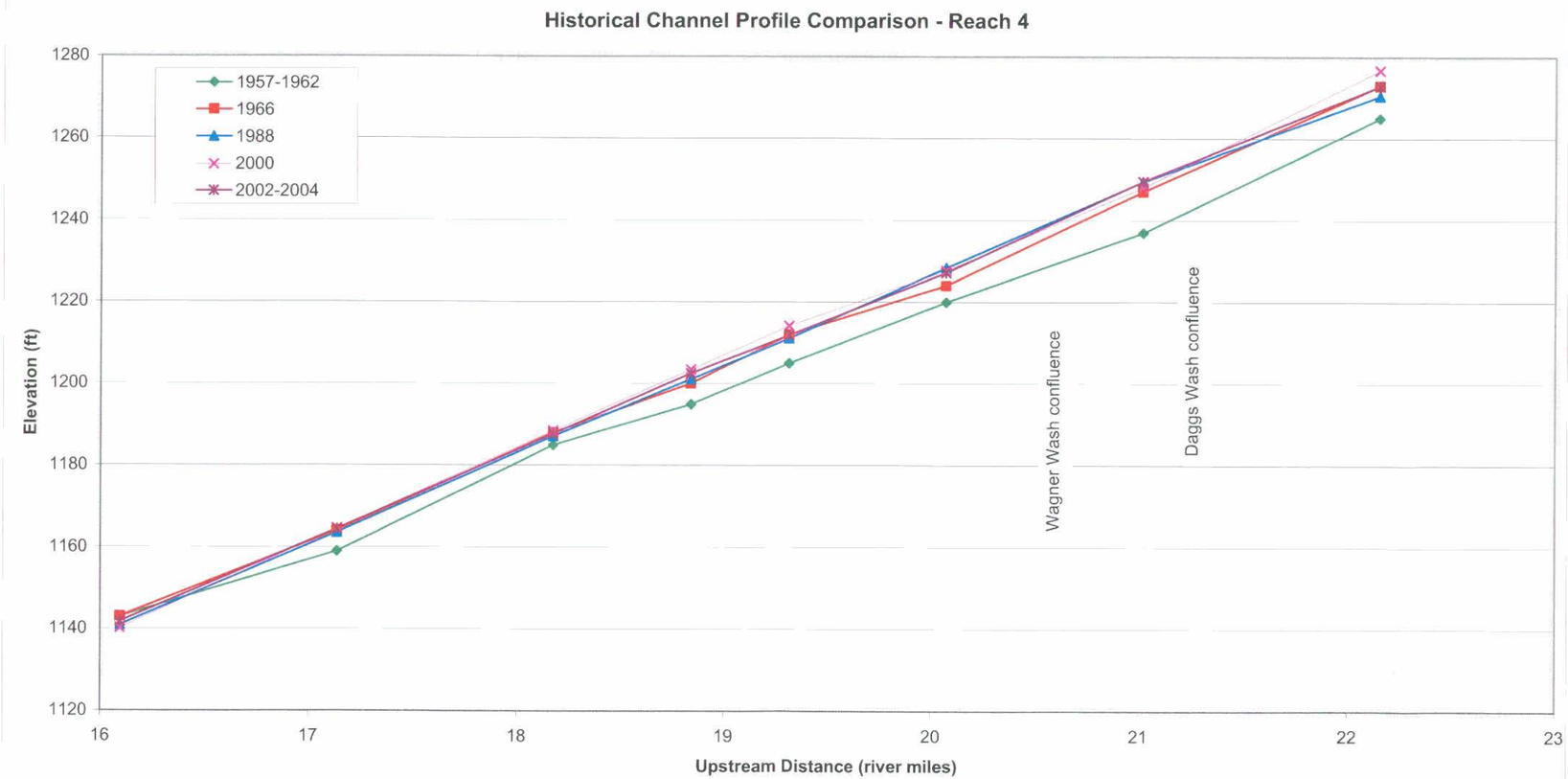

Figure 4-41. Reach 4 Longitudinal Profile

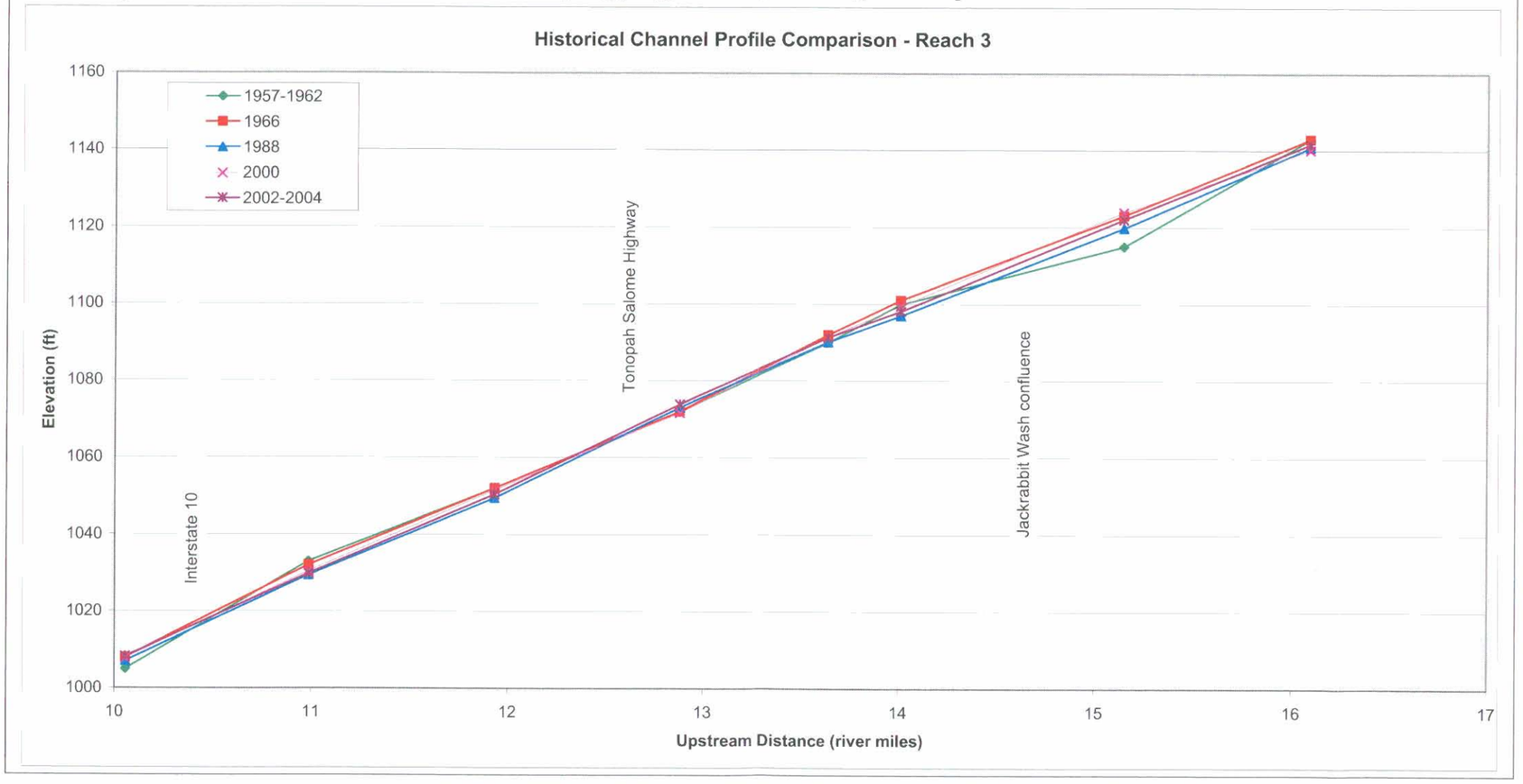

Figure 4-42. Reach 3 Longitudinal Profile

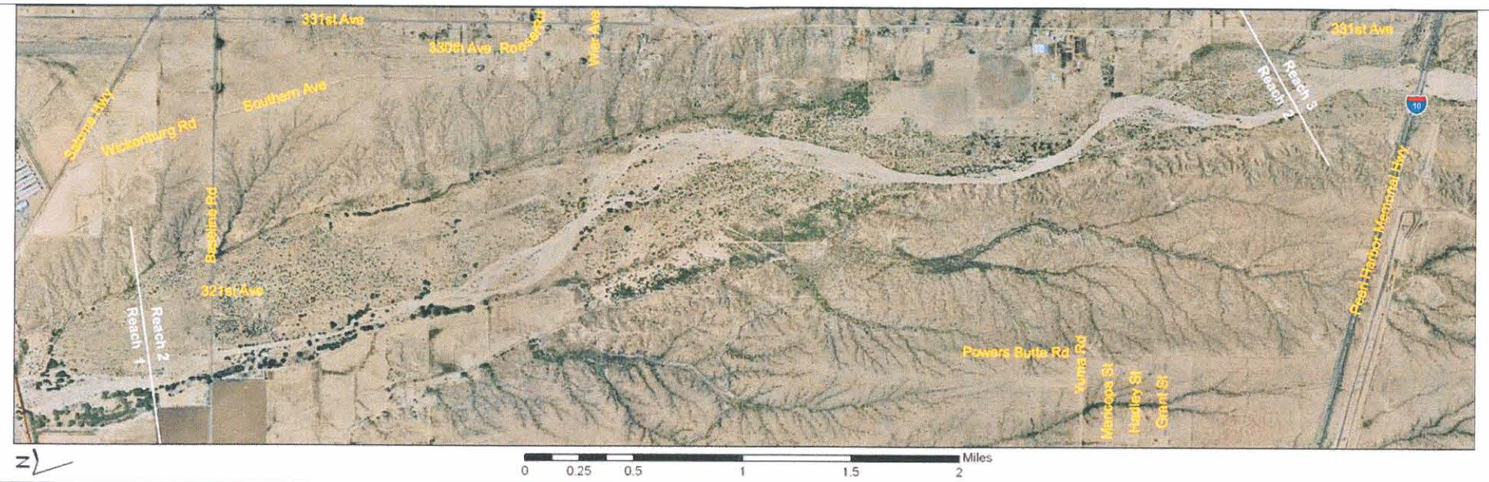

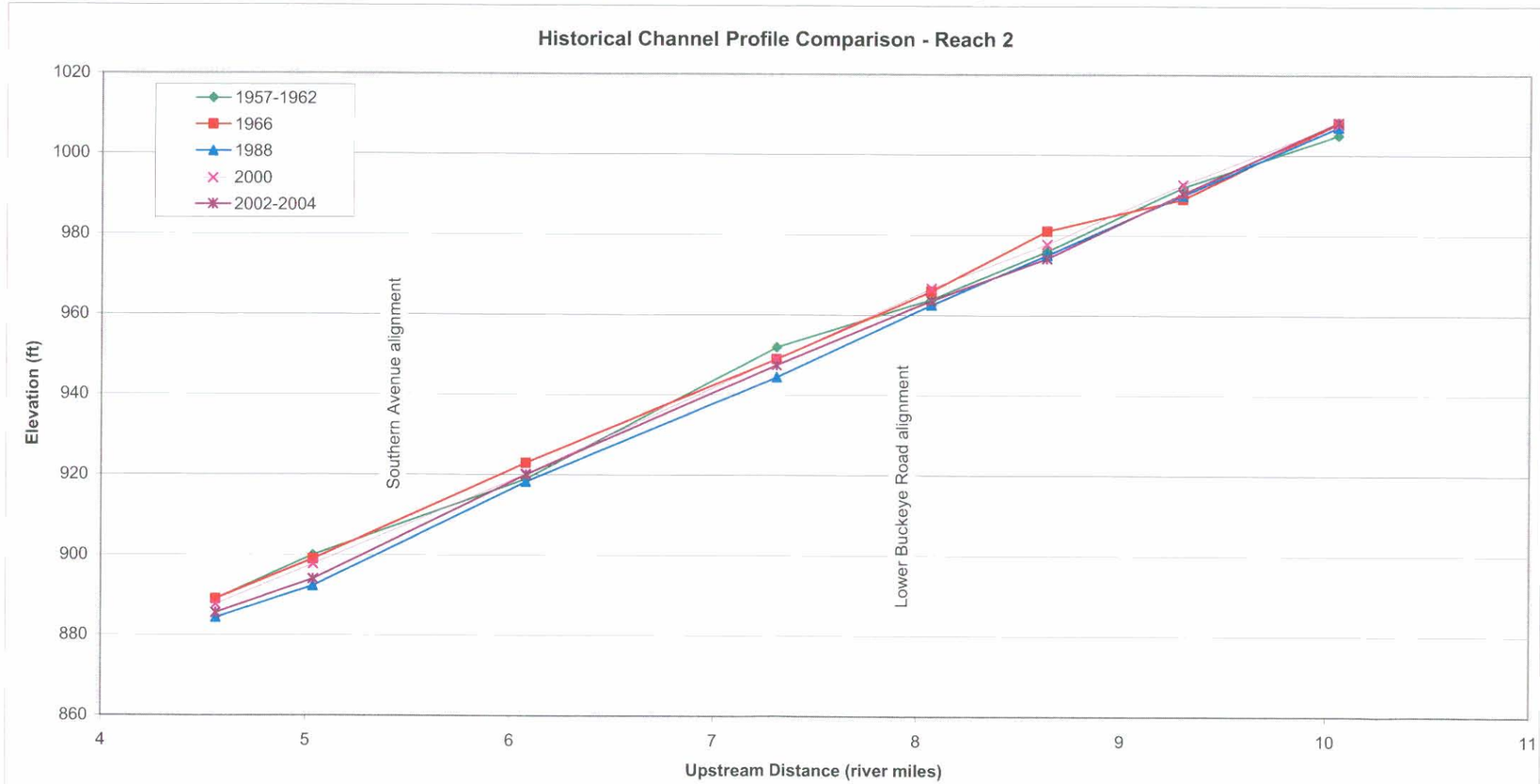

Figure 4-43. Reach 2 Longitudinal Profile

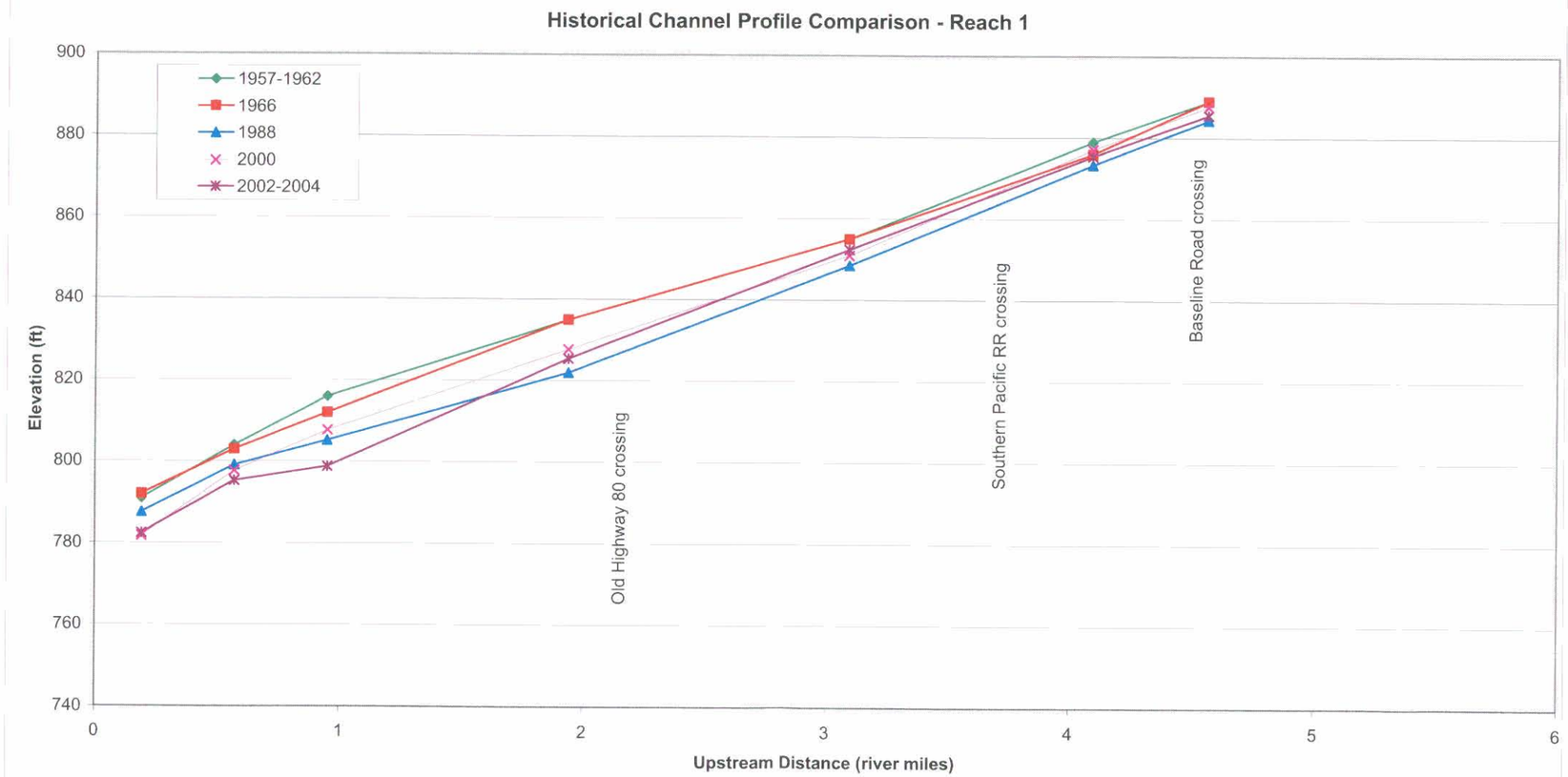

Figure 4-44. Reach 1 Longitudinal Profile

4.6.3.3 Interpretation

The longitudinal profile plots shown in Figure 4-40 through Figure 4-44 suggest the Lower Hassayampa River has experienced some moderate bed elevation change of the active channel. Profile changes also impact channel slope. Slope changes over time suggest disequilibrium. If the slope becomes flatter, a typical response might include degradation of the active channel and vertical, unstable cutbanks. Other evidence of degradation might include headcutting in tributaries in response to a change in their local base level. If the slope becomes steeper, a typical response might include channel aggradation, which might in turn cause higher flood water surface elevations. A slope analysis was performed for the Lower Hassayampa River; and is summarized in Table 4-8.

Table 4-8. Historical Channel Slopes

1957-1962	1966	1988	2000	2002-2004
0.00421 ft/ft	0.00415 ft/ft	0.00418 ft/ft	0.00422 ft/ft	0.00422 ft/ft

The minimum and maximum values shown in Table 4-8 vary by only 2%, suggesting the Lower Hassayampa River had maintained a consistent overall slope during the 47-year period of record. The slope values vary more dramatically by reaches, as shown in Table 4-9.

Table 4-9. Historical Channel Slopes By Reach

Topographic Data Set	Reach 5 (ft/ft)	Reach 4 (ft/ft)	Reach 3 (ft/ft)	Reach 2 (ft/ft)	Reach 1 (ft/ft)
1957-62	0.00491	0.00362	0.00409	0.00412	0.00427
1966	0.00434	0.00400	0.00432	0.00400	0.00408
1988	0.00442	0.00417	0.00419	0.00422	0.00417
2000	0.00419	0.00415	0.00432	0.00420	0.00463
2002-2004	0.00436	0.00415	0.00423	0.00419	0.00452
% Difference between min and max	15	13	5	5	12

Although the percent differences between the minimum and maximum values for each reach are higher than that calculated for the entire study area, no specific longitudinal patterns or trends were identified, as shown in Figure 4-45. Trends such as increasing or decreasing in slope in the downstream direction can provide insight into long-term river bed elevation behavior. The slope values for each reach fluctuate between topographic data sets with apparent randomness. Thus, no prediction of future bed elevation behavior can be made from these data sets. Furthermore, the slope data indicate slight fluctuations in bed elevation that locally affect channel slope probably occur locally within the study reach.

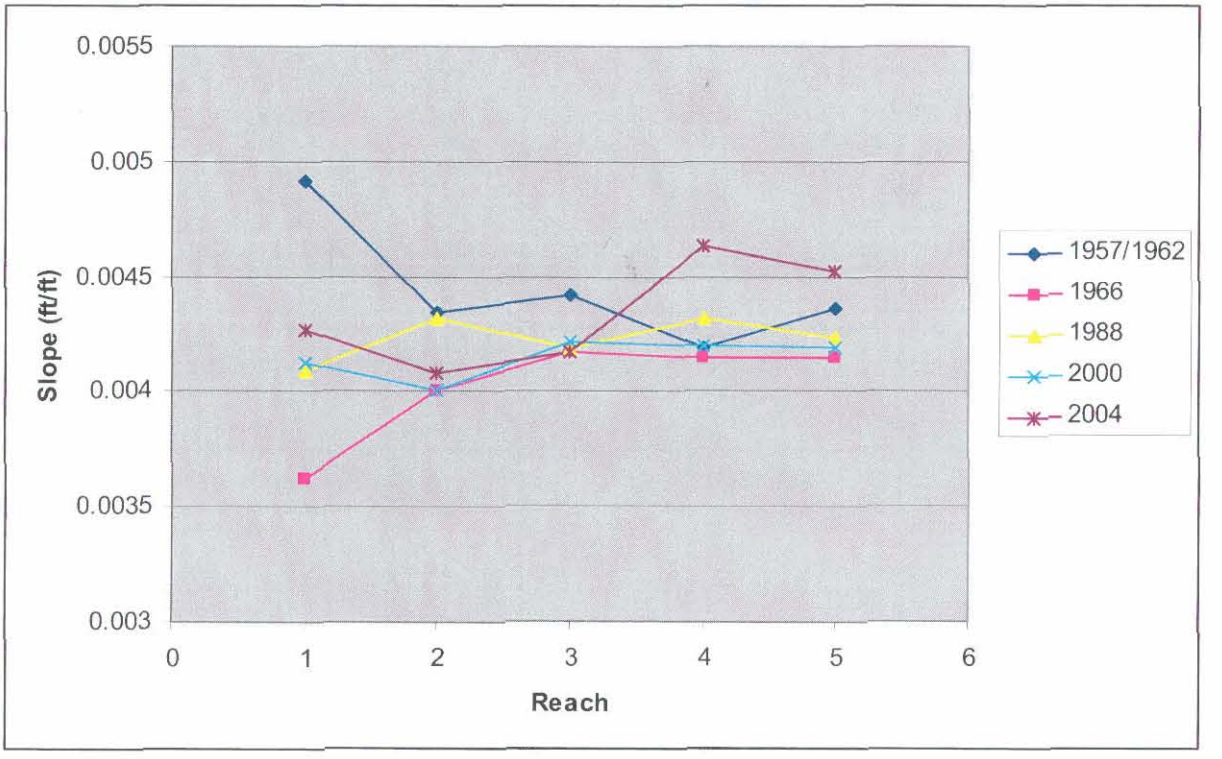

Figure 4-45. Slope Change by Reach, 1957-2004

4.6.3.3.1 *Reach 5*

No consistent pattern of either channel aggradation or degradation over the period of record is evident from the longitudinal plot. The 1957-1962 and 1966 data consistently plot as either the highest or lowest values, perhaps reflecting their relatively low data precision. There is no field evidence to support such dramatic changes in bed elevation within Reach 5. The other data plots indicate bed elevation changes between four feet and less than one foot between 1988 and 2004, with no consistent pattern of bed change, but rather alternating degradation and aggradation.

4.6.3.3.2 *Reach 4*

The post-1966 data indicate very minimal changes in bed elevation between dates of coverage. With the exception of the upstream-most section, the bed elevations vary by less than four feet, with smaller differences in the downstream direction, reaching less than one foot of difference just upstream of the Jackrabbit Wash delta. The lack of channel elevation change in the width-restricted reach at the Jackrabbit Wash delta is interesting, given that the relatively narrow channel width would normally result in higher flow velocities, scour, and a flatter slope. However, sediment supplied from Jackrabbit Wash probably controls the local Hassayampa River base level.

4.6.3.3.3 *Reach 3*

Longitudinal profile plots in Reach 3 indicate consistent trends like those described for

the reaches upstream. Recently, Reach 3 has been mined for aggregate with no discernable impact on the profile to date. Post-2004 flood observations indicate that some progressive bed elevation change in now underway.

4.6.3.3.4 Reach 2

Differences in historical bed elevations in Reach 2 are greater than the elevation differences in Reach 3. The data plots suggest net aggradation from 1988 to 2004. Some of the highest cutbanks within the study area were observed within the upper portion of Reach 2. Normally, high cut banks indicate degradation, but given the profile data, they are more likely to be the result of lateral erosion through high floodplain surfaces. Downstream of Baseline Road, the cutbank heights decreased significantly and the bank slopes were stable, which suggests that the river has had no net trend toward degradation in Reach 2.

4.6.3.3.5 Reach 1

The longitudinal profile plots for Reach 1 diverge just upstream of the Old US 80 crossing. Upstream of Old US 80, the river experienced net aggradation from 1988 to 2004. Downstream of Old US 80, the river degraded. Not coincidently, Reach 1 is the most modified portion of the river within the study area. The longitudinal profile plot suggests the channel bed within the channelized portion degraded approximately 11 feet between 1957 and 1988, and degraded an additional 6 feet between 1988 and 2004. Several large floods which could likely have scoured out the leveed channel occurred between the time periods of the topographic data. Anecdotal accounts from long term residents record that historically, prior to failure of Gillespie Dam, local farmers periodically "cleaned out" the main channel to remove vegetation and sediment deposition. Since Gillespie Dam failed in 1993, long-term residents report that the river has degraded with each flow. High, vertical cutbanks observed downstream of the Arlington Canal crossing are evidence of channel degradation near the Gila River confluence.

4.6.4 Conclusions

Comparisons of cross-section profiles within the study reach indicate that the channel and floodplain have experienced only minor changes in elevation over the period of the topographic record. The earliest sets of topographic data used in the analysis were not reliable due to their low resolution and large contour interval. The more recent topographic data sets produced more consistent, reliable results, although resolution variability complicated their interpretation. For the majority of the cross-section profile plots, the changes in channel and floodplain elevations were within the margin of error of the topographic data sets. No significant regional patterns or trends in channel and floodplain form were identified through the profile analysis. Significant changes were generally localized and were not consistent between adjacent profile plots.

The field analyses described in Chapter 2 indicate that the river is in a relatively stable equilibrium slope condition. None of the classic evidence associated with slope adjustments described previously in this chapter were found on a regional scale. Areas of local scour and fill were found, but the extents were generally short, suggesting that

the processes were not regional. The results of the HEC-6 analysis (Chapter 5) indicate the Lower Hassayampa River is likely to experience slight net, long-term aggradation on the order of less than one foot over the next 67 years. The results from Table 4-8 indicating the historical channel slope has not varied significantly over the period of the topographic record is consistent with what was observed in the field analysis.

4.7 Summary

The bed elevation analysis describe in this chapter included predictive analysis of scour, equilibrium slope, and armoring in addition to cross-section and longitudinal profile analyses. The results of these analyses included the following:

- In general, the largest component of scour other than long-term scour is either the antidune or bend scour. Given the potential for future channel movement within the stream corridor, consideration of bend scour at any point within the reach is prudent for design of any structure with an extended design life.

- Local scour was estimated as zero for the study, since reach-averaged values for a local condition could not be justified. Bridge scour was computed for the four bridges in the study reach using the HEC-RAS Hydraulic Design module. The I-10 and UPRR Bridges are likely to be scour critical, but the Old US 80 has recently been modified to include scour mitigation measures.

- The total scour along the study reach is about five to six feet for the 2-year event, eight to ten feet for the 10-year event, and greater than 10 feet for the 100-year event.

- Given an average height of the Holocene floodplain of about six feet, the maximum net rate of long-term degradation in the study reach is about 6×10^{-4} ft/yr (< 1 inch/century).

- In general, the equilibrium slope equations predict long-term aggradation, although the geologic, field and historical evidence do not support this conclusion.

- The actual magnitude of the expected bed elevation changes will be based in part on sediment supply, and the magnitude and frequency of the flows experienced in the future.

- The channel bed scour depth and long-term scour will not be limited by armoring during floods or over the long term. Sediments observed in the gravel pits were not significantly more coarse-grained than the material exposed on the surface. That is, effective armor layers were not observed in the field at gravel pits.

- The channel bed material is mobile, and will be transported during even small flows.

- The Lower Hassayampa River historically has adjusted its geometry predominantly by horizontal adjustments of its braided channel. Vertical scour has been limited to a few feet based on field observations of exposures of channel alluvium in gravel pits and soil pits.

- The engineering analyses predict that scour is likely during floods, as well as potential long-term scour, particularly if the sediment supply is reduced from the existing condition.

- Comparisons of cross-section profiles throughout the study area indicated the channel and floodplain have experienced minor changes in elevation over the period of the topographic record.

- No significant regional patterns or trends in channel and floodplain form were identified through the cross-section profile analysis.

- Areas of local scouring and filling of the channel were found in the cross-section profile analysis, but the upstream and downstream extents were generally short, suggesting those processes were not regional.

- Historical channel slope has been relatively consistent throughout the topographic record, suggesting a near equilibrium slope condition.

- No identifiable regional trends or patterns of slope change were found in the longitudinal profile analysis.

- The majority of the elevations changes identified in the longitudinal profile analysis were within the potential margin of error of the topographic data.

CHAPTER 5 - SEDIMENT TRANSPORT ANALYSIS

The objective of the sediment transport analysis was to simulate the long-term streambed profile response to the Lower Hassayampa River based on natural and existing conditions within the river corridor. This objective was accomplished via the following tasks:

- HEC-6 Modeling
- Sediment Continuity Routing
- Mining Impact Analysis

The results of the sediment transport analysis are presented in this chapter.

5.1 Sediment Data

The sediment samples were collected from the bed of the Hassayampa River over the entire length of the study reach. Sampling sites were located in the active channel and were taken approximately one mile apart. Sediment samples were obtained from soil pits excavated in the channel, with the sediment sample material integrated over the four to six feet depth of the pit. Samples were also collected from the active channel at the confluences with Jackrabbit Wash and Wagner/Daggs Wash to capture the effect of sediments flowing from these tributaries. The approximate locations of the sediment sampling sites were shown in Figure 3-7.

Sieve analyses of the sediment samples were performed by Speedie & Associates to obtain the sediment gradation curves shown in Figure 5-1. Inspection of the data revealed no consistent trend in sediment size by reach or with distance along the study reach. Figure 5-1 shows that the variation from the mean is not significant except at the confluences of Jackrabbit Wash and Wagner/Daggs Wash. Therefore, the sediment gradation curves for all five reaches were averaged together to obtain a composite reach-averaged curve for the Hassayampa River main stem, and the confluence samples were used as representative of the tributary inflow.

Sediment sample gradation data and plots showing the sediment distribution curves for each reach are provided in Appendix 5.4.

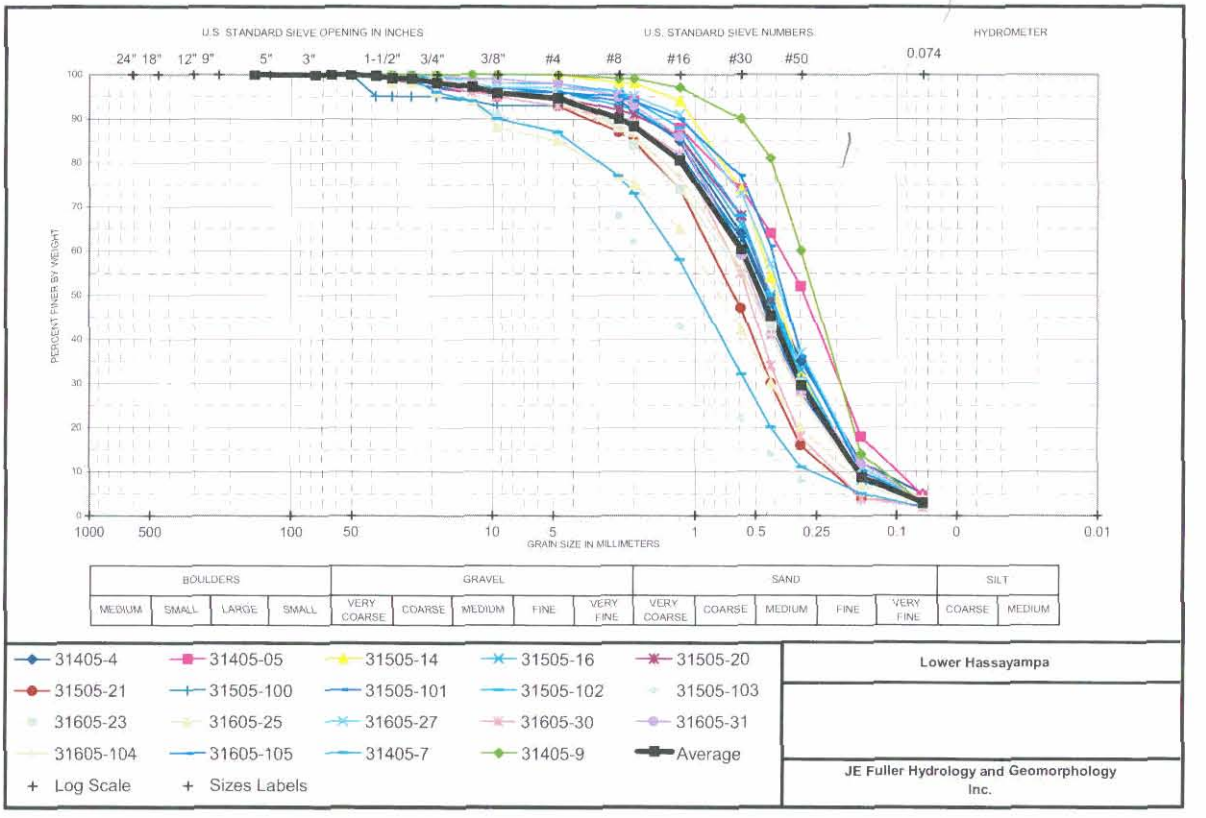

Figure 5-1. Sediment gradation curve

5.2 Sediment Transport Function

The selection of the sediment transport functions used in the sediment transport analyses described in this chapter was based on a comparison of parameters describing the study reach conditions with the published range of the data used to develop individual sediment transport functions. The US Army Corps of Engineers (USACE) SAM software provides the parameter ranges for a range of available sediment transport functions. The parameter and data for the study reach were obtained from HEC-RAS modeling (Chapter 3), sediment sieve data described above, topographic information (Chapter 2), field observations (Chapter 2), and recent aerial photographs (Chapter 3). Table 5-1 summarizes data for the Hassayampa River study reach compared to the data ranges used to evaluate sediment transport functions.

Three equations, Ackers-White, Colby and Yang, were initially considered because they compared reasonably well with the HEC-RAS results and the measured sediment data. However, based on the data summarized in Table 5-1, engineering judgment, and past HEC-6 modeling experience, the Ackers-White, Toffaleti, Yang, and the Toffaleti-Meyer-Peter-Muller combination (TMPM) equations were advanced for final evaluation for use in HEC-6 modeling. The former three equations were developed for sand-bed rivers. The Ackers-White equation was developed for sand-bed rivers with subcritical flow while the Toffaleti equation was developed for large sand-bed rivers. In addition to these equations, the Colby equation and Laursen-Copeland equations were also considered. However, preliminary runs using the Colby equation resulted in numerical problems and a fatal error in the HEC-6 model. The Laursen-Copeland equation was

found to over-predict the transport of fine material and in the absences of armoring can lead to erroneous results and was therefore abandoned. SAM-AID software also predicted good matches for the Engelund-Hansen and Van Rijn equations, but these equations are not supported by HEC-6, and were therefore dropped from further consideration.

Table 5-1. Transport function equation data

Parameter	Median Value: Study Reach	Ackers White	Yang Transport Function	Toffaleti Transport Function	MPM Transport Function
Particle Size (mm)	0.5	0.04-7	0.15-1.7	0.095-0.76	0.4-29
Velocity (fps)	7.0	0.07-7.1	0.8-6.4	0.7-7.8	1.2-9.4
Slope (ft/ft)	0.004	0.00006-0.037	0.000043-0.028	0.000002-0.0011	0.0004-0.02
Depth (ft)	2.7	0.01-1.4	0.04-50	0.7-56	0.03-3.9
Top Width (ft)	1866	0.23-4	0.44-1750	0.8-3640	0.5-6.6

The field observations and sediment sampling data reveal the presence of mostly sand in the channel for the entire study area with a median diameter of approximately 0.5 mm. The sediment sampling data show the presence of some gravel in the samples, with a maximum diameter of 50 mm. Based on these observations, District staff directed the team to use the Toffaleti-Meyer-Peter-Muller combination equation (TMPM). The TMPM equation uses the Toffaleti method for the sandy sediment fraction and the Meyer-Peter-Muller method for gravel transport. As a result, the TMPM combination is able to model both sand and gravel transport. The TMPM combination was used for past District HEC-6 models on the Salt River (high gravel content) and the Gila River (high sand content).

5.3 Model Hydrology

Hydrologic data used in the sediment transport modeling were obtained from the LHWCMP Hydrology Report, and are based primarily on USGS stream gauge records for the Hassayampa River and Jackrabbit Wash and hydrologic modeling principles for Wagner Wash and Daggs Wash.

5.3.1 Hassayampa River

5.3.1.1 Hydrology Boundary Conditions

The flow discharges in the Hassayampa River and the tributaries are input as boundary conditions at the upstream end of the HEC-6 model. The following two types of hydrographs were considered for the simulations:

- Long-Term Flow (Mean Daily Discharge)
- Design Flood (100-Year Hydrograph)

The USGS mean daily discharges for the Hassayampa River were obtained for the period from 1937 to 2004 for the USGS stream gauges in the study reach, as described in the LHWCMP Hydrology Report. The mean daily discharge dataset provided the flow

records used to evaluate the long-term impacts. The 100-year flood hydrograph was derived as described in the LHWCMP Hydrology Report, and was appended to the long-term flow records based on mean daily discharge records. Use of the combined long-term mean daily records with the 100-year hydrograph was done per the direction of District staff. Figure 5-2 shows the long-term hydrograph and Figure 5-3 shows the 100-year hydrograph. The 100-year hydrographs shown in Figure 5-3 were obtained by scaling the hydrographs from the HEC-1 hydrologic model to the FDS peak flows. In other words, the shapes of the hydrographs were obtained from the hydrologic modeling (see LHWCMP Hydrology report) and were scaled to give peak flows that matched the FIS study peak flows. This matching was done for the upstream Hassayampa River, the Wagner-Daggs tributary system and Jackrabbit Wash. The flow hydrograph at the downstream end of the HEC-6 model near the Gila River was obtained by adding these three hydrographs. This was done since the HEC-6 model does not have the capability to attenuate the hydrograph as flow goes downstream. The downstream hydrograph obtained through summation of upstream hydrographs provides a resulting hydrograph with flows that are higher than the attenuated hydrograph. This approach was adopted as it represents more conservative approach with respect to sedimentation results. The flow data were incorporated into the HEC-6 model on Q records. Flows less than 500 cfs were not included to reduce the time taken to perform the simulation. The results did not have any perceivable changes due to the elimination of the flows under 500 cfs.

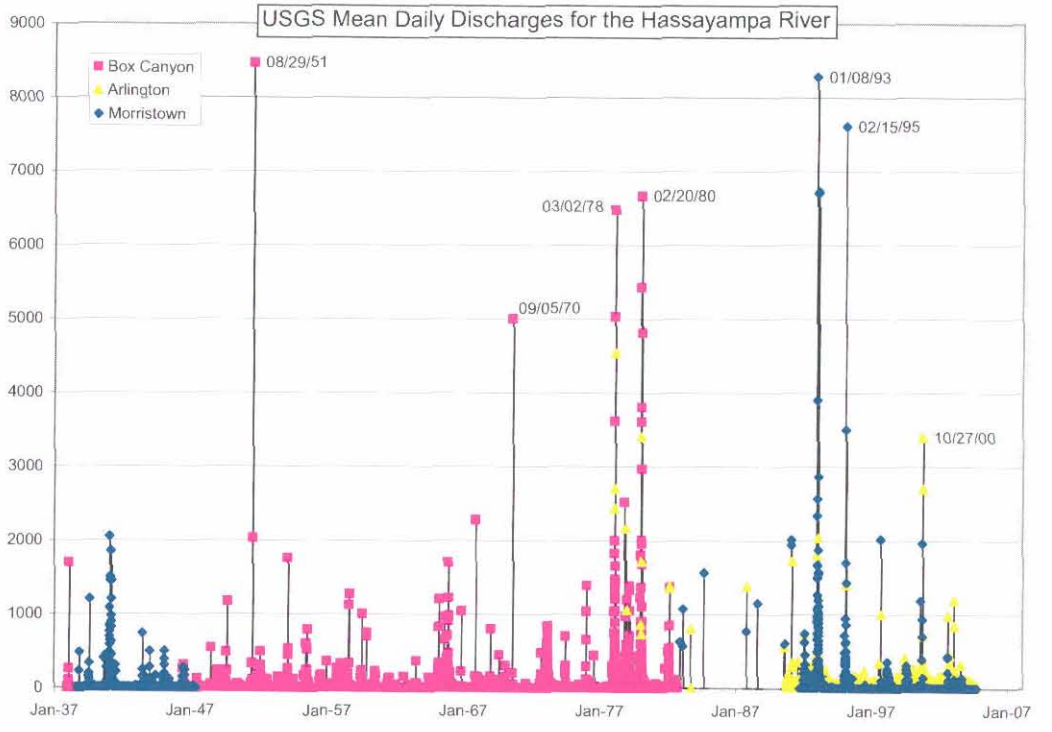

Figure 5-2. Long-Term Hydrographs

5.3.1.2 Tributary Inflow Hydrology

The 100-year hydrographs for the tributary inflows to the study reach were derived by scaling the HEC-1 model results presented in the LHWCMP Hydrology Report to the peak discharges established by FEMA in the effective Flood Insurance Study (FIS) for

each tributary. The following two tributary inflow points were considered:

- Daggs Wash-Wagner Wash
- Jackrabbit Wash

Daggs Wash and Wagner Wash were considered as a single inflow point for the HEC-6 model because their confluences are located within several thousand feet of each other, and because they have a similar hydrologic response. The FDS peak discharges for Daggs Wash and Wagner Wash were added together (3041 cfs + 15700 cfs = 18750 cfs) to create a single value to scale the HEC-1 model results. For Jackrabbit Wash, the HEC-1 hydrograph was scaled to 32,500 cfs, the FDS 100-year peak.

Tributary inflows for the period of record (long-term) simulation were assumed to be reflected in the USGS gage data used for that analysis. The flow data for the Jackrabbit Wash and Wagner-Daggs tributary systems were input on Q records as "local inflows."

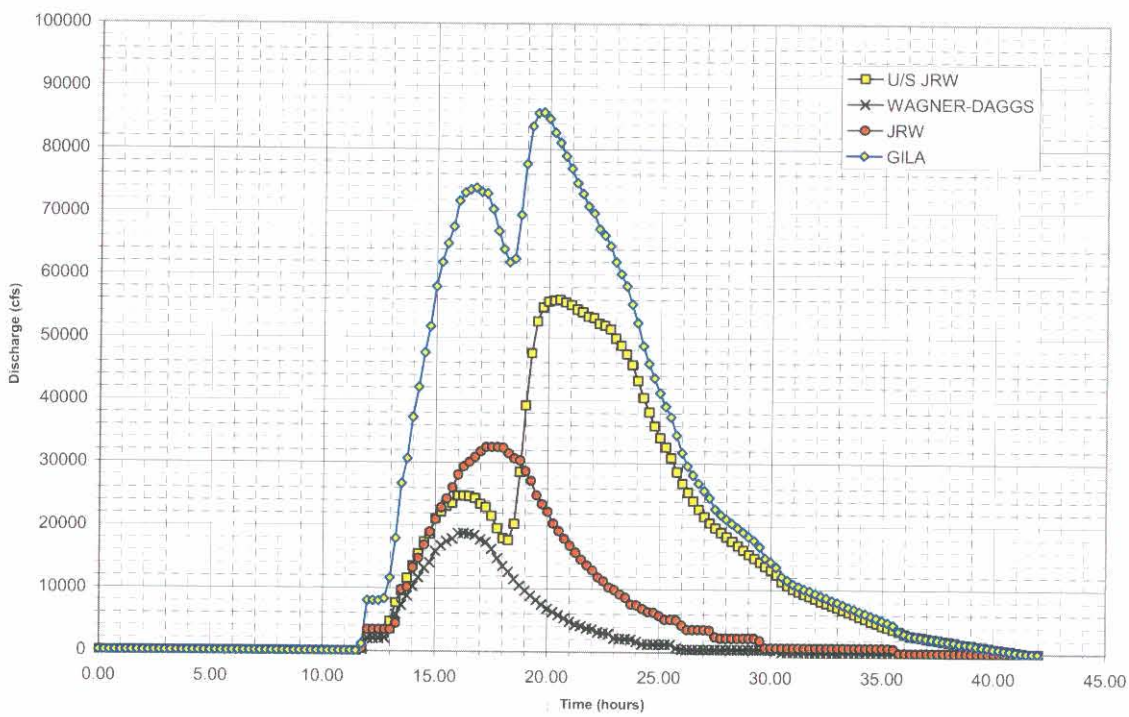

Figure 5-3. 100-Year Hydrographs

5.3.1.3 Leveed Reach

The presence of the levees in Reach 1 of the Hassayampa River creates the possibility of overtopping for flows larger than the channel and levee capacity. In HEC-RAS, the overtopping was modeled using lateral weirs, multiple models, and parallel flow paths. Unfortunately, few of the HEC-RAS modeling options are available in HEC-6. Therefore, a simpler approach was adopted. The flows leaving the main channel over the levees, as determined by the HEC-RAS results, were modeled in HEC-6 by changing the

discharge using QT records. That is, the change in flow rate along the main channel was simulated using the change of flow option.

The amount of flow that is be diverted out of the main channel was determined using the results from the HEC-RAS model. Since the simulated hydrographs involve a range of flows, a relationship between the incoming flow and diverted flow was established using HEC-RAS modeling of the following flow rates: 5,000 cfs, 20,000 cfs, 50,000 cfs and 75,000 cfs. The outflow for any given inflow was then determined by interpolation using the results for these four flow discharges. The outflow was incorporated into the HEC-6 model as a flow change by specifying the location of the outflow using the QT record and the flow change using the Q record.

In the HEC-RAS model, it may be noted that the flow changes due to lateral weirs occur at almost every cross-section in the leveed reach. Modeling such continuous flow change is not possible in HEC-6 since a total of only 10 flow changes can be used on the Q record. The two tributary inflow points also required space on the Q record, leaving only eight possible flow changes in the levee reach. By iteration of results and engineering judgment, it was determined that three flow change points (four flow rates) in Reach 1 were sufficient to model flow changes. Figure 5-4 shows the flow distribution in the main channel as estimated by HEC-RAS and as incorporated into the HEC-6 model. Four upstream flows of 15000 cfs, 20000 cfs, 50000 cfs and 75000 cfs are considered. Figure 5-4 shows how the flows are reduced at three locations (river-stations 2.19, 3.53, 4.0) for each of these four flows. Interpolation was used to determine the flow reduction pattern for upstream flows other than the four flows considered here. The interpolation process gives a peak flow rate of 35802 cfs for the main stem levee reach (below cross-section 2.19). This is the first entry in the Q record and it is not for the entire river. The flow rates for location upstream of the levee reach is obtained by including the flow changes. This results in a peak flow flow for the entire cross-section including the main stem and overbank flows of 85800 cfs which is higher than 74100 cfs (the FEMA effective).

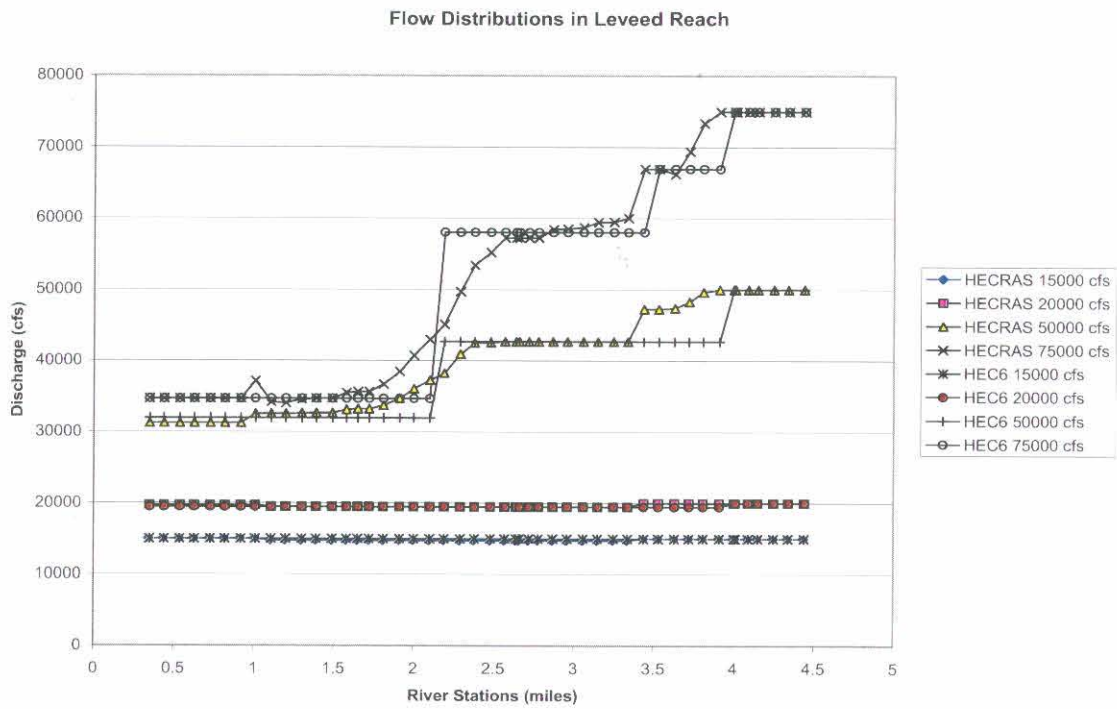

Figure 5-4. Flow Distribution in Leveed Reach

5.4 Sediment Inflow

The Hassayampa River is a free-flowing stream in which field evidence and flood observations suggest that sediment is readily transported from the upper watershed into the study reach. Sediment inflow points include the upstream study limit and the three major tributaries that join the river within the study limits.

5.4.1 Methodology

Sediment data for the Lower Hassayampa River are extremely scarce. Only one source of sediment measurements was identified for the lower Hassayampa River, and none were found for any of the Hassayampa River tributaries. Water quality data from the USGS gauging station on the Hassayampa River at Arlington, AZ include suspended concentrations, but no bedload measurements. There are 52 suspended sediment records in the USGS dataset for a period ranging from 1996 to 1997. The flow rates covered by this USGS dataset are extremely low and, hence, cannot be readily used to obtain an adequate sediment rating curve. In addition, the dataset contains only suspended sediment data and does not include any bedload component.

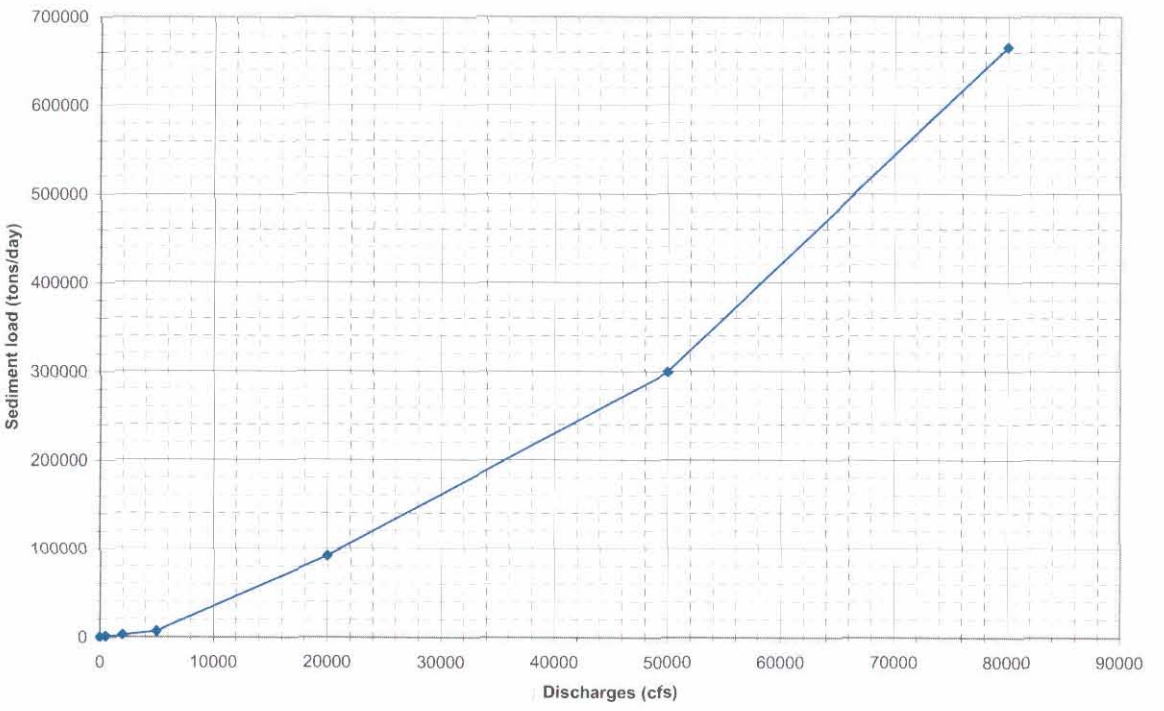

Figure 5-5. Sediment Inflow Rating Curve for the Hassayampa River

Due to lack of available measured sediment concentration data, the sediment inflow rating curves were developed using the assumption that the sediment supply reach is in equilibrium. If the upstream reach is in equilibrium, the sediment transport capacity estimates can be used to derive the sediment inflow rates. Sediment transport capacity for the supply reach was estimated by developing a separate HEC-6 model for the supply reach which extended upstream approximately one river mile of the upper study limit. Cross section data for the reach upstream of the LHWCMP study limit were

obtained from the FIS HEC-2 model. This HEC-6 model was run in an iterative fashion (a.k.a., a "recirculation model") by changing the inflowing sediment until the inflowing load approximately matched the sediment outflow, which by definition represents a state of equilibrium for the supply reach. Separate HEC-6 models were used over a range of flows to develop a relationship between water discharge and sediment inflow, as well as a gradation for the sediment inflow. The HEC-6 results were assembled into a table describing sediment inflow for flow rates of 500, 2,000, 5,000, 20,000, 50,000 and 80,000 cfs, and was entered into HEC-6 model using the "LT", "LQ" and "LF" records. A minimum value of 1 cfs was included in the table to cover the entire range of 1 to 80,000 cfs. These flows were selected to cover the entire range of flows possible during a single 100-year event. The sediment inflow rating curve for the Hassayampa River is shown in Figure 5-5.

5.4.2 Jackrabbit Wash

The HEC-6 recirculation model procedure was also used to develop the inflow sediment rating curve for Jackrabbit Wash. Cross-section geometry for the Jackrabbit Wash recirculation HEC-6 model was obtained from the HEC-RAS hydraulic model developed by WEST Consultants, Inc. for the LHWCMP floodplain delineation task. The sediment inflow table consists of the following flows: 1, 500, 2000, 5000, 12500, 20000 and 35000 cfs. These flows were selected to cover the entire range of flows possible during a single 100-year event, as well as the period of record flows.

5.4.3 Wagner Wash and Daggs Wash

The HEC-6 recirculation model procedure was also used to develop the inflow sediment rating curve for Wagner Wash/Daggs Wash confluence. The cross-section geometry used was based on Wagner Wash, and was obtained from the previous FIS HEC2 model developed for the District by HDR Engineering in 1991. The sediment inflow table consists of the following flows: 1, 500, 1000, 2000, 4000, 6000, 8000 and 20000 cfs. These flows were selected to cover the entire range of flows possible during a single 100-year event, as well as the period of record flows.

5.4.4 Other Tributaries

No other tributaries were included in the sediment modeling effort because of their small watershed size and limited contribution of flow and/or sediment to the stream system.

5.5 HEC-6 Sediment Transport Modeling

The HEC-6 computer model was designed to simulate long-term trends of scour and/or deposition in a stream channel that result from changing the natural hydrology, channel geometry, or sediment supply. The U.S. Army Corps of Engineers describes the HEC-6 computer program as follows:

> *HEC-6 is a one-dimensional movable boundary open channel flow numerical model designed to simulate and predict changes in river profiles resulting from scour and deposition over moderate time periods. Continuous flow records may be partitioned into a series of steady flows of variable discharge and duration. For each flow, a water surface profile is calculated providing hydraulic data at*

each cross section. These hydraulic data, combined with the discharge and flow duration information, allow volumetric accounting of sediment within stream reaches. The amount of scour or deposition at each section may then be computed and the cross section bed elevation adjusted accordingly. Hydraulic data associated with the next discharge are then computed using the updated geometry, and the channel geometry is again updated. This process is repeated through the entire duration of flows. (Paraphrased, p. 1, USACOE, 1993)

HEC-6 models were prepared for the LHWCMP study reach to assess potential reaches of aggradation or degradation and to estimate the range of general scour for the various conditions. The overall objectives of the HEC-6 modeling task include the following:

- Establish base condition models that can be used and/or modified for evaluating management alternatives in Phase 2 of the Watercourse Master Plan.
- Establish base condition models and modeling guidelines that can be used by or conveyed to consulting engineers working for private developers in the floodplain or sand and gravel mining interests.
- Provide a tool for assessing the expected streambed profile response of the Hassayampa River in natural and existing conditions. In particular, the model will be used to help identify aggrading or degrading stream reaches, and to assess the impact of sediment transport and deposition on regulatory water surface elevations and flood hazards.
- Test the effectiveness of assessing headcut/tailcut potential at in-stream sand and gravel excavations, as well as estimating safe yield from aggrading reaches.

5.5.1 Model Limitations

The following limitations or assumptions of the HEC-6 model are listed below:

- One Dimensional. HEC-6 assumes that flow in the stream is one dimensional, i.e., the model does not account for secondary currents from meandering, eddying, or turbulence that cannot be addressed through the use of energy loss coefficients. Gradually-varied flow conditions usually are modeled adequately using a one-dimensional model.

- Steady Discharge. The HEC-6 model simulates passage of a flood or annual hydrograph (unsteady flow) as a series of discrete steady flows of known duration. HEC-6 is best suited to simulating channel changes from hydrographs that rise and fall gradually over a relatively long duration.

- Uniform Scour or Deposition. Any change in bed elevation resulting from scour or deposition is applied uniformly across the entire moveable portion of channel. That is, a uniform depth of sediment is added to, or subtracted from, each station (GR) point used to describe the geometry of the active channel. The formation of point or lateral bars, bend scour holes, and local scour is not simulated.

- Sediment Continuity. HEC-6 computes changes in bed elevation based on the

principal of conservation of sediment volume:

Sediment (in) – Sediment (out) = Change in Sediment Volume
Change in Bed Elevation = Change in Sediment Volume / Reach Length

- Initial Conditions. The initial concentration of sediment material is assumed to be negligible. That is, all bed material is contained in the sediment reservoir at the start of the computational interval and is returned to the sediment reservoir at the end of the interval.

- Time Scale. HEC-6 was developed "to predict changes in river profiles from scour and/ or deposition over moderate time periods (typically years, although applications to single flood events are possible)." HEC-6 performs best for gradually changing hydraulic conditions, e.g. for large rivers with slow rising and falling hydrographs.

- Sediment sources. The model assumes that there are only two sediment sources – inflowing water and movable portion of the stream bed. HEC-6 does not consider lateral channel (bank) erosion – no sediment is supplied from the banks.

- Sediment Calculations. A number of transport functions are coded in HEC-6, all of which apply the transport function by grain size.

- Equilibrium. The HEC-6 sediment transport function algorithms assume that sediment equilibrium conditions are reached during each time step of a single event, a condition which, probably, is not met for very short events. If equilibrium conditions are probably not established, then the modeling results should be interpreted in a qualitative manner.

- Time-step. Reach hydraulics and sediment transport potential are based on the channel geometry. Generally, a change in bed elevation of 1 foot or 10 percent of the flow depth within a single time step is considered significant. In addition, the time step must be long enough that the flow would have sufficient time to travel through the longest stream segment.

- Lateral Weirs and Bridge Hydraulics. HEC-6 does not have the capability of modeling the lateral weirs or the bridge hydraulics.

Table 5-2 lists these assumptions and indicates which assumptions may or may not be valid for the Lower Hassayampa River study reach. Given the assumptions and conditions that are not valid specifically for the study reach area, the HEC-6 modeling results are best suited to predicting relative trends of expected changes rather than calculating precise topographical changes.

Table 5-2. Model Limitations	
Assumptions/Limitations	**Valid for Study Reach?**
One Dimensional	*Yes/No. Probably Gradually Varying Definitely not valid near confluences*
Uniform scour or deposition	*No. Braided system with bars*
No Bank Erosion	*No. Historically, banks have moved*
Steady Flow conditions model	*Probably valid for low flows. Larger flow events tend to have steep variations in time.*
Sediment Continuity	*Yes*
Initial conditions for suspended sediment	*Yes. Ephemeral stream*
Time scale of hydrograph	*No. Flash flood conditions*
Sediment sources	*Yes/No. Some sediment may come from lateral bank erosions*
Sediment Calculations	*Yes. Toffaleti-MPM Equation is used which is based on grain size distributions*
Equilibrium achieved in Time step	*Yes/No. Daily mean values are used. Variations within the day are ignored. It is likely that equilibrium conditions are reached in the time-step time-frame.*
Time step length	*Yes. Scour limited in time steps* *Yes. Adequate travel time*
Lateral Weirs and Bridge Hydraulics	*Lateral weirs and bridges are model indirectly relying on HEC-RAS results.*

Another limitation of the HEC-6 model is its ease of use relative to the difficulty of generating reasonable results. Significant experience on the part of the modeler is required to produce realistic results and interpret model output correctly. For example, initial HEC-6 runs frequently generate thalweg profiles with a zigzag pattern, which is often interpreted as simple variation between deposition and scour. Unfortunately, the zigzag pattern may be the result of numerical instability in the model, although no error or warning message is generated by the program. The numerical instability can often be overcome by reducing the duration of internal calculation time-steps, as well as by increasing the distance between cross-sections. The zigzag pattern is also more pronounced for steeper channels. Reducing the time-steps increases the total number of computations while reducing the number of cross-sections, which in turn results in reduced computational accuracy. The weighting factors for numerical integration on the I4 record also provide another mechanism for fine-tuning the numerical stability. Novice or impatient users may be unfamiliar with the techniques necessary to produce accurate, realistic results and may therefore terminate their analysis before realizing the model potential.

5.5.2 HEC-6 Model Parameters

5.5.2.1 Base Geometry Data

HEC-RAS channel geometry was the basis for the HEC-6 model, with the same cross-section locations and station/elevation. In the HEC-RAS model, the river was divided into three reaches in Reach 1, where the river is leveed. In HEC-RAS, flow overtopping

the levees was modeled using lateral weirs and the overtopping flows can enter the neighboring reaches. In HEC-6, only the main reach was considered; the two side reaches present in HEC-RAS model were not modeled.

The process of converting HEC-RAS geometry to HEC-6 format involved the following steps:

- Section Geometry. HEC-RAS cross-section geometry points were imported into the HEC-6 input file.

- Interpolated Section Geometry. New points were inserted into the cross-section geometry using linear interpolation to obtain at least one point every 50 feet horizontally and every one foot vertically. Addition of interpolated points was done to enable the cross-section shape to evolve evenly as the sediment erosion and deposition is simulated.

- Section Point Reduction. The number of cross-section geometry points was reduced to 190 to be less than the maximum allowable number HEC-6 of 200, and to allow room to add any additional points during the simulation. The reduction was achieved by filtering points mostly near the far ends on the overbanks and through elimination of points close to each other, while retaining the overall shape of the cross-section geometry and an even vertical and horizontal distribution of points.

- Ineffective Flow Areas. The ineffective flow areas modeled in HEC-RAS were imported and set as conveyance limits using the "XL" records. The ineffective area option in HEC-RAS changes the conveyance while retaining the wetted perimeter, which is similar to how the HEC-6 conveyance limits option functions, although ineffective area vertical extents cannot be specified in HEC-6. In addition, HEC-RAS allows multiple ineffective areas within a cross section, while in HEC-6 only allows two, with one on each side of the main channel. Appropriate procedures were followed to work within the HEC-6 limitations and incorporate known ineffective flow areas.

- Manning's N. Conveyance-weighted Manning's N values were extracted from the HEC-RAS output table. These values were used as starting point for the hydraulics calibration runs. Further details on the hydraulics calibration and Manning's N values are provided in the following section.

5.5.2.2 Manning's N Values - Hydraulics Calibration

A hydraulics calibration exercise was performed to obtain a reasonable match between water surface elevations and velocities computed by HEC-6 and the values computed by HEC-RAS. First, the HEC-RAS model was run for a range of flows (5,000 cfs, 20,000 cfs, 50,000 cfs and 75,000 cfs), the conveyance-weighted Manning's N values for each flow rate were extracted from the output, and the values were input into the HEC-6 model on NV records. Second, a fixed-bed HEC-6 model was developed to obtain hydraulics results from HEC-6 without any influence by sediment transport.

Third, the HEC-6 Manning's values on NV records were modified through repeated runs of the HEC-6 model.

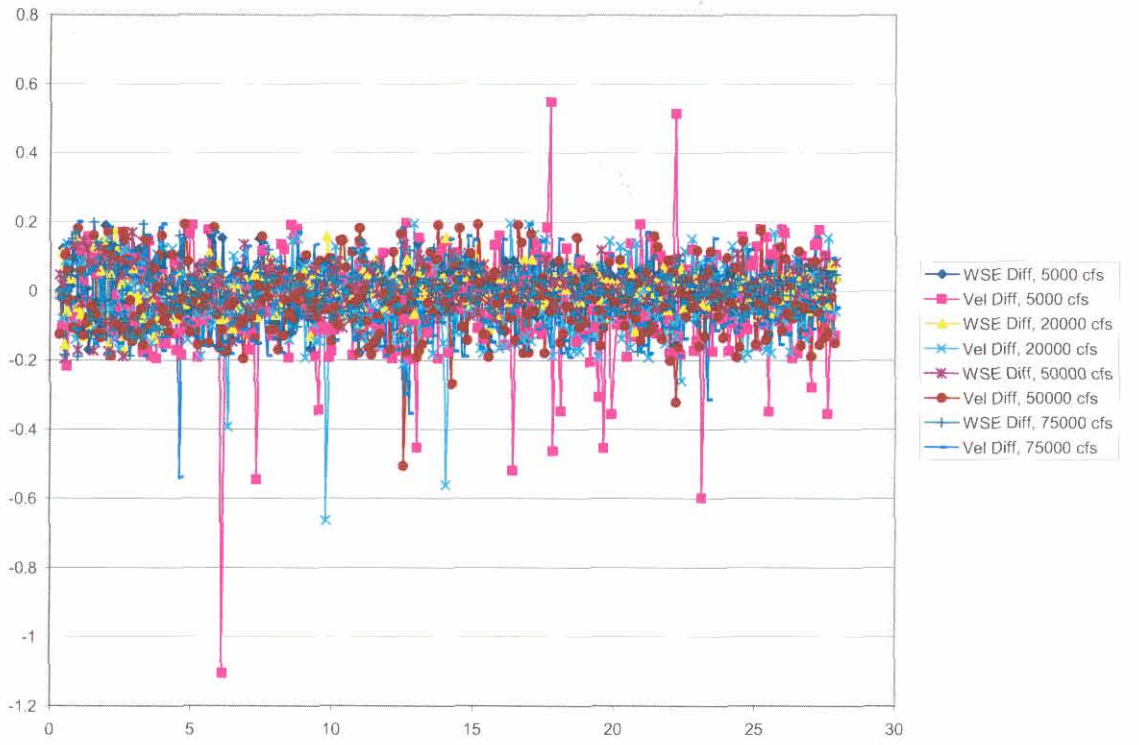

Figure 5-6. Hydraulics Calibration

This process was performed for 5,000 cfs, 20,000 cfs, 50,000 cfs and 75,000 cfs, until the water surface elevations and velocities matched the HEC-RAS values for the same flow rates within a tolerance of 0.2 ft and 0.2 ft/sec, respectively, in most places, as shown on Figure 5-6. A difference of up to 1 ft/sec was seen at a few locations for the 5,000 and 20,000 cfs runs where flow was critical, and matching of both the velocity and water surface elevations at the specified tolerance was not possible. These differences occur only at few locations and the velocities were within 0.6 ft/s at all except one location. The results of the hydraulics comparison in tabular format are presented in Appendix 5.5.

5.5.2.3 Moveable Bed Limits

The moveable bed limits determine which part of the channel HEC-6 allows to move vertically when subject to erosion or sedimentation. HEC-6 computations adjust the channel bed within moveable bed limits. The H/HD record option in HEC-6 is used to specify lateral and vertical limits on bed movement. The process used to adjust the bed is summarized as follows:

- Deposition (no scour) is allowed outside the conveyance limits on the XL record.
- Scour occurs only is within the movable bed limits, within the conveyance limits, within the effective flow limits defined by the X3 record, and below the water

surface elevation.

- Once the scour or deposition limits are determined, the volume of scour or deposition is divided by the effective width and length of the control volume to obtain the bed elevation change.

The Lower Hassayampa River has a wide river channel with an indistinct low flow channel with subtle transitions to bars, floodplains and terraces, divided flow around low islands, and surfaces that function as depositional zones during some flow events, but that are mobilized during large floods. The braided condition indicates that the main channel changes location, as does the flow distribution. While the smaller flows may be restricted to a narrow channel, the larger flows such as the 100 year flow event may submerge the entire river channel. In the absence of a specified moveable bed limit, HEC-6 would adjust only the wetted part of the cross-section. Therefore, for this study reach, it was deemed appropriate not to set moveable bed limits, but rather to let HEC-6 use the wetted perimeter to determine the moveable limits as flow rates vary during the hydrograph.

5.5.2.4 Water Temperature

The model water temperature of 67°F was estimated based on the results of published USGS water quality sampling at Morristown and Arlington.

5.5.2.5 Downstream Rating Curve

The downstream depth-discharge rating curve was derived from HEC-RAS, using a range of flows and a normal depth boundary condition. The WEST HEC-RAS model included only the 100-year simulation and used the "Known WS" water surface elevation as the boundary condition. For the purpose of HEC-6 modeling where the flow varies with the hydrographs, the normal depth option was used as the downstream boundary condition.

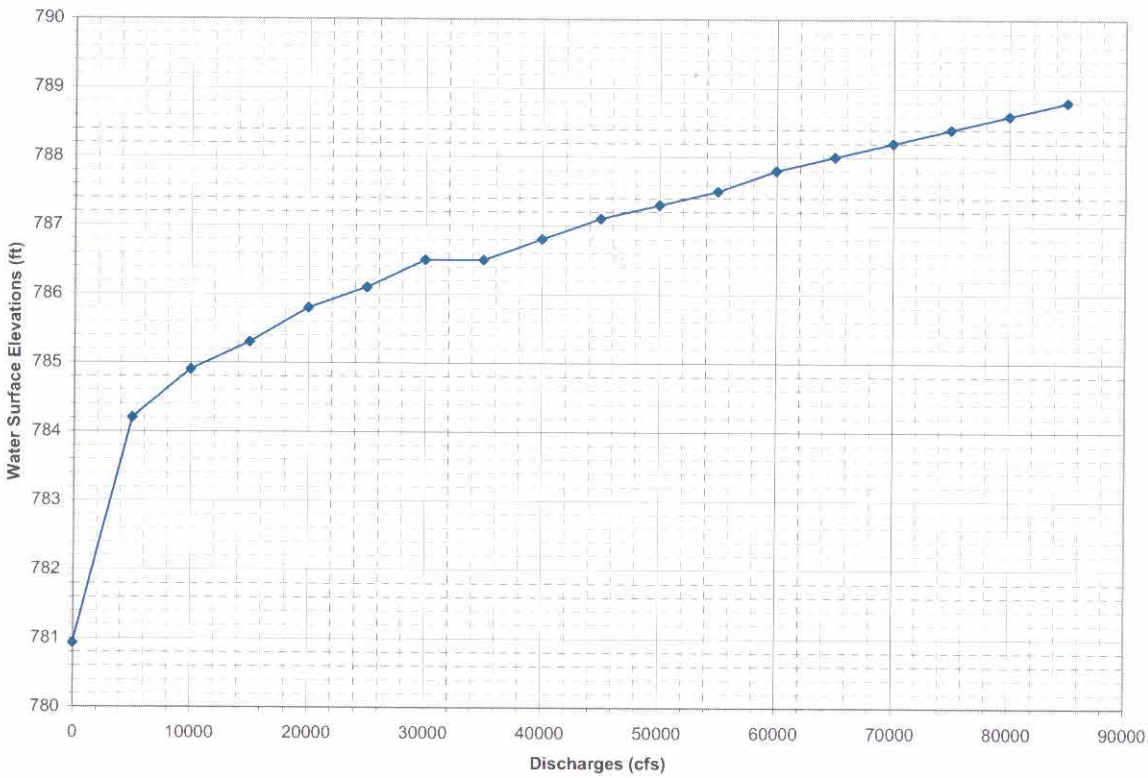

Figure 5-7. Downstream Rating Curve

5.5.2.6 Depth to Bedrock

Field evidence documented in Chapter 2, which includes observations of numerous in-channel soil pits and visits to in-stream sand and gravel excavations, indicates that bedrock occurs at depths well below the expected depth scour. Thus, it was assumed that an unlimited sediment supply was available from the bed for sediment transport. In HEC-6, the HD record was used specifying a value of 20 feet to bed-rock. The value of 20 feet was sufficient to simulate unrestrained sediment supply.

5.5.2.7 Bridges

Unlike the HEC-RAS model, the option to specify bridges is not available in the HEC-6 sediment transport model. As a result, the hydraulics losses at bridge locations cannot be modeled in HEC-6. However, the hydraulic calibration (discussed in Section 5.5.2.2) ensures that hydraulics in HEC-6 mirrors closely the hydraulics computed with HEC-RAS model. Since the HEC-RAS model incorporates the bridge and performs the hydraulic calculations accordingly, it can be anticipated that the hydraulic effects of the bridge are somewhat included in the HEC-6 model. This procedure was used for the bridges located at Old US 80, I-10, and the SPRR.

5.5.3 HEC-6 Model Scenarios

The following four HEC-6 modeling scenarios were selected by District staff for the LHWCMP:

- Scenario #1 - Sediment Inflow Calibration Model. The sediment inflow calibration of the HEC-6 model was performed using the existing FDS model to simulate the floods between the periods 1987 to 2004. A comparison between the previous FDS topography from 1987 to the latest 2004 topography provided the basis for the calibration.

- Scenario #2 - Manning's N Calibration Model. A calibration effort similar to that described for the sediment inflow calibration (Scenario #1) was performed by varying the Manning's N values.

- Scenario #3 - Tributary Sediment Inflow Impact Model. The impact of varying tributary sediment inflow on sediment transport along the Hassayampa River main stem was analyzed.

- Scenario #4 - Existing Conditions Model. An existing conditions HEC-6 model was prepared to simulate the sediment transport and channel response to recurrence of the period of record gauged long-term (mean daily) flow hydrograph followed by a 100-year hydrograph. The existing conditions model (Scenario #4) is intended for use in alternatives evaluation in Phase 2 of the LHWCMP.

District staff determined that other modeling scenarios listed in Task 9.6 of the scope of services should not be performed and developed the scenario list shown above.

Base modeling results are summarized in Table 5-3 and the results for modeling Scenarios #1 and #2 are described below in Sections 5.5.3.1 and 5.5.3.2. The base modeling results indicate that only minimal bed elevation changes occurred between 1987 and 2004, as shown by the average root mean square (RMS) of 1.39 for the observed elevation difference on the 1987 and 2004 topographic data (Table 5-3). The period from 1987 to 2004 included several moderate floods the 1993 and 1995. The results summarized in Table 5-3 also indicate the following:

- Most of the study reach had slight net degradation between 1987 and 2004, with an average bed elevation change of 0.2 feet.

- The maximum average observed degradation occurred in Reach 1 where some evidence suggests recent degradation is linked to failure of Gillespie Dam.

- The greatest net aggradation occurred in Reach 2 between RM 3.53 and 7.75, which is upstream of the constricted levee reach.

- Almost all of the observed and predicted average elevation change estimates are less than the accuracy of the mapping used to generate the estimates, and should therefore be considered as approximate. The 1987 mapping had a 4-foot contour interval (±2 ft) and the 2004 mapping had a 2-foot contour interval (±1 ft).

Table 5-3. 1987 and 2004 Topography Comparisons									
			Observed Topography Data				Predicted Topography From HEC-6 Modeling		
XS ID	Left Stn	Right Stn	1987 Average Bed	2004 Average Bed	04-87 Differ-ence	Differ-ence^2	2004 Average Bed	04-87 Differ-ence	Differ-ence^2
1.11	9837.9	10155.8	808.0	804.5	-3.5	12.00	808.6	0.60	0.36
1.49	9830.3	10132.6	816.1	812.3	-3.8	14.41	815.6	-0.50	0.25
2.48	9839.4	10126.7	831.8	831.3	-0.5	0.29	832.1	0.30	0.09
3.53	9908	10507.5	852.4	855.1	2.7	7.38	854.5	2.10	4.41
4.53	9307.8	10756.6	878.4	878.7	0.3	0.12	878.8	0.40	0.16
5.00	9561.9	10586.6	890.0	890.2	0.2	0.04	890.1	0.10	0.01
5.48	9730	10964.9	899.1	900.0	0.9	0.78	899.2	0.10	0.01
6.52	9208.1	10240.8	919.3	922.6	3.3	10.96	920.4	1.10	1.21
7.75	8788.9	10132.6	948.5	950.6	2.1	4.36	948.0	-0.50	0.25
8.51	9768.4	11123.6	967.7	967.5	-0.2	0.02	966.6	-1.10	1.21
9.08	9905.3	10815.1	979.7	979.5	-0.2	0.03	980.1	0.40	0.16
9.74	9230.9	10348	993.4	993.3	-0.1	0.00	994.4	1.00	1.00
10.5	9846.8	10864.5	1011.4	1011.1	-0.3	0.07	1011.8	0.40	0.16
11.43	8853.1	10452.1	1033.2	1033.3	0.1	0.01	1033.7	0.50	0.25
12.37	8381.8	10079.5	1055.6	1054.1	-1.5	2.21	1055.1	-0.50	0.25
13.32	8530.6	10986.6	1077.6	1077.4	-0.2	0.03	1078.2	0.60	0.36
14.08	9095.4	10400.3	1094.4	1095.0	0.6	0.42	1094.8	0.40	0.16
14.45	9625.8	10374.1	1102.4	1102.6	0.2	0.06	1102.8	0.40	0.16
15.59	9382.1	10535.8	1125.2	1124.5	-0.7	0.55	1125.4	0.20	0.04
16.53	9180.3	10159.6	1145.0	1144.3	-0.7	0.46	1144.7	-0.30	0.09
17.58	9459.7	10112.8	1167.6	1167.3	-0.3	0.09	1168.8	1.20	1.44
18.62	8064.1	10310.6	1191.3	1189.8	-1.5	2.25	1190.8	-0.50	0.25
19.28	9300.6	10775.8	1204.9	1205.3	0.4	0.16	1205.5	0.60	0.36
19.75	9211.5	10128.9	1215.7	1215.6	-0.1	0.02	1215.6	-0.10	0.01
20.51	8372.1	10153.1	1232.1	1230.3	-1.8	3.39	1232.2	0.10	0.01
21.46	9494.4	10614.6	1253.2	1251.8	-1.4	2.08	1253.3	0.10	0.01
22.59	8539.3	10464.2	1277.0	1277.3	0.3	0.08	1277.2	0.20	0.04
23.63	9662.8	10972.8	1297.6	1298.2	0.6	0.32	1297.0	-0.60	0.36
24.20	9155.1	10421.6	1310.4	1310.4	0.0	0.00	1310.8	0.40	0.16
24.77	8645.1	10086	1324.3	1323.7	-0.6	0.41	1324.4	0.10	0.01
25.72	7512.7	10759.9	1348.6	1348.1	-0.5	0.28	1348.6	0.00	0.00
26.67	9924.3	13922.8	1370.9	1370.6	-0.3	0.07	1370.8	-0.10	0.01
27.61	9960.5	14331.7	1393.2	1392.4	-0.8	0.64	1392.9	-0.30	0.09
Root Mean Square of Difference (RMS)						1.39			0.64

- The volume of sediment deficit indicated by the net average observed bed elevation change from 1987 to 2004 was about 660 acre-feet (1.1 million yards) over the entire study reach, or 94 AF/yr. The sediment volume excess predicted

by the HEC-6 base model during the 1987 to 2004 period was 650 (1.1 million yards), or 94 AF/yr.

The results in Table 5-3 regarding Modeling Scenarios #1 and #2 are discussed below.

5.5.3.1 Scenario #1: Sediment Inflow Calibration Model

The Scenario #1 HEC-6 model used the 1987 FIS topographic data as the starting channel geometry, simulated the known flow records for the study reach during the period from 1987 to 2004. This was done to simulate the changes that occurred during 1987 to 2004 and calibrate the model by comparing the simulated forecast of the 2004 channel topography with the surveyed 2004 topography by varying the sediment inflow rating curve. The sediment inflows were varied from the base values calculated using the procedures described in Section 5.4 by +40%, +20%, -20%, and -40%. As shown in Figure 5-8, the HEC-6 model was not sensitive to sediment flow. Past HEC-6 modeling experiences on streams in Arizona demonstrate that model sensitivity to sediment inflow is general limited to the upstream-most cross sections, if an adequate sediment reservoir exists along the moveable bed, which is the case on the Hassayampa River. In general, an increase or decrease in the sediment inflow rate resulted in less than 0.1 foot of difference in the predicted average bed elevation.

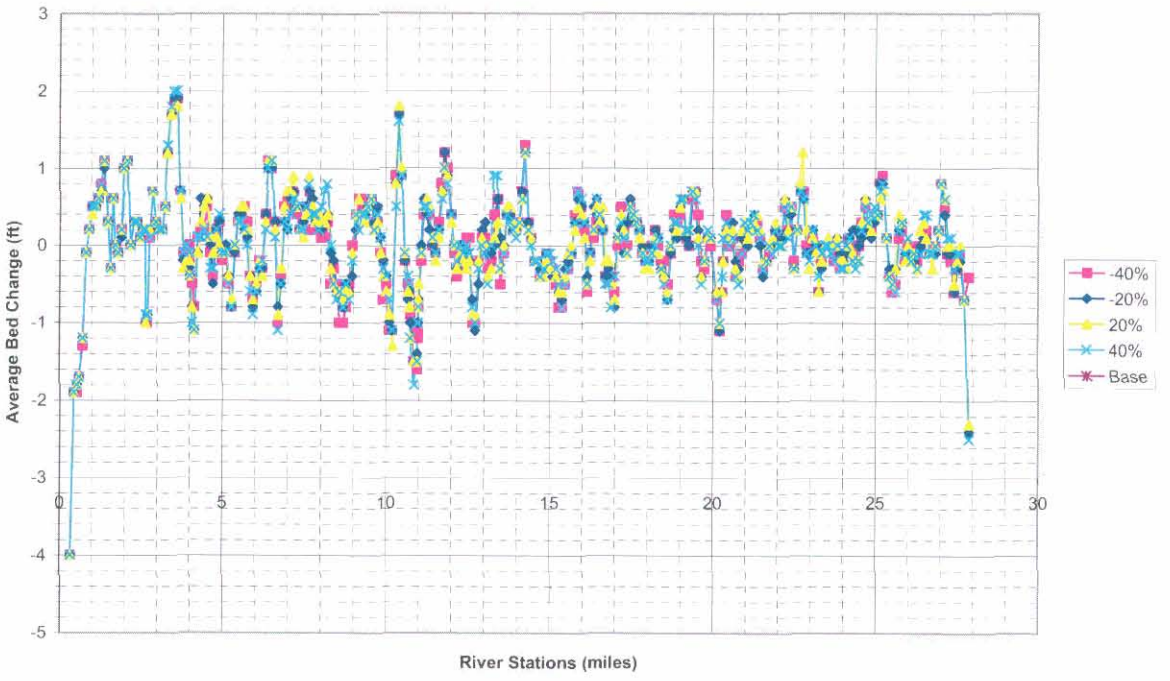

Figure 5-8. Sediment Inflow model calibration

Based on the HEC-6 modeling results summarized in Figure 5-8, it was concluded that the HEC-6 model of the Hassayampa River is not sensitive to sediment inflow for the existing condition, at least for the period of record modeled.

5.5.3.2 Scenario #2 - Manning's N Model Calibration

The Scenario #2 HEC-6 model used the 1987 FIS topographic data as the starting channel geometry, simulated the known flow records for the study reach during the period from 1987 to 2004, and attempted to improve the forecast of the 2004 channel topography by varying the Manning's N values. The Manning's N values were varied from the base values determined using the procedures described in Section 5.5.2.2 by +40%, +20%, -20%, and -40%. As shown in Figure 5-9, the HEC-6 model was not sensitive to Manning's N value. In general, an increase or decrease in the Manning's N value over the moveable bed portion of the cross section resulted in less than 0.2 foot of difference in the predicted average bed elevation.

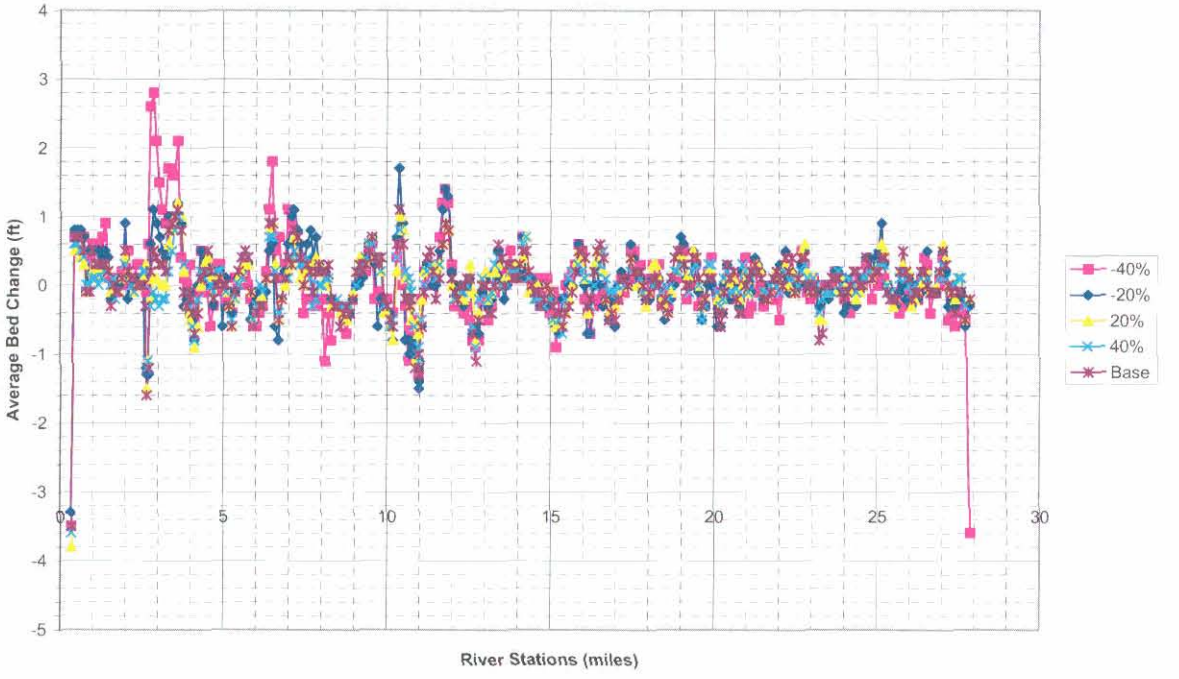

Figure 5-9. Manning's N model calibration

Based on the HEC-6 modeling results summarized in Figure 5-9, it was concluded that the HEC-6 model of the Hassayampa River is not sensitive to Manning's N value for the existing condition, at least for the period of record modeled.

5.5.3.3 Scenario #3 - Tributary Sediment Inflow Impact Model

Modeling Scenario #3 was intended to test the HEC-6 model sensitivity to sediment supplied from the tributaries. Tributary sediment inflow is considered important because floodplain management strategies applied within the watershed such as storm water retention may have adverse impacts on sediment supply. Conversely, grading associated with new construction tends to increase sediment supply. Field and historical evidence suggests that tributary sediment supply does impact morphology.

However, as might be expected from the results of Modeling Scenario #1, the HEC-6

model for the LHWCMP study reach is not sensitive to the supply provided from the tributaries, as shown in Figure 5-10. Note that these results do not necessarily mean that the Hassayampa River is not influenced by tributary sediment supply, since the historical channel morphology analysis clearly demonstrated that the tributaries control lateral channel position to a large degree; it merely indicates that the HEC-6 model is able to tap the reservoir of sediment available in the channel to make up the difference in supply, and/or that the sediment supply from the main stem is significantly larger than the sediment supply from the tributaries.

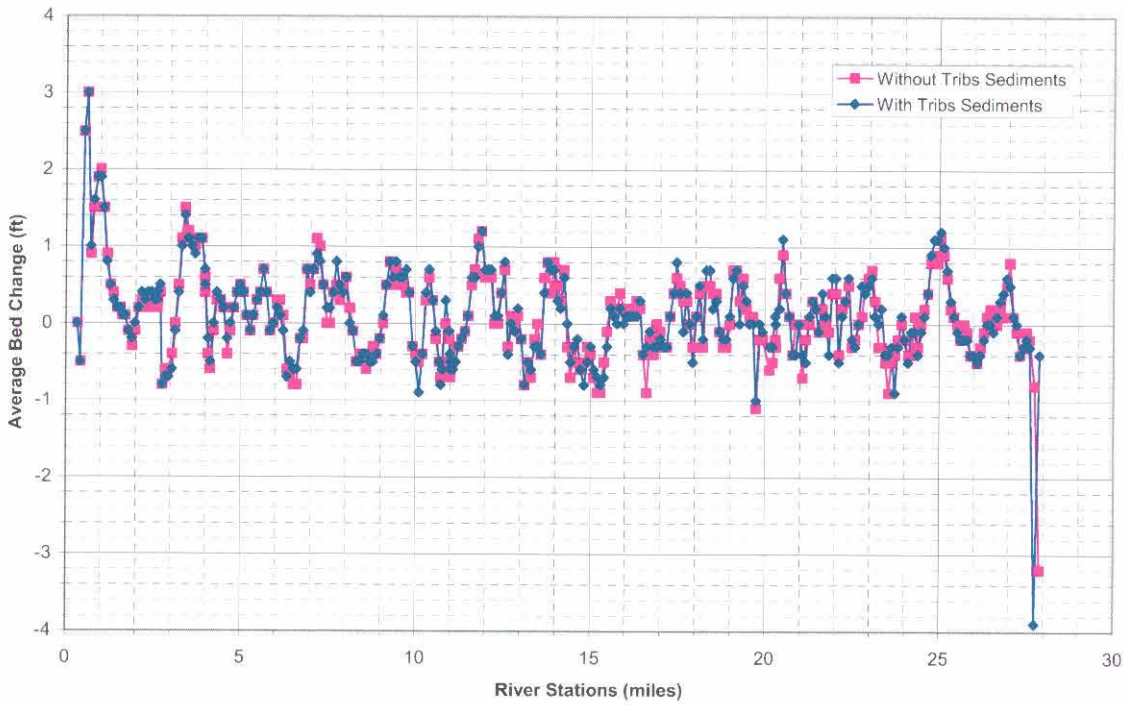

Figure 5-10. Influence of Tributary sediments

5.5.3.4 Scenario #4 - Existing Conditions Model

The existing conditions HEC-6 model was developed using the 2004 topography as the base topographic condition and the WEST HEC-RAS model. The hydrologic data used in the model consisted of the entire period of record mean daily discharges and 100-year hydrograph described in Section 5.3.1.1. The Scenario #4 HEC-6 model reflects the current conditions and is intended for predicting sediment trends and future river behavior.

A number of sensitivity analyses were performed on the Scenario #4 HEC-6 model to test the model sensitivity to various derived or assumed input parameters. A base condition simulation was performed using the long-term hydrograph with the 100-year hydrograph appended to the end of the long-term hydrograph, the results from which are shown in Figure 5-11. Figure 5-11 shows the changes in the average bed elevations as measured up to the 10-year and the 50-year discharges. In other words,

the average bed elevation change is presented by averaging the elevations for the wetted portion of the cross-section during the 10-year and 50-year flow rates. Figure 5-11 shows the average bed computations using 10-year and the 50-year wetted portions of the cross-section give similar results. Predicted net bed elevation changes in the base condition HEC-6 model are uniformly less than one foot throughout the study reach. Table 5-4 shows the sediment load passing through the system. The results also indicate a net deficit of 129 ac. ft. after passage of the long-term hydrograph and a single 100-year event. This result can be interpreted as an average bed change of 0.02 ft for the entire system. The relatively muted response to the long-term flow record and a 100-year flood indicates that the study reach is relatively stable. The general trend shows an overall net aggradation rather than net degradation. The most significant departure from the mean occurs in Reach 1 at the confluence with the Gila River. Predicted deposition is this reach is probably due to loss of flow by levee overtopping, without loss of sediment supply. As the flow rate decreases in the downstream direction, the sediment transport capacity also decreases and sediment is deposited. This reach is also potentially impacted by backwater from the Gila and some flattening of slope on the historic delta of the Hassayampa River in the Gila River floodplain. Interestingly, historical data indicate that this reach has experienced long-term degradation, rather than aggradation, probably due to decreased base level along the Gila River. Base level adjustments are not simulated very well by HEC-6.

Table 5-4. Sediment load passing through the system

Flow Description	Sediment leaving the system at downstream end of the model (tons)	Load Through System (ac. ft)
Long-term flows Only	591092	173
Long-term flows and 100-year event	839589	265

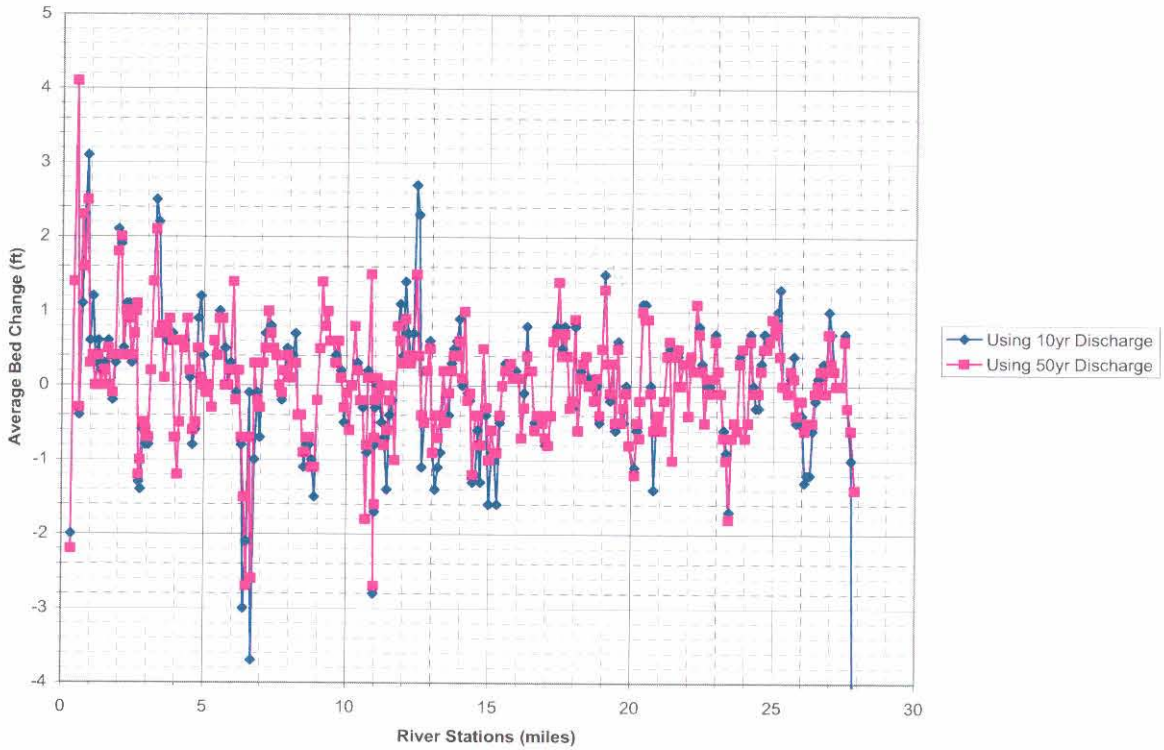

Figure 5-11. Average Bed Change – Base Conditions Model

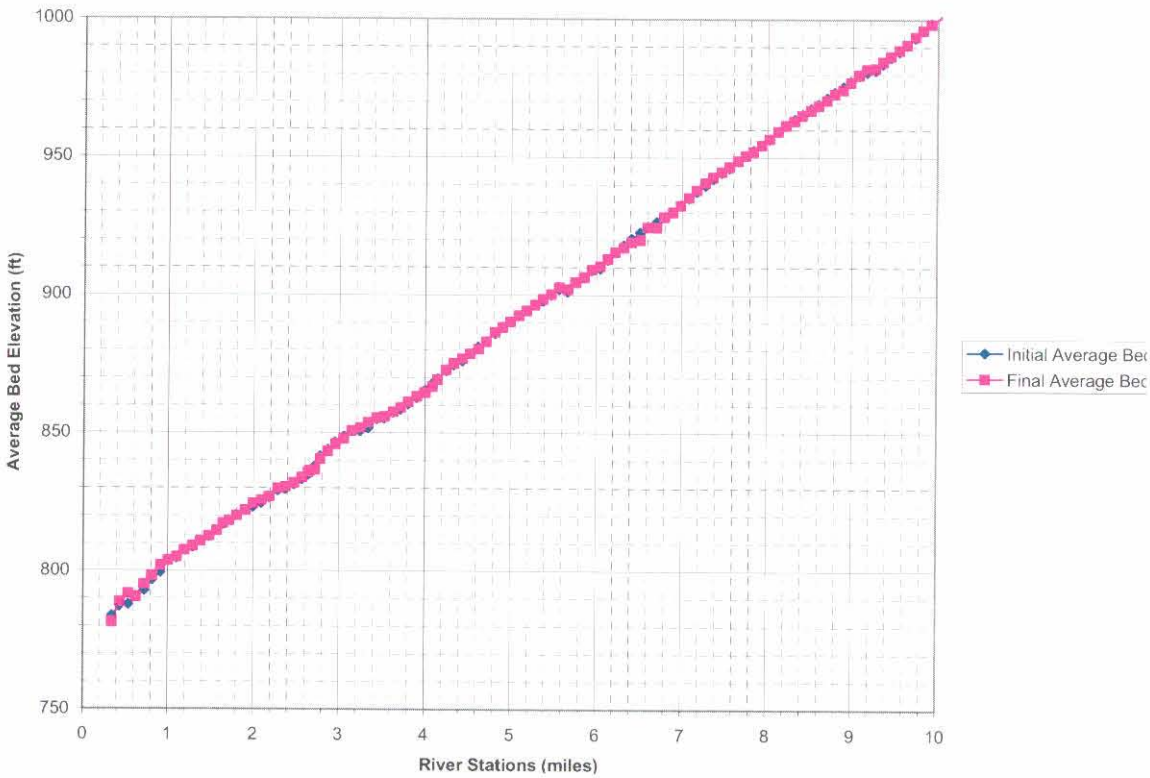

Figure 5-12. Initial and Final Average Bed Elevations (1 of 3)

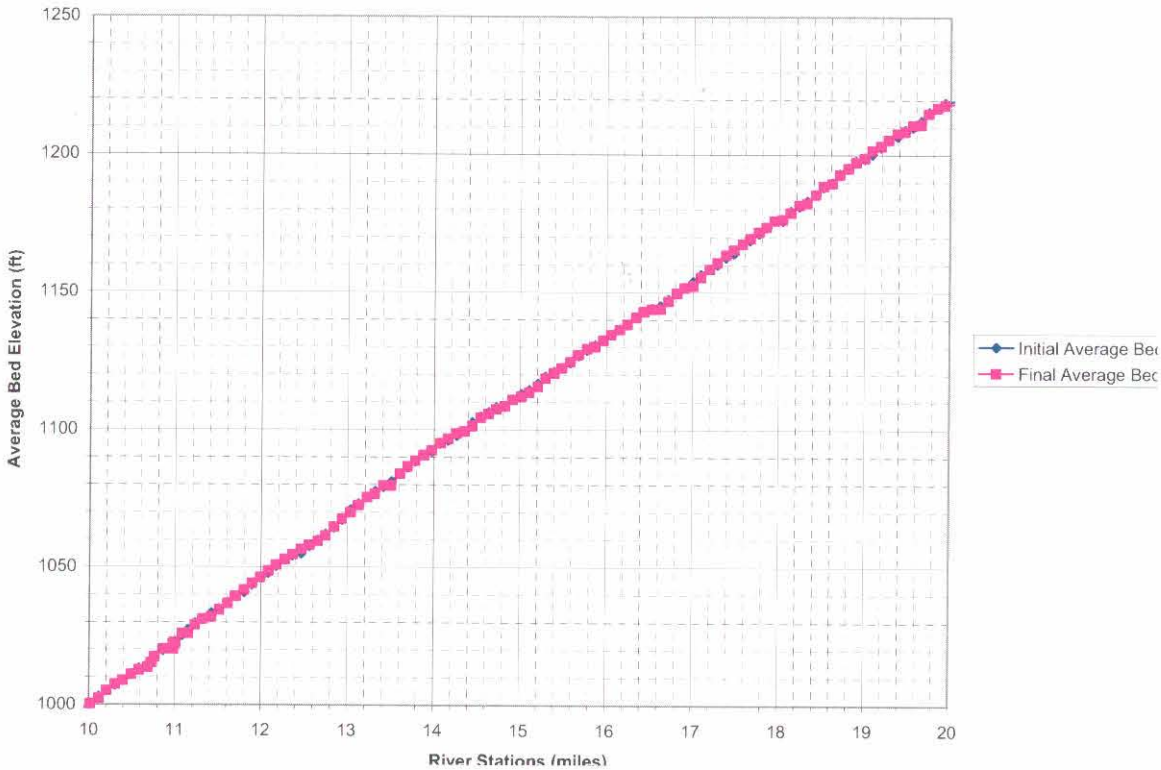

Figure 5-13. Initial and Final Average Bed Elevations (2 of 3)

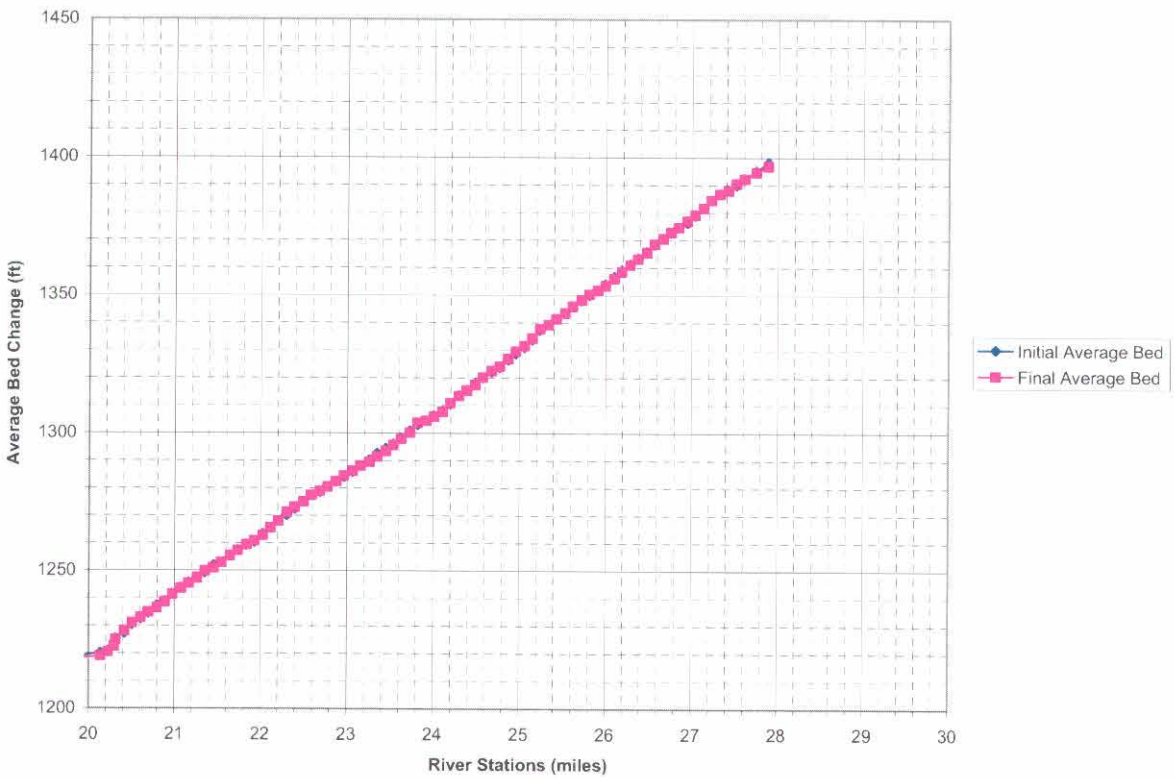

Figure 5-14. Initial and Final Average Bed Elevations (3 of 3)

The following sensitivity analyses were performed on the Scenario #4 base model to evaluate various input parameters:

- Manning's N Value
- Sediment Inflows
- Sediment Particle Size

The results of the sensitivity analyses are described in the following sections.

5.5.3.4.1 Manning's N Value Sensitivity Analysis

The Manning's N values were changed from the base values by ±20% and ±40%. The values were varied to investigate the effect of changes in vegetative cover, formation of channel bed forms, or other alternations of the channel and floodplain. As shown in Figure 5-15, changes in the predicted net bed elevation were observed only at the upstream and downstream ends where the model is influenced by the boundary conditions, with no discernable changes in the rest of the study reach. Thus, the results indicate that the model is not very sensitive to changes in Manning's N.

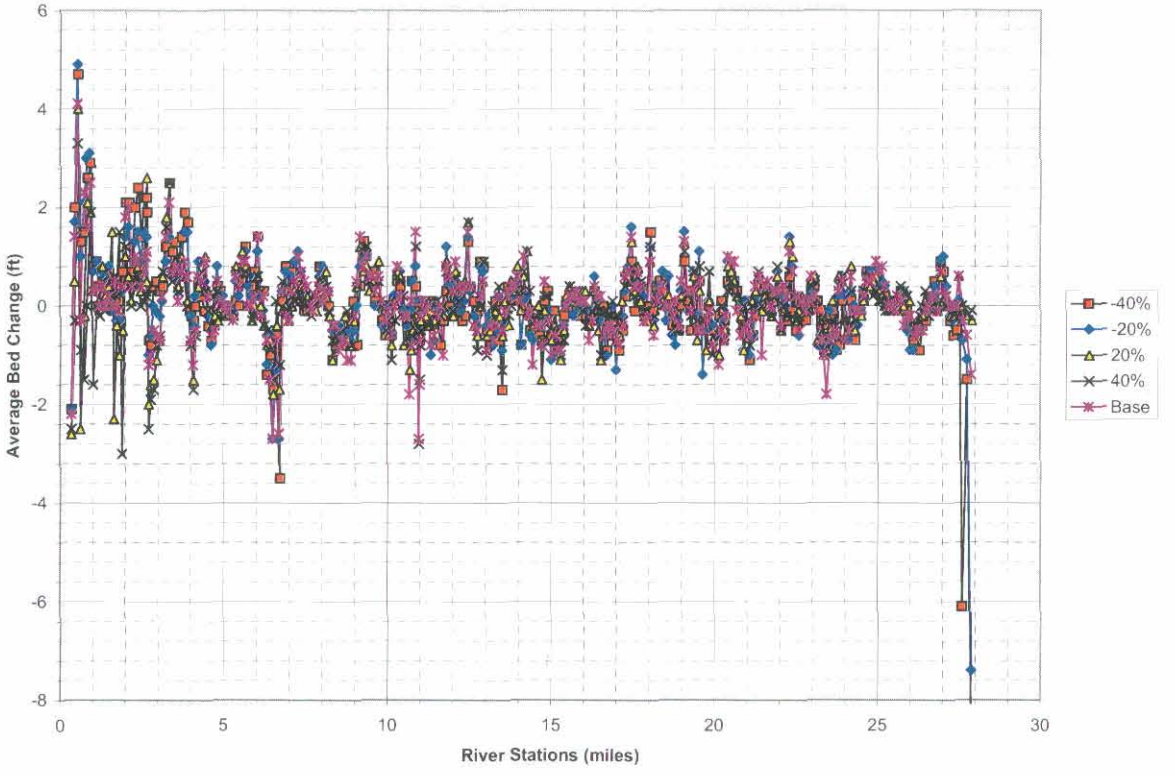

Figure 5-15. Manning's n value sensitivity

5.5.3.4.2 Sediment inflow sensitivity analyses

The sediment inflow values were varied from the base values by ±20% and ±40%, with

the results shown in Figure 5-16. As with the Scenario #1 results, no discernable changes in the predicted net bed elevation change were observed in the study reach due to increases or decreases in sediment inflow. These results indicate that the model is not sensitive to changes in sediment inflow rate. The adjustment to the sediment deficit or surplus occurs in the upstream few cross-sections so that the sediment transport capacity is achieved for most of the study reach.

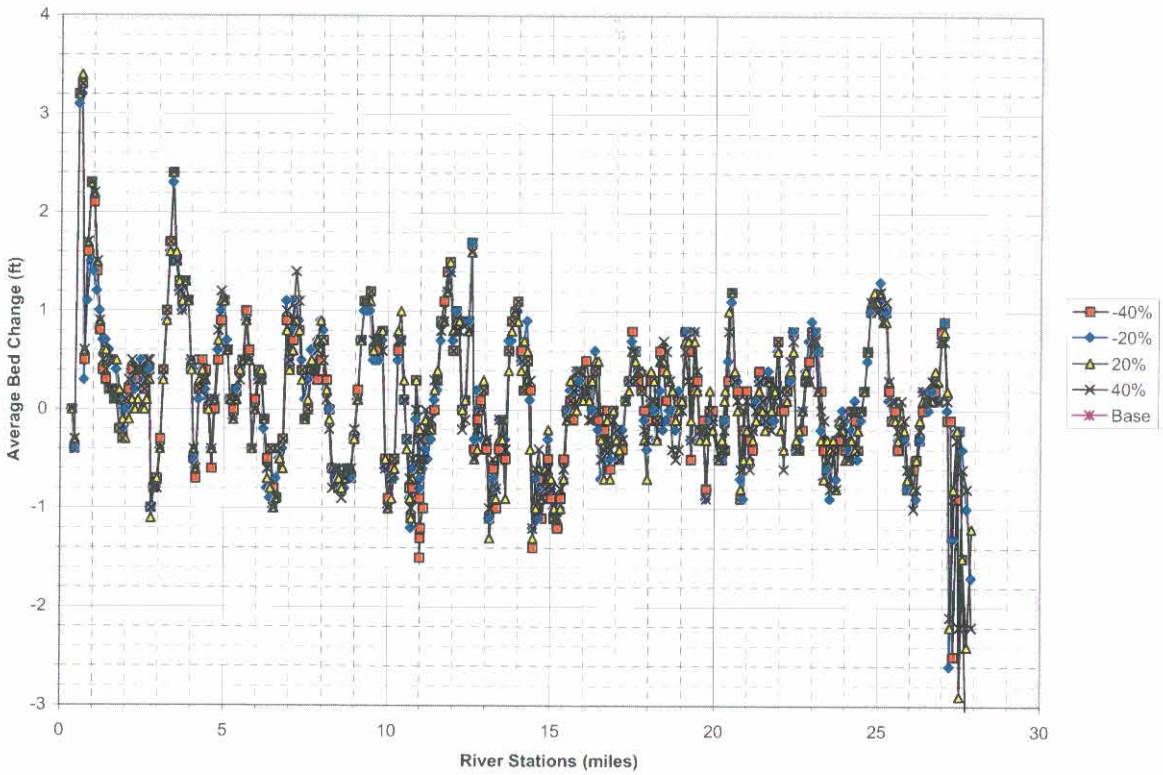

Figure 5-16. Sediment Inflow Sensitivity

5.5.3.4.3 *Particle size sensitivity analysis*

Base model sensitivity to changes in particle size was tested by shifting the reach-average sediment gradation curve along the logarithmic scale in two directions. This procedure preserves the shape of the curve which, in turn, preserves relative sediment distribution, but increases or decreases the particle size. Two adjusted sediment distribution curves were generated, one representing smaller sediment sizes and the other representing larger sediment sizes. Figure 5-17 shows the three gradation curves. The median (d50) grain sizes of the three curves are approximately 0.3 mm, 0.45 mm and 0.73 mm. The sensitivity of the model to these three gradation curves is presented in Figure 5-18. It can be seen that the model is behaving as anticipated with finer sediments resulting in larger bed change and coarser smaller. However, the variations from the base conditions is not significant in most locations and, therefore, it is concluded that the HEC-6 base model results are not sensitive to particle size.

5.5.3.4.4 *Transport function*

District staff requested that no sensitivity analysis be performed for the sediment

transport function.

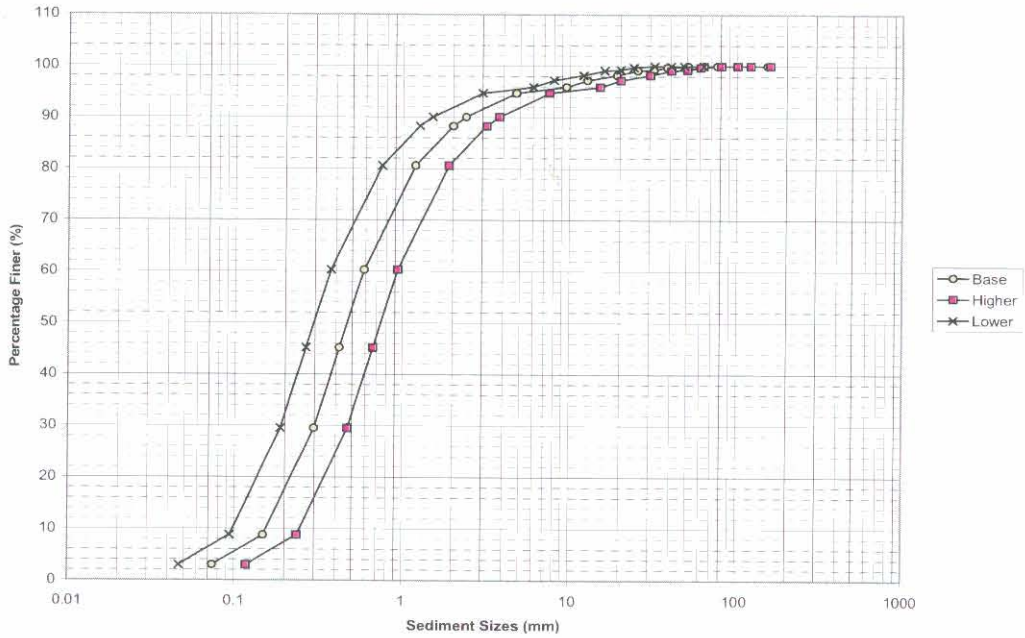

Figure 5-17. Particle size sensitivity

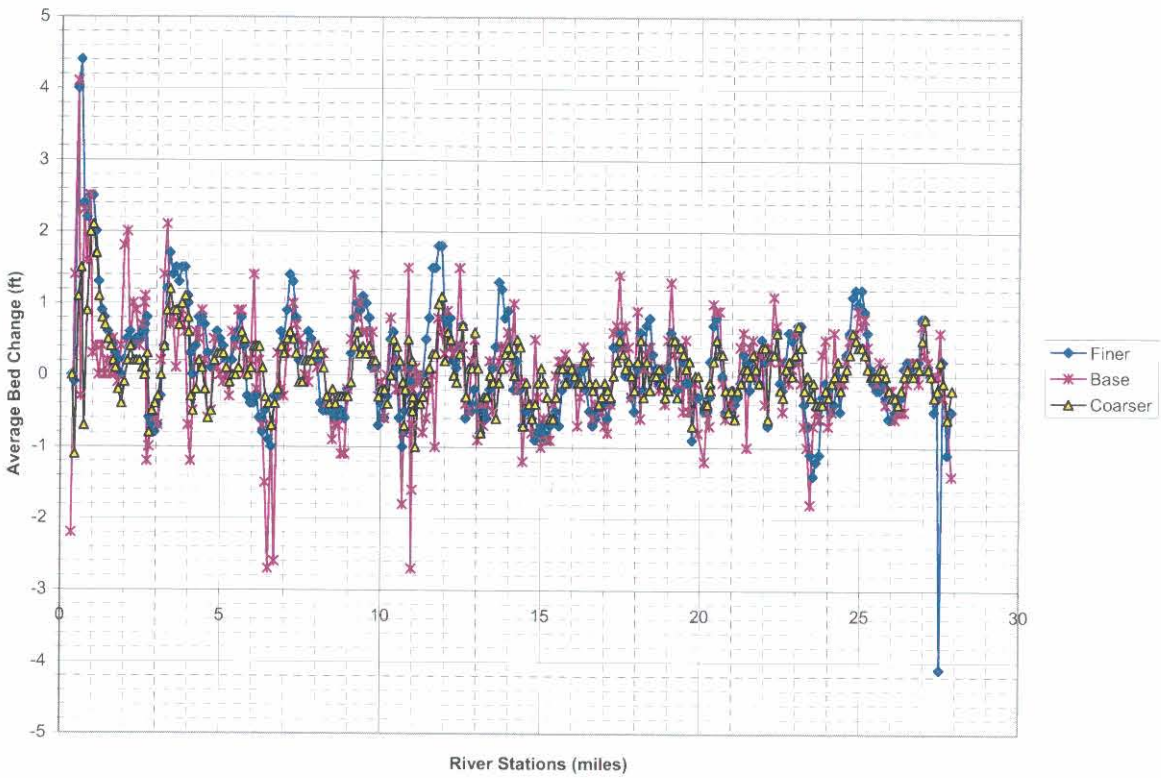

Figure 5-18. Particle size sensitivity

5.5.4 HEC-6 Modeling Results

The following conclusions can be drawn from the HEC-6 modeling summarized above:

- Model Sensitivity. The HEC-6 model of the LHWMCP study reach is not sensitive to Manning's N value, main stem sediment inflow, tributary sediment inflow, and sediment particle size.

- Aggradation. The HEC-6 model predicts slight net sediment deposition (aggradation) in the Lower Hassayampa River study reach.

- Vertical Stability. The HEC-6 model predicts that net vertical channel change will be minor if the watershed and channel remains undisturbed. The relatively muted predicted response is probably due to low annual flow volumes and/or relatively flashy flood hydrographs.

- Sediment Transport. The Hassayampa River moves very large volumes of sediment through the study reach, but transport is balanced to a near equilibrium state under existing conditions.

- Expected Trend. Neither significant degradation nor aggradation is expected for the study reach if existing channel and watershed conditions are preserved.

- Alternative Evaluation. The existing conditions model (Scenario #4) is intended for use in alternatives evaluation in Phase 2 of the LHWCMP.

These results are generally consistent with the field and historical observations summarized in Chapters 2 and 3, and the bed elevation data in Chapter 4.

5.6 Reach Equation Analysis

A sediment transport analysis using the same sediment transport function used in the HEC-6 modeling was applied on a reach-by-reach basis to compare with the HEC-6 modeling results.

5.6.1 Transport functions

5.6.1.1 Methodology

A simplified approach to evaluate sediment transport in the study reach was applied using sediment transport functions. The purpose of this procedure is to determine the transport characteristics using reach-averaged approach. The adopted procedure consisted of the following steps:

1. The study reach was divided into 10 subreaches. The subreaches were defined so that the computed HEC-RAS hydraulic characteristics did not vary significantly within any one reach.

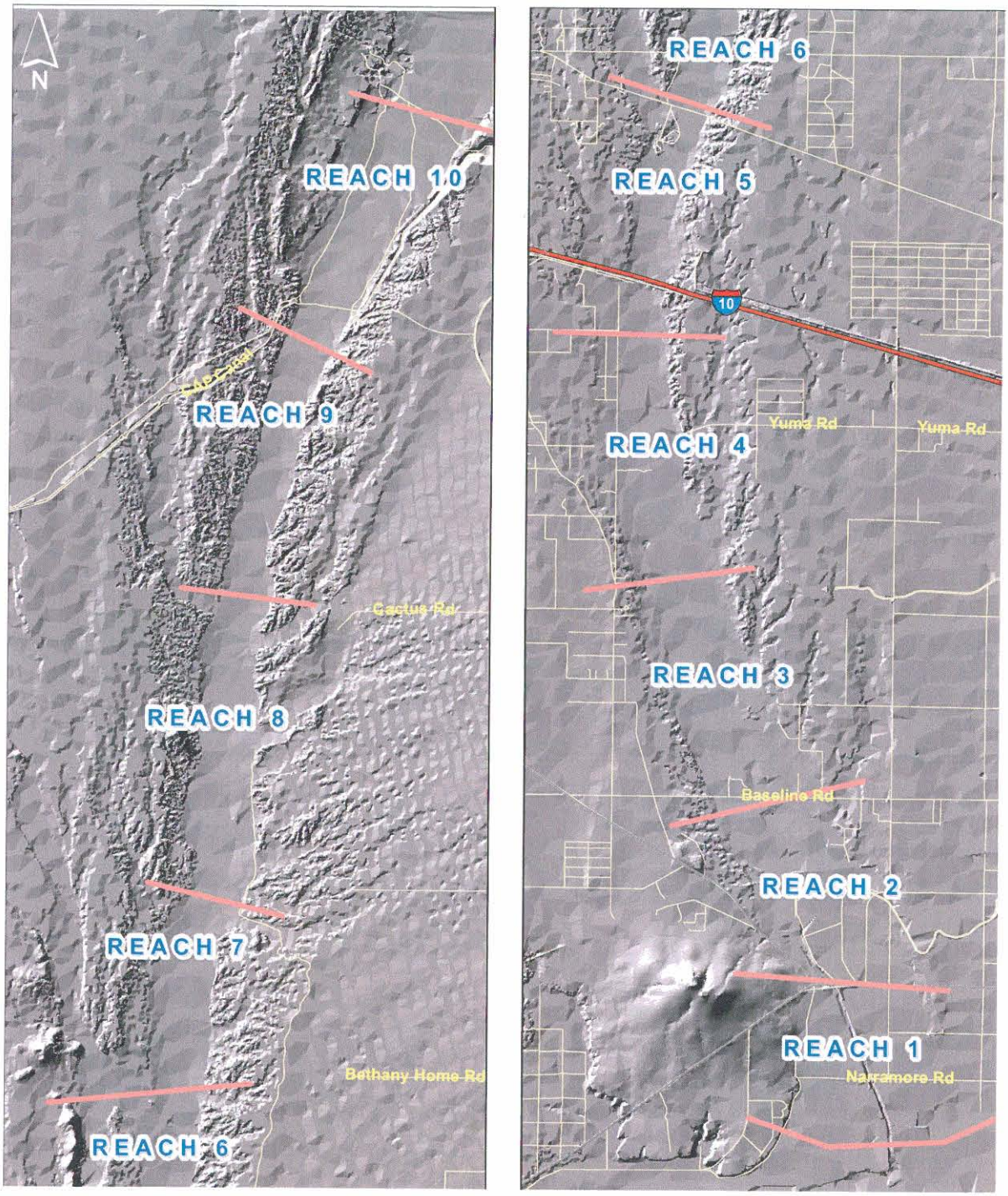

Figure 5-19. Reach limits

The 100-year design hydrograph was discretized into a histogram of constant discharges for defined time intervals. The discretization was performed using the following flow rates: 250 cfs, 500 cfs, 1,000 cfs, 2,000 cfs, 5,000 cfs, 20,000 cfs, 50,000 cfs and 75,000 cfs. The duration for each flow interval was determined from the histogram. Table 5-5 and Table 5-6 show the discretizations of the hydrographs, as

well as where the duration of the segment of the hydrograph between the minimum and maximum value is determined and applied to the corresponding flow value.

Table 5-5. Long-Term Hydrograph Discretizations			
Flow (cfs)	Minimum value (cfs)	Maximum value (cfs)	Duration(days)
250	0	300	1304
500	300	750	202
1000	750	1300	71
2000	1300	3500	49
5000	3500	6500	9
10000	6500	13500	6
20000	13500	30000	0
50000	30000	60000	0
75000	60000	85000	0

Table 5-6. 100-year Event Hydrograph Discretizations			
Flow (cfs)	Minimum value (cfs)	Maximum value (cfs)	Duration(hours)
250	0	300	1.5
500	300	750	3.6
1000	750	1300	3.3
2000	1300	3500	10.9
5000	3500	6500	7.6
10000	6500	13500	12.9
20000	13500	30000	19.6
50000	30000	60000	20.9
75000	60000	85000	9.3

2. HEC-RAS model developed for the LHWCMP described in Chapter 3 was used to generate hydraulic data for each subreach. The HEC-RAS results were imported into a spreadsheet.

3. Using the estimated hydraulic parameters, such as velocity, hydraulic depth, Manning's N value, and energy slope, the Tofaleti-MPM sediment transport function was used to compute sediment transport capacity at each cross-section. The sediment transport function was used to derive the sediment transport capacity, and the average sediment transport capacity for each subreach was determined.

4. The Exner equation was used to determine the change in the bed sediment volume for each subreach for each time segment. The individual volume changes for each time segment were summed to give net volume changed in the sub-reach.

5. The net volume change was applied the subreach, using the average width and reach length to estimate the average bed elevation change.

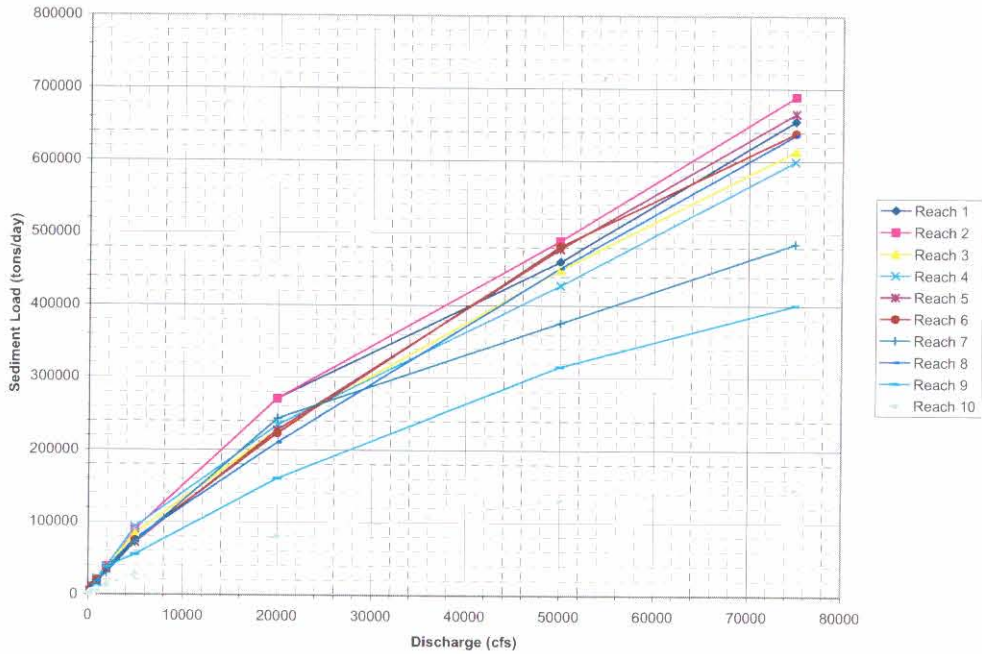

Figure 5-20. Sediment Transport Capacity by Subreach

5.6.1.2 Results & Interpretation

The computed sediment transport rating curves for each of the 10 subreaches are shown in Figure 5-20. The subreaches are numbered from upstream to downstream (i.e., Subreach 10 is at the Gila River confluence). From Figure 5-20, it can be seen that the sediment transport capacity is relatively uniform throughout the LHWCMP study reach except in the subreach between the Gila River confluence and the SPRR Bridge. The subreaches at the downstream end of model are leveed and the flow overtops the levees, leading to reduction in the flow. This discharge reduction decreases sediment transport capacity. In general, transport capacity reduction causes deposition, which is apparent in the subsequent bed-change calculations presented below.

The Table 5-7 and Table 5-8 present the results for the long-term hydrograph and the 100 year hydrograph, respectively. The results show that the flows smaller than 500 cfs cause most of the long-term bed changes, probably because most of the historical flow volume occurred at flow rates less than 500 cfs. In addition, the results indicate that significant deposition occurs at the downstream end of the study reach. A similar trend was observed in the HEC-6 modeling. The driving mechanism for this deposition is the effect on reach hydraulics of loss of flow overtopping the levee. The reaches where degradation is predicted (Subreach 3-4, 5-6, and 7-8) occur in no particular geomorphic setting.

Table 5-7. Long-Term Reach-By-Reach Bed Change (ft)									
Flow (cfs)	Reach 1-2	Reach 2-3	Reach 3-4	Reach 4-5	Reach 5-6	Reach 6-7	Reach 7-8	Reach 8-9	Reach 9-10
250	10	16	-2	5	-1	5	-3	-1	2
500	5	4	0	1	-1	1	-1	1	0
1000	3	2	0	0	0	1	-1	0	0
2000	3	0	-1	1	0	0	0	0	0
5000	1	0	0	0	0	0	0	0	0
20000	1	0	0	0	0	0	0	0	0
50000	0	0	0	0	0	0	0	0	0
75000	0	0	0	0	0	0	0	0	0
Total	23	22	-3	7	-2	7	-5	0	2

For the 100-year hydrograph response shown in Table 5-8, the results indicate no net change is predicted except at the very highest flow rates, or at least the predicted changes are smaller than one significant figure. Like the HEC-6 results, deposition is predicted in the downstream leveed reach. Net scour is predicted upstream of the Jackrabbit Wash, upstream of the I-10 Bridge, and in Reach 2 upstream of the SPRR Bridge. The predicted trends for the long-term flow analysis were dissimilar to the predicted trends for the 100-year event simulation.

Table 5-8. 100-Year Event Reach-By-Reach Bed Change **(ft)**									
Flow (cfs)	Reach 1-2	Reach 2-3	Reach 3-4	Reach 4-5	Reach 5-6	Reach 6-7	Reach 7-8	Reach 8-9	Reach 9-10
250	0.00	0.00	0.00	0.00	0.00	0.00	0.00	0.00	0.00
500	0.00	0.00	0.00	0.00	0.00	0.00	0.00	0.00	0.00
1000	0.01	0.00	0.00	0.00	0.00	0.00	0.00	0.00	0.00
2000	0.03	0.00	0.00	0.01	0.00	0.00	0.00	0.00	0.00
5000	0.03	0.01	0.00	0.00	0.00	0.01	0.00	0.00	0.00
20000	0.08	0.02	0.01	-0.01	0.00	0.00	0.00	0.01	0.00
50000	0.20	0.05	-0.02	0.03	0.00	-0.02	0.01	0.01	-0.01
75000	0.27	0.07	-0.03	0.04	0.01	-0.02	0.00	0.02	-0.01
Total	0.62	0.15	-0.05	0.08	0.01	-0.02	0.00	0.04	-0.01

5.6.1.3 Comparison with HEC-6 Model Results

The subreach-averages from the HEC-6 model results are presented in Table 5-9. A comparison of the HEC-6 modeling results and the spreadsheet-based results shows that the approximate method generated higher estimates of net deposition or scour than the HEC-6 model results. From the results, it can be concluded that the spreadsheet based method provides reasonable qualitative estimates which can be used to determine whether a reach is stable, eroding or aggrading. This could be significant due to the ease of applying the spreadsheet-based method compared to the extensive efforts involved in HEC-6 modeling.

Table 5-9. HEC-6 Reach-By-Reach Net Bed Change									
Reach 1	Reach 2	Reach 3	Reach 4	Reach 5	Reach 6	Reach 7	Reach 8	Reach 9	Reach 10
0.04	-0.02	0.03	0.09	-0.15	0.16	0.07	0.16	0.33	0.76

5.6.2 Safe Yield Recommendation

The concept of safe yield implies that a certain volume of "excess" sediment can be removed from the river without impacting the overall stream system. Neglecting the theoretical deficiencies of the existence of "excess" sediment in a self-formed, natural river system like the Lower Hassayampa River, the HEC-6 base model results indicate that no significant long-term trend towards aggradation is expected in the Lower Hassayampa River. Field evidence clearly demonstrates that in-stream excavations lead to significant headcutting and that no physical evidence of long-term aggradation exists. However, HEC-6 sensitivity analyses and field observations at the in-stream excavations during the floods of December 2004 indicate that a significant sediment reservoir exists in the bed, banks and floodplain of the study reach. According to those results, isolated pits will have little impact on the short-term overall morphology of the river. Therefore, it is concluded that there is no safe yield for the Lower Hassayampa River.

5.7 In-Stream Mining Impact Analyses

An analysis was performed to assess the effectiveness of using HEC-6 to model sand and gravel mining impacts, and to identify alternative methods for assessing the impacts of sand and gravel mining in the flood and erosion hazard zone.

5.7.1 Methodologies

An evaluation of the capabilities of the models to predict the headcut and tailcut development for in-stream gravel pits was performed. The presence of sand and gravel mining pits was investigated by using the following methods:

- ADOT Procedure (Simons, Li and Associates , 1986)
- HEC-6 Modeling

Additional models were evaluated as dictated by the LHWCMP scope of work (Task 9.6.8), but were not included in this report at the direction of District staff. The details of the two analyses listed above are presented below.

5.7.2 Model Geometry Data

The mining impact analysis evaluates the effectiveness of the selected models to predict pit scour. To allow an effective comparison, simple model geometry was used for both the channel and overbank. A rectangular channel and rectangular in-stream pit were simulated. The dimensions of the rectangular channel and the pit were chosen to approximately represent a typical mining scenario in the Lower Hassayampa River. The following three typical mining scenarios were evaluated:

- Mining Pit Occupies Entire Floodplain Width (Figure 5-21)
- Mining Pit Occupies Part of Floodway in Center of Channel (Figure 5-22)
- Mining Pit Occupies Part of Floodway Fringe On One Side of River (Figure 5-23)

A summary of the selected parameters is presented in Table 5-10.

Table 5-10. Pit Analyses Parameters (ft)

Description	Side	Middle	Full
Width of the Channel (ft)	1,800	1,800	1,800
Pit width (ft)	800	800	1,800
Pit length (ft)	1,000	1,000	1,000
Pit Depth (ft)	30	30	30
Slope of the channel	0.004	0.004	0.004
Downstream Reach Length (ft)	15,000	15,000	15,000
Upstream Reach Length (ft)	15,000	15,000	15,000
Manning's n	0.035	0.035	0.035

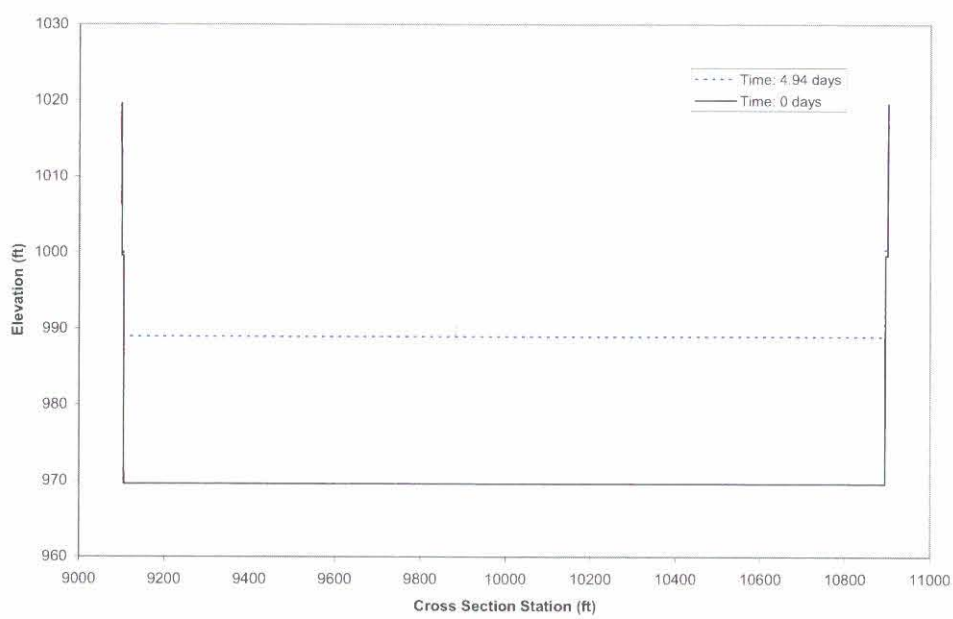

Figure 5-21. Cross Section for Pit Occupying Entire Floodplain.

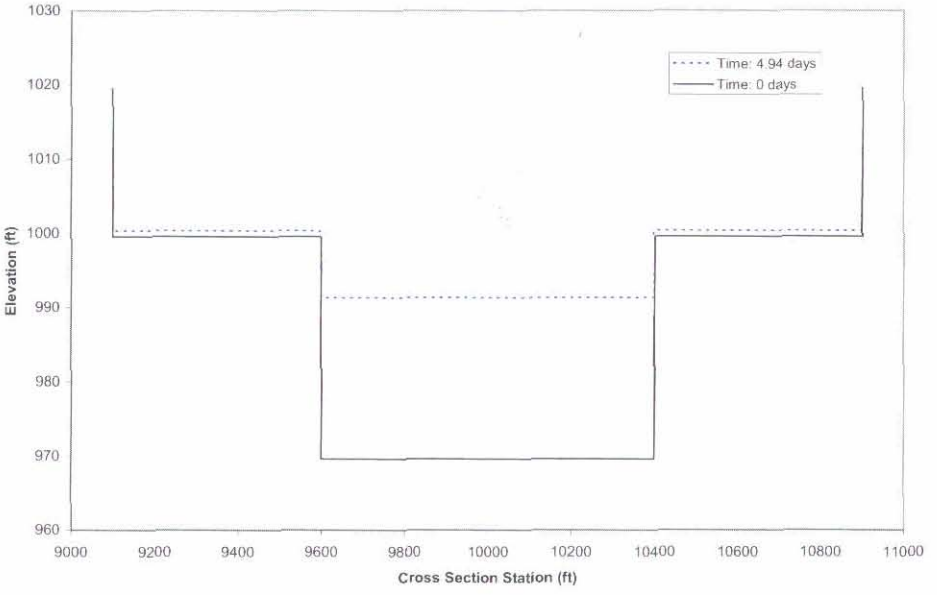

Figure 5-22. Cross Section for Pit Occupying Part of Channel

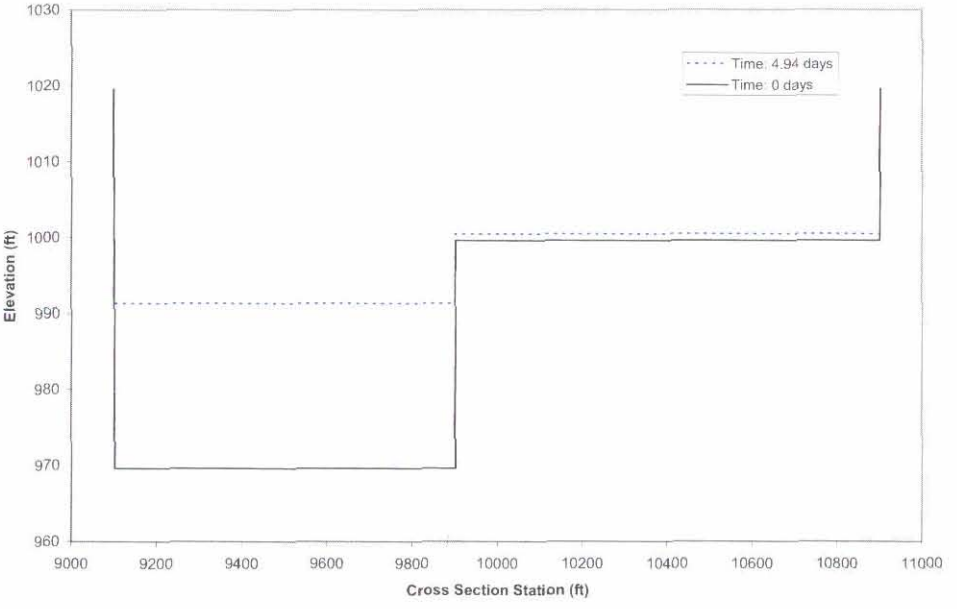

Figure 5-23. Cross Section for Pit Located in Floodway Fringe.

5.7.3 Flow Hydrograph

The flow hydrographs for a 100-year and 10-year event were analyzed. The recent flood event of 2004-2005 was also considered to simulate a typical runoff event. The flood hydrographs were discretized as needed in the each of the selected models.

5.7.4 Sediment Data

The reach-average sediment gradation curve presented in Section 5.1 was used to perform the pit analyses.

5.7.5 ADOT Procedure

Simons, Li and Associates (1986) developed a procedure for the Arizona Department of Transportation (ADOT). The procedure calculates long-term scour and short-term pit scour in the reaches adjacent to an in-stream mine, as documented in the ADOT Report (SLA, 1986). A numerical model was developed by SLA to investigate various scenarios of upstream and downstream scour caused by in-stream mining. Based on the results from the SLA numerical model, SLA developed regression equations to predict scour upstream (headcutting) and downstream (tailcutting) of the pit.

A spreadsheet was developed by JEF to perform the ADOT method calculations. The calculation details are presented in Appendix 5.6. The ADOT procedure is independent of the pit location and position within the channel. As a result, all three scenarios are represented by single set of calculations, the results of which are summarized in **Table 5-11** for the 100-year, 10-year, and the typical runoff events. The results indicate that the 10 year, 100-year and typical events with long durations can have similar headcut and tailcut geometry.

Table 5-11. ADOT Procedure Pit Analysis Results

Flow Event	Headcut		Tailcut	
	Length of Scour (ft)	Scour Depth (ft)	Length of Scour (ft)	Scour Depth (ft)
Typical Event	139	7	4948	14.4
10-Year	154	14.2	4929	14.6
100-Year	189	15	4675	18

The advantages of the ADOT method include the following:

- The procedure was specifically developed to analyze pit scour
- The procedure incorporates arid conditions where the flow enters an empty pit, fills it and then flows downstream
- The procedure is relatively simple
- The procedure includes consideration of potential armoring
- The headcut and tailcut channel geometry is based on regime equations
- The method accounts for water volume and the time to fill the excavation
- Tailcutting is not computed unless the pit fills and overflows

The disadvantages of the ADOT method include the following:

- The model is applicable only to pits unaffected by scour from previous flow events. That is, cumulative affects of multiple events or mining in between events is not simulated.
- The model is developed based on simple pit and channel geometries and does

not include site specific geometries, unique pit layouts, or pit alignments.
- The mathematical procedures are somewhat complex and required iterative solutions or spreadsheet programming.
- The model assumes headcutting ceases when the pit fills with water
- The model limits the headcut depth to one-half the pit depth
- Sediment supply and upstream transport capacity are not accounted for

In general, field observations made during the December 2004 flood and the smaller floods preceding it do not support the ADOT method results. Observed headcuts were longer, deeper, and wider than predicted. In addition, during the larger flood sediment completely filled the in-channel excavation due to the high sediment load in the river.

5.7.6 HEC-6

HEC-6 was also used to assess potential scour near the hypothetical in-stream mine described above for the same set of flow events. Sample HEC-6 model results are presented in Figure 5-24 to Figure 5-26, which show the predicted changes in thalweg elevation. The results predict some sediment accumulation inside the pit, and headcut or tailcut development where expected. Initial model runs did not predict either headcutting or tailcutting and had significant model instabilities indicated by a "zigzag" bed elevation pattern observed in the post-sedimentation thalweg profiles. The zigzag pattern is a typical outcome of numerical instability in the model and is generally overcome by reducing the duration of internal calculation time-steps, as well as by increasing the distance between cross-sections. In this case, the steps taken to reduce numerical stability had the effect of enabling the model to generate a headcut and tailcut profile.

The zigzag pattern is also more pronounced for steeper channels. Reducing the time-steps increases the total number of computations, while reducing the number of cross-sections decrease the computational accuracy. The weighting factors for numerical integration provide another mechanism for fine-tuning the numerical stability. Experimenting with the time-step, the cross-section spacing, and weighting factors revealed that most of the zigzag developments in the model could be eliminated with patience and numerous trials.

The advantages of the HEC-6 model for modeling sand and gravel impacts include the following:

- HEC-6 can use site specific pit and channel geometric data
- HEC-6 is widely used and is available for free
- HEC-6 allows selection of several sediment transport equations
- HEC-6 performs sediment volume accounting
- HEC-6 accounts for variation in upstream sediment supply
- HEC-6 computes headcutting after the pit fills with water and does not limit the headcut depth to one-half the pit depth

The disadvantages of the HEC-6 for modeling sand and gravel impacts include the following:

- Model instability may prevent the model from showing headcut and tailcut erosion. Significant time investment, patience, and modeler experience may be required to eliminate model instability.
- HEC-6 is a steady state model and computes the backwater profile as if the pit were filled by water at the first time step (Q>0 cfs). Consequently, the model does not account for the time to fill the pit with floodwater before computing tailcut erosion. In addition, it does not properly model the hydraulics of flow entering an empty pit.
- HEC-6 may run without an error message but generate nonsensical results, causing difficulty for inexperienced users and reviewers.
- The hydraulics and sediment continuity computations are not clearly explained in the model documentation to demonstrate how the model considers a partially excavated channel. For example, HEC-6 averages the bed elevation change over the entire cross section. Where the pit only occupies a small part of the channel it is not clear whether the model subroutines accurately depict channel processes.
- HEC-6 spreads the sediment deficit across the entire mobile bed width upstream and downstream of the pit, thus muting the predicted headcut and tailcut profiles.
- Additional HEC-6 limitations and assumptions were discussed in Section 5.5.1

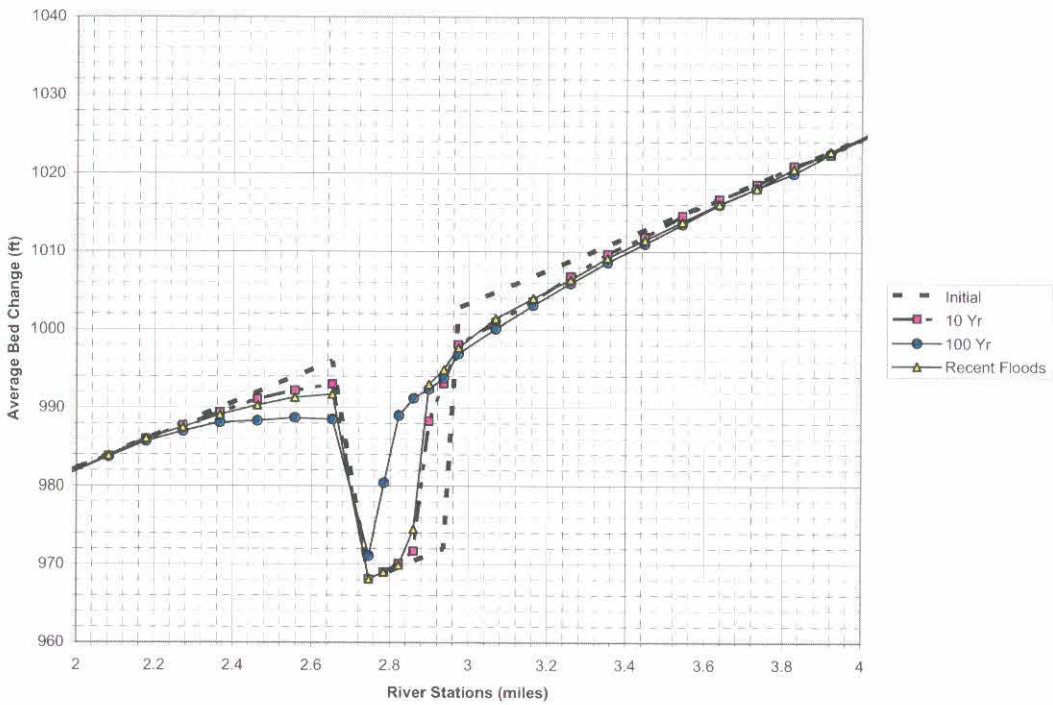

Figure 5-24. Gravel Pit Analysis – Pit Occupying Full Width Of Channel

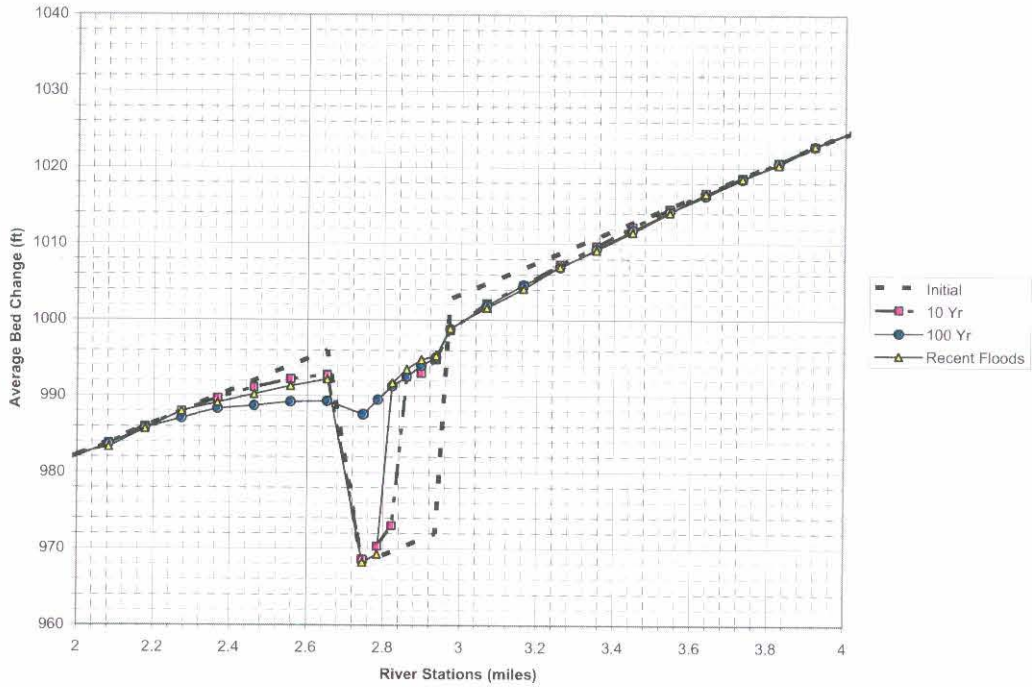

Figure 5-25. Gravel Pit Analysis – Pit Located At One Side Of Channel

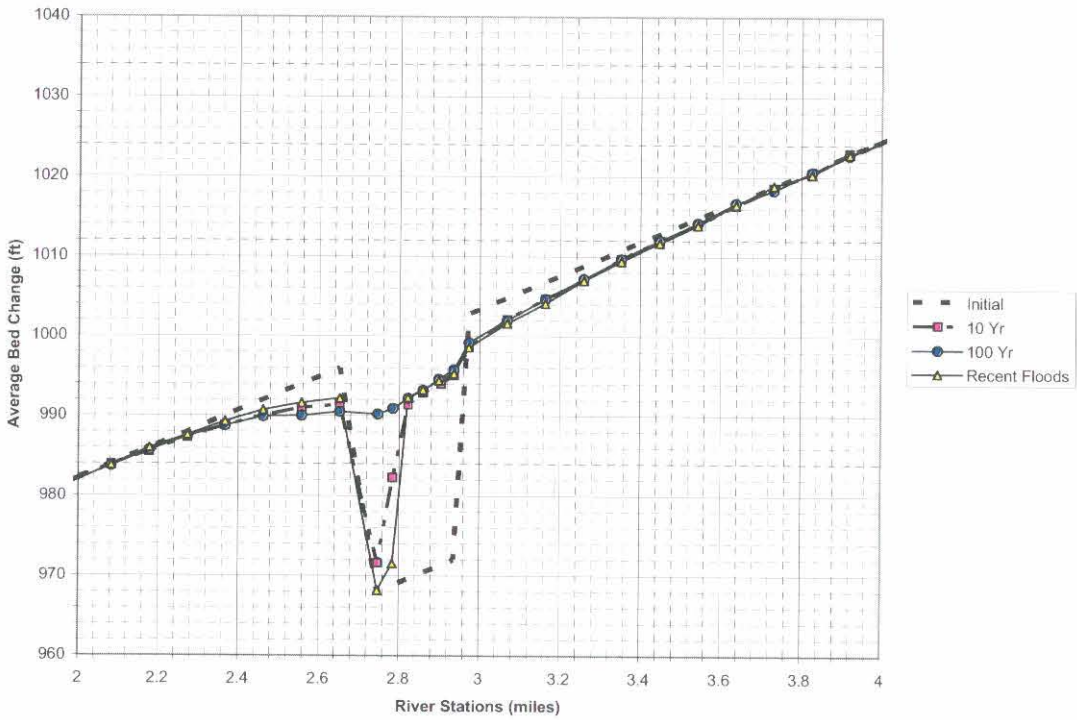

Figure 5-26. Gravel Pit Analysis – Pit Located At Middle Of Channel

From the results presented in Figure 5-24, Figure 5-21, and Figure 5-26, it can be seen that the cases in which the pit occupies the entire channel and the case in which the pit is in the middle show significantly more deposition than the case in which the pit is located on one side of the channel. For 100-year flow, the smaller pit fills entirely, unlike the pit occupying the entire channel. It can also be observed that the headcut and tailcut developments are similar for all the three cases.

The HEC-6 model results presented in the previous sections indicate some capability of the modeling to simulate the headcut and tailcut development. One of the main drawbacks of the HEC-6 modeling is the need for the flow to exist in the entire study reach. In reality, the flow would enter the pit first, which is of great significance in ephemeral river systems in which the channel is dry most of the time. In such a case, the pit will fill with water while the headcut develops simultaneously. Since no outflow occurs during the time the pit is filling, the tailcutting should not begin until outflow from the pit begins. Meanwhile, significant deposition could occur inside the pit. The model's requirement for steady flow (same amount of flow exists in the entire study reach) potentially distorts the sedimentation that can occur at the pits. In contrast, the ADOT procedure is based on the numerical results from a model that considers the sequence of pit filling before any occurrence of outflow.

5.7.7 In-Stream Mining Impact Analysis Summary

The pit-scour analyses were performed using the ADOT procedure and HEC-6. The results indicate significantly differing predictions of headcut/tailcut length, depth and width. HEC-6 predicted headcut/tailcut lengths that far exceed the estimates generated using the ADOT equations, but the ADOT equations predicted much greater maximum headcut/tailcut depths. The ADOT equations predicted relatively narrow, regime-geometry headcut/tailcut channel widths, while HEC-6 necessarily predicted adjustments that span the entire mobile bed width.

The evaluation indicates that each method has advantages and disadvantages. HEC-6 modeling requires significant effort to develop hydraulic data and specialized expertise to interpret the results. HEC-6 is not specifically developed for analysis for pit scour and may result in erroneous results.

5.8 Summary

Sediment transport models were developed for the Lower Hassayampa River. The existing conditions HEC-6 model (Scenario #4) is intended for use in alternatives evaluation in Phase 2 of the LHWCMP. Results generally indicate that the existing condition of the river is stable, and some resiliency to changes in sediment supply, at least for the short-term. For existing condition, sediment deposition or scour are not likely to significantly impact regulatory water surface elevations, at least on a regional scale. In-stream mining is likely to cause headcutting and tailcutting in the vicinity of the excavations.

CHAPTER 6 - LATERAL MIGRATION ANALYSIS

6.1 Objectives

The objectives of the lateral migration analysis were to estimate the potential for future lateral migration of the Lower Hassayampa River and to develop regulatory erosion hazard zone boundaries within the study area. In addition to the analyses and results described in Chapters 2 to 5 of this report, the lateral migration analysis relied on the following evaluations described in this Chapter:

- Historical Channel Change Analysis
- Historical Flood Impact Analysis
- Channel Locational Probability Analysis

An existing conditions erosion hazard zone was also developed for Jackrabbit Wash from the Central Arizona Project (CAP) Siphon to the Hassayampa River confluence. This chapter describes the methodology used to define the recommended erosion hazard boundaries for the Hassayampa River and Jackrabbit Wash.

6.2 Historical Channel Change Analysis

Mapping of existing and historical functional surfaces within the floodplain and historical avulsive channel changes was described in Chapter 3. The historical channel change analysis described in this Section focuses on movement of the active channel during the period of record. The maximum measured channel movement within the 70-year period of record for each reach was determined by comparing active channel positions on the semi-rectified historical aerial photographs. This historical channel change can be quantified as either change during single flood events or cumulative change observed over the entire period of record. The baseline from which the lateral migration distances described in this chapter are computed is the left bank (or Station 0) from the HEC-RAS cross-sections derived from the Hydraulics Report for the Lower Hassayampa Watercourse Master Plan prepared by WEST Consultants.

6.2.1 Single-Event Channel Change Analysis

The maximum single-event channel change for the active channel corridor in each reach was measured from the historical aerial photographs. These measurements were performed for the left and right active channel banks independently. The bank movement information was determined by calculating the maximum lateral change that occurred between consecutive sets of aerial photography that bracket a large flood event. Once the maximum active channel movement in each set of photographs was measured, the maximum measurement in each reach was determined from measurements for all the sets of aerial photographs. The maximum value is significant in that it represents the maximum single-event change known to have occurred, and thus can be used as a reasonable prediction of the minimum magnitude of future single event change. Larger changes could be induced by floods larger than those in the period of record, or by human impacts to the watershed or watercourse. Table 6-1 lists the results of the maximum single-event channel change analysis for each reach.

Table 6-1. Maximum single-event channel change summary				
Reach	Aerial Photo Set	Max Lateral Change (ft)	River Station	Bank
5	1964-1972	478	25.72	Right
4	1964-1972	511	21.27	Left
3	1988-1992	540	13.32	Right
2	1949-1953	1,329	10.12	Left
1	1949-1953	665	between 1.91 and 2	Left

The results shown in Table 6-1indicate that the Lower Hassayampa River has experienced dynamic lateral changes within the period of record. The maximum single-event lateral change values shown in Table 6-1 were used as the minimum starting buffer distance for the Severe Erosion Hazard Zone delineation, as discussed later in this chapter.

6.2.2 Long-Term Channel Change Analysis

In addition to the maximum single-event changes, the long-term or cumulative channel change was calculated for the left and right banks in each reach of the Lower Hassayampa River study reach. The long-term channel change was determined by measuring the maximum change in active channel position by reach between the earliest and most recent set of historical aerial photography. The estimates of long-term active channel change aid in defining long-term trends of channel migration. For example, the maximum lateral change that occurred between 1949 and 2004 in Reach 2 occurred in the direction of the right bank and was approximately 1,554 feet (about 28 ft/yr), which indicates a reasonable estimate of a minimum lateral distance in which future migration of the active channel might occur over moderate time durations. In several cases, the comparison of channel position over the period of record failed to capture the real magnitude of channel movement because channel migration back and forth over the floodplain returned the channel to a position close to the initial position, resulting in a relatively low cumulative estimate of movement. Table 6-2 summarizes the results of the long-term channel change analysis.

Table 6-2. Cumulative channel change summary					
Reach	Time Span	Cumulative Max Lateral Change (ft)	River Station	Bank	Migration Rate (ft/year)
5	1949-2004	352	25.91	Right	6
4	1949-2004	366	16.82	Right	7
3	1949-2004	1,911	13.23	Right	35
2	1949-2004	1,554	10.12	Right	28
1	1934-2004	929	4.44	Right	13

The maximum long-term channel change measurements shown in Table 6-2 reflect the net change within the period of record, as well as the particular flood series events during that period. Some of the lateral change values in Table 6-2 are lower than those in Table 6-1 for the same reach. The low change value is a result of bi-directional (back and forth) lateral movement of the river over the period of record. For example, the

1970 flood caused the river to migrate 511 feet in Reach 4 during that single event. The maximum cumulative change for Reach 4 (1949-2004) was only 366 feet, which means the bank(s) partially recovered to their pre-flood locations or migrated toward river left during subsequent floods.

Figure 6-1 and Figure 6-2 summarize the lateral migration analysis for each bank. In the plots, negative values indicate lateral migration of the bank toward river right, while positive values indicate lateral migration of the bank toward river left. The plots provide insight into the historical lateral migration of the river, but they can be misleading in that they include channel narrowing following large magnitude floods. Channel narrowing does not necessarily indicate lateral instability, but rather is usually flood recovery to a more equilibrium channel width. To represent true channel movement, the bank position data were filtered to show only bank movement outside the footprint of the previous channel position, as shown in Figure 6-3. In Figure 6-3, the positive values indicate the right bank movement only when the channel migrated outside of its former position. The negative values indicate the left bank movement only in the leftward direction when the channel migrated outside its former position. The higher the variability in the plot lines, the more laterally unstable the river has been. Where the variability in the plot lines is low, the river has been more laterally stable within the period of record.

6.2.3 Width Change Analysis

Changes in channel width can occur independently, but often occur in conjunction with lateral channel migration. Changes in width can be the result of natural processes or human impacts (e.g. encroachment, levees, bridges, etc.). Channel width changes often create adverse conditions by disrupting sediment continuity, as at bridge constrictions that increase flow velocities, or along levees that cut off normal floodplain storage. Natural channel width changes often occur during floods as the river adjusts to the increased discharge and sediment load. Whether natural or human caused, changes in channel width are a direct reflection of the system adjusting to the imposed water and sediment discharges. A width change analysis was performed for the Lower Hassayampa River to identify and quantify areas of historical lateral stability. Width measurements were calculated for each set of historical aerial photography using the HEC-6 cross-section locations as measuring points (Chapter 5). Figure 6-4 shows the summary of the width change analysis. Large magnitude variability in the plot lines indicates high variability in historical channel width. This variability suggests overall lateral instability of the channel (as shown by the yellow, horizontal arrows). The areas where the plot lines are concurrent indicate historical stability of the channel (as shown by the red, horizontal arrows). Note that the two major areas of stability are located at the major tributary confluence areas.

6.2.4 Summary

Bank movement and width changes were measured from semi-rectified historical aerial photographs. The maximum single event and long-term change in channel position and active channel width in the study reach were over 1,300 feet, 1,900 feet, and 1,200 feet, respectively. These data were used as fundamental tools in defining the erosion hazard zone boundaries described later in this chapter.

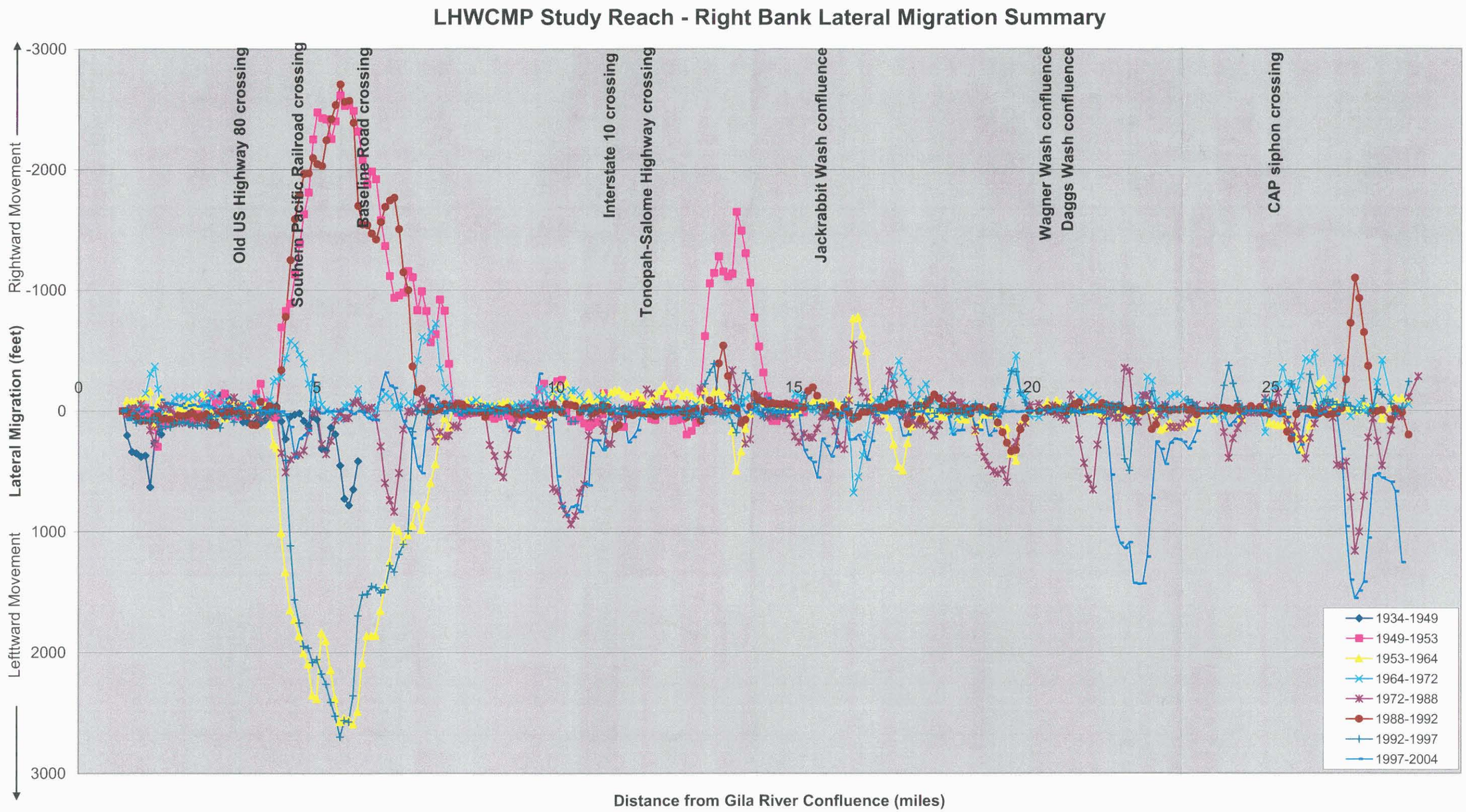

Figure 6-1. Right bank lateral migration summary

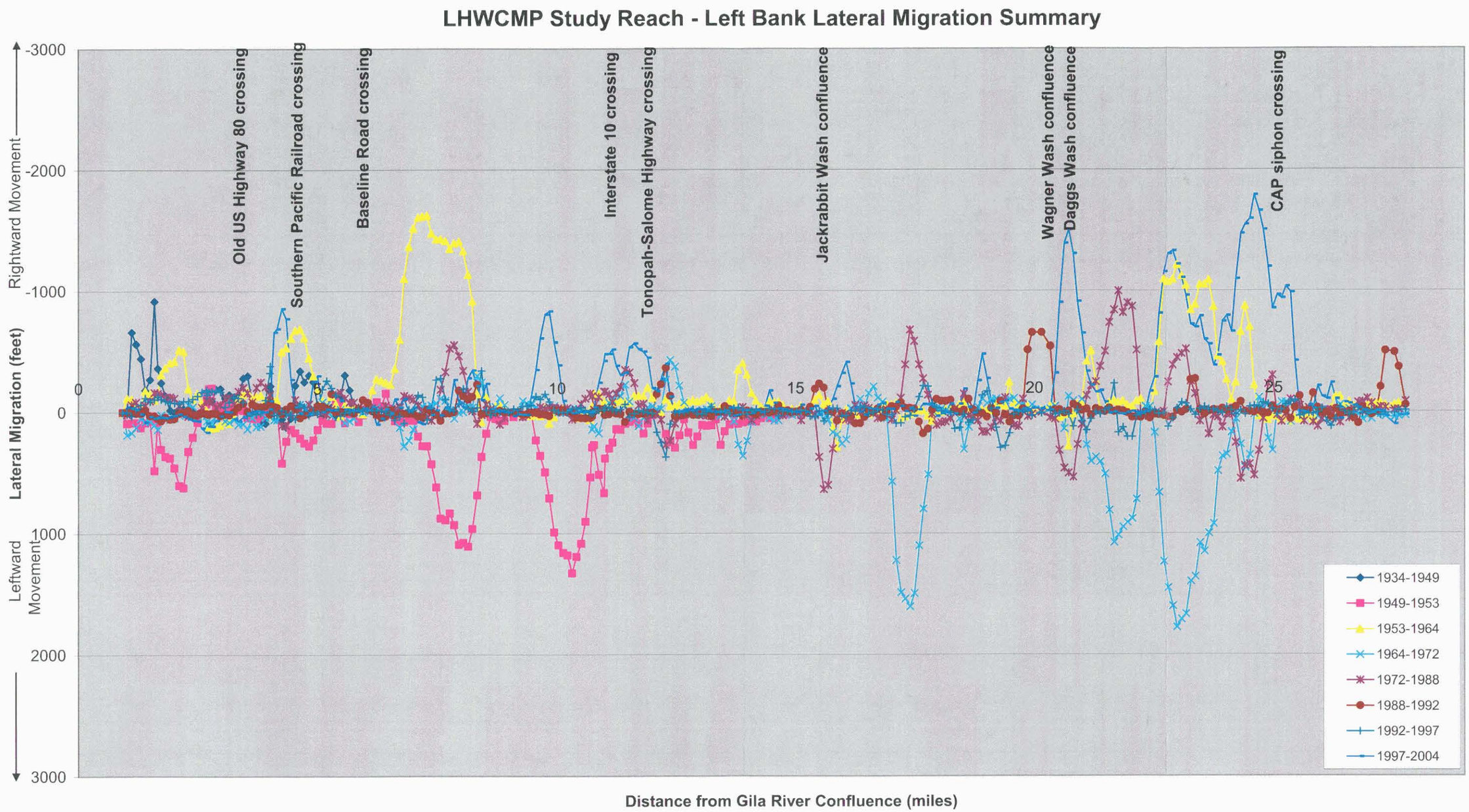

Figure 6-2. Left bank lateral migration summary

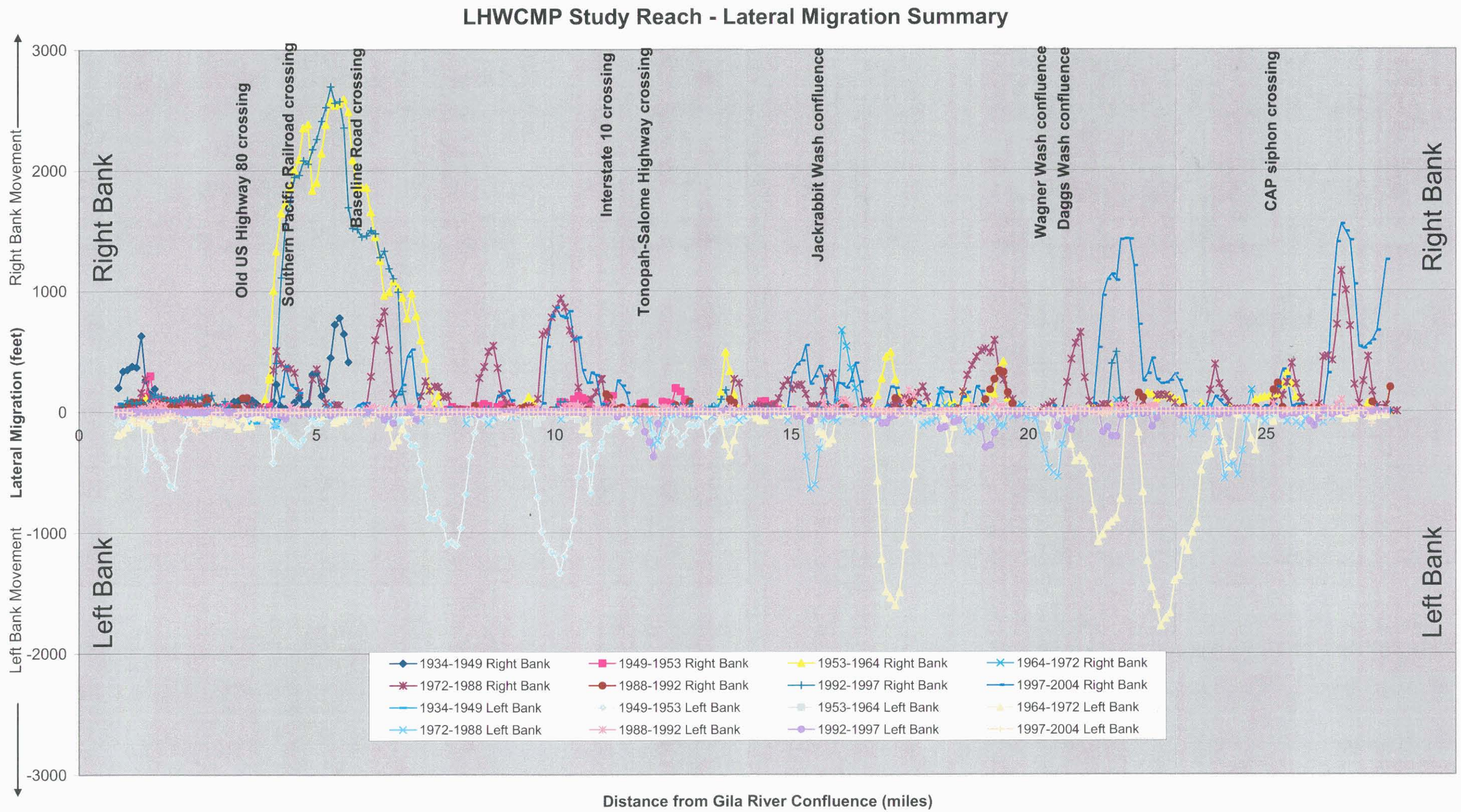

Figure 6-3. Lower Hassayampa lateral migration summary

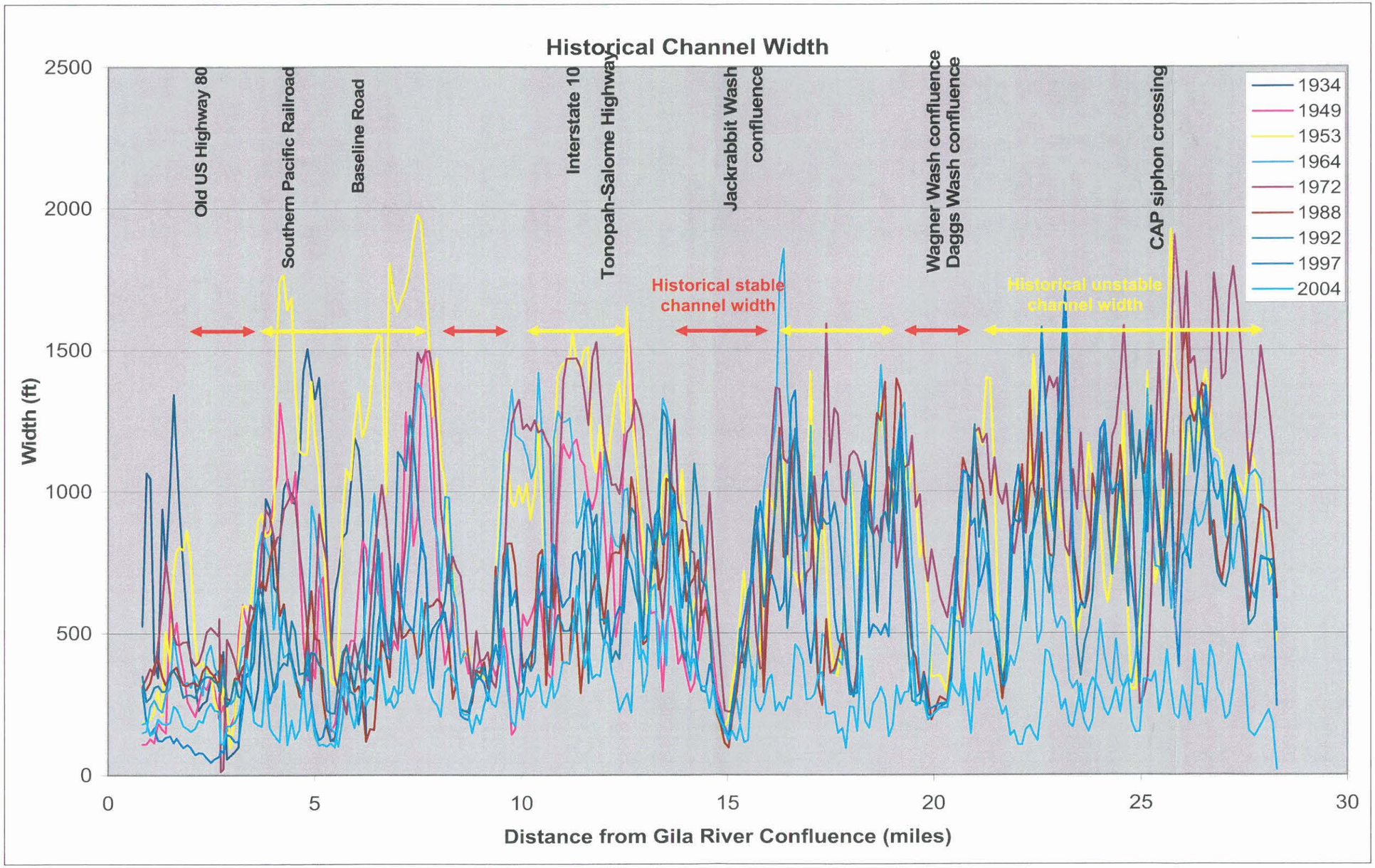

Figure 6-4. Width change analysis summary

6.3 Historical Flood Impact Analysis

6.3.1 Flood Chronology

Although it would be ideal to have historical aerial photography that brackets each flood within the period of record so that the impact of each flood could be quantified, such temporally sequential photography was not available for the Lower Hassayampa River. However, combining the historical gage record with the available aerial photography can provide insight into the impacts of individual floods. Table 6-3 lists the largest floods that have occurred on the Hassayampa River within the period of record and the subsequent bracket of available aerial photography.

Table 6-3. List of floods and subsequent aerial photo coverage

Flood Date	Peak Estimate (cfs)	USGS Gage ID (nearest to LHWCMP study area)	Aerial Photo Sets (years)
August 29, 1951	27,000	09515500 (near Wickenburg)	1949-1953
September 5, 1970	47,500	09516500 (near Morristown)	1964-1972
March 2, 1978	20,000	09517000 (near Arlington)	1972-1988
February 20, 1980	11,200	09517000 (near Arlington)	1972-1988
January 8, 1993	11,400	09517000 (near Arlington)	1992-1997
September 26, 1997	11,800	09516500 (near Morristown)	1997-2001
October 27, 2000	22,200	09517000 (near Arlington)	1997-2001

As shown in Table 6-3, some floods are more tightly bracketed by historical aerial photography than others. Impacts from individual floods were estimated by comparing the gage record for the years other than the flood year, but within the period represented by the aerial photo sets. For example, the 1949-1953 photo set spans five years, with a large flood in 1951. Between 1951 (the date of the flood) and 1953 (the date of the next photo), the USGS gage #09515500 near Wickenburg recorded peaks flows of 1,600 and 900 in 1952 and 1953, respectively. The relatively small floods between 1951 and 1953 probably had little or no impact on channel change caused by the much larger 1951 flood, thus making the 1953 photos reasonably representative of the post-1951 flood channel. In contrast, the 1980 flood is bracketed by photos from 1972 to 1988 (a 16-year time span). Between 1972 and 1988 the USGS gaging station near Arlington #09517000 recorded the following peak discharges:

- 1972 = 225 cfs
- 1973 = 12,300 cfs
- 1974 = 250 cfs
- 1975 = 0 cfs
- 1976 = 13,000 cfs
- 1977 = 4,300 cfs
- 1978 = 20,000 cfs
- 1979 = 3,300 cfs
- 1980 = 11,200 cfs
- 1983 = 3,300 cfs
- 1984 = 2,850 cfs
- 1985 = 372 cfs
- 1986 = 2,610 cfs
- 1987 = 404 cfs
- 1988 = 2,800 cfs

Several floods occurred between the 1978 flood and the date of the aerial photo (1988). Therefore, the impacts from the 1978 flood are less likely to be observed and quantified from the 1988 photo. Measurements were made for those sets of photos that bracketed large floods and are discussed below.

6.3.2 Impacts of Historical Floods

One method of quickly quantifying the change in channel morphology caused by a flood is to look at the change in channel width from pre- and post-flood conditions. This technique was applied for each of the floods discussed in this section. The 1949 aerial coverage extended only up to river station 15.21. Therefore, the mean width determined from the 1953 aerial photos was estimated only up to station 15.21. Table 6-4 summarizes the results of the quantitative impacts of the historical floods.

Table 6-4. Historical Flood Impacts on the Active Corridor

Flood Date	Aerial Photo Set	Pre-flood Mean Active Corridor Width (ft)	Post-flood Mean Active Corridor Width (ft)	Difference (ft)
August 29, 1951	1949 - 1953	711	1,116	405
September 5, 1970	1964 - 1972	891	1,067	176
January 8, 1993	1992 - 1997	936	889	-47
September 26, 1997	1997[1] - 2001[2]	889	657	-232
October 27, 2000	1997 - 2001	889	657	-232

6.3.3 Lateral Migration Constraints

The historical analysis and field investigations identified locations in the study area that, within the period of record, were stable due to bedrock outcrops, erosion-resistant soils, tributary deposits, or manmade structures. The locations of historical channel stability are important for determining erosion hazard zones. Some factors such as locations of bedrock and erosion-resistant soils are reliable indicators of future lateral stability. Other features such as tributary deposits and manmade structures are less reliable because of the potential for human intervention. Tributary deposits have provided lateral stability to the Lower Hassayampa by the input of sediment which forms deltaic deposits within the floodplain. As long as the rate of sediment influx from the tributaries is greater than the ability of the Hassayampa River to remove the sediments during flood events, then the tributary sediments will continue to accumulate. If the rate of sediment-influx decreases or the transport rate in the main stem increases, due to human impacts on the channel and/or watershed, control provided by the tributaries will vanish. Additionally, if changes in tributary mouth location resulting from avulsions occur, the locus of sediment supply to the main stem will change. This process has occurred historically at the Jackrabbit Wash and Wagner Wash confluences, leaving large deltaic deposits that no longer receive the same volumes of sediment, thus no longer actively provide lateral stability (Figure 6-5). Field investigations indicated the tributary sediments are erodible.

[1] 1997 aerial photos were taken between January and May, thus pre-September 1997 flood

[2] Minimal channel change occurred between 2001 and 2004, thus only 2004 active channel limits were delineated

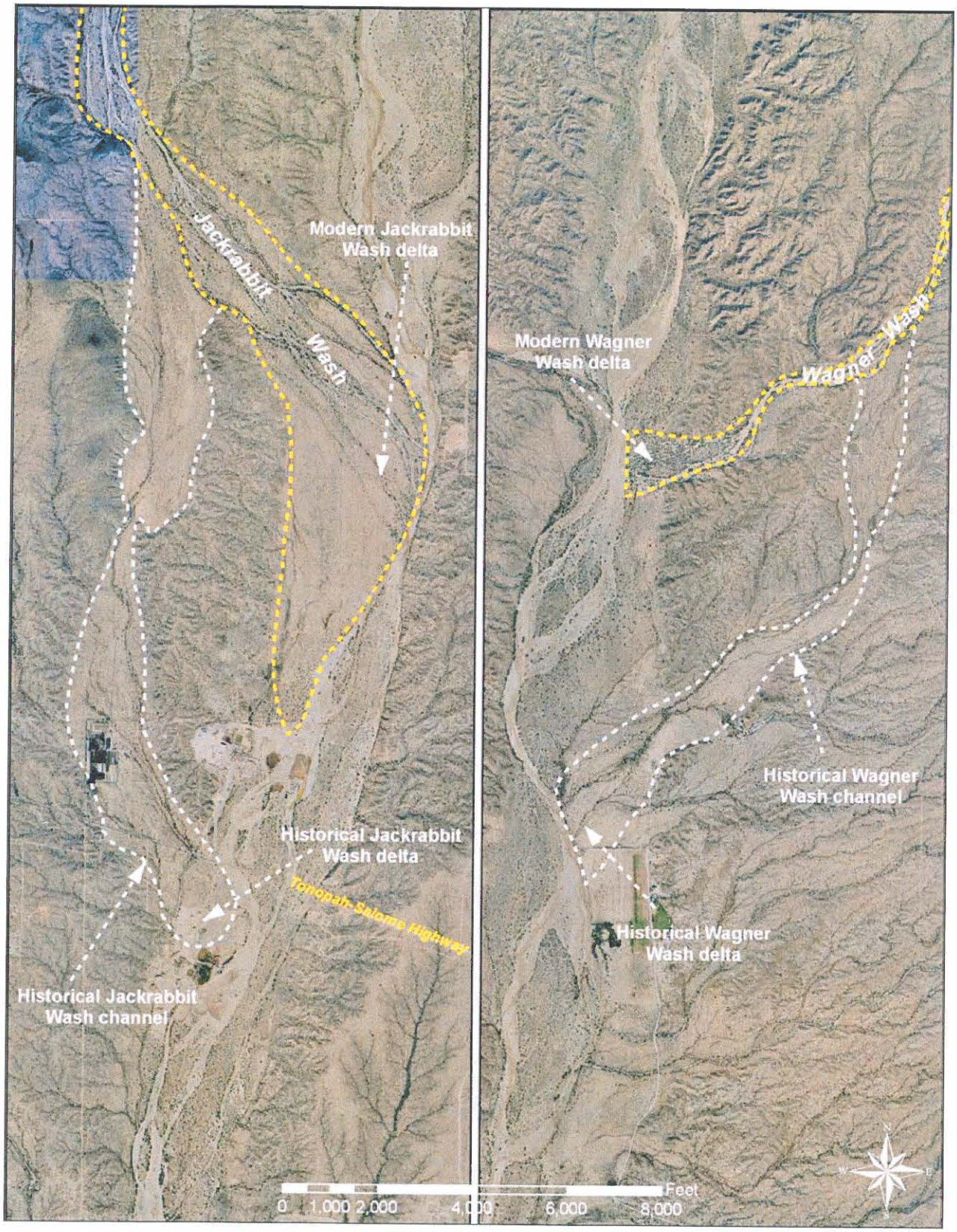

Figure 6-5. Major tributary avulsion locations

Manmade structures can provide reliable, lateral stability when properly engineered and maintained. The four bridges within the study area (Interstate 10, Union Pacific Railroad, and Old US 80) have provided lateral stability within the period of record. However, given the magnitude of historical channel change, the relatively small floods in the record relative to the FIS peak discharge, future floods could potentially erode abutments or other structure elements (Figure 6-6), as has occurred at other rivers in the Phoenix metropolitan area.

Alma School Road Bridge during the January 2005 floods on the Salt River, Tempe, Arizona. View downstream.

Figure 6-6. Alma School Road Bridge abutment erosion.

6.4 Locational Probability Analysis

Another quantitative evaluation of historical channel movement performed was locational probability analysis. Location probability is defined as the percentage of time that the active channel of the Hassayampa River was observed in a particular location during the period of photographic record. In other words, if the active channel was delineated in the earliest aerial photograph set and remained in that location throughout all of the subsequent aerial photos, the locational probability assigned to that location was 100 percent. Therefore, locational probability is a measure of historical channel stability and instability.

6.4.1 Methodology

Channel positions were mapped on historical aerial photographs described previously in this report. The location of the active channel in each aerial photo set was digitized in ArcGIS on the semi-rectified aerial photographs to create a polygon showing the channel boundaries. The resulting polygon shape files were overlain using the 'union' function in ArcGIS. Prior to the union processing, an attribute field was added to each historic active channel shape file, quantifying the number of years between that photo set and the previous photo set. For example, the field added to the 1972 active channel shape file was given a value of 8 years, since the next previous historic aerial photo set was dated 1964. So, the assumption was that the active channel was present the entire period between the two dates. The earliest aerial photo set in 1934 was assigned a value of zero years.

Each photo set was overlain one at a time until all the photo sets were "unioned." The resulting shape file was then further refined to add attributes via another union process to assign the limits of the 1934 and 1949 photo sets, since those aerials only partially covered the study reach. Therefore, the 100 percent potential maximum locational probability value represents different lengths of time for different parts of the study area. The 1934 photo set extends from the lower study limit to a point just upstream of Baseline Road. The 1949 photo set extends from the lower study limit to about the confluence with Jackrabbit Wash.

Locational probability was then calculated as the sum of years present for each individual polygon record divided by the total potential time (e.g. 51 years for the reach upstream of Jackrabbit Wash, 55 years from Baseline to Jackrabbit, and 70 years for the reach from just upstream of Baseline Road to the Gila River).

6.4.2 Results and Interpretation

Figure 6-7 through Figure 6-12 show the results of the locational probability analysis for each reach. Not surprisingly, the locational probability analysis results are similar to the other historical and geomorphic channel position results, since they rely on the same data sets. The locational probability merely quantifies the historical data. The following observations are made regarding the locational probability plots shown in Figure 6-7 through Figure 6-12:

- The existing thalweg location has shown some persistence in the landscape over the 70-year period of record, as can be seen from a consistent narrow corridor of 70 to 90 percent locational probability.

- In most of the study area, the active channel has been located on either side of the floodplain during some part of the relatively short period of record, indicating the potential for extreme channel relocations within the geologic floodplain.

- Numerous islands where the active channel has not been located have persisted through the period of record, confirming field observations of moderate levels of historical permanence of these island features.

- The island features indicate that much of the most extreme channel movement has been avulsive, rather than accretive.

- Flow bifurcation points, or splays, exist along the active channel. These splays have very low locational probability and are the sites of most active low flow channel movement.

- The active channel position has been most stable near major tributary confluences.

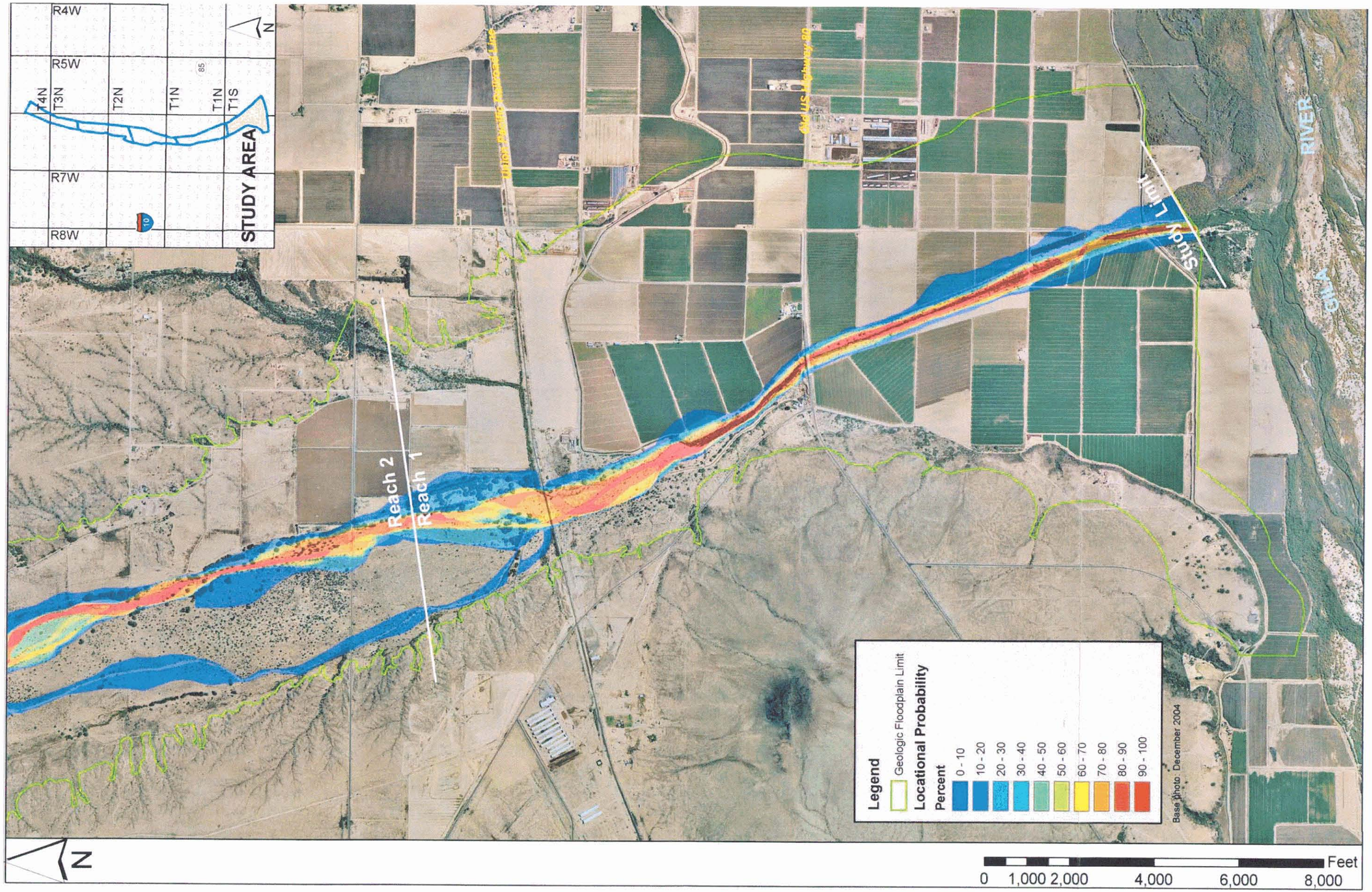

Figure 6-7. Locational Probability for Reach 1 (maximum potential number of years = 70 years)

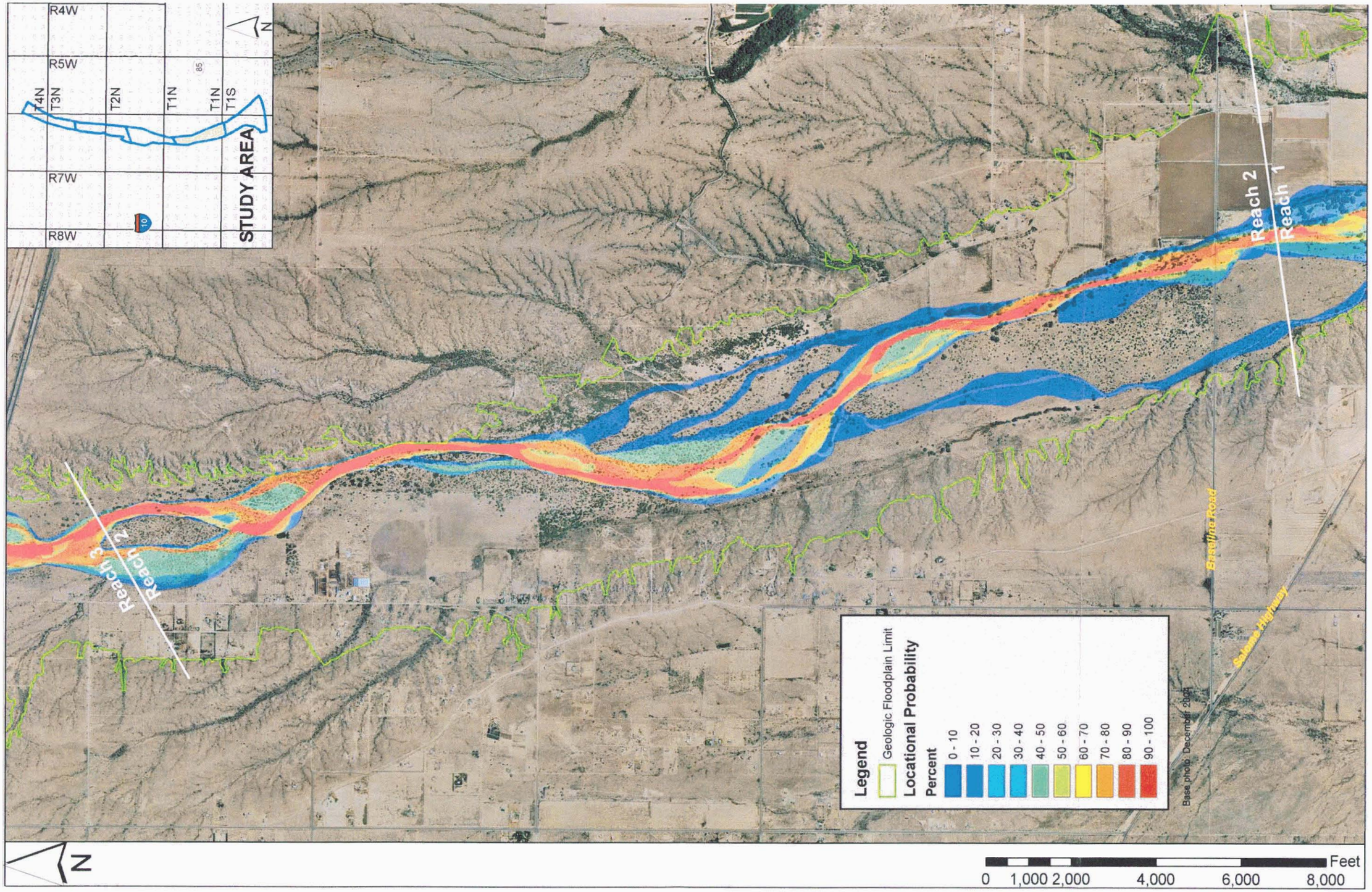

Figure 6-8. Locational Probability for Reach 2 (maximum potential number of years = 55 years)

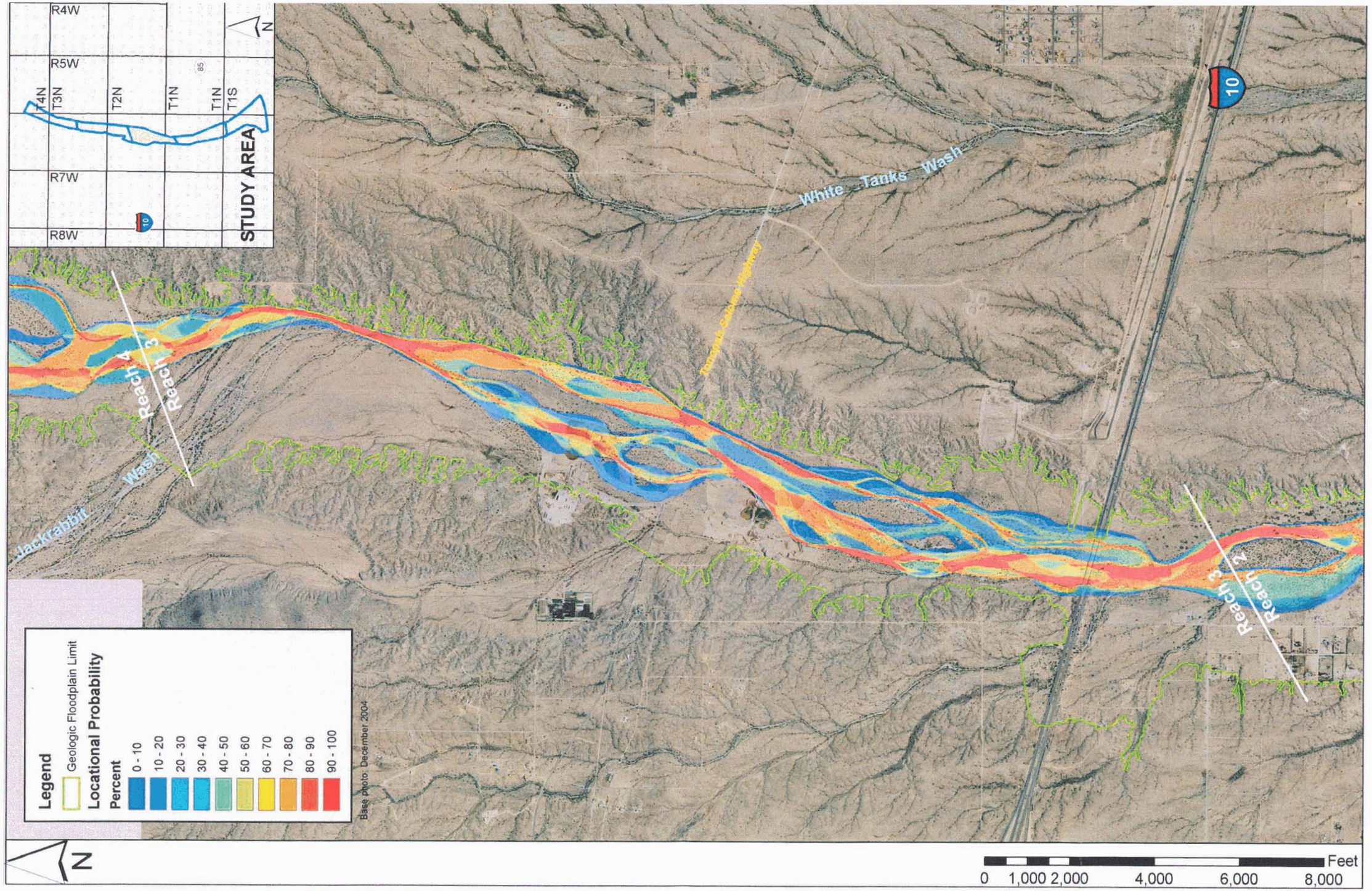

Figure 6-9. Locational Probability for Reach 3 (maximum potential number of years = 55 years)

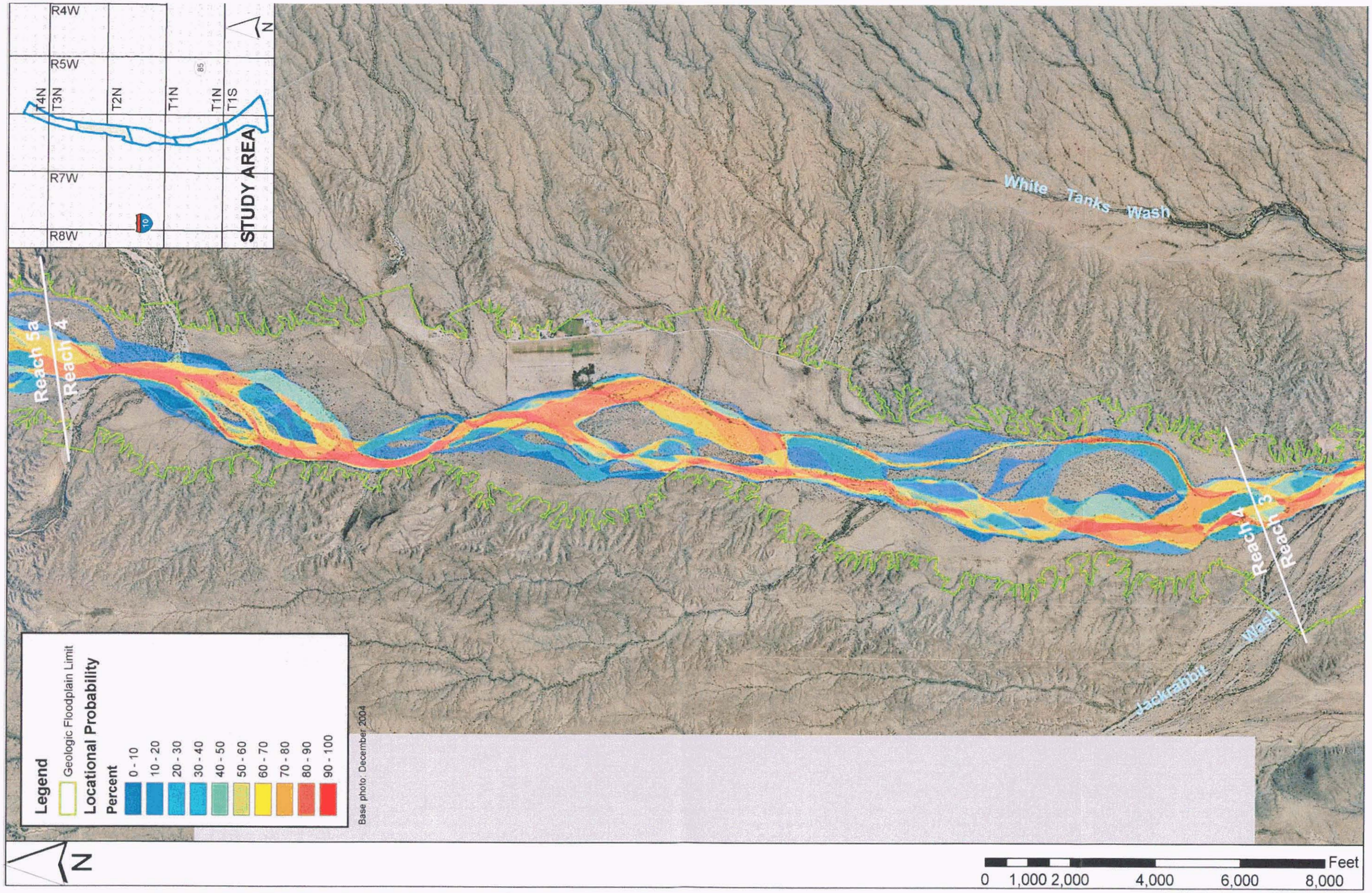

Figure 6-10. Locational Probability for Reach 4 (maximum potential number of years = 51 years)

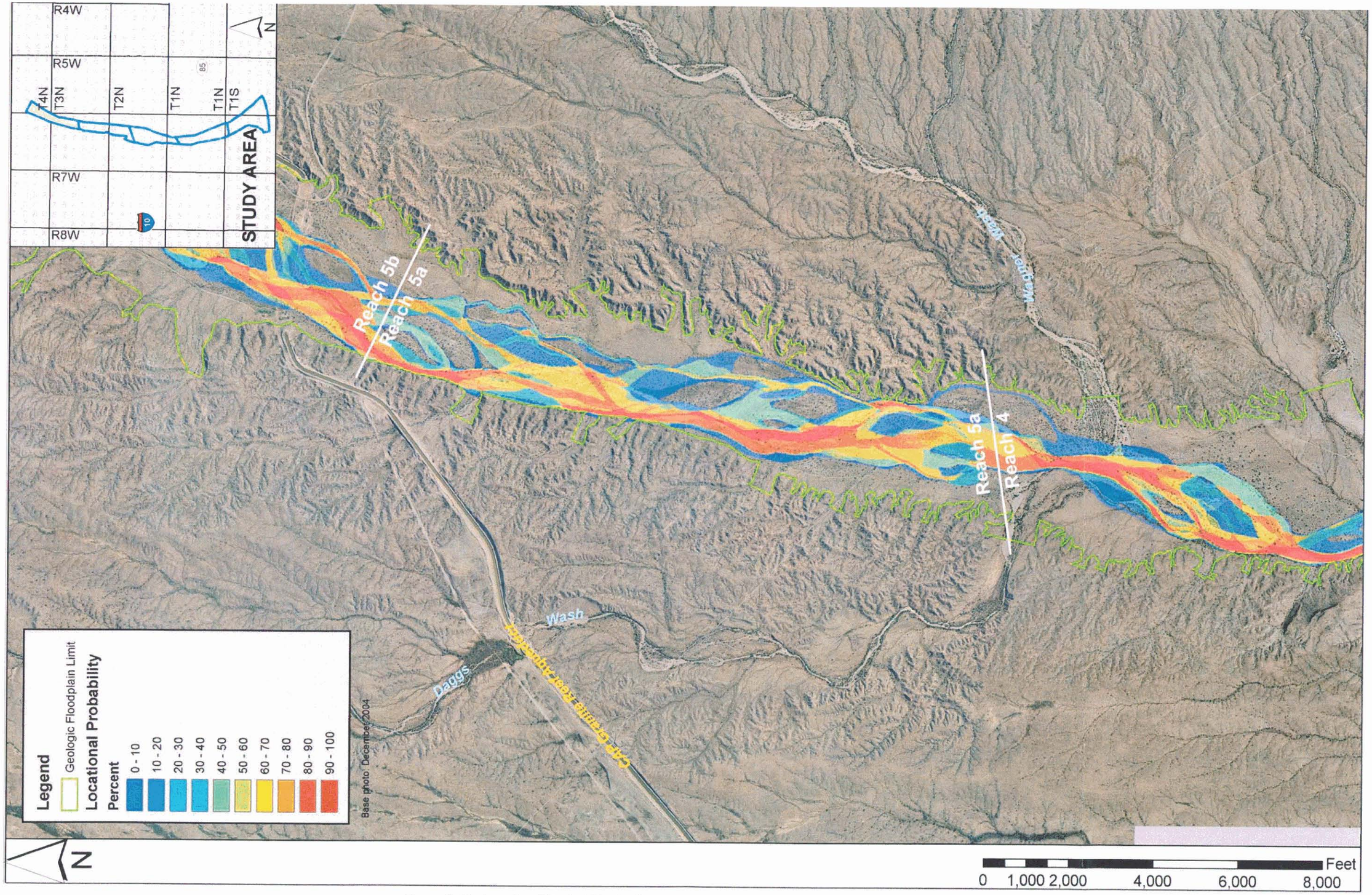

Figure 6-11. Locational Probability for Reach 5a (maximum potential number of years = 51 years)

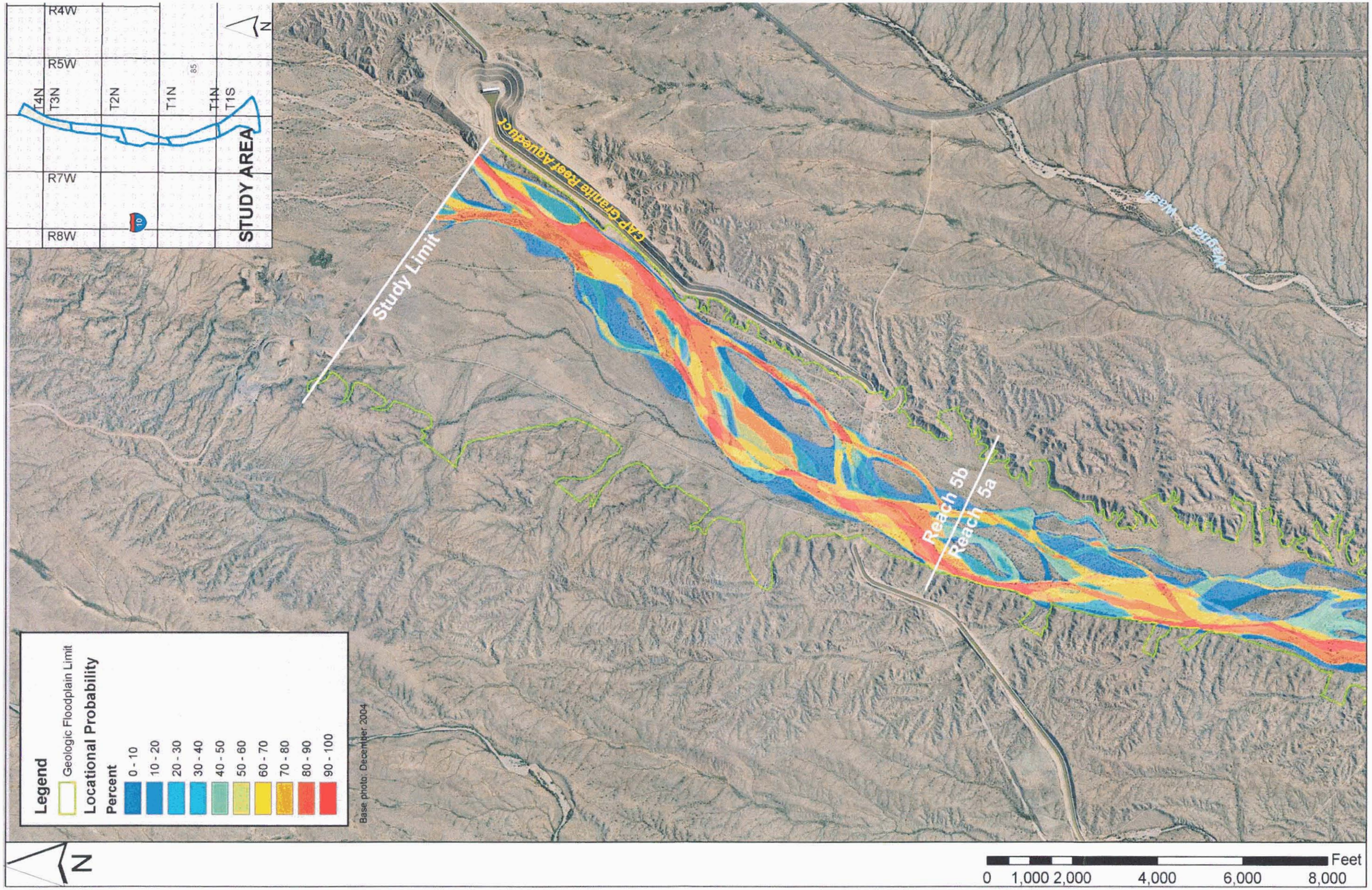

Figure 6-12. Locational Probability for Reach 5b (maximum potential number of years = 51 years)

6.5 Erosion Hazard Zones

Erosion hazard zones were delineated for the Lower Hassayampa River and Jackrabbit Wash within the LHWCMP study limits. The erosion hazard zones for the Hassayampa River were based on Level 3 methodologies as defined in the District's draft Erosion Hazard Zone Delineation and Development Guidelines. The following three lateral erosion hazard zones were defined for the Hassayampa River:

- Severe Erosion Hazard Zone (SEHZ)
- Lateral Migration Erosion Hazard Zone (LMEHZ)
- Long-Term Erosion Hazard Zone (LTEHZ)

The Jackrabbit Wash erosion hazard zones were delineated based on the Level 3 Limited-Detail Methodology.

6.5.1 Methodologies

The following types of information were considered in defining the erosion hazard boundaries, as described in this Chapter and Chapters 2 to 5:

- Field Data
- Stream Classification
- Mapping Of Geomorphic Surfaces
- Historical Channel Changes
- Empirical Geomorphic Analysis
- Engineering Analysis
- HEC-6 Modeling Results
- Bed Elevation Analysis Results
- Lateral Constraints

In addition, engineering judgment and past experience was relied on when defining the erosion hazard zone boundaries, particularly for reaches where conflicting information exists. Finally, it is noted that the scale of analysis for a watercourse master plan precludes detailed analysis of each parcel within the 28-mile study limit. Therefore, it is possible that more detailed, site-specific engineering and geomorphic analyses might result in refinement of the erosion hazard delineation. Guidelines for the types of more detailed analyses are provided in Chapter 8.

6.5.1.1 Field Data

Field observations and interpretations were described in Chapter 2. Detailed field inspections of the study reach were conducted over a 10-month period. Field visits consisted of walking the active channel and floodplain areas, photographing and mapping key features, and recording descriptions of existing channel conditions. Field data were used to identify areas of lateral stability, as well as to identify actively eroding areas outside the main channel. Geomorphic indicators of instability such as cutbanks, headcuts, and avulsions were documented during the field investigations.

Field information was used primarily for delineating the LMEHZ and LTEHZ.

Specifically, field data were used to identify avulsive overbank flow paths, evidence of high flow velocities and sediment transport on floodplains, and to distinguish depositional surfaces from transport surfaces.

6.5.1.2 Stream Classification

Stream classification data were described in Chapter 3. Based on the stream classification methodologies, the Lower Hassayampa River was determined to be highly unstable and is subject to high rates of lateral erosion. The stream classification data were most useful for delineating the LHEHZ.

6.5.1.3 Geomorphic Mapping

The geomorphic mapping analysis was described in Chapter 3. Based on interpretation of aerial photographs, field investigations, surficial soil characteristics, channel and floodplain topography, published surficial mapping, and detailed soil profile descriptions of soil pits, detailed geomorphic mapping was performed. The geomorphic mapping was used to estimate the relative age of the floodplain terraces in the study area, and to distinguish geologically recent geomorphic surfaces from older, more stable surfaces. Geomorphic age data were useful for distinguishing areas of active and inactive channel movement, and for constraining the maximum and minimum rates of channel evolution. The geomorphic surface map was overlaid on a set of the orthorectified photograph base maps for the study area. Areas with geomorphically active, young surfaces were included in the erosion hazard zone.

Geomorphic mapping was used primarily for delineating the SEHZ and LMEHZ. Evidence of past single event erosion such as cut banks, bar formation, and flotsam were used to identify areas subject to severe erosion hazards. Surficial mapping of geologically young floodplain surfaces was used to identify areas subject to active channel and floodplain processes that should be mapped within the LMEHZ. Similarly, channel pattern interpretations were made to distinguish areas at imminent risk of erosion from areas that might be at risk at some point in the near future. The Pleistocene-Holocene boundary and functional landform surface analysis was used as the primary basis for identifying the LMEHZ and the LTEHZ.

6.5.1.4 Historical Channel Changes

Mapping of historical channel movement was described previously in this Chapter and in Chapter 3. The maximum long-term measured channel movement per-reach within the 70-year period of photographic record was used as a minimum predicted erosion distance for the LMEHZ. Because the magnitude and direction of future erosion cannot be predicted with 100 percent certainty, the maximum erosion distance was plotted as the lateral distance across the channel from each of the banks. That is, it was assumed future erosion could occur in either direction. This distance represents a minimum setback distance from which erosion hazard was defined, unless a physical boundary to lateral erosion existed, such as a geologically older, more resistant terrace, bedrock, or a manmade structure.

The maximum measured single event erosion distance in each reach was used on the minimum predicted erosion distance for the SEHZ, and was also measured from either

bank or incipient avulsive channel path.

6.5.1.5 Empirical Geomorphic Analysis

The empirical geomorphic analyses were described in Chapter 3. These analyses attempt to relate measurable stream characteristics such as sediment size, channel geometry, and hydraulic information to equilibrium channel geometry characteristics using regime equations. Expected trends of channel change (or stability) interpreted from the empirical equations were factored into the erosion hazard delineations. In general, the information gleaned from the empirical geomorphic analyses did not control placement of the SEHZ, LMEHZ, or LTEHZ boundaries, because of the wide active floodplain surfaces and the rather large measured historical channel movement.

6.5.1.6 Engineering Analysis

Engineering analyses of river stability performed for the Lower Hassayampa River included general scour calculation, allowable velocity estimates, equilibrium slope determination, and armoring potential analyses. Reaches of stability and instability defined by these engineering approaches were factored into the erosion hazard zone delineation. The analyses indicated that the existing channel banks and beds are highly erodible with no potential for armoring or physical constraint of lateral erosion, except in the few isolated areas where bedrock occurs. In general, while the engineering analyses predicted a high degree of vulnerability to lateral erosion, they did not provide diagnostic data for determining where the EHZ boundaries should be placed. Furthermore, the engineering analyses tended to predict long-term vertical equilibrium for the study reach, at least for the existing condition.

6.5.1.7 Velocity and Depth-Velocity Product Analyses

A new type of spatial analysis developed by JEF for the LHWCMP was conducted using HEC-RAS hydraulic data and ArcGIS map techniques to identify reaches with erodible flow depths and velocities. The plots of the HEC-RAS hydraulic data provide a visual representation of velocity and depth to aid in identifying potential avulsion areas and to estimate the limits of erosive processes during the simulated 100-year flood. The potential avulsion zones were then defined using the District's *Erosion Hazard Delineation and Development Guidelines* (FCDMC, 2003), which define the following characteristics as indicative of avulsion potential:

- *100-year maximum (not average) floodplain flow depth greater than two feet.*
- *100-year maximum floodplain velocity greater than four ft/sec, or the product of 100-year floodplain depth and velocity squared greater than 18 ($dv^2 > 18$).*

A velocity and depth distribution for each cross-section was calculated in HEC-RAS using the flow distribution value of 43. From this, three output reports representing the channel and both overbank areas were generated using HEC-RAS. The output data was listed by left and right of each of the 43 intervals across the section. Using a Python macro, the center of each distribution was calculated and a geographic coordinate assigned. This technique resulted in a spatial coordinate (X,Y) at each interval along the cross-sections. A grid was then generated in ArcMap using the (X,Y) coordinates for the lateral position and the velocity or depth value at each interval for

the Z value. A contour map was created from the grid data. Finally, a TIN was generated from the contour data.

The result was a spatial distribution plot of velocity "zones" that were definable by the velocity unit value (ft/s). This same process was then repeated while substituting depth for velocity to create a spatial depth distribution, and finally a depth-velocity (DV) product input value was used to generate a spatial DV plot. Figure 6-13 shows examples of each of these plots. The individual classes for each plot were determined by using the FCDMC guidelines listed above. Velocities of 4 ft/s or greater were considered erosive velocities, thus areas for potential avulsion. Additionally, DV values of six or greater (velocity=4 ft/s * depths=2 ft) were considered erosive values, and the underlying areas were included in the erosion hazard zone. 100-year velocity, depth, and depth-velocity product plots for the entire study area are shown in Figure 6-14 to Figure 6-16.

The depth-velocity plots were used primarily for delineating the SEHZ, which includes the floodplain areas with high probabilities of avulsion. In many cases, the LHEHZ was measured from the margin of the high depth-velocity zone, rather than the existing channel bank because of the high potential for avulsion and the highly erodible soils in the floodplain. The depth-velocity plots were also useful for identifying near-channel high velocity zones to be included in the SEHZ.

6.5.1.8 HEC-6 Modeling

HEC-6 modeling is not directly applicable to lateral channel stability evaluations. The HEC-6 model is useful for identifying reaches of vertical channel stability or instability, or reaches with sediment deficits or surpluses, from which inferences about lateral stability can be made. However, because the HEC-6 modeling results indicate that the existing condition of the Hassayampa River is relatively stable, little information relating to lateral stability could be derived from it. The vertical stability and insensitivity to Manning's N value, sediment inflow, and sediment gradation predicted by the HEC-6 modeling results, as described in Chapter 5, were interpreted to indicate that the river uses the large sediment reservoir to maintain stability. Much of the sediment reservoir is tapped by channel width adjustments (bank erosion) or floodplain deposition (sediment storage).

6.5.1.9 Bed Elevation Analysis

Historical topographic data were used to identify trends in bed elevation change. These data indicated that moderate fluctuations in bed elevation occur at any given location due to pulses of sediment transport, changes in low flow channel position, or flood response. However, no consistent long-term trend was identified that would affect lateral stability.

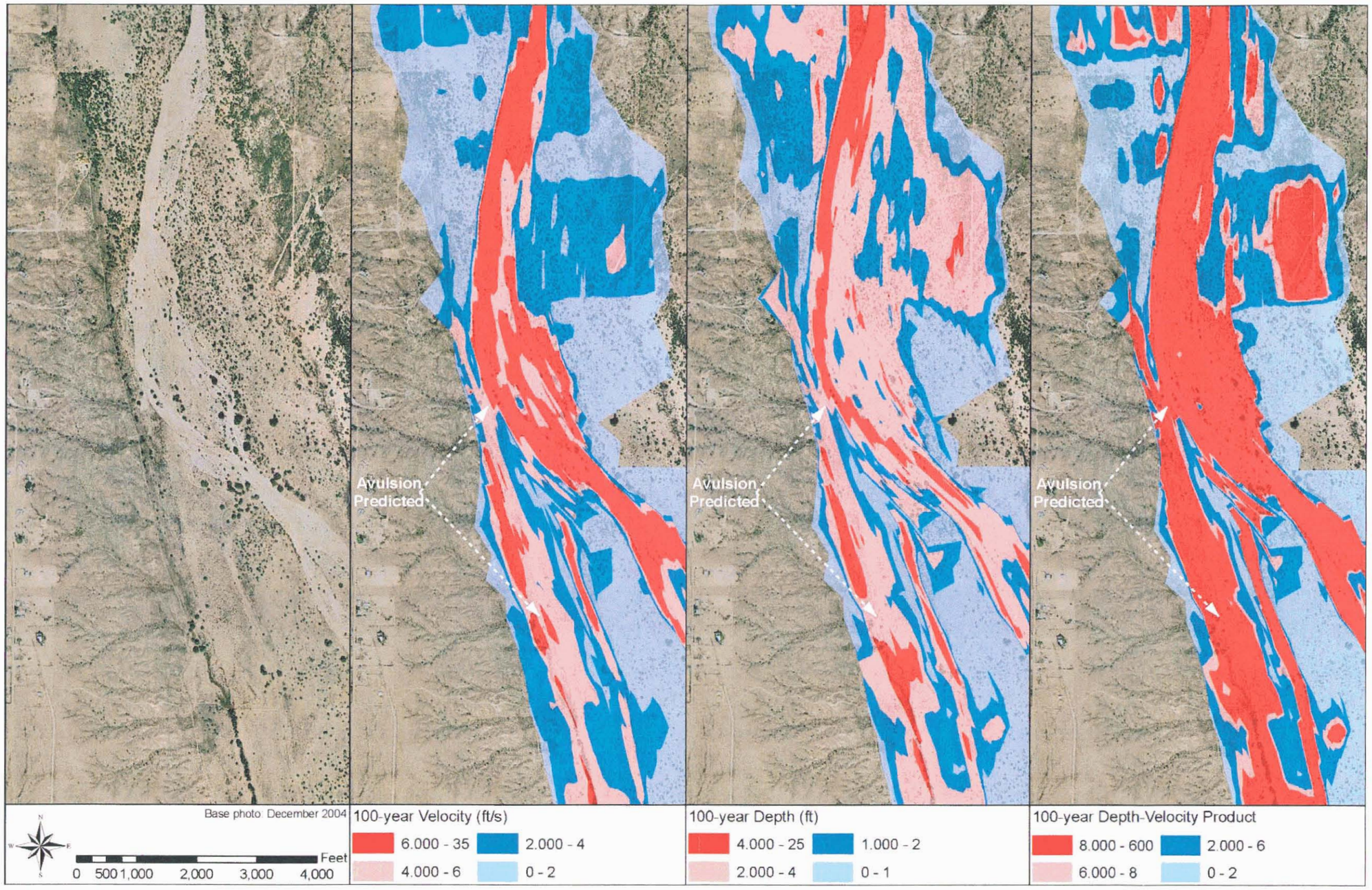

Figure 6-13. Hydraulic data spatial plots

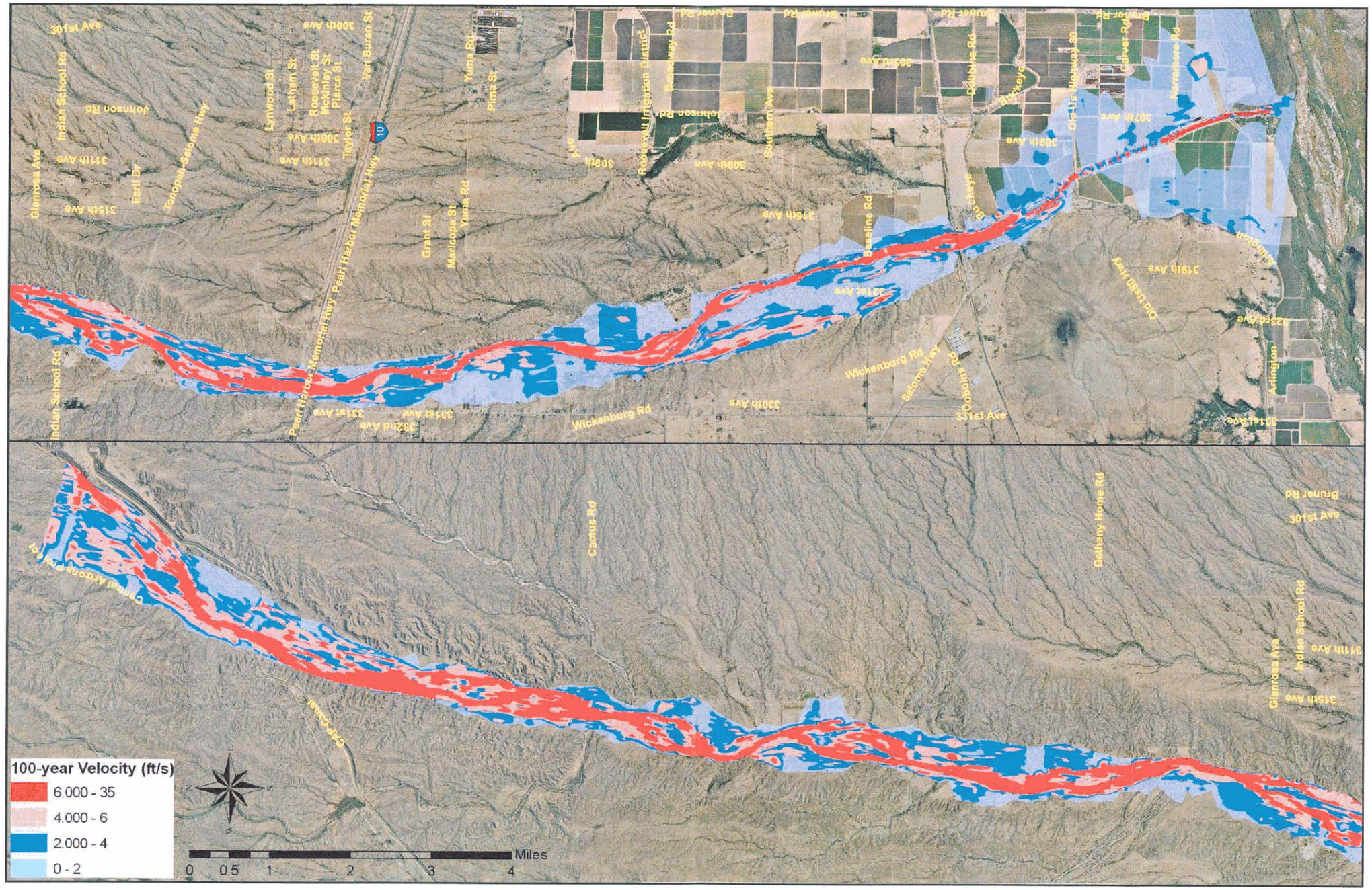

Figure 6-14. Velocity data spatial plots

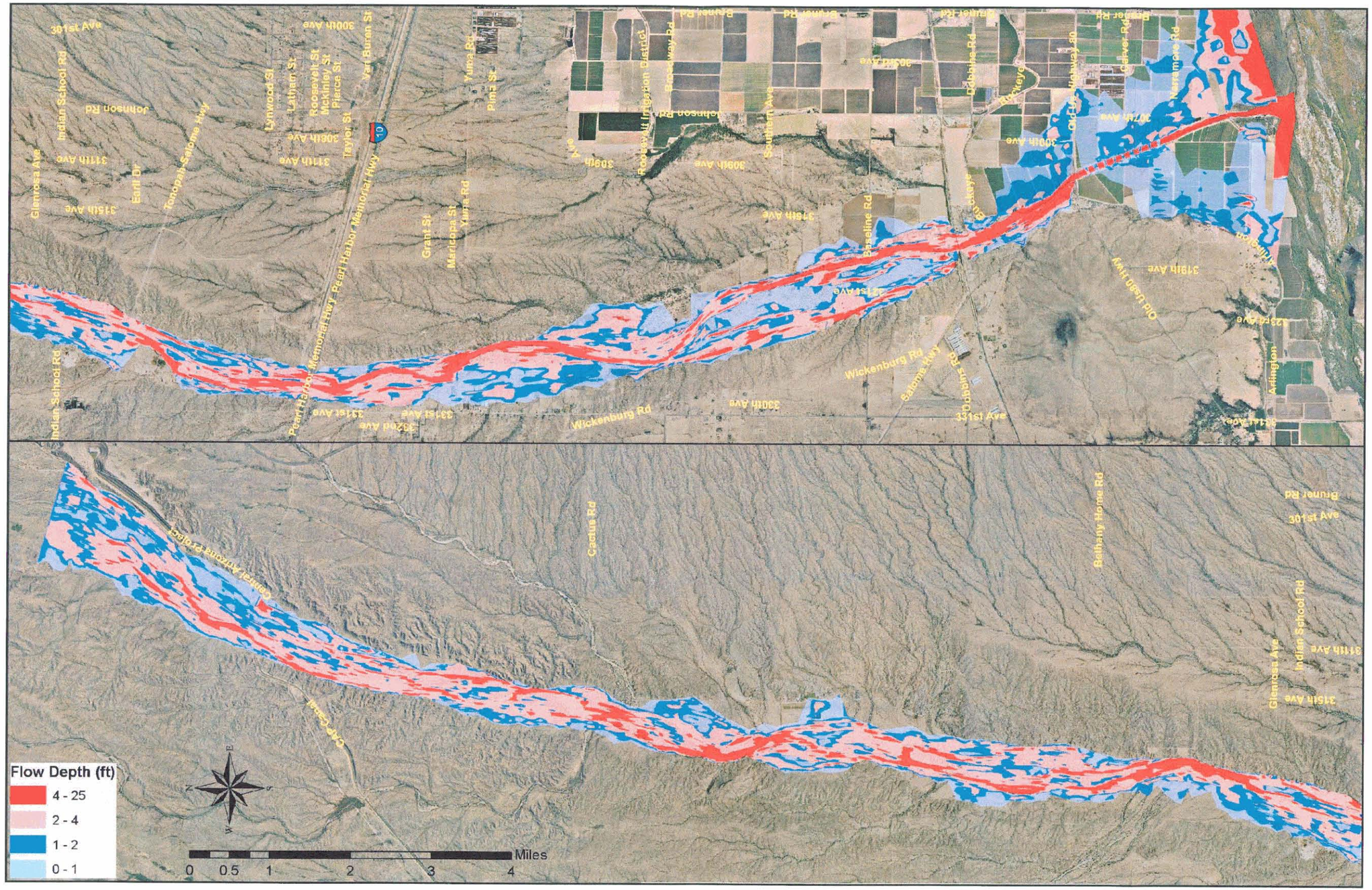

Figure 6-15. Depth data spatial plots

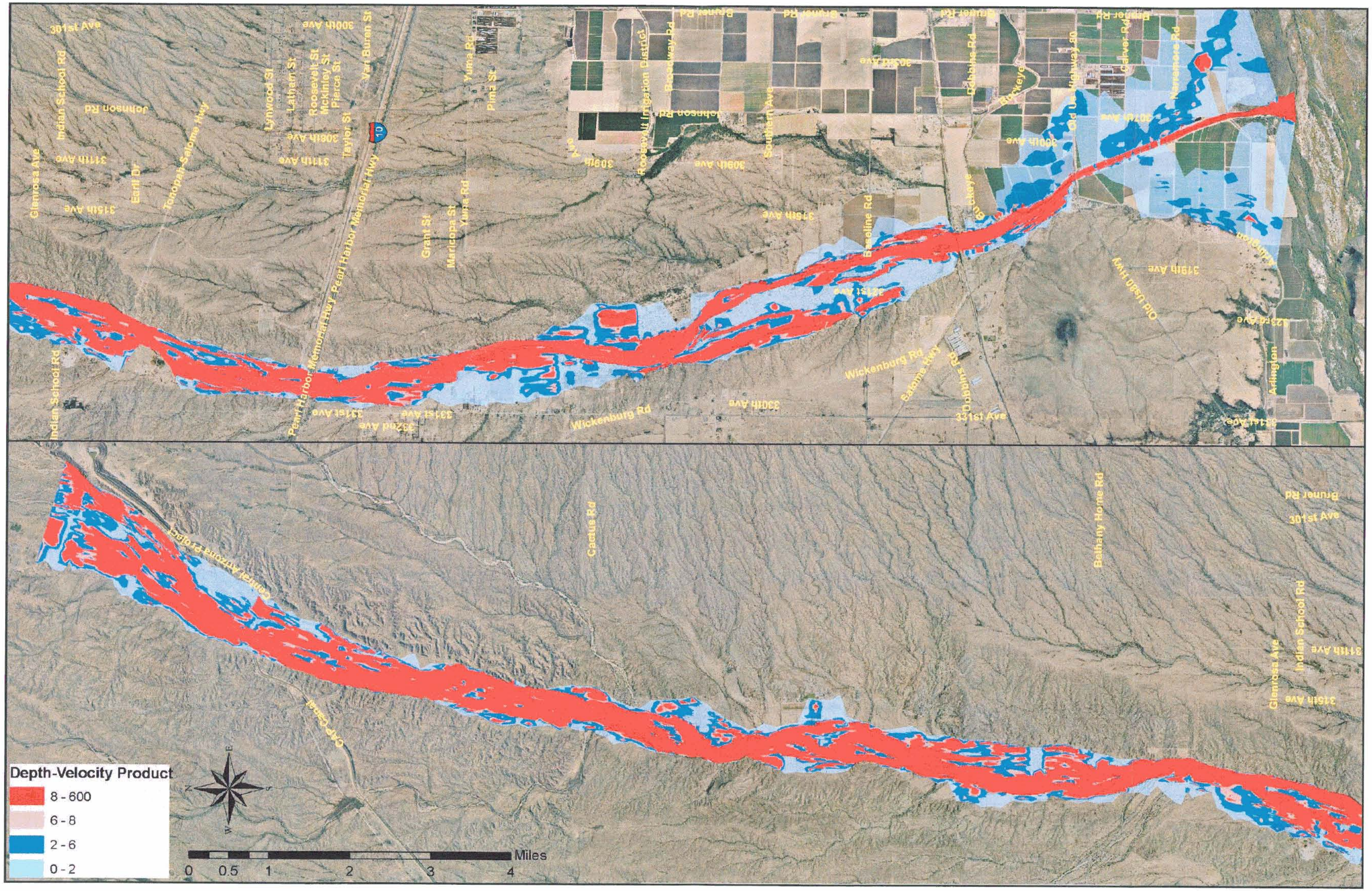

Figure 6-16. Depth-velocity product data spatial plots

6.5.2 Severe Erosion Hazard Zone

The severe erosion hazard zone is comprised of the active stream channels and bar deposit areas in addition to the channel margin areas likely to be eroded during a single 100-year flood. Because of the high susceptibility of the Hassayampa River to avulsive channel change, areas vulnerable to avulsion were included in the severe erosion hazard zone. The basis of mapping for the severe erosion hazard zone also included the following:

- Maximum historical, single-event lateral change of the active channel corridor (including active channels and bars) for each reach.
- Maximum, historical lateral extent of the active channel corridor.
- Spatial distribution of erosive 100-year velocities as predicted by one-dimensional, hydraulic modeling, including erosive velocities in overbank areas that will lead to channel avulsions.
- Spatial distribution of erosive depth-velocity product values as predicted by one-dimensional, hydraulic modeling, including potential overbank avulsion areas.
- Natural and manmade physical constraints on lateral erosion.
- Field data, such as channel pattern, which indicates bend angle, preferred direction of erosion, and evidence of recent bank erosion (or stability).

In addition, areas within the limits of existing sand and gravel mining operations were considered by definition to be in the severe erosion hazard zone, since no engineered erosion protection was observed near the mines during field visits. The mining footprint at the time of the field investigation was used, unless specific information about the future build out of the mine was available.

6.5.3 Lateral Migration Erosion Hazard Zone

The lateral migration erosion hazard zone consists of the channel margin area likely to be eroded by a "typical" series of floods over a sixty-year period, plus the erosion that would be caused by a 100-year flood. The lateral migration erosion hazard zone also includes the natural channel movement due to geomorphic processes such as meander migration and channel avulsions that occur over the course of several events or in response to future changes in floodplain morphology. The basis of mapping for the lateral migration erosion hazard zone included the following:

- Maximum, historical lateral channel change considering multiple mechanisms (single-event change, multiple-event change, and cumulative change).
- Spatial distribution of erosive 100-year velocities as predicted by one-dimensional, hydraulic modeling.
- Spatial distribution of erosive depth-velocity product values as predicted by HEC-RAS hydraulic modeling.
- Geomorphic mapping of functional surfaces that indicate the long-term active area of the river valley.
- Natural and manmade physical constraints on lateral erosion
- Field data, such as channel pattern, which indicates bend angle, preferred direction of erosion, and evidence of recent bank erosion (or stability), as well as

evidence of sediment transport and scour on the non-channel floodplain surfaces.

The limits of the lateral migration erosion hazard zone were widened in reaches where the field assessments and spatial distribution of erosive velocities and depth-velocity products indicated a potential for future erosion, where evidence of ongoing erosion was observed, and in reaches where accelerated erosion was expected due to channel bends or over-steepened banks. The LMEHZ is usually considered the regulatory erosion hazard zone by the District.

6.5.4 Long-Term Erosion Hazard Zone

The long-term erosion hazard zone consists of the channel margin area defined by geologic evidence of channel movement over the past 100 to 1,000 years, and represents expected or potential channel movement over the next 60 to 1,000 years in the future. The boundary of the expected long-term erosion hazard zone envelopes the results of all the predictive methods used to assess channel stability, in addition to application of engineering judgment and interpretation of the site geomorphology. The basis of mapping included the following:

- Field investigations of the extent of the Holocene floodplain.
- Evidence of geologic age within the Holocene floodplain.

The Holocene floodplain was generally included within the long-term erosion hazard zone, with the LTEHZ boundary placed at the top of the terrace scarp at the Pleistocene-Holocene boundary, subject to the qualifications and guidelines described below.

6.5.5 Erosion Zone Delineation at the Pleistocene-Active Channel Contact

Field data clearly demonstrate that the active channel is able to erode the older Pleistocene terraces. Where the active channel abuts these surfaces, the banks are typically cut to a vertical or near-vertical slope. However, comparisons of historical aerial photographs indicate that the rate of erosion of these surfaces by the active channel is well within the measurement accuracy, or less than about 30 to 70 feet over the 65 period of record. Therefore, predictions of single event and long term lateral movement relied on regional estimates of erosion rates of less than 1 ft/year (JEF, 2000; 2002, 2003) for these types of resistant, older surfaces, and an assumed maximum lateral migration rate of less than 1 ft/yr (70 feet in 65 years). Therefore, where the active channel abuts the Pleistocene terrace, the following erosion hazard zone delineation techniques were used:

- SEHZ: The minimum recommended setback of 15 feet in the ADWR State Standard 5-95 was used from the top of the nearest active channel bank.
- LMEHZ: A setback was established based on a projected 4:1 slope from the toe of the closest active channel bank, or 15 feet, whichever was greater.
- LTEHZ: The LTHEZ was defined at a point 150 feet from the LMEHZ.

In addition, the LMEHZ was generally placed at the top of Pleistocene terrace scarp if

the limit fell on the scarp itself. Typically the scarp slopes are too steep for development. Also, some smoothing of the EHZ boundaries was employed to reflect the relatively smooth linear tendencies of river processes.

6.5.6 Erosion Hazard Zone Delineation

Figure 6-17 through Figure 6-22 show the erosion hazard zone delineations for the Hassayampa River within the LHWCMP study area. Where the three zones plotted coincidently, only the severe erosion hazard zone is shown.

6.6 Jackrabbit Wash Erosion Hazard Delineation

The Jackrabbit Wash erosion hazard zone was determined using a Level 3 – Limited Scope analysis as described in the *Erosion Hazard Delineation and Development Guidelines* (FCDMC, 2003). The guidelines describe a Level 3 – Limited Scope analysis as follows:

> *If the proposed development will be located outside the Holocene floodplain, or the modern geologic floodplain, the risk of lateral erosion is generally less than if the development is located within the Holocene floodplain. For development outside the Holocene floodplain a less detailed erosion hazard evaluation consisting of the following elements is required to characterize the erosion hazard:*

- *Geomorphic and Geologic Mapping. Mapping of Holocene (Qy, < 10,000 years before present) and Pleistocene landforms and geomorphic surfaces (Qm, > 10,000 years before present), as well as mapping of the locations of bedrock outcrops, is required. Geomorphic mapping shall extend upstream and downstream of the proposed development a distance of at least four times the regulatory floodplain width. Photographic documentation and written descriptions of field and soils characteristics used to differentiate Holocene and Pleistocene surfaces are required to support the geomorphic mapping. The extent and lithology of bedrock shall be clearly described and delineated. Surficial geologic mapping for many parts of Arizona is available from the Arizona Geological Survey (www.azgs.us.az). Detailed soils mapping may be available in published soil surveys by the Soil Conservation Service or U.S. Forest Service.[3]. References to publications describing procedures for mapping geomorphic surfaces are provided in Section 6.*
- *Field Investigation. Documentation of each of the Level 2 site characteristics is required. Field data shall be succinctly summarized and the investigator shall provide a clear conclusion regarding the relevance of the field data for determining stream stability and erosion hazard.*
- *Qm Surface Lateral Erosion Rate. Estimation of the rate of lateral erosion of the Qm surfaces based on field data, historical documentation of long-term channel movement, interpretation of hydraulic modeling results, and/or geotechnical analysis of erosion potential is required, especially where the main channel abuts the Qm terrace.*

[3] SCS soils mapping coverage is at: http://data4.ftw.nrcs.usda.gov/website/archived_ssurgo/viewer.htm.

- *Floodplain/Floodway Delineation. If no regulatory floodplain exists, the 100-year floodplain and floodway shall be delineated within the project limits using, at minimum, the procedures described in Section 2.2.2. Hydraulic data from the floodplain delineation shall be used to support the geomorphic mapping and estimate of the Qm surface lateral erosion rate.*
- Delineate Erosion Hazard Zone. Based on the analyses described above, an erosion hazard zone for the study area shall be delineated.

The methodology used in delineating the recommended erosion hazard zone for Jackrabbit Wash was slightly modified from the Guidelines. The approach used to delineate the erosion hazard boundary was to identify the Pleistocene (Qm)-Holocene boundary, wherein the boundary would become the erosion hazard zone. Field investigations were conducted to identify locations of bedrock and other lateral constraints, in addition to identifying the Holocene limits. Figure 6-23 shows the erosion hazard zone for Jackrabbit Wash.

6.6.1 Summary

Erosion hazard zones were delineated for the Hassayampa River and Jackrabbit Wash downstream of the CAP siphons. Both rivers are subject to extreme rates and magnitudes of lateral erosion during individual floods and over the long term. Significant erosion hazards exist along both rivers within their entire modern geologic floodplain.

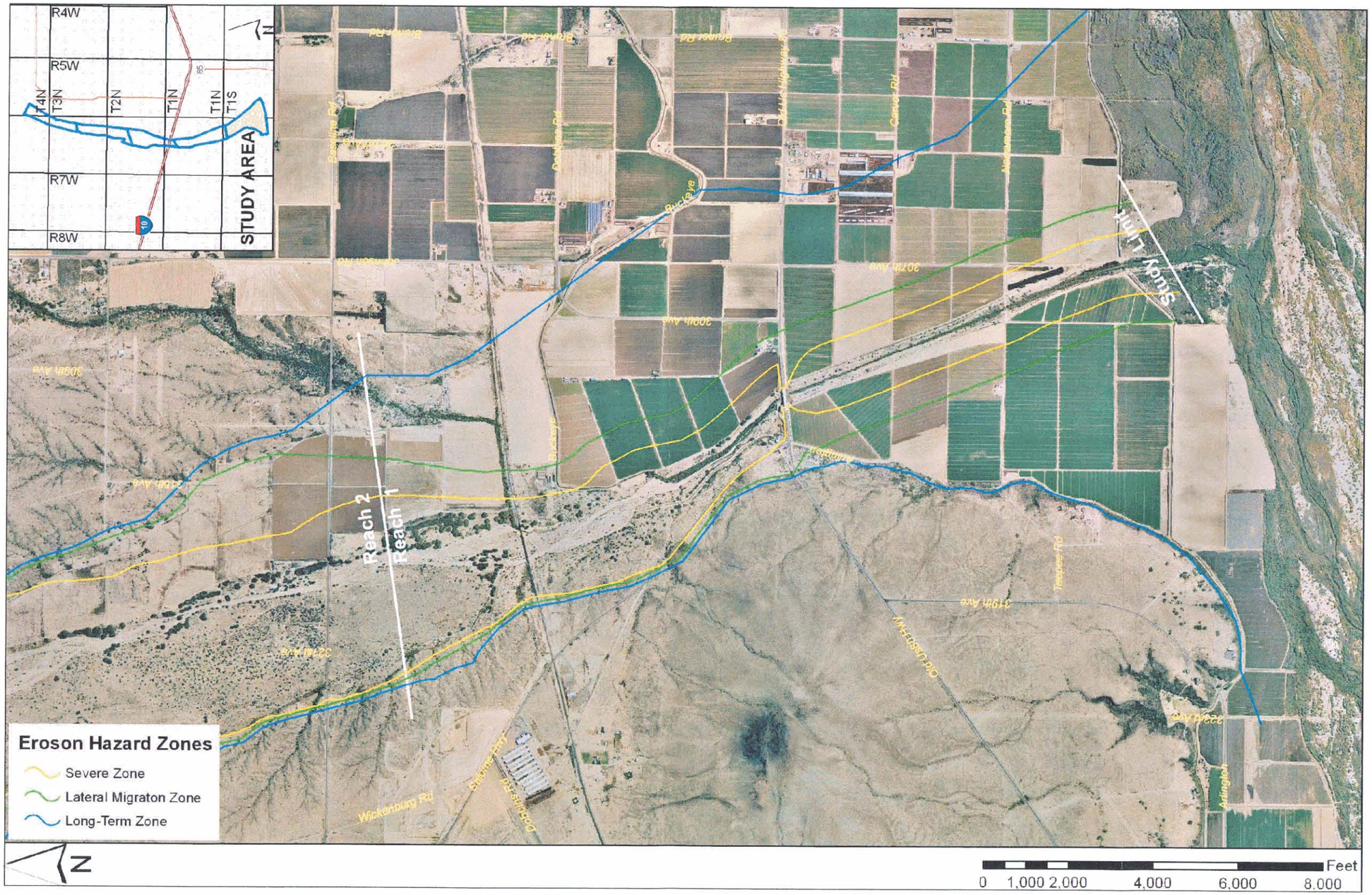

Figure 6-17. Lower Hassayampa River Erosion Hazard Zones - Reach 1

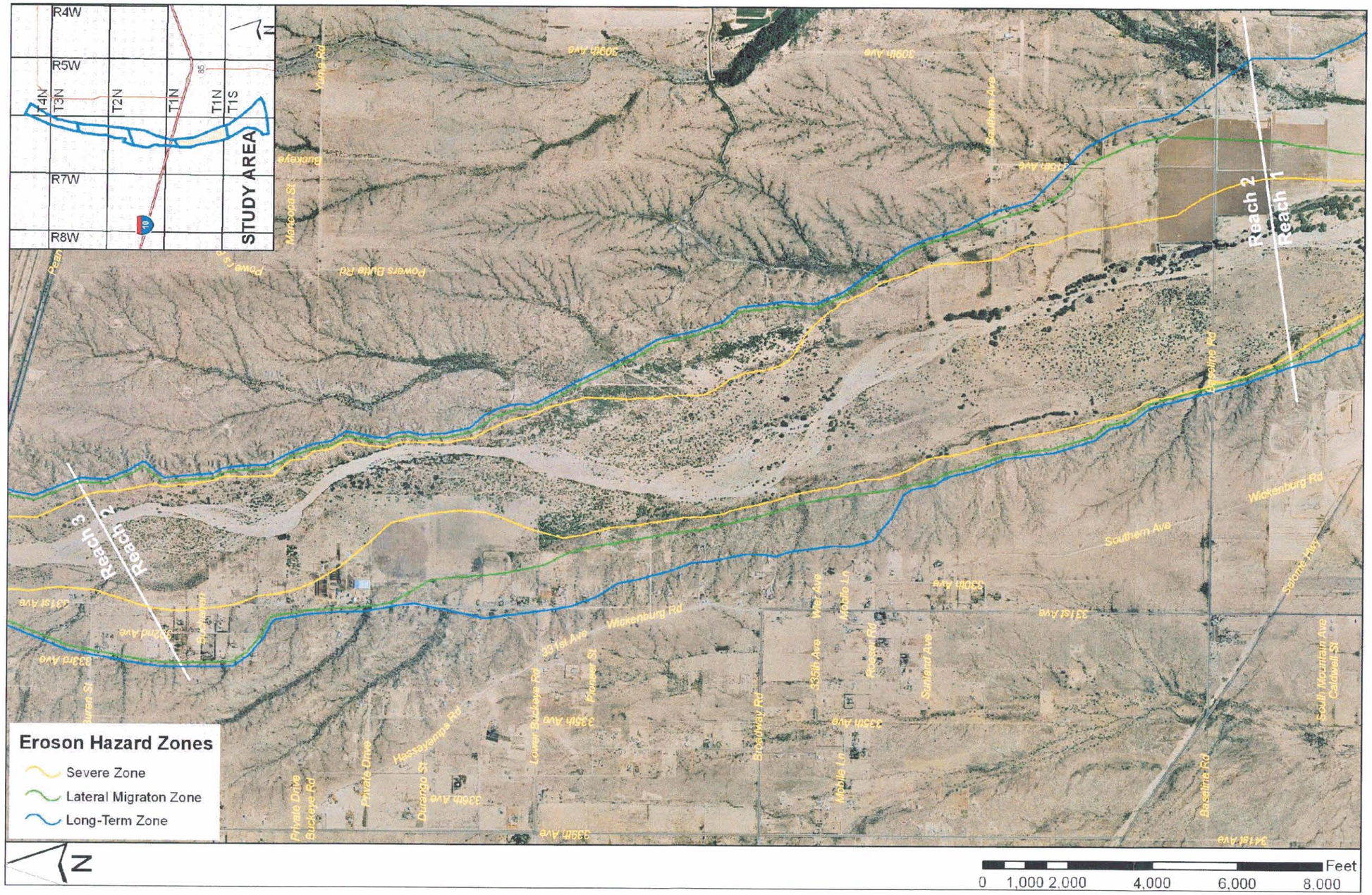

Figure 6-18. Lower Hassayampa River Erosion Hazard Zones - Reach 2

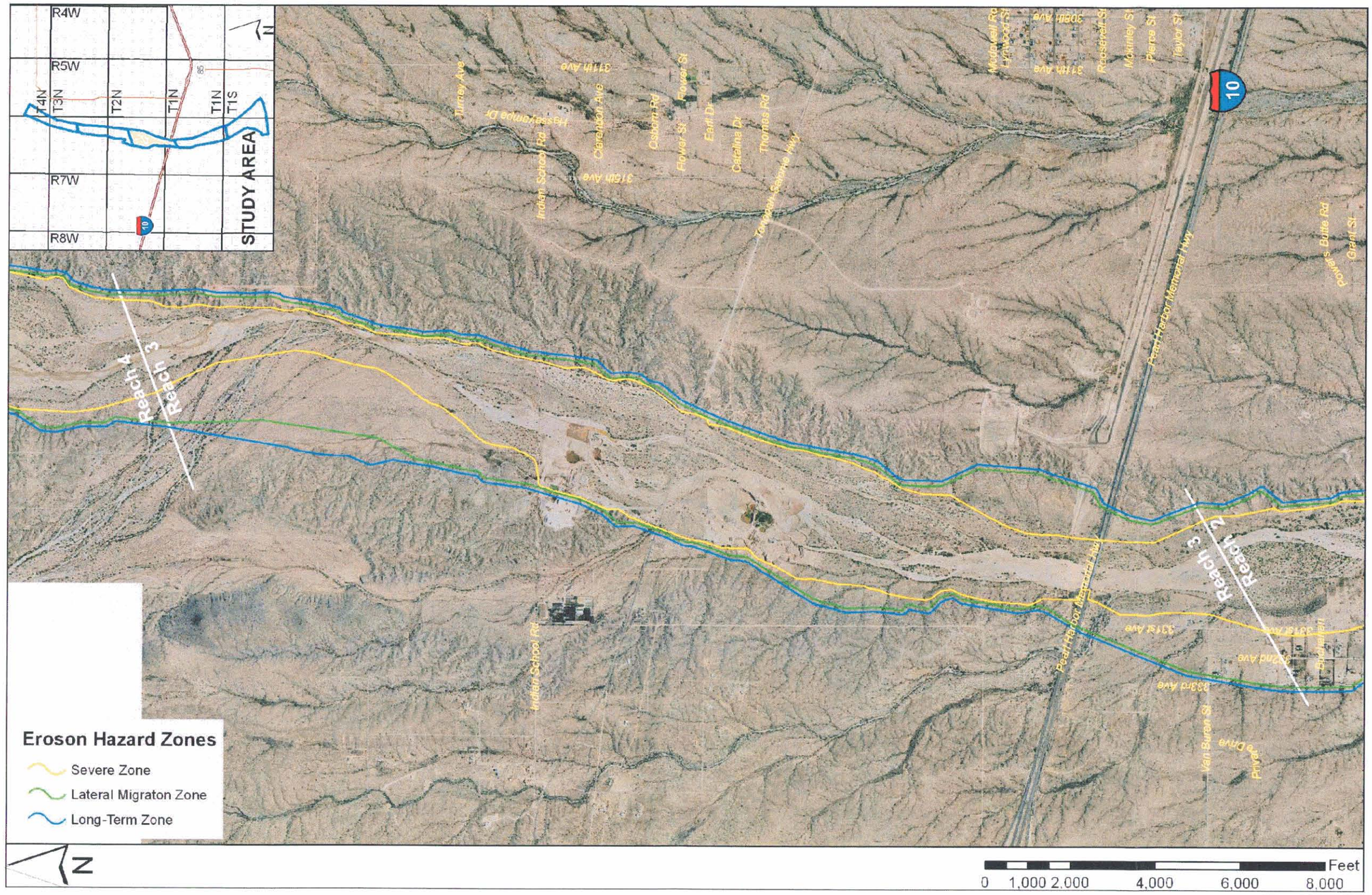

Figure 6-19. Lower Hassayampa River Erosion Hazard Zones - Reach 3

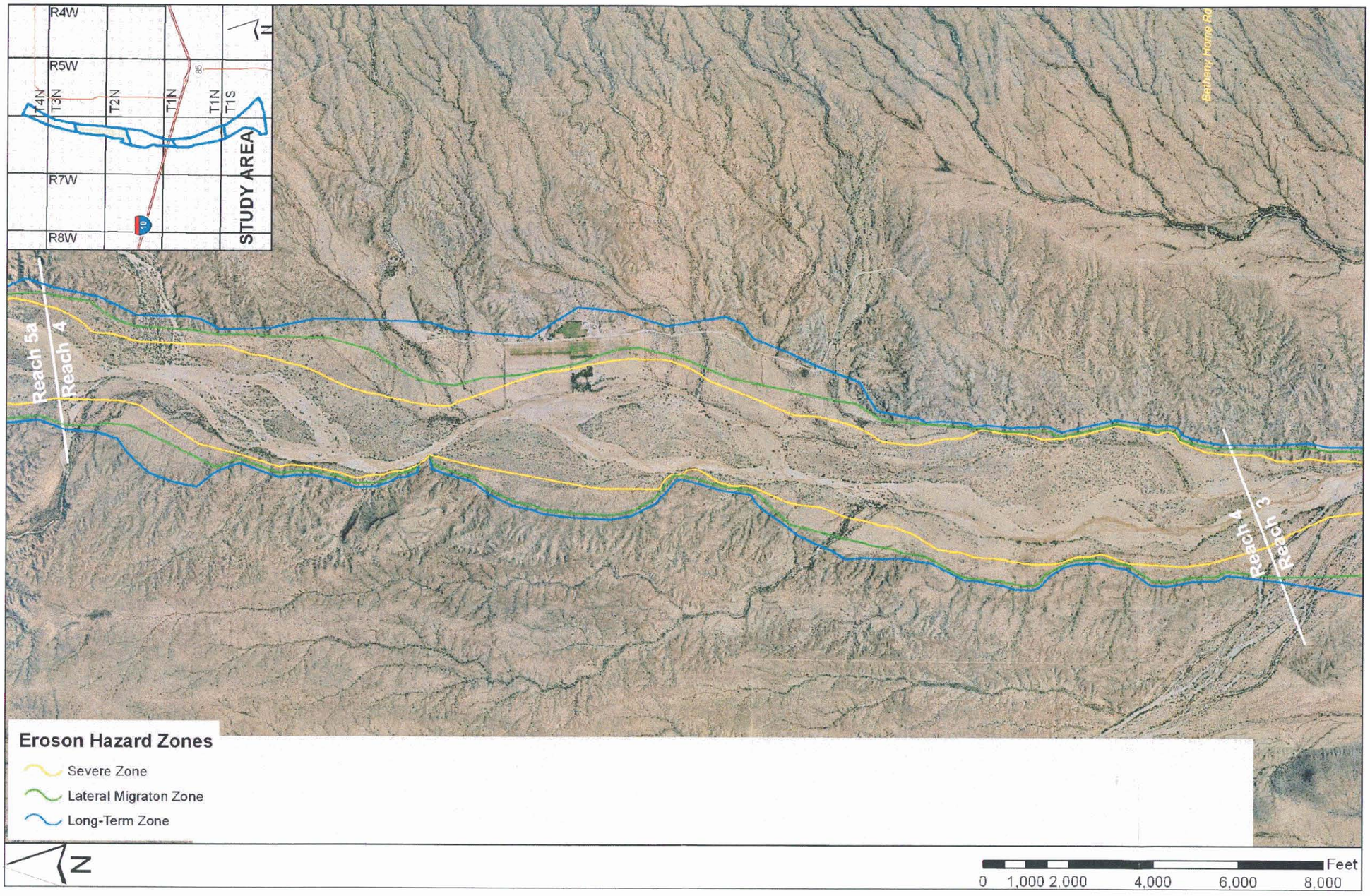

Figure 6-20. Lower Hassayampa River Erosion Hazard Zones - Reach 4

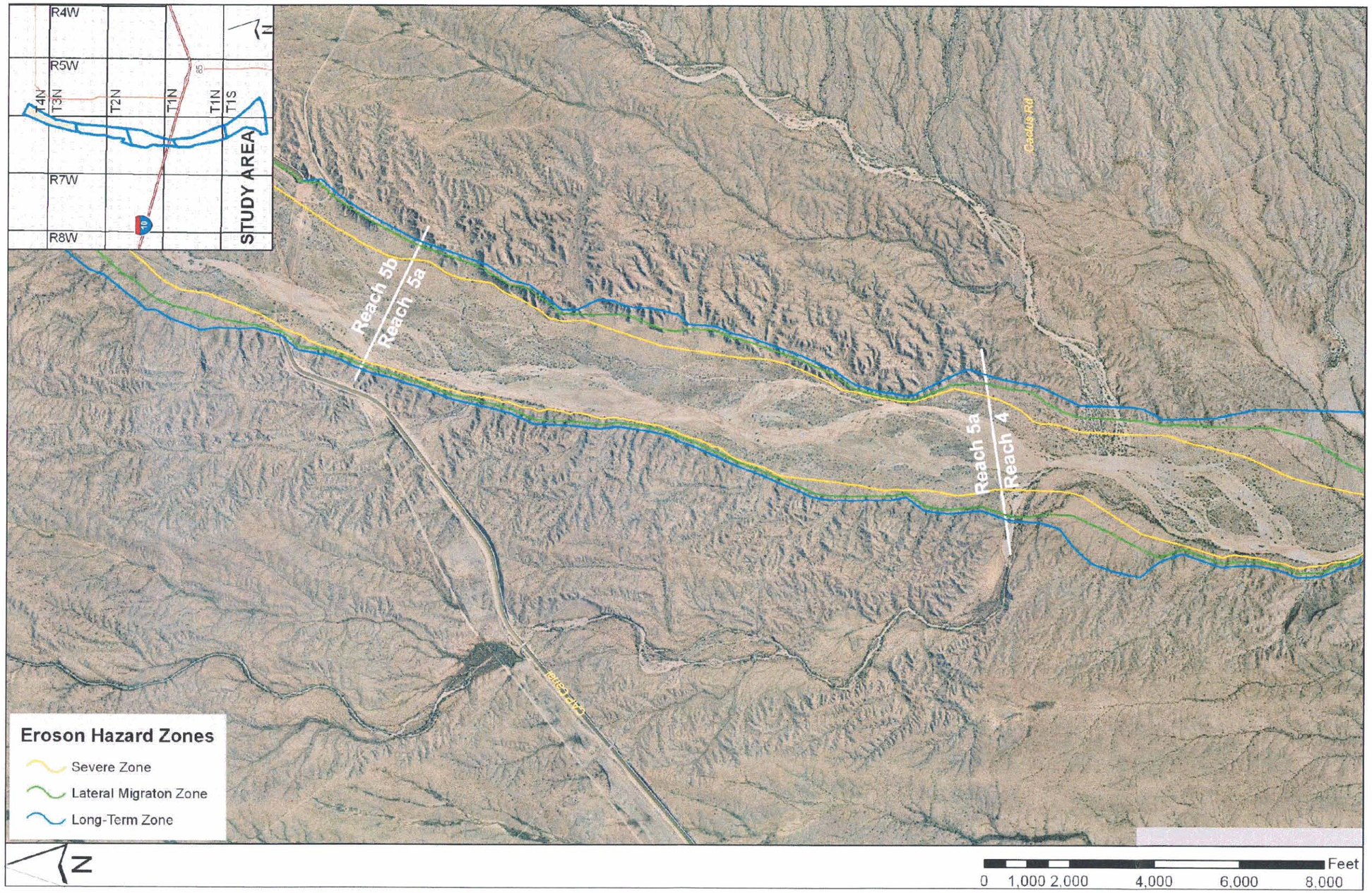

Figure 6-21. Lower Hassayampa River Erosion Hazard Zones - Reach 5a

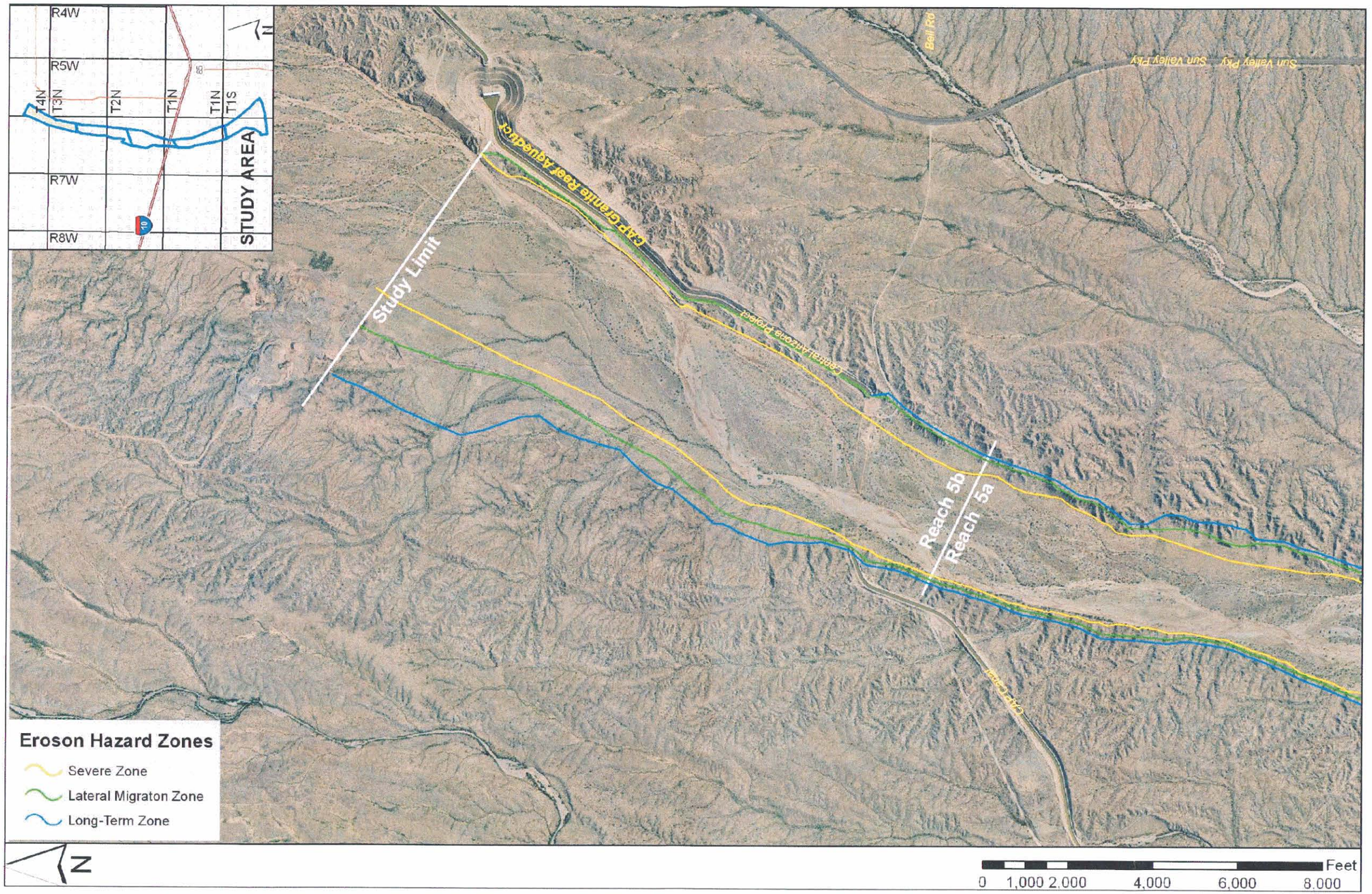

Figure 6-22. Lower Hassayampa River Erosion Hazard Zones - Reach 5b

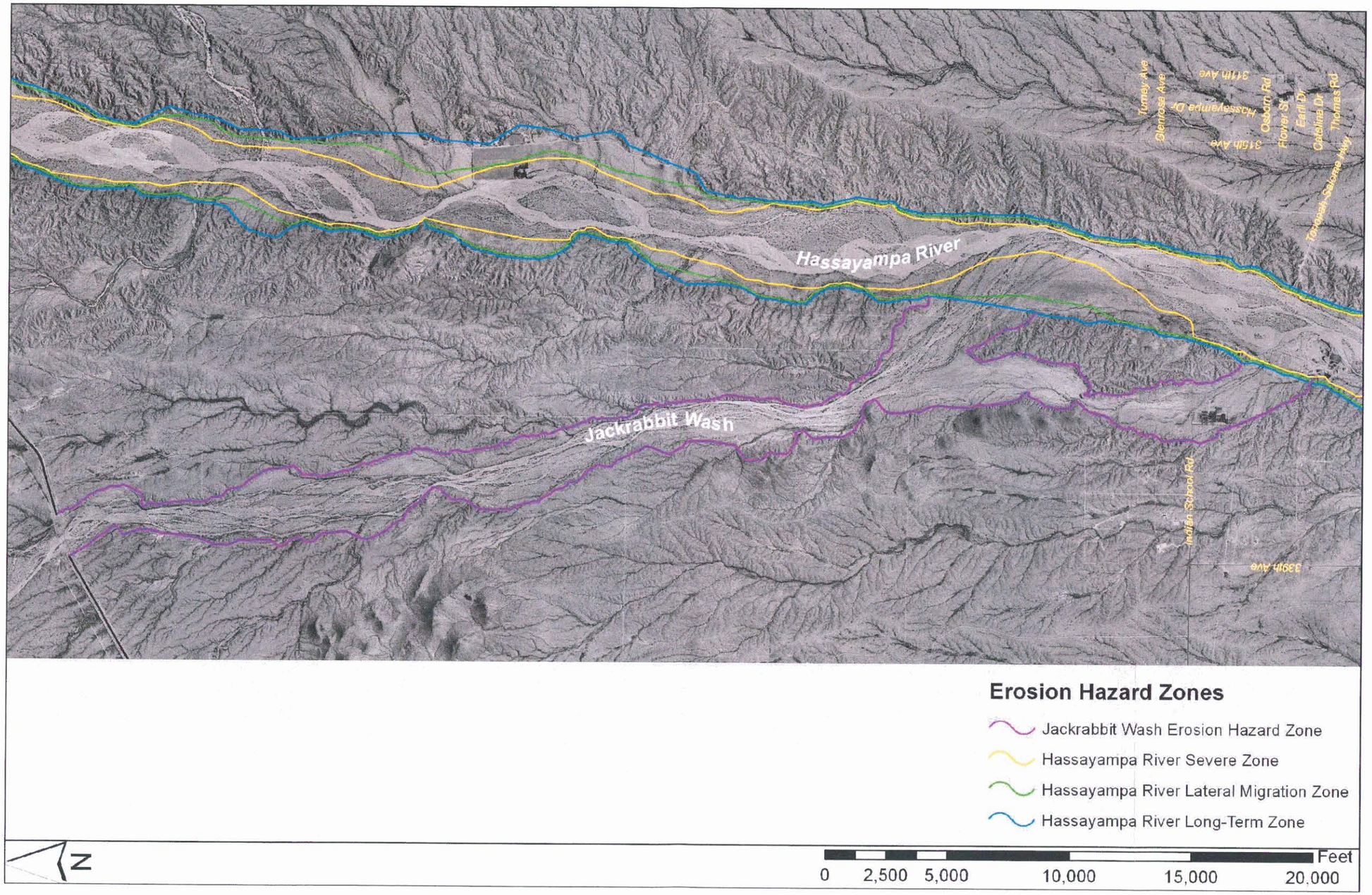

Figure 6-23. Jackrabbit Wash Erosion Hazard Zone

CHAPTER 7 - SEDIMENT TREND ANALYSIS

The purpose of the sediment trend analysis was to develop a management tool based on the results of the analyses described in Chapters 2 to 6 of this report. The sediment trend is intended to be used to evaluate the impacts of future activities and infrastructure in the channel corridor. The sediment trend analysis focused on predicting the following potential channel responses:

- Aggradation and Degradation
- Lateral Channel Movement
- Response to Urbanization and Channelization

The sediment trend analysis also serves as a summary and synthesis of the various methodologies presented in the previous chapters of the LHWCMP River Behavior Report.

7.1 River Behavior Trends: Vertical Channel Change

Rivers respond to fluctuations in water and sediment supply by adjusting their bed elevation through aggradation or degradation. Aggradation is a progressive rise in bed elevation characterized by net deposition. Degradation is a progressive decline in bed elevation characterized by net scour. Trends in expected vertical channel change for the existing condition of the Lower Hassayampa River study reach were evaluated using the following types of information:

- Functional Surface Analysis
- Geomorphic Mapping
- HEC-6 Modeling
- Sediment Transport Calculations
- Observed River Responses

The existing condition trend for the study reach is long-term vertical stability, except in Reach 1 where degradation is occurring.

7.1.1 Functional Surface Analysis

The functional surface analysis described in Chapter 3 concluded that a majority of the Holocene floodplain in the study reach has been subject to active channel and floodplain processes during the 70-year period of record. Active channel and floodplain processes in the study area include channel scour and deposition, bar formation, and floodplain sedimentation. The functional surface analysis results, as well as the lack of high, relict terraces within the Holocene floodplain, reveals that the Hassayampa River uses its entire geologic floodplain to maintain its natural form and function. The bed elevation analysis also supports that interpretation. Absence of long-term degradation makes floodplain surfaces accessible to critical riverine processes such as floodplain sedimentation (storage), flow attenuation (floodplain storage), channel avulsions, and

high rates of lateral movement. The functional surface analysis also provides the following information regarding existing condition trends in vertical channel change for the LHWCMP study reach:

- The relatively low floodplain terraces are evidence of limited or no long-term scour. As a river degrades, its former floodplains are transformed into perched, relict terraces. No such segregation of terraces occurs in the Lower Hassayampa River geologic floodplain.

- The relative permanence of the active channel position demonstrated in the locational probability analysis is evidence of a lack of long-term aggradation. As a river aggrades, the active channel rises relative to the floodplain, which deflects high flow into the floodplain, causes new avulsive channels to form, and distributes the channel across the geologic floodplain. While a high potential for avulsion exists in the study reach, the historical record indicates that such changes occur infrequently during the large floods, rather than in response to gradual aggradation of the main channel.

- The large width of the active channel and floodplain absorbs and mutes potential vertical responses. Sediment deficits or surpluses can be made up by slight scour, widening, or shallow deposition over a very large area. That is, the wide floodplain serves as a large reservoir of sediment storage or supply that helps preserve the existing condition of the river.

7.1.2 Geomorphic Mapping

The geomorphic analyses provided the following clues to existing trends of vertical channel behavior for the study reach:

- Bank Height. There is no definitive trend in active channel bank height with respect to longitudinal distance along the study reach that suggests aggradation or degradation. Bank height typically increases in degrading rivers, and decreases in aggrading rivers. In contrast, the height of the Pleistocene terraces does decrease in the downstream direction, indicating a slight aggradational, valley filling trend in geologic time in the downstream portion of the reach.

- Tributary Confluence Elevations. Major tributaries flowing into the Hassayampa River join at an equal grade to the main stem. Tributaries to degrading rivers typically have hanging or over-steepened channels at their mouths. Tributaries to aggrading rivers typically are backfilled by main stem sedimentation. Neither condition occurs in the study reach. At the Gila River confluence, the Hassayampa River has experienced recent degradation, probably in response to a local base level fall on the Gila River.

- Tributary Terraces. The tributaries terraces that line much of the study reach typically are not inundated by the 100-year flood, and do not appear to be actively flooded by Hassayampa River floods. Degrading rivers typically actively

erode tributary sediments and remove their terraces. Aggrading rivers typically bury tributary deposits.

- Profile. The longitudinal profile of the Hassayampa River is very uniform through the study reach, indicating a history of vertical stability.

- Channel Pattern. The channel pattern is temporally persistent and not strongly braided, indicating that no significant aggradation has occurred.

- Geologic Control. No evidence was identified to indicate that the existing vertical channel stability is due to geologic control of slope by bedrock, hardpan, or other resistant subsurface layers. Although some anecdotal evidence exists for a basalt layer under the channel of Reach 1 upstream of the Old US 80 Bridge, and the SPRR Bridge as-builts note that the piers are founded on a hardpan, neither of these features crops out in the channel bed..

In Reach 1, the river appears to be degrading in response to either base level fall in the Gila River and/or channelization impacts due to the levees located downstream of Old US 80. Historical topographic data are the strongest evidence of recent degradation, but other evidence includes bed sediment coarsening along the perennial low flow channel, vertical drops in the low flow channel at the farm crossings, and high cut banks downstream of the Arlington Canal crossing.

7.1.3 HEC-6 Modeling

The HEC-6 models predict net channel change of less than one foot of either aggradation or degradation, regardless of the time period or flood frequency considered. The lack of vertical response, as predicted by the HEC-6 model, is partly due to the low flood peaks in the historical record, as well as the small flow volumes of the (flashy) 100-year design flood. The low predicted vertical response is also due to the fact that the river has a wide, poorly defined main channel (for sediment modeling purposes). Because of the width, sediment movement is spread over a large area, muting the potential response. In addition, the river's available sediment conveyance areas are spatially discontinuous within the floodplain, with low areas not linearly connected to upstream low areas, making modeling difficult.

The HEC-6 predicted deposition in Reach 1 levee area may be a modeling artifact, rather than a true depiction of past or expected channel behavior. Longitudinal profiles of the reach indicate degradation has occurred recently in the lower part of Reach 1, in response to base level change at Gila River. Base level changes are not modeled well by HEC-6. No field evidence of long-term aggradation in Reach 1 was observed, although local farmers recount past efforts to periodically clean the channel of vegetation and increase capacity. It is possible that increased roughness due to vegetative growth adjacent to the tailwater channel could induce deposition, although field evidence suggests the area of densest vegetation has degraded.

The HEC-6 model insensitivity to upstream and tributary sediment inflow may under-predict the actual response. HEC-6 programming code allows the model to obtain the full capacity of sediment transport at any section, regardless of whether river could actually pick up that load within the time step or distance between cross sections. This modeling assumption may lead to impractical or unrealistic consequences. For example, the model will compute scour below the invert of the next downstream section, which would create an adverse slope (zero velocity, and thus zero transport) in a single time step. In reality, such a vertical adjustment could not occur. The huge reservoir of available sediment in the wide cross sections of the Hassayampa River makes the model insensitive to variations in sediment inflow at the upstream end or at tributaries. In reality, a sediment deficit at an inflow point would be made up over a longer reach, over a longer time period, and would generally be limited to the areas nearest the main channel.

The HEC-6 modeling results for vertical channel change near gravel pits was not conclusive. While the model correctly depicted headcut and tailcut formation, the results were very different from those predicted by the ADOT equations, as well as from the field observations during the December 2004 floods. No calibration data were available from which to evaluate the accuracy of the HEC-6 or ADOT model results.

7.1.4 Sediment Transport Calculations

Sedimentation engineering analyses indicated that the Hassayampa River flows at a steeper slope than most other rivers of its size and sediment characteristics. Because of the fine-grained sediment composition in the channel and floodplains, scour is not prevented by armoring, and the bed and banks are highly vulnerable to scour and erosion. Regime equations predict that the equilibrium channel will be deeper and flatter than the existing channel. Allowable velocity results indicate that erosion should be expected. Despite these tendencies toward scour, the channel has not experienced any known vertical adjustments, except near in-stream mining. High sediment transport rates and the large available sediment reservoir are probably responsible for preserving an apparent equilibrium state. The engineering analyses that predict extensive long-term degradation could be interpreted to mean that the existing river condition is near an erosive threshold and that it may be vulnerable to future changes in sediment or water supply.

7.1.5 Observed River Responses

The vertical characteristics of the Hassayampa River have responded to natural floods in the following ways:

- No Net Vertical Change. No substantive changes in channel or floodplain elevation were observed by field, historical, or modeling analyses.
- Scour and Fill. Flood scour appears to be balanced by fill in the study reach, either temporally or spatially.
- Non-Scouring Layer. Observations of the walls of active sand & gravel excavations, and at an excavation that temporarily exposed the CAP siphon, indicate that there is a non-scoured layer at a depth of about 10 feet below the

active channel bed. Evidence for this layer includes the degree of compaction, soil reddening, and carbonate accumulation at depth. The presence of such a layer at depth beneath the active channel suggests that no long-term degradation has occurred in the recent past, since degradation would have removed the overlying loose sediment.

- Channel Soil Pits. Soil pits excavated in the main channel indicated that the active transport layer is at least six feet deep in most places, and that no scour resistant layer exists below the channel bed.

There are few existing long-term human activities in the study reach from which to assess the observed impact on the river. The following types of human activities were observed:

- Bridges. The three bridges in the study reach have had no obvious impact on the vertical stability of the river. Neither aggradation nor degradation appears to have occurred at any bridge or in the adjacent stream reaches. Channel changes observed at the Old US 80 Bridge are interpreted to be responses to channelization, rather than bridge construction.
- Dip Crossings. Paved dip crossings at Baseline Road and the Tonopah-Salome Highway may provide grade control during small flows, but are usually eroded during floods of any significance. Bed elevation adjustments observed during or after floods at the dip crossings are interpreted as natural processes or response to adjacent mining, rather than related to the dip crossings themselves.
- Levees. Historical data suggest that the river has not degraded or aggraded in the levee reach in spite of the flow constriction. Recent degradation (and possible historical aggradation) is probably more related to local base level fluctuation in the Gila River than to the levee channelization.
- Structures. Local scour occurs at structures such as power poles or bank protection, but no significant long-term changes were observed.
- Mines. In-stream mines are a relatively recent feature in the study reach, but appear to have cause local degradation by direct excavation, headcutting, and tailcutting, as well as capture of the low flow channel.

In general, the river has had few significant, wide-spread, observed vertical responses to the natural or imposed environment.

7.1.6 Aggradation/Degradation Trend

The river behavior analysis tasks completed for the LHWCMP indicate that in its existing condition, the Lower Hassayampa River has experienced neither significant aggradation nor degradation. The river experienced slight net aggradation from 1987 to 2004, but at levels well within the measurement accuracy. Recently, the downstream end of Reach 1 near the Gila River confluence has degraded.

7.2 River Behavior Trends: Lateral Channel Change

Rivers respond to fluctuations in water and sediment supply by adjusting their channel geometry, channel pattern, and stream width through lateral erosion or channel

deposition. Trends in expected lateral channel change in the Lower Hassayampa River study reach were evaluated using the following types of information:

- Functional Surface Analysis
- Geomorphic Mapping
- HEC-6 Modeling
- Sediment Transport Calculations
- Observed River Responses

The existing condition trend for the study reach is active channel movement, channel widening during floods, and infrequent but significant channel avulsions.

7.2.1 Functional Surface Analysis

The functional surface analysis described in Chapter 3 concluded that a majority of the Holocene floodplain in the study reach has been subject to active channel and floodplain processes during the 70-year period of record. All of the functional surfaces are of very recent geologic age and are composed of highly erodible fine-grained alluvium. Tributary terraces have been relatively persistent landforms during the past 70 years, but the functional surface analysis indicates that the small tributary terrace deposits are readily eroded when the main stem active channel abuts them. A primary geomorphic response to flooding is the expansion of the area occupied by the active channel and bars. Channel widening and formation of new avulsive channels should be expected in future floods.

The differences between Reach 1 and the other Lower Hassayampa River study reaches are readily apparent from the functional surface analysis. There are essentially no bar deposits in Reach 1, while bars and low floodplains comprise a significant part of the geologic floodplain in the remainder of the study area. The Reach 1 floodplain consists solely of the active channel and the (disturbed) floodplain.

7.2.2 Geomorphic Mapping

The geomorphic mapping analysis revealed that the entire geologic floodplain is composed of very young surfaces, which indicates that none of the floodplain has been stable for any significant period of time. The Pleistocene terraces that bound the river valley offer some resistance to lateral erosion, but are themselves subject to some degree of erosion. While no measurable erosion of the Pleistocene (Qm) surfaces occurred during the 70-year period of record, even where low flow channel abuts it, field evidence suggests they are trimmed by lateral channel erosion. Based on the photographic record and field evidence, a maximum rate of less then one foot per year was assumed. Certainly, the Pleistocene terraces are more resistant than the Holocene floodplain surfaces on the opposite bank of the main channel, leading to preferential erosion of the younger surfaces.

Comparison of historical aerial photographs revealed the magnitude of potential lateral movement during large floods and over time. Lateral erosion of more than 1,400 feet during a single flood and more than 1,900 feet during the period of record was

documented. This degree of lateral erosion is more than sufficient to allow channel movement across the geologic floodplain within any reasonable planning period. Despite the magnitude of measured channel movement in some locations, overall the locational probability analysis indicated a tendency for the low flow channel to occupy or re-occupy the same position during the period of record, a conclusion which is supported by field observations of large saguaro stands on mid-channel islands.

Locational probability analysis also reveals a chute and splay pattern to alternating stable and unstable reaches. This chute and splay pattern of the existing low flow channel may provide a useful analog for assessing potential channelization impacts. The "chute" sections consist of single, well-defined channels that flow toward wider "splay" reaches that distribute the low flow into a multiple-channel network. The chute and splay pattern appears to be relatively persistent in the landscape, and part of the river's natural form and function. Short channelized reaches might be designed using the chute length and characteristics as a template, as long an opportunity for a downstream splay were preserved.

7.2.3 HEC-6 Modeling

HEC-6 models provide no information directly applicable to assessing lateral stability trends. However, given the HEC-6 model prediction of near stability for the study reach, it may be concluded that the extreme lateral movement observed along the river corridor is not a function of a sediment deficit or surplus. The model results may also indicate that the low flow channel is at its regime depth, so that any sediment deficit or surplus will be satisfied by channel width adjustments.

7.2.4 Sediment Transport Calculations

The sedimentation engineering methodologies used indicate that the channel bed and banks have no inherent stability. Therefore, any long-term persistence of low flow channel position, as seen by locational probability analysis, is surprising. The locational stability may be due in part to high sediment supply rates that reduce the erosive force, transmission losses that reduce flow rates relative to the sediment supply over the reach length, and dumping of excess sediment upstream of the study reach where the stream is more braided.

7.2.5 Observed Lateral Channel Responses

The lateral characteristics of the Hassayampa River have responded to natural floods in the following ways:

- Widening. The primary response to flooding in the study reach is channel widening. Channel widening is expressed as expansion of the low flow channel or by formation of wide bars adjacent to the channel. During most floods, the main channel tends to widen rather than cut new channels elsewhere within the floodplain.
- Lateral Erosion. Accretive lateral erosion also occurs during floods, and is primarily expressed as meander movement on bends.

- Avulsion. Channel avulsions are a rare, because floods are rare, but are an observed outcome of flood inundation of the floodplain. Avulsive channel paths include tributary channel alignments, overbank swales, and channels formed by on-surface internal drainage.
- Tributary Control. The most laterally stable and spatially persistent low flow channel reaches on the Lower Hassayampa River are those that are adjacent to major tributary deltas. Tributary terraces at the Wagner/Daggs Wash confluence and the Jackrabbit Wash confluence have controlled channel width and location for nearly 70 years, in contrast to highly mobile reaches upstream and downstream.
- Drainage Pattern Persistence. Flood flows tend to follow existing channel paths rather than create new ones, thus providing some degree of long-term lateral stability.

One of the more interesting observed features of the study reach is the apparent lack of response to channelization in Reach 1 and to bridge construction in Reaches 2 and 3. The lack of an adverse lateral response in Reach 1 is more surprising given that the natural form in Reach 1 was probably a distributary channel pattern on the Hassayampa River confluence delta. The classic response to channelization, especially where the channel and floodplain are significantly narrowed, is long-term degradation, increased sinuosity, and/or bank failure. However, the channelization in Reach 1 has been very stable laterally, despite the fact that the channel is contained by only non-engineered levees composed highly erodible floodplain alluvium. The lack of response in Reach 1 may be due to any or all of the following:

- Limited Flow Volume. Few days of flow during most years means few opportunities for the river to do significant geomorphic work. Hydrologic records indicate that approximately 1300 days of flow greater than 100 cfs occurred during the 60-year record (6% of time).
- Rare Floods. On arid region streams, much of the geomorphic work is accomplished during floods. The period of record is characterized by few large floods.
- High Sediment Supply. The very high sediment supply and transport rate means no sediment deficit exists, and thus there is no need for erosion to reach the transport capacity. In fact, bank collapses during floods probably produce excess sediment loads that must be deposited as bars or on the floodplain.
- Transmission Losses. The study reach is a losing stream, with significant loss of surface water to infiltration and floodplain storage. As the water discharge decreases with distance along the reach, the transport capacity decreases resulting in sediment deposition rather than erosion.
- Channel Maintenance. Field and anecdotal evidence suggests that local residents may periodically repair levees and grade the narrow floodplain.

The lack of lateral channel response in Reach 1 may be functionally similar to the long-term lack of widening in the tributary delta reaches. The reasons listed above may

cause the river to be more tolerant of localized impositions on the natural form than other, sediment deprived rivers in urbanized watersheds.

7.2.6 Lateral Movement Trends

The river behavior analysis tasks completed for the LHWCMP indicate that in its existing condition, the Lower Hassayampa River has experienced periodic large magnitude lateral channel change, especially during large floods, but that the river may be tolerant of localized channelization as long as sediment supply remains high relative to transport capacity.

7.3 Implications of Sediment Trends

The sediment trends identified for the existing condition of the Lower Hassayampa River for the LHWCMP Phase 1 River Behavior Analysis can be used to predict the expected future behavior of the river.

7.3.1 Flood Response

Floods have been the primary mechanism for channel change within the LHWCMP study reach. There is no reason to expect any change in the existing channel pattern as long as the flood hydrology is unchanged. Because the normal condition of the river is a dry riverbed, no channel change occurs during normal conditions. During floods, energy is supplied to the system to do the geomorphic work imposed by the water and sediment inputs, as well as the work required to move the stream toward its dynamic equilibrium state. Historically, the typical flood response in the study reach has been channel widening, bank erosion, and floodplain sediment deposition. If sediment supply rates and transmission losses remain high, then the erosive response to floods will be limited to that experienced historically.

7.3.2 Natural Channel Controls

No permanent natural channel controls were found in the LHWCMP study reach, except for a small area of bedrock on the right bank of Reach 4. No natural vertical channel controls exist in the study reach, and except for the recently constructed channel lining at the Old US 80 Bridge section, no vertical control of any kind exists. The Pleistocene terraces that bound the river valley in Reaches 2 to 5 are more resistant than the floodplain soils, and thus provide some degree of lateral control. However, the terraces show evidence of being eroded when the main channel flows directly against them. Therefore, if changes are imposed on the natural river system, or if development occurs within the lateral migration erosion hazard zone, structural measures will be required to prevent damage to development by natural riverine processes because no natural barriers exist.

7.3.3 Encroachment & Channelization

Encroachment and channelization may have a profound impact on channel stability in the LHWCMP study reach. While the existing channelized reach has had few known responses to its limited areas of channelization, the sediment trend analysis identified the following scenarios in which encroachment and/or channelization would adversely affect channel stability:

- Decreased Sediment Reservoir. Channelization and encroachment, if protected from lateral erosion and flood inundation, would decrease the size of the large sediment reservoir that is comprised by the wide active channel and floodplain. This sediment reservoir acts as a buffer that mutes potential channel responses to local changes in the sediment balance. Without access to the buffering sediment reservoir, sediment deficits and surpluses would be more strongly expressed vertically in a narrowed river corridor.
- Decreased Transmission Loss. Channelization and encroachment would decrease the wetted perimeter of the channel and floodplain and reduce opportunities for infiltration and floodplain storage. Without these types of flow attenuation, peak discharges and thus, sediment transport capacity, would remain high over the length of the study reach. High sediment transport capacity translates to increased scour and erosion.
- Increased Flow Velocity. Sediment transport is exponentially related to flow velocity. Encroachment or channelization that increases flow velocities would increase sediment transport rates, flatten equilibrium slopes (scour), and accelerate lateral erosion rates.
- Decreased Floodplain Width. Narrowing the river corridor increases the sediment transport rate relative to the sediment supply, reduces available sediment supply from the banks and floodplain, increases velocities, and decreases flow attenuation, all of which tend to increases erosion potential.

It is important to note that the restricted active channel widths at the major tributary deltas have not had adverse consequences on main stem stability, probably because the sediment supply remained high. Furthermore, the floodway encroachment analyses performed by WEST Consultants indicated only minimal increases in velocity, flow depth, and peak discharge by encroachment of the floodway fringe.

7.3.4 Bridge Crossings

Mathematical modeling of bridge hydraulics and sedimentation was not part of the LHWCMP Phase 1 scope of services. Therefore, the sediment trend analysis for bridge crossings relies on observations of impacts (or lack thereof) at the few existing bridges in the study reach. Given the high probability that numerous new bridges will be constructed in the rapidly developing watershed, more detailed evaluation of bridge impacts should be included in the LHWCMP Phase 2 scope of services. Specifically, the Phase 2 analysis should investigate the expected long-term scour relative to existing and future bridge foundation depths for various encroachment, channelization, and hydrologic scenarios. Impacts on long-term vertical stability at utility crossings should also be considered.

The I-10 and SPRR Bridges show minimal or no discernable impacts from long-term river processes or from specific floods. In addition, the river reaches adjacent to the bridges appear to be similarly unaffected by the bridge modifications to the natural system. Therefore, if the sediment transport, flood characteristics, and hydraulics in the river system remain substantially unchanged, then bridges with similar widths, pier

configurations, abutment designs, and freeboard should respond similarly to the existing bridges' response.

7.3.5 Sand & Gravel Mining

It is well documented that in-stream aggregate mining creates local sediment deficits that cause headcutting and tailcutting. In no case does in-stream mining increase the stability of a natural river system. However, if in-stream mining is adequately engineered, the impacts to the stream system may be reduced to a level at which no adverse impacts to adjacent properties occur. For the Hassayampa River, the sediment trends identified relative to in-stream mining indicate the following:

- Headcut. Given the fine-grained channel and floodplain sediments, the Hassayampa River is especially susceptible to headcutting during small floods. During large floods, if the mines are spaced adequately, the large sediment reservoir and high sediment supply rate will tend to fill shallow pits and bury headcuts, at least in the short term.
- Tailcut. Tailcutting downstream of in-stream excavations will occur in the study reach. However, the large sediment reservoir can act to limit the effective zone of tailcut channel, if the mines are spaced adequately to prevent a domino effect of intersecting tailcuts and headcuts.
- Potential Capture. The wide erosion hazard zones along the Hassayampa River indicate that any excavation within the geologic floodplain is subject to capture by the main channel if it experiences lateral migration. In addition, because of the tendency for headcuts to propagate long distances upstream, there is increased risk that small braids that flow into channel excavations will lead to headcuts that capture the main channel upstream, diverting it toward the excavation.

Some potential may exist to establish mining districts along short channelized reaches between bridges, as long as they are structurally isolated from the main channel, as discussed in Section 7.3.3 for channelization. Using the tributary delta reaches as a reference template, and/or matching the channel chute and splay distribution, reach lengths which may have minimal impacts on the channel might be defined.

7.3.6 Watershed Urbanization

If the natural flood hydrology of the watershed is altered, the river's flood response is likely to be altered as well. Probable flood responses to the following types of hydrologic alterations are suggested by the observed and predicted sediment trends:

- Flood Frequency. Flood frequency may increase if watersheds urbanize without enforcing retention or detention standards. An increase in the number of runoff events will increase the rate of channel adjustment, including lateral erosion and long-term degradation. A decrease in flood frequency due to retention of is likely to make the channel more vulnerable to lateral erosion, but decrease the opportunity for such erosion to occur.
- Flood Volume. Runoff volume may increase if no retention or detention standards are applied to the urbanizing upland watersheds. Increases in runoff

volume will increase the potential for, and rate of, long-term degradation by increasing the sediment transport rate and decreasing the sediment supply.

- Effluent Discharge. Discharge of treated effluent to the normally dry Hassayampa River channel will undoubtedly impact channel morphology. Discharge rates below the threshold of sediment movement will have minimal direct impacts but will likely increase vegetative growth, channel roughness, and avulsion potential. Discharge to floodplain areas will have less impact than discharge directly to the active channel areas.

Watershed impacts are most likely to be expressed in the portions of the Hassayampa River that are within the LHWCMP study reach. Upstream of the study reach, much of the watershed lies within National Forest boundaries and is unlikely to be urbanized.

7.4 Recommendations for Future Sediment Analyses

The following sedimentation engineering analyses are recommended for Phase 2 of the LHWCMP, based on the results of the sediment trend analysis:

- HEC-6 Channelization Model. The relative trend of channel change should be assessed by comparing the base condition HEC-6 model developed for this study with HEC-6 models that depict various channelization options.
- HEC-6 Sand & Gravel Spacing Impact Model. HEC-6 models with varying densities, spacing, and sizes of in-stream excavations should be prepared to assess the ability of the river to absorb the impact of in-stream mining. Headcut and tailcut profiles for pits should be prepared using the ADOT methodology in conjunction with the HEC-6 modeling to assess potential impacts to reaches between pits.
- Bridge Scour. Local and long-term scour at bridges should be computed to determine potential impacts to bridge stability for the recommended future channel condition.

7.5 Summary

Sediment trends for the Lower Hassayampa River were identified based on the river behavior analyses performed for the LHWMCP. The existing condition of the study reach is vertically stable and subject to high rates of lateral migration. The high rates of expected lateral erosion should not be viewed as instability, but rather as the natural tendency of the river. Attempts to control the naturally high lateral erosion rates will likely have long-term consequences for vertical channel stability, sediment continuity with adjacent reaches, and public expenditure for maintenance and repair.

CHAPTER 8 - SUMMARY

The historic and geologic records indicate that the Lower Hassayampa River is vulnerable to extreme rates of lateral channel movement. Population growth in the Phoenix west valley has increased the pressure to develop flood and erosion prone lands along the major stream corridors. A watercourse management plan is required to prevent flood damages and preserve the natural function of the streams. The analyses summarized in the previous chapters have shown that lateral migration is not a new phenomenon in the LHWCMP study area. The recommended management alternatives are intended to promote safe development of the river corridor in the fugure.

The River Behavior Report prepared in support of the LHWCMP included the following six primary types of analyses, each of which was discussed in the preceding chapters:

- Field Reconnaissance Analysis
- Geomorphic Analysis
- Bed Elevation Analysis
- Sediment Transport Analysis
- Lateral Migration Analysis
- Sediment Trend Analysis

In addition, erosion hazard zones were delineated for the entire study reach.

8.1 General Recommendations

The following general recommendations are intended for management of the Lower Hassayampa River and Jackrabbit Wash with the study area:

1. Adopt the recommended lateral migration erosion hazard zone for floodplain management purposes.

2. Proceed with Phase 2 of the LHWCMP to identify effective management guidelines for the Lower Hassayampa River.

3. Regulate all new development within the severe and lateral migration erosion hazard zones by requiring a special use permit. To obtain a permit, the development within the corridor must do the following:

    - Meet the National Flood Insurance Program (NFIP) requirements for development within a floodplain.
    - Provide an engineering and geomorphic study certifying that the proposed development will not be affected by erosion over a 60-year planning period.
    - Demonstrate that any proposed bank stabilization will not deleteriously affect reaches or development upstream and downstream.

- Demonstrate the stability of any proposed bank stabilization. Local scour, long-term degradation, channel movement, and bank erosion shall be explicitly addressed in the design reports for any proposed bank protection.
- Hold the Town of Buckeye, the Flood Control District of Maricopa County, and Maricopa County harmless from any and all claims resulting from erosion or any other flood related damage to development within the erosion corridor.
- Provide for perpetual maintenance of bank stabilization at no cost to any public agency. Provide for maintenance and access easement adjacent to any bank stabilization.
- Obtain necessary floodplain, wetlands (404), and water quality (401) permits or approvals for any construction activities at no cost to any public agency.

4. Design Guidelines for Single Lot Development in Erosion Hazard Zones. The high lateral erosion hazard on the Lower Hassayampa River will create difficulties for management of erosion hazards in areas outside of master planned communities and large subdivisions due to the cost of mitigation measures. Plans for acceptable erosion management measures should be developed as soon as possible.

5. Regulation of In-Stream Sand & Gravel Mining. Sand and gravel mining is likely to result in channel degradation and increased bank erosion if it is not properly engineered and managed. The following minimum requirements should be fulfilled:

    - A mining reclamation plan should be established prior to the initiation of mining or leasing of land.
    - An assessment of potential upstream and downstream impacts should be prepared that certifies that no adverse impacts will occur under normal and extreme flow conditions. The assessment should include detailed consideration of the full range of possible discharges (normal low flow to 100-year flood), application of the types of geomorphic analyses summarized in this report, and mathematical modeling of sediment transport, headcut progression, and scour. The assessment should also include consideration of cumulative impacts that could be caused if similar mining were allowed everywhere on the watercourse.
    - In-stream mining or other excavation that intercepts, blocks or diverts the main channel should be prohibited. Excavation within the 100-year floodplain or lateral migration erosion hazard zone should be avoided, and should include engineered bank stabilization and grade control where permitted.

6. Future Monitoring. Channel stability should be monitored periodically to assess impacts of floods, to determine whether erosion hazard zones should be updated, and to document continued channel change for application to other stream systems in Maricopa County. The monitoring effort should include the following:

    - Establish monitoring stations at the field sections established for this study. Cross sections should be inspected and photo-documented during the fall of

every year, and immediately after any flood that exceeds the 5-year recurrence interval.

- Controlled aerial photography should be collected every other year or after any flood that exceeds the 10-year recurrence interval.

CHAPTER 9 – REFERENCES

Ackers, P. & Charlton, F.G., 1971, "The Slope and Resistance of Small Meandering Channels," Institute of Civil Engineers, Proceedings, Supplement 15, 1970, Paper 7362S.

Birkeland, P. W., 1984, Soils and geomorphology: New York, Oxford University Press, 372 p.

Birkeland, P. W., Machette, M. N., and Haller, K. M., 1991, Soils as a tool for applied Quaternary geology: Utah Geological and Mineral Survey Miscellaneous Publication 91-3, 63 p.

Blench, T., 1951, "Regime Theory for Self-Formed Sediment-Bearing Channels," ASCE Proceedings, Vol. 77.

Brice, J.C., and Blodgett, J.C., 1978, Countermeasures for Hydraulic Problems at Bridges," Volumes 1 & 2, FHWA/RD-78-162,163. Federal Highway Administration, Washington, D.C.

FCDMC, 2003, *Erosion Hazard Zone Delineation and Development Guidelines*, Flood Control District of Maricopa County, Arizona.

FHWA, Federal Highway Administration, 1991, Stream Stability at Highway Structures, Hydrologic Engineering Circular No. 20. FHWA Publication No. FHWA-IP-90-014. McLean, Virginia.

JE Fuller/Hydrology & Geomorphology, Inc., "Lower Hassayampa River Watercourse Master Plan, Hydrology Report," Submitted to: Flood Control District of Maricopa County, February 2005

Kennedy, R.G., 1895, The Prevention of Silting in Irrigation Canals, Min. Proc., Inst. Civil Engineers, Vol. CXIX.

Ritter, D.F, 1979, *Process Geomorphology*, Wm. C. Brown Publishers, Dubuque, Iowa.

Rosgen, D., 1996, *Applied River Morphology*. Wildland Hydrology, Pagosa Springs, Colorado.

Schumm, S.A., 1977, *The Fluvial System*, The Blackburn Press, Caldwell, NJ.

Simons, Li and Associates, "Effects of In-Stream Mining on Channel Stability," FHWA Report Number: FHWA-AZ89-250, Arizona Department of Transportation (ADOT), June 1989 (3 Volumes).

US Army Corps of Engineers, "HEC-6, Scour and Deposition in Rivers and Reservoirs," User's Manual, Aug 93, 286 pp.

WEST Consultants, Inc. "Lower Hassayampa River Watercourse Master Plan, Final Hydraulics Report, Hassayampa River" Submitted to: Flood Control District of Maricopa County, August 2005.

CHAPTER 10 - GLOSSARY

Agglomerate – Sedimentary rock type formed of detrital volcanic material explosively ejected from a volcanic vent, with clasts larger than 32 millimeters.

Alluvial Fan - A fan-shaped deposit of sediment located where a stream issues from a narrow valley of high slope onto a plane or broad valley of low slope.

Alluvium – Deposits of clay, silt, sand, gravel, or other particulate material in a streambed , on a floodplain or delta, or at the base of a mountain.

Altithermal – A period of time within the Holocene epoch characterized by higher than average temperatures and/or decreased precipitation.

Anabranching – A river channel pattern in which the width of islands is more than three times the river width at average discharge.

Anastomosing – A stream pattern charcterized by a net-like or interwoven channel pattern, with individual flow paths better defined or permanent than braided channel flow paths.

Andesite – A volcanic rock type mostly composed of plagioclase and other mafic materials.

Angle of Repose – The maximum angle of a slope that can be maintained by an accumulation of material.

Argillic – Descriptive of a detrital sedimentary rock with particles less than 4 mm in diameter.

Arkosic – Rock type, generally sandstone, composed of more than 25 percent silica-feldspar minerals.

Armor – A natural layer of particles, usually gravel and cobble sizes, that may cover the surface of the streambed as a coarse residue after erosion of the finer bed materials. The layer, often just one to three particles thick, inhibits the erosion of underlying particles.

Avulsion – The sudden relocation of a stream away from its original flow path, usually due to catastrophic sediment deposition in the original flow path.

Bajada – A piedmont comprised of coalescing alluvial fans.

Bankfull Elevation – The elevation on the bank where flooding begins. Bankfull discharge is defined as the flow rate which fills the active channel just prior to inundating the floodplain.

Bed Load – The portion of sediment in a stream which is transported by rolling, bouncing, or sliding on the stream bed.

Bifurcation – The division of a stream into two or more channels in the downstream direction.

Bioturbation – The disruption of sediments mainly by the burrowing activities of organisms.

Boundary Shear Stress – A frictional resistance at the marginal area of a flow which results in a decrease in velocity at the boundary areas.

Breccia – A rock unit composed of coarse highly angular fragments.

Calcareous – Calcium-rich.

Caliche – Calcium Carbonate ($CaCO_3$) deposited and illuviated in arid region soils cemented into a petrocalcic horizon; often as Stage IV carbonate.

Carbonate Stage – Stage I carbonate is loose disseminated $CaCO_3$ in the soil matrix. State II carbonate is thin, discontinuous coatings of $CaCO_3$ on the bottoms of coarse clasts in the

soil matrix. Stage III carbonate is continuous coatings of $CaCO_3$ on the majority of coarse clasts in the soil matrix. Stage IV carbonate is replacement of the original soil matrix by a thick, well-cemented layer of $CaCO_3$. Stage V carbonate has strongly expressed laminar and/or platey structure.

Clastic – Rock fragments or other material which has been transported.

Contraction Scour – A form of scour frequently occurring in rivers at bridge crossings where stream width rapidly contracts causing an increase in stream velocity and/or turbulence.

Crenulation Index – The ratio of the topographic contour length to the straight line distance along the arc of the contour. A low crenulation index indicates low relief and a uniform surface.

Critical Shear Stress – The component of shear stress parallel to a slip plane in a slip system which controls the activity along that plane.

Cut Bank – The outside bank of a channel bend, often eroding and on the opposite side of the stream from a point bar.

Dendritic Drainage Pattern – A drainage system with tributaries which join at all angles, similar to the branching pattern of a tree. The number of flow paths decrease in the downstream direction.

Desert Pavement – A layer of tightly packed coarse sediment found on the surface of desert soils formed by winnowing away finer sediment by wind, rainfall, or local runoff. Degree of pavement development is related to the intensity of the formative processes.

Desert Varnish – A dark stain substance with a glistening luster, composed of manganese or iron oxide, found on the exposed surfaces of coarse rock material in arid climates. Desert varnish is formed as microbiotic organisms fix eolian cations with oxygen during infrequent wetting by rain.

Discharge – The volume of water passing through a channel during a given time, usually measured in cubic feet per second.

Dynamic Equilibrium – A natural state of regular, expected channel change with time where stream characteristics naturally adjust to the physical conditions of the environment.

Embayment – Fault-bounded mountain ranges have highly linear mountain fronts upon formation. Headward erosion along stream forms canyons. With time, these canyons cause the mountain front to be increasingly non-linear or "embayed".

Entrenchment Ratio – A computed index value which is used to describe the degree of vertical containment of a river channel (width of the flood-prone area at an elevation twice the maximum bankfull depth/bankfull width).

Ephemeral Stream – A stream that only experiences flow in times of heavy runoff and precipitation. An ephemeral stream does not have a base flow, as the channel is always above groundwater.

Evaporites – Sedimentary rock types formed by evaporation of water; for example, halite and gypsum.

Facies – A grouping of sediments, rocks, or soils with a common or related origin.

Fanglomerate – Rock and soil material originally deposited as an alluvial fan which has since been transformed into bedrock. Fanglomerates are characterized by a wide range of grain sizes and bedding types.

Felsic – A term applied to K-feldspar and silica rich rock types.

Fluvial – Of or pertaining to rivers and stream flow.

Froude Number – A number describing the ratio of inertial to gravitational forces in flowing water. A Froude number greater than one indicates supercritical flow.

Geomorphology – The study of the shape and form of the Earth's surface.

Graywacke – A type of sandstone characterized by detrital sand grains in a clay matrix. A dirty hard sandstone.

Headcutting – Channel degradation associated with abrupt changes in the bed elevation (headcut) that migrate in an upstream direction.

Holocene – Recent; that period of geologic history (an epoch) since the last ice age in North America (the past 10,000 years); also the series of strata deposited during that epoch.

Hydraulic Geometry – The description of the graphical relations between plot points of the hydraulic characteristics of a stream, typically width, depth, velocity and discharge.

Illuviation – The downward transport of mineral or other material in a soil layer, usually the B or C soil horizon.

Imbrication – Overlapping alignment of pebbles and cobbles due to transport in water. The tail of one clast overlies the head of the next clast downstream.

Incised Channel – A channel that cuts vertically downward, below the level at which it originally formed.

Inselbergs – Isolated remnants of bedrock exposed as small hills or buttes in the alluvial plain or pediment.

Intermittent Streams – A stream or part of a stream that flows only in direct response to precipitation, receiving little or no water from springs, snowmelt or other sources. It may be dry for a large part of the year, generally more than three months. Its course may be marked by an eroded channel, sediment deposits, scour, or transport of leaf litter or soil.

Interrupted Stream – A stream which has short perennial segments with intervening ephemeral or intermittent segments.

Interfluves – The area between braided flow channels. The area is usually vegetated in contrast to the sandy channel beds.

Normal Fault – A fault in which the hanging-wall block moved down relative to the footwall block.

Paleoflood – any flood that occurred prior to, or without, human records.

Patina – a coating or layer of corrosion formed by oxidation. Desert varnish forms a patina on the surface of rocks.

Pediment – A gently sloped erosion surface composed of bedrock with a thin veneer of alluvium, often formed by mountain front planation.

Pedogenic Clay – Clay that forms as a result of in place weathering within a soil column.

Perennial Streams – A stream that normally has water in its channel at all times.

Petrocalcic – Calcium-rich rock material

Piedmont – A general term for the sloping land area adjacent to a mountain front.

Planform – The form or pattern contour of an object as viewed from above; map view.

Pool – A section of the river with relatively deep water and low flow velocities.

Riffle – A relatively shallow section of a river with high-velocity, turbulent flow.

Riparian – Pertaining to anything connected with or adjacent to the banks of a river or stream.

Riprap – Rock material placed on stream banks to protect a structure or embankment from erosion.

Runoff – That part of precipitation that appears in surface-water bodies. It is the same as streamflow unaffected by artificial diversions, storage or other human works in or on the stream channels.

Scour – Excessive erosion of a streambed or a bank.

Sediment Yield – The total sediment outflow from a watershed or a drainage area at a point of reference and in a specified period of time. This is equal to the sediment discharge from the drainage area.

Sherds – Broken pieces of pottery or ceramic ware.

Sinuous – The "curviness" of planform of a river channel, the degree of meandering.

Slackwater – A low-energy zone in a stream characterized by near-zero velocity and sediment deposition.

Strath Terrace - A stream terrace formed by erosion, rather than deposition.

Stratigraphy – The study of layered sedimentary or metamorphic rock, especially their relative ages and correlation between different areas.

Stream Order – A geomorphic parameter used to describe the complexity of a drainage system. A first order stream has no tributaries. A second order stream is formed by the confluence of two first order streams. A third order stream is formed by the confluence of two second order streams. No stream order system exists specifically for alluvial fans.

Stream Power – A technical term relating shear stress and velocity. The units signify power per unit area of stream bed.

Supply Reach. The reach located upstream of the reach studied in detail. Since water flows downstream, sediment and water are supplied from reaches upstream.

Suspended Load – The part of the total sediment load that moves above the bed load. The weight of the suspended sediment is totally supported by the fluid.

Swale – A small channel, ditch, or depression.

Tensional Cracks – Cracks that are elongate and that form as forces work to pull apart a soil or rock unit.

Thalweg – An imaginary line along the length of the river connecting the deepest points.

Torrifluvents – A type of soil characterized by stream deposits of gravelly, sandy material, and lack of significant soil horizon development.

Tuff – A rock type formed of compacted volcanic fragments and ash.

Watershed – An area confined by drainage divides, usually having only one streamflow outlet.

APPENDIX 5.1

Field forms

BANK DESCRIPTIONS

Symbols

Map Location	Cutbanks	Bedrock	Caliche
Mb1		v v v v v v v v v	+ + + + + + + + +

Descriptions

1.	Height	(+2 - cumulative height from A/C)		
2.	Slope	(2/1)		
3.	Veg%	(30%)		
4.	Struct	A. Cutbank	m=massive	g=graded
			s=stratified	b=bioturbated
		B. Sloping bank		
5.	Cohes	n=none	m=moderate	
		l=low	h=high	
6.	Cohes type	carb	clay	
7.	Sed	si fs gr co		
		s cs		
8.	Veg type			

Symbols

Avulsion Pot	Headcuts	Ground photo	S.W. Dep
		5	SWD

FLOODPLAIN DESCRIPTIONS

Symbols

Map Location

Mf1

Descriptions

1.	Height				
2.	Sed	si	fs	gr	co
		s	cs		
3.	Energy Env.	D	E		
4.	Drainage Net.	Y	N		
5.	Firmness	s=soft	f=firm		
6	Topo	s=sculpted	h=hummocky		
		p=planar			
7.	Veg density	n=none	m=moderate		
		l=low	d=dense		
8.	Veg maturity	l=low	h=high		
		m=med			
9.	Gravel lag	Y	N		
10.	Pavement	Y	N		
11.	Varnish	Y	N		
12.	Geomorph unit				
13.	Veg type				

CHANNEL DESCRIPTIONS

Symbols

Map Location

Mc1

channel descr. taken at U/S edge of map sheet and in center of map sheet

Descriptions

1.	Sed%	si	s	
		gr	co	
2.	Sed size	d_{50}		d_{90}
		d_{10}		
3.	Equilibrium	deg		agg
4.	Veg%			
5.	Veg type			

Unit Description Matrix

	Qac	Qy2a	Qy2	Qy1	Qt
Veg	tumble weed	snakeweed, low brush	snakeweed, immature PV/mesq	mature PV/ mesq, some creosote, saguaro, cholla	creosote dominated, saguaro
Height	0	<1 to 3	2 to 5	varies	varies
Sed	med/coarse sand	med/coarse sand	fine/med sand cap	fine to coarse sand	fine/med sand with gravel lag
Topo	-	fluv sculpted, active flood channels	fluv sculpted, hummocky	planar	hummocky, perp flow path
Drainage net	No	No	No	Immature	Immature to moderate
Energy env	Erosional	Erosional	Erosional	Depositional	Varies
Function	Low-flow corridor	Low flow=sed storage High flow=sed transport/re-worked	Sed transport, active floodplain	Sed deposition	Varies

Qy2a

Qy2

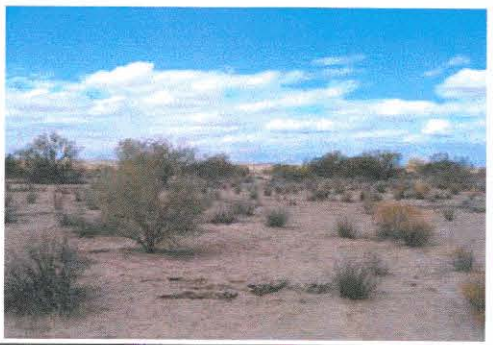

Qy1

Qt

Project _____ Date _____ Pit ID ____ GPS _____ Field Crew _____

Time _____

Vegetation Descr. _____

Gemorph. Surface _____ Descr. by _____

Slope _____ Parent Mat. _____

Pavement ❑ Archeological ❑

Varnish ❑ Moisture cond. dry❑ moist❑ wet❑

Depth (in)	Sketch	Color	Structure			% Gravel	Consistence			Texture		Clay Films	Boundary		$CaCO_3$		Notes
		Moist	Grade	Size	Form		Dry	Wet				Freq.	Dist.	Outline	Efferv.	Stage	d_{50}=
			M	vf	gr	0 50	lo	*Stick.*	*Plast.*	S	SiCL	vf	abrupt	smooth	ne	I +	
			Sg	f	pl	<10 65	so	so	po	LS	SiL	f1	sharp	wavy	ve	II	
to		Dry	1	m	pr	10 75	sh	ss	ps	SL	Si	c2	clear	lobate	e	III	
			2	c	cpr	15 >75	h	s	p	SCL	SiC	m3	gradual	irregular	es	IV	
			3	vc	abk	25	vh	vs	vp	S	C	c4	diffuse	tongued	ev	V	
					sbk	35	eh			CL	SC					VI	
Depth (in)	Sketch	Color	Structure			% Gravel	Consistence			Texture		Clay Films	Boundary		$CaCO_3$		Notes
		Moist	Grade	Size	Form		Dry	Wet				Freq.	Dist.	Outline	Efferv.	Stage	d_{50}=
			M	vf	gr	0 50	lo	*Stick.*	*Plast.*	S	SiCL	vf	abrupt	smooth	ne	I +	
			Sg	f	pl	<10 65	so	so	po	LS	SiL	f1	sharp	wavy	ve	II	
to		Dry	1	m	pr	10 75	sh	ss	ps	SL	Si	c2	clear	lobate	e	III	
			2	c	cpr	15 >75	h	s	p	SCL	SiC	m3	gradual	irregular	es	IV	
			3	vc	abk	25	vh	vs	vp	S	C	c4	diffuse	tongued	ev	V	
					sbk	35	eh			CL	SC					VI	
Depth (in)	Sketch	Color	Structure			% Gravel	Consistence			Texture		Clay Films	Boundary		$CaCO_3$		Notes
		Moist	Grade	Size	Form		Dry	Wet				Freq.	Dist.	Outline	Efferv.	Stage	d_{50}=
			M	vf	gr	0 50	lo	*Stick.*	*Plast.*	S	SiCL	vf	abrupt	smooth	ne	I +	
			Sg	f	pl	<10 65	so	so	po	LS	SiL	f1	sharp	wavy	ve	II	
to		Dry	1	m	pr	10 75	sh	ss	ps	SL	Si	c2	clear	lobate	e	III	
			2	c	cpr	15 >75	h	s	p	SCL	SiC	m3	gradual	irregular	es	IV	
			3	vc	abk	25	vh	vs	vp	S	C	c4	diffuse	tongued	ev	V	
					sbk	35	eh			CL	SC					VI	
Depth (in)	Sketch	Color	Structure			% Gravel	Consistence			Texture		Clay Films	Boundary		$CaCO_3$		Notes
		Moist	Grade	Size	Form		Dry	Wet				Freq.	Dist.	Outline	Efferv.	Stage	d_{50}=
			M	vf	gr	0 50	lo	*Stick.*	*Plast.*	S	SiCL	vf	abrupt	smooth	ne	I +	
			Sg	f	pl	<10 65	so	so	po	LS	SiL	f1	sharp	wavy	ve	II	
to		Dry	1	m	pr	10 75	sh	ss	ps	SL	Si	c2	clear	lobate	e	III	
			2	c	cpr	15 >75	h	s	p	SCL	SiC	m3	gradual	irregular	es	IV	
			3	vc	abk	25	vh	vs	vp	S	C	c4	diffuse	tongued	ev	V	
					sbk	35	eh			CL	SC					VI	
Depth (in)	Sketch	Color	Structure			% Gravel	Consistence			Texture		Clay Films	Boundary		$CaCO_3$		Notes
		Moist	Grade	Size	Form		Dry	Wet				Freq.	Dist.	Outline	Efferv.	Stage	d_{50}=
			M	vf	gr	0 50	lo	*Stick.*	*Plast.*	S	SiCL	vf	abrupt	smooth	ne	I +	
			Sg	f	pl	<10 65	so	so	po	LS	SiL	f1	sharp	wavy	ve	II	
to		Dry	1	m	pr	10 75	sh	ss	ps	SL	Si	c2	clear	lobate	e	III	
			2	c	cpr	15 >75	h	s	p	SCL	SiC	m3	gradual	irregular	es	IV	
			3	vc	abk	25	vh	vs	vp	S	C	c4	diffuse	tongued	ev	V	
					sbk	35	eh			CL	SC					VI	

Photographs

Photo #	Description
	Pre-excavation
	Spoil material
	Pit profile
	Vegetation
	General geomorphic surface

Photo #	Description

SKETCH / NOTES

APPENDIX 5.2

Soil description sheets

Project Huxmp Date 3-14 Pit ID 1 GPS _____ Field Crew CEH DEF

Time 12:30

Vegetation Descr. Creosote, grass, minor cacti

Gemorph. Surface floodplain Descr. by CEH

Slope flat Parent Mat. Alluvium

SKETCH ON BACK

Pavement ☐ Archeological ☐

Varnish ☐ Moisture cond. dry☒ moist☒ wet☐

dry ← → wet

(SV) (P)

Depth (in)	Horiz.	Color	Structure			% Gravel	Consistence			Texture		Clay Films	Boundary		$CaCO_3$		Notes
		Moist	Grade	Size	Form		Dry	Wet				Freq.	Dist.	Outline	Efferv.	Stage	fine sand
6.9	A	7.5 3/4	M	vf	gr	0 50	lo	Stick.	Plast.	S	SiCL	vf	abrupt	smooth	ne	I +	
	Bt		Sg	f	pl	<10 65	so	so	po	LS	SiL	f1	sharp	wavy	ve	II	(5.5) (7)
to	Bk	Dry	1	m	pr	10 75	sh	ss	ps	SL	Si	c2	clear	lobate	e	III	
	C	7.5YR	2	c	cpr	15 >75	h	s	p	SCL	SiC	m3	gradual	irregular	es	IV	
5.9	E	4/4	3	vc	abk	25	vh	vs	vp	S	C	c4	diffuse	tongued	ev	V	← max CO_3 @ 6.2'
					sbk	35	eh			CL	SC	(N)				VI	

Depth (in)	Horiz.	Color	Structure			% Gravel	Consistence			Texture		Clay Films	Boundary		$CaCO_3$		Notes
		Moist	Grade	Size	Form		Dry	Wet				Freq.	Dist.	Outline	Efferv.	Stage	med sand
5.9	A	7.5YR 4/3	M	vf	gr	0 50	lo	Stick.	Plast.	S	SiCL	vf	abrupt	smooth	ne	I +	
	Bt		Sg	f	pl	<10 65	so	so	po	LS	SiL	f1	sharp	wavy	ve	II	(5)
to	Bk	Dry	1	m	pr	10 75	sh	ss	ps	SL	Si	c2	clear	lobate	e	III	(4.9)
	C	10YR	2	c	cpr	15 >75	h	s	p	SCL	SiC	m3	gradual	irregular	es	IV	
3.9	E	4/3	3	vc	abk	25	vh	vs	vp	S	C	c4	diffuse	tongued	ev	V	
					sbk	35	eh			CL	SC	(N)				VI	

Depth (in)	Horiz.	Color	Structure			% Gravel	Consistence			Texture		Clay Films	Boundary		$CaCO_3$		Notes
		Moist	Grade	Size	Form		Dry	Wet				Freq.	Dist.	Outline	Efferv.	Stage	med sand
3.9	A	7.5YR 4/3	M	vf	gr	0 50	lo	Stick.	Plast.	S	SiCL	vf	abrupt	smooth	ne	I +	
	Bt		Sg	f	pl	<10 65	so	so	po	LS	SiL	f1	sharp	wavy	ve	II	(3) (19)
to	Bk	Dry	1	m	pr	10 75	sh	ss	ps	SL	Si	c2	clear	lobate	e	III	
	C	2.5YR	2	c	cpr	15 >75	h	s	p	SCL	SiC	m3	gradual	irregular	es	IV	
3.5	E	6/2	3	vc	abk	25	vh	vs	vp	S	C	c4	diffuse	tongued	ev	V	
					sbk	35	eh			CL	SC	(N)				VI	

Depth (in)	Horiz.	Color	Structure			% Gravel	Consistence			Texture		Clay Films	Boundary		$CaCO_3$		Notes
		Moist	Grade	Size	Form		Dry	Wet				Freq.	Dist.	Outline	Efferv.	Stage	coarse sand
3.5	A	7.5YR 5/4	M	vf	gr	0 50	lo	Stick.	Plast.	S	SiCL	vf	abrupt	smooth	ne	I +	
	Bt		Sg	f	pl	<10 65	so	so	po	LS	SiL	f1	sharp	wavy	ve	II	(4) (20+)
to	Bk	Dry	1	m	pr	10 75	sh	ss	ps	SL	Si	c2	clear	lobate	e	III	
	C	2.5YR	2	c	cpr	15 >75	h	s	p	SCL	SiC	m3	gradual	irregular	es	IV	
2.9	E	7/2	3	vc	abk	25	vh	vs	vp	S	C	c4	diffuse	tongued	ev	V	
					sbk	35	eh			CL	SC	(N)				VI	

Depth (in)	Horiz.	Color	Structure			% Gravel	Consistence			Texture		Clay Films	Boundary		$CaCO_3$		Notes
		Moist	Grade	Size	Form		Dry	Wet				Freq.	Dist.	Outline	Efferv.	Stage	well layered, horizontal
2.9	A	7.5YR 4/2	M	vf	gr	0 50	lo	Stick.	Plast.	S	SiCL	vf	abrupt	smooth	ne	I +	slightly reddened
	Bt		Sg	f	pl	<10 65	so	so	po	LS	SiL	f1	sharp	wavy	ve	II	coarse sand
to	Bk	Dry	1	m	pr	10 75	sh	ss	ps	SL	Si	c2	clear	lobate	e	III	
	C	2.5YR	2	c	cpr	15 >75	h	s	p	SCL	SiC	m3	gradual	irregular	es	IV	(5) (20+)
1.2	E	6/2	3	vc	abk	25	vh	vs	vp	S	C	c4	diffuse	tongued	ev	V	
					sbk	35	eh			CL	SC	(N)				VI	

Photographs

Photo #	Description
52	Pre-excavation
7	Spoil material
7	Pit profile
	Vegetation
8	General geomorphic surface

Photo #	Description

Project LHWCMS Date 3.14 Pit ID 1 GPS _____ Field Crew JEF, CEH

Time 12:30

Vegetation Descr. _____

Gemorph. Surface _____ see pg 1

Descr. by CEH

Slope _____ Parent Mat. _____

Pavement ☐ Archeological ☐

Varnish ☐ Moisture cond. dry☐ moist☐ wet☐

Depth (in)	Horiz.	Color	Structure			% Gravel	Consistence			Texture	Clay Films	Boundary		$CaCO_3$		Notes
		Moist	Grade	Size	Form		Dry	Wet			Freq.	Dist.	Outline	Efferv.	Stage	
1.2	A		M	vf	gr	0 50	lo	Stick.	Plast.	S SiCL	vf	abrupt	smooth	ne	I +	fi sand
	Bt		Sg	f	pl	<10 65	so	so	po	LS SiL	f1	sharp	wavy	ve	II	
to	Bk	Dry	1	m	pr	10 75	sh	ss	ps	SL Si	c2	clear	lobate	e	III	3.5 20+
	C	2.5YR	2	c	cpr	15 >75	h	s	p	SCL SiC	m3	gradual	irregular	es	IV	
	E	6/3	3	vc	abk	25	vh	vs	vp	S C	c4	diffuse	tongued	ev	V	
BASE					sbk	35	eh			CL SC					VI	

Depth (in)	Horiz.	Color	Structure			% Gravel	Consistence			Texture	Clay Films	Boundary		$CaCO_3$		Notes
		Moist	Grade	Size	Form		Dry	Wet			Freq.	Dist.	Outline	Efferv.	Stage	
	A		M	vf	gr	0 50	lo	Stick.	Plast.	S SiCL	vf	abrupt	smooth	ne	I +	
	Bt		Sg	f	pl	<10 65	so	so	po	LS SiL	f1	sharp	wavy	ve	II	
to	Bk	Dry	1	m	pr	10 75	sh	ss	ps	SL Si	c2	clear	lobate	e	III	
	C		2	c	cpr	15 >75	h	s	p	SCL SiC	m3	gradual	irregular	es	IV	
	E		3	vc	abk	25	vh	vs	vp	S C	c4	diffuse	tongued	ev	V	
					sbk	35	eh			CL SC					VI	

Depth (in)	Horiz.	Color	Structure			% Gravel	Consistence			Texture	Clay Films	Boundary		$CaCO_3$		Notes
		Moist	Grade	Size	Form		Dry	Wet			Freq.	Dist.	Outline	Efferv.	Stage	
	A		M	vf	gr	0 50	lo	Stick.	Plast.	S SiCL	vf	abrupt	smooth	ne	I +	
	Bt		Sg	f	pl	<10 65	so	so	po	LS SiL	f1	sharp	wavy	ve	II	
to	Bk	Dry	1	m	pr	10 75	sh	ss	ps	SL Si	c2	clear	lobate	e	III	
	C		2	c	cpr	15 >75	h	s	p	SCL SiC	m3	gradual	irregular	es	IV	
	E		3	vc	abk	25	vh	vs	vp	S C	c4	diffuse	tongued	ev	V	
					sbk	35	eh			CL SC					VI	

Depth (in)	Horiz.	Color	Structure			% Gravel	Consistence			Texture	Clay Films	Boundary		$CaCO_3$		Notes
		Moist	Grade	Size	Form		Dry	Wet			Freq.	Dist.	Outline	Efferv.	Stage	
	A		M	vf	gr	0 50	lo	Stick.	Plast.	S SiCL	vf	abrupt	smooth	ne	I +	
	Bt		Sg	f	pl	<10 65	so	so	po	LS SiL	f1	sharp	wavy	ve	II	
to	Bk	Dry	1	m	pr	10 75	sh	ss	ps	SL Si	c2	clear	lobate	e	III	
	C		2	c	cpr	15 >75	h	s	p	SCL SiC	m3	gradual	irregular	es	IV	
	E		3	vc	abk	25	vh	vs	vp	S C	c4	diffuse	tongued	ev	V	
					sbk	35	eh			CL SC					VI	

Depth (in)	Horiz.	Color	Structure			% Gravel	Consistence			Texture	Clay Films	Boundary		$CaCO_3$		Notes
		Moist	Grade	Size	Form		Dry	Wet			Freq.	Dist.	Outline	Efferv.	Stage	
	A		M	vf	gr	0 50	lo	Stick.	Plast.	S SiCL	vf	abrupt	smooth	ne	I +	
	Bt		Sg	f	pl	<10 65	so	so	po	LS SiL	f1	sharp	wavy	ve	II	
to	Bk	Dry	1	m	pr	10 75	sh	ss	ps	SL Si	c2	clear	lobate	e	III	
	C		2	c	cpr	15 >75	h	s	p	SCL SiC	m3	gradual	irregular	es	IV	
	E		3	vc	abk	25	vh	vs	vp	S C	c4	diffuse	tongued	ev	V	
					sbk	35	eh			CL SC					VI	

Photographs

Photo #	Description
	Pre-excavation
	Spoil material
	Pit profile
	Vegetation
	General geomorphic surface

Photo #	Description

Project LHWCMP Date 3-14 Pit ID 2 GPS _____ Field Crew JEF MJK CH

Time ~11am

Vegetation Descr. Creosote & grass

Gemorph. Surface TRib Descr. by MJK

Slope up to West Parent Mat. alluvium

Pavement ☐ Archeological ☐

Varnish ☐ Moisture cond. dry☒ moist☒ wet☐

Sketch on back

SV PEN

Depth (in)	Horiz.	Color	Structure Grade	Size	Form	% Gravel	Consistence Dry	Wet Stick.	Wet Plast.	Texture	Clay Films Freq.	Boundary Dist.	Boundary Outline	$CaCO_3$ Efferv.	$CaCO_3$ Stage	Notes
ft 6.3		Moist 7.5YR 4/3	M	vf	gr	0 50	lo			S SiCL	vf	abrupt	smooth	ne	I +	slight gravel lag on surface
	A		Sg	f	pl	<10 65	so	so	po	LS SiL	f1	sharp	wavy	ve	II	
to	Bt	Dry	1	m	pr	10 75	sh	ss	ps	SL Si	c2	clear	lobate	e	III	3
	Bk	7.5YR	2	c	cpr	15 >75	h	s	p	SCL SiC	m3	gradual	irregular	es	IV	0
	C	5/3	3	vc	abk	25	vh	vs	vp	S C	c4	diffuse	tongued	ev	V	
6.1	E				sbk	35	eh			CL SC	NO				VI	

Depth (in)	Horiz.	Color	Structure Grade	Size	Form	% Gravel	Consistence Dry	Wet Stick.	Wet Plast.	Texture	Clay Films Freq.	Boundary Dist.	Boundary Outline	$CaCO_3$ Efferv.	$CaCO_3$ Stage	Notes
6.1		Moist 7.5YR 4/3	M	vf	gr	10% 0 50	lo			S SiCL	vf	abrupt	smooth	ne	I +	ES @ base less gravel
	A		Sg	f	pl	<10 65	so	so	po	LS SiL	f1	sharp	wavy	ve	II	1
to	Bt	Dry	1	m	pr	10 75	sh	ss	ps	SL Si	c2	clear	lobate	e	III	4
	Bk	7.5YR	2	c	cpr	15 >75	h	s	p	SCL SiC	m3	gradual	irregular	es	IV	
	C	4/4	3	vc	abk	25	vh	vs	vp	S C	c4	diffuse	tongued	ev	V	main difference in gravel content
4.6	E				sbk	35	eh			CL SC	NO				VI	

Depth (in)	Horiz.	Color	Structure Grade	Size	Form	% Gravel	Consistence Dry	Wet Stick.	Wet Plast.	Texture	Clay Films Freq.	Boundary Dist.	Boundary Outline	$CaCO_3$ Efferv.	$CaCO_3$ Stage	Notes
4.6		Moist 7.5YR 4/4	M	vf	gr	0 50	lo			S SiCL	vf	abrupt	smooth	ne	I +	more gravel
	A		Sg	f	pl	<10 65	so	so	po	LS SiL	f1	sharp	wavy	ve	II	
to	Bt	Dry	1	m	pr	10 75	sh	ss	ps	SL Si	c2	clear	lobate	e	III	3 12
	Bk	7.5YR	2	c	cpr	15 >75	h	s	p	SCL SiC	m3	gradual	irregular	es	IV	
	C	4/4	3	vc	abk	25	vh	vs	vp	S C	c4	diffuse	tongued	ev	V	
2.6	E				sbk	35	eh			CL SC	H				VI	thin discontinuous

Depth (in)	Horiz.	Color	Structure Grade	Size	Form	% Gravel	Consistence Dry	Wet Stick.	Wet Plast.	Texture	Clay Films Freq.	Boundary Dist.	Boundary Outline	$CaCO_3$ Efferv.	$CaCO_3$ Stage	Notes
2.6		Moist 7.5YR 4/4	M	vf	gr	0 50	lo			S SiCL	vf	abrupt	smooth	ne	I +	thin continuous
	A		Sg	f	pl	<10 65	so	so	po	LS SiL	f1	sharp	wavy	ve	II	poor structure
to	Bt	Dry	1	m	pr	10 75	sh	ss	ps	SL Si	c2	clear	lobate	e	III	peds are rare
	Bk	7.5YR	2	c	cpr	15 >75	h	s	p	SCL SiC	m3	gradual	irregular	es	IV	mostly loose gravel
	C	5/4	3	vc	abk	25	vh	vs	vp	S C	c4	diffuse	tongued	ev	V	D90 = 2 cm 20
2.2	E				sbk	35	eh			CL SC	NO				VI	3

Depth (in)	Horiz.	Color	Structure Grade	Size	Form	% Gravel	Consistence Dry	Wet Stick.	Wet Plast.	Texture	Clay Films Freq.	Boundary Dist.	Boundary Outline	$CaCO_3$ Efferv.	$CaCO_3$ Stage	Notes
2.2		Moist 7.5YR 4/4	M	vf	gr	0 50	lo			S SiCL	vf	abrupt	smooth	ne	I +	$CaCO_3$ - more disseminated in matrix
	A		Sg	f	pl	<10 65	so	so	po	LS SiL	f1	sharp	wavy	ve	II	
to	Bt	Dry	1	m	pr	10 75	sh	ss	ps	SL Si	c2	clear	lobate	e	III	20+
	Bk	7.5YR	2	c	cpr	15 >75	h	s	p	SCL SiC	m3	gradual	irregular	es	IV	5
	C	5/3	3	vc	abk	25	vh	vs	vp	S C	c4	diffuse	tongued	ev	V	
1.9	E				sbk	35	eh			CL SC					VI	

Photographs

Photo #	Description
53	Pre-excavation
6	Spoil material
5	Pit profile
	Vegetation
4	General geomorphic surface

Photo #	Description

Project Lthwcmp Date 3.14 Pit ID 2 GPS _____ Field Crew JEF, CH

Time ~11 am

Vegetation Descr. See pg. 1

Gemorph. Surface _____ Descr. by MJK

Slope _____ Parent Mat. _____

Pavement ☐ Archeological ☐

Varnish ☐ Moisture cond. dry☒ moist☐ wet☐

(SV) (P)

Depth (in)	Horiz.	Color	Structure			% Gravel	Consistence			Texture	Clay Films	Boundary		$CaCO_3$		Notes
		Moist	Grade	Size	Form		Dry	Wet			Freq.	Dist.	Outline	Efferv.	Stage	
1.9	A	7.5YR	M	vf	gr	0 50	lo	Stick.	Plast.	S SiCL	vf	abrupt	smooth	ne	I +	
	Bt	4/4	Sg	f	pl	<10 65	so	so	po	LS SiL	f1	sharp	wavy	ve	II	
to	Bk	Dry	1	m	pr	10 75	sh	ss	ps	SL Si	c2	clear	lobate	e	III	
	C	7.5YR	2	c	cpr	15 >75	h	s	p	SCL SiC	m3	gradual	irregular	es	IV	(4) 20+
	E	5/3	3	vc	abk	25	vh	vs	vp	S C	c4	diffuse	tongued	ev	V	
0					sbk	35	eh			CL SC	No	PIT			VI	
		bottom of PIT														

Depth (in)	Horiz.	Color	Structure			% Gravel	Consistence			Texture	Clay Films	Boundary		$CaCO_3$		Notes
		Moist	Grade	Size	Form		Dry	Wet			Freq.	Dist.	Outline	Efferv.	Stage	
	A		M	vf	gr	0 50	lo	Stick.	Plast.	S SiCL	vf	abrupt	smooth	ne	I +	
	Bt		Sg	f	pl	<10 65	so	so	po	LS SiL	f1	sharp	wavy	ve	II	
to	Bk	Dry	1	m	pr	10 75	sh	ss	ps	SL Si	c2	clear	lobate	e	III	
	C		2	c	cpr	15 >75	h	s	p	SCL SiC	m3	gradual	irregular	es	IV	
	E		3	vc	abk	25	vh	vs	vp	S C	c4	diffuse	tongued	ev	V	
					sbk	35	eh			CL SC					VI	

Depth (in)	Horiz.	Color	Structure			% Gravel	Consistence			Texture	Clay Films	Boundary		$CaCO_3$		Notes
		Moist	Grade	Size	Form		Dry	Wet			Freq.	Dist.	Outline	Efferv.	Stage	
	A		M	vf	gr	0 50	lo	Stick.	Plast.	S SiCL	vf	abrupt	smooth	ne	I +	
	Bt		Sg	f	pl	<10 65	so	so	po	LS SiL	f1	sharp	wavy	ve	II	
to	Bk	Dry	1	m	pr	10 75	sh	ss	ps	SL Si	c2	clear	lobate	e	III	
	C		2	c	cpr	15 >75	h	s	p	SCL SiC	m3	gradual	irregular	es	IV	
	E		3	vc	abk	25	vh	vs	vp	S C	c4	diffuse	tongued	ev	V	
					sbk	35	eh			CL SC					VI	

Depth (in)	Horiz.	Color	Structure			% Gravel	Consistence			Texture	Clay Films	Boundary		$CaCO_3$		Notes
		Moist	Grade	Size	Form		Dry	Wet			Freq.	Dist.	Outline	Efferv.	Stage	
	A		M	vf	gr	0 50	lo	Stick.	Plast.	S SiCL	vf	abrupt	smooth	ne	I +	
	Bt		Sg	f	pl	<10 65	so	so	po	LS SiL	f1	sharp	wavy	ve	II	
to	Bk	Dry	1	m	pr	10 75	sh	ss	ps	SL Si	c2	clear	lobate	e	III	
	C		2	c	cpr	15 >75	h	s	p	SCL SiC	m3	gradual	irregular	es	IV	
	E		3	vc	abk	25	vh	vs	vp	S C	c4	diffuse	tongued	ev	V	
					sbk	35	eh			CL SC					VI	

Depth (in)	Horiz.	Color	Structure			% Gravel	Consistence			Texture	Clay Films	Boundary		$CaCO_3$		Notes
		Moist	Grade	Size	Form		Dry	Wet			Freq.	Dist.	Outline	Efferv.	Stage	
	A		M	vf	gr	0 50	lo	Stick.	Plast.	S SiCL	vf	abrupt	smooth	ne	I +	
	Bt		Sg	f	pl	<10 65	so	so	po	LS SiL	f1	sharp	wavy	ve	II	
to	Bk	Dry	1	m	pr	10 75	sh	ss	ps	SL Si	c2	clear	lobate	e	III	
	C		2	c	cpr	15 >75	h	s	p	SCL SiC	m3	gradual	irregular	es	IV	
	E		3	vc	abk	25	vh	vs	vp	S C	c4	diffuse	tongued	ev	V	
					sbk	35	eh			CL SC					VI	

Photographs

Photo #	Description
	Pre-excavation
	Spoil material
	Pit profile
	Vegetation
	General geomorphic surface

Photo #	Description

Project _____ Date 3-14-05 Pit ID 3 GPS _____ Field Crew JF, CH

Time _____

Vegetation Descr. Cr (20%) grass < 5 (80%)

Gemorph. Surface Flood plain Descr. by JF

Slope level Parent Mat. _____

Pavement ☐ Archeological ☐

Varnish ☐ Moisture cond. dry☐ moist☐ wet☐

All colors from 7.5y

Depth (in)	Horiz.	Color (Moist)	Structure Grade	Size	Form	% Gravel	Consistence Dry	Wet Stick.	Wet Plast.	Texture	Clay Films Freq.	Boundary Dist.	Boundary Outline	$CaCO_3$ Efferv.	$CaCO_3$ Stage	Notes
5.7	A	2.5y	M	vf	gr	0 50	lo	Stick.	Plast.	S SiCL	vf	abrupt	smooth	ne	I +	PM 0
	Bt	4/3	Sg	f	pl	<10 65	so	so	po	LS SiL	f1	sharp	wavy	ve	II	TM 4
to	Bk	Dry	1	m	pr	10 75	sh	ss	ps	SL Si	c2	clear	lobate	e	III	
	C	7.5y	2	c	cpr	15 >75	h	s	p	SCL SiC	m3	gradual	irregular	es	IV none	
5.4	E	5/3	3	vc	abk	25	vh	vs	vp	S C	c4	diffuse	tongued	ev	V	
					sbk	35	eh			CL SC	No				VI	

Depth (in)	Horiz.	Color (Moist)	Structure Grade	Size	Form	% Gravel	Consistence Dry	Wet Stick.	Wet Plast.	Texture	Clay Films Freq.	Boundary Dist.	Boundary Outline	$CaCO_3$ Efferv.	$CaCO_3$ Stage	Notes
5.4	A	7.5y	M	vf	gr	0 50	lo	Stick.	Plast.	S SiCL	vf	abrupt	smooth	ne	I +	PM 3
	Bt	3/3	Sg	f	pl	<10 65	so	so	po	LS SiL	f1	sharp	wavy	ve	II	TM 3
to	Bk	Dry	1	m	pr	10 75	sh	ss	ps	SL Si	c2	clear	lobate	e	III	
2	C	7.5y	2	c	cpr	15 >75	h	s	p	SCL SiC	m3	gradual	irregular	es	IV none	
4.8	E	5/2	3	vc	abk	25	vh	vs	vp	S C	c4	diffuse	tongued	ev	V	
					sbk	35	eh			CL SC	No				VI	

Depth (in)	Horiz.	Color (Moist)	Structure Grade	Size	Form	% Gravel	Consistence Dry	Wet Stick.	Wet Plast.	Texture	Clay Films Freq.	Boundary Dist.	Boundary Outline	$CaCO_3$ Efferv.	$CaCO_3$ Stage	Notes
4.8	A	7.5y 4/2	M	vf	gr	0 50	lo	Stick.	Plast.	S SiCL	vf	abrupt	smooth	ne	I +	PM 2
	Bt		Sg	f	pl	<10 65	so	so	po	LS SiL	f1	sharp	wavy	ve	II	TM 4
to	Bk	Dry	1	m	pr	10 75	sh	ss	ps	SL Si	c2	clear	lobate	e	III	
3	C	7.5y	2	c	cpr	15 >75	h	s	p	SCL SiC	m3	gradual	irregular	es	IV none	
3.7	E	4/3	3	vc	abk	25	vh	vs	vp	S C	c4	diffuse	tongued	ev	V	
					sbk	35	eh			CL SC	No				VI	

Depth (in)	Horiz.	Color (Moist)	Structure Grade	Size	Form	% Gravel	Consistence Dry	Wet Stick.	Wet Plast.	Texture	Clay Films Freq.	Boundary Dist.	Boundary Outline	$CaCO_3$ Efferv.	$CaCO_3$ Stage	Notes
3.7	A	7.5 4/2	M	vf	gr	0 50	lo	Stick.	Plast.	S SiCL	vf	abrupt	smooth	ne	I +	PM 0
	Bt		Sg	f	pl	<10 65	so	so	po	LS SiL	f1	sharp	wavy	ve	II	TM 10
to	Bk	Dry	1	m	pr	10 75	sh	ss	ps	SL Si	c2	clear	lobate	e	III	
4	C	3/2 darkest	2	c	cpr	15 >75	h	s	p	SCL SiC	m3	gradual	irregular	es	IV none	
2.6	E	Varies in Color	3	vc	abk	25	vh	vs	vp	S C	c4	diffuse	tongued	ev	V	
					sbk	35	eh			CL SC	C2				VI	

Depth (in)	Horiz.	Color (Moist)	Structure Grade	Size	Form	% Gravel	Consistence Dry	Wet Stick.	Wet Plast.	Texture	Clay Films Freq.	Boundary Dist.	Boundary Outline	$CaCO_3$ Efferv.	$CaCO_3$ Stage	Notes
2.6	A	4/3	M	vf	gr	0 50	lo	Stick.	Plast.	S SiCL	vf	abrupt	smooth	ne	I +	PM 8
	Bt		Sg	f	pl	<10 65	so	so	po	LS SiL	f1	sharp	wavy	ve	II	TM 3
to	Bk	Dry	1	m	pr	10 75	sh	ss	ps	SL Si	c2	clear	lobate	e	III	
5	C	5/2	2	c	cpr	15 >75	h	s	p	SCL SiC	m3	gradual	irregular	es	IV none	
2.1	E		3	vc	abk	25	vh	vs	vp	S C	c4	diffuse	tongued	ev	V	
					sbk	35	eh			CL SC					VI	

Photographs

Photo #	Description
54	Pre-excavation
14	Spoil material ~p
12	Pit profile
13	Vegetation
13	General geomorphic surface

Photo #	Description

sheet 2 of 2

Project _____ Date _____ Pit ID 3 GPS _____ Field Crew _____

Time _____

Vegetation Descr. _____

Gemorph. Surface _____ Descr. by _____

Slope _____ Parent Mat. _____

Pavement ❑ Archeological ❑

Varnish ❑ Moisture cond. dry❑ moist❑ wet❑

Depth (in)	Horiz.	Color	Structure			% Gravel		Consistence			Texture		Clay Films	Boundary		$CaCO_3$		Notes
		Moist	Grade	Size	Form			Dry	Wet				Freq.	Dist.	Outline	Efferv.	Stage	
2.1	A	4/2	M	vf	gr	0	50	lo	Stick.	Plast.	S	SiCL	vf	abrupt	smooth	ne	I +	probacetal 7
	Bt		Sg	f	pl	<10	65	so	so	po	LS	SiL	f1	sharp	wavy	ve	II	Stage 1 TM = 6
to	Bk	Dry	1	m	pr	10	75	sh	ss	ps	SL	Si	c2	clear	lobate	e	III	none
6	C	5/3	2	c	cpr	15	>75	h	s	p	SCL	SiC	m3	gradual	irregular	es	IV	
1.7	E		3	vc	abk	25		vh	vs	vp	S	C	c4	diffuse	tongued	ev	V	
					sbk	35		eh			CL	SC					VI	

Depth (in)	Horiz.	Color	Structure			% Gravel		Consistence			Texture		Clay Films	Boundary		$CaCO_3$		Notes
		Moist	Grade	Size	Form			Dry	Wet				Freq.	Dist.	Outline	Efferv.	Stage	
1.7	A		M	vf	gr	0	50	lo	Stick.	Plast.	S	SiCL	vf	abrupt	smooth	ne	~~II~~ +	PM 9
	Bt	5/3	Sg	f	pl	<10	65	so	so	po	LS	SiL	f1	sharp	wavy	ve	II	Stage one TM 0
to	Bk	Dry	1	m	pr	10	75	sh	ss	ps	SL	Si	c2	clear	lobate	e	III	
7	C		2	c	cpr	15	>75	h	s	p	SCL	SiC	m3	gradual	irregular	es	IV	none
Bt	E	6/3	3	vc	abk	25		vh	vs	vp	S	C	c4	diffuse	tongued	ev	V	
					sbk	35		eh			CL	SC					VI	

Depth (in)	Horiz.	Color	Structure			% Gravel		Consistence			Texture		Clay Films	Boundary		$CaCO_3$		Notes
		Moist	Grade	Size	Form			Dry	Wet				Freq.	Dist.	Outline	Efferv.	Stage	
	A		M	vf	gr	0	50	lo	Stick.	Plast.	S	SiCL	vf	abrupt	smooth	ne	I +	2
	Bt		Sg	f	pl	<10	65	so	so	po	LS	SiL	f1	sharp	wavy	ve	II	
to	Bk	Dry	1	m	pr	10	75	sh	ss	ps	SL	Si	c2	clear	lobate	e	III	
	C		2	c	cpr	15	>75	h	s	p	SCL	SiC	m3	gradual	irregular	es	IV	none
	E		3	vc	abk	25		vh	vs	vp	S	C	c4	diffuse	tongued	ev	V	
					sbk	35		eh			CL	SC					VI	

Depth (in)	Horiz.	Color	Structure			% Gravel		Consistence			Texture		Clay Films	Boundary		$CaCO_3$		Notes
		Moist	Grade	Size	Form			Dry	Wet				Freq.	Dist.	Outline	Efferv.	Stage	
	A		M	vf	gr	0	50	lo	Stick.	Plast.	S	SiCL	vf	abrupt	smooth	ne	I +	8
	Bt		Sg	f	pl	<10	65	so	so	po	LS	SiL	f1	sharp	wavy	ve	II	
to	Bk	Dry	1	m	pr	10	75	sh	ss	ps	SL	Si	c2	clear	lobate	e	III	
	C		2	c	cpr	15	>75	h	s	p	SCL	SiC	m3	gradual	irregular	es	IV	
	E		3	vc	abk	25		vh	vs	vp	S	C	c4	diffuse	tongued	ev	V	
					sbk	35		eh			CL	SC					VI	

Depth (in)	Horiz.	Color	Structure			% Gravel		Consistence			Texture		Clay Films	Boundary		$CaCO_3$		Notes
		Moist	Grade	Size	Form			Dry	Wet				Freq.	Dist.	Outline	Efferv.	Stage	
	A		M	vf	gr	0	50	lo	Stick.	Plast.	S	SiCL	vf	abrupt	smooth	ne	I +	
	Bt		Sg	f	pl	<10	65	so	so	po	LS	SiL	f1	sharp	wavy	ve	II	
to	Bk	Dry	1	m	pr	10	75	sh	ss	ps	SL	Si	c2	clear	lobate	e	III	
	C		2	c	cpr	15	>75	h	s	p	SCL	SiC	m3	gradual	irregular	es	IV	
	E		3	vc	abk	25		vh	vs	vp	S	C	c4	diffuse	tongued	ev	V	
					sbk	35		eh			CL	SC					VI	

Photographs

Photo #	Description
	Pre-excavation
	Spoil material
	Pit profile
	Vegetation
	General geomorphic surface

Photo #	Description

Project LHWCMP Date 3/14/04 Pit ID 6 GPS _____ Field Crew JF, MK

Time _____

Vegetation Descr. _____

Gemorph. Surface Qyl Descr. by JF

Slope Flat Parent Mat. Alluvium

Pavement ☐ Archeological ☐

Varnish ☐ Moisture cond. dry☐ moist☑ wet☐

SKETCH ON BACK

Depth (in)	Horiz.	Color	Structure: Grade	Size	Form	% Gravel	Consistence: Dry	Wet: Stick.	Plast.	Texture	Clay Films: Freq.	Boundary: Dist.	Outline	CaCO3: Efferv.	Stage	Notes
		Moist														Penetrometer
6.1	A	7.5yr	M	vf	gr	0 50	lo	Stick.	Plast.	S SiCL	vf	abrupt	smooth	ne	I +	0
	Bt	4/2 wet	Sg	f	pl	<10 65	so	so	po	LS SiL	f1	sharp	wavy	ve	II	
to	Bk	Dry	1	m	pr	10 75	sh	ss	ps	SL Si	c2	clear	lobate	e	III	Shear
	C	7.5yR	2	c	cpr	15 >75	h	s	p	SCL SiC	m3	gradual	irregular	es	IV	
6.0	E	6/3	3	vc	abk	25	vh	vs	vp	S C	c4	diffuse	tongued	ev	V	N/A
		moist			sbk	35	eh			CL SC	No				VI	

Depth (in)	Horiz.	Color	Structure: Grade	Size	Form	% Gravel	Consistence: Dry	Wet: Stick.	Plast.	Texture	Clay Films: Freq.	Boundary: Dist.	Outline	CaCO3: Efferv.	Stage	Notes
		Moist														
6.0	A	7.5yr	M	vf	gr	0 50	lo	Stick.	Plast.	S SiCL	vf	abrupt	smooth	ne	I +	0
	Bt	5/3 wet	Sg	f	pl	<10 65	so	so	po	LS SiL	f1	sharp	wavy	ve	II	
to	Bk	Dry	1	m	pr	10 75	sh	ss	ps	SL Si	c2	clear	lobate	e	III	
	C	7.5yr	2	c	cpr	15 >75	h	s	p	SCL SiC	m3	gradual	irregular	es	IV	2
4.6	E	6/3	3	vc	abk	25	vh	vs	vp	S C	c4	diffuse	tongued	ev	V	
		moist			sbk	35	eh			CL SC	No				VI	

Depth (in)	Horiz.	Color	Structure: Grade	Size	Form	% Gravel	Consistence: Dry	Wet: Stick.	Plast.	Texture	Clay Films: Freq.	Boundary: Dist.	Outline	CaCO3: Efferv.	Stage	Notes
		Moist														
4.6	A	7.5yr	M	vf	gr	0 50	lo	Stick.	Plast.	S SiCL	vf	abrupt	smooth	ne	I +	
	Bt	5/3 wet	Sg	f	pl	<10 65	so	so	po	LS SiL	f1	sharp	wavy	ve	II	
to	Bk	Dry	1	m	pr	10 75	sh	ss	ps	SL Si	c2	clear	lobate	e	III	3
	C	7.5yr	2	c	cpr	15 >75	h	s	p	SCL SiC	m3	gradual	irregular	es	IV	
4.3	E	5/3	3	vc	abk	25	vh	vs	vp	S C	c4	diffuse	tongued	ev	V	3
		moist			sbk	35	eh			CL SC	No				VI	

Depth (in)	Horiz.	Color	Structure: Grade	Size	Form	% Gravel	Consistence: Dry	Wet: Stick.	Plast.	Texture	Clay Films: Freq.	Boundary: Dist.	Outline	CaCO3: Efferv.	Stage	Notes
		Moist														
4.3	A	7.5yr	M	vf	gr	0 50	lo	Stick.	Plast.	S SiCL	vf	abrupt	smooth	ne	I +	
	Bt	4/3 moist	Sg	f	pl	<10 65	so	so	po	LS SiL	f1	sharp	wavy	ve	II	
to	Bk	~~Dry~~ wet	1	m	pr	10 75	sh	ss	ps	SL Si	c2	clear	lobate	e	III	0
	C	7.5yr	2	c	cpr	15 >75	h	s	p	SCL SiC	m3	gradual	irregular	es	IV	
3.9	E	4/2	3	vc	abk	25	vh	vs	vp	S C	c4	diffuse	tongued	ev	V	3
					sbk	35	eh			CL SC					VI	

Depth (in)	Horiz.	Color	Structure: Grade	Size	Form	% Gravel	Consistence: Dry	Wet: Stick.	Plast.	Texture	Clay Films: Freq.	Boundary: Dist.	Outline	CaCO3: Efferv.	Stage	Notes
		Moist														
3.9	A	7.5yr	M	vf	gr	0 50	lo	Stick.	Plast.	S SiCL	vf	abrupt	smooth	ne	I +	
	Bt	4/3	Sg	f	pl	<10 65	so	so	po	LS SiL	f1	sharp	wavy	ve	II	
to	Bk	~~Dry~~ wet	1	m	pr	10 75	sh	ss	ps	SL Si	c2	clear	lobate	e	III	0
	C	7.5yr	2	c	cpr	15 >75	h	s	p	SCL SiC	m3	gradual	irregular	es	IV	
2.95	E	5/2	3	vc	abk	25	vh	vs	vp	S C	c4	diffuse	tongued	ev	V	4
					sbk	35	eh			CL SC					VI	

Photographs

Photo #	Description
55	Pre-excavation (last week
1	Spoil material
2	Pit profile
3	Vegetation
3	General geomorphic surface

Photo #	Description

P2

Project _____ Date _____ Pit ID 6 GPS _____ Field Crew MJL, CAF

Time _____

Vegetation Descr. _____

Gemorph. Surface Alluvial _____ Descr. by JAF

Slope flat Parent Mat. _____ See fill

Pavement ☐ Archeological ☐

Varnish ☐ Moisture cond. dry☐ moist☒ wet☐

Depth (in)	Horiz.	Color	Structure			% Gravel	Consistence			Texture		Clay Films	Boundary		$CaCO_3$		Notes
		Moist	Grade	Size	Form		Dry	Wet				Freq.	Dist.	Outline	Efferv.	Stage	
2.95	A	7.5yr	M	vf	gr	0 50	lo	Stick.	Plast.	S	SiCL	vf	abrupt	smooth	ne	I +	
	Bt	4/3 wet	Sg	f	pl	<10 65	so	so	po	LS	SiL	f1	sharp	wavy	ve	II	0
to	Bk	Dry	1	m	pr	10 75	sh	ss	ps	SL	Si	c2	clear	lobate	e	III	3
	C	7.5yr	2	c	cpr	15 >75	h	s	p	SCL	SiC	m3	gradual	irregular	es	IV	
2.7	E	3/3 moist	3	vc	abk	25	vh	vs	vp	S	C	c4	diffuse	tongued	ev	V	
					sbk	35	eh			CL	SC					VI	

Depth (in)	Horiz.	Color	Structure			% Gravel	Consistence			Texture		Clay Films	Boundary		$CaCO_3$		Notes
		Moist	Grade	Size	Form		Dry	Wet				Freq.	Dist.	Outline	Efferv.	Stage	
2.7	A	7.5yr	M	vf	gr	0 50	lo	Stick.	Plast.	S	SiCL	vf	abrupt	smooth	ne	I +	
	Bt	4/3	Sg	f	pl	<10 65	so	so	po	LS	SiL	f1	sharp	wavy	ve	II	3
to	Bk	Dry	1	m	pr	10 75	sh	ss	ps	SL	Si	c2	clear	lobate	e	III	3
	C	7.5yr	2	c	cpr	15 >75	h	s	p	SCL	SiC	m3	gradual	irregular	es	IV	
1.8	E	5/3 wet	3	vc	abk	25	vh	vs	vp	S	C	c4	diffuse	tongued	ev	V	
					sbk	35	eh			CL	SC					VI	

Depth (in)	Horiz.	Color	Structure			% Gravel	Consistence			Texture		Clay Films	Boundary		$CaCO_3$		Notes
		Moist	Grade	Size	Form		Dry	Wet				Freq.	Dist.	Outline	Efferv.	Stage	
1.8	A	7.5yr	M	vf	gr	0 50	lo	Stick.	Plast.	S	SiCL	vf	abrupt	smooth	ne	I +	
	Bt	4/3	Sg	f	pl	<10 65	so	so	po	LS	SiL	f1	sharp	wavy	ve	II	3
to	Bk	Dry	1	m	pr	10 75	sh	ss	ps	SL	Si	c2	clear	lobate	e	III	4
	C	7.5yr	2	c	cpr	15 >75	h	s	p	SCL	SiC	m3	gradual	irregular	es	IV	
0.6	E	4/3 wet	3	vc	abk	25	vh	vs	vp	S	C	c4	diffuse	tongued	ev	V	
					sbk	35	eh			CL	SC					VI	

Depth (in)	Horiz.	Color	Structure			% Gravel	Consistence			Texture		Clay Films	Boundary		$CaCO_3$		Notes
		Moist	Grade	Size	Form		Dry	Wet				Freq.	Dist.	Outline	Efferv.	Stage	
0.6	A	7.5yr	M	vf	gr	0 50	lo	Stick.	Plast.	S	SiCL	vf	abrupt	smooth	ne	I +	
	Bt	6/3	Sg	f	pl	<10 65	so	so	po	LS	SiL	f1	sharp	wavy	ve	II	13
to	Bk	Dry	1	m	pr	10 75	sh	ss	ps	SL	Si	c2	clear	lobate	e	III	0
	C	7.5yr	2	c	cpr	15 >75	h	s	p	SCL	SiC	m3	gradual	irregular	es	IV	
0	E	4/4 wet	3	vc	abk	25	vh	vs	vp	S	C	c4	diffuse	tongued	ev	V	
					sbk	35	eh			CL	SC					VI	

Depth (in)	Horiz.	Color	Structure			% Gravel	Consistence			Texture		Clay Films	Boundary		$CaCO_3$		Notes
		Moist	Grade	Size	Form		Dry	Wet				Freq.	Dist.	Outline	Efferv.	Stage	
	A		M	vf	gr	0 50	lo	Stick.	Plast.	S	SiCL	vf	abrupt	smooth	ne	I +	
	Bt		Sg	f	pl	<10 65	so	so	po	LS	SiL	f1	sharp	wavy	ve	II	
to	Bk	Dry	1	m	pr	10 75	sh	ss	ps	SL	Si	c2	clear	lobate	e	III	
	C		2	c	cpr	15 >75	h	s	p	SCL	SiC	m3	gradual	irregular	es	IV	
	E		3	vc	abk	25	vh	vs	vp	S	C	c4	diffuse	tongued	ev	V	
					sbk	35	eh			CL	SC					VI	

Photographs

Photo #	Description
	Pre-excavation
	Spoil material
	Pit profile
	Vegetation
	General geomorphic surface

Photo #	Description

Project Lthumcs Date 3/15/05 Pit ID 8 GPS _____ Field Crew JF, CH

Time _____

Vegetation Descr. Cr (10%), grasses/flowers (90%)

Gemorph. Surface Floodplain Qyl Descr. by JF

Slope _____ Parent Mat. _____

Pavement ☐ Archeological ☐ SKETCH ON BACK

Varnish ☐ Moisture cond. dry☐ moist☐ wet☐

*7.5y for all co

Depth (in)	Horiz.	*Color (Moist)	Structure Grade	Size	Form	% Gravel	Consistence Dry	Wet Stick.	Wet Plast.	Texture	Clay Films Freq.	Boundary Dist.	Boundary Outline	CaCO3 Efferv.	CaCO3 Stage	Notes
1																
7.8 to 7.2	A	4/3	M	vf	gr	0 50	lo	Stick.	Plast.	S SiCL	vf	abrupt	smooth	ne	I +	PM = 4
	Bt		Sg	f	pl	<10 65	so	so	po	LS SiL	f1	sharp	wavy	ve	II	TM = 5
	Bk	Dry	1	m	pr	10 75	sh	ss	ps	SL Si	c2	clear	lobate	e	III	
	C		2	c	cpr	15 >75	h	s	p	SCL SiC	m3	gradual	irregular	es	IV no	
	E	4/3	3	vc	abk	25	vh	vs	vp	S C	c4	diffuse	tongued	ev	V	
					sbk	35	eh			CL SC	no				VI	
2																
7.2 to 6.1	A	4/3	M	vf	gr	0 50	lo	Stick.	Plast.	S SiCL	vf	abrupt	smooth	ne	I +	peds (may not be true PM = 0 TM = 7
	Bt		Sg	f	pl	<10 65	so	so	po	LS SiL	f1	sharp	wavy	ve	II	
	Bk	Dry	1	m	pr	10 75	sh	ss	ps	SL Si	c2	clear	lobate	e	III	
	C		2	c	cpr	15 >75	h	s	p	SCL SiC	m3	gradual	irregular	es	IV no	
	E	4/3	3	vc	abk	25	vh	vs	vp	S C	c4	diffuse	tongued	ev	V	
					sbk	35	eh			CL SC					VI	
3																
to 4.9	A	4/3	M	vf	gr	0 50	lo	Stick.	Plast.	S SiCL	vf	abrupt	smooth	ne	I +	*peds (may not be true peds)
	Bt		Sg	f	pl	<10 65	so	so	po	LS SiL	f1	sharp	wavy	ve	II	*little more gravel than 2
	Bk	Dry	1	m	pr	10 75	sh	ss	ps	SL Si	c2	clear	lobate	e	III	*capped by 2/10 ft. layer
	C		2	c	cpr	15 >75	h	s	p	SCL SiC	m3	gradual	irregular	es	IV no	with ~~more~~ clay
	E	4/3	3	vc	abk	25	vh	vs	vp	S C	c4	diffuse	tongued	ev	V	↳ eff = es PM = 0
					sbk	35	eh			CL SC	no				VI	TM = 4
4																
to 4.1	A	4/3	M	vf	gr	0 50	lo	Stick.	Plast.	S ~~SiCL~~	vf	abrupt	smooth	ne	1 +	Texture = SCL
	Bt		Sg	f	pl	<10 65	so	so	po	LS SiL	f1	sharp	wavy	ve	II	PM = 0
	Bk	Dry	1	m	pr	10 75	sh	ss	ps	SL Si	c2	clear	lobate	e	III	TM = 5
	C		2	c	cpr	15 >75	h	s	p	~~SCL~~ ~~SiC~~	m3	gradual	irregular	es	IV	
	E	4/4	3	vc	abk	25	vh	vs	vp	S C	c4	diffuse	tongued	ev	V	
					sbk	35	eh			CL SC					VI	
5																
to 3.5	A	4/3	M	vf	gr	0 50	lo	Stick.	Plast.	S SiCL	vf	abrupt	smooth	ne	1 +	PM = 0
	Bt		Sg	f	pl	<10 65	so	so	po	LS SiL	f1	sharp	wavy	ve	II	TM = 5
	Bk	Dry	1	m	pr	10 75	sh	ss	ps	SL Si	c2	clear	lobate	e	III	
	C		2	c	cpr	15 >75	h	s	p	SCL SiC	m3	gradual	irregular	es	IV	
	E	4/3	3	vc	abk	25	vh	vs	vp	S C	c4	diffuse	tongued	ev	V	
					sbk	35	eh			CL SC					VI	

Photographs

Photo #	Description
[illegible]	Pre-excavation
	Spoil material
	Pit profile
	Vegetation
	General geomorphic surface

Photo #	Description

Project _____ Date _____ Pit ID 8 GPS _____ Field Crew _____

Time _____

Vegetation Descr. _____

Gemorph. Surface _____ Descr. by _____

Slope _____ Parent Mat. _____

Pavement ☐ Archeological ☐

Varnish ☐ Moisture cond. dry☐ moist☐ wet☐

Depth (in)	Horiz.	Color	Structure			% Gravel	Consistence			Texture		Clay Films	Boundary		$CaCO_3$		Notes
		Moist	Grade	Size	Form		Dry	Wet				Freq.	Dist.	Outline	Efferv.	Stage	pocket soil (dark clay)
	A	4/3	M	vf	gr	0 50	lo	Stick.	Plast.	S	SiCL	vf	abrupt	smooth	ne	I +	charcoal found
	Bt		Sg	f	pl	<10 65	so	~~ss~~	~~po~~	~~LS~~	SiL	~~f1~~	sharp	wavy	ve	II	capped by pockets of darker
to	Bk	Dry	1	m	pr	10 75	sh	ss	ps	SL	Si	c2	clear	lobate	e	III	PM = 4
	C		2	c	cpr	15 >75	h	s	p	SCL	SiC	m3	gradual	irregular	es	IV no	TM = 6
6 2.8	E	4/4	3	vc	abk	25	vh	vs	vp	S	C	c4	diffuse	tongued	ev	V	
					sbk	35	eh			CL	SC					VI	

Depth (in)	Horiz.	Color	Structure			% Gravel	Consistence			Texture		Clay Films	Boundary		$CaCO_3$		Notes
		Moist	Grade	Size	Form		Dry	Wet				Freq.	Dist.	Outline	Efferv.	Stage	PM = 14
	A	5/3	M	vf	gr	0 50	lo	Stick.	Plast.	S	SiCL	vf	abrupt	smooth	ne	I +	TM = 4
	Bt		Sg	f	pl	<10 65	so	so	po	LS	SiL	f1	sharp	wavy	ve	II	
to	Bk	Dry	1	m	pr	10 75	sh	ss	ps	SL	Si	c2	clear	lobate	e	III no	
	C		2	c	cpr	15 >75	h	s	p	SCL	SiC	m3	gradual	irregular	es	IV	
7 1.8	E	5/3	3	vc	abk	25	vh	vs	vp	S	C	c4	diffuse	tongued	ev	V	
					sbk	35	eh			CL	SC	no				VI	

Depth (in)	Horiz.	Color	Structure			% Gravel	Consistence			Texture		Clay Films	Boundary		$CaCO_3$		Notes
1.8		Moist	Grade	Size	Form		Dry	Wet				Freq.	Dist.	Outline	Efferv.	Stage	PM = 17
	A	5/4	M	vf	gr	0 50	lo	Stick.	Plast.	S	SiCL	vf	abrupt	smooth	ne	I +	TM = 5
	Bt		Sg	f	pl	<10 65	so	so	po	LS	SiL	f1	sharp	wavy	ve	II	
to	Bk	Dry	1	m	pr	10 75	sh	ss	ps	SL	Si	c2	clear	lobate	e	III no	
	C		2	c	cpr	15 >75	h	s	p	SCL	SiC	m3	gradual	irregular	es	IV	
8 1.4	E	5/4	3	vc	abk	25	vh	vs	vp	S	C	c4	diffuse	tongued	ev	V	
					sbk	35	eh			CL	SC	no				VI	

Depth (in)	Horiz.	Color	Structure			% Gravel	Consistence			Texture		Clay Films	Boundary		$CaCO_3$		Notes
1.4		Moist	Grade	Size	Form		Dry	Wet				Freq.	Dist.	Outline	Efferv.	Stage	PM = 14
	A	5/3	M	vf	gr	0 50	lo	Stick.	Plast.	S	SiCL	vf	abrupt	smooth	ne	I +	TM = 0
	Bt		Sg	f	pl	<10 65	so	so	po	LS	SiL	f1	sharp	wavy	ve	II	
to	Bk	Dry	1	m	pr	10 75	sh	ss	ps	SL	Si	c2	clear	lobate	e	III no	
	C		2	c	cpr	15 >75	h	s	p	SCL	SiC	m3	gradual	irregular	es	IV	
9 Bottom	E	5/4	3	vc	abk	25	vh	vs	vp	S	C	c4	diffuse	tongued	ev	V	
					sbk	35	eh			CL	SC	no				VI	

Depth (in)	Horiz.	Color	Structure			% Gravel	Consistence			Texture		Clay Films	Boundary		$CaCO_3$		Notes
		Moist	Grade	Size	Form		Dry	Wet				Freq.	Dist.	Outline	Efferv.	Stage	
	A		M	vf	gr	0 50	lo	Stick.	Plast.	S	SiCL	vf	abrupt	smooth	ne	I +	
	Bt		Sg	f	pl	<10 65	so	so	po	LS	SiL	f1	sharp	wavy	ve	II	
to	Bk	Dry	1	m	pr	10 75	sh	ss	ps	SL	Si	c2	clear	lobate	e	III	
	C		2	c	cpr	15 >75	h	s	p	SCL	SiC	m3	gradual	irregular	es	IV	
	E		3	vc	abk	25	vh	vs	vp	S	C	c4	diffuse	tongued	ev	V	
					sbk	35	eh			CL	SC					VI	

Photographs

Photo #	Description
56	Pre-excavation
20	Spoil material
21	Pit profile
see pic	Vegetation
	General geomorphic surface

Photo #	Description

Project LHWCMP Date 3/15/05 Pit ID 13 GPS _____ Field Crew JF, MK, CH

Time _____

Vegetation Descr. _____

Gemorph. Surface Qt - tributary Descr. by JF

Slope _____ Parent Mat. _____

Pavement ☐ Archeological ☐

Varnish ☐ Moisture cond. dry ☑ moist ☐ wet ☐

Depth (in)	Horiz.	Color	Structure			% Gravel	Consistence			Texture	Clay Films	Boundary		$CaCO_3$		Notes
		~~Moist~~ Wet	Grade	Size	Form		Dry	Wet			Freq.	Dist.	Outline	Efferv.	Stage	
7.4	A	7.5yr	M	vf	gr	0 50	lo	Stick.	Plast.	S SiCL	vf	abrupt	smooth	ne	I +	$CaCO_3$ nodules
	Bt	5/4	Sg	f	pl	<10 65	so	so	po	LS SiL	f1	sharp	wavy	ve	II	Bioturbated zone
to	Bk	Dry	1	m	pr	10 75	sh	ss	ps	SL Si	c2	clear	lobate	e	III	
	C	7.5yr	2	c	cpr	15 >75	h	s	p	SCL SiC	m3	gradual	irregular	es	IV	Penet. 4 Shear 6
6.8	E	6/4	3	vc	abk	25	vh	vs	vp	S C	c4	diffuse	tongued	ev	V	
					sbk	35	eh			CL SC	N/A				VI	

Depth (in)	Horiz.	Color	Structure			% Gravel	Consistence			Texture	Clay Films	Boundary		$CaCO_3$		Notes
		~~Moist~~ Wet	Grade	Size	Form		Dry	Wet			Freq.	Dist.	Outline	Efferv.	Stage	
6.8	A	7.5yr	M	vf	gr	0 50	lo	Stick.	Plast.	S SiCL	vf	abrupt	smooth	ne	I +	$CaCO_3$ nods.
	Bt	5/4	Sg	f	pl	<10 65	so	so	po	LS SiL	f1	sharp	wavy	ve	II	
to	Bk	Dry	1	m	pr	10 75	sh	ss	ps	SL Si	c2	clear	lobate	e	III	
	C	7.5yr	2	c	cpr	15 >75	h	s	p	SCL SiC	m3	gradual	irregular	es	IV	
5.1	E	6/4	3	vc	abk	25	vh	vs	vp	S C	c4	diffuse	tongued	ev	V	Penet. 10 Shear 6
					sbk	35	eh			CL SC	N/A				VI	

Depth (in)	Horiz.	Color	Structure			% Gravel	Consistence			Texture	Clay Films	Boundary		$CaCO_3$		Notes
		~~Moist~~ Wet	Grade	Size	Form		Dry	Wet			Freq.	Dist.	Outline	Efferv.	Stage	
5.1	A	7.5yr	M	vf	gr	0 50	lo	Stick.	Plast.	S SiCL	vf	abrupt	smooth	ne	I +	~~$CaCO_3$ nods~~.
	Bt	4/4	Sg	f	pl	<10 65	so	so	po	LS SiL	f1	sharp	wavy	ve	II	Fewer $CaCO_3$ nods
to	Bk	Dry	1	m	pr	10 75	sh	ss	ps	SL Si	c2	clear	lobate	e	III	
	C	7.5yr	2	c	cpr	15 >75	h	s	p	SCL SiC	m3	gradual	irregular	es	IV	
1.1	E	6/4	3	vc	abk	25	vh	vs	vp	S C	c4	diffuse	tongued	ev	V	Penet. 17 Shear 8
					sbk	35	eh			CL SC					VI	

Depth (in)	Horiz.	Color	Structure			% Gravel	Consistence			Texture	Clay Films	Boundary		$CaCO_3$		Notes
		~~Moist~~ Wet	Grade	Size	Form		Dry	Wet			Freq.	Dist.	Outline	Efferv.	Stage	
1.1	A	7.5yr	M	vf	gr	0 50	lo	Stick.	Plast.	S SiCL	vf	abrupt	smooth	ne	I +	
	Bt	5/4	Sg	f	pl	<10 65	so	so	po	LS SiL	f1	sharp	wavy	ve	II	
to	Bk	Dry	1	m	pr	10 75	sh	ss	ps	SL Si	c2	clear	lobate	e	III	
	C	7.5yr	2	c	cpr	15 >75	h	s	p	SCL SiC	m3	gradual	irregular	es	IV	
0	E	6/4	3	vc	abk	25	vh	vs	vp	S C	c4	diffuse	tongued	ev	V	Penet. 20 Shear 5
					sbk	35	eh			CL SC	N/A				VI	

Depth (in)	Horiz.	Color	Structure			% Gravel	Consistence			Texture	Clay Films	Boundary		$CaCO_3$		Notes
		Moist	Grade	Size	Form		Dry	Wet			Freq.	Dist.	Outline	Efferv.	Stage	
	A		M	vf	gr	0 50	lo	Stick.	Plast.	S SiCL	vf	abrupt	smooth	ne	I +	
	Bt		Sg	f	pl	<10 65	so	so	po	LS SiL	f1	sharp	wavy	ve	II	
to	Bk	Dry	1	m	pr	10 75	sh	ss	ps	SL Si	c2	clear	lobate	e	III	
	C		2	c	cpr	15 >75	h	s	p	SCL SiC	m3	gradual	irregular	es	IV	
	E		3	vc	abk	25	vh	vs	vp	S C	c4	diffuse	tongued	ev	V	
					sbk	35	eh			CL SC					VI	

Photographs

Photo #	Description
57	Pre-excavation
28	Spoil material
27, 28	Pit profile
28	Vegetation
29	General geomorphic surface

Photo #	Description

East side f/p series of 3 pits - right after lunch

Project LHWCMP Date 3-15 Pit ID 15 GPS _____ Field Crew MJK, CKH, JEF

Time 1 pm

Vegetation Descr. Creosote - PV - brush - grass

Gemorph. Surface floodplain Q12 Descr. by MJK

Slope flat / undulating Parent Mat. _____

Pavement ☐ Archeological ☐

Varnish ☐ Moisture cond. dry☐ moist☐ wet☐

NO SHADES IN SHADE

SKETCH ON BACK

< 1 except ↓ (SV) (P)

Depth (in)	Horiz.	Color	Structure Grade	Size	Form	% Gravel	Consistence Dry	Wet Stick.	Plast.	Texture	Clay Films Freq.	Boundary Dist.	Outline	CaCO3 Efferv.	Stage	Notes
6.3		Moist 7.5YR														
	A	4/3	M	vf	gr	0 50	lo	Stick.	Plast.	S SiCL	vf	abrupt	smooth	ne	I +	(0) (0)
	Bt		Sg	f	pl	<10 65	so	so	po	LS SiL	f1	sharp	wavy	ve	II	
to	Bk	Dry*	1	m	pr	10 75	sh	ss	ps	SL Si	c2	clear	lobate	e	III	
	C	7.5YR	2	c	cpr	15 >75	h	s	p	SCL SiC	m3	gradual	irregular	es	IV	
	E	6/2	3	vc	abk	25	vh	vs	vp	S C	c4	diffuse	tongued	ev	V	
6.2					sbk	35	eh			CL SC	NO				VI	

Depth (in)	Horiz.	Color	Structure Grade	Size	Form	% Gravel	Consistence Dry	Wet Stick.	Plast.	Texture	Clay Films Freq.	Boundary Dist.	Outline	CaCO3 Efferv.	Stage	Notes
6.2		Moist														~~silt cap c top~~
	A	4/3	M	vf	gr	0 50	lo	Stick.	Plast.	S SiCL	vf	abrupt	smooth	ne	I +	
	Bt		Sg	f	pl	<10 65	so	so	po	LS SiL	f1	sharp	wavy	ve	II	(0)
to	Bk	Dry	1	m	pr	10 75	sh	ss	ps	SL Si	c2	clear	lobate	e	III	
	C	7.5YR	2	c	cpr	15 >75	h	s	p	SCL SiC	m3	gradual	irregular	es	IV	
	E	4/3	3	vc	abk	25	vh	vs	vp	S C	c4	diffuse	tongued	ev	V	(3)
5.5					sbk	35	eh			CL SC	NO				VI	

Depth (in)	Horiz.	Color	Structure Grade	Size	Form	% Gravel	Consistence Dry	Wet Stick.	Plast.	Texture	Clay Films Freq.	Boundary Dist.	Outline	CaCO3 Efferv.	Stage	Notes
5.5		Moist														silt cap c top some clay films
	A	4/3	M	vf	gr	0 50	lo	Stick.	Plast.	S SiCL	vf	abrupt	smooth	ne	I +	
	Bt		Sg	f	pl	<10 65	so	so	po	LS SiL	f1	sharp	wavy	ve	II	
to	Bk	Dry	1	m	pr	10 75	sh	ss	ps	SL Si	c2	clear	lobate	e	III	(2)
	C	7.5YR	2	c	cpr	15 >75	h	s	p	SCL SiC	m3	gradual	irregular	es	IV	
	E	4/3	3	vc	abk	25	vh	vs	vp	S C	c4	diffuse	tongued	ev	V	(3)
4.9					sbk	35	eh			CL SC	NO				VI	

Depth (in)	Horiz.	Color	Structure Grade	Size	Form	% Gravel	Consistence Dry	Wet Stick.	Plast.	Texture	Clay Films Freq.	Boundary Dist.	Outline	CaCO3 Efferv.	Stage	Notes
4.9		Moist														
	A	4/3	M	vf	gr	0 50	lo	Stick.	Plast.	S SiCL	vf	abrupt	smooth	ne	I +	
	Bt		Sg	f	pl	<10 65	so	so	po	LS SiL	f1	sharp	wavy	ve	II	(6)
to	Bk	Dry	1	m	pr	10 75	sh	ss	ps	SL Si	c2	clear	lobate	e	III	
	C	7.5YR	2	c	cpr	15 >75	h	s	p	SCL SiC	m3	gradual	irregular	es	IV	(2.5)
	E	4/3	3	vc	abk	25	vh	vs	vp	S C	c4	diffuse	tongued	ev	V	
3.8					sbk	35	eh			CL SC	NO				VI	

Depth (in)	Horiz.	Color	Structure Grade	Size	Form	% Gravel	Consistence Dry	Wet Stick.	Plast.	Texture	Clay Films Freq.	Boundary Dist.	Outline	CaCO3 Efferv.	Stage	Notes
3.8		Moist														
	A	4/3	M	vf	gr	0 50	lo	Stick.	Plast.	S SiCL	vf	abrupt	smooth	ne	I +	
	Bt		Sg	f	pl	<10 65	so	so	po	LS SiL	f1	sharp	wavy	ve	II	(4)
to	Bk	Dry	1	m	pr	10 75	sh	ss	ps	SL Si	c2	clear	lobate	e	III	
	C	7.5YR	2	c	cpr	15 >75	h	s	p	SCL SiC	m3	gradual	irregular	es	IV	(2.5)
	E	4/3	3	vc	abk	25	vh	vs	vp	S C	c4	diffuse	tongued	ev	V	
1.9					sbk	35	eh			CL SC	NO				VI	

Photographs

Photo #	Description
58	Pre-excavation
23	Spoil material
22	Pit profile
23	Vegetation
24	General geomorphic surface

Photo #	Description

* NO REAL DRY COLORS - MOIST

Project LHCWMP Date 3-15 Pit ID 15 GPS _____ Field Crew JEF, MJK, CEH

Time 1 pm

Vegetation Descr. _____

Gemorph. Surface Qyz / Sangs 1 Descr. by MJK

Slope _____ Parent Mat. _____

Pavement ☐ Archeological ☐

Varnish ☐ Moisture cond. dry☐ moist☐ wet☐

all less than I except

Depth (in)	Horiz.	Color	Structure			% Gravel	Consistence			Texture	Clay Films	Boundary		$CaCO_3$		Notes
19		Moist	Grade	Size	Form		Dry	Wet			Freq.	Dist.	Outline	Efferv.	Stage	- possible clay films when smeared
	A	4/5	M	vf	gr	0 50	lo	Stick.	Plast.	S SiCL	vf	abrupt	smooth	ne	I +	
	Bt		Sg	f	pl	<10 65	so	so	po	LS SiL	f1	sharp	wavy	ve	II	
to	Bk	Dry	1	m	pr	10 75	sh	ss	ps	SL Si	c2	clear	lobate	e	III	
	C	7.5YR	2	c	cpr	15 >75	h	s	p	SCL SiC	m3	gradual	irregular	es	IV	3
Bottom	E	3/3	3	vc	abk	25	vh	vs	vp	S C	c4	diffuse	tongued	ev	V	
Pit 0.8					sbk	35	eh			CL SC	no				VI	5.5

Depth (in)	Horiz.	Color	Structure			% Gravel	Consistence			Texture	Clay Films	Boundary		$CaCO_3$		Notes
0.8		Moist	Grade	Size	Form		Dry	Wet			Freq.	Dist.	Outline	Efferv.	Stage	No coatings
	A	4/3	M	vf	gr	0 50	lo	Stick.	Plast.	S SiCL	vf	abrupt	smooth	ne	I +	
	Bt		Sg	f	pl	<10 65	so	so	po	LS SiL	f1	sharp	wavy	ve	II	
to	Bk	Dry	1	m	pr	10 75	sh	ss	ps	SL Si	c2	clear	lobate	e	III	
	C	7.5YR	2	c	cpr	15 >75	h	s	p	SCL SiC	m3	gradual	irregular	es	IV	11
Bottom	E	4/3	3	vc	abk	25	vh	vs	vp	S C	c4	diffuse	tongued	ev	V	
Pit					sbk	35	eh			CL SC	no				VI	5

Depth (in)	Horiz.	Color	Structure			% Gravel	Consistence			Texture	Clay Films	Boundary		$CaCO_3$		Notes
		Moist	Grade	Size	Form		Dry	Wet			Freq.	Dist.	Outline	Efferv.	Stage	
	A		M	vf	gr	0 50	lo	Stick.	Plast.	S SiCL	vf	abrupt	smooth	ne	I +	
	Bt		Sg	f	pl	<10 65	so	so	po	LS SiL	f1	sharp	wavy	ve	II	
to	Bk	Dry	1	m	pr	10 75	sh	ss	ps	SL Si	c2	clear	lobate	e	III	
	C		2	c	cpr	15 >75	h	s	p	SCL SiC	m3	gradual	irregular	es	IV	
	E		3	vc	abk	25	vh	vs	vp	S C	c4	diffuse	tongued	ev	V	
					sbk	35	eh			CL SC					VI	

Depth (in)	Horiz.	Color	Structure			% Gravel	Consistence			Texture	Clay Films	Boundary		$CaCO_3$		Notes
		Moist	Grade	Size	Form		Dry	Wet			Freq.	Dist.	Outline	Efferv.	Stage	
	A		M	vf	gr	0 50	lo	Stick.	Plast.	S SiCL	vf	abrupt	smooth	ne	I +	
	Bt		Sg	f	pl	<10 65	so	so	po	LS SiL	f1	sharp	wavy	ve	II	
to	Bk	Dry	1	m	pr	10 75	sh	ss	ps	SL Si	c2	clear	lobate	e	III	
	C		2	c	cpr	15 >75	h	s	p	SCL SiC	m3	gradual	irregular	es	IV	
	E		3	vc	abk	25	vh	vs	vp	S C	c4	diffuse	tongued	ev	V	
					sbk	35	eh			CL SC					VI	

Depth (in)	Horiz.	Color	Structure			% Gravel	Consistence			Texture	Clay Films	Boundary		$CaCO_3$		Notes
		Moist	Grade	Size	Form		Dry	Wet			Freq.	Dist.	Outline	Efferv.	Stage	
	A		M	vf	gr	0 50	lo	Stick.	Plast.	S SiCL	vf	abrupt	smooth	ne	I +	
	Bt		Sg	f	pl	<10 65	so	so	po	LS SiL	f1	sharp	wavy	ve	II	
to	Bk	Dry	1	m	pr	10 75	sh	ss	ps	SL Si	c2	clear	lobate	e	III	
	C		2	c	cpr	15 >75	h	s	p	SCL SiC	m3	gradual	irregular	es	IV	
	E		3	vc	abk	25	vh	vs	vp	S C	c4	diffuse	tongued	ev	V	
					sbk	35	eh			CL SC					VI	

Photographs

Photo #	Description
	Pre-excavation
	Spoil material
	Pit profile
	Vegetation
	General geomorphic surface

Photo #	Description

Project LAWCMP Date 3/15/05 Pit ID 18 GPS _____ Field Crew JF, CH

Time _____

Vegetation Descr. Cr (40%) grasses

Gemorph. Surface floodplain Qyl – Jackrabbit fan Descr. by JF

Slope _____ Parent Mat. _____

Pavement ☐ Archeological ☐

Varnish ☐ Moisture cond. dry☐ moist☐ wet☐

SKETCH ON BACK

	Depth (in)	Horiz.	Color	Structure Grade	Size	Form	% Gravel	Consistence Dry	Wet Stick.	Wet Plast.	Texture	Clay Films Freq.	Boundary Dist.	Boundary Outline	$CaCO_3$ Efferv.	$CaCO_3$ Stage	Notes
			Moist	Grade	Size	Form		Dry	Wet			Freq.	Dist.	Outline	Efferv.	Stage	
1	6.3 to 5.8	A		M	vf	gr	0 50	lo	Stick.	Plast.	S SiCL	vf	abrupt	smooth	ne	I +	Bioturbated Hassy Dep
		Bt		Sg	f	pl	<10 65	so	so	po	LS SiL	f1	sharp	wavy	ve	II	
		Bk	Dry	1	m	pr	10 75	sh	ss	ps	SL Si	c2	clear	lobate	e	III	pm = 0
		C		2	c	cpr	15 >75	h	s	p	SCL SiC	m3	gradual	irregular	es	IV no	Tm = 4
		E	6/3	3	vc	abk	25	vh	vs	vp	S C	c4	diffuse	tongued	ev	V	
						sbk	35	eh			CL SC	no				VI	
2	5.2 to 4.6	A		M	vf	gr	0 50	lo	Stick.	Plast.	S SiCL	vf	abrupt	smooth	ne	I +	Hassy Dep Irregular Sand cap w/ greenish color
		Bt		Sg	f	pl	<10 65	so	so	po	LS SiL	f1	sharp	wavy	ve	II	
		Bk	Dry	1	m	pr	10 75	sh	ss	ps	SL Si	c2	clear	lobate	e	III	pm = 7
		C		2	c	cpr	15 >75	h	s	p	SCL SiC	m3	gradual	irregular	es	IV no	Tm = 4
		E	5/4	3	vc	abk	25	vh	vs	vp	S C	c4	diffuse	tongued	ev	V	
						sbk	35	eh			CL SC	no				VI	
3	4.6 to 4.2	A		M	vf	gr	0 50	lo	Stick.	Plast.	S SiCL	vf	abrupt	smooth	ne	I +	JWT Dep has a rooting layer
		Bt		Sg	f	pl	<10 65	so	so	po	LS SiL	f1	sharp	wavy	ve	II	
		Bk	Dry	1	m	pr	10 75	sh	ss	ps	SL Si	c2	clear	lobate	e	III	pm = 7
		C		2	c	cpr	15 >75	h	s	p	SCL SiC	m3	gradual	irregular	es	IV no	Tm = 3
		E	5/3	3	vc	abk	25	vh	vs	vp	S C	c4	diffuse	tongued	ev	V	
						sbk	35	eh			CL SC	no				VI	
4	4.2 to	A		M	vf	gr	0 50	lo	Stick.	Plast.	S SiCL	vf	abrupt	smooth	ne	I +	Hassy Dep.
		Bt		Sg	f	pl	<10 65	so	so	po	LS SiL	f1	sharp	wavy	ve	II	
		Bk	Dry	1	m	pr	10 75	sh	ss	ps	SL Si	c2	clear	lobate	e	III	pm = 7
		C		2	c	cpr	15 >75	h	s	p	SCL SiC	m3	gradual	irregular	es	IV no	Tm = 5
		E	4/3	3	vc	abk	25	vh	vs	vp	S C	c4	diffuse	tongued	ev	V	
						sbk	35	eh			CL SC	no				VI	
5	3.8 to	A		M	vf	gr	0 50	lo	Stick.	Plast.	S SiCL	vf	abrupt	smooth	ne	I +	JWT Dep rooting layer
		Bt		Sg	f	pl	<10 65	so	so	po	LS SiL	f1	sharp	wavy	ve	II	
		Bk	Dry	1	m	pr	10 75	sh	ss	ps	SL Si	c2	clear	lobate	e	III no	
		C		2	c	cpr	15 >75	h	s	p	SCL SiC	m3	gradual	irregular	es	IV	pm = 8
		E	5/3	3	vc	abk	25	vh	vs	vp	S C	c4	diffuse	tongued	ev	V	Tm = 4
						sbk	35	eh			CL SC					VI	

Photographs

Photo #	Description
59	Pre-excavation
36	Spoil material
35	Pit profile
36	Vegetation
37	General geomorphic surface

Photo #	Description

Project Lthn Cmx Date 3/15 Pit ID 1F GPS _____ Field Crew CH

Time _____

Vegetation Descr. _____

Gemorph. Surface / See pg. 1 Descr. by JF

Slope _____ Parent Mat. _____

Pavement ☐ Archeological ☐

Varnish ☐ Moisture cond. dry☐ moist☐ wet☐

Depth (in)	Horiz.	Color	Structure			% Gravel	Consistence			Texture	Clay Films	Boundary		$CaCO_3$		Notes
		Moist	Grade	Size	Form		Dry	Wet			Freq.	Dist.	Outline	Efferv.	Stage	
	A		M	vf	gr	0 50	lo	Stick.	Plast.	S SiCL	vf	abrupt	smooth	ne	I +	Hassy Dep
	Bt		Sg	f	pl	<10 65	so	so	po	LS SiL	f1	sharp	wavy	ve	II	PM: 12
to	Bk	Dry	1	m	pr	10 75	sh	ss	ps	SL Si	c2	clear	lobate	e	III no	TM: 5
6	C		2	c	cpr	15 >75	h	s	p	SCL SiC	m3	gradual	irregular	es	IV	
3.6	E	5/3	3	vc	abk	25	vh	vs	vp	S C	c4	diffuse	tongued	ev	V	
					sbk	35	eh			CL SC	no				VI	

Depth (in)	Horiz.	Color	Structure			% Gravel	Consistence			Texture	Clay Films	Boundary		$CaCO_3$		Notes
		Moist	Grade	Size	Form		Dry	Wet			Freq.	Dist.	Outline	Efferv.	Stage	
	A		M	vf	gr	0 50	lo	Stick.	Plast.	S SiCL	vf	abrupt	smooth	ne	I +	~~Fwf~~ Dep
	Bt		Sg	f	pl	<10 65	so	so	po	LS SiL	f1	sharp	wavy	ve	II	~~Hassy~~
to	Bk	Dry	1	m	pr	10 75	sh	ss	ps	SL Si	c2	clear	lobate	e	III	JWT PM: 10
7	C		2	c	cpr	15 >75	h	s	p	SCL SiC	m3	gradual	irregular	es	IV no	TM: 4
3.3	E	5/3	3	vc	abk	25	vh	vs	vp	S C	c4	diffuse	tongued	ev	V	
					sbk	35	eh			CL SC					VI	

Depth (in)	Horiz.	Color	Structure			% Gravel	Consistence			Texture	Clay Films	Boundary		$CaCO_3$		Notes
		Moist	Grade	Size	Form		Dry	Wet			Freq.	Dist.	Outline	Efferv.	Stage	
	A		M	vf	gr	0 50	lo	Stick.	Plast.	S SiCL	vf	abrupt	smooth	ne	I +	Hassy Dep? w/ sands
	Bt		Sg	f	pl	<10 65	so	so	po	LS SiL	f1	sharp	wavy	ve	II	
to	Bk	Dry	1	~~m~~	pr	10 75	sh	ss	ps	SL Si	c2	clear	lobate	e	III	PM = 8
8	C		2	c	cpr	15 >75	h	s	p	SCL SiC	m3	gradual	irregular	es	IV no	TM = 5
3.1	E	4.3	3	vc	abk	25	vh	vs	vp	S C	c4	diffuse	tongued	ev	V	
					sbk	35	eh			CL SC					VI	

Depth (in)	Horiz.	Color	Structure			% Gravel	Consistence			Texture	Clay Films	Boundary		$CaCO_3$		Notes
		Moist	Grade	Size	Form		Dry	Wet			Freq.	Dist.	Outline	Efferv.	Stage	
	A		M	vf	gr	0 50	lo	Stick.	Plast.	S SiCL	vf	abrupt	smooth	ne	I +	JWT Dep
	Bt		Sg	f	pl	<10 65	so	so	po	LS SiL	f1	sharp	wavy	ve	II	
to	Bk	Dry	1	m	pr	10 75	sh	ss	ps	SL Si	c2	clear	lobate	e	III no	PM = 15
9	C		2	c	cpr	15 >75	h	s	p	SCL SiC	m3	gradual	irregular	es	IV	
2.3	E	5/3	3	vc	abk	25	vh	vs	vp	S C	c4	diffuse	tongued	ev	V	TM = 1
					sbk	35	eh			CL SC					VI	

Depth (in)	Horiz.	Color	Structure			% Gravel	Consistence			Texture	Clay Films	Boundary		$CaCO_3$		Notes
		Moist	Grade	Size	Form		Dry	Wet			Freq.	Dist.	Outline	Efferv.	Stage	
	A		M	vf	gr	0 50	lo	Stick.	Plast.	S SiCL	vf	abrupt	smooth	ne	I +	Hassy Dep
	Bt		Sg	f	pl	<10 65	so	so	po	LS SiL	f1	sharp	wavy	ve	II	
to	Bk	Dry	1	m	pr	10 75	sh	ss	ps	SL Si	c2	clear	lobate	e	III no	PM = 6
10	C		2	c	cpr	15 >75	h	s	p	SCL SiC	m3	gradual	irregular	es	IV	
1.1	E	4/4	3	vc	abk	25	vh	vs	vp	S C	c4	diffuse	tongued	ev	V	TM = 4
					sbk	35	eh			CL SC					VI	

Photographs

Photo #	Description
	Pre-excavation
	Spoil material
	Pit profile
	Vegetation
	General geomorphic surface

Photo #	Description

Project LHWCMP Date 3/15 Pit ID 18 GPS Field Crew CH

Time

Vegetation Descr.

Gemorph. Surface / see pg 1 Descr. by JF

Slope Parent Mat.

Pavement ☐ Archeological ☐

Varnish ☐ Moisture cond. dry☐ moist☐ wet☐

Depth (in)	Horiz.	Color	Structure Grade	Size	Form	% Gravel	Consistence Dry	Wet Stick.	Plast.	Texture	Clay Films Freq.	Boundary Dist.	Outline	$CaCO_3$ Efferv.	Stage	Notes
		Moist														JWT Dep
	A		M	vf	gr	0 50	lo			S SiCL	vf	abrupt	smooth	ne	I +	pM = 3
	Bt		Sg	f	pl	<10 65	so	so	po	LS SiL	f1	sharp	wavy	ve	II	TM = 4
to	Bk	Dry	1	m	pr	10 75	sh	ss	ps	SL Si	c2	clear	lobate	e	III	
	C		2	c	cpr	15 >75	h	s	p	SCL SiC	m3	gradual	irregular	es	IV no	
0.8	E	5/3	3	vc	abk	25	vh	vs	vp	S C	c4	diffuse	tongued	ev	V	
					sbk	35	eh			CL SC					VI	

Depth (in)	Horiz.	Color	Structure Grade	Size	Form	% Gravel	Consistence Dry	Wet Stick.	Plast.	Texture	Clay Films Freq.	Boundary Dist.	Outline	$CaCO_3$ Efferv.	Stage	Notes
		Moist														Hassy Dep
	A		M	vf	gr	0 50	lo			S SiCL	vf	abrupt	smooth	ne	I +	pM = 8
	Bt		Sg	f	pl	<10 65	so	so	po	LS SiL	f1	sharp	wavy	ve	II	TM = 3
to	Bk	Dry	1	m	pr	10 75	sh	ss	ps	SL Si	c2	clear	lobate	e	III	
	C		2	c	cpr	15 >75	h	s	p	SCL SiC	m3	gradual	irregular	es	IV no	
0.4	E	4/3	3	vc	abk	25	vh	vs	vp	S C	c4	diffuse	tongued	ev	V	
					sbk	35	eh			CL SC					VI	

Depth (in)	Horiz.	Color	Structure Grade	Size	Form	% Gravel	Consistence Dry	Wet Stick.	Plast.	Texture	Clay Films Freq.	Boundary Dist.	Outline	$CaCO_3$ Efferv.	Stage	Notes
		Moist														JWT Dep
	A		M	vf	gr	0 50	lo			S SiCL	vf	abrupt	smooth	ne	I +	pM = 20
	Bt		Sg	f	pl	<10 65	so	so	po	LS SiL	f1	sharp	wavy	ve	II	
to	Bk	Dry	1	m	pr	10 75	sh	ss	ps	SL Si	c2	clear	lobate	e	III	TM = too coarse
	C		2	c	cpr	15 >75	h	s	p	SCL SiC	m3	gradual	irregular	es	IV no	
Bt.	E	5/3	3	vc	abk	25	vh	vs	vp	S C	c4	diffuse	tongued	ev	V	
					sbk	35	eh			CL SC					VI	

Depth (in)	Horiz.	Color	Structure Grade	Size	Form	% Gravel	Consistence Dry	Wet Stick.	Plast.	Texture	Clay Films Freq.	Boundary Dist.	Outline	$CaCO_3$ Efferv.	Stage	Notes
		Moist														
	A		M	vf	gr	0 50	lo			S SiCL	vf	abrupt	smooth	ne	I +	
	Bt		Sg	f	pl	<10 65	so	so	po	LS SiL	f1	sharp	wavy	ve	II	
to	Bk	Dry	1	m	pr	10 75	sh	ss	ps	SL Si	c2	clear	lobate	e	III	
	C		2	c	cpr	15 >75	h	s	p	SCL SiC	m3	gradual	irregular	es	IV	
	E		3	vc	abk	25	vh	vs	vp	S C	c4	diffuse	tongued	ev	V	
					sbk	35	eh			CL SC					VI	

Depth (in)	Horiz.	Color	Structure Grade	Size	Form	% Gravel	Consistence Dry	Wet Stick.	Plast.	Texture	Clay Films Freq.	Boundary Dist.	Outline	$CaCO_3$ Efferv.	Stage	Notes
		Moist														
	A		M	vf	gr	0 50	lo			S SiCL	vf	abrupt	smooth	ne	I +	
	Bt		Sg	f	pl	<10 65	so	so	po	LS SiL	f1	sharp	wavy	ve	II	
to	Bk	Dry	1	m	pr	10 75	sh	ss	ps	SL Si	c2	clear	lobate	e	III	
	C		2	c	cpr	15 >75	h	s	p	SCL SiC	m3	gradual	irregular	es	IV	
	E		3	vc	abk	25	vh	vs	vp	S C	c4	diffuse	tongued	ev	V	
					sbk	35	eh			CL SC					VI	

Photographs

Photo #	Description
	Pre-excavation
	Spoil material
	Pit profile
	Vegetation
	General geomorphic surface

Photo #	Description

Project LHWCMP Date 3/16/05 Pit ID 22 GPS _____ Field Crew JF, MK, CH

Time _____

Vegetation Descr. _____

Gemorph. Surface Gyl Descr. by CH

Slope _____ Parent Mat. _____

Pavement ☐ Archeological ☐

Varnish ☐ Moisture cond. dry☐ moist☑ wet☐

Depth (in)	Horiz.	Color	Structure			% Gravel	Consistence			Texture	Clay Films	Boundary		$CaCO_3$		Notes
		Moist	Grade	Size	Form		Dry	Wet			Freq.	Dist.	Outline	Efferv.	Stage	
6.7	A	7.5yr	M	vf	gr	0 50	lo	Stick.	Plast.	S SiCL	vf	abrupt	smooth	ne	I +	Penet.
	Bt	5/2	Sg	f	pl	<10 65	so	so	po	LS SiL	f1	sharp	wavy	ve	II	0
to	Bk	Dry Wet	1	m	pr	10 75	sh	ss	ps	SL Si	c2	clear	lobate	e	III	Shear
	C		2	c	cpr	15 >75	h	s	p	SCL SiC	m3	gradual	irregular	es	IV	
6.3	E	4/3	3	vc	abk	25	vh	vs	vp	S C	c4	diffuse	tongued	ev	V	7
					sbk	35	eh			CL SC	NA				VI	

Depth (in)	Horiz.	Color	Structure			% Gravel	Consistence			Texture	Clay Films	Boundary		$CaCO_3$		Notes
		Moist Wet	Grade	Size	Form		Dry	Wet			Freq.	Dist.	Outline	Efferv.	Stage	
6.3	A	3/4	M	vf	gr	0 50	lo	Stick.	Plast.	S SiCL	vf	abrupt	smooth	ne	I +	Penet.
	Bt		Sg	f	pl	<10 65	so	so	po	LS SiL	f1	sharp	wavy	ve	II	3
to	Bk	Dry Moist	1	m	pr	10 75	sh	ss	ps	SL Si	c2	clear	lobate	e	III	Shear
	C	7.5yr	2	c	cpr	15 >75	h	s	p	SCL SiC	m3	gradual	irregular	es	IV	
4.9	E	4/3	3	vc	abk	25	vh	vs	vp	S C	c4	diffuse	tongued	ev	V	4
					sbk	35	eh			CL SC					VI	

Depth (in)	Horiz.	Color	Structure			% Gravel	Consistence			Texture	Clay Films	Boundary		$CaCO_3$		Notes
		Moist	Grade	Size	Form		Dry	Wet			Freq.	Dist.	Outline	Efferv.	Stage	
4.9	A	7.5yr	M	vf	gr	0 50	lo	Stick.	Plast.	S SiCL	vf	abrupt	smooth	ne	I +	Penet.
	Bt	4/3	Sg	f	pl	<10 65	so	so	po	LS SiL	f1	sharp	wavy	ve	II	0
to	Bk	Dry Wet	1	m	pr	10 75	sh	ss	ps	SL Si	c2	clear	lobate	e	III	Shear
	C		2	c	cpr	15 >75	h	s	p	SCL SiC	m3	gradual	irregular	es	IV	
4.5	E	4/4	3	vc	abk	25	vh	vs	vp	S C	c4	diffuse	tongued	ev	V	5
					sbk	35	eh			CL SC	NA				VI	

Depth (in)	Horiz.	Color	Structure			% Gravel	Consistence			Texture	Clay Films	Boundary		$CaCO_3$		Notes
		Moist	Grade	Size	Form		Dry	Wet			Freq.	Dist.	Outline	Efferv.	Stage	
4.5	A	Wet	M	vf	gr	0 50	lo	Stick.	Plast.	S SiCL	vf	abrupt	smooth	ne	I +	Penet.
	Bt	4/3	Sg	f	pl	<10 65	so	so	po	LS SiL	f1	sharp	wavy	ve	II	20
to	Bk	Dry	1	m	pr	10 75	sh	ss	ps	SL Si	c2	clear	lobate	e	III	
	C	7.5yr	2	c	cpr	15 >75	h	s	p	SCL SiC	m3	gradual	irregular	es	IV	Shear
4.2	E	4/3	3	vc	abk	25	vh	vs	vp	S C	c4	diffuse	tongued	ev	V	4
					sbk	35	eh			CL SC	NA				VI	

Depth (in)	Horiz.	Color	Structure			% Gravel	Consistence			Texture	Clay Films	Boundary		$CaCO_3$		Notes
		Moist	Grade	Size	Form		Dry	Wet			Freq.	Dist.	Outline	Efferv.	Stage	
4.2	A	Wet	M	vf	gr	0 50	lo	Stick.	Plast.	S SiCL	vf	abrupt	smooth	ne	I +	Penet.
	Bt	3/4	Sg	f	pl	<10 65	so	so	po	LS SiL	f1	sharp	wavy	ve	II	1
to	Bk	Dry	1	m	pr	10 75	sh	ss	ps	SL Si	c2	clear	lobate	e	III	
	C	7.5yr	2	c	cpr	15 >75	h	s	p	SCL SiC	m3	gradual	irregular	es	IV	Shear
3.5	E	4/3	3	vc	abk	25	vh	vs	vp	S C	c4	diffuse	tongued	ev	V	4
					sbk	35	eh			CL SC	NA				VI	

Photographs

Photo #	Description
60	Pre-excavation
42	Spoil material
41	Pit profile
43	Vegetation
43	General geomorphic surface

Photo #	Description

Project _____ Date _____ Pit ID 22 GPS _____ Field Crew _____

Time _____

Vegetation Descr. _____

Gemorph. Surface _____ Descr. by _____

Slope _____ Parent Mat. _____

Pavement ☐ Archeological ☐

Varnish ☐ Moisture cond. dry☐ moist☐ wet☐

Depth (in)	Horiz.	Color	Structure			% Gravel	Consistence			Texture	Clay Films	Boundary		$CaCO_3$		Notes
		~~Moist~~ Wet	Grade	Size	Form		Dry	Wet			Freq.	Dist.	Outline	Efferv.	Stage	Penet.
3.5	A	4/3	M	vf	gr	0 50	lo	Stick.	Plast.	S SiCL	vf	abrupt	smooth	~~ne~~	I +	9
	Bt		Sg	f	pl	<10 65	so	so	po	LS SiL	f1	sharp	wavy	ve	II	
to	Bk	Dry	1	m	pr	10 75	sh	ss	ps	SL Si	c2	clear	lobate	e	III	
	C	7.5yr	2	c	cpr	15 >75	h	s	p	SCL SiC	m3	gradual	irregular	es	IV	Shear
2.7	E	5/3	3	vc	abk	25	vh	vs	vp	S C	c4	diffuse	tongued	ev	V	2
					sbk	35	eh			CL SC	N/A				VI	

Depth (in)	Horiz.	Color	Structure			% Gravel	Consistence			Texture	Clay Films	Boundary		$CaCO_3$		Notes
		~~Moist~~ Wet	Grade	Size	Form		Dry	Wet			Freq.	Dist.	Outline	Efferv.	Stage	Penet.
2.7	A	4/3	M	vf	gr	0 50	lo	Stick.	Plast.	S SiCL	vf	abrupt	smooth	ne	I +	8
	Bt		Sg	f	pl	<10 65	so	so	po	LS SiL	f1	sharp	wavy	ve	II	
to	Bk	Dry	1	m	pr	10 75	sh	ss	ps	SL Si	c2	clear	lobate	e	III	Shear
	C	7.5yr	2	c	cpr	15 >75	h	s	p	SCL SiC	m3	gradual	irregular	es	IV	4
1.7	E	4/3	3	vc	abk	25	vh	vs	vp	S C	c4	diffuse	tongued	ev	V	
					sbk	35	eh			CL SC	N/A				VI	

Depth (in)	Horiz.	Color	Structure			% Gravel	Consistence			Texture	Clay Films	Boundary		$CaCO_3$		Notes
		~~Moist~~ Wet	Grade	Size	Form		Dry	Wet			Freq.	Dist.	Outline	Efferv.	Stage	Penet.
1.7	A	4/3	M	vf	gr	0 50	lo	Stick.	Plast.	S SiCL	vf	abrupt	smooth	ne	I +	10
	Bt		Sg	f	pl	<10 65	so	so	po	LS SiL	f1	sharp	wavy	ve	II	
to	Bk	Dry 7.5yr	1	m	pr	10 75	sh	ss	ps	SL Si	c2	clear	lobate	e	III	Shear
	C	5/3	2	c	cpr	15 >75	h	s	p	SCL SiC	m3	gradual	irregular	es	IV	3
0.8	E		3	vc	abk	25	vh	vs	vp	S C	c4	diffuse	tongued	ev	V	
					sbk	35	eh			CL SC					VI	

Depth (in)	Horiz.	Color	Structure			% Gravel	Consistence			Texture	Clay Films	Boundary		$CaCO_3$		Notes
		~~Moist~~ Wet	Grade	Size	Form		Dry	Wet			Freq.	Dist.	Outline	Efferv.	Stage	Penet.
2.5	A	4/2	M	vf	gr	0 50	lo	Stick.	Plast.	S SiCL	vf	abrupt	smooth	ne	I +	20
	Bt		Sg	f	pl	<10 65	so	so	po	LS SiL	f1	sharp	wavy	ve	II	
to	Bk	Dry 7.5yr	1	m	pr	10 75	sh	ss	ps	SL Si	c2	clear	lobate	e	III	Shear
	C		2	c	cpr	15 >75	h	s	p	SCL SiC	m3	gradual	irregular	es	IV	3
0	E	4/3	3	vc	abk	25 20	vh	vs	vp	S C	c4	diffuse	tongued	ev	V	
					sbk	35	eh			CL SC	N/A				VI	

Depth (in)	Horiz.	Color	Structure			% Gravel	Consistence			Texture	Clay Films	Boundary		$CaCO_3$		Notes
		Moist	Grade	Size	Form		Dry	Wet			Freq.	Dist.	Outline	Efferv.	Stage	
	A		M	vf	gr	0 50	lo	Stick.	Plast.	S SiCL	vf	abrupt	smooth	ne	I +	
	Bt		Sg	f	pl	<10 65	so	so	po	LS SiL	f1	sharp	wavy	ve	II	
to	Bk	Dry	1	m	pr	10 75	sh	ss	ps	SL Si	c2	clear	lobate	e	III	
	C		2	c	cpr	15 >75	h	s	p	SCL SiC	m3	gradual	irregular	es	IV	
	E		3	vc	abk	25	vh	vs	vp	S C	c4	diffuse	tongued	ev	V	
					sbk	35	eh			CL SC					VI	

Photographs

Photo #	Description
	Pre-excavation
	Spoil material
	Pit profile
	Vegetation
	General geomorphic surface

Photo #	Description

Project: HWOMP Date 3/16/05 Pit ID 24 GPS _____ Field Crew JF, MK, CH

Time _____

Vegetation Descr. _____

Gemorph. Surface Qy2 Descr. by JF

Slope _____ Parent Mat. _____

Pavement ☐ Archeological ☐

Varnish ☐ Moisture cond. dry☑ moist☐ wet☐

Depth (in)	Horiz.	Color	Structure: Grade	Size	Form	% Gravel	Consistence: Dry	Wet: Stick.	Plast.	Texture	Clay Films	Boundary: Dist.	Outline	$CaCO_3$: Efferv.	Stage	Notes
6.9	A	~~Moist~~ Wet 4/3	~~1~~	vf	gr	0 50	lo	Stick.	Plast.	L	Freq.	Dist.	Outline	ne	I +	Silt cap, platy structure. 1mm organic crust.
	Bt		Sg	f	pl	<10 65	so	so	po	S SiCL	vf	abrupt	smooth	ve	II	
to	Bk	Dry	1	m	pr	10 75	sh	ss	ps	LS SiL	f1	sharp	wavy	e	III	Penet. Shear
	C	7.5yr	2	c	cpr	15 >75	h	s	p	SL Si	c2	clear	lobate	es	IV	
6.85	E	6/3	3	vc	abk	25	vh	vs	vp	SCL SiC	m3	gradual	irregular	ev	V	2
					sbk	35	eh			S C	c4	diffuse	tongued		VI	
										CL SC	NA					

Depth (in)	Horiz.	Color	Structure: Grade	Size	Form	% Gravel	Consistence: Dry	Wet: Stick.	Plast.	Texture	Clay Films	Boundary: Dist.	Outline	$CaCO_3$: Efferv.	Stage	Notes
6.85	A	~~Moist~~ Wet 4/3	M	vf	gr	0 50	lo	Stick.	Plast.	~~S~~	Freq.	Dist.	Outline	ne	I +	Bioturbated, rooting layer.
	Bt		Sg	f	pl	<10 65	so	so	po	S SiCL	vf	abrupt	smooth	ve	II	
to	Bk	Dry	1	m	pr	10 75	sh	ss	~~ps~~	LS SiL	f1	sharp	wavy	e	III	Penet. Shear
	C	7.5yr	2	c	cpr	15 >75	h	s	p	SL Si	c2	clear	lobate	es	IV	
6.0	E	5/4	3	vc	abk	25	vh	vs	vp	SCL SiC	m3	gradual	irregular	ev	V	4 4
					sbk	35	eh			S C	c4	diffuse	tongued		VI	
										CL SC	NA					

Depth (in)	Horiz.	Color	Structure: Grade	Size	Form	% Gravel	Consistence: Dry	Wet: Stick.	Plast.	Texture	Clay Films	Boundary: Dist.	Outline	$CaCO_3$: Efferv.	Stage	Notes
6.0	A	~~Moist~~ Wet 4/3	M	vf	gr	0 50	lo	Stick.	Plast.	S	Freq.	Dist.	Outline	ne	I +	
	Bt		Sg	f	pl	<10 65	so	so	po	S SiCL	vf	abrupt	smooth	ve	II	
to	Bk	Dry	1	m	pr	10 75	sh	ss	ps	LS SiL	f1	sharp	wavy	e	III	Penet. Shear
	C	7.5yr	2	c	cpr	15 >75	h	s	p	SL Si	c2	clear	lobate	es	IV	
5.7	E	6/4	3	vc	abk	25	vh	vs	vp	SCL SiC	m3	gradual	irregular	ev	V	7 3
					sbk	35	eh			S C	c4	diffuse	tongued		VI	
										CL SC	NA					

Depth (in)	Horiz.	Color	Structure: Grade	Size	Form	% Gravel	Consistence: Dry	Wet: Stick.	Plast.	Texture	Clay Films	Boundary: Dist.	Outline	$CaCO_3$: Efferv.	Stage	Notes
5.7	A	~~Moist~~ Wet 4/3	M	vf	gr	0 50	lo	Stick.	Plast.	S	Freq.	Dist.	Outline	ne	I +	Penet.
	Bt		Sg	f	pl	<10 65	so	so	po	S SiCL	vf	abrupt	smooth	ve	II	~~2~~ 1
to	Bk	Dry	1	m	pr	10 75	sh	ss	ps	LS SiL	f1	sharp	wavy	e	III	Shear
	C	7.5yr	2	c	cpr	15 >75	h	s	p	SL Si	c2	clear	lobate	es	IV	~~1~~ 2
4.4	E	5/4	3	vc	abk	25	vh	vs	vp	SCL SiC	m3	gradual	irregular	ev	V	
					sbk	35	eh			S C	c4	diffuse	tongued		VI	
										CL SC	NA					

Depth (in)	Horiz.	Color	Structure: Grade	Size	Form	% Gravel	Consistence: Dry	Wet: Stick.	Plast.	Texture	Clay Films	Boundary: Dist.	Outline	$CaCO_3$: Efferv.	Stage	Notes
4.4	A	~~Moist~~ Wet 5/3	M	vf	gr	0 50	lo	Stick.	Plast.	S	Freq.	Dist.	Outline	ne	I +	Penet.
	Bt		Sg	f	pl	<10 65	so	so	po	S SiCL	vf	abrupt	smooth	ve	II	5
to	Bk	Dry	1	m	pr	10 75	sh	ss	ps	LS SiL	f1	sharp	wavy	e	III	Shear
	C	7.5yr	2	c	cpr	15 >75	h	s	p	SL Si	c2	clear	lobate	es	IV	2
2.9	E	6/3	3	vc	abk	25	vh	vs	vp	SCL SiC	m3	gradual	irregular	ev	V	
					sbk	35	eh			S C	c4	diffuse	tongued		VI	
										CL SC	NA					

Photographs

Photo #	Description
	Pre-excavation
45	Spoil material
46	Pit profile
48	Vegetation
47, 48	General geomorphic surface

Photo #	Description

Project _____ Date _____ Pit ID 24 GPS _____ Field Crew _____

Time _____

Vegetation Descr. _____

Gemorph. Surface _____ Descr. by _____

Slope _____ Parent Mat. _____

Pavement ❑ Archeological ❑

Varnish ❑ Moisture cond. dry❑ moist❑ wet❑

Depth (in)	Horiz.	Color	Structure			% Gravel	Consistence			Texture	Clay Films	Boundary		$CaCO_3$		Notes
		~~Moist~~	Grade	~~Size~~	~~Form~~		Dry	Wet			Freq.	Dist.	Outline	Efferv.	Stage	
2.9	A	Wet	M	vf	gr	0 50	lo	Stick.	Plast.	S SiCL	vf	abrupt	smooth	ne	I +	Perch
	Bt	4/3	Sg	f	pl	<10 65	so	so	po	LS SiL	f1	sharp	wavy	ve	II	6
to	Bk	Dry	1	m	pr	10 75	sh	ss	ps	SL Si	c2	clear	lobate	e	III	
	C	7.5yr	2	c	cpr	15 >75	h	s	p	SCL SiC	m3	gradual	irregular	es	IV	Shear
1.7	E	5/3	3	vc	abk	25	vh	vs	vp	S C	c4	diffuse	tongued	ev	V	0
					sbk	35	eh			CL SC	NA				VI	

Depth (in)	Horiz.	Color	Structure			% Gravel	Consistence			Texture	Clay Films	Boundary		$CaCO_3$		Notes
		~~Moist~~	Grade	Size	Form		Dry	Wet			Freq.	~~Dist.~~	~~Outline~~	Efferv.	Stage	
1.7	A	5/3 Wet	M	vf	gr	0 50	lo	Stick.	Plast.	S SiCL	vf	abrupt	smooth	ne	I +	Perch.
	Bt		Sg	f	pl	<10 65	so	so	po	LS SiL	f1	sharp	wavy	ve	II	15
to	Bk	Dry	1	m	pr	10 75	sh	ss	ps	SL Si	c2	clear	lobate	e	III	
	C	7.5yr	2	c	cpr	15 >75	h	s	p	SCL SiC	m3	gradual	irregular	es	IV	Shear
0	E	5/3	3	vc	abk	25	vh	vs	vp	S C	c4	diffuse	tongued	ev	V	1
					sbk	35	eh			CL SC	NA				VI	

Depth (in)	Horiz.	Color	Structure			% Gravel	Consistence			Texture	Clay Films	Boundary		$CaCO_3$		Notes
		Moist	Grade	Size	Form		Dry	Wet			Freq.	Dist.	Outline	Efferv.	Stage	
	A		M	vf	gr	0 50	lo	Stick.	Plast.	S SiCL	vf	abrupt	smooth	ne	I +	
	Bt		Sg	f	pl	<10 65	so	so	po	LS SiL	f1	sharp	wavy	ve	II	
to	Bk	Dry	1	m	pr	10 75	sh	ss	ps	SL Si	c2	clear	lobate	e	III	
	C		2	c	cpr	15 >75	h	s	p	SCL SiC	m3	gradual	irregular	es	IV	
	E		3	vc	abk	25	vh	vs	vp	S C	c4	diffuse	tongued	ev	V	
					sbk	35	eh			CL SC					VI	

Depth (in)	Horiz.	Color	Structure			% Gravel	Consistence			Texture	Clay Films	Boundary		$CaCO_3$		Notes
		Moist	Grade	Size	Form		Dry	Wet			Freq.	Dist.	Outline	Efferv.	Stage	
	A		M	vf	gr	0 50	lo	Stick.	Plast.	S SiCL	vf	abrupt	smooth	ne	I +	
	Bt		Sg	f	pl	<10 65	so	so	po	LS SiL	f1	sharp	wavy	ve	II	
to	Bk	Dry	1	m	pr	10 75	sh	ss	ps	SL Si	c2	clear	lobate	e	III	
	C		2	c	cpr	15 >75	h	s	p	SCL SiC	m3	gradual	irregular	es	IV	
	E		3	vc	abk	25	vh	vs	vp	S C	c4	diffuse	tongued	ev	V	
					sbk	35	eh			CL SC					VI	

Depth (in)	Horiz.	Color	Structure			% Gravel	Consistence			Texture	Clay Films	Boundary		$CaCO_3$		Notes
		Moist	Grade	Size	Form		Dry	Wet			Freq.	Dist.	Outline	Efferv.	Stage	
	A		M	vf	gr	0 50	lo	Stick.	Plast.	S SiCL	vf	abrupt	smooth	ne	I +	
	Bt		Sg	f	pl	<10 65	so	so	po	LS SiL	f1	sharp	wavy	ve	II	
to	Bk	Dry	1	m	pr	10 75	sh	ss	ps	SL Si	c2	clear	lobate	e	III	
	C		2	c	cpr	15 >75	h	s	p	SCL SiC	m3	gradual	irregular	es	IV	
	E		3	vc	abk	25	vh	vs	vp	S C	c4	diffuse	tongued	ev	V	
					sbk	35	eh			CL SC					VI	

Photographs

Photo #	Description
	Pre-excavation
	Spoil material
	Pit profile
	Vegetation
	General geomorphic surface

Photo #	Description

Project LHwmp Date 3·16 Pit ID 26 GPS _____ Field Crew JF, CH, KAG, MD

Time 1pm

Vegetation Descr. grass & brush

Gemorph. Surface abandoned farm field floodplain? Descr. by MK

Slope flat Parent Mat. Alluvium

Pavement ☐ Archeological ☐

Varnish ☐ Moisture cond. dry☐ moist☐ wet☐

No SKETCH - very uniform, massive (chl not here in record) <5k

Depth (in)	Horiz.	Color	Structure			% Gravel	Consistence			Texture	Clay Films	Boundary		$CaCO_3$		Notes
		Moist	Grade	Size	Form		Dry	Wet			Freq.	Dist.	Outline	Efferv.	Stage	
6.1	A	5/4	M	vf	gr	0 50	lo	Stick.	Plast.	S SiCL	vf	abrupt	smooth	ne	I +	rooting layer
	Bt		Sg	f	pl	<10 65	so	so	po	LS SiL	f1	sharp	wavy	ve	II	4.5 13
to	Bk	Dry 7.5YR	1	m	pr	10 75	sh	ss	ps	SL Si	c2	clear	lobate	e	III	
	C		2	c	cpr	15 >75	h	s	p	SCL SiC	m3	gradual	irregular	es	IV	
	E	6/4	3	vc	abk	25	vh	vs	vp	S C	c4	diffuse	tongued	ev	V	
5.8					sbk	35	eh			CL SC					VI	

Depth (in)	Horiz.	Color	Structure			% Gravel	Consistence			Texture	Clay Films	Boundary		$CaCO_3$		Notes
		Moist	Grade	Size	Form		Dry	Wet			Freq.	Dist.	Outline	Efferv.	Stage	
5.8	A	5/4	M	vf	gr	0 50	lo	Stick.	Plast.	S SiCL	vf	abrupt	smooth	ne	I +	
	Bt		Sg	f	pl	<10 65	so	so	po	LS SiL	f1	sharp	wavy	ve	II	5
to	Bk	~~Dry~~ Moist 7.5YR	1	m	pr	10 75	sh	ss	ps	SL Si	c2	clear	lobate	e	III	20
	C		2	c	cpr	15 >75	h	s	p	SCL SiC	m3	gradual	irregular	es	IV	
	E	5/4	3	vc	abk	25	vh	vs	vp	S C	c4	diffuse	tongued	ev	V	
0					sbk	35	eh			CL SC					VI	

Depth (in)	Horiz.	Color	Structure			% Gravel	Consistence			Texture	Clay Films	Boundary		$CaCO_3$		Notes
		Moist	Grade	Size	Form		Dry	Wet			Freq.	Dist.	Outline	Efferv.	Stage	
	A		M	vf	gr	0 50	lo	Stick.	Plast.	S SiCL	vf	abrupt	smooth	ne	I +	
	Bt		Sg	f	pl	<10 65	so	so	po	LS SiL	f1	sharp	wavy	ve	II	
to	Bk	Dry	1	m	pr	10 75	sh	ss	ps	SL Si	c2	clear	lobate	e	III	
	C		2	c	cpr	15 >75	h	s	p	SCL SiC	m3	gradual	irregular	es	IV	
	E		3	vc	abk	25	vh	vs	vp	S C	c4	diffuse	tongued	ev	V	
					sbk	35	eh			CL SC					VI	

Depth (in)	Horiz.	Color	Structure			% Gravel	Consistence			Texture	Clay Films	Boundary		$CaCO_3$		Notes
		Moist	Grade	Size	Form		Dry	Wet			Freq.	Dist.	Outline	Efferv.	Stage	
	A		M	vf	gr	0 50	lo	Stick.	Plast.	S SiCL	vf	abrupt	smooth	ne	I +	
	Bt		Sg	f	pl	<10 65	so	so	po	LS SiL	f1	sharp	wavy	ve	II	
to	Bk	Dry	1	m	pr	10 75	sh	ss	ps	SL Si	c2	clear	lobate	e	III	
	C		2	c	cpr	15 >75	h	s	p	SCL SiC	m3	gradual	irregular	es	IV	
	E		3	vc	abk	25	vh	vs	vp	S C	c4	diffuse	tongued	ev	V	
					sbk	35	eh			CL SC					VI	

Depth (in)	Horiz.	Color	Structure			% Gravel	Consistence			Texture	Clay Films	Boundary		$CaCO_3$		Notes
		Moist	Grade	Size	Form		Dry	Wet			Freq.	Dist.	Outline	Efferv.	Stage	
	A		M	vf	gr	0 50	lo	Stick.	Plast.	S SiCL	vf	abrupt	smooth	ne	I +	
	Bt		Sg	f	pl	<10 65	so	so	po	LS SiL	f1	sharp	wavy	ve	II	
to	Bk	Dry	1	m	pr	10 75	sh	ss	ps	SL Si	c2	clear	lobate	e	III	
	C		2	c	cpr	15 >75	h	s	p	SCL SiC	m3	gradual	irregular	es	IV	
	E		3	vc	abk	25	vh	vs	vp	S C	c4	diffuse	tongued	ev	V	
					sbk	35	eh			CL SC					VI	

Photographs

Photo #	Description
	Pre-excavation
50	Spoil material
49	Pit profile
51	Vegetation
	General geomorphic surface

Photo #	Description

APPENDIX 5.3

Results of geomorphic mapping & soils analysis

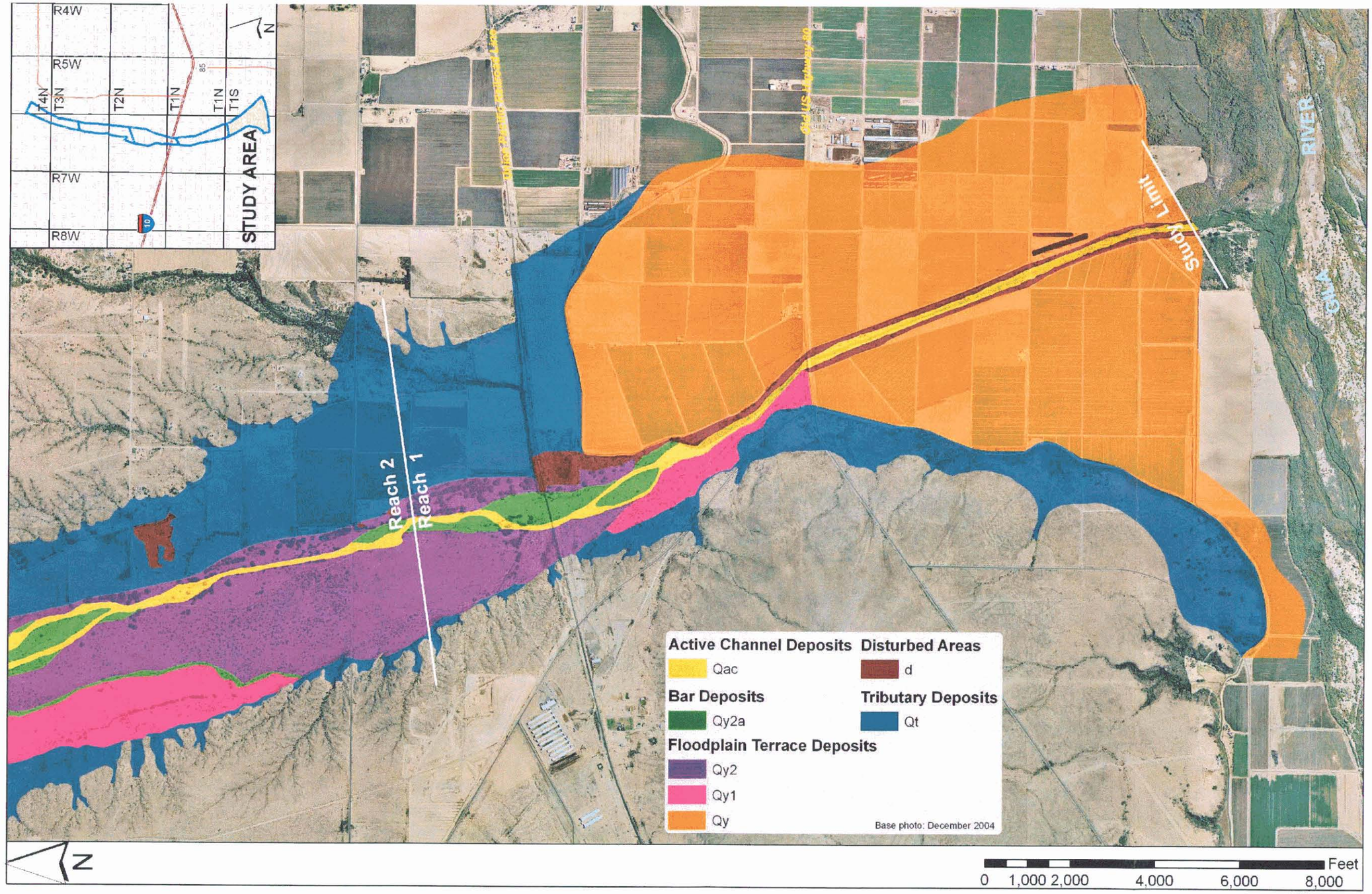

Reach 1 mapped geomorphology

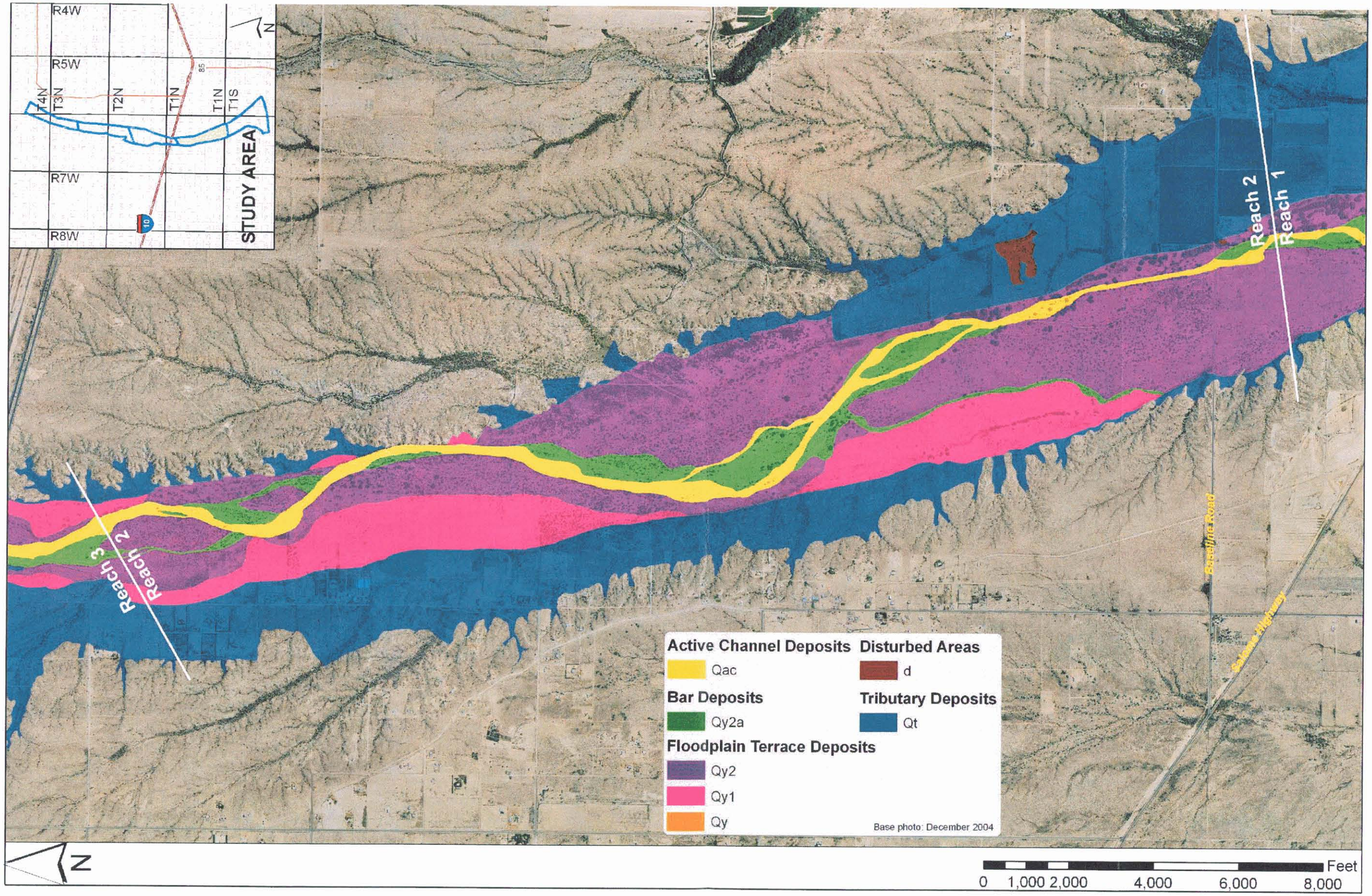

Reach 2 mapped geomorphology

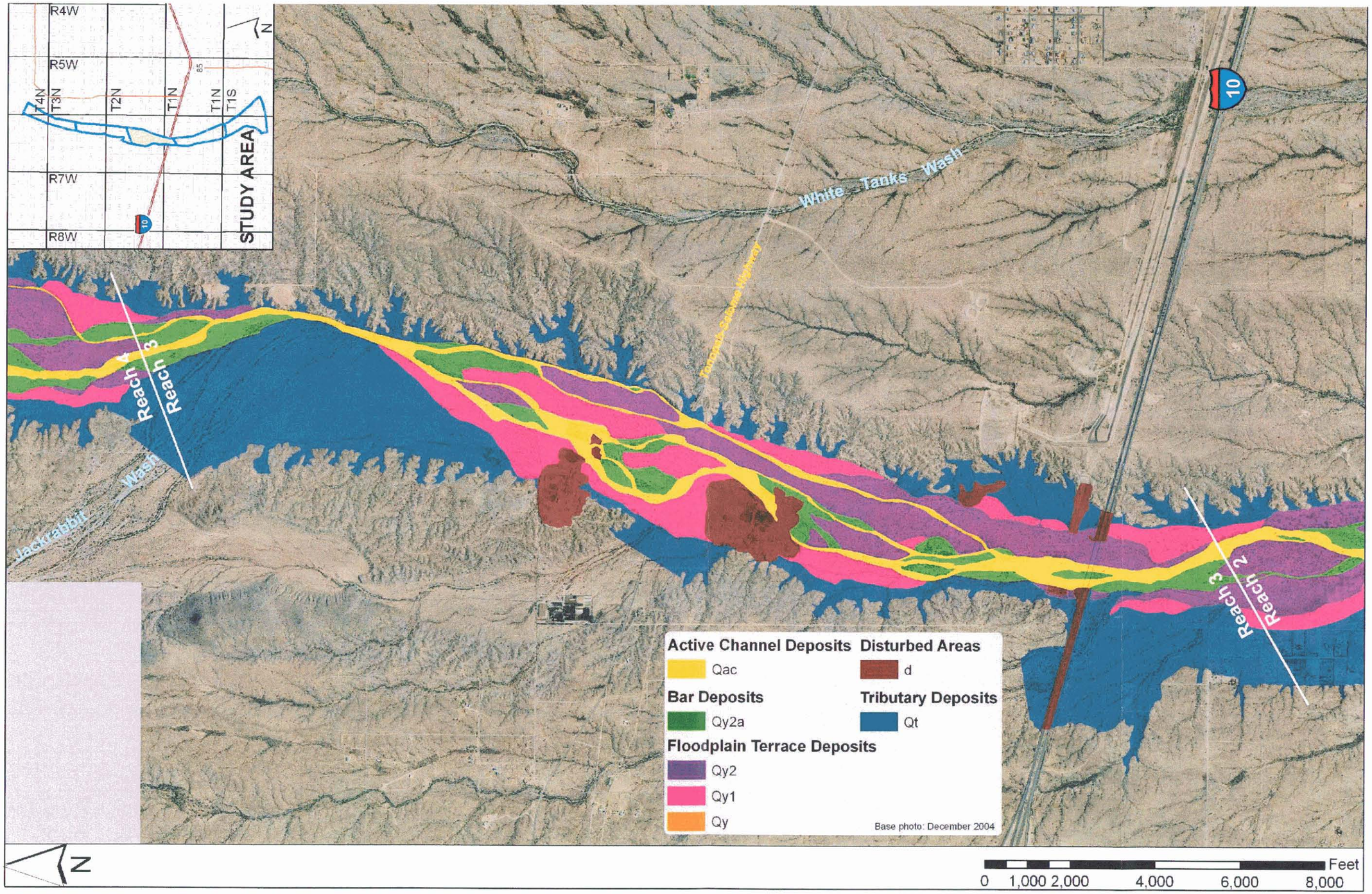

Reach 3 mapped geomorphology

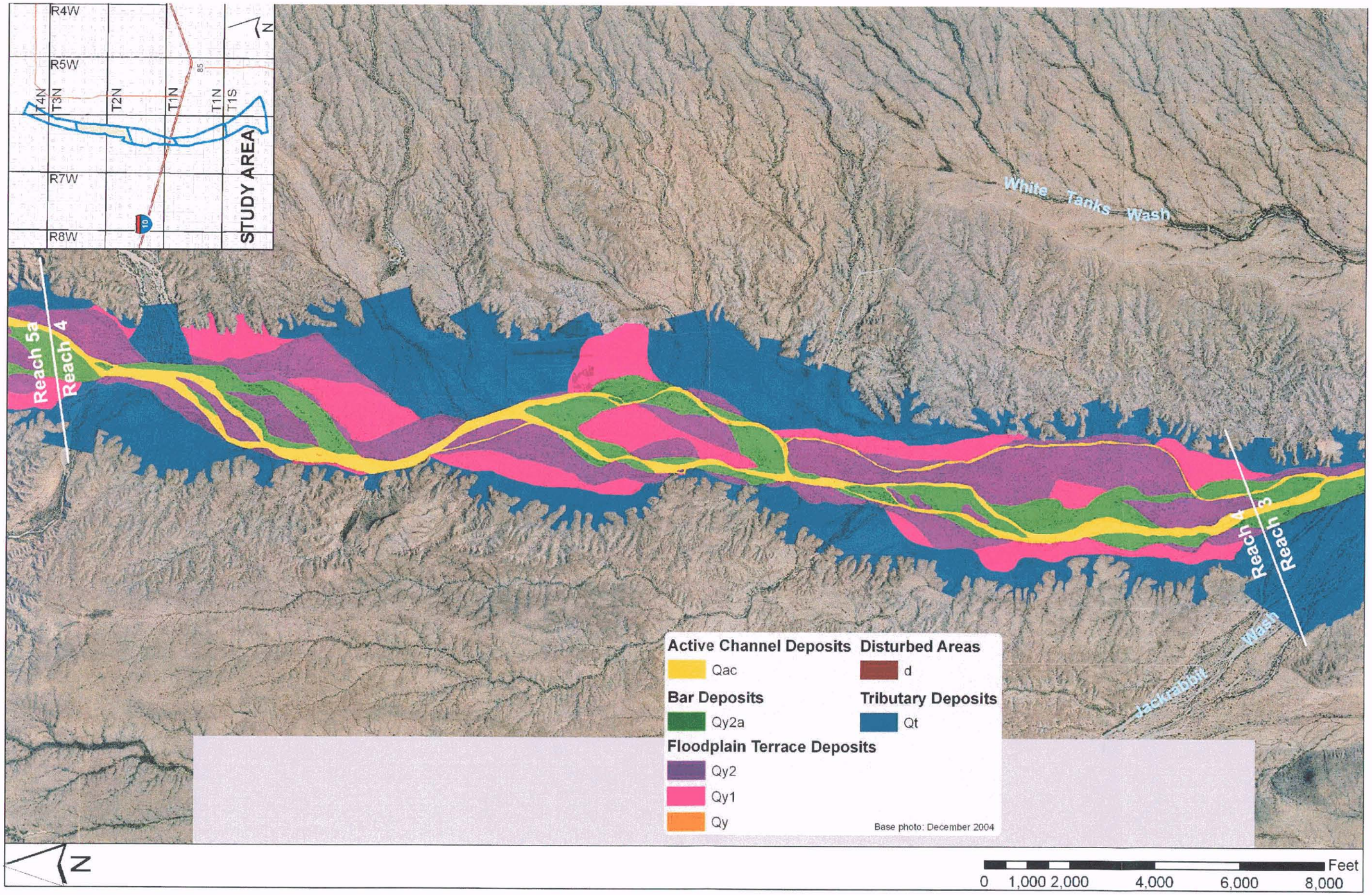

Reach 4 mapped geomorphology

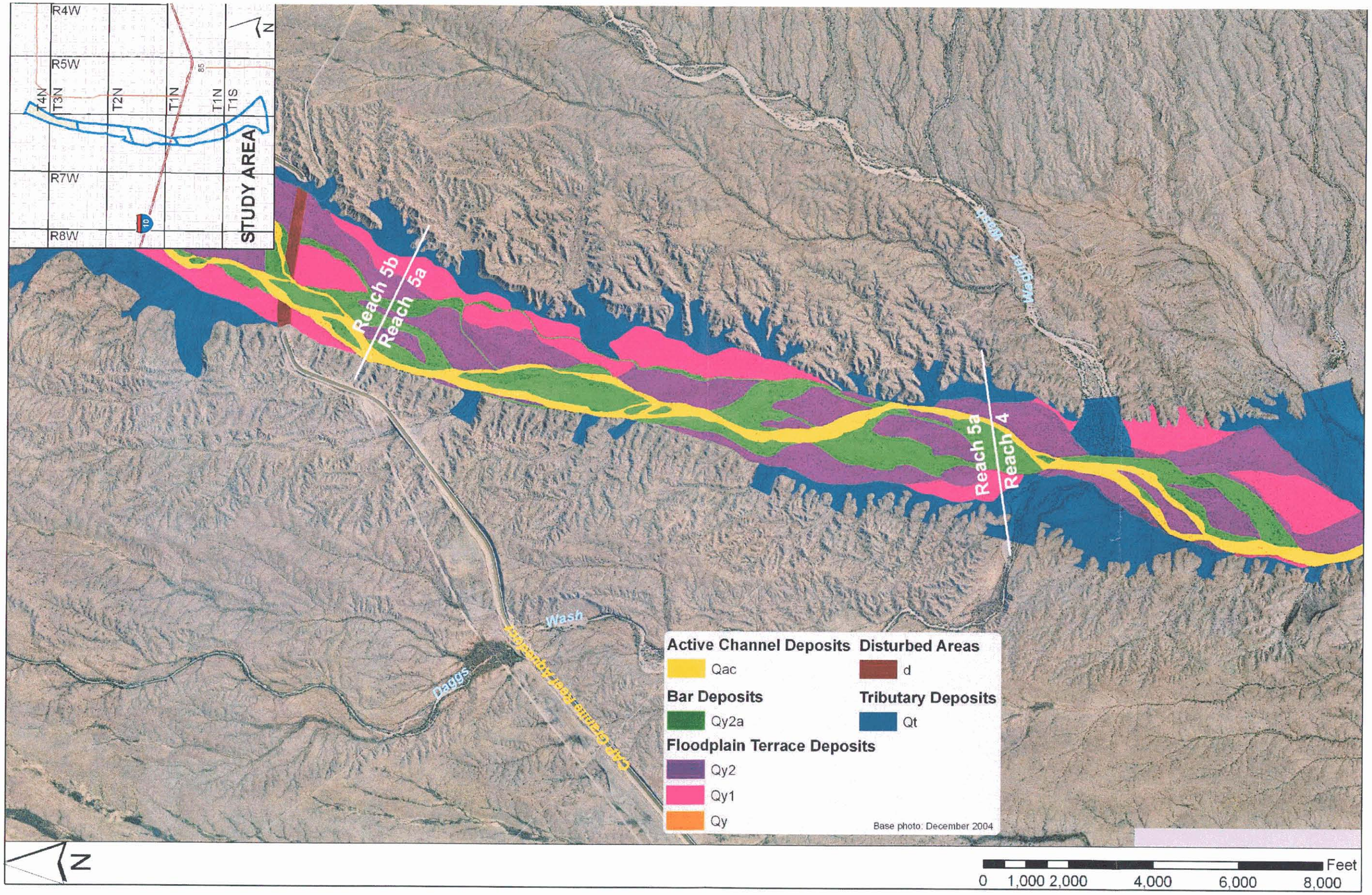

Reach 5a mapped geomorphology

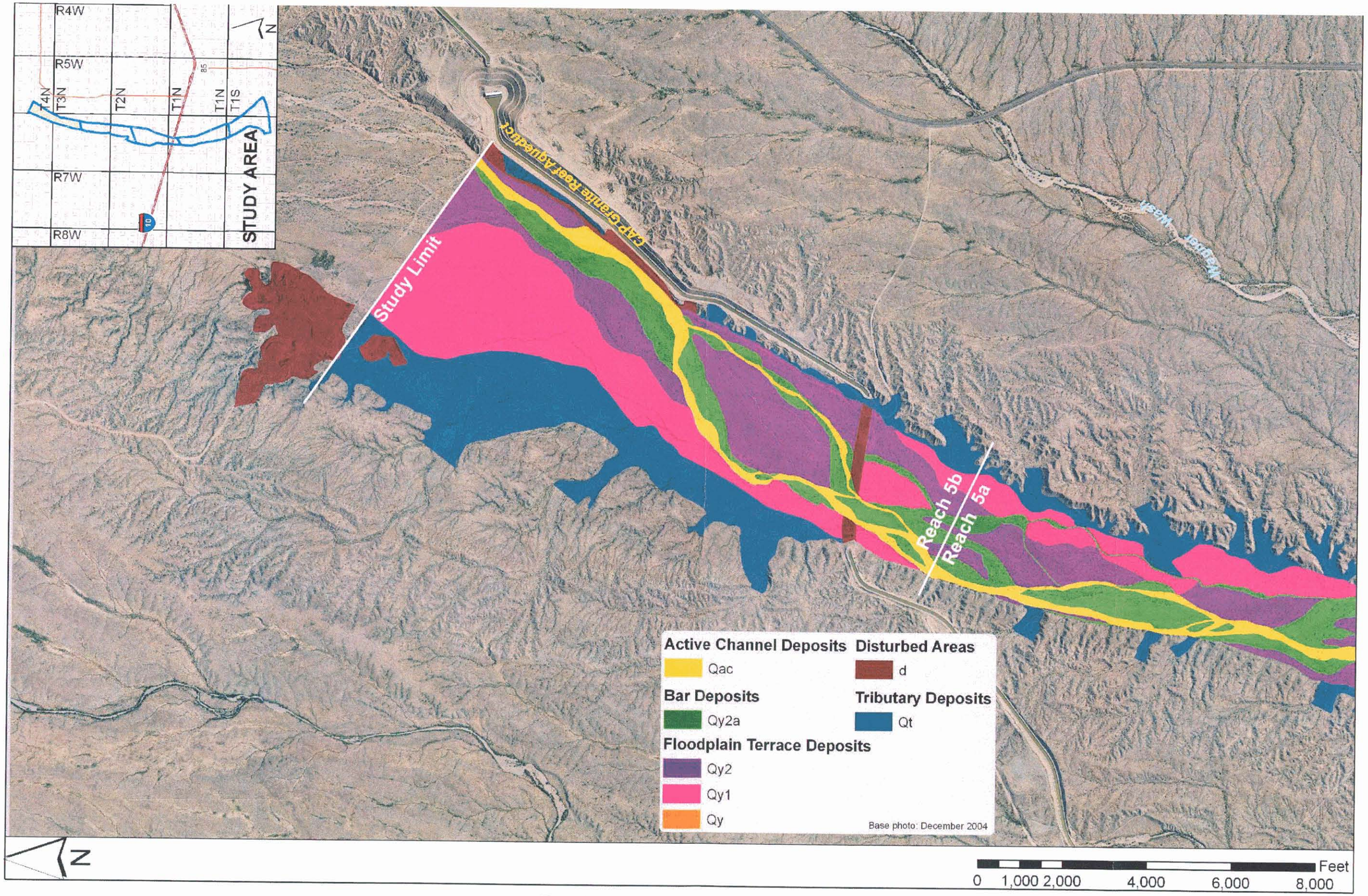

Reach 5b mapped geomorphology

APPENDIX 5.4

Sediment sample gradation data

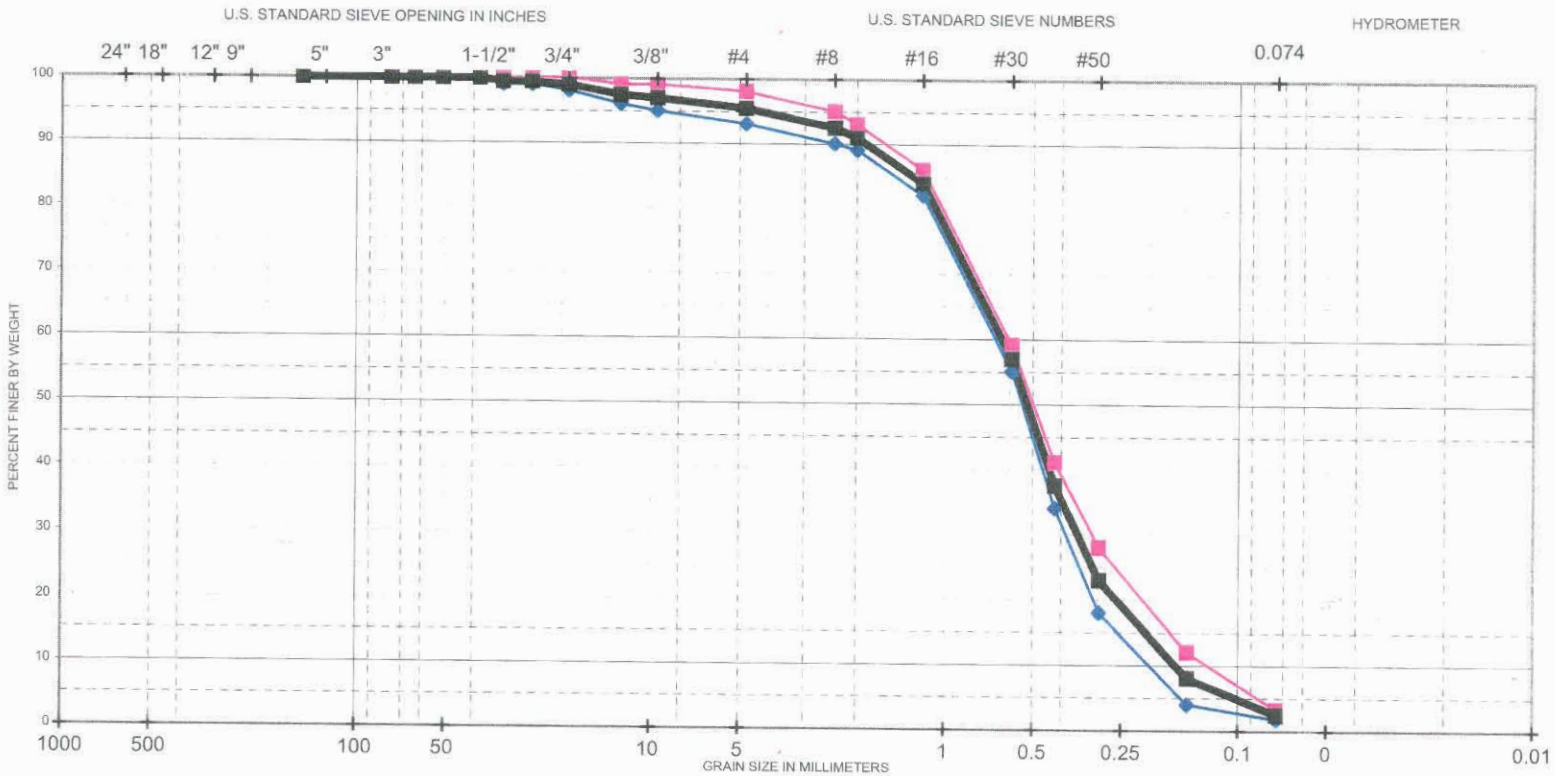

BOULDERS				GRAVEL					SAND					SILT	
MEDIUM	SMALL	LARGE	SMALL	VERY COARSE	COARSE	MEDIUM	FINE	VERY FINE	VERY COARSE	COARSE	MEDIUM	FINE	VERY FINE	COARSE	MEDIUM

31605-30 31605-31 Average + Log Scale + Sizes Labels

Lower Hassayampa - Reach 1

JE Fuller Hydrology and Geomorphology Inc.

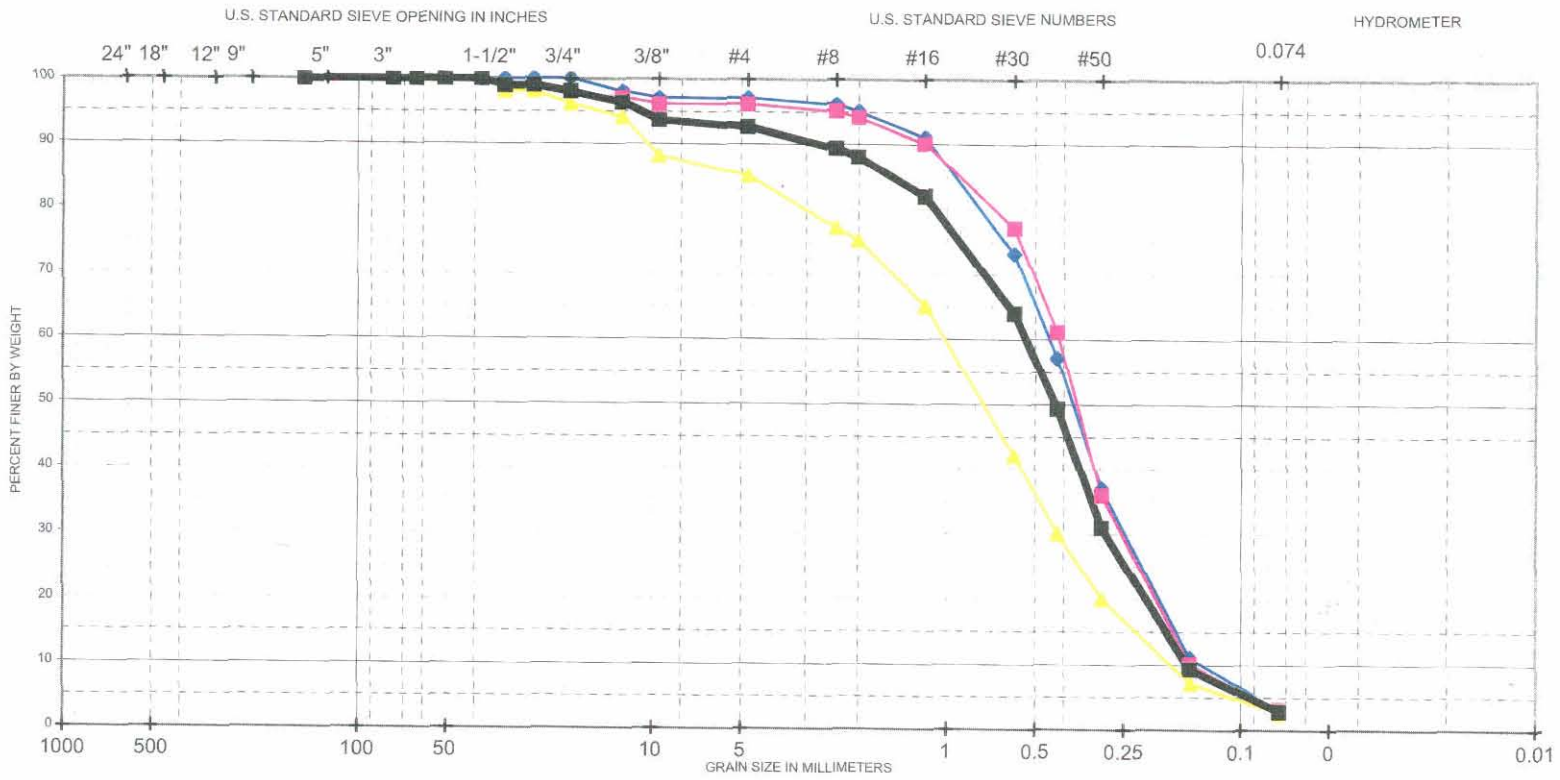

BOULDERS				GRAVEL					SAND					SILT	
MEDIUM	SMALL	LARGE	SMALL	VERY COARSE	COARSE	MEDIUM	FINE	VERY FINE	VERY COARSE	COARSE	MEDIUM	FINE	VERY FINE	COARSE	MEDIUM

31605-27 31605-105 31605-25 Average + Log Scale + Sizes Labels

Lower Hassayampa - Reach 2

JE Fuller Hydrology and Geomorphology Inc.

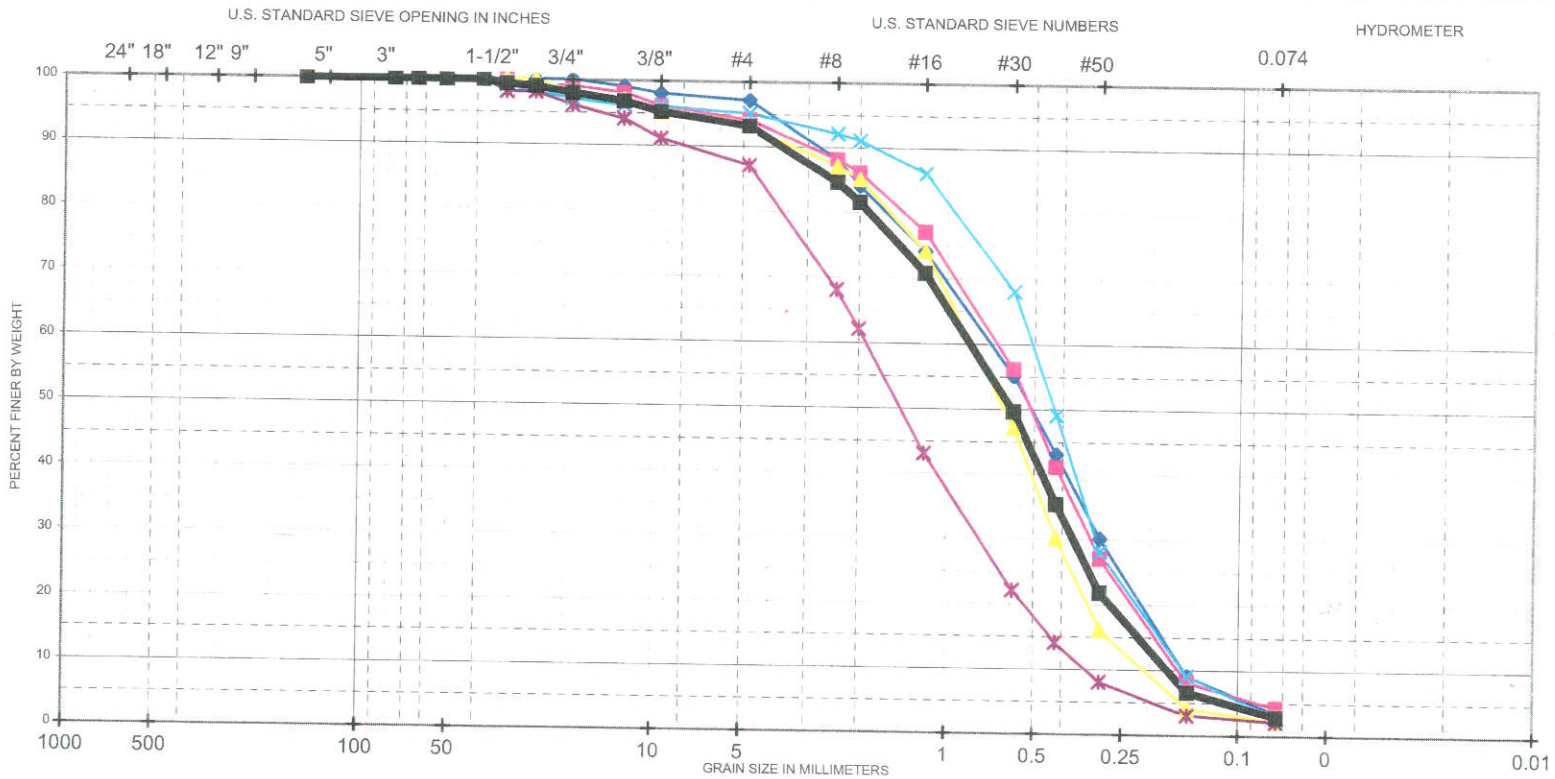

BOULDERS				GRAVEL					SAND					SILT	
MEDIUM	SMALL	LARGE	SMALL	VERY COARSE	COARSE	MEDIUM	FINE	VERY FINE	VERY COARSE	COARSE	MEDIUM	FINE	VERY FINE	COARSE	MEDIUM

31605-23 31605-104 31505-21 31505-20

31505-103 Average + Log Scale + Sizes Labels

Lower Hassayampa - Reach 3

JE Fuller Hydrology and Geomorphology Inc.

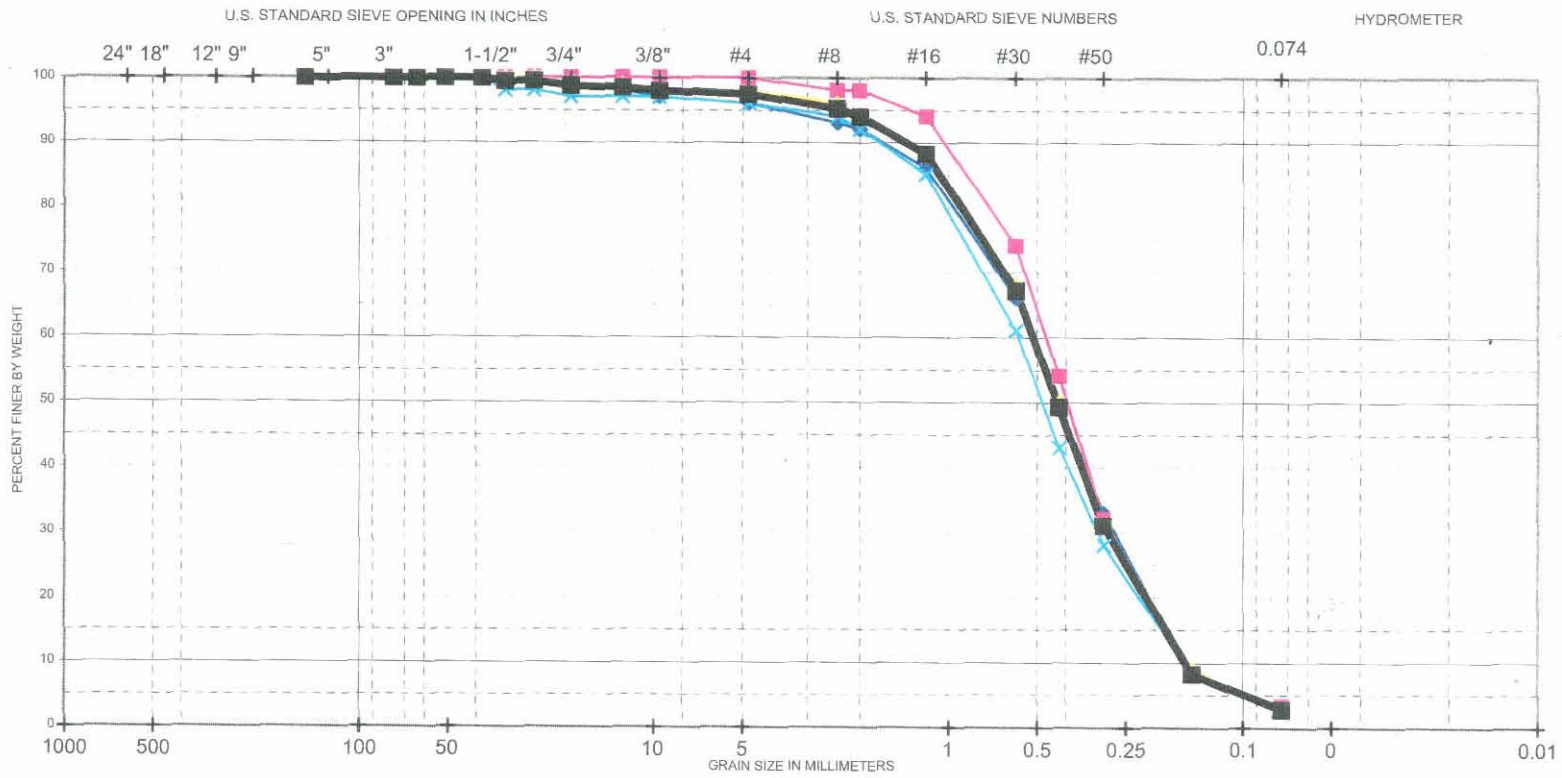

BOULDERS				GRAVEL					SAND					SILT	
MEDIUM	SMALL	LARGE	SMALL	VERY COARSE	COARSE	MEDIUM	FINE	VERY FINE	VERY COARSE	COARSE	MEDIUM	FINE	VERY FINE	COARSE	MEDIUM

31505-16 31505-14 31505-102 31505-101

Average + Log Scale + Sizes Labels

Lower Hassayampa - Reach 4

JE Fuller Hydrology and Geomorphology Inc.

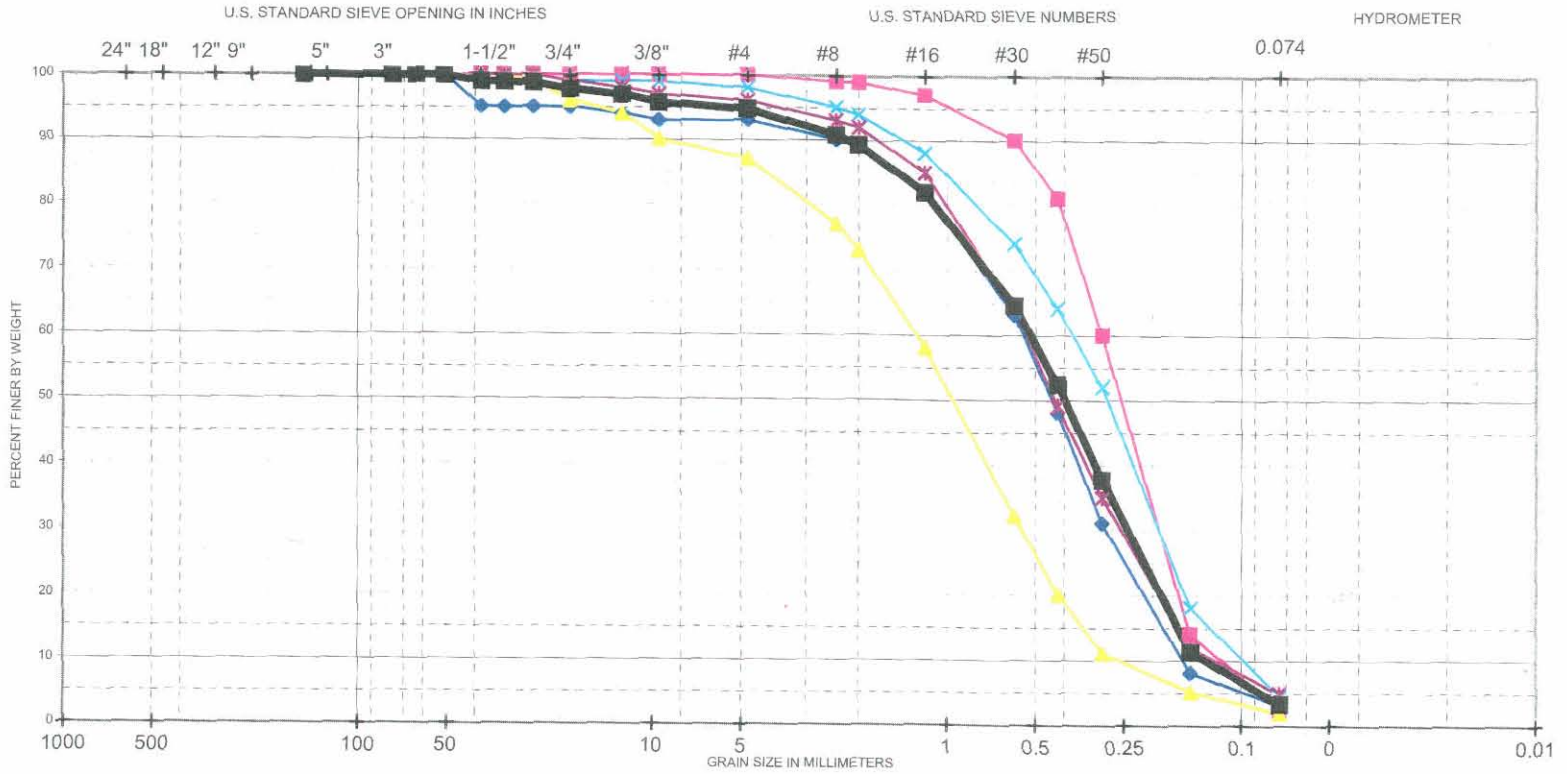

BOULDERS				GRAVEL					SAND					SILT	
MEDIUM	SMALL	LARGE	SMALL	VERY COARSE	COARSE	MEDIUM	FINE	VERY FINE	VERY COARSE	COARSE	MEDIUM	FINE	VERY FINE	COARSE	MEDIUM

31505-100 31405-9 31405-7 31405-05

31405-4 Average + Log Scale + Sizes Labels

Lower Hassayampa - Reach 5

JE Fuller Hydrology and Geomorphology Inc.

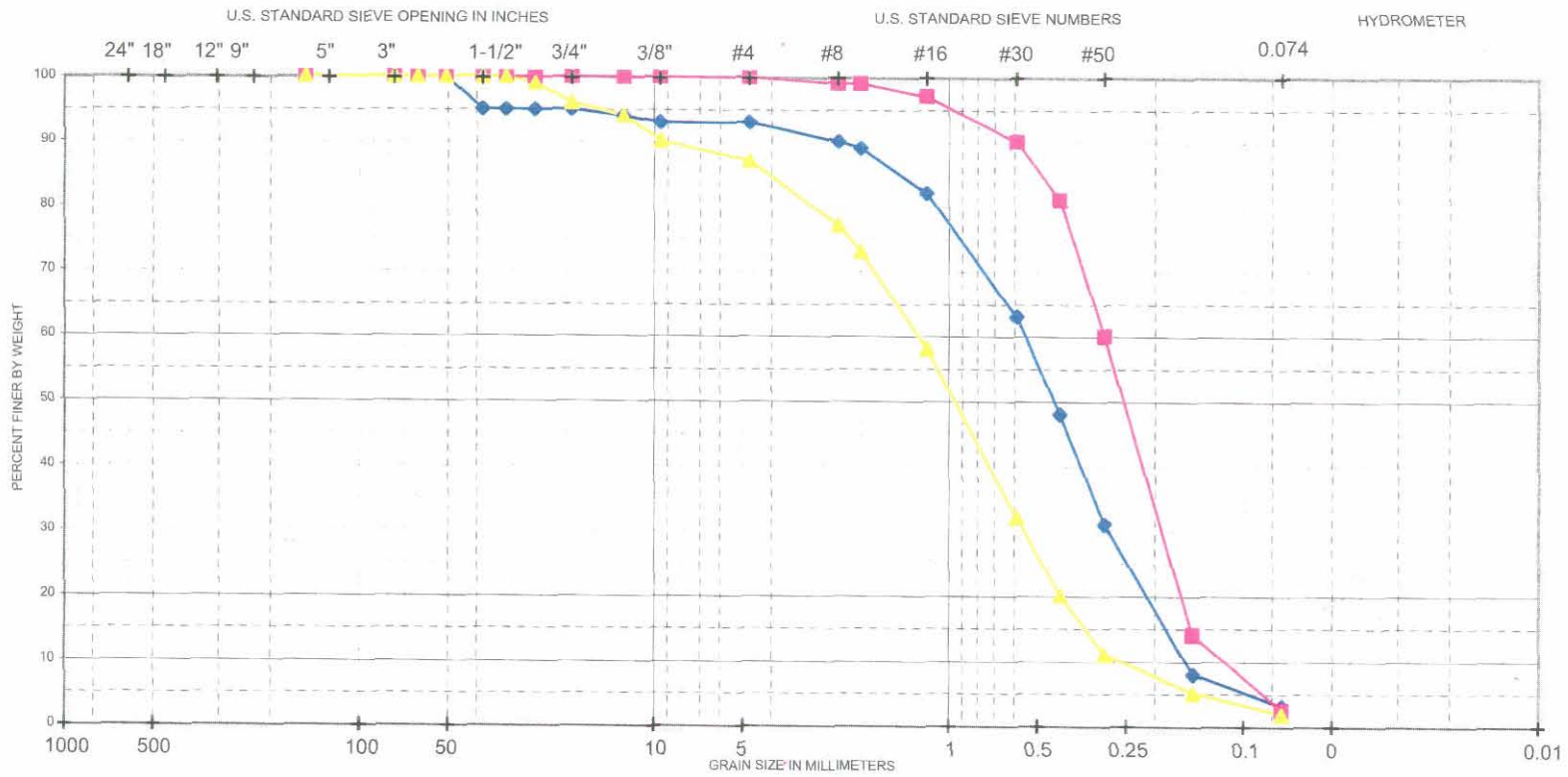

31505-100 31405-9 31405-7 + Log Scale + Sizes Labels

Lower Hassayampa - Reach 5a

JE Fuller Hydrology and Geomorphology Inc.

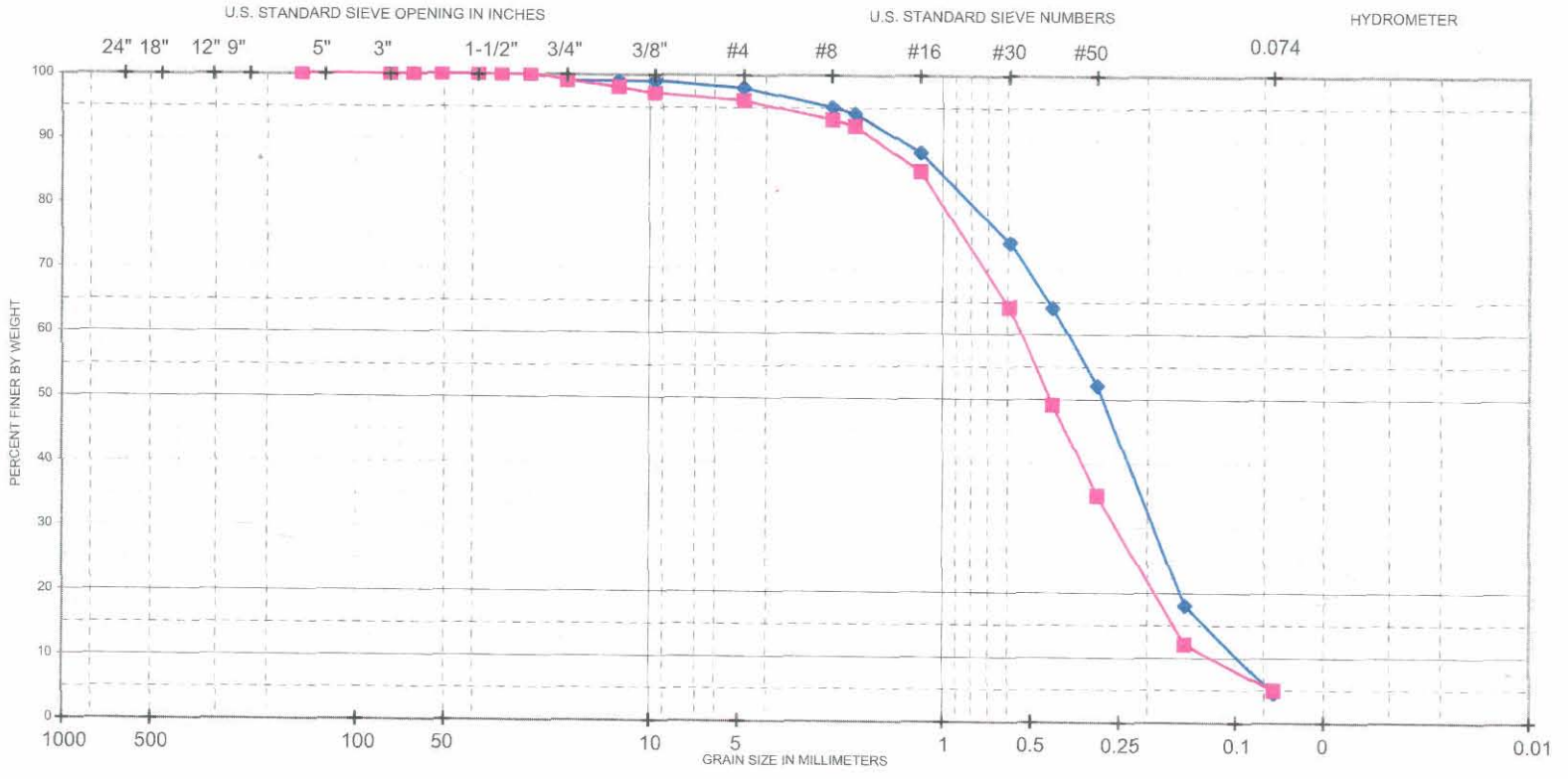

BOULDERS				GRAVEL					SAND					SILT	
MEDIUM	SMALL	LARGE	SMALL	VERY COARSE	COARSE	MEDIUM	FINE	VERY FINE	VERY COARSE	COARSE	MEDIUM	FINE	VERY FINE	COARSE	MEDIUM

31405-05 31405-4 + Log Scale + Sizes Labels

Lower Hassayampa - Reach 5b

JE Fuller Hydrology and Geomorphology Inc.

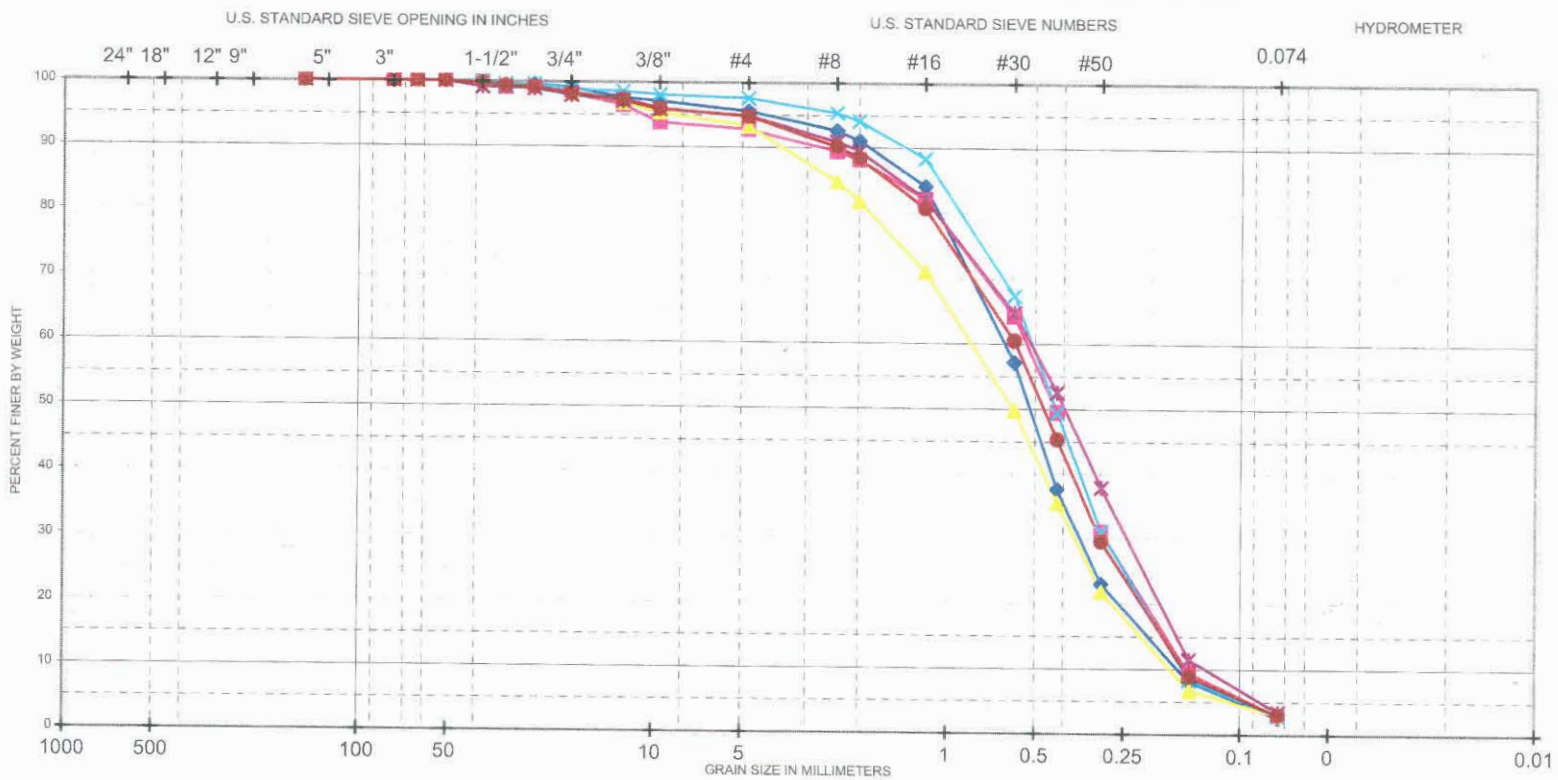

Reach 1 Reach 2 Reach 3 Reach 4

Reach 5 Reach 1 - 5 + Log Scale + Sizes Labels

Lower Hassayampa - Reach Averages

JE Fuller Hydrology and Geomorphology Inc.

APPENDIX 5.5

HEC-6 vs. RAS comparison tables

HYDRAULIC CALIBRATION USING MANNINGS VALUES

	HEC-RAS RESULTS			HEC-6 RESULTS			
River Sta	Q Total	W.S. Elev	Vel Chnl	WSE	VEL C	WS DIFF	VEL DIFF
	(cfs)	(ft)	(ft/s)				
0.35	34640	786.78	7.11	786.778	7.088	-0.002	-0.022
0.44	34640	794.13	3.92	794.107	3.919	-0.023	-0.001
0.54	34640	795.93	5.77	795.745	5.908	-0.185	0.138
0.63	34640	797.37	13.13	797.366	13.137	-0.004	0.007
0.73	34640	803.78	7.57	803.824	7.537	0.044	-0.033
0.82	34640	808.18	9.59	808.331	9.48	0.151	-0.11
0.92	34640	811.78	10.14	811.949	10.025	0.169	-0.115
1.01	34640	813.55	10.42	813.36	10.62	-0.19	0.2
1.11	34640	815.25	10.15	815.262	10.155	0.012	0.005
1.2	34640	818.27	9.18	818.317	9.171	0.047	-0.009
1.3	34640	820.55	9.06	820.527	9.108	-0.023	0.048
1.39	34640	822.26	10.69	822.193	10.748	-0.067	0.058
1.49	34640	824.34	9.45	824.257	9.518	-0.083	0.068
1.58	34640	825.98	8.54	826.179	8.386	0.199	-0.154
1.65	34640	827.32	9.75	827.46	9.618	0.14	-0.132
1.72	34640	828.88	10.54	828.972	10.454	0.092	-0.086
1.81	34640	830.79	10.66	830.758	10.689	-0.032	0.029
1.91	34640	832.96	11.11	833.035	11.081	0.075	-0.029
2	34640	835.26	10.43	835.129	10.553	-0.131	0.123
2.1	34640	836.51	10.89	836.33	11.075	-0.18	0.185
2.19	58000	837.52	18.48	837.555	18.415	0.035	-0.065
2.29	58000	842.88	11.91	842.764	12.017	-0.116	0.107
2.38	58000	844.09	11.94	844.161	11.871	0.071	-0.069
2.48	58000	845.23	13.64	845.362	13.488	0.132	-0.152
2.57	58000	847.12	13.73	847.121	13.668	0.001	-0.062
2.64	58000	849.01	11	848.93	11.062	-0.08	0.062
2.66	58000	849.15	11.92	849.063	12.014	-0.087	0.094
2.72	58000	849.39	18.63	849.39	18.639	0	0.009
2.78	58000	856.06	10.76	855.933	10.853	-0.127	0.093
2.87	58000	858.05	8.31	857.862	8.424	-0.188	0.114
2.96	58000	859.35	6.17	859.219	6.21	-0.131	0.04
3.06	58000	859.95	6.32	859.811	6.395	-0.139	0.075
3.15	58000	860.73	5.35	860.648	5.406	-0.082	0.056
3.25	58000	861.25	6.11	861.112	6.216	-0.138	0.106
3.34	58000	861.74	6.18	861.933	5.992	0.193	-0.188
3.44	58000	861.89	10.13	861.766	10.292	-0.124	0.162
3.53	66933	862.94	12.85	862.99	12.733	0.05	-0.117
3.63	66933	864.65	12.32	864.678	12.27	0.028	-0.05
3.72	66933	867.08	9.83	866.976	9.931	-0.104	0.101
3.81	66933	868.06	10.42	867.95	10.469	-0.11	0.049
3.91	66933	869.36	11.56	869.247	11.743	-0.113	0.183
4	75000	871.48	13.15	871.609	12.978	0.129	-0.172
4.01	75000	873.28	10.4	873.145	10.594	-0.135	0.194
4.09	75000	875.11	9.18	875.111	9.047	0.001	-0.133
4.15	75000	876.88	5.58	876.858	5.541	-0.022	-0.039
4.25	75000	878.02	5.88	878.053	5.879	0.033	-0.001
4.34	75000	879.78	7.24	879.719	7.293	-0.061	0.053
4.44	75000	881.39	7.44	881.371	7.397	-0.019	-0.043
4.53	75000	883.43	8.32	883.385	8.345	-0.045	0.025
4.63	75000	885.88	10.75	886.041	10.21	0.161	-0.54
4.72	75000	888.76	7.61	888.7	7.759	-0.06	0.149
4.82	75000	890.15	9.95	890.152	9.863	0.002	-0.087
4.91	75000	892.36	9.34	892.329	9.374	-0.031	0.034
5	75000	894.93	8.17	894.92	8.074	-0.01	-0.096
5.1	75000	897.28	8.09	897.303	8.074	0.023	-0.016
5.19	75000	899.39	8.64	899.414	8.501	0.024	-0.139
5.29	75000	901.47	7.15	901.476	7.091	0.006	-0.059
5.38	75000	903.28	6.27	903.276	6.294	-0.004	0.024
5.48	75000	904.95	6.55	905.021	6.39	0.071	-0.16
5.57	75000	906.69	6.81	906.698	6.806	0.008	-0.004
5.67	75000	908.15	12.07	908.24	11.979	0.09	-0.091
5.76	75000	910.19	11.84	910.162	11.68	-0.028	-0.16
5.86	75000	912.51	10.96	912.444	11.129	-0.066	0.169
5.95	75000	914.73	7.08	914.788	6.911	0.058	-0.169
6.05	75000	915.81	11.16	915.779	10.991	-0.031	-0.169
6.14	75000	917.85	9.83	917.905	9.68	0.055	-0.15
6.23	75000	919.47	9.5	919.4	9.526	-0.07	0.026
6.33	75000	921.62	9.53	921.61	9.572	-0.01	0.042
6.42	75000	924.21	10.48	924.248	10.298	0.038	-0.182
6.52	75000	926.97	10.03	926.877	10.088	-0.093	0.058
6.61	75000	928.76	10.57	928.688	10.65	-0.072	0.08
6.71	75000	930.62	9.29	930.608	9.142	-0.012	-0.148
6.8	75000	932.81	7.36	932.784	7.248	-0.026	-0.112
6.9	75000	934.52	11.57	934.542	11.632	0.022	0.062

	HEC-RAS RESULTS			HEC-6 RESULTS			
River Sta	Q Total	W.S. Elev	Vel Chnl	WSE	VEL C	WS DIFF	VEL DIFF
	(cfs)	(ft)	(ft/s)				
6.99	75000	937.29	10.03	937.179	10.159	-0.111	0.129
7.09	75000	939.68	10.37	939.616	10.39	-0.064	0.02
7.18	75000	942.06	10.11	942.059	9.964	-0.001	-0.146
7.28	75000	944.41	9.12	944.39	9.199	-0.02	0.079
7.37	75000	946.34	8.73	946.328	8.578	-0.012	-0.152
7.47	75000	948.46	7.62	948.512	7.562	0.052	-0.058
7.56	75000	950.12	7.31	950.052	7.449	-0.068	0.139
7.66	75000	952.18	8.92	952.206	8.828	0.026	-0.092
7.75	75000	954.63	7.7	954.749	7.513	0.119	-0.187
7.84	75000	956.85	8.12	956.886	8.08	0.036	-0.04
7.94	75000	958.86	7.64	958.899	7.501	0.039	-0.139
8.03	75000	961.08	10.47	961.052	10.533	-0.028	0.063
8.13	75000	964.03	8.74	963.978	8.747	-0.052	0.007
8.22	75000	966.03	9.52	966.116	9.342	0.086	-0.178
8.32	75000	968.6	7.68	968.55	7.717	-0.05	0.037
8.41	75000	970.42	7	970.436	6.908	0.016	-0.092
8.51	75000	972.39	7.75	972.402	7.712	0.012	-0.038
8.6	75000	974.76	7.71	974.802	7.604	0.042	-0.106
8.7	75000	977.24	6.77	977.258	6.725	0.018	-0.045
8.79	75000	979.17	7.82	979.066	7.99	-0.104	0.17
8.89	75000	981.16	7.03	981.18	6.954	0.02	-0.076
8.98	75000	982.95	6.55	982.886	6.633	-0.064	0.083
9.08	75000	984.94	7.67	984.927	7.661	-0.013	-0.009
9.17	75000	987.08	9.25	987.043	9.305	-0.037	0.055
9.27	75000	989.41	12.05	989.393	11.961	-0.017	-0.089
9.36	75000	991.47	11.16	991.463	11.293	-0.007	0.133
9.45	75000	993.42	9.61	993.453	9.604	0.033	-0.006
9.55	75000	995.25	8.16	995.2	8.202	-0.05	0.042
9.64	75000	996.23	10.48	996.193	10.556	-0.037	0.076
9.74	75000	999.11	8.73	999.094	8.787	-0.016	0.057
9.83	75000	1001.08	10.23	1001.08	10.197	0	-0.033
9.93	75000	1003.56	9.54	1003.48	9.632	-0.08	0.092
10.02	75000	1006.12	8.93	1006.148	8.904	0.028	-0.026
10.12	75000	1008.25	9.03	1008.289	8.886	0.039	-0.144
10.21	75000	1010.62	7.36	1010.64	7.385	0.02	0.025
10.31	75000	1012.59	7.97	1012.529	8.009	-0.061	0.039
10.4	75000	1014.26	11.86	1014.198	11.855	-0.062	-0.005
10.5	75000	1016.57	11.31	1016.572	11.25	0.002	-0.06
10.59	75000	1019.02	11.65	1019.01	11.604	-0.01	-0.046
10.69	75000	1021.22	13.03	1021.251	12.978	0.031	-0.052
10.73	75000	1023.42	8.67	1023.345	8.789	-0.075	0.119
10.77	75000	1024.1	8.59	1024.15	8.446	0.05	-0.144
10.87	75000	1025.43	8.73	1025.477	8.597	0.047	-0.133
10.98	75000	1027.28	12.83	1027.315	12.73	0.035	-0.1
10.99	75000	1029.04	9.96	1028.99	10.105	-0.05	0.145
11	75000	1029.27	10.08	1029.378	9.902	0.108	-0.178
11.01	75000	1029.85	9.36	1029.759	9.476	-0.091	0.116
11.09	75000	1031.32	8.91	1031.278	9.004	-0.042	0.094
11.16	75000	1032.68	10.11	1032.612	10.231	-0.068	0.121
11.24	75000	1034.74	9.1	1034.812	8.977	0.072	-0.123
11.33	75000	1036.51	8.37	1036.504	8.382	-0.006	0.012
11.43	75000	1037.79	10.1	1037.819	10.013	0.029	-0.087
11.52	75000	1040.1	8.02	1040.172	7.962	0.072	-0.058
11.62	75000	1041.59	9.24	1041.625	9.153	0.035	-0.087
11.71	75000	1044.03	7.95	1044.098	7.789	0.068	-0.161
11.81	75000	1045.9	7.66	1045.865	7.676	-0.035	0.016
11.9	75000	1047.53	9.04	1047.557	8.853	0.027	-0.187
12	75000	1050.24	8.48	1050.218	8.484	-0.022	0.004
12.09	75000	1052.32	7.57	1052.311	7.494	-0.009	-0.076
12.18	75000	1054.12	9.63	1054.139	9.518	0.019	-0.112
12.28	75000	1056.95	8.08	1056.904	8.039	-0.046	-0.041
12.37	75000	1058.47	9.39	1058.425	9.22	-0.045	-0.17
12.47	75000	1060.37	8.65	1060.234	8.832	-0.136	0.182
12.56	75000	1062.64	10.93	1062.64	10.632	0	-0.298
12.66	75000	1065.38	11.25	1065.399	11.089	0.019	-0.161
12.75	75000	1068.18	10.87	1068.298	10.515	0.118	-0.355
12.85	75000	1070.96	8.14	1070.919	8.126	-0.041	-0.014
12.94	75000	1072.35	9.3	1072.353	9.287	0.003	-0.013
13.04	75000	1075.02	8.78	1075.018	8.746	-0.002	-0.034
13.13	75000	1077.29	7.35	1077.315	7.29	0.025	-0.06
13.23	75000	1079.44	7.04	1079.499	6.939	0.059	-0.101
13.32	75000	1081.14	7.75	1081.069	7.842	-0.071	0.092
13.42	75000	1083.08	7.27	1083.102	7.121	0.022	-0.149
13.51	75000	1085.25	11.36	1085.25	11.287	0	-0.073
13.61	75000	1088.96	6.04	1089.084	5.911	0.124	-0.129

	HEC-RAS RESULTS			HEC-6 RESULTS			
River Sta	Q Total	W.S. Elev	Vel Chnl	WSE	VEL C	WS DIFF	VEL DIFF
	(cfs)	(ft)	(ft/s)				
13.7	75000	1090.22	7.78	1090.224	7.79	0.004	0.01
13.79	75000	1092.39	9.18	1092.369	9.213	-0.021	0.033
13.89	75000	1094.79	8.17	1094.806	8.08	0.016	-0.09
13.98	75000	1096.51	9.53	1096.459	9.635	-0.051	0.105
14.08	75000	1099.2	9.98	1099.195	9.966	-0.005	-0.014
14.17	75000	1101.3	10.61	1101.231	10.759	-0.069	0.149
14.27	75000	1103.5	11.09	1103.497	11.095	-0.003	0.005
14.36	75000	1106.56	12.2	1106.649	12.025	0.089	-0.175
14.45	75000	1108.41	12.12	1108.423	12.151	0.013	0.031
14.55	75000	1110.73	10.02	1110.769	10.007	0.039	-0.013
14.64	75000	1112.7	12.07	1112.771	11.88	0.071	-0.19
14.73	75000	1115.18	11.82	1115.275	11.63	0.095	-0.19
14.83	75000	1117.66	10.42	1117.65	10.579	-0.01	0.159
14.92	75000	1118.8	11.44	1118.774	11.475	-0.026	0.035
15.02	75000	1120.01	13.65	1120.017	13.798	0.007	0.148
15.11	75000	1122.71	9.62	1122.772	9.584	0.062	-0.036
15.21	75000	1123.48	12.11	1123.466	12.186	-0.014	0.076
15.3	75000	1125.32	12.5	1125.375	12.334	0.055	-0.166
15.4	75000	1127.95	9.3	1127.958	9.216	0.008	-0.084
15.49	75000	1128.95	9.86	1128.955	9.769	0.005	-0.091
15.59	75000	1130.2	10.13	1130.148	10.026	-0.052	-0.104
15.68	75000	1131.83	11.87	1131.837	11.722	0.007	-0.148
15.78	75000	1134.5	9.05	1134.437	9.028	-0.063	-0.022
15.87	75000	1135.65	10.89	1135.65	10.779	0	-0.111
15.97	75000	1137.61	9.51	1137.616	9.388	0.006	-0.122
16.06	75000	1139.47	8.81	1139.415	8.959	-0.055	0.149
16.16	75000	1141.03	10.37	1141.071	10.353	0.041	-0.017
16.25	75000	1143.06	9	1143.069	9.03	0.009	0.03
16.35	75000	1144.76	8.19	1144.812	8.124	0.052	-0.066
16.44	75000	1146.63	10.58	1146.58	10.538	-0.05	-0.042
16.53	75000	1149.06	11.61	1149.09	11.486	0.03	-0.124
16.63	75000	1150.64	11.73	1150.709	11.58	0.069	-0.15
16.72	75000	1152.7	10.83	1152.69	10.881	-0.01	0.051
16.82	75000	1154.92	9.22	1154.926	9.271	0.006	0.051
16.91	75000	1156.63	10.05	1156.66	9.881	0.03	-0.169
17.01	75000	1158.48	11.36	1158.459	11.554	-0.021	0.194
17.1	75000	1161.04	9.95	1161.055	9.939	0.015	-0.011
17.2	75000	1162.92	9.45	1162.915	9.551	-0.005	0.101
17.29	75000	1164.78	9.96	1164.813	9.849	0.033	-0.111
17.39	75000	1166.88	10.91	1166.844	11.055	-0.036	0.145
17.48	75000	1168.97	11.38	1168.996	11.278	0.026	-0.102
17.58	75000	1171.88	11.03	1171.904	11.02	0.024	-0.01
17.67	75000	1174.6	8.73	1174.658	8.622	0.058	-0.108
17.77	75000	1176.51	9.19	1176.567	9.03	0.057	-0.16
17.86	75000	1178.73	9.97	1178.724	9.967	-0.006	-0.003
17.95	75000	1181.28	9.39	1181.263	9.298	-0.017	-0.092
18.05	75000	1182.69	8.26	1182.623	8.411	-0.067	0.151
18.14	75000	1183.74	10.92	1183.797	10.741	0.057	-0.179
18.24	75000	1186.39	9	1186.453	8.857	0.063	-0.143
18.33	75000	1188.04	9.29	1188.119	9.125	0.079	-0.165
18.43	75000	1190.21	10.26	1190.249	10.069	0.039	-0.191
18.52	75000	1192.89	7.57	1192.907	7.507	0.017	-0.063
18.62	75000	1193.99	7.45	1193.919	7.553	-0.071	0.103
18.71	75000	1196.19	9.36	1196.189	9.339	-0.001	-0.021
18.81	75000	1198.96	8.69	1198.874	8.713	-0.086	0.023
18.9	75000	1201.18	9.16	1201.169	9.028	-0.011	-0.132
19	75000	1203.31	6.86	1203.31	6.829	0	-0.031
19.09	75000	1204.63	8.04	1204.655	8.036	0.025	-0.004
19.19	75000	1206.72	9.9	1206.763	9.757	0.043	-0.143
19.28	75000	1210.22	8.33	1210.263	8.275	0.043	-0.055
19.38	75000	1212.42	8.29	1212.411	8.278	-0.009	-0.012
19.47	75000	1214.04	10.53	1214.057	10.53	0.017	0
19.56	75000	1216.75	8.21	1216.821	8.101	0.071	-0.109
19.66	75000	1218.02	10.31	1218.012	10.277	-0.008	-0.033
19.75	75000	1222.17	9.27	1222.231	9.201	0.061	-0.069
19.85	75000	1224.26	7.8	1224.212	7.901	-0.048	0.101
19.94	75000	1225.5	8.72	1225.496	8.66	-0.004	-0.06
20.14	75000	1226.94	9.57	1226.888	9.62	-0.052	0.05
20.23	75000	1227.96	9.75	1227.893	9.805	-0.067	0.055
20.3	75000	1228.89	9.92	1228.871	9.886	-0.019	-0.034
20.32	75000	1230.42	9.3	1230.467	9.235	0.047	-0.065
20.42	75000	1232.22	7.92	1232.244	7.918	0.024	-0.002
20.51	75000	1234.02	8.71	1234.026	8.722	0.006	0.012
20.61	75000	1236.55	7.65	1236.537	7.673	-0.013	0.023
20.7	75000	1238.51	8.54	1238.516	8.475	0.006	-0.065

	HEC-RAS RESULTS			HEC-6 RESULTS			
River Sta	Q Total	W.S. Elev	Vel Chnl	WSE	VEL C	WS DIFF	VEL DIFF
	(cfs)	(ft)	(ft/s)				
20.8	75000	1241.06	9.69	1241.026	9.59	-0.034	-0.1
20.89	75000	1244.05	9.19	1243.875	9.093	-0.175	-0.097
20.98	75000	1246.4	9.98	1246.464	9.804	0.064	-0.176
21.08	75000	1249.36	9.51	1249.396	9.353	0.036	-0.157
21.17	75000	1251.65	8.48	1251.549	8.65	-0.101	0.17
21.27	75000	1253.29	9.68	1253.366	9.499	0.076	-0.181
21.36	75000	1255.32	8.32	1255.335	8.419	0.015	0.099
21.46	75000	1256.87	9.28	1256.867	9.268	-0.003	-0.012
21.55	75000	1258.41	10.33	1258.378	10.37	-0.032	0.04
21.65	75000	1259.9	9.97	1259.95	9.89	0.05	-0.08
21.74	75000	1261.7	10.05	1261.748	9.945	0.048	-0.105
21.84	75000	1263.71	8.74	1263.744	8.687	0.034	-0.053
21.93	75000	1264.96	8.73	1264.931	8.769	-0.029	0.039
22.03	75000	1267.51	11	1267.552	10.895	0.042	-0.105
22.12	75000	1270.44	8.47	1270.407	8.54	-0.033	0.07
22.21	75000	1272.11	11.01	1272.136	10.903	0.026	-0.107
22.31	75000	1275.19	8.05	1275.279	7.861	0.089	-0.189
22.4	75000	1276.23	10.15	1276.255	10.123	0.025	-0.027
22.5	75000	1278.89	9.35	1278.938	9.211	0.048	-0.139
22.59	75000	1281.33	8.91	1281.292	8.924	-0.038	0.014
22.69	75000	1282.99	8.08	1283.008	8.094	0.018	0.014
22.78	75000	1284.35	8.87	1284.405	8.86	0.055	-0.01
22.88	75000	1286.15	9.83	1286.162	9.741	0.012	-0.089
22.97	75000	1288.31	9.16	1288.29	9.058	-0.02	-0.102
23.07	75000	1289.95	10.97	1289.939	11.025	-0.011	0.055
23.16	75000	1292.46	12.83	1292.486	12.768	0.026	-0.062
23.26	75000	1295.63	13.26	1295.627	13.353	-0.003	0.093
23.35	75000	1298.26	12.46	1298.253	12.146	-0.007	-0.314
23.45	75000	1300.14	11	1300.144	10.911	0.004	-0.089
23.54	75000	1301.53	9.63	1301.494	9.783	-0.036	0.153
23.63	75000	1302.84	10.08	1302.88	9.966	0.04	-0.114
23.73	75000	1305.05	10.93	1305.027	10.976	-0.023	0.046
23.82	75000	1307.63	9.99	1307.641	9.886	0.011	-0.104
23.92	75000	1309.27	10.73	1309.275	10.634	0.005	-0.096
24.01	75000	1311.25	9.23	1311.231	9.297	-0.019	0.067
24.11	75000	1312.93	9.5	1312.942	9.409	0.012	-0.091
24.2	75000	1315.14	8.63	1315.131	8.612	-0.009	-0.018
24.3	75000	1317.36	10.07	1317.375	9.948	0.015	-0.122
24.39	75000	1320.24	6.99	1320.275	6.882	0.035	-0.108
24.49	75000	1321.81	8.35	1321.842	8.261	0.032	-0.089
24.58	75000	1324.13	8.03	1324.057	8.049	-0.073	0.019
24.68	75000	1326.23	8.05	1326.163	8.048	-0.067	-0.002
24.77	75000	1327.98	9.55	1327.913	9.669	-0.067	0.119
24.87	75000	1330.3	9.65	1330.309	9.684	0.009	0.034
24.96	75000	1332.91	8.71	1332.891	8.702	-0.019	-0.008
25.06	75000	1334.71	9.23	1334.723	9.162	0.013	-0.068
25.15	75000	1337.41	9.01	1337.355	8.948	-0.055	-0.062
25.24	75000	1340.69	10.23	1340.736	10.132	0.046	-0.098
25.34	75000	1343.83	6.84	1343.808	6.807	-0.022	-0.033
25.43	75000	1345.24	7.42	1345.179	7.471	-0.061	0.051
25.53	75000	1347.13	7.49	1347.136	7.362	0.006	-0.128
25.62	75000	1349.66	6.77	1349.655	6.729	-0.005	-0.041
25.72	75000	1351.65	6.41	1351.692	6.324	0.042	-0.086
25.81	75000	1353.14	7.82	1353.154	7.772	0.014	-0.048
25.91	75000	1355.24	7.99	1355.266	7.835	0.026	-0.155
26	75000	1357.34	8.15	1357.327	8.106	-0.013	-0.044
26.1	75000	1360.04	7.82	1360.069	7.694	0.029	-0.126
26.19	75000	1362.67	6.81	1362.739	6.682	0.069	-0.128
26.29	75000	1364.85	6.76	1364.836	6.792	-0.014	0.032
26.38	75000	1366.99	6.65	1367.017	6.571	0.027	-0.079
26.48	75000	1368.86	7.1	1368.808	7.188	-0.052	0.088
26.57	75000	1371.32	6.94	1371.396	6.805	0.076	-0.135
26.67	75000	1373.72	6.1	1373.734	6.073	0.014	-0.027
26.76	75000	1375.54	6.49	1375.599	6.374	0.059	-0.116
26.85	75000	1377.69	6.55	1377.71	6.516	0.02	-0.034
26.95	75000	1379.67	5.74	1379.664	5.692	-0.006	-0.048
27.04	75000	1381.72	6.92	1381.73	6.809	0.01	-0.111
27.14	75000	1384.45	6.48	1384.401	6.637	-0.049	0.157
27.23	75000	1387.12	6.77	1387.147	6.739	0.027	-0.031
27.33	75000	1389.56	6.08	1389.61	5.999	0.05	-0.081
27.43	75000	1391.18	5.75	1391.177	5.665	-0.003	-0.085
27.52	75000	1392.86	5.53	1392.872	5.502	0.012	-0.028
27.61	75000	1394.74	7.26	1394.735	7.199	-0.005	-0.061
27.75	75000	1398.17	5.38	1398.216	5.475	0.046	0.095
27.89	75000	1400.65	5.39	1400.697	5.342	0.047	-0.048

HYDRAULIC CALIBRATION USING MANNINGS VALUES

	HEC-RAS RESULTS			HEC-6 RESULTS			
River Sta	Q Total	W.S. Elev	Vel Chnl	WSE	VEL C	WS DIFF	VEL DIFF
	(cfs)	(ft)	(ft/s)				
0.35	31950	786.57	7.02	786.617	6.894	0.047	-0.126
0.44	31950	793.84	3.77	793.856	3.749	0.016	-0.021
0.54	31950	795.61	5.54	795.414	5.644	-0.196	0.104
0.63	31950	797.05	12.71	797.021	12.765	-0.029	0.055
0.73	31950	803.26	7.32	803.311	7.292	0.051	-0.028
0.82	31950	807.58	9.28	807.711	9.172	0.131	-0.108
0.92	31950	811.11	9.84	811.24	9.73	0.13	-0.11
1.01	31950	812.88	10.28	812.709	10.461	-0.171	0.181
1.11	31950	814.66	9.89	814.624	9.946	-0.036	0.056
1.2	31950	817.69	8.96	817.835	8.831	0.145	-0.129
1.3	31950	820.01	8.77	820.133	8.677	0.123	-0.093
1.39	31950	821.72	10.34	821.799	10.264	0.079	-0.076
1.49	31950	823.74	9.19	823.821	9.146	0.081	-0.044
1.58	31950	825.4	8.31	825.227	8.471	-0.173	0.161
1.65	31950	826.81	9.46	826.878	9.393	0.068	-0.067
1.72	31950	828.4	10.19	828.527	10.068	0.127	-0.122
1.81	31950	830.31	10.32	830.399	10.184	0.089	-0.136
1.91	31950	832.52	10.69	832.631	10.562	0.111	-0.128
2	31950	834.78	10.04	834.692	10.159	-0.088	0.119
2.1	31950	836.02	10.5	835.846	10.674	-0.174	0.174
2.19	42680	836.51	15	836.587	14.812	0.077	-0.188
2.29	42680	840.21	10.9	840.105	11.003	-0.105	0.103
2.38	42680	841.55	10.88	841.633	10.784	0.083	-0.096
2.48	42680	842.93	12.34	843.021	12.234	0.091	-0.106
2.57	42680	844.98	12.24	845.027	12.133	0.047	-0.107
2.64	42680	846.52	10.18	846.331	10.351	-0.189	0.171
2.66	42680	846.57	11.2	846.451	11.349	-0.119	0.149
2.72	42680	847.01	17.31	846.922	17.401	-0.088	0.091
2.78	42680	853.49	9.74	853.648	9.61	0.158	-0.13
2.87	42680	855.41	7.6	855.484	7.573	0.074	-0.027
2.96	42680	856.63	6.24	856.801	6.095	0.171	-0.145
3.06	42680	857.46	6.46	857.544	6.386	0.084	-0.074
3.15	42680	858.53	5.49	858.632	5.367	0.102	-0.123
3.25	42680	859.25	5.84	859.282	5.788	0.032	-0.052
3.34	42680	859.82	5.9	859.963	5.743	0.143	-0.157
3.44	42680	860.02	11.23	859.984	11.381	-0.036	0.151
3.53	47246	862.14	10.4	862.219	10.29	0.079	-0.11
3.63	47246	863.36	10.9	863.403	10.804	0.043	-0.096
3.72	47246	865.56	8.75	865.55	8.813	-0.01	0.063
3.81	47246	866.59	9.33	866.545	9.343	-0.045	0.013
3.91	47246	868.01	10.36	867.962	10.465	-0.048	0.105
4	50000	870.29	10.79	870.319	10.738	0.029	-0.052
4.01	50000	871.43	9.03	871.351	9.191	-0.079	0.161
4.09	50000	873.12	8.61	873.071	8.524	-0.049	-0.086
4.15	50000	874.97	5.08	874.98	5.01	0.01	-0.07
4.25	50000	876.43	5.87	876.466	5.751	0.036	-0.119
4.34	50000	878.7	6.56	878.673	6.665	-0.027	0.105
4.44	50000	880.33	6.55	880.295	6.503	-0.035	-0.047
4.53	50000	882.39	7.7	882.36	7.649	-0.03	-0.051
4.63	50000	885	9.18	885.073	9.113	0.073	-0.067
4.72	50000	887.72	7.28	887.691	7.257	-0.029	-0.023
4.82	50000	889.24	9.19	889.146	9.383	-0.094	0.193
4.91	50000	891.49	8.64	891.499	8.725	0.009	0.085
5	50000	894.04	7.51	894.074	7.39	0.034	-0.12
5.1	50000	896.34	7.96	896.376	7.93	0.036	-0.03
5.19	50000	898.47	7.88	898.504	7.865	0.034	-0.015
5.29	50000	900.42	6.63	900.482	6.475	0.062	-0.155
5.38	50000	902.22	5.65	902.246	5.598	0.026	-0.052
5.48	50000	903.89	6.06	903.958	6.044	0.068	-0.016
5.57	50000	905.67	6.33	905.69	6.308	0.02	-0.022
5.67	50000	907.16	10.45	907.247	10.299	0.087	-0.151
5.76	50000	909.04	11.24	909.04	11.315	0	0.075
5.86	50000	911.44	10.84	911.396	11.024	-0.044	0.184
5.95	50000	913.86	6.4	913.888	6.33	0.028	-0.07
6.05	50000	914.88	10.28	914.929	10.115	0.049	-0.165
6.14	50000	917.01	8.49	917.03	8.376	0.02	-0.114
6.23	50000	918.54	8.51	918.496	8.337	-0.044	-0.173
6.33	50000	920.7	8.05	920.693	7.875	-0.007	-0.175
6.42	50000	923.25	8.69	923.209	8.648	-0.041	-0.042
6.52	50000	926.04	9.3	925.893	9.266	-0.147	-0.034
6.61	50000	927.96	9.24	927.869	9.296	-0.091	0.056
6.71	50000	929.66	8.28	929.635	8.196	-0.025	-0.084
6.8	50000	931.79	6.55	931.829	6.452	0.039	-0.098
6.9	50000	933.63	10.6	933.765	10.404	0.135	-0.196

	HEC-RAS RESULTS			HEC-6 RESULTS			
River Sta	Q Total	W.S. Elev	Vel Chnl	WSE	VEL C	WS DIFF	VEL DIFF
	(cfs)	(ft)	(ft/s)				
6.99	50000	936.47	8.31	936.46	8.23	-0.01	-0.08
7.09	50000	938.68	9.1	938.623	9.034	-0.057	-0.066
7.18	50000	941.13	8.69	941.059	8.615	-0.071	-0.075
7.28	50000	943.34	8.19	943.356	8.052	0.016	-0.138
7.37	50000	945.4	7.9	945.348	7.918	-0.052	0.018
7.47	50000	947.6	6.71	947.674	6.686	0.074	-0.024
7.56	50000	949.25	6.47	949.215	6.628	-0.035	0.158
7.66	50000	951.39	7.92	951.404	7.932	0.014	0.012
7.75	50000	953.8	6.78	953.85	6.763	0.05	-0.017
7.84	50000	955.98	7.35	956.061	7.236	0.081	-0.114
7.94	50000	958.01	6.92	958.069	6.808	0.059	-0.112
8.03	50000	960.35	9.2	960.37	9.231	0.02	0.031
8.13	50000	963.09	7.83	963.119	7.66	0.029	-0.17
8.22	50000	965.07	8.68	965.05	8.742	-0.02	0.062
8.32	50000	967.63	7.16	967.651	7.03	0.021	-0.13
8.41	50000	969.52	6.44	969.531	6.412	0.011	-0.028
8.51	50000	971.5	7.16	971.508	7.095	0.008	-0.065
8.6	50000	973.82	7.01	973.857	6.929	0.037	-0.081
8.7	50000	976.32	6.2	976.325	6.181	0.005	-0.019
8.79	50000	978.22	7.16	978.197	7.124	-0.023	-0.036
8.89	50000	980.24	6.29	980.253	6.329	0.013	0.039
8.98	50000	982.1	5.85	982.106	5.845	0.006	-0.005
9.08	50000	984.09	6.76	984.02	6.864	-0.07	0.104
9.17	50000	986.2	8.32	986.19	8.291	-0.01	-0.029
9.27	50000	988.49	10.64	988.469	10.592	-0.021	-0.048
9.36	50000	990.35	9.71	990.409	9.681	0.059	-0.029
9.45	50000	992.12	8.56	992.189	8.481	0.069	-0.079
9.55	50000	993.94	6.9	993.863	6.986	-0.077	0.086
9.64	50000	994.94	9.2	994.954	9.163	0.014	-0.037
9.74	50000	997.73	8.3	997.733	8.247	0.003	-0.053
9.83	50000	1000.02	9.49	1000.01	9.435	-0.01	-0.055
9.93	50000	1002.61	8.33	1002.605	8.424	-0.005	0.094
10.02	50000	1004.96	8.1	1005.018	7.954	0.058	-0.146
10.12	50000	1007.09	8.23	1007.095	8.182	0.005	-0.048
10.21	50000	1009.53	6.26	1009.615	6.16	0.085	-0.1
10.31	50000	1011.46	6.87	1011.368	7.015	-0.092	0.145
10.4	50000	1013.2	10.28	1013.093	10.428	-0.107	0.148
10.5	50000	1015.47	9.94	1015.448	10.007	-0.022	0.067
10.59	50000	1017.86	10.54	1017.82	10.541	-0.04	0.001
10.69	50000	1020.13	11.23	1020.159	11.188	0.029	-0.042
10.73	50000	1022.01	7.52	1021.93	7.633	-0.08	0.113
10.77	50000	1022.69	7.49	1022.698	7.407	0.008	-0.083
10.87	50000	1024.08	7.65	1024.065	7.613	-0.015	-0.037
10.98	50000	1026.19	10.85	1026.223	10.67	0.033	-0.18
10.99	50000	1027.6	8.51	1027.473	8.654	-0.127	0.144
11	50000	1027.83	8.63	1027.831	8.609	0.001	-0.021
11.01	50000	1028.36	7.93	1028.231	8.112	-0.129	0.182
11.09	50000	1029.74	7.99	1029.725	8.082	-0.015	0.092
11.16	50000	1031.32	9.1	1031.333	9.102	0.013	0.002
11.24	50000	1033.53	8	1033.551	7.912	0.021	-0.088
11.33	50000	1035.25	7.35	1035.313	7.185	0.063	-0.165
11.43	50000	1036.66	9.09	1036.734	8.906	0.074	-0.184
11.52	50000	1038.94	6.92	1038.979	6.77	0.039	-0.15
11.62	50000	1040.49	8.31	1040.481	8.238	-0.009	-0.072
11.71	50000	1043.04	6.76	1043.127	6.635	0.087	-0.125
11.81	50000	1044.79	6.64	1044.773	6.666	-0.017	0.026
11.9	50000	1046.47	8.35	1046.465	8.339	-0.005	-0.011
12	50000	1049.31	7.56	1049.324	7.528	0.014	-0.032
12.09	50000	1051.3	6.84	1051.32	6.671	0.02	-0.169
12.18	50000	1053.27	8.81	1053.227	8.923	-0.043	0.113
12.28	50000	1056.11	6.99	1056.115	6.965	0.005	-0.025
12.37	50000	1057.59	8.12	1057.538	8.061	-0.052	-0.059
12.47	50000	1059.38	7.21	1059.265	7.376	-0.115	0.166
12.56	50000	1061.51	10.06	1061.647	9.553	0.137	-0.507
12.66	50000	1064.34	10.04	1064.387	9.864	0.047	-0.176
12.75	50000	1067.05	10.04	1067.039	9.99	-0.011	-0.05
12.85	50000	1069.95	6.98	1069.951	6.963	0.001	-0.017
12.94	50000	1071.31	7.76	1071.303	7.791	-0.007	0.031
13.04	50000	1073.84	8.06	1073.944	7.868	0.104	-0.192
13.13	50000	1076.31	6.41	1076.402	6.237	0.092	-0.173
13.23	50000	1078.52	6.14	1078.605	5.986	0.085	-0.154
13.32	50000	1080.35	6.69	1080.268	6.758	-0.082	0.068
13.42	50000	1082.26	6.13	1082.279	6.096	0.019	-0.034
13.51	50000	1084.27	9.96	1084.202	10.074	-0.068	0.114
13.61	50000	1087.8	5.37	1087.825	5.308	0.025	-0.062

	HEC-RAS RESULTS			HEC-6 RESULTS			
River Sta	Q Total	W.S. Elev	Vel Chnl	WSE	VEL C	WS DIFF	VEL DIFF
	(cfs)	(ft)	(ft/s)				
13.7	50000	1089.27	7.06	1089.246	7.152	-0.024	0.092
13.79	50000	1091.64	7.79	1091.559	7.982	-0.081	0.192
13.89	50000	1093.88	7.21	1093.889	7.223	0.009	0.013
13.98	50000	1095.69	8.25	1095.688	8.219	-0.002	-0.031
14.08	50000	1098.36	8.91	1098.375	8.86	0.015	-0.05
14.17	50000	1100.48	9.09	1100.459	9.09	-0.021	0
14.27	50000	1102.53	9.93	1102.638	9.661	0.108	-0.269
14.36	50000	1105.61	10.62	1105.557	10.696	-0.053	0.076
14.45	50000	1107.5	10.53	1107.492	10.561	-0.008	0.031
14.55	50000	1109.49	9.23	1109.455	9.412	-0.035	0.182
14.64	50000	1111.02	11.48	1111.084	11.375	0.064	-0.105
14.73	50000	1114.02	10	1114.072	9.978	0.052	-0.022
14.83	50000	1116.11	9.35	1116.22	9.207	0.11	-0.143
14.92	50000	1117.32	10.47	1117.247	10.577	-0.073	0.107
15.02	50000	1118.85	11.23	1118.899	11.262	0.049	0.032
15.11	50000	1120.95	9.05	1120.967	9.022	0.017	-0.028
15.21	50000	1122.01	11.27	1121.946	11.463	-0.064	0.193
15.3	50000	1123.97	10.89	1123.951	10.914	-0.019	0.024
15.4	50000	1126.38	8.22	1126.457	8.094	0.077	-0.126
15.49	50000	1127.52	8.64	1127.567	8.512	0.047	-0.128
15.59	50000	1128.82	9.51	1128.792	9.319	-0.028	-0.191
15.68	50000	1130.75	10.55	1130.702	10.585	-0.048	0.035
15.78	50000	1133.31	7.83	1133.233	7.884	-0.077	0.054
15.87	50000	1134.5	9.98	1134.482	9.945	-0.018	-0.035
15.97	50000	1136.64	8.35	1136.614	8.329	-0.026	-0.021
16.06	50000	1138.49	7.69	1138.539	7.576	0.049	-0.114
16.16	50000	1140.1	9.06	1140.161	8.944	0.061	-0.116
16.25	50000	1142	8.01	1142.011	8.005	0.011	-0.005
16.35	50000	1143.79	7.15	1143.85	7.073	0.06	-0.077
16.44	50000	1145.86	9.02	1145.836	8.995	-0.024	-0.025
16.53	50000	1148.1	10.41	1148.121	10.267	0.021	-0.143
16.63	50000	1149.61	10.48	1149.617	10.672	0.007	0.192
16.72	50000	1151.73	9.44	1151.705	9.581	-0.025	0.141
16.82	50000	1153.88	8.21	1153.945	8.031	0.065	-0.179
16.91	50000	1155.7	8.81	1155.715	8.744	0.015	-0.066
17.01	50000	1157.6	10.22	1157.591	10.042	-0.009	-0.178
17.1	50000	1160.19	8.69	1160.135	8.855	-0.055	0.165
17.2	50000	1162.07	8.39	1162.091	8.332	0.021	-0.058
17.29	50000	1163.98	8.64	1163.971	8.626	-0.009	-0.014
17.39	50000	1166.07	9.58	1166.056	9.602	-0.014	0.022
17.48	50000	1168.13	10.01	1168.13	10.048	0	0.038
17.58	50000	1171.01	9.52	1171.101	9.341	0.091	-0.179
17.67	50000	1173.55	7.74	1173.611	7.73	0.061	-0.01
17.77	50000	1175.44	8.08	1175.462	8.023	0.022	-0.057
17.86	50000	1177.67	9.02	1177.642	9.002	-0.028	-0.018
17.95	50000	1180.21	8.26	1180.236	8.238	0.026	-0.022
18.05	50000	1181.53	7.16	1181.476	7.248	-0.054	0.088
18.14	50000	1182.78	9.73	1182.828	9.581	0.048	-0.149
18.24	50000	1185.41	7.6	1185.434	7.476	0.024	-0.124
18.33	50000	1186.96	8	1186.981	7.956	0.021	-0.044
18.43	50000	1189.14	9.22	1189.158	9.176	0.018	-0.044
18.52	50000	1191.8	6.64	1191.838	6.557	0.038	-0.083
18.62	50000	1192.94	6.72	1192.93	6.751	-0.01	0.031
18.71	50000	1195.5	8.19	1195.444	8.345	-0.056	0.155
18.81	50000	1198.16	7.53	1198.145	7.426	-0.015	-0.104
18.9	50000	1200.3	8.31	1200.289	8.224	-0.011	-0.086
19	50000	1202.4	5.79	1202.466	5.699	0.066	-0.091
19.09	50000	1203.69	7.2	1203.678	7.21	-0.012	0.01
19.19	50000	1205.95	8.58	1205.941	8.633	-0.009	0.053
19.28	50000	1209.26	7.4	1209.3	7.376	0.04	-0.024
19.38	50000	1211.44	7.19	1211.465	7.172	0.025	-0.018
19.47	50000	1213.04	9.58	1213.043	9.524	0.003	-0.056
19.56	50000	1215.62	7.01	1215.738	6.852	0.118	-0.158
19.66	50000	1216.84	9.18	1216.849	9.072	0.009	-0.108
19.75	50000	1220.95	8.05	1221.003	8.045	0.053	-0.005
19.85	50000	1222.9	7.05	1222.83	7.133	-0.07	0.083
19.94	50000	1224.21	8.07	1224.218	8.039	0.008	-0.031
20.14	50000	1225.77	8.7	1225.77	8.669	0	-0.031
20.23	50000	1226.84	8.48	1226.779	8.57	-0.061	0.09
20.3	50000	1227.75	9.18	1227.776	9.111	0.026	-0.069
20.32	50000	1229.54	8.01	1229.593	7.984	0.053	-0.026
20.42	50000	1231.23	6.92	1231.271	6.818	0.041	-0.102
20.51	50000	1233.1	8.25	1233.06	8.228	-0.04	-0.022
20.61	50000	1235.76	6.5	1235.768	6.523	0.008	0.023
20.7	50000	1237.6	7.65	1237.609	7.581	0.009	-0.069

	HEC-RAS RESULTS			HEC-6 RESULTS			
River Sta	Q Total	W.S. Elev	Vel Chnl	WSE	VEL C	WS DIFF	VEL DIFF
	(cfs)	(ft)	(ft/s)				
20.8	50000	1240.26	8.36	1240.214	8.279	-0.046	-0.081
20.89	50000	1243.11	7.75	1243.065	7.774	-0.045	0.024
20.98	50000	1245.39	8.59	1245.429	8.446	0.039	-0.144
21.08	50000	1248.26	8.35	1248.295	8.229	0.035	-0.121
21.17	50000	1250.49	7.44	1250.463	7.496	-0.027	0.056
21.27	50000	1252.15	8.5	1252.179	8.382	0.029	-0.118
21.36	50000	1254.1	7.43	1254.133	7.326	0.033	-0.104
21.46	50000	1255.77	8.23	1255.658	8.39	-0.112	0.16
21.55	50000	1257.39	8.88	1257.341	9.008	-0.049	0.128
21.65	50000	1258.87	8.94	1258.876	8.939	0.006	-0.001
21.74	50000	1260.88	8.44	1260.913	8.301	0.033	-0.139
21.84	50000	1262.7	7.64	1262.701	7.594	0.001	-0.046
21.93	50000	1264.01	7.39	1263.977	7.479	-0.033	0.089
22.03	50000	1266.52	9.88	1266.583	9.679	0.063	-0.201
22.12	50000	1269.46	7.15	1269.44	7.205	-0.02	0.055
22.21	50000	1271.12	9.93	1271.211	9.608	0.091	-0.322
22.31	50000	1274.19	6.81	1274.286	6.648	0.096	-0.162
22.4	50000	1275.25	9.31	1275.27	9.304	0.02	-0.006
22.5	50000	1278.13	7.86	1278.113	7.893	-0.017	0.033
22.59	50000	1280.44	7.7	1280.473	7.626	0.033	-0.074
22.69	50000	1282.04	6.89	1282.028	6.878	-0.012	-0.012
22.78	50000	1283.39	7.92	1283.416	7.872	0.026	-0.048
22.88	50000	1285.35	8.33	1285.334	8.315	-0.016	-0.015
22.97	50000	1287.37	7.72	1287.331	7.837	-0.039	0.117
23.07	50000	1288.99	9.19	1289.016	9.03	0.026	-0.16
23.16	50000	1291.55	11.27	1291.544	11.309	-0.006	0.039
23.26	50000	1294.68	11.28	1294.711	11.148	0.031	-0.132
23.35	50000	1297.05	11.01	1296.982	11.063	-0.068	0.053
23.45	50000	1298.9	10.54	1298.888	10.655	-0.012	0.115
23.54	50000	1300.65	8	1300.66	7.987	0.01	-0.013
23.63	50000	1301.87	8.7	1301.878	8.656	0.008	-0.044
23.73	50000	1304.16	9.44	1304.176	9.367	0.016	-0.073
23.82	50000	1306.66	8.71	1306.624	8.692	-0.036	-0.018
23.92	50000	1308.35	9.26	1308.34	9.125	-0.01	-0.135
24.01	50000	1310.25	8.03	1310.192	8.125	-0.058	0.095
24.11	50000	1311.98	8.3	1311.978	8.268	-0.002	-0.032
24.2	50000	1314.19	7.48	1314.21	7.445	0.02	-0.035
24.3	50000	1316.5	9.08	1316.461	9.146	-0.039	0.066
24.39	50000	1319.31	5.91	1319.418	5.719	0.108	-0.191
24.49	50000	1320.88	7.3	1320.95	7.138	0.07	-0.162
24.58	50000	1323.3	6.94	1323.223	7.084	-0.077	0.144
24.68	50000	1325.4	6.97	1325.406	6.918	0.006	-0.052
24.77	50000	1327.15	8.36	1327.139	8.361	-0.011	0.001
24.87	50000	1329.47	8.57	1329.482	8.567	0.012	-0.003
24.96	50000	1332.09	7.5	1332.088	7.521	-0.002	0.021
25.06	50000	1333.87	8.2	1333.899	8.045	0.029	-0.155
25.15	50000	1336.62	8	1336.531	7.962	-0.089	-0.038
25.24	50000	1339.9	9	1339.899	9.175	-0.001	0.175
25.34	50000	1342.77	6.21	1342.823	6.164	0.053	-0.046
25.43	50000	1344.32	6.84	1344.368	6.698	0.048	-0.142
25.53	50000	1346.29	6.66	1346.329	6.532	0.039	-0.128
25.62	50000	1348.72	6.15	1348.721	6.12	0.001	-0.03
25.72	50000	1350.75	5.73	1350.767	5.705	0.017	-0.025
25.81	50000	1352.31	7.39	1352.331	7.363	0.021	-0.027
25.91	50000	1354.5	6.99	1354.413	7.117	-0.087	0.127
26	50000	1356.48	7.45	1356.491	7.334	0.011	-0.116
26.1	50000	1359.26	6.94	1359.198	7.033	-0.062	0.093
26.19	50000	1361.89	5.85	1361.918	5.783	0.028	-0.067
26.29	50000	1364.08	5.79	1364.096	5.809	0.016	0.019
26.38	50000	1366.24	5.73	1366.299	5.65	0.059	-0.08
26.48	50000	1368.19	6.14	1368.167	6.096	-0.023	-0.044
26.57	50000	1370.68	5.93	1370.675	6.045	-0.005	0.115
26.67	50000	1373.04	5.22	1373.109	5.062	0.069	-0.158
26.76	50000	1374.9	5.55	1374.937	5.499	0.037	-0.051
26.85	50000	1377.05	5.54	1377.078	5.503	0.028	-0.037
26.95	50000	1378.95	4.85	1379.034	4.799	0.084	-0.051
27.04	50000	1381.03	6.14	1381.111	5.951	0.081	-0.189
27.14	50000	1383.84	5.5	1383.804	5.586	-0.036	0.086
27.23	50000	1386.51	5.86	1386.53	5.801	0.02	-0.059
27.33	50000	1388.93	5.24	1388.988	5.085	0.058	-0.155
27.43	50000	1390.52	4.96	1390.551	4.933	0.031	-0.027
27.52	50000	1392.2	4.77	1392.299	4.636	0.099	-0.134
27.61	50000	1394.18	6.41	1394.195	6.29	0.015	-0.12
27.75	50000	1397.57	4.58	1397.587	4.563	0.017	-0.017
27.89	50000	1400.08	4.67	1400.164	4.52	0.084	-0.15

HYDRAULIC CALIBRATION USING MANNINGS VALUES

	HEC-RAS RESULTS			HEC-6 RESULTS			
River Sta	Q Total	W.S. Elev	Vel Chnl	WSE	VEL C	WS DIFF	VEL DIFF
	(cfs)	(ft)	(ft/s)				
0.35	19466	785.75	5.87	785.747	5.856	-0.003	-0.014
0.44	19466	792.26	2.99	792.372	2.91	0.112	-0.08
0.54	19466	793.84	4.3	793.684	4.386	-0.156	0.086
0.63	19466	795.25	10.68	795.19	10.815	-0.06	0.135
0.73	19466	800.56	5.89	800.595	5.857	0.035	-0.033
0.82	19466	804.36	7.56	804.498	7.463	0.138	-0.097
0.92	19466	807.45	8.19	807.604	8.049	0.154	-0.141
1.01	19466	809.29	9.74	809.243	9.806	-0.047	0.066
1.11	19466	811.66	8.26	811.593	8.346	-0.067	0.086
1.2	19466	814.28	7.79	814.147	7.935	-0.133	0.145
1.3	19466	816.59	7.5	816.515	7.564	-0.075	0.064
1.39	19466	818.36	8.75	818.275	8.826	-0.085	0.076
1.49	19466	820.23	8	820.133	8.082	-0.097	0.082
1.58	19466	822.09	7.25	822.216	7.143	0.126	-0.107
1.65	19466	823.98	7.89	824.129	7.739	0.149	-0.151
1.72	19466	825.58	8.48	825.458	8.62	-0.122	0.14
1.81	19466	827.52	8.66	827.579	8.593	0.059	-0.067
1.91	19466	829.93	8.57	830.072	8.437	0.142	-0.133
2	19466	832.01	8.05	832.167	7.925	0.157	-0.125
2.1	19466	833.16	8.56	833.008	8.712	-0.152	0.152
2.19	19466	834.25	8.81	834.295	8.758	0.045	-0.052
2.29	19466	835.78	7.91	835.956	7.768	0.176	-0.142
2.38	19466	837.05	7.92	837.167	7.819	0.117	-0.101
2.48	19466	838.7	9.09	838.817	8.921	0.117	-0.169
2.57	19466	840.91	8.7	840.93	8.682	0.02	-0.018
2.64	19466	841.99	7.36	841.82	7.471	-0.17	0.111
2.66	19466	842.86	7.45	842.729	7.573	-0.131	0.123
2.72	19466	843.06	13.01	843.088	12.947	0.028	-0.063
2.78	19466	848.18	7.57	848.168	7.586	-0.012	0.016
2.87	19466	850.2	6.34	850.195	6.345	-0.005	0.005
2.96	19466	851.58	6.29	851.646	6.157	0.066	-0.133
3.06	19466	853.24	6.08	853.217	6.116	-0.023	0.036
3.15	19466	854.86	4.96	854.843	4.992	-0.017	0.032
3.25	19466	855.82	4.81	855.774	4.821	-0.046	0.011
3.34	19466	856.47	4.91	856.392	4.99	-0.078	0.08
3.44	19466	856.99	11.17	856.985	11.162	-0.005	-0.008
3.53	20000	860.01	6.8	859.901	6.725	-0.109	-0.075
3.63	20000	860.97	7.74	860.948	7.59	-0.022	-0.15
3.72	20000	862.67	6.44	862.534	6.479	-0.136	0.039
3.81	20000	863.82	7.65	863.724	7.756	-0.096	0.106
3.91	20000	865.76	7.89	865.686	7.829	-0.074	-0.061
4	20000	868.22	7.2	868.256	7.143	0.036	-0.057
4.01	20000	868.68	6.5	868.566	6.626	-0.114	0.126
4.09	20000	870.43	7.49	870.314	7.466	-0.116	-0.024
4.15	20000	872.41	3.96	872.397	3.845	-0.013	-0.115
4.25	20000	874.28	4.75	874.28	4.678	0	-0.072
4.34	20000	876.86	5.04	876.788	5.163	-0.072	0.123
4.44	20000	878.41	4.99	878.392	4.964	-0.018	-0.026
4.53	20000	880.51	6.34	880.431	6.314	-0.079	-0.026
4.63	20000	883.25	7.08	883.309	7.14	0.059	0.06
4.72	20000	885.67	6.01	885.64	6.091	-0.03	0.081
4.82	20000	887.26	7.64	887.22	7.679	-0.04	0.039
4.91	20000	889.39	7.56	889.434	7.417	0.044	-0.143
5	20000	891.85	7.56	891.849	7.437	-0.001	-0.123
5.1	20000	894.4	6.97	894.398	7.014	-0.002	0.044
5.19	20000	896.39	7.69	896.369	7.728	-0.021	0.038
5.29	20000	898.4	6.31	898.448	6.242	0.048	-0.068
5.38	20000	900.18	4.33	900.237	4.141	0.057	-0.189
5.48	20000	901.78	6.09	901.771	6.112	-0.009	0.022
5.57	20000	903.81	5.29	903.834	5.321	0.024	0.031
5.67	20000	905.24	8.1	905.349	8.032	0.109	-0.068
5.76	20000	907.52	8.45	907.584	8.348	0.064	-0.102
5.86	20000	909.78	8.91	909.735	8.948	-0.045	0.038
5.95	20000	911.97	6.15	912.045	6.079	0.075	-0.071
6.05	20000	913.24	8.06	913.159	8.024	-0.081	-0.036
6.14	20000	915.33	6.62	915.373	6.435	0.043	-0.185
6.23	20000	916.89	6.6	916.812	6.621	-0.078	0.021
6.33	20000	919.09	6.77	919.103	6.376	0.013	-0.394
6.42	20000	921.81	6.92	921.822	6.854	0.012	-0.066
6.52	20000	924.45	6.97	924.341	7.071	-0.109	0.101
6.61	20000	926.27	6.55	926.291	6.58	0.021	0.03
6.71	20000	927.77	6.27	927.722	6.297	-0.048	0.027
6.8	20000	929.93	5.37	929.921	5.311	-0.009	-0.059
6.9	20000	932.08	7.91	932.119	8.02	0.039	0.11

	HEC-RAS RESULTS			HEC-6 RESULTS			
River Sta	Q Total	W.S. Elev	Vel Chnl	WSE	VEL C	WS DIFF	VEL DIFF
	(cfs)	(ft)	(ft/s)				
6.99	20000	934.78	6.17	934.758	6.157	-0.022	-0.013
7.09	20000	937.12	6.43	937.102	6.402	-0.018	-0.028
7.18	20000	939.47	6.74	939.399	6.678	-0.071	-0.062
7.28	20000	941.69	6.24	941.737	6.19	0.047	-0.05
7.37	20000	943.89	6.51	943.814	6.583	-0.076	0.073
7.47	20000	946.2	5.08	946.268	5.064	0.068	-0.016
7.56	20000	947.85	5.05	947.878	5.052	0.028	0.002
7.66	20000	950.14	6.28	950.148	6.312	0.008	0.032
7.75	20000	952.43	5.17	952.434	5.163	0.004	-0.007
7.84	20000	954.5	6.03	954.594	5.915	0.094	-0.115
7.94	20000	956.55	5.74	956.613	5.674	0.063	-0.066
8.03	20000	958.75	7.66	958.681	7.75	-0.069	0.09
8.13	20000	961.43	6.22	961.416	6.23	-0.014	0.01
8.22	20000	963.28	7.82	963.239	7.822	-0.041	0.002
8.32	20000	966.02	6.27	965.976	6.264	-0.044	-0.006
8.41	20000	967.96	5.47	967.955	5.467	-0.005	-0.003
8.51	20000	969.86	6.14	969.887	5.999	0.027	-0.141
8.6	20000	971.99	5.35	971.988	5.494	-0.002	0.144
8.7	20000	974.38	5.35	974.428	5.33	0.048	-0.02
8.79	20000	976.34	5.7	976.311	5.852	-0.029	0.152
8.89	20000	978.35	5.45	978.389	5.477	0.039	0.027
8.98	20000	980.64	4.27	980.663	4.344	0.023	0.074
9.08	20000	982.57	5.31	982.637	5.117	0.067	-0.193
9.17	20000	984.64	6.12	984.659	6.124	0.019	0.004
9.27	20000	986.13	8.77	986	8.852	-0.13	0.082
9.36	20000	988.18	6.28	988.231	6.185	0.051	-0.095
9.45	20000	989.3	6.76	989.352	6.613	0.052	-0.147
9.55	20000	991.23	5.55	991.281	5.404	0.051	-0.146
9.64	20000	992.72	7.76	992.701	7.707	-0.019	-0.053
9.74	20000	995.84	6.59	995.821	6.652	-0.019	0.062
9.83	20000	998.16	8.29	998.316	7.625	0.156	-0.665
9.93	20000	1000.88	6.81	1000.89	6.774	0.01	-0.036
10.02	20000	1003.05	6.75	1003.038	6.716	-0.012	-0.034
10.12	20000	1005.12	7.12	1005.074	7.248	-0.046	0.128
10.21	20000	1007.77	4.41	1007.767	4.36	-0.003	-0.05
10.31	20000	1009.65	4.9	1009.65	4.905	0	0.005
10.4	20000	1011.42	7.52	1011.34	7.496	-0.08	-0.024
10.5	20000	1013.64	7.39	1013.578	7.473	-0.062	0.083
10.59	20000	1015.88	7.91	1015.851	7.831	-0.029	-0.079
10.69	20000	1017.91	8.64	1017.889	8.676	-0.021	0.036
10.73	20000	1019.54	5.7	1019.474	5.814	-0.066	0.114
10.77	20000	1020.31	5.75	1020.352	5.696	0.042	-0.054
10.87	20000	1021.95	5.92	1021.934	5.861	-0.016	-0.059
10.98	20000	1024.53	7.33	1024.57	7.217	0.04	-0.113
10.99	20000	1025.43	5.85	1025.425	5.885	-0.005	0.035
11	20000	1025.66	6.01	1025.7	5.922	0.04	-0.088
11.01	20000	1026.11	5.35	1026.014	5.43	-0.096	0.08
11.09	20000	1027.5	6.2	1027.455	6.326	-0.045	0.126
11.16	20000	1029.42	6.54	1029.482	6.406	0.062	-0.134
11.24	20000	1031.41	6.76	1031.451	6.606	0.041	-0.154
11.33	20000	1033.34	5.37	1033.382	5.292	0.042	-0.078
11.43	20000	1034.8	7.79	1034.794	7.748	-0.006	-0.042
11.52	20000	1037.08	5.07	1037.169	4.929	0.089	-0.141
11.62	20000	1038.67	7.05	1038.719	6.889	0.049	-0.161
11.71	20000	1041.45	4.73	1041.447	4.699	-0.003	-0.031
11.81	20000	1042.97	5	1042.956	4.93	-0.014	-0.07
11.9	20000	1044.66	7.67	1044.611	7.721	-0.049	0.051
12	20000	1047.71	6.27	1047.731	6.192	0.021	-0.078
12.09	20000	1049.49	5.73	1049.464	5.756	-0.026	0.026
12.18	20000	1051.71	7.3	1051.748	7.138	0.038	-0.162
12.28	20000	1054.48	5.41	1054.469	5.434	-0.011	0.024
12.37	20000	1055.89	6.37	1055.912	6.235	0.022	-0.135
12.47	20000	1057.3	5.18	1057.188	5.328	-0.112	0.148
12.56	20000	1058.85	9.78	1058.912	9.568	0.062	-0.212
12.66	20000	1061.97	8.59	1062.061	8.451	0.091	-0.139
12.75	20000	1064.97	7.27	1064.979	7.159	0.009	-0.111
12.85	20000	1067.61	5.08	1067.602	5.081	-0.008	0.001
12.94	20000	1069.15	6.3	1069.084	6.496	-0.066	0.196
13.04	20000	1072.3	6.3	1072.289	6.308	-0.011	0.008
13.13	20000	1074.76	4.82	1074.815	4.659	0.055	-0.161
13.23	20000	1076.9	4.77	1076.905	4.73	0.005	-0.04
13.32	20000	1078.97	5.19	1078.945	5.148	-0.025	-0.042
13.42	20000	1080.96	4.16	1080.972	4.11	0.012	-0.05
13.51	20000	1082.95	6.87	1082.893	6.966	-0.057	0.096
13.61	20000	1086.03	4.24	1086.138	4.058	0.108	-0.182

	HEC-RAS RESULTS			HEC-6 RESULTS			
River Sta	Q Total	W.S. Elev	Vel Chnl	WSE	VEL C	WS DIFF	VEL DIFF
	(cfs)	(ft)	(ft/s)				
13.7	20000	1087.9	5.26	1087.882	5.331	-0.018	0.071
13.79	20000	1090.21	5.97	1090.222	5.921	0.012	-0.049
13.89	20000	1092.25	5.99	1092.286	5.903	0.036	-0.087
13.98	20000	1094.15	6.2	1094.189	6.05	0.039	-0.15
14.08	20000	1096.7	7.87	1096.855	7.308	0.155	-0.562
14.17	20000	1099.05	6.43	1099.052	6.456	0.002	0.026
14.27	20000	1100.71	7.51	1100.725	7.456	0.015	-0.054
14.36	20000	1102.94	10.33	1102.966	10.251	0.026	-0.079
14.45	20000	1105.7	8.35	1105.742	8.229	0.042	-0.121
14.55	20000	1107.51	6.71	1107.489	6.803	-0.021	0.093
14.64	20000	1108.75	8.81	1108.791	8.69	0.041	-0.12
14.73	20000	1111.48	7.3	1111.454	7.405	-0.026	0.105
14.83	20000	1113.37	6.74	1113.414	6.678	0.044	-0.062
14.92	20000	1114.54	8.42	1114.493	8.52	-0.047	0.1
15.02	20000	1116.39	8.64	1116.502	8.588	0.112	-0.052
15.11	20000	1118.38	6.43	1118.359	6.364	-0.021	-0.066
15.21	20000	1119.53	8.7	1119.565	8.718	0.035	0.018
15.3	20000	1121.87	7.93	1121.894	7.764	0.024	-0.166
15.4	20000	1124.01	6.18	1124.088	6	0.078	-0.18
15.49	20000	1125.38	6.37	1125.36	6.404	-0.02	0.034
15.59	20000	1126.91	7.01	1126.799	6.968	-0.111	-0.042
15.68	20000	1129.04	7.98	1129.024	7.883	-0.016	-0.097
15.78	20000	1131.33	6.08	1131.284	6.062	-0.046	-0.018
15.87	20000	1132.9	7.29	1132.829	7.334	-0.071	0.044
15.97	20000	1134.87	6.13	1134.907	5.964	0.037	-0.166
16.06	20000	1136.68	6.15	1136.673	6.199	-0.007	0.049
16.16	20000	1138.6	6.78	1138.636	6.621	0.036	-0.159
16.25	20000	1140.28	6.19	1140.299	6.106	0.019	-0.084
16.35	20000	1142.22	5.82	1142.188	6.016	-0.032	0.196
16.44	20000	1144.68	6.22	1144.657	6.253	-0.023	0.033
16.53	20000	1146.52	7.88	1146.529	7.726	0.009	-0.154
16.63	20000	1148.11	7.06	1148.099	7.035	-0.011	-0.025
16.72	20000	1149.81	7.7	1149.794	7.76	-0.016	0.06
16.82	20000	1152.3	6.14	1152.39	5.997	0.09	-0.143
16.91	20000	1154.22	6.52	1154.223	6.39	0.003	-0.13
17.01	20000	1156.14	7.75	1156.162	7.943	0.022	0.193
17.1	20000	1158.67	6.55	1158.761	6.404	0.091	-0.146
17.2	20000	1160.7	6.3	1160.686	6.463	-0.014	0.163
17.29	20000	1162.63	6.56	1162.647	6.534	0.017	-0.026
17.39	20000	1164.79	7.11	1164.747	7.156	-0.043	0.046
17.48	20000	1166.68	7.42	1166.643	7.358	-0.037	-0.062
17.58	20000	1169.46	7.04	1169.432	7.189	-0.028	0.149
17.67	20000	1171.83	6.08	1171.887	5.988	0.057	-0.092
17.77	20000	1173.69	6.27	1173.748	6.211	0.058	-0.059
17.86	20000	1175.91	7.6	1175.912	7.412	0.002	-0.188
17.95	20000	1178.47	6.52	1178.465	6.472	-0.005	-0.048
18.05	20000	1179.64	4.8	1179.673	4.773	0.033	-0.027
18.14	20000	1181.26	7.56	1181.28	7.474	0.02	-0.086
18.24	20000	1183.73	5.31	1183.776	5.212	0.046	-0.098
18.33	20000	1185.15	6.15	1185.156	6.109	0.006	-0.041
18.43	20000	1187.54	6.78	1187.614	6.658	0.074	-0.122
18.52	20000	1189.99	5.36	1190.003	5.334	0.013	-0.026
18.62	20000	1191.41	5.22	1191.461	5.047	0.051	-0.173
18.71	20000	1194.3	6.27	1194.269	6.308	-0.031	0.038
18.81	20000	1196.71	6.18	1196.68	6.006	-0.03	-0.174
18.9	20000	1198.89	6.5	1198.879	6.478	-0.011	-0.022
19	20000	1200.79	4.12	1200.856	3.979	0.066	-0.141
19.09	20000	1202.15	5.62	1202.141	5.683	-0.009	0.063
19.19	20000	1204.64	6.2	1204.633	6.212	-0.007	0.012
19.28	20000	1207.61	5.6	1207.677	5.458	0.067	-0.142
19.38	20000	1209.65	5.47	1209.669	5.468	0.019	-0.002
19.47	20000	1211.34	8.08	1211.381	7.888	0.041	-0.192
19.56	20000	1213.65	4.92	1213.624	4.993	-0.026	0.073
19.66	20000	1214.68	8.04	1214.664	7.955	-0.016	-0.085
19.75	20000	1219.08	5.47	1219.107	5.442	0.027	-0.028
19.85	20000	1220.59	5.57	1220.513	5.714	-0.077	0.144
19.94	20000	1222	7.03	1222.022	6.946	0.022	-0.084
20.14	20000	1223.86	6.76	1223.88	6.712	0.02	-0.048
20.23	20000	1224.94	6.02	1224.886	6.149	-0.054	0.129
20.3	20000	1225.85	7.42	1225.878	7.402	0.028	-0.018
20.32	20000	1227.94	5.59	1228.022	5.451	0.082	-0.139
20.42	20000	1229.49	5.02	1229.489	5.044	-0.001	0.024
20.51	20000	1231.76	6.92	1231.719	7.032	-0.041	0.112
20.61	20000	1234.31	5.04	1234.364	4.875	0.054	-0.165
20.7	20000	1236.1	6.35	1236.127	6.299	0.027	-0.051

	HEC-RAS RESULTS			HEC-6 RESULTS			
River Sta	Q Total	W.S. Elev	Vel Chnl	WSE	VEL C	WS DIFF	VEL DIFF
	(cfs)	(ft)	(ft/s)				
20.8	20000	1238.94	6.38	1238.822	6.517	-0.118	0.137
20.89	20000	1241.53	5.24	1241.522	5.206	-0.008	-0.034
20.98	20000	1243.69	6.42	1243.697	6.406	0.007	-0.014
21.08	20000	1246.56	6.01	1246.542	6.016	-0.018	0.006
21.17	20000	1248.57	5.31	1248.584	5.364	0.014	0.054
21.27	20000	1250.15	6.34	1250.2	6.147	0.05	-0.193
21.36	20000	1252.01	5.8	1252.044	5.734	0.034	-0.066
21.46	20000	1253.97	6.48	1253.964	6.442	-0.006	-0.038
21.55	20000	1255.75	6.08	1255.787	6	0.037	-0.08
21.65	20000	1257.18	7	1257.153	6.992	-0.027	-0.008
21.74	20000	1259.49	5.92	1259.504	5.927	0.014	0.007
21.84	20000	1261.17	5.36	1261.25	5.208	0.08	-0.152
21.93	20000	1262.42	5.19	1262.365	5.216	-0.055	0.026
22.03	20000	1265.08	7.38	1265.115	7.262	0.035	-0.118
22.12	20000	1267.82	5.05	1267.862	4.953	0.042	-0.097
22.21	20000	1269.59	7.6	1269.619	7.469	0.029	-0.131
22.31	20000	1272.46	4.93	1272.46	4.853	0	-0.077
22.4	20000	1273.9	7.18	1273.964	6.919	0.064	-0.261
22.5	20000	1276.77	5.8	1276.72	5.915	-0.05	0.115
22.59	20000	1279.12	5.38	1279.12	5.306	0	-0.074
22.69	20000	1280.48	5.02	1280.5	4.938	0.02	-0.082
22.78	20000	1281.84	6.63	1281.801	6.781	-0.039	0.151
22.88	20000	1284.11	5.26	1284.14	5.315	0.03	0.055
22.97	20000	1285.78	5.58	1285.83	5.509	0.05	-0.071
23.07	20000	1287.56	6.14	1287.592	6.222	0.032	0.082
23.16	20000	1290.11	8.11	1290.073	8.148	-0.037	0.038
23.26	20000	1293.04	7.55	1293.043	7.567	0.003	0.017
23.35	20000	1295.2	7.96	1295.154	8.051	-0.046	0.091
23.45	20000	1297.1	7.5	1297.084	7.472	-0.016	-0.028
23.54	20000	1298.6	5.92	1298.555	6.015	-0.045	0.095
23.63	20000	1300.2	6.48	1300.164	6.527	-0.036	0.047
23.73	20000	1302.8	6.44	1302.779	6.457	-0.021	0.017
23.82	20000	1305.09	6.46	1305.105	6.452	0.015	-0.008
23.92	20000	1306.89	6.52	1306.853	6.598	-0.037	0.078
24.01	20000	1308.63	5.9	1308.639	5.899	0.009	-0.001
24.11	20000	1310.46	5.89	1310.482	5.874	0.022	-0.016
24.2	20000	1312.6	5.78	1312.606	5.909	0.006	0.129
24.3	20000	1315.12	7.07	1315.09	7.067	-0.03	-0.003
24.39	20000	1317.71	4.29	1317.747	4.222	0.037	-0.068
24.49	20000	1319.41	5.64	1319.424	5.563	0.014	-0.077
24.58	20000	1321.95	4.85	1321.981	4.655	0.031	-0.195
24.68	20000	1323.97	5.17	1323.923	5.295	-0.047	0.125
24.77	20000	1325.7	6.3	1325.725	6.118	0.025	-0.182
24.87	20000	1328.05	6.83	1328.034	6.847	-0.016	0.017
24.96	20000	1330.75	5.42	1330.765	5.366	0.015	-0.054
25.06	20000	1332.47	6.87	1332.496	6.706	0.026	-0.164
25.15	20000	1335.34	6.14	1335.265	6.181	-0.075	0.041
25.24	20000	1338.04	7.99	1338.082	8.008	0.042	0.018
25.34	20000	1340.93	5.32	1340.97	5.223	0.04	-0.097
25.43	20000	1342.61	6.36	1342.662	6.188	0.052	-0.172
25.53	20000	1344.57	5.95	1344.608	5.811	0.038	-0.139
25.62	20000	1346.9	5.7	1346.95	5.52	0.05	-0.18
25.72	20000	1349.04	4.99	1348.975	5.157	-0.065	0.167
25.81	20000	1350.7	6.67	1350.714	6.597	0.014	-0.073
25.91	20000	1353.01	5.7	1352.981	5.646	-0.029	-0.054
26	20000	1354.97	6.34	1355.005	6.232	0.035	-0.108
26.1	20000	1357.84	5.71	1357.836	5.625	-0.004	-0.085
26.19	20000	1360.47	4.52	1360.458	4.478	-0.012	-0.042
26.29	20000	1362.73	4.47	1362.788	4.293	0.058	-0.177
26.38	20000	1365.02	4.22	1365.012	4.229	-0.008	0.009
26.48	20000	1367.06	4.6	1367.054	4.691	-0.006	0.091
26.57	20000	1369.6	4.36	1369.627	4.344	0.027	-0.016
26.67	20000	1371.89	3.84	1371.921	3.741	0.031	-0.099
26.76	20000	1373.72	4.21	1373.758	4.161	0.038	-0.049
26.85	20000	1375.89	4.06	1375.944	3.919	0.054	-0.141
26.95	20000	1377.63	3.52	1377.67	3.47	0.04	-0.05
27.04	20000	1379.64	5.24	1379.584	5.288	-0.056	0.048
27.14	20000	1382.75	4.06	1382.744	4.054	-0.006	-0.006
27.23	20000	1385.56	4.4	1385.535	4.477	-0.025	0.077
27.33	20000	1387.91	3.87	1387.921	3.912	0.011	0.042
27.43	20000	1389.45	3.59	1389.452	3.548	0.002	-0.042
27.52	20000	1391.03	3.6	1391.038	3.575	0.008	-0.025
27.61	20000	1393.14	5.29	1393.1	5.444	-0.04	0.154
27.75	20000	1396.53	3.16	1396.606	3.039	0.076	-0.121
27.89	20000	1399.08	3.73	1399.119	3.67	0.039	-0.06

HYDRAULIC CALIBRATION USING MANNINGS VALUES

	HEC-RAS RESULTS			HEC-6 RESULTS			
River Sta	Q Total	W.S. Elev	Vel Chnl	WSE	VEL C	WS DIFF	VEL DIFF
	(cfs)	(ft)	(ft/s)				
0.35	5000	784.2	3.91	784.2	3.898	0	-0.012
0.44	5000	789.53	1.61	789.652	1.509	0.122	-0.101
0.54	5000	790.67	2.13	790.506	2.237	-0.164	0.107
0.63	5000	791.92	8.22	791.977	8.003	0.057	-0.217
0.73	5000	795.82	3.16	795.834	3.131	0.014	-0.029
0.82	5000	798.42	4.21	798.515	4.117	0.095	-0.093
0.92	5000	800.69	4.87	800.851	4.779	0.161	-0.091
1.01	5000	802.48	9.05	802.457	8.988	-0.023	-0.062
1.11	5000	805.32	5.49	805.207	5.607	-0.113	0.117
1.2	5000	807.45	5.77	807.478	5.795	0.028	0.025
1.3	5000	809.93	4.94	809.937	4.911	0.007	-0.029
1.39	5000	811.63	5.81	811.46	5.968	-0.17	0.158
1.49	5000	813.22	5.6	813.105	5.725	-0.115	0.125
1.58	5000	815.43	5.65	815.332	5.749	-0.098	0.099
1.65	5000	818.33	4.93	818.297	4.979	-0.033	0.049
1.72	5000	819.83	5.59	819.729	5.684	-0.101	0.094
1.81	5000	822.12	5.4	822.016	5.496	-0.104	0.096
1.91	5000	824.82	4.63	824.947	4.499	0.127	-0.131
2	5000	826.46	4.33	826.65	4.206	0.19	-0.124
2.1	5000	827.39	5.18	827.25	5.336	-0.14	0.156
2.19	5000	828.52	5.94	828.656	5.755	0.136	-0.185
2.29	5000	830.22	4.85	830.337	4.717	0.117	-0.133
2.38	5000	831.72	5.1	831.744	5.088	0.024	-0.012
2.48	5000	834.29	5.35	834.353	5.29	0.063	-0.06
2.57	5000	836.46	4.85	836.437	4.876	-0.023	0.026
2.64	5000	837.18	4.47	837.053	4.642	-0.127	0.172
2.66	5000	837.83	4.57	837.751	4.696	-0.079	0.126
2.72	5000	838.54	8.11	838.512	8.134	-0.028	0.024
2.78	5000	842.61	4.34	842.677	4.285	0.067	-0.055
2.87	5000	843.93	4.76	843.825	4.86	-0.105	0.1
2.96	5000	845.26	5.81	845.306	5.736	0.046	-0.074
3.06	5000	847.87	4.81	847.984	4.72	0.114	-0.09
3.15	5000	849.68	4.35	849.8	4.222	0.12	-0.128
3.25	5000	851.03	4.4	850.999	4.455	-0.031	0.055
3.34	5000	852.19	4.01	852.257	3.833	0.067	-0.177
3.44	5000	854.11	8.06	854.159	7.899	0.049	-0.161
3.53	5000	856.9	4.5	856.806	4.647	-0.094	0.147
3.63	5000	858.26	6.58	858.336	6.392	0.076	-0.188
3.72	5000	860.33	3.62	860.304	3.669	-0.026	0.049
3.81	5000	861.47	5.94	861.522	5.745	0.052	-0.195
3.91	5000	863.78	5.08	863.782	5.05	0.002	-0.03
4	5000	865.86	5.67	865.926	5.542	0.066	-0.128
4.01	5000	866.3	4.64	866.276	4.688	-0.024	0.048
4.09	5000	867.94	7.51	868.044	7.36	0.104	-0.15
4.15	5000	870.1	3.67	870.067	3.519	-0.033	-0.151
4.25	5000	872.37	3.72	872.359	3.704	-0.011	-0.016
4.34	5000	874.92	4.46	874.923	4.337	0.003	-0.123
4.44	5000	876.56	4.27	876.49	4.354	-0.07	0.084
4.53	5000	878.88	5.16	878.861	4.99	-0.019	-0.17
4.63	5000	881.18	4.5	881.287	4.38	0.107	-0.12
4.72	5000	883.35	3.99	883.32	3.805	-0.03	-0.185
4.82	5000	885.33	4.8	885.349	4.709	0.019	-0.091
4.91	5000	887.48	5.19	887.424	5.166	-0.056	-0.024
5	5000	889.44	6.05	889.461	6.215	0.021	0.165
5.1	5000	891.57	7.44	891.526	7.631	-0.044	0.191
5.19	5000	893.54	7.11	893.577	7.017	0.037	-0.093
5.29	5000	895.03	9.35	895.101	9.158	0.071	-0.192
5.38	5000	897.56	5.63	897.604	5.577	0.044	-0.053
5.48	5000	898.71	8.92	898.667	8.998	-0.043	0.078
5.57	5000	901.2	5.14	901.25	5.054	0.05	-0.086
5.67	5000	902.76	6.32	902.762	6.498	0.002	0.178
5.76	5000	904.93	6.36	905.091	6.333	0.161	-0.027
5.86	5000	906.97	8.01	906.988	7.94	0.018	-0.07
5.95	5000	909.49	5.49	909.541	5.508	0.051	0.018
6.05	5000	911.03	4.87	910.987	4.809	-0.043	-0.061
6.14	5000	913.2	6.66	913.353	5.554	0.153	-1.106
6.23	5000	915.35	4.2	915.328	4.029	-0.022	-0.171
6.33	5000	917.2	6.24	917.177	6.164	-0.023	-0.076
6.42	5000	920.36	4.28	920.374	4.295	0.014	0.015
6.52	5000	922.92	4.47	922.777	4.45	-0.143	-0.02
6.61	5000	924.79	3.25	924.746	3.282	-0.044	0.032
6.71	5000	926.13	3.6	926.072	3.522	-0.058	-0.078
6.8	5000	928.27	3.67	928.22	3.556	-0.05	-0.114
6.9	5000	930.51	5.11	930.568	5.123	0.058	0.013

	HEC-RAS RESULTS			HEC-6 RESULTS			
River Sta	Q Total	W.S. Elev	Vel Chnl	WSE	VEL C	WS DIFF	VEL DIFF
	(cfs)	(ft)	(ft/s)				
6.99	5000	933.01	5.07	932.999	5.081	-0.011	0.011
7.09	5000	935.42	4.91	935.425	4.74	0.005	-0.17
7.18	5000	937.68	5.71	937.727	5.586	0.047	-0.124
7.28	5000	939.95	5.56	939.977	5.518	0.027	-0.042
7.37	5000	942.41	5.84	942.478	5.294	0.068	-0.546
7.47	5000	944.69	4.18	944.84	4.142	0.15	-0.038
7.56	5000	946.52	4.02	946.532	4.136	0.012	0.116
7.66	5000	948.8	4.38	948.85	4.32	0.05	-0.06
7.75	5000	950.89	4.94	950.891	4.878	0.001	-0.062
7.84	5000	953.04	4.8	953.036	4.863	-0.004	0.063
7.94	5000	954.93	4.96	954.974	4.83	0.044	-0.13
8.03	5000	957.07	5.03	956.978	5.005	-0.092	-0.025
8.13	5000	959.36	4.89	959.394	4.915	0.034	0.025
8.22	5000	961.4	5.43	961.367	5.566	-0.033	0.136
8.32	5000	963.81	6.15	963.687	6.272	-0.123	0.122
8.41	5000	965.92	4.45	965.872	4.484	-0.048	0.034
8.51	5000	967.42	5.9	967.476	5.708	0.056	-0.192
8.6	5000	969.24	5.92	969.118	6.112	-0.122	0.192
8.7	5000	971.88	4.45	971.794	4.602	-0.086	0.152
8.79	5000	973.42	5.36	973.35	5.541	-0.07	0.181
8.89	5000	975.08	5.78	975.163	5.78	0.083	0
8.98	5000	977.95	4.47	977.968	4.451	0.018	-0.019
9.08	5000	980.08	4.96	980.067	4.905	-0.013	-0.055
9.17	5000	981.8	4.22	981.725	4.231	-0.075	0.011
9.27	5000	982.96	6.25	982.793	6.314	-0.167	0.064
9.36	5000	984.69	6.34	984.681	6.222	-0.009	-0.118
9.45	5000	986.7	6.63	986.73	6.442	0.03	-0.188
9.55	5000	988.97	5.04	989.05	4.695	0.08	-0.345
9.64	5000	990.74	6.36	990.826	6.27	0.086	-0.09
9.74	5000	993.67	6	993.69	5.894	0.02	-0.106
9.83	5000	996.2	6.84	996.268	6.726	0.068	-0.114
9.93	5000	998.75	7.39	998.732	7.198	-0.018	-0.192
10.02	5000	1000.98	5.02	1001.044	4.847	0.064	-0.173
10.12	5000	1002.72	7.21	1002.75	7.097	0.03	-0.113
10.21	5000	1006.02	2.93	1005.998	2.937	-0.022	0.007
10.31	5000	1007.82	3.96	1007.791	3.908	-0.029	-0.052
10.4	5000	1009.7	4.91	1009.673	4.948	-0.027	0.038
10.5	5000	1012.15	4.58	1012.118	4.601	-0.032	0.021
10.59	5000	1014.16	4.72	1014.142	4.69	-0.018	-0.03
10.69	5000	1015.83	5.16	1015.828	5.171	-0.002	0.011
10.73	5000	1017.05	4.29	1017.052	4.298	0.002	0.008
10.77	5000	1018.17	4.37	1018.214	4.185	0.044	-0.185
10.87	5000	1020.17	4.59	1020.067	4.593	-0.103	0.003
10.98	5000	1023.03	4.3	1023.019	4.3	-0.011	0
10.99	5000	1023.66	3.39	1023.622	3.467	-0.038	0.077
11	5000	1023.87	3.6	1023.852	3.653	-0.018	0.053
11.01	5000	1024.28	2.96	1024.236	3.096	-0.044	0.136
11.09	5000	1025.63	4.59	1025.658	4.472	0.028	-0.118
11.16	5000	1027.89	3.99	1027.87	4.021	-0.02	0.031
11.24	5000	1029.63	4.44	1029.599	4.466	-0.031	0.026
11.33	5000	1031.22	4.05	1031.255	3.999	0.035	-0.051
11.43	5000	1032.9	6.56	1032.935	6.469	0.035	-0.091
11.52	5000	1035.08	3.66	1035.125	3.497	0.045	-0.163
11.62	5000	1036.71	5.85	1036.751	5.778	0.041	-0.072
11.71	5000	1039.64	3.91	1039.693	3.797	0.053	-0.113
11.81	5000	1041.11	3.56	1041.028	3.671	-0.082	0.111
11.9	5000	1042.82	6.51	1042.83	6.451	0.01	-0.059
12	5000	1045.61	5.45	1045.654	5.268	0.044	-0.182
12.09	5000	1047.16	5.48	1047.156	5.436	-0.004	-0.044
12.18	5000	1049.32	7.24	1049.382	7.045	0.062	-0.195
12.28	5000	1051.75	6.91	1051.753	6.738	0.003	-0.172
12.37	5000	1053.57	5.19	1053.565	5.161	-0.005	-0.029
12.47	5000	1054.37	2.77	1054.411	2.744	0.041	-0.026
12.56	5000	1055.78	8.07	1055.777	7.988	-0.003	-0.082
12.66	5000	1059.05	7.41	1058.986	7.608	-0.064	0.198
12.75	5000	1062.15	5.21	1062.21	5.014	0.06	-0.196
12.85	5000	1064.59	4.28	1064.558	4.288	-0.032	0.008
12.94	5000	1066.57	6.58	1066.596	6.494	0.026	-0.086
13.04	5000	1070.91	5.39	1071.048	4.937	0.138	-0.453
13.13	5000	1073.09	3.54	1073.067	3.695	-0.023	0.155
13.23	5000	1075.23	3.62	1075.202	3.615	-0.028	-0.005
13.32	5000	1077.62	3.54	1077.59	3.621	-0.03	0.081
13.42	5000	1079.47	2.85	1079.487	2.729	0.017	-0.121
13.51	5000	1081.65	4.42	1081.584	4.477	-0.066	0.057
13.61	5000	1084.37	3.21	1084.343	3.287	-0.027	0.077

	HEC-RAS RESULTS			HEC-6 RESULTS			
River Sta	Q Total	W.S. Elev	Vel Chnl	WSE	VEL C	WS DIFF	VEL DIFF
	(cfs)	(ft)	(ft/s)				
13.7	5000	1086.35	4.15	1086.324	4.252	-0.026	0.102
13.79	5000	1088.43	4.08	1088.509	3.885	0.079	-0.195
13.89	5000	1090.38	4.82	1090.319	4.939	-0.061	0.119
13.98	5000	1092.47	4.15	1092.515	4.146	0.045	-0.004
14.08	5000	1094.77	6.18	1094.763	6.326	-0.007	0.146
14.17	5000	1097.09	4.51	1097.144	4.334	0.054	-0.176
14.27	5000	1098.72	4.81	1098.699	4.838	-0.021	0.028
14.36	5000	1100.63	6.48	1100.596	6.591	-0.034	0.111
14.45	5000	1102.67	6.78	1102.68	6.761	0.01	-0.019
14.55	5000	1104.46	5.96	1104.525	5.905	0.065	-0.055
14.64	5000	1105.76	7.08	1105.795	7.078	0.035	-0.002
14.73	5000	1108.14	6.06	1108.131	6.103	-0.009	0.043
14.83	5000	1110.42	4.26	1110.441	4.239	0.021	-0.021
14.92	5000	1111.66	6.5	1111.675	6.528	0.015	0.028
15.02	5000	1113.46	6.03	1113.534	6.004	0.074	-0.026
15.11	5000	1115.49	4.85	1115.46	4.856	-0.03	0.006
15.21	5000	1117.53	6.28	1117.543	6.172	0.013	-0.108
15.3	5000	1120.19	4.59	1120.214	4.525	0.024	-0.065
15.4	5000	1122	4.65	1122.023	4.511	0.023	-0.139
15.49	5000	1123.67	3.81	1123.686	3.788	0.016	-0.022
15.59	5000	1125.33	4.59	1125.153	4.572	-0.177	-0.018
15.68	5000	1127.7	4.87	1127.717	4.79	0.017	-0.08
15.78	5000	1129.5	4.32	1129.452	4.454	-0.048	0.134
15.87	5000	1131.12	5.64	1131.133	5.577	0.013	-0.063
15.97	5000	1133.09	4.18	1133.07	4.341	-0.02	0.161
16.06	5000	1135.07	5.2	1135.06	5.209	-0.01	0.009
16.16	5000	1137.13	4.87	1137.215	4.714	0.085	-0.156
16.25	5000	1138.61	5.2	1138.606	5.257	-0.004	0.057
16.35	5000	1140.56	4.59	1140.589	4.615	0.029	0.025
16.44	5000	1142.92	5.87	1143.007	5.35	0.087	-0.52
16.53	5000	1145.21	4.51	1145.188	4.451	-0.022	-0.059
16.63	5000	1146.45	4.05	1146.439	4.049	-0.011	-0.001
16.72	5000	1148.26	5.64	1148.279	5.499	0.019	-0.141
16.82	5000	1150.82	3.95	1150.783	3.976	-0.037	0.026
16.91	5000	1152.47	4.97	1152.453	5.004	-0.017	0.034
17.01	5000	1154.39	5.13	1154.392	5.008	0.002	-0.122
17.1	5000	1157.1	4.7	1157.128	4.654	0.028	-0.046
17.2	5000	1159.28	4.42	1159.288	4.527	0.008	0.107
17.29	5000	1161.07	4.16	1160.996	4.299	-0.074	0.139
17.39	5000	1163.3	5.48	1163.338	5.372	0.038	-0.108
17.48	5000	1165.15	4.54	1165.192	4.415	0.042	-0.125
17.58	5000	1167.74	6.24	1167.733	6.34	-0.007	0.1
17.67	5000	1170.16	4.19	1170.099	4.375	-0.061	0.185
17.77	5000	1171.95	5.98	1171.898	6.528	-0.052	0.548
17.86	5000	1174.08	7.07	1174.159	6.607	0.079	-0.463
17.95	5000	1176.48	6.51	1176.414	6.533	-0.066	0.023
18.05	5000	1177.75	2.49	1177.737	2.458	-0.013	-0.032
18.14	5000	1179.89	5.39	1179.955	5.043	0.065	-0.347
18.24	5000	1182.03	3.47	1182.013	3.453	-0.017	-0.017
18.33	5000	1183.41	5.32	1183.41	5.445	0	0.125
18.43	5000	1186.1	4.1	1186.13	4.12	0.03	0.02
18.52	5000	1188.25	5.02	1188.211	5.077	-0.039	0.057
18.62	5000	1190.16	3.32	1190.197	3.36	0.037	0.04
18.71	5000	1192.56	5.6	1192.59	5.455	0.03	-0.145
18.81	5000	1195.07	4.76	1195.023	4.851	-0.047	0.091
18.9	5000	1197.34	4.33	1197.378	4.31	0.038	-0.02
19	5000	1199.07	3	1199.143	2.873	0.073	-0.127
19.09	5000	1200.51	3.95	1200.483	3.946	-0.027	-0.004
19.19	5000	1203.01	5.47	1203.055	5.265	0.045	-0.205
19.28	5000	1206.04	3.77	1206.024	3.714	-0.016	-0.056
19.38	5000	1207.68	3.98	1207.688	3.874	0.008	-0.106
19.47	5000	1209.43	6.99	1209.499	6.683	0.069	-0.307
19.56	5000	1211.39	3.14	1211.406	3.124	0.016	-0.016
19.66	5000	1212.99	6.17	1213.038	5.715	0.048	-0.455
19.75	5000	1216.58	3.82	1216.547	3.786	-0.033	-0.034
19.85	5000	1217.87	4.33	1217.833	4.43	-0.037	0.1
19.94	5000	1219.51	6.95	1219.554	6.593	0.044	-0.357
20.14	5000	1221.72	4.29	1221.757	4.193	0.037	-0.097
20.23	5000	1222.63	3.57	1222.656	3.506	0.026	-0.064
20.3	5000	1223.95	5.93	1223.921	5.831	-0.029	-0.099
20.32	5000	1226.37	3.35	1226.43	3.302	0.06	-0.048
20.42	5000	1227.82	3.5	1227.872	3.539	0.052	0.039
20.51	5000	1230.15	5.9	1230.189	5.71	0.039	-0.19
20.61	5000	1232.39	5.32	1232.338	5.458	-0.052	0.138
20.7	5000	1234.29	6.19	1234.265	6.221	-0.025	0.031

	HEC-RAS RESULTS			HEC-6 RESULTS			
River Sta	Q Total	W.S. Elev	Vel Chnl	WSE	VEL C	WS DIFF	VEL DIFF
	(cfs)	(ft)	(ft/s)				
20.8	5000	1237.42	4.68	1237.466	4.548	0.046	-0.132
20.89	5000	1239.77	3.32	1239.827	3.225	0.057	-0.095
20.98	5000	1242.2	4.8	1242.16	4.994	-0.04	0.194
21.08	5000	1245.03	3.48	1245.051	3.504	0.021	0.024
21.17	5000	1246.75	3.48	1246.729	3.408	-0.021	-0.072
21.27	5000	1248.31	4.38	1248.296	4.398	-0.014	0.018
21.36	5000	1249.94	4.75	1249.858	4.908	-0.082	0.158
21.46	5000	1252.45	5.3	1252.438	5.327	-0.012	0.027
21.55	5000	1254.3	3.13	1254.347	3.007	0.047	-0.123
21.65	5000	1255.65	5.33	1255.669	5.434	0.019	0.104
21.74	5000	1258.3	3.63	1258.298	3.62	-0.002	-0.01
21.84	5000	1259.87	3.39	1259.809	3.48	-0.061	0.09
21.93	5000	1261.06	3.16	1261.068	3.081	0.008	-0.079
22.03	5000	1263.87	5.11	1263.9	4.932	0.03	-0.178
22.12	5000	1266.13	3.35	1266.12	3.369	-0.01	0.019
22.21	5000	1267.7	6.9	1267.544	7.414	-0.156	0.514
22.31	5000	1270.69	3.62	1270.683	3.489	-0.007	-0.131
22.4	5000	1272.56	5.65	1272.595	5.467	0.035	-0.183
22.5	5000	1275.21	5.41	1275.195	5.465	-0.015	0.055
22.59	5000	1277.63	3.83	1277.592	3.893	-0.038	0.063
22.69	5000	1278.77	3.6	1278.756	3.61	-0.014	0.01
22.78	5000	1280.2	5.71	1280.165	5.831	-0.035	0.121
22.88	5000	1282.63	3.74	1282.664	3.568	0.034	-0.172
22.97	5000	1284.15	5.44	1284.099	5.296	-0.051	-0.144
23.07	5000	1285.88	4.93	1285.826	4.969	-0.054	0.039
23.16	5000	1288.53	6.63	1288.596	6.031	0.066	-0.599
23.26	5000	1291.62	4.24	1291.62	4.202	0	-0.038
23.35	5000	1293.63	4.7	1293.594	4.716	-0.036	0.016
23.45	5000	1295.61	4.4	1295.567	4.492	-0.043	0.092
23.54	5000	1297.05	3.78	1297.11	3.606	0.06	-0.174
23.63	5000	1298.96	3.87	1298.97	3.977	0.01	0.107
23.73	5000	1301.38	4.05	1301.402	3.978	0.022	-0.072
23.82	5000	1303.67	4.05	1303.683	3.971	0.013	-0.079
23.92	5000	1305.47	3.72	1305.492	3.732	0.022	0.012
24.01	5000	1307.11	3.33	1307.141	3.299	0.031	-0.031
24.11	5000	1309.03	3.55	1309.078	3.377	0.048	-0.173
24.2	5000	1311.1	3.27	1311.13	3.177	0.03	-0.093
24.3	5000	1313.46	5.02	1313.395	5.087	-0.065	0.067
24.39	5000	1315.91	3.58	1315.88	3.557	-0.03	-0.023
24.49	5000	1317.89	4.07	1317.919	3.948	0.029	-0.122
24.58	5000	1320.35	3.39	1320.305	3.548	-0.045	0.158
24.68	5000	1322.52	3.57	1322.537	3.471	0.017	-0.099
24.77	5000	1324.11	4.41	1324.132	4.298	0.022	-0.112
24.87	5000	1326.55	5.81	1326.528	5.883	-0.022	0.073
24.96	5000	1329.43	3.74	1329.385	3.828	-0.045	0.088
25.06	5000	1331.11	5.33	1331.092	5.459	-0.018	0.129
25.15	5000	1333.9	4.32	1333.869	4.161	-0.031	-0.159
25.24	5000	1336.29	5.35	1336.257	5.529	-0.033	0.179
25.34	5000	1338.63	6.54	1338.668	6.441	0.038	-0.099
25.43	5000	1340.56	5.46	1340.468	5.616	-0.092	0.156
25.53	5000	1341.8	8.39	1341.885	8.041	0.085	-0.349
25.62	5000	1344.86	4.83	1344.79	4.936	-0.07	0.106
25.72	5000	1347.03	5.63	1347.023	5.569	-0.007	-0.061
25.81	5000	1349.18	5.7	1349.141	5.821	-0.039	0.121
25.91	5000	1351.3	4.75	1351.313	4.662	0.013	-0.088
26	5000	1353.36	4.88	1353.302	5.059	-0.058	0.179
26.1	5000	1356.33	4.49	1356.257	4.659	-0.073	0.169
26.19	5000	1358.91	3.33	1358.95	3.226	0.04	-0.104
26.29	5000	1361.23	3.43	1361.188	3.505	-0.042	0.075
26.38	5000	1363.74	2.91	1363.767	2.717	0.027	-0.193
26.48	5000	1365.65	3.76	1365.718	3.587	0.068	-0.173
26.57	5000	1368.14	3.74	1368.233	3.56	0.093	-0.18
26.67	5000	1370.29	3.1	1370.297	3.202	0.007	0.102
26.76	5000	1372.02	3.65	1372.035	3.622	0.015	-0.028
26.85	5000	1374.49	3.41	1374.506	3.452	0.016	0.042
26.95	5000	1376.24	2.23	1376.312	2.11	0.072	-0.12
27.04	5000	1378.3	3.91	1378.36	3.632	0.06	-0.278
27.14	5000	1381.52	3.15	1381.468	3.284	-0.052	0.134
27.23	5000	1384.45	3.77	1384.437	3.911	-0.013	0.141
27.33	5000	1386.83	2.91	1386.816	3.087	-0.014	0.177
27.43	5000	1388.25	2.87	1388.3	2.738	0.05	-0.132
27.52	5000	1389.77	2.59	1389.725	2.694	-0.045	0.104
27.61	5000	1392.11	4.63	1392.157	4.275	0.047	-0.355
27.75	5000	1395.49	2.01	1395.557	1.943	0.067	-0.067
27.89	5000	1398.11	2.87	1398.144	2.742	0.034	-0.128

APPENDIX 5.6

ADOT scour example details

Headcut Analysis for Sand Beds - Short-Term

Excavation Width	Wp	800 ft
Excavation Length	Lp	1000 ft
Excavation Depth	Yp	30 ft
Channel Slope	S	0.004
Excavation Volume:	Vf	2.4000E+07 ft^3
Initial Fill Period	Tf	2.2522 hrs

Time Interval (hours)	DT t (secs)	Discharge Q (cfs)	Flow Volume at Time Step (ft^3)	Cumulative Flow Volume (ft^3)	Dimensionless Time T* = t/Tf	Inflow/Outflow Channel Width Wc (ft)	Dimensionless Excavation Width W* = Wp/Wc	qp = Q/Wp (cfs/ft)	qc = Q/Wc (cfs/ft)	Max. possible Scour depth Ysmax (ft)	Scour Depth from Eq. Ys-eq (ft)	Estimated Scour Depth Ys	Scour Length at 5% Ys Ls5 (ft)
0.2500	900	200	1.8000E+05	1.8000E+05	0.1110	25.4	31.5264	0.2500	7.8816	15.0	0.3	0.3	23
0.5000	900	1000	9.0000E+05	1.0800E+06	0.2220	50.7	15.7804	1.2500	19.7254	15.0	2.4	2.4	51
0.7500	900	1000	9.0000E+05	1.9800E+06	0.3330	50.7	15.7804	1.2500	19.7254	15.0	3.1	3.1	59
1.0000	900	1200	1.0800E+06	3.0600E+06	0.4440	54.8	14.5905	1.5000	21.8857	15.0	4.3	4.3	70
1.2500	900	2500	2.2500E+06	5.3100E+06	0.5550	75.2	10.6415	3.1250	33.2547	15.0	7.7	7.7	101
1.5000	900	3600	3.2400E+06	8.5500E+06	0.6660	87.9	9.0972	4.5000	40.9373	15.0	10.3	10.3	125
1.7500	900	4700	4.2300E+06	1.2780E+07	0.7770	98.6	8.1118	5.8750	47.6565	15.0	12.8	12.8	148
2.0000	900	5700	5.1300E+06	1.7910E+07	0.8880	107.2	7.4660	7.1250	53.1956	15.0	15.1	15.0	169
2.2500	900	6700	6.0300E+06	2.3940E+07	0.9990	114.9	6.9647	8.3750	58.3296	15.0	17.3	15.0	189

Tailcut Analysis - Short-Term

Excavation Width	Wp	800 ft
Excavation Length	Lp	1000 ft
Excavation Depth	Yp	30 ft
Channel Slope	S	0.004

Excavation Volume:	Vf	2.4000E+07 ft^3

Time Interval (hours)	DT t (secs)	Discharge Q (cfs)	Flow Volume at Time Step (ft^3)	Cumulative Flow Volume (ft^3)	Sand Wave Celerity Cs (ft/s)	Dimensionless Time T*	Inflow/Outflow Channel Width Wc (ft)	Dimensionless Excavation Width W* = Wp/Wc	qp = Q/Wp (cfs/ft)	qc = Q/Wc (cfs/ft)	Scour Depth from Eq. Ys-eq (ft)	Scour Length at 5% Ys Ls5 (ft)
0.2492	897	200	1.7945E+05	1.7945E+05	3.0450E-04	0.0003	25.4	31.5264	0.2500	7.8816	0.2	36
0.2500	900	1000	9.0000E+05	1.0794E+06	1.8173E-03	0.0019	50.7	15.7804	1.2500	19.7254	0.7	116
0.2500	900	1000	9.0000E+05	1.9794E+06	1.8173E-03	0.0035	50.7	15.7804	1.2500	19.7254	1.0	171
0.2500	900	1200	1.0800E+06	3.0594E+06	2.2250E-03	0.0055	54.8	14.5905	1.5000	21.8857	1.2	225
0.2500	900	2500	2.2500E+06	5.3094E+06	5.0252E-03	0.0101	75.2	10.6415	3.1250	33.2547	1.7	320
0.2500	900	3600	3.2400E+06	8.5494E+06	7.5324E-03	0.0168	87.9	9.0972	4.5000	40.9373	2.3	436
0.2500	900	4700	4.2300E+06	1.2779E+07	1.0127E-02	0.0260	98.6	8.1118	5.8750	47.6565	2.8	568
0.2500	900	5700	5.1300E+06	1.7909E+07	1.2545E-02	0.0373	107.2	7.4660	7.1250	53.1956	3.4	708
0.2500	900	6700	6.0300E+06	2.3939E+07	1.5010E-02	0.0508	114.9	6.9647	8.3750	58.3296	4.0	856
0.2500	900	7500	6.7500E+06	3.0689E+07	1.7012E-02	0.0661	120.6	6.6350	9.3750	62.2030	4.5	1007
0.2500	900	8300	7.4700E+06	3.8159E+07	1.9038E-02	0.0832	125.9	6.3520	10.3750	65.9024	5.1	1161
0.2500	900	8700	7.8300E+06	4.5989E+07	2.0059E-02	0.1013	128.5	6.2248	10.8750	67.6944	5.6	1311
0.2500	900	9200	8.2800E+06	5.4269E+07	2.1342E-02	0.1205	131.6	6.0770	11.5000	69.8853	6.1	1460
0.2500	900	9200	8.2800E+06	6.2549E+07	2.1342E-02	0.1397	131.6	6.0770	11.5000	69.8853	6.5	1603
0.2500	900	9000	8.1000E+06	7.0649E+07	2.0828E-02	0.1584	131.6	6.0770	11.2500	68.3660	6.8	1738
0.2500	900	8600	7.7400E+06	7.8389E+07	1.9803E-02	0.1762	131.6	6.0770	10.7500	65.3275	7.0	1865
0.2500	900	8000	7.2000E+06	8.5589E+07	1.8275E-02	0.1927	131.6	6.0770	10.0000	60.7698	7.2	1982
0.2500	900	7600	6.8400E+06	9.2429E+07	1.7264E-02	0.2082	131.6	6.0770	9.5000	57.7313	7.3	2088
0.2500	900	10100	9.0900E+06	1.0152E+08	2.3672E-02	0.2295	137.0	5.8379	12.6250	73.7038	8.1	2186
0.2500	900	19800	1.7820E+07	1.1934E+08	4.9973E-02	0.2745	183.0	4.3707	24.7500	108.1747	9.7	2390
0.2500	900	32400	2.9160E+07	1.4850E+08	8.6326E-02	0.3522	226.2	3.5366	40.5000	143.2311	11.6	2748
0.2500	900	41300	3.7170E+07	1.8567E+08	1.1302E-01	0.4539	251.1	3.1861	51.6250	164.4819	13.4	3197
0.2500	900	45900	4.1310E+07	2.2698E+08	1.2707E-01	0.5683	262.8	3.0446	57.3750	174.6867	14.9	3671
0.2500	900	48500	4.3650E+07	2.7063E+08	1.3509E-01	0.6899	269.1	2.9734	60.6250	180.2600	16.4	4140
0.2500	900	50400	4.5360E+07	3.1599E+08	1.4097E-01	0.8167	273.5	2.9246	63.0000	184.2519	17.7	4599
0.2500	900	52200	4.6980E+07	3.6297E+08	1.4657E-01	0.8400	277.7	2.8808	65.2500	187.9745	18.0	4675

Short-Term Scour Profiles

Headcut Scour Profile

y_s/y_{sbrink}	Scour depth y_s	L_s/L_{s5}	Scour Distance L_s
	(ft)		(ft)
0.05	0.75	1.00	189
0.25	3.75	0.60	114
0.50	7.50	0.30	57
0.75	11.25	0.15	28
1.00	15.00	0.00	0

Tailcut Scour Profile

y_s/y_{sbrink}	Scour depth y_s	L_s/L_{s5}	Scour Distance L_s
	(ft)		(ft)
0.05	1	1.00	4675
0.25	5	0.50	2338
0.50	9	0.25	1169
0.75	14	0.10	468
1.00	18	0.00	0

Headcut Analysis for Sand Beds - Short-Term

Excavation Width	Wp	800 ft
Excavation Length	Lp	1000 ft
Excavation Depth	Yp	30 ft
Channel Slope	S	0.004
Excavation Volume:	Vf	2.4000E+07 ft^3
Initial Fill Period	Tf	4.9644 hrs

Time Interval	DT	Discharge	Flow Volume at Time Step	Cumulative Flow Volume	Dimensionless Time	Inflow/Outflow Channel Width	Dimensionless Excavation Width	qp = Q/Wp	qc = Q/Wc	Max. possible Scour depth	Scour Depth from Eq.	Estimated Scour Depth	Scour Length at 5% Ys
(hours)	t (secs)	Q (cfs)	(ft^3)	(ft^3)	T* = t/Tf	Wc (ft)	W* = Wp/Wc	(cfs/ft)	(cfs/ft)	Ysmax (ft)	Ys-eq (ft)	Ys	Ls5 (ft)
0.2500	900	41	3.6986E+04	3.6986E+04	0.0504	12.9	62.2563	0.0514	3.1981	15.0	0.0	0.0	10
0.5000	900	205	1.8493E+05	2.2192E+05	0.1007	25.7	31.1621	0.2568	8.0040	15.0	0.3	0.3	22
0.7500	900	205	1.8493E+05	4.0685E+05	0.1511	25.7	31.1621	0.2568	8.0040	15.0	0.4	0.4	25
1.0000	900	247	2.2192E+05	6.2877E+05	0.2014	27.8	28.8123	0.3082	8.8805	15.0	0.6	0.6	29
1.2500	900	514	4.6233E+05	1.0911E+06	0.2518	38.1	21.0142	0.6421	13.4937	15.0	1.5	1.5	41
1.5000	900	740	6.6575E+05	1.7569E+06	0.3022	44.5	17.9645	0.9247	16.6110	15.0	2.3	2.3	51
1.7500	900	966	8.6918E+05	2.6260E+06	0.3525	49.9	16.0186	1.2072	19.3375	15.0	3.1	3.1	59
2.0000	900	1171	1.0541E+06	3.6801E+06	0.4029	54.3	14.7435	1.4640	21.5851	15.0	3.9	3.9	67
2.2500	900	1377	1.2390E+06	4.9192E+06	0.4532	58.2	13.7535	1.7209	23.6683	15.0	4.7	4.7	74
2.5000	900	1541	1.3870E+06	6.3062E+06	0.5036	61.1	13.1024	1.9264	25.2400	15.0	5.5	5.5	80
2.7500	900	1705	1.5349E+06	7.8411E+06	0.5539	63.8	12.5436	2.1318	26.7411	15.0	6.2	6.2	86
3.0000	900	1788	1.6089E+06	9.4500E+06	0.6043	65.1	12.2923	2.2346	27.4682	15.0	6.7	6.7	91
3.2500	900	1890	1.7014E+06	1.1151E+07	0.6547	66.7	12.0004	2.3630	28.3572	15.0	7.3	7.3	96
3.5000	900	1890	1.7014E+06	1.2853E+07	0.7050	66.7	12.0004	2.3630	28.3572	15.0	7.7	7.7	98
3.7500	900	1849	1.6644E+06	1.4517E+07	0.7554	66.7	12.0004	2.3116	27.7408	15.0	7.9	7.9	100
4.0000	900	1767	1.5904E+06	1.6108E+07	0.8057	66.7	12.0004	2.2089	26.5078	15.0	8.0	8.0	101
4.2500	900	1644	1.4795E+06	1.7587E+07	0.8561	66.7	12.0004	2.0548	24.6585	15.0	8.0	8.0	102
4.5000	900	1562	1.4055E+06	1.8992E+07	0.9065	66.7	12.0004	1.9521	23.4255	15.0	8.0	8.0	103
4.7500	900	2075	1.8678E+06	2.0860E+07	0.9568	69.4	11.5284	2.5942	29.9067	15.0	9.9	9.9	114
4.9644	772	4068	3.1397E+06	2.4000E+07	1.0000	92.7	8.6310	5.0856	43.8939	15.0	14.2	14.2	154

Tailcut Analysis - Short-Term

Excavation Width	Wp	800 ft
Excavation Length	Lp	1000 ft
Excavation Depth	Yp	30 ft
Channel Slope	S	0.004

Excavation Volume: Vf 2.4000E+07 ft^3

Time Interval (hours)	DT t (secs)	Discharge Q (cfs)	Flow Volume at Time Step (ft^3)	Cumulative Flow Volume (ft^3)	Sand Wave Celerity Cs (ft/s)	Dimensionless Time T* = t/Tf	Inflow/Outflow Channel Width Wc (ft)	Dimensionless Excavation Width W* = Wp/Wc	qp = Q/Wp (cfs/ft)	qc = Q/Wc (cfs/ft)	Scour Depth from Eq. Ys-eq (ft)	Scour Length at 5% Ys Ls5 (ft)
0.2463	887	41	3.6435E+04	3.6435E+04	5.2572E-05	0.0000	12.9	62.2563	0.0514	3.1981	0.1	12
0.2500	900	205	1.8493E+05	2.2137E+05	3.1377E-04	0.0003	25.7	31.1621	0.2568	8.0040	0.3	40
0.2500	900	205	1.8493E+05	4.0630E+05	3.1377E-04	0.0006	25.7	31.1621	0.2568	8.0040	0.4	60
0.2500	900	247	2.2192E+05	6.2822E+05	3.8415E-04	0.0010	27.8	28.8123	0.3082	8.8805	0.4	79
0.2500	900	514	4.6233E+05	1.0905E+06	8.6761E-04	0.0017	38.1	21.0142	0.6421	13.4937	0.6	112
0.2500	900	740	6.6575E+05	1.7563E+06	1.3005E-03	0.0029	44.5	17.9645	0.9247	16.6110	0.8	152
0.2500	900	966	8.6918E+05	2.6255E+06	1.7484E-03	0.0045	49.9	16.0186	1.2072	19.3375	1.0	198
0.2500	900	1171	1.0541E+06	3.6796E+06	2.1659E-03	0.0064	54.3	14.7435	1.4640	21.5851	1.3	247
0.2500	900	1377	1.2390E+06	4.9186E+06	2.5915E-03	0.0088	58.2	13.7535	1.7209	23.6683	1.5	299
0.2500	900	1541	1.3870E+06	6.3056E+06	2.9372E-03	0.0114	61.1	13.1024	1.9264	25.2400	1.7	352
0.2500	900	1705	1.5349E+06	7.8405E+06	3.2869E-03	0.0144	63.8	12.5436	2.1318	26.7411	1.9	405
0.2500	900	1788	1.6089E+06	9.4495E+06	3.4632E-03	0.0175	65.1	12.2923	2.2346	27.4682	2.1	458
0.2500	900	1890	1.7014E+06	1.1151E+07	3.6848E-03	0.0208	66.7	12.0004	2.3630	28.3572	2.3	510
0.2500	900	1890	1.7014E+06	1.2852E+07	3.6848E-03	0.0241	66.7	12.0004	2.3630	28.3572	2.4	560
0.2500	900	1849	1.6644E+06	1.4517E+07	3.5960E-03	0.0274	66.7	12.0004	2.3116	27.7408	2.5	607
0.2500	900	1767	1.5904E+06	1.6107E+07	3.4190E-03	0.0304	66.7	12.0004	2.2089	26.5078	2.6	651
0.2500	900	1644	1.4795E+06	1.7586E+07	3.1553E-03	0.0333	66.7	12.0004	2.0548	24.6585	2.7	692
0.2500	900	1562	1.4055E+06	1.8992E+07	2.9807E-03	0.0360	66.7	12.0004	1.9521	23.4255	2.7	729
0.2500	900	2075	1.8678E+06	2.0860E+07	4.0870E-03	0.0396	69.4	11.5284	2.5942	29.9067	3.0	764
0.2500	900	4068	3.6616E+06	2.4521E+07	8.6280E-03	0.0474	92.7	8.6310	5.0856	43.8939	3.6	835
0.2500	900	6658	5.9918E+06	3.0513E+07	1.4904E-02	0.0608	114.6	6.9838	8.3219	58.1186	4.3	960
0.2500	900	8486	7.6377E+06	3.8151E+07	1.9513E-02	0.0784	127.2	6.2917	10.6079	66.7415	5.0	1117
0.2500	900	9432	8.4884E+06	4.6639E+07	2.1939E-02	0.0981	133.1	6.0124	11.7894	70.8823	5.6	1282
0.2500	900	9966	8.9692E+06	5.5608E+07	2.3323E-02	0.1191	136.2	5.8716	12.4572	73.1438	6.1	1446
0.2500	900	10356	9.3205E+06	6.4929E+07	2.4339E-02	0.1410	138.5	5.7754	12.9452	74.7636	6.6	1606
0.2500	900	10726	9.6534E+06	7.4582E+07	2.5306E-02	0.1638	140.6	5.6889	13.4075	76.2741	7.1	1763
0.2500	900	10993	9.8938E+06	8.4476E+07	2.6007E-02	0.1872	142.1	5.6290	13.7414	77.3511	7.5	1917
0.2500	900	11199	1.0079E+07	9.4555E+07	2.6547E-02	0.2111	143.3	5.5844	13.9983	78.1719	7.9	2066
0.2500	900	11281	1.0153E+07	1.0471E+08	2.6763E-02	0.2352	143.7	5.5669	14.1010	78.4984	8.3	2211
0.2500	900	11301	1.0171E+07	1.1488E+08	2.6817E-02	0.2593	143.8	5.5625	14.1267	78.5799	8.7	2352
0.2500	900	11219	1.0097E+07	1.2498E+08	2.6601E-02	0.2832	143.8	5.5625	14.0240	78.0084	9.0	2488
0.2500	900	11116	1.0005E+07	1.3498E+08	2.6330E-02	0.3069	143.8	5.5625	13.8955	77.2940	9.3	2619

0.2500	900	10993	9.8938E+06	1.4487E+08	2.6007E-02	0.3304	143.8	5.5625	13.7414	76.4368	9.6	2745
0.2500	900	11055	9.9493E+06	1.5482E+08	2.6168E-02	0.3539	143.8	5.5625	13.8185	76.8654	9.9	2866
0.2500	900	11281	1.0153E+07	1.6498E+08	2.6763E-02	0.3780	143.8	5.5625	14.1010	78.4370	10.2	2983
0.2500	900	11671	1.0504E+07	1.7548E+08	2.7793E-02	0.4030	145.8	5.4860	14.5890	80.0356	10.6	3103
0.2500	900	12267	1.1040E+07	1.8652E+08	2.9373E-02	0.4294	149.0	5.3698	15.3339	82.3398	11.0	3224
0.2500	900	12884	1.1595E+07	1.9812E+08	3.1015E-02	0.4574	152.2	5.2578	16.1045	84.6734	11.3	3349
0.2500	900	13541	1.2187E+07	2.1030E+08	3.2777E-02	0.4869	155.4	5.1464	16.9264	87.1103	11.7	3477
0.2500	900	14116	1.2705E+07	2.2301E+08	3.4327E-02	0.5177	158.3	5.0552	17.6455	89.2011	12.1	3609
0.2500	900	14548	1.3093E+07	2.3610E+08	3.5493E-02	0.5497	160.3	4.9901	18.1849	90.7452	12.5	3744
0.2500	900	14856	1.3371E+07	2.4947E+08	3.6329E-02	0.5824	161.8	4.9453	18.5702	91.8361	12.9	3881
0.2500	900	15000	1.3500E+07	2.6297E+08	3.6720E-02	0.6154	162.4	4.9249	18.7500	92.3419	13.2	4017
0.2500	900	14979	1.3482E+07	2.7645E+08	3.6664E-02	0.6484	162.4	4.9249	18.7243	92.2154	13.5	4152
0.2500	900	14836	1.3352E+07	2.8981E+08	3.6273E-02	0.6811	162.4	4.9249	18.5445	91.3299	13.8	4285
0.2500	900	14630	1.3167E+07	3.0297E+08	3.5716E-02	0.7132	162.4	4.9249	18.2877	90.0649	14.0	4415
0.2500	900	14342	1.2908E+07	3.1588E+08	3.4937E-02	0.7447	162.4	4.9249	17.9281	88.2940	14.2	4543
0.2500	900	14055	1.2649E+07	3.2853E+08	3.4160E-02	0.7754	162.4	4.9249	17.5685	86.5231	14.4	4666
0.2500	900	13747	1.2372E+07	3.4090E+08	3.3330E-02	0.8054	162.4	4.9249	17.1832	84.6256	14.5	4786
0.2500	900	13438	1.2095E+07	3.5300E+08	3.2501E-02	0.8347	162.4	4.9249	16.7979	82.7282	14.7	4902
0.2500	900	13110	1.1799E+07	3.6480E+08	3.1620E-02	0.8400	162.4	4.9249	16.3870	80.7043	14.6	4929

Short-Term Scour Profiles

Headcut Scour Profile

y_s/y_{sbrink}	Scour depth y_s	L_s/L_{s5}	Scour Distance L_s
	(ft)		(ft)
0.05	0.71	1.00	154
0.25	3.55	0.60	92
0.50	7.10	0.30	46
0.75	10.65	0.15	23
1.00	14.20	0.00	0

Tailcut Scour Profile

y_s/y_{sbrink}	Scour depth y_s	L_s/L_{s5}	Scour Distance L_s
	(ft)		(ft)
0.05	1	1.00	4929
0.25	4	0.50	2465
0.50	7	0.25	1232
0.75	11	0.10	493
1.00	15	0.00	0

Headcut Analysis for Sand Beds - Short-Term

Excavation Width	Wp	800 ft
Excavation Length	Lp	1000 ft
Excavation Depth	Yp	30 ft
Channel Slope	S	0.004
Excavation Volume:	Vf	2.4000E+07 ft^3
Initial Fill Period	Tf	7.0759 hrs

Time Interval (hours)	DT t (secs)	Discharge Q (cfs)	Flow Volume at Time Step (ft^3)	Cumulative Flow Volume (ft^3)	Dimensionless Time T* = t/Tf	Inflow/Outflow Channel Width Wc (ft)	Dimensionless Excavation Width W* = Wp/Wc	qp = Q/Wp (cfs/ft)	qc = Q/Wc (cfs/ft)	Max. possible Scour depth Ysmax (ft)	Estimated Scour Depth Ys
7.0759	25473	942	2.4000E+07	2.4000E+07	1.0000	204.0	3.9219	1.1777	4.6189	11.8	6.9

Tailcut Analysis - Short-Term

Excavation Width	Wp	800 ft
Excavation Length	Lp	1000 ft
Excavation Depth	Yp	30 ft
Channel Slope	S	0.004

Excavation Volume: Vf 2.4000E+07 ft^3

Time Interval (hours)	DT t (secs)	Discharge Q (cfs)	Flow Volume at Time Step (ft^3)	Cumulative Flow Volume (ft^3)	Sand Wave Celerity Cs (ft/s)	Dimensionless Time T* = t/Tf	Inflow/Outflow Channel Width Wc (ft)	Dimensionless Excavation Width W* = Wp/Wc	qp = Q/Wp (cfs/ft)	qc = Q/Wc (cfs/ft)	Scour Depth from Eq. Ys-eq (ft)	Scour Length at 5% Ys Ls5 (ft)
23.9998	86399	942	8.1402E+07	8.1402E+07	1.7010E-03	0.1470	49.4	16.1899	1.1777	19.0668	4.8	1796
24.0000	86400	10623	9.1784E+08	9.9924E+08	2.5037E-02	0.8400	140.0	5.7125	13.2789	75.8562	14.4	4948

Short-Term Scour Profiles

Headcut Scour Profile

y_s/y_{sbrink}	Scour depth y_s	L_s/L_{s5}	Scour Distance L_s
	(ft)		(ft)
0.05	0.34	1.00	139
0.25	1.72	0.60	84
0.50	3.45	0.30	42
0.75	5.17	0.15	21
1.00	6.89	0.00	0

Tailcut Scour Profile

y_s/y_{sbrink}	Scour depth y_s	L_s/L_{s5}	Scour Distance L_s
	(ft)		(ft)
0.05	1	1.00	4948
0.25	4	0.50	2474
0.50	7	0.25	1237
0.75	11	0.10	495
1.00	14	0.00	0